

UC San Diego

UC San Diego Electronic Theses and Dissertations

Title

New convertible isocyanides for the Ugi Reaction : application to the stereoselective synthesis of omuralide

Permalink

<https://escholarship.org/uc/item/9g1346tj>

Author

Gilley, Cynthia Brooke

Publication Date

2008

Peer reviewed|Thesis/dissertation

UNIVERSITY OF CALIFORNIA, SAN DIEGO

**New Convertible Isocyanides for the Ugi Reaction;
Application to the Stereoselective Synthesis of Omuralide**

A Dissertation submitted in partial satisfaction of the
Requirements for the degree Doctor of Philosophy

in

Chemistry

by

Cynthia Brooke Gilley

Committee in charge:

Professor Yoshihisa Kobayashi, chair
Professor Yitzhak Tor
Professor Jerry Yang
Professor Wei Wang
Professor William Fenical

2008

©

Cynthia Brooke Gilley, 2008

All rights reserved.

The Dissertation of Cynthia Brooke Gilley is approved, and it is
acceptable in quality and form for publication on microfilm:

chair

University of California, San Diego

2008

*To my mother, Laurie
I feel as though I am the luckiest daughter alive*

and

*To the rest of my family
Thank you for your encouragement and love*

TABLE OF CONTENTS

Signature Page.....	iii
Dedication.....	iv
Table of Contents.....	v
List of Abbreviations.....	xi
List of Figures.....	xv
List of Schemes.....	xvi
List of Tables.....	xxi
Acknowledgments.....	xxii
Vita.....	xxiv
Abstract.....	xxv

CHAPTER ONE

1.1 Fused γ -Lactam- β -lactone Natural Products:	
Structure, Isolation, & Bioactivity.....	1
1.1.1 Lactacystin.....	1
1.1.1.1 Omuralide: Biologically Active Form.....	2
1.1.2 The Salinosporamides.....	3
1.1.3 The Cinnabaramides.....	4
1.2 Proteasome Inhibition.....	5
1.2.1 The Proteasome: Structure and Function.....	5
1.2.1.1 Mechanism of Peptide Hydrolysis.....	7
1.2.2 Existing and Theoretical Biomedical Implications.....	7
1.2.2.1 Apoptosis.....	8
1.2.2.2 Induction of Heat Shock Response.....	8
1.2.2.3 Inhibition of the Immune System.....	9
1.2.2.4 Anticancer Therapy.....	9
1.2.2.5 Antiviral Effect.....	10
1.2.2.6 Anti-inflammatory Effect.....	11

1.2.3	Classes of Proteasome Inhibitors.....	11
1.2.3.1	Peptide Aldehydes.....	12
1.2.3.2	Peptide Vinyl Sulfones.....	14
1.2.3.3	Peptide Boronates.....	15
1.2.3.4	Peptide Epoxyketones.....	16
1.2.3.5	β -Lactones.....	18
1.2.3.5.1	The Belactosines.....	18
1.2.3.5.2	Lactacystin/Omuralide.....	19
1.2.3.5.3	Salinosporamide A.....	22
1.2.3.6	Noncovalent Proteasome Inhibitors: TMC-95.....	23
1.3	Biosynthesis of Lactacystin.....	24
1.4	Relevant Synthetic Efforts.....	26
1.4.1	Corey's First Total Synthesis of Lactacystin.....	26
1.4.2	Corey's Second Total Synthesis of Lactacystin.....	27
1.4.3	Corey's Synthesis of α -Methylomuralide.....	29
1.5	Conclusions.....	30
1.6	Notes and References.....	32

CHAPTER TWO

2.1	Pyroglutamic Acid.....	40
2.1.1	Natural Products.....	41
2.1.2	Synthesis of 2-Alkylpyroglutamic Acids.....	42
2.1.2.1	Amidation (Bond A).....	42
2.1.2.2	Stereoselective Functionalization of C2 (Bond B).....	43
2.1.2.3	Formation of C3-C4 Bond (Bond C).....	44
2.1.2.4	Formation of C2-C3 Bond (Bond D).....	47
2.2	The Ugi Reaction.....	52
2.2.1	History of Multicomponent Reactions.....	52

2.2.2	Ugi Reaction with γ -Ketoacids.....	54
2.2.3	Mechanism.....	56
2.2.4	Stereochemical Aspects.....	58
2.2.5	Drug Discovery.....	61
2.2.6	Natural Product Synthesis.....	62
2.3	Convertible Isocyanides.....	64
2.3.1	Definition.....	64
2.3.2	Known Convertible Isocyanides.....	65
2.3.2.1	Armstrong's Universal Isocyanide.....	65
2.3.2.2	Ugi's Isocyanide.....	68
2.3.2.3	Marten's Isocyanide.....	68
2.3.2.4	Linderman's Isocyanide.....	69
2.3.3	Limitations of Existing Convertible Isocyanides.....	70
2.3.4	New Convertible Isocyanide.....	73
2.3.4.1	Activated Amides.....	73
2.3.4.2	Activation of Anilide via <i>N</i> -Acylindole.....	75
2.3.4.3	Strategy.....	76
2.4	Conclusions.....	77
2.5	Notes and References.....	78

CHAPTER THREE

3.1	1-Isocyano-2-(2,2-dimethoxyethyl)benzene.....	85
3.1.1	Preparative Synthesis.....	86
3.1.2	Application as Convertible Isocyanide.....	87
3.1.1.1	Pyroglutamic Acid Synthesis.....	88
3.1.1.2	Pyroglutamic Acid Derivatives.....	89
3.1.1.3	Linear Substrates.....	90
3.2	Preliminary Studies.....	91
3.2.1	General Strategy Towards β -Hydroxy- γ -ketoacids.....	92
3.2.2	Ugi Reaction of β -Hydroxy- γ -ketoacids.....	93

3.2.2.1	The Amadori Rearrangement.....	95
3.2.3	Ugi Reaction of β -Hydroxy- β -methyl- γ -ketoacids.....	96
3.3	Stereocontrolled Formal Total Synthesis of Proteasome Inhibitor Omuralide	98
3.3.1	Retrosynthetic Analysis.....	98
3.3.1.1	Nucleophilic Additions to 1,3-Dioxan-5-ones.....	99
3.3.2	Synthesis of (<i>E</i>)-2-hydroxymethylcinnamaldehyde (276)..	102
3.3.3	Synthesis of γ -ketoacid 274	103
3.3.4	Stereoselective Ugi Reaction of γ -ketoacid 274	105
3.3.4.1	Proposed Explanation of Diastereoselectivity.....	107
3.3.5	Failure of Indole Formation.....	107
3.3.6	Formation of <i>N</i> -Acylindole 302	109
3.3.7	Completion of Formal Synthesis of Omuralide.....	110
3.3.8	Corey's Endgame.....	111
3.4	Expanded Stereoselective Ugi Reaction of γ -ketoacids.....	112
3.4.1	Objective.....	112
3.4.2	Enantioselective Synthesis of γ -ketoacid 310	113
3.4.3	Racemic Synthesis of γ -ketoacid 311	114
3.4.4	Racemic Synthesis of γ -ketoacid 312	115
3.4.5	Stereoselectivity in the Ugi Reaction.....	116
3.5	Conclusions.....	118
3.6	Acknowledgments.....	120
3.7	Experimental.....	120
3.7.1	Materials and Methods.....	120
3.7.2	Preparative Procedures.....	122
3.8	Notes and References.....	149
APPENDIX ONE: Spectra Relevant to Chapter Three.....		152
APPENDIX TWO: X-ray Crystallography Reports Relevant to Chapter Three....		237

CHAPTER FOUR

4.1	New Convertible Isocyanide.....	272
4.1.1	Strategy.....	273
4.1.2	4-Methoxy-2-Nitrophenyl Isocyanide.....	275
4.2	<i>N</i> -Acylbenzotriazoles.....	275
4.2.1	Preparation.....	276
4.2.1.1	Direct Coupling of Benzotriazole with Acid Chlorides.....	276
4.2.1.2	Reaction with 1-(Methanesulfonyl)benzotriazole.....	277
4.2.1.3	Reaction with Thionyl Chloride.....	277
4.2.2	Utility.....	278
4.3	Preparation of 2- Nitrophenyl Isocyanide.....	280
4.4	2- Nitrophenyl Isocyanide as a Convertible Isocyanide.....	281
4.4.1	<i>N</i> -Acylbenzotriazole.....	281
4.4.2	Synthetic Utility.....	282
4.4.3	Synthesis of Amino Acid.....	285
4.5	Synthesis of the Fused γ -Lactam- β -lactone Bicycle.....	286
4.5.1	Retrosynthetic Analysis.....	286
4.5.2	Enantioselective Synthesis of Fused γ -Lactam- β -lactone 354	287
4.6	Conclusions.....	290
4.7	Acknowledgments.....	291
4.8	Experimental.....	292
4.8.1	Materials and Methods.....	292
4.8.2	Preparative Procedures.....	293
4.9	Notes and References.....	305

APPENDIX THREE: Spectra Relevant to Chapter Four.....	308
APPENDIX FOUR: X-ray Structure Reports Relevant to Chapter Four.....	342

LIST OF ABBREVIATIONS

Ac	acetyl, acetate
AcOH	acetic acid
Al	aldehyde
<i>i</i> -Am	<i>iso</i> -Amyl
aq.	aqueous
Ar	aryl
Arg	arginine
Asn	asparagine
ATP	adenosine triphosphate
Bn	benzyl
BOC	<i>tert</i> -butyloxycarbonyl
BOPCl	bis(2-oxo-3-oxazolidinyl)phosphinic chloride
bp	boiling point
br	broad
<i>n</i> -Bu	<i>normal</i> -butyl
<i>t</i> -Bu	<i>tertiary</i> -butyl
calcd	calculated
CAN	ceric ammonium nitrate
cat.	catalytic amount
CoA	coenzyme A
CSA	camphorsulfonic acid
d	doublet
<i>de</i>	diastereomeric excess
<i>dr</i>	diastereomeric ratio
Da	daltons
DBU	1,8-diazabicyclo[5.4.0]undec-7-ene
DCC	dicyclohexylcarbodiimide
DCM	dichloromethane

DMAP	4-dimethylaminopyridine
DMF	<i>N,N</i> -dimethylformamide
DMP	dess-martin periodinane
2,2-DMP	2,2-dimethoxypropane
DMS	dimethylsulfide
DMSO	dimethylsulfoxide
E ⁺	electrophile
<i>ee</i>	enantiomeric excess
EI	electron impact
equiv. (eq.)	equivalent
Et	ethyl
Gly	glycine
h	hour
Hz	hertz
IBX	2-iodoxybenzoic acid
IC	inhibitor concentration
IR	infrared (spectrum)
KHMDS	potassium bis(trimethylsilyl)amide
LDA	lithium diisopropylamine
Leu	leucine
LHMDS	lithium bis(trimethylsilyl)amide
m	multiplet
μm	micromolar
Me	methyl
min	minutes
mol	mole
MOM	methoxymethyl
mp	melting point
mRNA	messenger ribonucleic acid
Ms	methanesulfonyl (mesyl)

MTM	methylthiomethyl
NAC	<i>N</i> -acetyl cysteine
NF	nuclear factor
nM	nanomolar
NMR	nuclear magnetic resonance
Nu	nucleophile
[O]	oxidation
Pd/C	palladium on charcoal
Ph	phenyl
PhH	benzene
Piv	pivoyl
PMB	<i>para</i> -methoxybenzyl
PMP	<i>para</i> -methoxyphenyl
ppm	parts per million
PPTs	pyridinium <i>para</i> -toluenesulfonate
<i>i</i> -Pr	<i>iso</i> -propyl
Pro	proline
Py	pyridine
Quant.	quantitative
rt	room temperature
s	singlet
SAMP	(<i>S</i>)-1-amino-2-methoxymethylpyrrolidine
SAR	structure-activity relationship
t	triplet
TBAF	tetrabutylammonium fluoride
TBAI	tetrabutylammonium iodide
TBDPS	<i>tertiary</i> -butyldiphenylsilyl
TBS	<i>tertiary</i> -butyldimethylsilyl
Tf	trifluoromethanesulfonyl
TFA	trifluoroacetic acid

TFAA	trifluoroacetic anhydride
TFE	2,2,2-trifluoroethanol
THF	tetrahydrofuran
TLC	thin-layer chromatography
TMS	trimethylsilyl
(<i>p</i> -)TsOH	<i>para</i> -toluenesulfonic acid
Δ	heat to reflux

LIST OF FIGURES

Figure 1.1.1	Structure of Lactacystin.....	1
Figure 1.1.1.1	Structure of Omuralide.....	2
Figure 1.1.2	Structure of Salinosporamides A,B.....	3
Figure 1.1.3	Structure of Cinnabaramides A-G.....	4
Figure 1.2.3.6	Structure of TMC-95A.....	24
Figure 2.1.1	Natural Products Containing Pyroglutamic Acid.....	41
Figure 2.1.2	2-Alkylpyroglutamic Acid.....	42
Figure 2.2.5	Compounds with GHS Agonist Activity.....	61
Figure 2.3.2.1	Stable Derivatives of 1-Cyclohexen-1-yl Isocyanide.....	67
Figure 3.2	Structure of Model β -Hydroxy- γ -Ketoacids 257-261	92
Figure 3.3.3	X-ray Crystal Structure of 291	104
Figure 3.3.4	X-Ray Crystal Structure of 294	106
Figure 3.3.4.1	Explanation of Diastereoselectivity in the Ugi reaction of γ -ketoacid 274 with Convertible Isocyanide 240	107
Figure 3.4.1a	Structures of <i>epi</i> -Omuralide (308), desmethyl-Omulalide (309), and α -Methyl-Omuralide (58).....	112
Figure 3.4.1	Structures of Targeted γ -Ketoacids 310-312 and Expected Stereochemical Output via U-4C-3CCR.....	113
Figure 3.4.5	X-Ray Crystal Structure of 314	118
Figure 4.5.2	X-Ray Crystal Structure of 350	289

LIST OF SCHEMES

Scheme 1.2.1.1	Mechanism of Peptide Hydrolysis.....	7
Scheme 1.2.3.1	Mechanism of Proteasome Inhibition by Calpain Inhibitor I.....	13
Scheme 1.2.3.2	Mechanism of Proteasome Inhibition by Ac-Pro-Arg-Leu-Asn-vs.....	14
Scheme 1.2.3.3	Mechanism of Proteasome Inhibition by PS-341.....	15
Scheme 1.2.3.4	Mechanism of Proteasome Inhibition by Epoxomicin.....	17
Scheme 1.2.3.5.1	Mechanism of Proteasome Inhibition by Homobelactosin C.....	19
Scheme 1.2.3.5.2a	Mechanism of Proteasome Inhibition by Lactacystin in Cultured Cells.....	20
Scheme 1.2.3.5.2b	Interaction of Thr10 ^γ of 20S Proteasome with Lactacystin.....	21
Scheme 1.2.3.5.3	Mechanism of Proteasome Inhibition by Salinosporamides A.....	22
Scheme 1.3	Biosynthesis of Lactacystin.....	25
Scheme 1.4.1	Corey's First Total Synthesis of Lactacystin.....	27
Scheme 1.4.2	Corey's Second Total Synthesis of Lactacystin.....	28
Scheme 1.4.3	Corey's Total Synthesis of α -Methylomuralide.....	30
Scheme 2.1	Structure of Pyroglutamic Acid.....	40
Scheme 2.1.2.2a	Synthesis of 2-Alkylpyroglutamic Acid via Direct Alkylation.....	43
Scheme 2.1.2.2b	Baldwin's Total Synthesis of Lactacystin: Synthesis of 2-Alkylpyroglutamic Acid From Silyloxypyrroles.....	44

Scheme 2.1.2.3a	Pattenden's Total Synthesis of Lactacystin: Radical Cyclization Strategy.....	45
Scheme 2.1.2.3b	Corey's Total Synthesis of Omuralide-Salinosporamide A Hybrid: Kulinkovich Reaction Strategy.....	46
Scheme 2.1.2.4a	Wardrop's Total Synthesis of Omuralide: Intramolecular C-H Insertion Strategy.....	48
Scheme 2.1.2.4b	Jacobsen's Total Synthesis of Lactacystin: Enantio- and Diastereoselective Conjugate Addition Strategy.....	49
Scheme 2.1.2.4c	Potts's Total Synthesis of Salinosporamide A: Intramolecular Aldol Reaction Strategy.....	50
Scheme 2.1.2.4d	Romo's Total Synthesis of Salinosporamide A: Intramolecular Bis-Cyclization Strategy.....	51
Scheme 2.2	Strategy Towards 2-Alkylpyroglutamic Acid Synthesis...	52
Scheme 2.2.1	Passerini and Ugi Reaction.....	53
Scheme 2.2.2a	Ketoacids in Ugi-4C-3CCR.....	55
Scheme 2.2.2b	Ugi's Synthesis of Pyroglutamic Acid Amide.....	56
Scheme 2.2.3a	Mechanism of Ugi-4CCR.....	57
Scheme 2.2.3b	Mechanism of Ugi-4C-3CCR.....	58
Scheme 2.2.4a	Chiral Phenethylamines in the Ugi Reaction.....	59
Scheme 2.2.4b	Chiral Sugar Derived Amines in the Ugi Reaction.....	60
Scheme 2.2.6	Fukuyama's Total Synthesis of Ecteinascidine 743.....	63
Scheme 2.3.1	Definition of Convertible Isocyanide.....	65
Scheme 2.3.2.1a	Ugi's Application of 1-Cyclohexen-1-yl Isocyanide.....	66
Scheme 2.3.2.1b	Armstrong's Application of 1-Cyclohexen-1-yl Isocyanide.....	66
Scheme 2.3.2.1c	Activated Azlactone/Münchnone Intermediate.....	67

Scheme 2.3.2.2	Ugi's Convertible Isocyanide.....	68
Scheme 2.3.2.3	Marten's Convertible Isocyanide.....	69
Scheme 2.3.2.4	Linderman's Convertible Isocyanide.....	70
Scheme 2.3.3a	Strategy for Application of Convertible Isocyanide to 2-Alkylpyroglutamic Acid Synthesis.....	70
Scheme 2.3.3b	Failed Application of Armstrong's Isocyanide.....	71
Scheme 2.3.3c	Cisoid and Transoid Amide Rotamers.....	72
Scheme 2.3.4	Hydrolysis of C-Terminal Amide of Pyroglutamic Acid Amides.....	73
Scheme 2.3.4.1a	Structure of Activated Amides.....	74
Scheme 2.3.4.1b	Resonance Structures of Activated Amides.....	75
Scheme 2.3.4.2	2,2-Dimethoxyethyl)aniline as a Carboxylic Acid Protecting Group.....	76
Scheme 2.3.4.3	Hypothesis of 1-Isocyano-2-(2,2-dimethoxyethyl)benzene.....	76
Scheme 3.1	Hypothesis of 1-Isocyano-2-(2,2-dimethoxyethyl)benzene.....	86
Scheme 3.1.1	Preparative Synthesis of Isocyanide 240	87
Scheme 3.1.2.1	Synthesis of Pyroglutamic Acid 249 with Convertible Isocyanide 240	88
Scheme 3.1.2.2	Utility of <i>N</i> -Acylindole 248 as a Coupling Agent.....	89
Scheme 3.1.2.3	Utility of Convertible Isocyanide 240 in the U-4CR by Wessjohann.....	91
Scheme 3.2.1	General Strategy towards the Synthesis of the β -Hydroxy- γ -Ketoacid Motif.....	93
Scheme 3.2.2.1	The Amadori Rearrangement of β -Hydroxy- γ -Ketoacid 260	96

Scheme 3.3.1	Retrosynthetic Analysis for the Stereocontrolled Synthesis of Omuralide (2).....	99
Scheme 3.3.1.1a	Nucleophilic Additions to 2-Phenyl-1,3-dioxan-5-one (278) and 4-Phenylcyclohexanone (280).....	100
Scheme 3.3.1.1b	Nucleophilic Additions to Substituted 1,3-dioxan-5-ones 282 and 285	101
Scheme 3.3.1.1c	Expected Stereochemical Outcome in the Ugi Reaction of γ -Ketoacid 274 with Convertible Isocyanide 240	102
Scheme 3.3.2	Synthesis of (<i>E</i>)-2-(Hydroxymethyl)cinnamaldehyde (276).....	103
Scheme 3.3.3a	Evans Aldol Reaction incorporating (<i>E</i>)-2-(hydroxymethyl)cinnamaldehyde (276).....	104
Scheme 3.3.3b	Synthesis of γ -Ketoester 291	104
Scheme 3.3.3c	Synthesis and Observed Structure of γ -Ketoacid 294	105
Scheme 3.3.4	Stereoselective Ugi Reaction of γ -Ketoacid 274 with Convertible Isocyanide 240	106
Scheme 3.3.5	Failure of <i>N</i> -Acylindole Formation from Ugi Anilide 294	108
Scheme 3.3.6	Synthesis of <i>N</i> -Acylindole 302	109
Scheme 3.3.7	Completion of the Formal Total Synthesis of Omuralide (2).....	110
Scheme 3.3.8	Conversion of Common Intermediate 305 to Omuralide (2) reported by Corey.....	111
Scheme 3.4.2	Enantioselective Synthesis of γ -Ketoacid 310	113
Scheme 3.4.3	Racemic Synthesis of γ -Ketoacid 311	115
Scheme 3.4.4	Racemic Synthesis of γ -Ketoacid 312	116
Scheme 4.1	Failed Intramolecular Conversion of the Activated <i>N</i> -Acylindole Intermediate 297 to β -lactone 325	273

Scheme 4.1.1a	Structures of <i>N</i> -acylindole 248 and <i>N</i> -acylbenzotriazole 326	274
Scheme 4.1.1b	Retrosynthetic Strategy Towards Synthesis of <i>N</i> -Acylbenzotriazole 326	274
Scheme 4.1.2	4-Methoxy-2-Nitrophenyl Isocyanide (206) as Convertible Isocyanide in the Ugi Reaction.....	275
Scheme 4.2.1.2	Synthesis of <i>N</i> -Acylbenzotriazoles via Reaction of 1-(Methanesulfonyl)benzotriazole (335).....	277
Scheme 4.2.2a	Synthetic Applications of <i>N</i> -acylbenzotriazoles.....	278
Scheme 4.4.2b	Hypothesis of Direct β -Lactone formation via Activated <i>N</i> -acylbenzotriazole.....	279
Scheme 4.3	Synthesis of 2-Nitrophenyl Isocyanide (330).....	280
Scheme 4.4.1a	Synthesis of <i>N</i> -Acylbenzotriazole 326	281
Scheme 4.4.1b	Methanolysis of <i>N</i> -Acylbenzotriazole 326	282
Scheme 4.4.3	Synthesis of Linear <i>N</i> -Acylbenzotriazole 346	285
Scheme 4.5.1	Retrosynthetic Analysis of the Stereocontrolled Synthesis of Fused γ -Lactam- β -Lactone Bicycle 347	287
Scheme 4.5.2	Stereocontrolled Synthesis of Fused γ -Lactam- β -Lactone Bicycle 354	288

LIST OF TABLES

Table 3.2.2	The Ugi reaction of β -Hydroxy- γ -Ketoacids 257-261 with Convertible Isocyanide 240	94
Table 3.2.3	Ugi Reaction of β -Hydroxy- β -Methyl- γ -Ketoacids 259a-c with Convertible Isocyanide 240	97
Table 3.4.5	Stereoselective Ugi reaction of β,δ -Dihydroxy- γ -Ketoacids 310-312	117
Table 4.4.2	Synthetic Utility of <i>N</i> -Acylbenzotriazole 326	283

ACKNOWLEDGEMENTS

I would like to start by thanking my advisor, Professor Yoshihisa Kobayashi, for his advice and support. When I met Yoshi, I was immediately impressed with his knowledge of synthetic chemistry and his unwavering excitement and pursuit of chemical understanding. It became obvious, in a short amount of time, that Yoshi was dedicated to teaching his students. Not only did he provide helpful advice concerning laboratory skills but he also actively guided our learning and understanding of chemical reactions and their mechanisms, and for that, I am genuinely grateful.

Additionally, I am grateful to the other members of my thesis committee, Professors Yitzhak Tor, Jerry Yang, William Fenical and Wei Wang. On numerous occasions both Dr. Tor and Dr. Yang provided an ear and a place to go for advice and support.

I would like to thank my undergraduate research advisors, Professors Gene Hiegel and Maria Linder, for taking me under their wing and providing a place for me in their labs. Professor Hiegel was the first to inspire my love of organic chemistry and my drive to succeed. He also took the time to unofficially introduce me to organic synthesis and natural product chemistry. I will forever be grateful to him for his unwavering belief in me. Professor Linder was an important female figure in my life who showed me how to be a strong woman.

During my time at UCSD, I had the privilege of working with a number of bright people who have contributed to my growth as a chemist and as a person. In the early days, Kristy Clarke, Aikomari Guzman, and Misha Golynskiy were there to provide their

support and friendship. In the later days, I would like to thank Thong Nguyen, Mitchell Vamos, and above all Matt Buller for offering their friendship and support. Thong was there for me when I needed him the most and for that he will always have a special place in my heart. Mitchell could always be counted on for a laugh. As for Matt, his presence in my life makes me feel complete.

Finally, I would like to thank my family, my grandma Pat, my papa Jim, my brothers Craig and Jeff, my sister Michelle, all my aunts, uncles, and cousins, and most of all, my mother Laurie. Without her support, emotionally and financially, I could not have accomplished any of this. She is the strongest woman I know. She is my rock.

CHAPTER THREE, in part, is a reprint of the material as it appears in (1) Gilley, C. B.; Buller, M. J.; Kobayashi, Y. "New Entry to Convertible Isocyanides for the Ugi Reaction and its Application to the Stereocontrolled Formal Total Synthesis of the Proteasome Inhibitor Omuralide" *Organic Letters* **2007**, *9*, 3631-3634 (2) Buller, M. J.; Gilley, C. B.; Nguyen, B.; Olshansky, L.; Fraga, B.; Kobayashi, Y. "Synthesis of Functionalized Pyroglutamic Acids. Part 1: The Synthetic Utility of *N*-Acylindole and the Ugi Reaction with a Chiral Levulinic Acid" *Synlett* (Manuscript in Revision) (3) Gilley, C. B.; Buller, M. J.; Kobayashi, Y. "Synthesis of Functionalized Pyroglutamic Acids. Part 2: The Stereoselective Condensation of Multi-Functional Groups with Chiral Levulinic Acids" *Synlett* (Manuscript in Revision). The dissertation author was the primary or secondary investigator and author of this paper.

CHAPTER FOUR, in part, is a reprint of the material as it appears in Gilley, C. B.; Kobayashi, Y. "2-Nitrophenyl Isocyanide as a Versatile Convertible Isocyanide: Rapid Access to a Fused γ -Lactam- β -lactone Bicycle" *J. Org. Chem.* **2008**, *73*, 4198-4204. The dissertation author was the primary investigator and author of this paper.

VITA

- 2003 B.A. Chemistry
California State University, Fullerton
Fullerton, CA
- 2003-2008 Teaching Assistant
Department of Chemistry and Biochemistry
University of California, San Diego
- 2003-2008 Research Assistant
University of California, San Diego
- 2008 M.S. Chemistry
University of California, San Diego
La Jolla, CA
- 2008 Ph.D. Chemistry
University of California, San Diego
La Jolla, CA

PUBLICATIONS

Gilley, C. B.; Buller, M. J.; Pereira, G. R.; Nguyen, B.; Kobayashi, Y. "Synthesis of Proteasome Inhibitor Omuralide Featuring Stereocontrolled Ugi Reaction and Novel Convertible Isocyanide" (Manuscript in Preparation)

Buller, M. J.; Gilley, C. B.; Nguyen, B.; Olshansky, L.; Fraga, B.; Kobayashi, Y. "Synthesis of Functionalized Pyroglutamic Acids. Part 1: The Synthetic Utility of *N*-Acyldiindole and the Ugi Reaction with a Chiral Levulinic Acid" *Synlett* (Manuscript in Revision)

Gilley, C. B.; Buller, M. J.; Kobayashi, Y. "Synthesis of Functionalized Pyroglutamic Acids. Part 2: The Stereoselective Condensation of Multi-Functional Groups with Chiral Levulinic Acids" *Synlett* (Manuscript in Revision)

Gilley, C. B.; Kobayashi, Y. "2-Nitrophenyl Isocyanide as a Versatile Convertible Isocyanide: Rapid Access to a Fused γ -Lactam- β -lactone Bicycle" *J. Org. Chem.* **2008**, *73*, 4198-4204.

Gilley, C. B.; Buller, M. J.; Kobayashi, Y. "New Entry to Convertible Isocyanides for the Ugi Reaction and its Application to the Stereocontrolled Formal Total Synthesis of the Proteasome Inhibitor Omuralide" *Organic Letters* **2007**, *9*, 3631-3634.

Isaacson, J.; Gilley, C. B.; Kobayashi, Y. "Expeditious Access to Unprotected Pyroglutamic Acids" *Journal of Organic Chemistry* **2007**, *72*, 3913-3916.

Linder, M. C.; Moriya M.; Whon A.; Kassa A.; Gilley C. "Vesicular transport of Fe and interaction with other metal ions in polarized Caco2 cell monolayers" *Biological Research* **2006**, *39*, 143-156.

Gilley, C. B.; Hiegel, G. "The Oxidation of Primary Alcohols to Methyl Esters and Diols to Lactones Using Trichloroisocyanuric Acid" *Synthetic Communications* **2003**, *33*, 2003-2009.

ABSTRACT OF THE DISSERTATION

New Convertible Isocyanides for the Ugi Reaction;
Application to the Stereoselective Synthesis of Omuralide

by

Cynthia Brooke Gilley

Doctor of Philosophy in Chemistry

University of California, San Diego, 2008

Professor Yoshihisa Kobayashi, Chair

Omuralide, derived from natural product lactacystin, is a member of a family of proteasome inhibitors, including the salinosporamides and the cinnabaramides, that all contain a novel fused γ -lactam- β -lactone core structure. A great deal of attention from the synthetic community has been paid to these natural products due to recent validation of proteasome inhibition as a novel therapeutic target in human cancer. A formal total synthesis of omuralide is introduced along with an efficient synthetic route to the shared common fused γ -lactam- β -lactone core structure among the aforementioned proteasome inhibitors. Key features of my synthetic studies include the development of two

convertible isocyanides for use in the Ugi 4-center 3-component condensation reaction, their application in pyroglutamic acid derivative synthesis, and the development of a novel stereoselective Ugi reaction.

CHAPTER ONE

An Introduction to Lactacystin/Omuralide

1.1 Fused γ -Lactam- β -Lactone Natural Products: Structure, Isolation, and Bioactivity

1.1.1 Lactacystin

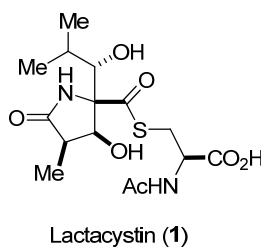


Figure 1.1.1 Structure of Lactacystin

In 1991, Omura reported the isolation and characterization of lactacystin (**1**, Figure 1.1.1), a natural compound isolated from the culture broth of *Streptomyces lactacystinaeus*.¹ The structure of lactacystin was elucidated by spectroscopic analyses, including NMR and X-ray crystallography,² and found to possess a non-peptide

consisting of two α -amino acids, an *N*-acetyl-cysteine and a novel pyroglutamic acid derivative.

Lactacystin was originally isolated and characterized as a result of its ability to induce neuritogenesis in neuroblastoma cell lines and was later identified as the first isolated natural proteasome inhibitor.^{3,4} Lactacystin, as well as other chemical compounds which are able to efficiently and selectively inhibit the proteasome, have found an application in biology and medicine as a means to investigate the proteasome and its cellular role.⁵ In addition, inhibition of proteasomal activity may eventually have applications in the treatment of many diseases including allergies,⁶ inflammation,⁷ viral infections,⁸ ischemic stroke,⁹ tuberculosis,¹⁰ and cancer.⁶

1.1.1.1 Omuralide: Biologically Active Form

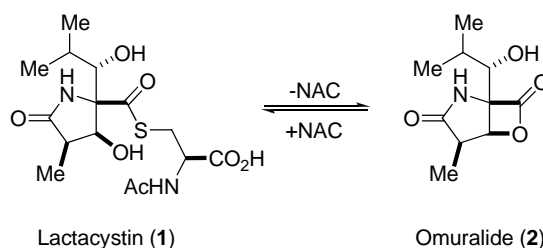


Figure 1.1.1.1 Structure of Omuralide

Surprisingly, subsequent *in vitro* studies revealed that lactacystin itself is not active against proteasomes. Further experiments showed that in aqueous solutions at pH 8, lactacystin is spontaneously converted into *clasto*-lactacystin β -lactone (Figure 1.1.1.1), later named omuralide (2), which is the active proteasome inhibitor.¹¹

1.1.2 The Salinosporamides

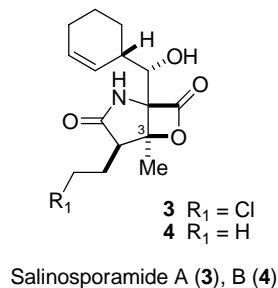


Figure 1.1.2 Structure of Salinosporamides A,B

In 2003, Fenical reported the discovery of salinosporamide A (**3**, Figure 1.1.2), a secondary metabolite of the marine actinomycete *Salinispora tropica*, as a highly potent and selective inhibitor of the proteasome.¹² In addition to being a more effective proteasome inhibitor than omuralide, approximately 35 times more potent, salinosporamide A displays high *in vitro* cytotoxic activity against many tumor cell lines (IC₅₀ values of 10 nM or less) and is currently undergoing clinical studies as a potential drug for anticancer treatment.¹³ The deschloro analog, salinosporamide B (**4**), was reported in 2005 as an additional secondary metabolite also produced by *Salinispora tropica*.^{14,15}

Structurally, the core of salinosporamide A, a fused γ -lactam- β -lactone, closely resembles omuralide.² However, salinosporamide A contains several unique substituents, including a cyclohexene ring in place of the isopropyl group, a chloroethyl group in place of the methyl group, and an additional methyl group attached to C3. Collectively, these

groups enhance its potency *in vitro* and *in vivo*.¹⁵ Remarkably, in contrast to omuralide, which exists in nature in the form of its precursor thioester lactacystin, thioesters of salinosporamide A have not been found in nature but have been prepared semisynthetically.¹⁶ Such a thioester would irreversibly give rise to chloride elimination with concurrent tetrahydrofuran formation, diminishing its biological activity (see section 1.2.3.5.3).

1.1.3 The Cinnabaramides

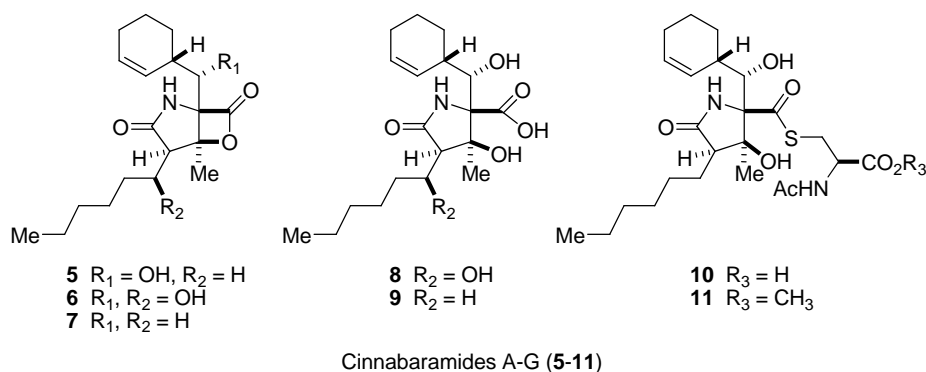


Figure 1.1.3 Structure of Cinnabaramides A-G

The cinnabaramides A-G (5-11) (Figure 1.1.3) were isolated from a terrestrial strain of *Streptomyces*, found in a Japanese soil sample, and identified as potent and selective inhibitors of the human 20S proteasome.¹⁷ The strain showed the closest similarity (99%) to three terrestrial *Streptomyces* spp. including *S. cinnabarinus* and two isolates not identified at species level. The absolute and relative configuration of cinnabaramide A was determined by X-ray crystallography.

Cinnabaramide A is structurally closely related to salinosporamide A and omuralide, sharing the fused γ -lactam- β -lactone core structure. However, when compared to salinosporamide A, cinnabaramide A contains an *n*-hexyl side chain in place of the chloro ethyl side chain of the latter. Interestingly, *N*-acetyl cysteine was incorporated in cinnabaramides F-G in an analogous manner as lactacystin.

The proteasomal inhibitory affects of the cinnabaramides A-C and F-G, determined using a human 20S proteasome inhibition assay, were determined to be in the low nM range which was similar in potency to that reported for salinosporamide A.

1.2 Proteasome Inhibition

1.2.1 The Proteasome: Structure and Function

The 26S proteasome complex⁵ is a multifunctional, 2,500 kDa intracellular proteolytic molecular machine, in which several enzymatic (proteolytic, ATPase, de-ubiquitinating) activities functional together with the ultimate goal of protein degradation.¹⁸ In eukaryotes, 26S proteasomes are composed of a cylinder shaped 20S core structure capped at each end by a regulatory component known as the 19S regulatory complex.¹⁹ The 19S complex is responsible for recognition, unfolding, and translocation of the selected substrates into the lumen of the 20S proteasome.²⁰ The 19S regulatory complex only recognizes proteins tagged by ubiquitin. This strictly controlled pathway,

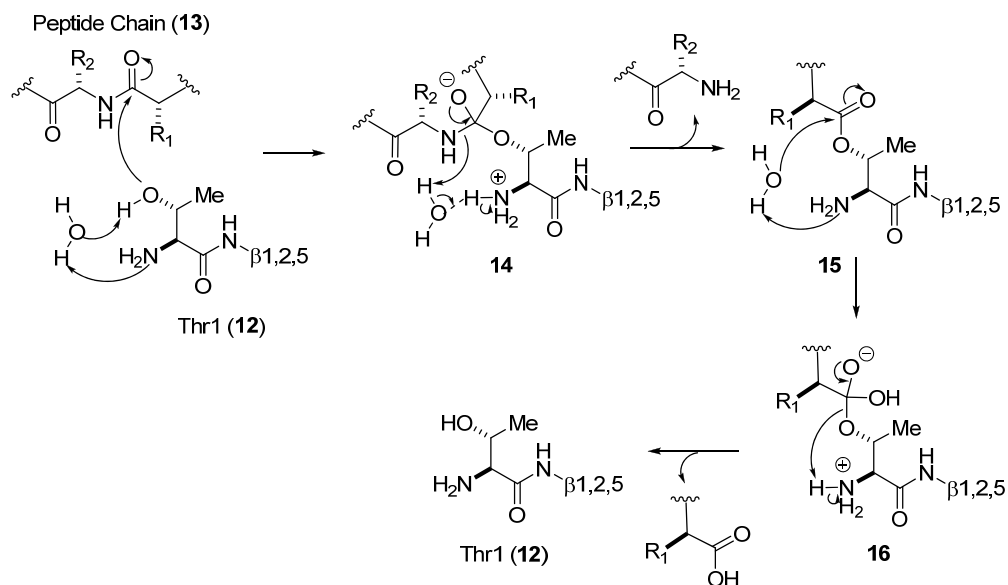
known as the ubiquitin-proteasome pathway,^{20,21} is the process by which the degradation of folded proteins into single amino acids begins. Once the unfolded protein has made it inside the inner cavity of the 20S proteasome, proteolytic cleavage can occur.

The 20S complex is formed by 28 protein subunits which are arranged in four stacked rings, two α -rings and two β -rings, each comprising seven subunits.²² The β -ring subunits contain the proteolytic active sites. Eukaryotic proteasomes contain only three proteolytically active β -subunits per β -ring (subunits β 1, β 2, and β 5), whereas the other β -subunits are inactive. Specifically, the *N*-terminal threonine of the proteolytically active β -subunits is the catalytic residue where proteolysis occurs.²³ Each active β -subunit has different proteolytic activity, designated caspase-, tryptic- and chymotrypic like active sites (subunits β 1, β 2, and β 5 respectively), which describes its affinity for proteolytic cleavage after certain types of amino acids.²⁴

1.2.1.1 Mechanism of Peptide Hydrolysis

Once a protein is unfolded and fed into the lumen of the 20S proteasome, protein hydrolytic cleavage occurs at the six active sites. Due to spacing between the active sites, protein chains are broken into oligomers which on average are 8-11 amino acids in length.²³ The mechanism of peptide hydrolysis via the proteasome²⁵ is suggested to involve the *N*-terminal threonine (**12**, Thr1) of the active β -subunits and a water molecule (Scheme 1.2.1.1). The water molecule serves as a hydrogen bonding bridge to activate the Thr1 β -hydroxyl group for nucleophilic attack to the peptide chain **13**. A tetrahedral intermediate **14** will result from the attack of the β -hydroxyl group of Thr1 on a carbonyl

belonging to an amide of the peptide chain. This tetrahedral intermediate can collapse to cleave the peptide chain. An acyl ester intermediate **15** linking the β -hydroxyl group on Thr1 will result and the same water molecule can facilitate the cleavage of the acyl ester bond to regenerate the free Thr1 **12** as well as releasing the peptide carboxylate.



Scheme 1.2.1.1 Mechanism of Peptide Hydrolysis

1.2.2 Existing and Theoretical Biomedical Implications

The proteasome is responsible for the non-lysosomal ATP-dependent proteolysis of most cellular proteins and is regulated by the ubiquitin-proteasome degradation pathway.²⁵ Proteolysis plays an important role in maintaining biological homeostasis and regulation of different cellular processes, such as cell differentiation, cell cycle control, antigen processing, and hormone metabolism. The following sections are dedicated to

the description of the effect of proteasome inhibitors on various essential cellular processes and the consequential existing and theoretical biomedical implications.

1.2.2.1 Apoptosis

The ubiquitin-proteasome pathway regulates cell death and survival by controlling the amounts of proteins, such as NF- κ B, which are critical for cell progression and transcriptional regulation as well as apoptosis.⁵ Consequently, changes in the intracellular level of these proteins, via proteasome inhibition, can have drastic effects on cell growth and survival. Proteasome inhibitors, at certain concentrations, can trigger apoptosis in cells. In general, rapidly dividing cells are more sensitive to pro-apoptotic effects of proteasome inhibitors than nondividing ones.²⁶ This selective and specific activation of apoptosis in rapidly dividing cells by proteasome inhibitors has allowed their use as tumor suppressors. Apoptosis was efficiently induced in the tumor cells, whereas the untransformed cells remained unharmed.

1.2.2.2 Induction of Heat Shock Response

At non-apoptotic concentrations, proteasome inhibitors have been shown to protect cells against apoptosis induced by other factors.²⁷ In a study, exposure of Madin-Darby canine kidney cells to lactacystin inhibited the degradation of short lived proteins and increased significantly the levels of mRNAs encoding cytosolic heat-shock proteins.²⁸ Moreover, this induction in the level of heat-shock proteins stimulated the

cells thermo-tolerance. Thus, proteasome inhibitors may have applications in protection against cell injury, various stress situations, and apoptosis.²⁹

1.2.2.3 Inhibition of the Immune System

Proteasome inhibitors could have strong potential as drugs for suppressing or modifying the cytotoxic immune response.³⁰ The proteasome plays an important role in cellular immune response, since they represent the main producer of antigenic peptides.³¹ An *in vivo* study showed that inhibition of the proteasome reduced the generation of peptides used in antigen formation.³² Consequently, the proteasome is recognized as a validated target for the modifying or silencing antigen processing and presentation to cytotoxic T-cells, which are important players in transplant rejection and autoimmune disease.

1.2.2.4 Anticancer Therapy

The development of new proteasome inhibitors with potential for cancer treatment is one of the fastest growing fields in modern biomedical science.⁶ The anticancer effects of proteasome inhibitors have been associated with the suppression of angiogenesis, which is the physiological process involving the growth of new blood vessels from pre-existing vessels. Angiogenesis is a normal process in growth and development, as well as in wound healing. However, this is also a fundamental step in the transition of tumors from a dormant state to a malignant state. Many of the factors involved in angiogenesis

are regulated by the proteasome. Thus, inhibition of proteasomal activity has been found to inhibit angiogenesis and induce apoptosis in human cancer cells with limited toxicity to normal cells. The dual action of blocking angiogenesis and inducing cell death makes proteasome inhibition attractive for chemotherapeutic purposes.

The proteasome inhibitor bortezomib has already been approved in the United States as a prescriptive drug for use against relapsed and/or refractory multiple myeloma.³³ Unfortunately, prolonged treatment is associated with toxicity and development of drug resistance. However, salinosporamide A induced apoptosis in multiple myeloma cells resistant to conventional and bortezomib therapies.^{12,13} In addition, salinosporamide A is orally bioactive and in animal tumor model studies is well tolerated and prolongs survival with significantly reduced tumor recurrence.

1.2.2.5 Antiviral Effect

The success of using proteasome inhibitors in cancer therapy stimulated clinical research toward treatment of other diseases including widespread diseases caused by various viruses. Initially, the Paramyxoviridae family of viruses were targeted because paramyxovirus infections are detected worldwide and there are currently no known therapeutic treatments or vaccines available for many of the diseases they cause. In a recent study, treatment of various virus-infected cells with different concentrations of lactacystin reduced viral growth in a dose dependant manner.⁸ In addition, the effect on viral maturation was shown to be highly cell specific and partly virus specific. These

early results provided the basis for further investigations of proteasome inhibitors as potential antiviral drugs.

Proteasome inhibitors may also be good therapeutic agents for malaria chemotherapy. A dipeptidyl boronic acid proteasome inhibitor, MLN-273, was tested on the blood and liver stages of a *Plasmodium* parasite species which cause malaria. The results showed the blocked development of the parasites at different stages but did not injure uninfected erythrocytes and hepatocytes.³⁴

Furthermore, proteasome inhibitors might represent a possible drug candidate for treatment of the human immunodeficiency virus (HIV) infection. It was demonstrated that HIV maturation and budding are reduced by proteasome inhibitors.³⁵

1.2.2.6 Anti-inflammatory Effect

The transcription factor NF- κ B plays a prominent role in inflammatory response. Proteasome inhibitors can potentially be used as anti-inflammatory agents then because they strongly stabilize the concentration of the inhibitor of NF- κ B, I κ -B α , through the ubiquitin-proteasome pathway.⁷

1.2.3 Classes of Proteasome Inhibitors

Classification of proteasome inhibitors is based on their characteristic binding mode to the proteolytically active sites, specificity, and reversibility of binding. Peptide aldehydes were the first discovered inhibitors of the 20S proteasome, and they are still

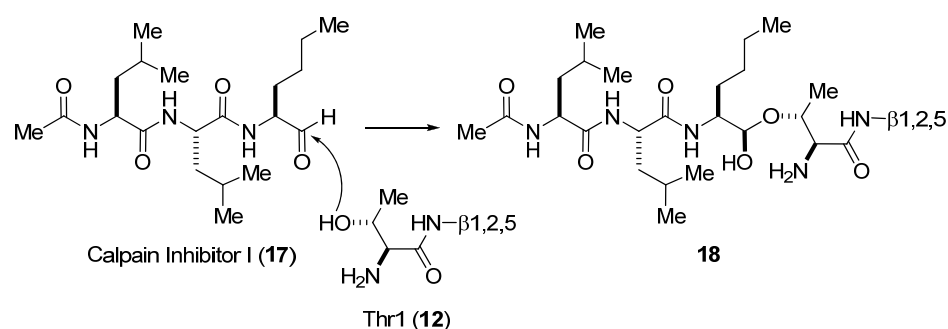
actively investigated.³⁶ Other classes of proteasome inhibitors include peptides containing a vinyl sulfone group,³⁷ and peptide boronates.³⁸ Peptide boronates are more potent inhibitors than peptide aldehydes and peptide vinyl sulfones and their high efficiency and selectivity as well as their low dissociation rates put these chemical compounds in the focus of medical research and drug development.

Besides synthetic peptide inhibitors, there exists a variety of natural compounds blocking proteasome activity, with three main groups being α,β -epoxyketones, β -lactones, and TMC-95s. Crystal structures of the inhibitor-proteasome complexes have provided valuable insight about the architecture and organization of substrate binding pockets near the proteolytically active centers. In the following sections, the main classes of proteasome inhibitors, focusing on structural and chemical aspects such as binding mode and mechanism, as well as specificity and selectivity, will be discussed.

1.2.3.1 Peptide Aldehydes

Generally, aldehyde inhibitors enter cells rapidly and their effect is reversible. These inhibitors have fast dissociation rates; they are rapidly oxidized into inactive carboxylic acids, and are then transported out of the cells.³⁹ However, the first structural information on the architecture of the proteasomal proteolytically active sites was obtained from the crystal structure of the *Thermoplasma acidophilum* proteasome in complex with calpain inhibitor I (**17**, Ac-Leu-Leu-nLeu-al, Scheme 1.2.3.1).²³ The data revealed that proteasomes belong to a novel class of proteases which use threonine as the nucleophilic residue in their active sites.

Calpain inhibitor I was found to be covalently bound to the β -hydroxy group of Thr1 (Thr1O^y) of the active proteasomal β -subunits (β 1, β 2, β 5) with the formation of hemiacetal bonds **18**. Although, the mechanism of proteolysis of all the active sites are identical, calpain inhibitor I binds with the highest affinity (IC_{50} of 2.1 μ M) to subunit β 5, carrying the chymotryptic-like active site, and has a low effect ($IC_{50} > 100 \mu$ M) on tryptic- and caspase-like activities (subunits β 2 and β 1, respectively). Due to the high reactivity of the aldehyde functional group, calpain inhibitors lack specificity and also inhibit a broad range of different serine and cysteine proteases.³⁹

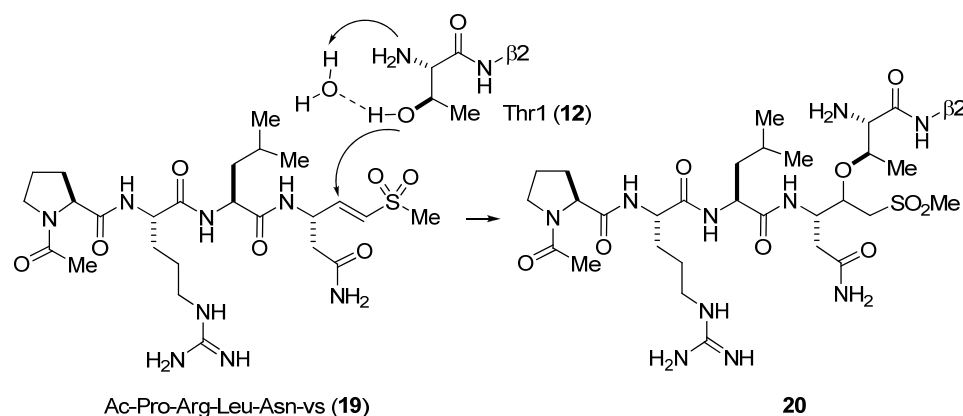


Scheme 1.2.3.1 Mechanism of Proteasome Inhibition by Calpain Inhibitor I

The crystal structure data helped to identify the specificity pockets in eukaryotic proteasomes and revealed that the active sites of subunits β 1, β 2, and β 5 differ significantly in the architecture of their binding pockets. In general, the chymotryptic-like active site is stabilized by hydrophobic residues and both the tryptic-like and the caspase-like active sites are stabilized by charged residues.²⁵

1.2.3.2 Peptide Vinyl Sulfones

Peptides possessing a vinyl sulfone moiety represent another class of proteasome inhibitors.⁴⁰ These compounds bind to the proteasome irreversibly but are less reactive than aldehydes. Vinyl sulfones act as Michael acceptors for soft nucleophiles such as thiols, leading to the formation of a covalent bond. They do not inhibit the activity of serine proteases, but they do show high specificity for intracellular cysteine proteases, which applies certain restrictions to their application *in vivo*, similar to peptide aldehydes. Vinyl sulfones are easier to synthesize than other irreversible inhibitors of the proteasome,⁴¹ but the main advantage of these covalent inhibitors is that they can be used as sensitive active site probes for mechanistic studies of proteasomes in different tissues and cells.⁴²



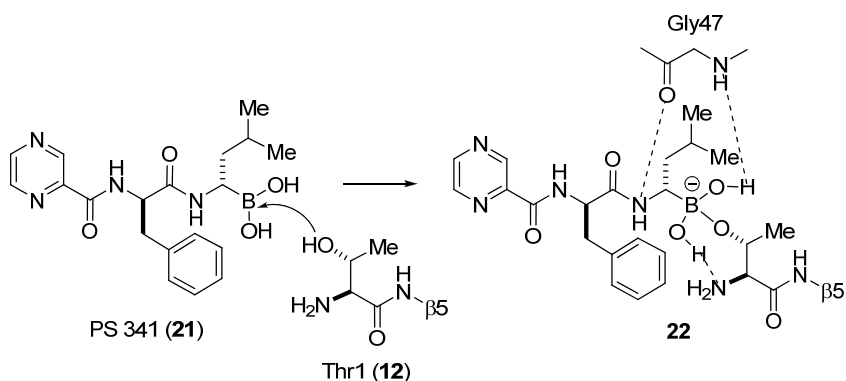
Scheme 1.2.3.2 Mechanism of Proteasome Inhibition by Ac-Pro-Arg-Leu-Asn-vs

A crystal structure of the proteasome complexed with the specific peptide vinyl sulfone inhibitor, Ac-Pro-Arg-Leu-Asn-vs **19**, was obtained and showed the inhibitor

irreversibly covalently bound to the Thr1O^γ of the active proteasomal β-subunit (β2) to the sulfones β-position (see **20**, Scheme 1.2.3.2).⁴¹ The proposed mechanism follows a typical Michael addition reaction with, in this case, a water molecule being used to increase the nucleophilicity of the hydroxyl group through a bridged hydrogen bonding network.

1.2.3.3 Peptide Boronates

Peptide boronates are much more potent inhibitors of the proteasome and have much slower dissociation rates than proteasome aldehyde adducts. Furthermore, peptide boronate derivatives are suitable for applications *in vivo*, being bioavailable and stable under physiological conditions.⁴³ Boronic acid peptides have been shown to inhibit some serine proteases but unlike aldehydes and sulfones, boronates are poor inhibitors of cysteine proteases, due to the weak interaction between sulfur and boron atoms.³⁸ Their selectivity makes boronic acid derivatives attractive candidates for drug development.

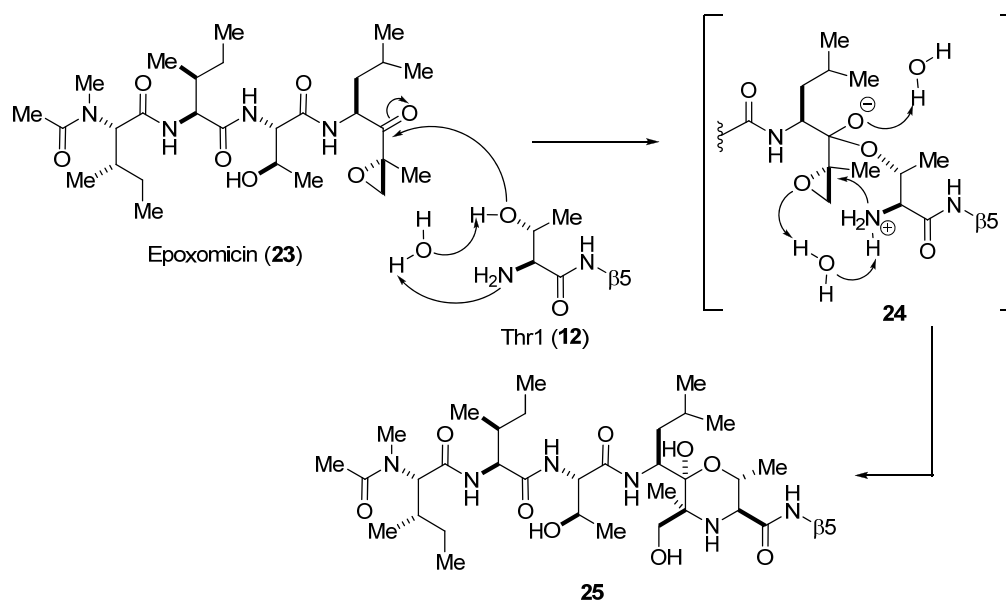


Scheme 1.2.3.3 Mechanism of Proteasome Inhibition by PS-341

The boronic acid dipeptide derivative, PS-341 (**21**, Scheme 1.2.3.3), later named bortezomib, demonstrates a high degree of selectivity for the proteasome ($K_i < 0.6$ nM).⁴⁴ An extensive investigation of bortezomib could not identify other targets of this inhibitor.⁴³ Under physiological conditions, bortezomib preferentially targets the proteasomal $\beta 5$ active site, and to a lesser extent the $\beta 1$ site, while the $\beta 2$ site is left relatively untouched.⁴⁵ Similar to the peptide aldehyde inhibitors, bortezomib's boron atom covalently interacts with the nucleophilic oxygens lone pair of Thr10⁷. The tetrahedral boronate adduct **22** is, furthermore, stabilized by hydrogen bonding of the two acidic boronate hydroxyl moieties. One hydrogen atom bridges the *N*-terminal threonine atom and the other is bridged to Gly47N.

1.2.3.4 Peptide Epoxyketones

Epoxomicin (**23**, Scheme 1.2.3.4), a natural peptidyl α',β' -epoxyketone, was isolated from the actinomycete strain Q966-17, and characterized based on its activity as an antitumor agent against B16 murine melanoma.⁴⁶ It was found to bind covalently to the proteolytically active subunits of the proteasome, primarily to the $\beta 5$ (chymotryptic-like) subunit, consequently inhibiting its activity.^{47,48} The tryptic- and caspase- like activities are inhibited at 100- and 1000- fold slower rates, respectively.⁴⁹ Unlike most other proteasome inhibitors, epoxomicin is highly specific for the proteasome and does not inhibit other proteases.⁴⁷



Scheme 1.2.3.4 Mechanism of Proteasome Inhibition by Epoxomicin

The crystal structure of the yeast 20S proteasome, in complex with epoxomicin, clarified this unique specificity of α',β' -epoxyketones for proteasomes.⁵⁰ Interestingly, the well defined electron density map of epoxomicin at the active site Thr1 reveals the presence of a unique six-membered morpholino ring system. This morpholino derivative **25** results from adduct formation between the α',β' -epoxyketone in epoxomicin and the amino terminal active site nucleophile Thr1O ^{γ} and N. The formation of the morpholino ring is proposed as a two-step process: first, activation of the Thr1O ^{γ} occurs by its *N*-terminal amino group directly or via a neighboring water molecule acting as the base. Subsequent nucleophilic attack of Thr1O ^{γ} on the carbonyl carbon atom of the epoxyketone produces a hemiacetal **24**, as observed in the structure of the proteasome-aldehyde inhibitor complexes. This hemiacetal bond facilitates the second step in the formation of the morpholino adduct. In this intramolecular cyclization, Thr1N opens the

epoxide ring an intramolecular displacement reaction. The nucleophilic attack of Thr1N occurs at the more substituted side of the epoxide. Thus, the resulting morpholino adduct formation is the favored 6 *exo*-tet ring closure⁵¹ instead of the 7 *endo*-tet ring closure, which would result from attack at the less hindered epoxy methylene.

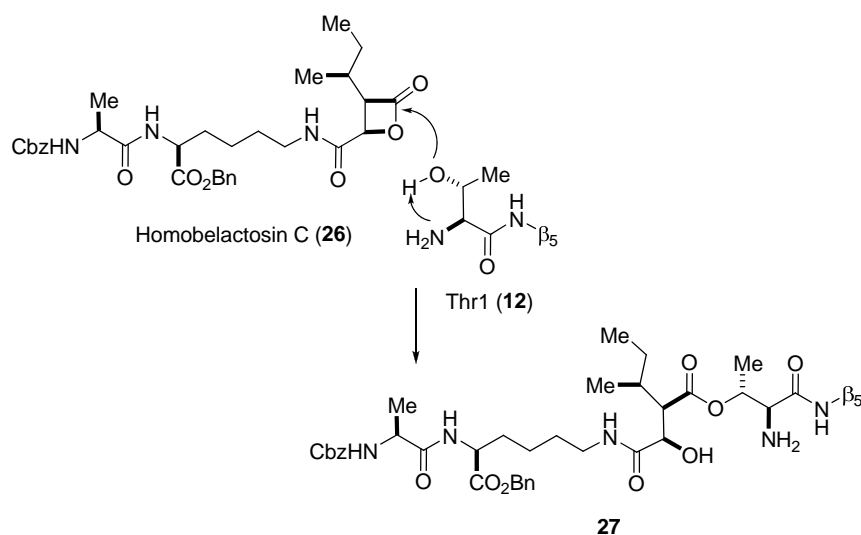
The unique binding mechanism of epoxyketones makes them one of the most selective inhibitors: it was shown that proteasomal subunits are the only cellular proteins covalently, and irreversibly, modified by epoxomicin.⁴⁷

1.2.3.5 β -Lactones

1.2.3.5.1 The Belactosines

Belactosin A and C, natural products from *Streptomyces* sp. UCK14, exhibit antitumor activity,(177,178) which has been shown to be significantly increased upon acetylation of the free amino group and esterification of the carboxyl group, as well as replacement of the ornithine moiety with lysine to furnish bis-benzyl-protected homobelactosin A and C.⁵² The latter, homobelactosin C (**26**, Scheme 1.2.3.5.1), shows IC₅₀ values against human pancreoma and colon cancer cells at the low nanomolar level.⁵³ The high antitumor activity of these compounds has been attributed to inhibition of the proteasomal activity. The crystal structure analysis of the yeast proteasome in complex with bis-benzyl-protected homobelactosin C reveals specific acylation to generate **27**, via reaction with the β -lactone, of Thr1O ^{γ} of the chymotryptic-like active site.⁵⁴ The crystal structure data reveal characteristic hydrophobic interactions of the

protecting groups, especially the benzyl groups, with protein residues, which offer a rational explanation of the observed IC₅₀ values.



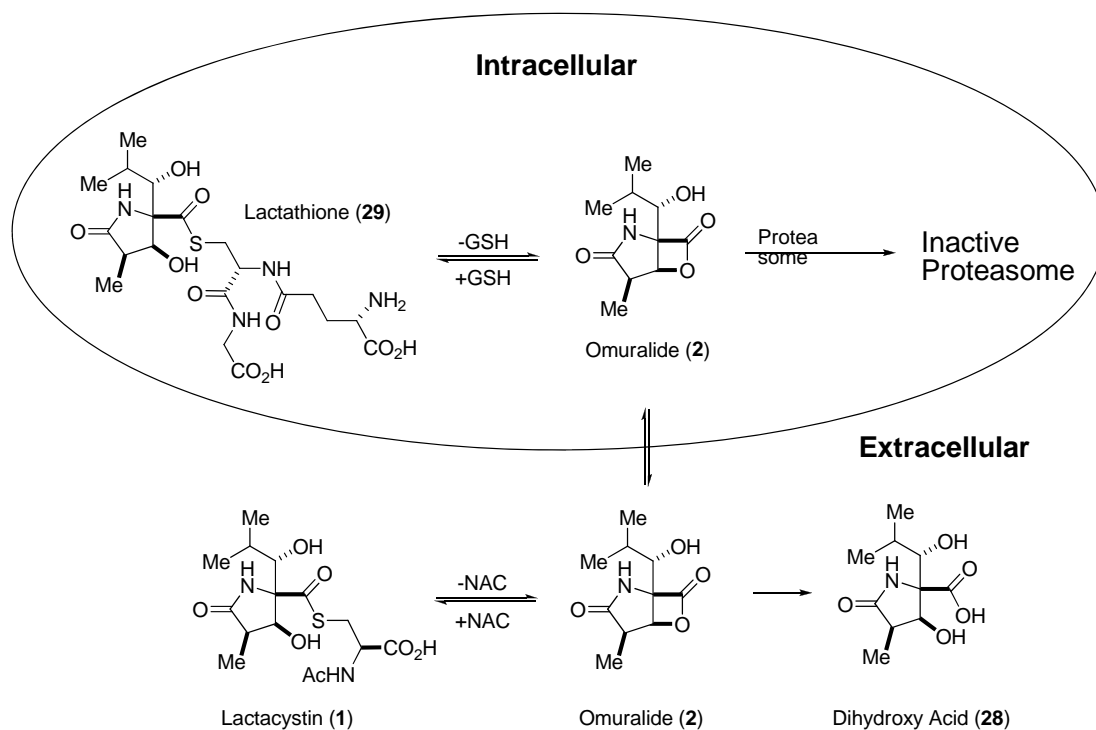
Scheme 1.2.3.5.1 Mechanism of Proteasome Inhibition by Homobelactosin C

1.2.3.5.2 Lactacystin/Omuralide

Studies carried out with radioactive lactacystin (**1**) revealed binding primarily to the β_5 proteasomal subunit which efficiently and irreversibly inhibits the chymotryptic-like activity of the proteasome.³ The tryptic-like and caspase-like activities are also blocked, but to a lesser extent.⁵⁵

As discussed earlier, *in vitro* studies revealed that omuralide (**2**), formed by spontaneous β -lactone formation and concurrent *N*-acetyl cysteine elimination of lactacystin (**1**), is the active proteasome inhibitor.¹¹ Those studies were then extended to examine the mechanism of proteasome inhibition by lactacystin in cultured cells (Scheme

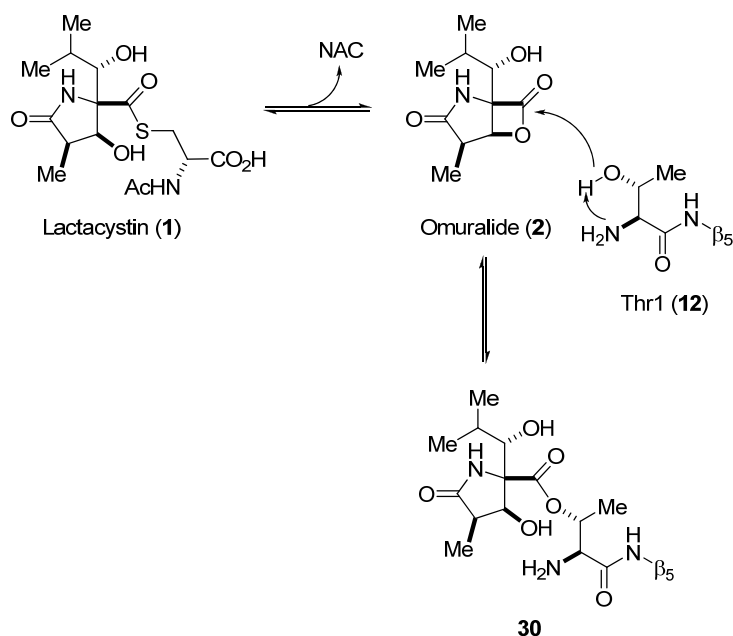
1.2.3.5.2a).⁵⁶ It was discovered that cells are relatively impermeable to lactacystin, but highly permeable to omuralide. While extracellular hydrolysis of omuralide to the dihydroxy acid **28** can occur, this process is offset to a large extent because of its rapid entry into cells. Thus, the efficacy of lactacystin as a proteasome inhibitor in cells will depend on the lactonization of lactacystin in the medium to generate omuralide.



Scheme 1.2.3.5.2a Mechanism of Proteasome Inhibition by Lactacystin in Cultured Cells

Once inside the cell, lactacystin has many fates. It can hydrolyze to the inactive dihydroxy acid, it can react with the proteasome, or it can react with the sulfhydryl of glutathione (GSH) to form a thioester adduct that is both structurally and functionally analogous to lactacystin. This thioester, which is called lactathione **29**, is inactive as a

proteasome inhibitor. Nevertheless, like lactacystin, it can spontaneously regenerate omuralide via intramolecular lactonization.

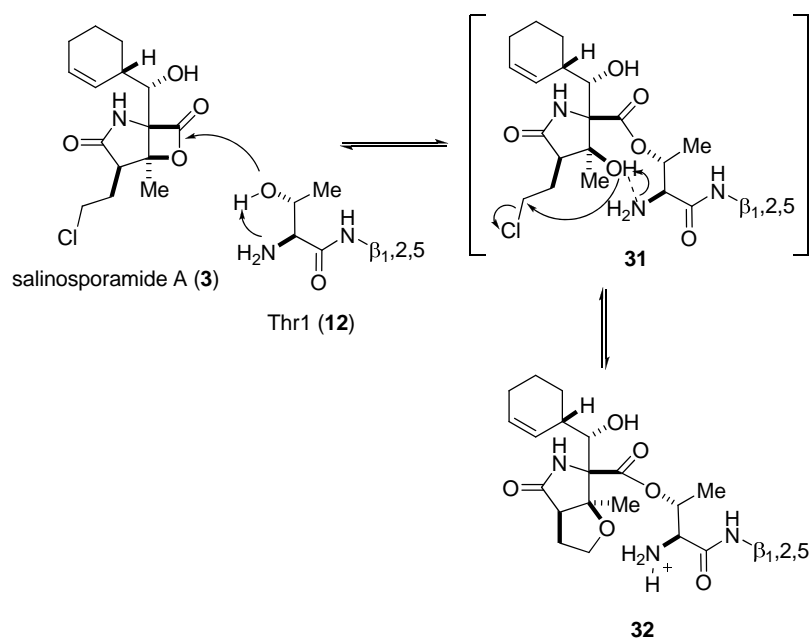


Scheme 1.2.3.5.2b Interaction of Thr1O^γ of 20S Proteasome with Lactacystin

An X-ray crystal structure of the yeast proteasome-omuralide complex demonstrated that the Thr1O^γ in the 20S proteasome is covalently bound as ester **30** to omuralide,⁵⁷ which is presumably formed from reaction of Thr1O^γ with the β-lactone (Scheme 1.2.3.5.2b). Furthermore, the nucleophilic water molecule, which is responsible for hydrolysis of the ester intermediate during normal peptide hydrolysis, is structurally distorted, which makes the process essentially irreversible.^{57,58}

1.2.3.5.3 Salinosporamide A

Given the structural similarities between omuralide and salinosporamide A, similar acyl ester binding of both inhibitors to the proteasome was expected which was indeed confirmed by crystal structure analysis.⁵⁹ However, the structural data revealed that, in contrast to omuralide, salinosporamide A was bound to all six catalytic subunits. Furthermore, the structure provided explanations for the enhanced potency of salinosporamide A compared to omuralide.



Scheme 1.2.3.5.3 Mechanism of Proteasome Inhibition by Salinosporamide A

The generated C3-O group in **31** of salinosporamide A (**3**), after ring opening of the β -lactone with Thr1O^y, subsequently forms a cyclic tetrahydrofuran ring **32** with the chloroethyl side chain, causing an enthalpically and entropically favorable binding mechanism associated with the release of HCl (Scheme 1.2.3.5.3). These findings

support the existence of a two-step mechanism in which addition of Thr1O γ to the β -lactone carbonyl is followed by nucleophilic addition of C3-O to the chloroethyl group to give rise to the cyclic ether.^{15,59} Thr1O γ is similarly acylated by the inhibitor, as has been described for the peptide substrate, and might similarly occur through a tetrahedral intermediate. Cleavage of the acyl ester intermediate by the nucleophilic water molecule is challenged by the special rearrangement of C3-O of the inhibitor at the active site. The *N*-terminus is positioned for hydrogen bonding with the inhibitor C3-OH. In the case of salinosporamide A, chlorine is eliminated and the *N*-terminus is fully protonated.⁵⁹

1.2.3.6 Non-covalent Proteasome inhibitors: TMC-95A

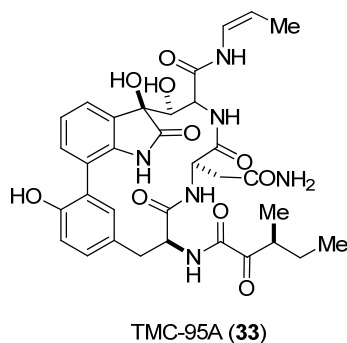


Figure 1.2.3.6 Structure of TMC-95A

All of the previously described proteasome inhibitors form a covalent bond with the active site Thr1O γ of the β -subunits. Application of these inhibitors *in vivo* often induces apoptosis and causes cell death.⁶⁰ It can be expected that the cytotoxic effects of proteasome inhibitors may be reduced by making their binding proteasomes reversible

and time-limited. Recently, it was shown that natural product TMC-95A (**33**, Figure 1.2.3.6), isolated from *Apiospora montagnei*, selectively and competitively block the proteolytic activity of the proteasome in the low nanomolar range.^{61,62} Furthermore, it was reported that TMC-95A does not inhibit other proteases.⁶²

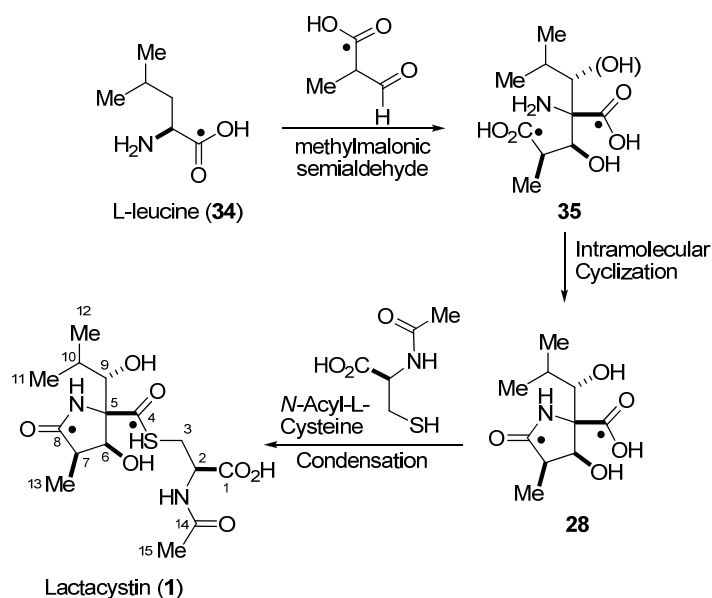
TMC-95A, which is not related to any previously mentioned proteasome inhibitor, consists of a heterocyclic ring system made of modified amino acids. The inhibitor binds to all three proteolytically active sites, as was elucidated from the crystal structure of the yeast proteasome in complex with TMC-95A.⁵⁰ All of the proteolytically active β -subunits were linked noncovalently to TMC-95A, not modifying their *N*-terminal threonines. A tight network of hydrogen bonds connects TMC-95A with the protein, thus stabilizing its position.

1.3 Biosynthesis of Lactacystin

A unique γ -lactam structure, as well as the hydroxyisobutyl and cysteinylthioester moieties, in lactacystin led to interest in the study of its biosynthesis.⁶³ In 1994, Nakagawa *et al* fed ¹³C-labeled compounds to cultures of *Streptomyces lactacystinaeus* and then isolated and characterized (¹³C-NMR) the ¹³C-enriched lactacystin produced.

The feeding of L-[2-¹³C] leucine (**34**) gave lactacystin (**1**) which showed a very intense signal for C5 indicating that the C₆ segment (C4, C5, C9, C10, C11, C12) is derived from L-leucine. The feeding experiment with sodium [1-¹³C] isobutyrate

revealed equal levels of enrichment for C1, C4, C8, C14. The incorporation at C8, in particular, provided unequivocal evidence that the γ -lactam ring of dihydroxyacid **28** is formed by a condensation of methylmalonic semialdehyde, derived from sodium [1- ^{13}C] isobutyrate and/or L-valine, with C5 of the C₆ unit from L-leucine, providing **35**, followed by intramolecular cyclization (Scheme 1.3). It was shown, additionally, that L-cysteine was also incorporated, via conversion to *N*-acyl-L-cysteine with acetyl-CoA, and then condensation to generate lactacystin (**1**).



Scheme 1.3 Biosynthesis of Lactacystin

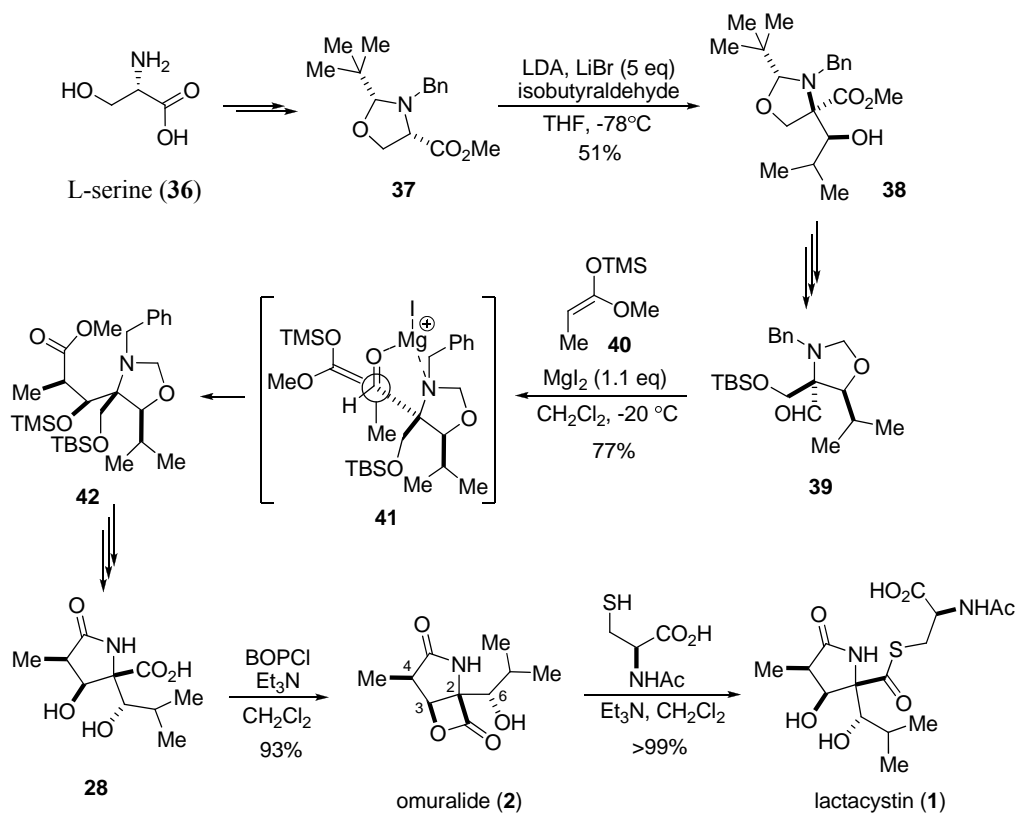
1.4 Relevant Synthetic Efforts

The unique structure and biological activity of lactacystin has attracted the attention of numerous chemists challenged to develop a synthetic route to the natural product. The first total synthesis was achieved by Corey in 1992.⁶⁴ Subsequently, two different synthetic routes, one to lactacystin,⁶⁵ and one to its hydrolytically more stable analog α -methylomuralide,⁶⁶ were reported by the same group.

1.4.1 Corey's First Total Synthesis of Lactacystin

The first Corey route (Scheme 1.4.1) utilized two aldol reactions to set all four stereocenters (C2, C3, C4, C6) of omuralide.⁶⁴ The stereochemistry of the tetrasubstituted C2 and trisubstituted C6 were controlled by utilizing Seebach's self-reproduction method. Thus, the aldol reaction between oxazolidinone **37** and isobutyraldehyde in the presence of LiBr gave aldol adduct **38** in 55% yield with greater than 98% diastereomeric purity after tituration of the crude product. After several steps, aldehyde **39** was obtained and the Mukaiyama MgI₂-mediated aldol reaction with *E*-trimethylsilyl enolate **40** was performed to yield the desired adduct **42** in 77% yield with a 9:1 diastereomeric ratio. The face selectivity of the aldehyde was in excess of 35:1 in this step. It was proposed that Mg chelates the aldehyde and the nitrogen of the oxozolidinone ring and that the enolated will approach from the less hindered side in a

synclinal fashion. After a few steps, dihydroxy acid **28** was obtained and the β -lactone ring was formed via a standard coupling reaction with BOPCl. Cysteine was introduced directly and the thioester lactacystin was obtained, completing the total synthesis.

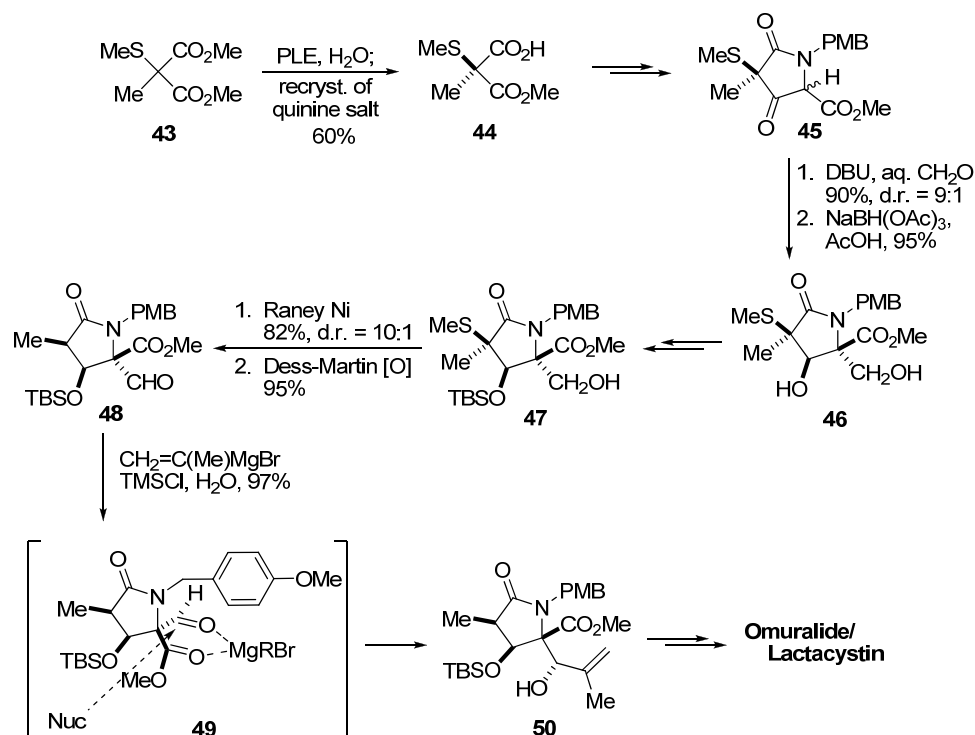


Scheme 1.4.1 Corey's First Total Synthesis of Lactacystin

1.4.2 Corey's Second Total Synthesis of Lactacystin

A second synthetic route to lactacystin, reported by Corey, where introduction of the isopropyl side chain would occur in the late-stage, was then disclosed (Scheme 1.4.2).⁶⁵ The interest was in synthesizing derivatives, whereby other lipophilic groups are introduced, in place of the isopropyl group, and determining what effect those changes

would have on the bioactivity. This synthesis required a bulky thiomethyl group on the γ -lactam ring as a directing group for the construction of the C2 and C3 stereocenters.



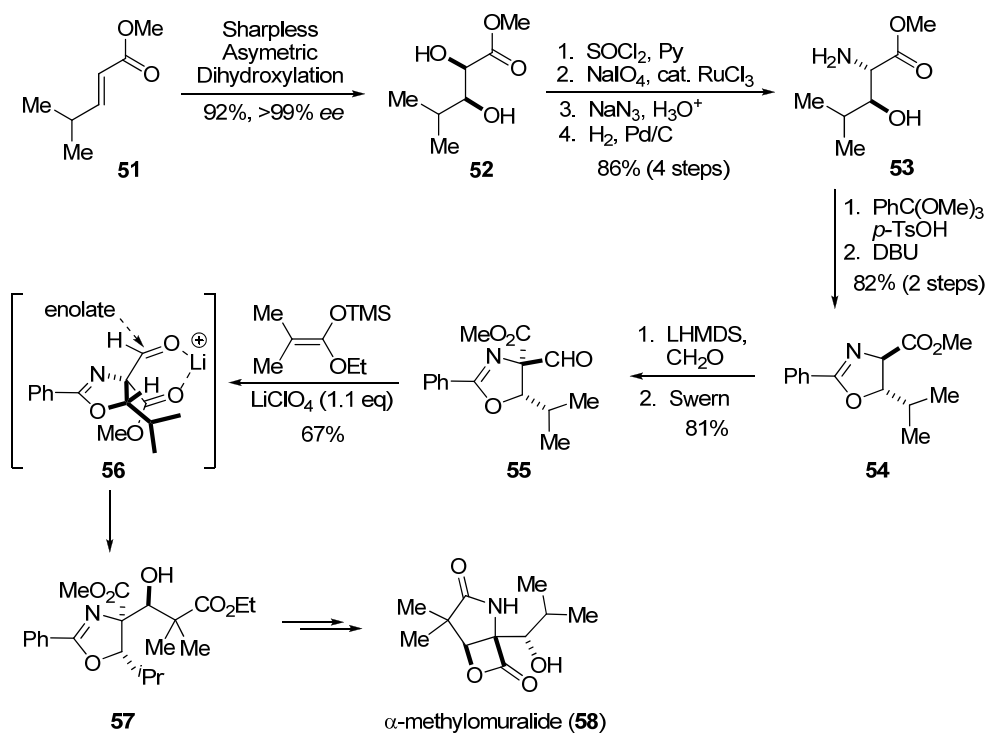
Scheme 1.4.2 Corey's Second Total Synthesis of Lactacystin

Asymmetric hydrolysis of diester **43** with porcine liver esterase (PLE) followed by recrystallization of the quinone salt of the resulting carboxylic acid produced **44** in 60% yield with 95% *ee*. After conversion into γ -lactam **45**, both the introduction of the hydroxymethyl group at C2 and reduction of C3 ketone proceeded from the less-hindered side opposite the thiomethyl group to give **46** in 99% *ee* after recrystallization. After a sequence of protecting group manipulations, desulfurization was performed with Raney Ni and the desired stereoisomer (not shown) was obtained in a 10:1 diastereomeric ratio.

Oxidation of the primary alcohol with DMP provided aldehyde **48**, which was subjected to the addition of isopropenyl magnesium bromide in the presence of TMSCl. The addition occurred selectively from the less hindered side of the six-membered chelate **49** to produce **50** as a single isomer. An additional five straightforward steps were required to complete the total synthesis of omuralide.

1.4.3 Corey's Synthesis of α -Methylomuralide

Lastly, Corey introduced a route to α -methylomuralide (**58**, Scheme 1.4.3), a hydrolytically more stable proteasome inhibitor when compared to omuralide and lactacystin.⁶⁶ Sharpless asymmetric dihydroxylation of *E*-ester **51** gave enantiomerically pure diol **52** in 92% yield after recrystallization. The *syn* diol **52** was then converted into *anti*-3-hydroxyleucine **53** via a cyclic sulfate. A two step sequence led to *trans*-oxazolidine **54** via *cis*-oxazolidine formation and epimerization of C2 with DBU. A hydroxymethyl group was introduced to C2 selectively from the opposite side of the isopropyl group and was subsequently oxidized to the corresponding aldehyde **55** via Swern oxidation. The aldehyde was then subjected to a Mukaiyama aldol reaction to produce adduct **57** selectively in 67% yield. The observed stereochemistry was rationalized from the chelate model **56**. Hydrolysis of the oxazolidine under acidic conditions and formation of the γ -lactam ring occurred in one step, followed by saponification of the methyl ester and β -lactone formation, produced α -methylomuralide (**58**).



Scheme 1.4.3 Corey's Total Synthesis of α -Methylomuralide

Since Corey's initial foray into the synthesis of lactacystin, several additional groups have published their strategies toward the same goal from 1992-2007.⁶⁴⁻⁶⁷ Due to the vast interest in the discovery of new proteasome inhibitors, and the validation of such a strategy as a novel therapeutic target associated with diseases such as cancer, interest is unlikely to wane.

1.5 Conclusions

Omuralide, derived from natural product lactacystin, is a member of a family of proteasome inhibitors, including the salinosporamides and the cinnabaramides, that all contain a novel fused γ -lactam- β -lactone core structure. A great deal of attention from the synthetic community has been paid to these natural products due to recent validation of proteasome inhibition as a novel therapeutic target in human cancer.

The proteasome is a large intracellular protease that is responsible for the orderly degradation of cellular proteins and is critical for normal cell cycling and function. Inhibition of the proteasome pathway results in changes at the cellular level that have existing and theoretical biomedical implications. In addition to anti-cancer therapy, proteasome inhibitors have potential applications in the inhibition of the immune system, anti-inflammatory response, and also in the treatment of viral diseases.

Several different classes of proteasome inhibitors exist that are classified based on their characteristic binding mode to the proteolytically active sites, specificity, and reversibility of binding. Peptide aldehydes, vinyl sulfones, and boronates are synthetic proteasome inhibitors that have aided in the elucidation of the structure, function, and mechanism of the proteolytically active sites. There are several classes of naturally occurring proteasome inhibitors, including α,β' -epoxyketones, β -lactones, and TMC-95s which all have different binding mechanisms providing distinct selectivity to these inhibitors.

The unique structure of lactacystin, containing a novel pyroglutamic acid derivative, led to interest in the study of its biosynthesis. It was discovered that L-leucine and malonic semialdehyde, derived biosynthetically from L-valine, were incorporated. Unequivocal evidence was provided that the two were involved in the formation of the γ -lactam ring via a condensation and intramolecular cyclization cascade sequence.

Corey introduced the first total synthesis of lactacystin in 1992, and later introduced two alternative routes, allowing for the synthesis of derivatives which have provided valuable structure-activity relationship information. Following his initial publication, several other groups published their alternative routes leading to vast array of knowledge on the many ways synthetic chemists can efficiently target and achieve the synthesis of members of this family of natural products.

However, despite the effort by synthetic chemists, there was still a lack of a unified synthetic strategy towards the synthesis of omuralide, α -methylomuralide, the salinosporamides, and the cinnabaramides. As a result, we sought the development of a mild and general strategy towards the synthesis of the common fused γ -lactam- β -lactone ring system of the aforementioned proteasome inhibitors.

1.6 Notes and References

(1) Omura, S.; Fujimoto, T.; Otaguro, K.; Matsuzaki, K.; Moriguchi, R.; Tanaka, H.; Sasaki, Y. *J. Antibiot.* **1991**, *44*, 113-116.

- (2) Omura, S.; Matsuzaki, K.; Fujimoto, T.; Kosuge, K.; Furuya, T.; Fujita, S.; Nakagawa, A. *J. Antibiot.* **1991**, *44*, 117-118.
- (3) Fenteany, G.; Standaert, R. F.; Lane, W. S.; Choi, S.; Corey, E. J.; Schreiber, S. L. *Science* **1995**, *268*, 726-731.
- (4) Fenteany, G.; Standaert, R. F.; Reichard, G. A.; Corey, E. J.; Schreiber, S. L. *Proc. Natl. Acad. Sci. U. S. A.* **1994**, *91*, 3358-3362.
- (5) Borissenko, L.; Groll, M. *Chem. Rev.* **2007**, *107*, 687-717.
- (6) Kisselev, A. F.; Goldberg, A. L. *Chem. Biol.* **2001**, *8*, 739-758.
- (7) Kalogeris, T. J.; Laroux, F. S.; Cockrell, A.; Ichikawa, H.; Okayama, N.; Phifer, T. J.; Alexander, J. S.; Grisham, M. B. *Am. J. Physiol.* **1999**, *276*, C856-C864.
- (8) Watanabe, H.; Tanaka, Y.; Shimazu, Y.; Sugahara, F.; Kuwayama, M.; Hiramatsu, A.; Kiyotani, K.; Yoshida, T.; Sakaguchi, T. *Microbiol. Immunol.* **2005**, *49*, 835-844.
- (9) Phillips, J. B.; Williams, A. J.; Adams, J.; Elliott, P. J.; Tortella, F. C. *Stroke* **2000**, *31*, 1686-1693.
- (10) Hu, G.; Lin, G.; Wang, M.; Dick, L.; Xu, R.-M.; Nathan, C.; Li, H. *Mol. Microbiol.* **2006**, *59*, 1417-1428.
- (11) Corey, E. J.; Li, W.-D. *Chem. Pharm. Bull. (Tokyo)* **1999**, *47*, 1-10; Dick, L. R.; Cruikshank, A. A.; Grenier, L.; Melandri, F. D.; Nunes, S. L.; Stein, R. L. *J. Biol. Chem.* **1996**, *271*, 7273-7276.
- (12) Feling, R. H.; Buchanan, G. O.; Mincer, T. J.; Kauffman, C. A.; Jensen, P. R.; Fenical, W. *Angew. Chem. Int. Ed.* **2003**, *42*, 355-357.
- (13) Chauhan, D.; Catley, L.; Li, G.; Podar, K.; Hideshima, T.; Velankar, M.; Mitsiades, C.; Mitsiades, N.; Yasui, H.; Letai, A.; Ova, H.; Berkers, C.; Nicholson, B.; Chao, T.-H.; Neuteboom, S. T. C.; Richardson, P.; Palladino, M. A.; Anderson, K. C. *Cancer Cell* **2005**, *8*, 407-419.

(14) Williams, P. G.; Buchanan, G. O.; Feling, R. H.; Kauffman, C. A.; Jensen, P. R.; Fenical, W. *J. Org. Chem.* **2005**, *70*, 6196-6203.

(15) Macherla, V. R.; Mitchell, S. S.; Manam, R. R.; Reed, K. A.; Chao, T.-H.; Nicholson, B.; Deyanat-Yazdi, G.; Mai, B.; Jensen, P. R.; Fenical, W. F.; Neuteboom, S. T. C.; Lam, K. S.; Palladino, M. A.; Potts, B. C. M. *J. Med. Chem.* **2005**, *48*, 3684-3687.

(16) Reed, K. A.; Manam, R. R.; Mitchell, S. S.; Xu, J.; Teisan, S.; Chao, T.-H.; Deyanat-Yazdi, G.; Neuteboom, S. T. C.; Lam, K. S.; Potts, B. C. M. *J. Nat. Prod.* **2007**, *70*, 269-276.

(17) Stadler, M.; Bitzer, J.; Mayer-Bartschmid, A.; Mueller, H.; Benet-Buchholz, J.; Gantner, F.; Tichy, H.-V.; Reinemer, P.; Bacon, K. B. *J. Nat. Prod.* **2007**, *70*, 246-252.

(18) Hough, R.; Pratt, G.; Rechsteiner, M. *J. Biol. Chem.* **1986**, *261*, 2400-2408.

(19) Eytan, E.; Ganoth, D.; Armon, T.; Hershko, A. *Proc. Natl. Acad. Sci. U. S. A.* **1989**, *86*, 7751-7755; Hough, R.; Pratt, G.; Rechsteiner, M. *J. Biol. Chem.* **1987**, *262*, 8303-8313.

(20) Voges, D.; Zwickl, P.; Baumeister, W. *Annu. Rev. Biochem.* **1999**, *68*, 1015-1068.

(21) Coux, O.; Tanaka, K.; Goldberg, A. L. *Annu. Rev. Biochem.* **1996**, *65*, 801-847.

(22) Hegerl, R.; Pfeifer, G.; Puehler, G.; Dahlmann, B.; Baumeister, W. *FEBS Lett.* **1991**, *283*, 117-121.

(23) Loewe, J.; Stock, D.; Jap, B.; Zwickl, P.; Baumeister, W.; Huber, R. *Science (Washington, D. C.)* **1995**, *268*, 533-539.

(24) Arendt, C. S.; Hochstrasser, M. *Proc. Natl. Acad. Sci. U. S. A.* **1997**, *94*, 7156-7161; Orlowski, M.; Cardozo, C.; Michaud, C. *Biochemistry* **1993**, *32*, 1563-1572.

- (25) Myung, J.; Kim, K. B.; Crews, C. M. *Med. Res. Rev.* **2001**, *21*, 245-273.
- (26) Lopes, U. G.; Erhardt, P.; Yao, R.; Cooper, G. M. *J. Biol. Chem.* **1997**, *272*, 12893-12896; Drexler, H. C. A. *Proc. Natl. Acad. Sci. U. S. A.* **1997**, *94*, 855-860.
- (27) Lin, K.-I.; Baraban, J. M.; Ratan, R. R. *Cell Death Differ.* **1998**, *5*, 577-583.
- (28) Bush, K. T.; Goldberg, A. L.; Nigam, S. K. *J. Biol. Chem.* **1997**, *272*, 9086-9092.
- (29) Meriin, A. B.; Gabai, V. L.; Yaglom, J.; Shifrin, V. I.; Sherman, M. Y. *J. Biol. Chem.* **1998**, *273*, 6373-6379; Lee, D. H.; Goldberg, A. L. *Mol. Cell. Biol.* **1998**, *18*, 30-38.
- (30) Groettrup, M.; Schmidtke, G. *Drug Discovery Today* **1999**, *4*, 63-71.
- (31) Rock, K. L.; Goldberg, A. L. *Annu. Rev. Immunol.* **1999**, *17*, 739-779.
- (32) Rock, K. L.; Gramm, C.; Rothstein, L.; Clark, K.; Stein, R.; Dick, L.; Hwang, D.; Goldberg, A. L. *Cell (Cambridge, Mass.)* **1994**, *78*, 761-771.
- (33) Richardson, P. G.; Sonneveld, P.; Schuster, M. W.; Irwin, D.; Stadtmauer, E. A.; Facon, T.; Harousseau, J.-L.; Ben-Yehuda, D.; Lonial, S.; Goldschmidt, H.; Reece, D.; San-Miguel, J. F.; Blade, J.; Boccadoro, M.; Cavenaugh, J.; Dalton, W. S.; Boral, A. L.; Esseltine, D. L.; Porter, J. B.; Schenkein, D.; Anderson, K. C. *New Engl. J. Med.* **2005**, *352*, 2487-2498.
- (34) Lindenthal, C.; Weich, N.; Chia, Y. S.; Heussler, V.; Klinkert, M. Q. *Parasitology* **2005**, *131*, 37-44.
- (35) Schubert, U.; Ott, D. E.; Chertova, E. N.; Welker, R.; Tessmer, U.; Princiotta, M. F.; Bennink, J. R.; Krausslich, H.-G.; Yewdell, J. W. *Proc. Natl. Acad. Sci. U. S. A.* **2000**, *97*, 13057-13062.
- (36) Vinitzky, A.; Michaud, C.; Powers, J. C.; Orłowski, M. *Biochemistry* **1992**, *31*, 9421-9428.

- (37) Palmer, J. T.; Rasnick, D.; Klaus, J. L.; Bromme, D. *J. Med. Chem.* **1995**, *38*, 3193-3196.
- (38) Adams, J.; Behnke, M.; Chen, S.; Cruickshank, A. A.; Dick, L. R.; Grenier, L.; Klunder, J. M.; Ma, Y.-T.; Plamondon, L.; Stein, R. L. *Bioorg. Med. Chem. Lett.* **1998**, *8*, 333-338.
- (39) Shaw, E. *Adv. Enzymol. Relat. Areas Mol. Biol.* **1990**, *63*, 271-347.
- (40) Bogyo, M.; McMaster, J. S.; Gaczynska, M.; Tortorella, D.; Goldberg, A. L.; Ploegh, H. *Proc. Natl. Acad. Sci. U. S. A.* **1997**, *94*, 6629-6634.
- (41) Nazif, T.; Bogyo, M. *Proc. Natl. Acad. Sci. U. S. A.* **2001**, *98*, 2967-2972.
- (42) Ovaa, H.; van Swieten, P. F.; Kessler, B. M.; Leeuwenburgh, M. A.; Fiebiger, E.; van den Nieuwendijk, A. M. C. H.; Galardy, P. J.; van der Marel, G. A.; Ploegh, H. L.; Overkleeft, H. S. *Angew. Chem. Int. Ed.* **2003**, *42*, 3626-3629.
- (43) Adams, J.; Palombella, V. J.; Sausville, E. A.; Johnson, J.; Destree, A.; Lazarus, D. D.; Maas, J.; Pien, C. S.; Prakash, S.; Elliott, P. J. *Cancer Res.* **1999**, *59*, 2615-2622.
- (44) Adams, J.; Stein, R. *Annu. Rep. Med. Chem.* **1996**, *31*, 279-288.
- (45) Berkers, C. R.; Verdoes, M.; Lichtman, E.; Fiebiger, E.; Kessler, B. M.; Anderson, K. C.; Ploegh, H. L.; Ovaa, H.; Galardy, P. J. *Nat. Methods* **2005**, *2*, 357-362.
- (46) Hanada, M.; Sugawara, K.; Kaneta, K.; Toda, S.; Nishiyama, Y.; Tomita, K.; Yamamoto, H.; Konishi, M.; Oki, T. *J. Antibiot.* **1992**, *45*, 1746-1752.
- (47) Meng, L.; Kwok, B. H. B.; Sin, N.; Crews, C. M. *Cancer Res.* **1999**, *59*, 2798-2801.
- (48) Elofsson, M.; Splittgerber, U.; Myung, J.; Mohan, R.; Crews, C. M. *Chem. Biol.* **1999**, *6*, 811-822.

- (49) Kim, K. B.; Myung, J.; Sin, N.; Crews, C. M. *Bioorg. Med. Chem. Lett.* **1999**, *9*, 3335-3340.
- (50) Groll, M.; Koguchi, Y.; Huber, R.; Kohno, J. *J. Mol. Biol.* **2001**, *311*, 543-548.
- (51) Baldwin, J. *Ciba Found. Symp.* **1978**, *53*, 85-99.
- (52) Larionov, O. V.; De Meijere, A. *Org. Lett.* **2004**, *6*, 2153-2156; Armstrong, A.; Scutt, J. N. *Org. Lett.* **2003**, *5*, 2331-2334.
- (53) Asai, A.; Tsujita, T.; Sharma, S. V.; Yamashita, Y.; Akinaga, S.; Funakoshi, M.; Kobayashi, H.; Mizukami, T. *Biochem. Pharmacol.* **2004**, *67*, 227-234.
- (54) Groll, M.; Larionov, O. V.; Huber, R.; de Meijere, A. *Proc. Natl. Acad. Sci. U. S. A.* **2006**, *103*, 4576-4579.
- (55) Craiu, A.; Gaczynska, M.; Akopian, T.; Gramm, C. F.; Fenteany, G.; Goldberg, A. L.; Rock, K. L. *J. Biol. Chem.* **1997**, *272*, 13437-13445.
- (56) Dick, L. R.; Cruikshank, A. A.; Destree, A. T.; Grenier, L.; McCormack, T. A.; Melandri, F. D.; Nunes, S. L.; Palombella, V. J.; Parent, L. A.; Plamondon, L.; Stein, R. L. *J. Biol. Chem.* **1997**, *272*, 182-188.
- (57) Groll, M.; Ditzel, L.; Lowe, J.; Stock, D.; Bochtler, M.; Bartunik, H. D.; Huber, R. *Nature* **1997**, *386*, 463-471.
- (58) Groll, M.; Berkers, C. R.; Ploegh, H. L.; Ovaa, H. *Structure (Cambridge, MA, U. S.)* **2006**, *14*, 451-456.
- (59) Groll, M.; Huber, R.; Potts, B. C. M. *J. Am. Chem. Soc.* **2006**, *128*, 5136-5141.
- (60) Hideshima, T.; Richardson, P.; Chauhan, D.; Palombella, V. J.; Elliott, P. J.; Adams, J.; Anderson, K. C. *Cancer Res.* **2001**, *61*, 3071-3076; Shinohara, K.; Tomioka, M.; Nakano, H.; Tone, S.; Ito, H.; Kawashima, S. *Biochem. J* **1996**, *317*, 385-

388; Imajoh-Ohmi, S.; Kawaguchi, T.; Sugiyama, S.; Tanaka, K.; Omura, S.; Kikuchi, H. *Biochem. Biophys. Res. Commun.* **1995**, *217*, 1070-1077.

(61) Kohno, J.; Koguchi, Y.; Nishio, M.; Nakao, K.; Kuroda, M.; Shimizu, R.; Ohnuki, T.; Komatsubara, S. *J. Org. Chem.* **2000**, *65*, 990-995.

(62) Koguchi, Y.; Kohno, J.; Nishio, M.; Takahashi, K.; Okuda, T.; Ohnuki, T.; Komatsubara, S. *J. Antibiot.* **2000**, *53*, 105-109.

(63) Nakagawa, A.; Takahashi, S.; Uchida, K.; Matsuzaki, K.; Omura, S.; Nakamura, A.; Kurihara, N.; Nakamatsu, T.; Miyake, Y.; et al. *Tetrahedron Lett.* **1994**, *35*, 5009-5012; Nakagawa, A.; Kainosho, M.; Omura, S. *Pure Appl. Chem.* **1994**, *66*, 2411-2413.

(64) Corey, E. J.; Li, W.; Reichard, G. A. *J. Am. Chem. Soc.* **1998**, *120*, 2330-2336; Corey, E. J.; Reichard, G. A. *J. Am. Chem. Soc.* **1992**, *114*, 10677-10678.

(65) Corey, E. J.; Li, W.; Nagamitsu, T. *Angew. Chem. Int. Ed.* **1998**, *37*, 1676-1679.

(66) Saravanan, P.; Corey, E. J. *J. Org. Chem.* **2003**, *68*, 2760-2764.

(67) Hayes, C. J.; Sherlock, A. E.; Green, M. P.; Wilson, C.; Blake, A. J.; Selby, M. D.; Prodger, J. C. *J. Org. Chem.* **2008**, *73*, 2041-2051; Yoon, C. H.; Flanigan, D. L.; Yoo, K. S.; Jung, K. W. *Eur. J. Org. Chem.* **2007**, 37-39; Shibasaki, M.; Kanai, M.; Fukuda, N. *Chem.--Asian J.* **2007**, *2*, 20-38; Hayes, C. J.; Sherlock, A. E.; Selby, M. D. *Org. Biomol. Chem.* **2006**, *4*, 193-195; Fukuda, N.; Sasaki, K.; Sastry, T. V. R. S.; Kanai, M.; Shibasaki, M. *J. Org. Chem.* **2006**, *71*, 1220-1225; Balskus, E. P.; Jacobsen, E. N. *J. Am. Chem. Soc.* **2006**, *128*, 6810-6812; Wardrop, D. J.; Bowen, E. G. *Chem. Commun. (Cambridge, U. K.)* **2005**, 5106-5108; Reddy, L. R.; Saravanan, P.; Fournier, J.-F.; Reddy, B. V. S.; Corey, E. J. *Org. Lett.* **2005**, *7*, 2703-2705; Reddy, L. R.; Fournier, J.-F.; Reddy, B. V. S.; Corey, E. J. *J. Am. Chem. Soc.* **2005**, *127*, 8974-8976; Reddy, L. R.; Fournier, J.-F.; Reddy, B. V. S.; Corey, E. J. *Org. Lett.* **2005**, *7*, 2699-2701; Donohoe, T. J.; Sintim, H. O.; Sisangia, L.; Ace, K. W.; Guyo, P. M.; Cowley, A.; Harling, J. D. *Chem. Eur. J.* **2005**, *11*, 4227-4238; Ooi, H.; Ishibashi, N.; Iwabuchi, Y.; Ishihara, J.; Hatakeyama, S. *J. Org. Chem.* **2004**, *69*, 7765-7768; Donohoe, T. J.; Sintim, H. O.; Sisangia, L.; Harling, J. D. *Angew. Chem. Int. Ed.* **2004**, *43*, 2293-2296; Brennan, C. J.; Pattenden, G.; Rescourio, G. *Tetrahedron Lett.* **2003**, *44*, 8757-8760; Green, M. P.; Prodger, J. C.; Hayes, C. J. *Tetrahedron Lett.* **2002**, *43*, 6609-6611; Iwama, S.; Gao, W.-G.; Shinada, T.; Ohfuné, Y. *Synlett* **2000**, 1631-1633; Soucy, F.; Grenier, L.; Behnke, M.

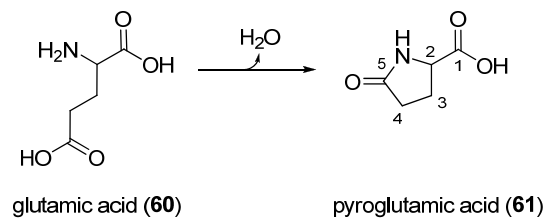
L.; Destree, A. T.; McCormack, T. A.; Adams, J.; Plamondon, L. *J. Am. Chem. Soc.* **1999**, *121*, 9967-9976; Panek, J. S.; Masse, C. E. *Angew. Chem. Int. Ed.* **1999**, *38*, 1093-1095; Kang, S. H.; Jun, H.-S. *Chemical Communications (Cambridge)* **1998**, 1929-1930; Chida, N.; Takeoka, J.; Ando, K.; Tsutsumi, N.; Ogawa, S. *Tetrahedron* **1997**, *53*, 16287-16298; Nagamitsu, T.; Sunazuka, T.; Tanaka, H.; Omura, S.; Sprengeler, P. A.; Smith, A. B., III *J. Am. Chem. Soc.* **1996**, *118*, 3584-3590; Chida, N.; Takeoka, J.; Tsutsumi, N.; Ogawa, S. *J. Chem. Soc., Chem. Commun.* **1995**, 793-794; Uno, H.; Baldwin, J. E.; Russell, A. T. *J. Am. Chem. Soc.* **1994**, *116*, 2139-2140; Sunazuka, T.; Nagamitsu, T.; Matsuzaki, K.; Tanaka, H.; Omura, S.; Smith, A. B., III *J. Am. Chem. Soc.* **1993**, *115*, 5302.

CHAPTER TWO

An Introduction to the Synthesis of Pyroglutamic Acid Derivatives via the Ugi Reaction

2.1 Pyroglutamic Acid

The pyroglutamic acid moiety is a common building block in asymmetric synthesis¹ and is also readily found in nature in the form of biologically active peptides such as gonadotrophin-² and thyrotrophin-releasing³ hormones, in depsipeptides such as didemnins,⁴ and naturally occurring peptides and pseudopeptides.⁵ Glutamic acid (**60**) is the natural precursor of pyroglutamic acid (**61**), easily prepared by direct dehydration⁶ (Scheme 2.1).



Scheme 2.1 Structure of Pyroglutamic Acid

2.1.1 Natural Products

Derivatives of the pyroglutamic acid moiety are found in a number of natural products including lactacystin,⁷ salinosporamides A-B,⁸ cinnabaramides A-C,⁹ dysibetaine,¹⁰ amathaspiramides B and D,¹¹ oxazolomycin A,¹² KSM-2690,¹³ and neooxazolomycin¹⁴ (Figure 2.1.1). Interestingly, the substituents on the pyroglutamic acid of these natural products are diverse. All are alkylated at the 2-position of the pyroglutamic acid, creating a tetrasubstituted chiral center. Other common substituents are hydroxy and alkyl groups variously placed on C3 and C4, and on nitrogen.

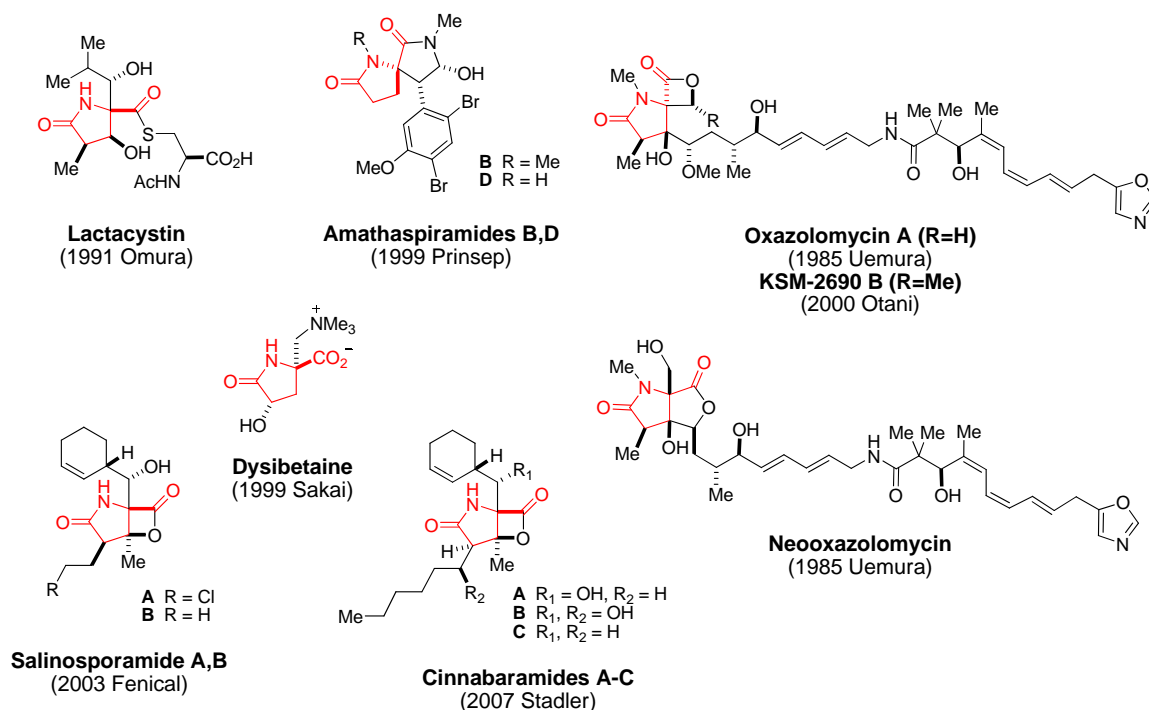


Figure 2.1.1 Natural Products Containing Pyroglutamic Acid

Due to the relative abundance of the 2-alkylpyroglutamic acid scaffold in nature, and the diverse substitution patterns present, a general and practical strategy towards their enantioselective construction is ideal. Summarized below are the known strategies toward the stereospecific synthesis of 2-alkylpyroglutamic acids, including those developed for the syntheses of lactacystin/ omuralide and salinosporamide A.

2.1.2 Synthesis of 2-Alkylpyroglutamic Acids

The discovery of proteasome inhibitors omuralide and salinosporamide A led to interest in the design of synthetic strategies towards the 2-alkylpyroglutamic acid (**62**) common core structure. Those strategies can be summarized into four main categories, involving formation of the four bonds labeled A, B, C, and D (Figure 2.1.2).

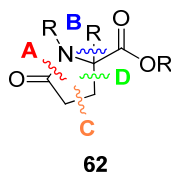


Figure 2.1.2 2-Alkylpyroglutamic Acid

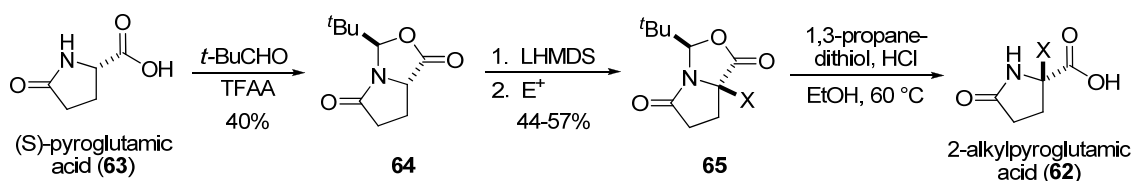
2.1.2.1 Amidation (Bond A)

The most common strategy towards the synthesis of 2-alkylpyroglutamic acid derivatives is late stage γ -lactam formation from the corresponding 2-alkylglutamic acid,

ester, or amide, which mimics the natural synthesis of pyroglutamic acids (see section 2.1). The first example of this strategy, reported by Corey (see section 1.4.1), utilized two aldol reactions to set all four stereocenters (C2, C3, C4, C6) of omuralide, followed by late stage cyclization to form the γ -lactam ring.¹⁵

2.1.2.2 Stereoselective Functionalization of C2 (Bond B)

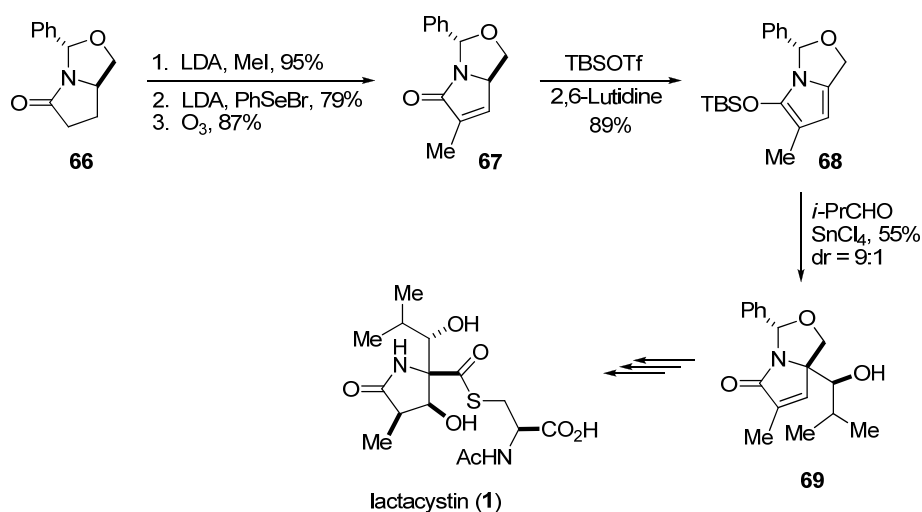
The 2-alkylation of alkyl pyroglutamates can be achieved via deprotonation of the 2-position with LHMDS when the nitrogen is unsubstituted¹⁶ or benzylated,¹⁷ but with loss of chiral information. However, when the nitrogen and carboxylic acid of (*S*)-pyroglutamic acid (**63**) are protected as an *N,O*-acetal, forming bicyclic derivative **64**, the 2-position can be deprotonated and alkylated, providing **65**, with benzylic bromides or carbonyl compounds with retention of configuration¹⁸ (Scheme 2.1.2.2a). However, yields are low to moderate and the variety of electrophiles is limited to activated alkyl halides and carbonyl compounds.



Scheme 2.1.2.2a Synthesis of 2-Alkylpyroglutamic Acid via Direct Alkylation

The first lactacystin synthesis reported using the C2 alkylation strategy was the second synthetic route reported by Corey (see section 1.4.2).¹⁹ An alternative strategy to

activation of the 2-position by deprotonation with base is the formation of a silyl enol ether, as the nucleophilic component, and subsequent Mukaiyama aldol reaction. Didehydroglutaminol **66**²⁰ was formed from oxazolidinone **67** by sequential methylation, selenation at C4, and ozonolysis (Scheme 2.1.2.2b). Transformation into silyloxypyrrole **68** was accomplished with TBSOTf and 2,6-lutidine. Mukaiyama aldol reaction at C2, performed with isobutyraldehyde in the presence of SnCl₄, afforded predominantly diastereomer **69** which is an intermediate in Baldwin's total synthesis of lactacystin (**1**).²¹

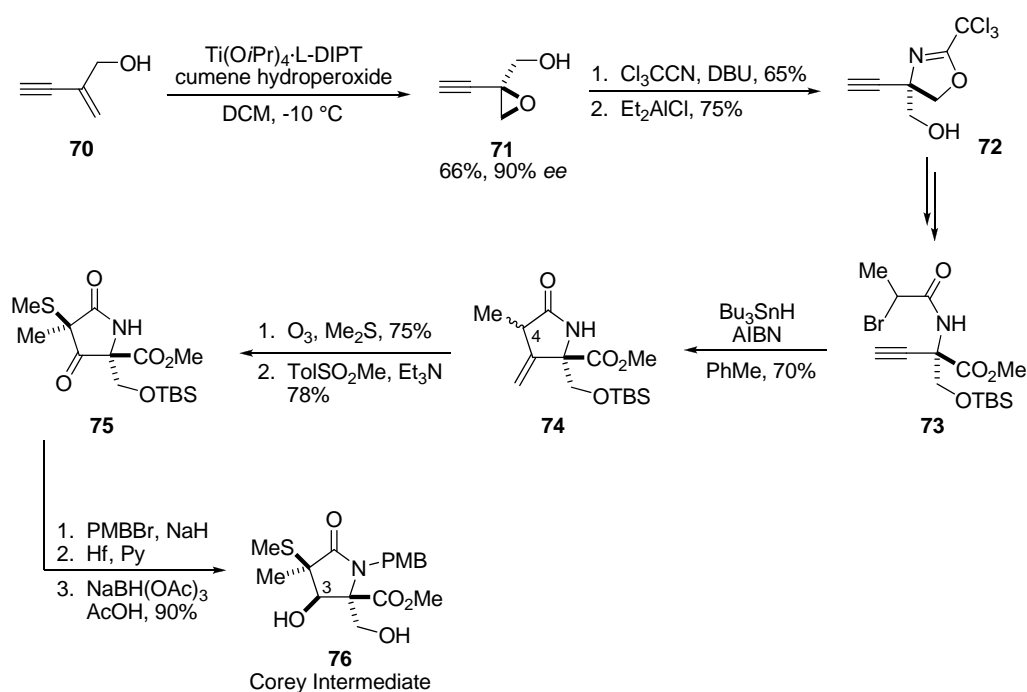


Scheme 2.1.2.2b Baldwin's Total Synthesis of Lactacystin: Synthesis of 2-Alkylpyroglutamic Acid From Silyloxypyrroles

2.1.2.3 Formation of C3-C4 Bond (Bond C)

It is also possible to synthesize 2-alkylpyroglutamic acids by formation of the C3-C4 bond. Pattenden reported a formal total synthesis of lactacystin/ omuralide where he introduced the strategy of utilizing a radical cyclization to form the 2-alkylpyroglutamic

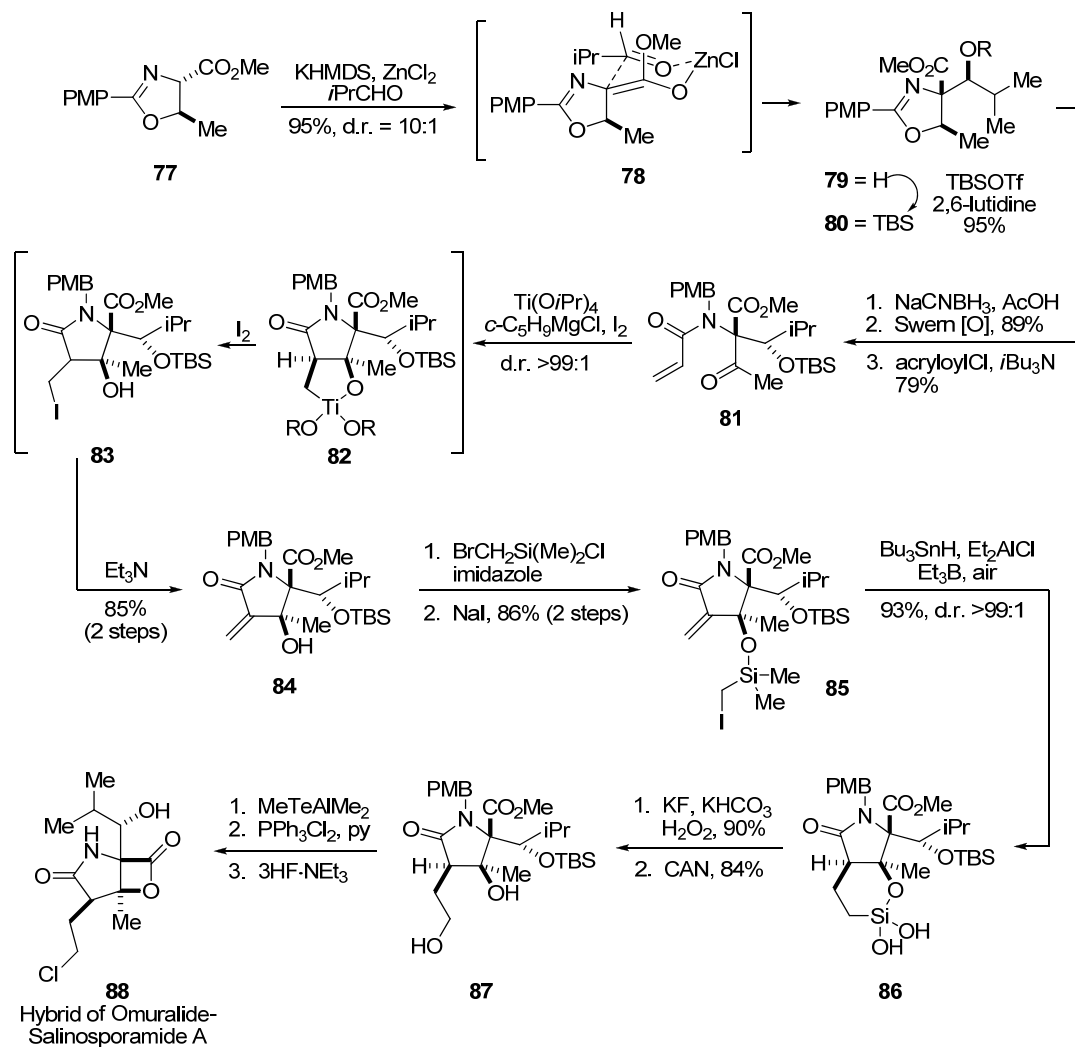
acid derivative **74** (Scheme 2.1.2.3a).²² The crucial radical cyclization of **73** proceeded with Bu_3SnH in the presence of a catalytic amount of AIBN under toluene reflux conditions to produce 2-alkylpyroglutamic acids derivative **74** in 70% yield as a 2:1 mixture of stereoisomers at C4. The stereochemistry of C4 was adjusted through sulfanylation of the β -ketolactam derived from **74**. Finally, Corey intermediate **76**¹⁹ (see section 1.4.2) was synthesized from **75** over three steps.



Scheme 2.1.2.3a Pattenden's Total Synthesis of Lactacystin: Radical Cyclization Strategy

During his first total synthesis of salinosporamide A, Corey introduced a key Baylis-Hillman reaction to construct the C3-C4 bond of the 2-alkylpyroglutamic acid core structure.²³ Unfortunately, the key Baylis-Hillman reaction was very slow (7 days).

As a result, during the synthesis of omuralide-salinosporamide A hybrid **88**²⁴ (Scheme 2.1.2.3b), he improved the synthetic efficiency by using the Kulinkovich reaction²⁵ in place of the Baylis-Hillman reaction.

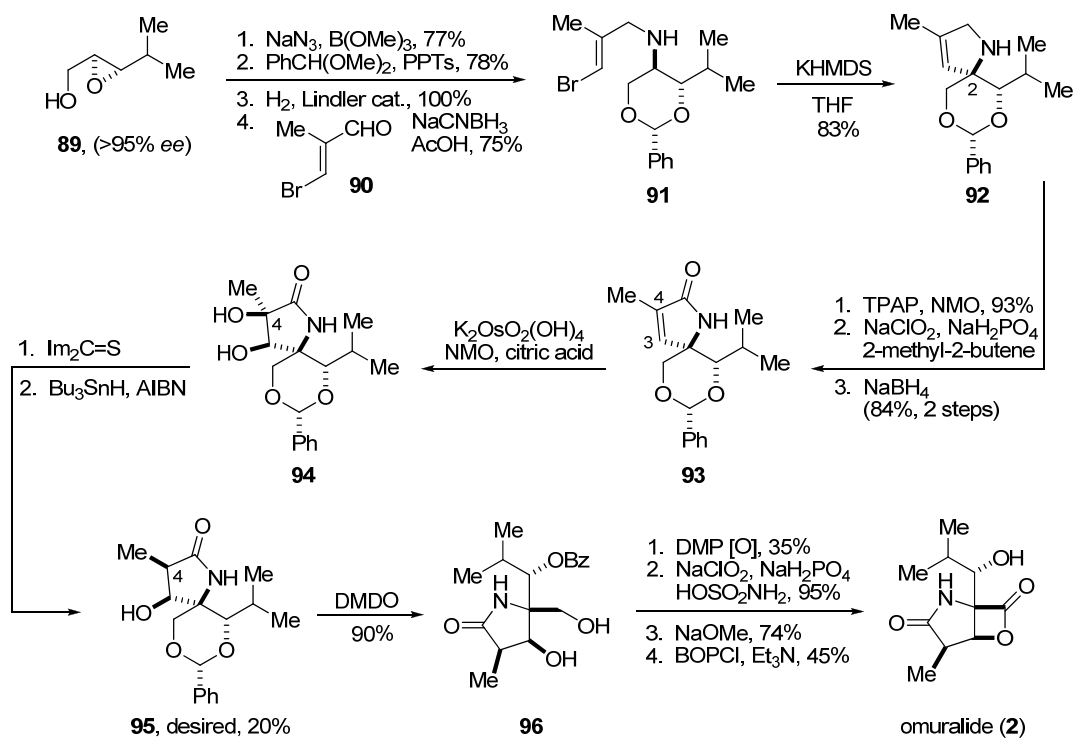


Scheme 2.1.2.3b Corey's Total Synthesis of Omuralide-Salinosporamide A Hybrid: Kulinkovich Reaction Strategy

Thus, treatment of **81** with the Kulinkovich reagent prepared from $\text{Ti}(\text{OiPr})_4$ and cyclopentylmagnesium chloride, followed by iodination of the resulting titanacycle **82** and elimination of HI with Et_3N produced **84** in 85% yield with greater than 99:1 selectivity. This excellent diastereoselectivity can be explained by considering the titanacycle formation from the less hindered side opposite the bulky isobutyl group at C2. The reaction time was only five hours throughout the sequence, in stark contrast to the seven day Baylis-Hillman reaction. Several more steps and the synthesis of omuralide-salinosporamide A hybrid **88** was accomplished.

2.1.2.4 Formation of C2-C3 Bond (Bond D)

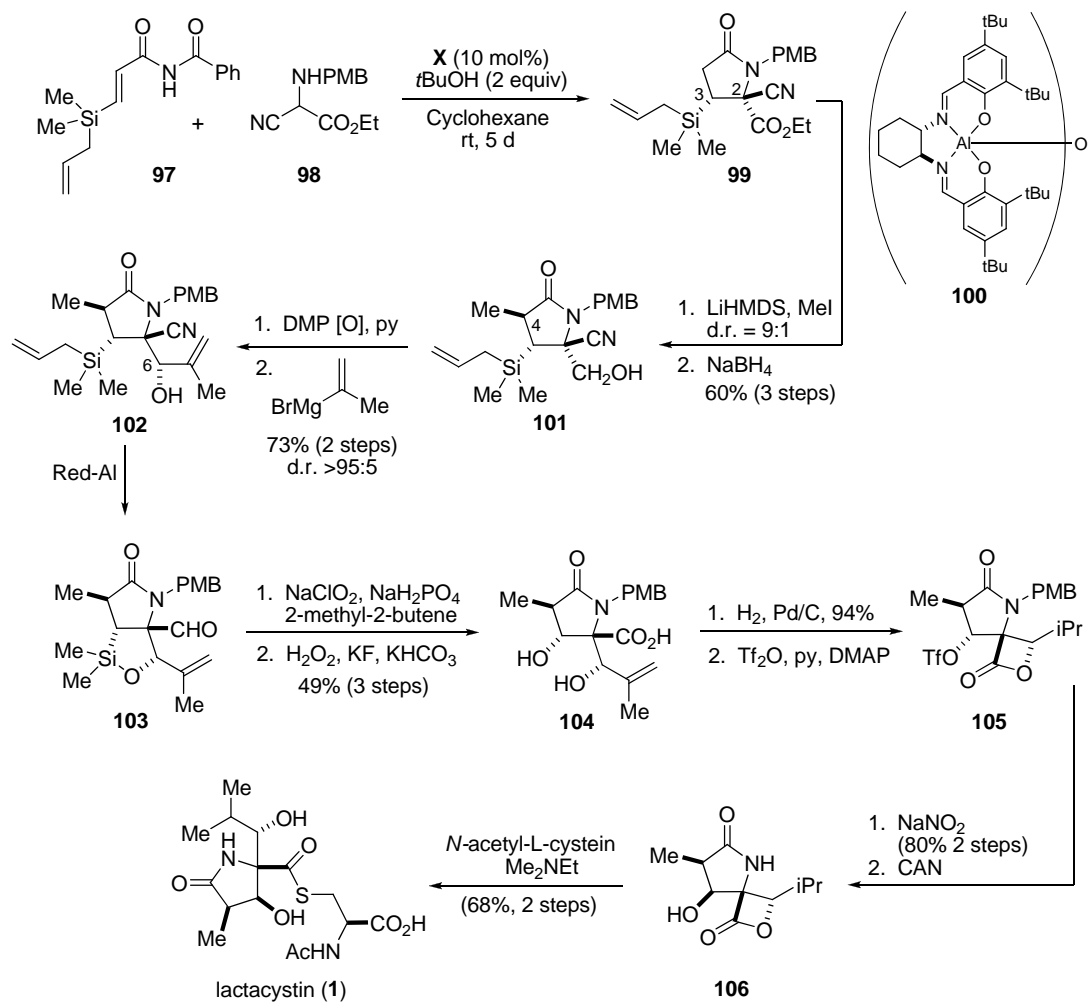
There are also several strategies for the construction of the C2-C3 bond of 2-alkylpyroglutamic acids. The first strategy involves an intramolecular C-H insertion of an alkylidene carbene, originally introduced by Hayes²⁶ but also independently developed by Wardrop.²⁷ The stereoselective C-H insertion proceeded from **91** to produce spiro pyrroline **92** in 83% yield (Scheme 2.1.2.4a). The undesired 1,2-methyl migration product was also observed (13%). α -Oxidation of the amine group with TPAP followed by Pinnick oxidation first produced the corresponding *N*-chlorolactam, and subsequent *N*-dechlorination with NaBH_4 gave the desired lactam **93**, which after several steps was elaborated to omuralide (**2**).



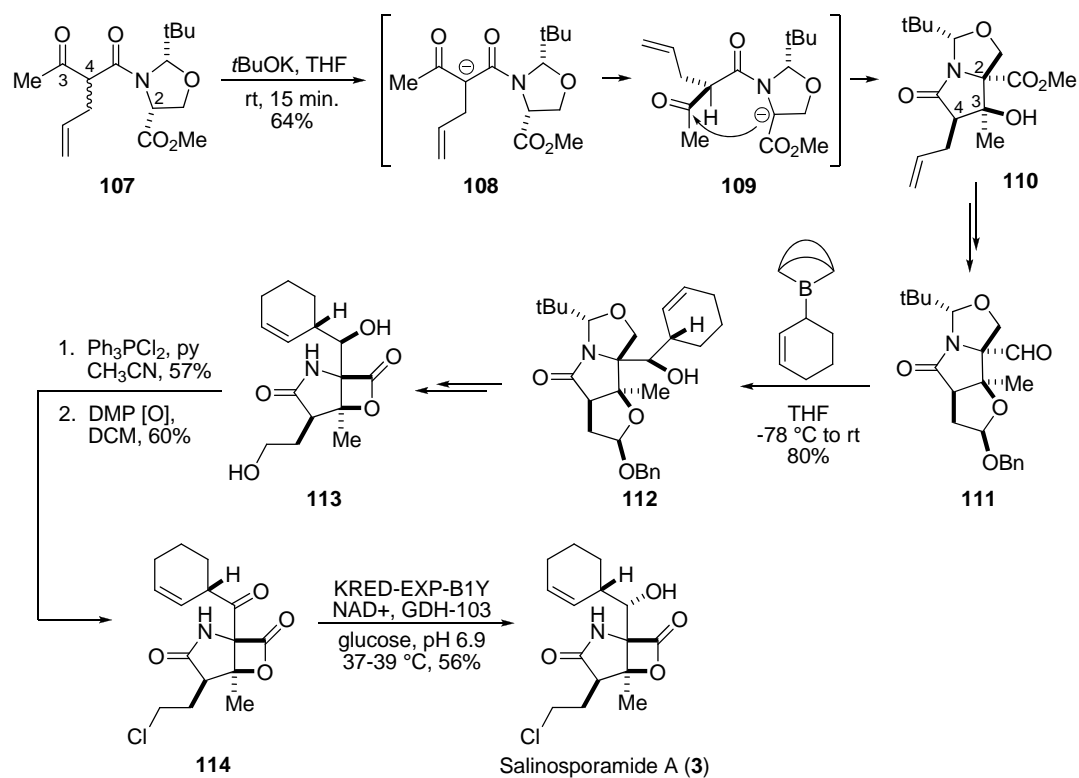
Scheme 2.1.2.4a Wardrop's Total Synthesis of Omuralide: Intramolecular C-H Insertion Strategy

A different approach to the generation of the C2-C3 bond of the 2-alkylpyroglutamic acid core of omuralide/ lactacystin was reported by Jacobsen.²⁸ His synthesis began with a catalytic enantio- and diastereoselective conjugate addition of α -amino cyanoacetate **98** to α,β -unsaturated β -silylimide **97** with 10 mol% of the μ -oxo dimer of salen-Al complex **100** to produce γ -lactam **99** with 98% *ee* and 9:1 *dr* (Scheme 2.1.2.4b). The reaction is noteworthy in that the 2-alkylpyroglutamic acid core of lactacystin is synthesized efficiently in one-pot, although the stereochemistry of C3 is opposite to that of the natural compound. Interestingly, it was found that synthetic

intermediate spiro- β -lactone **106** is a comparably potent inhibitor of the 20S-proteasome relative to omuralide (**2**).



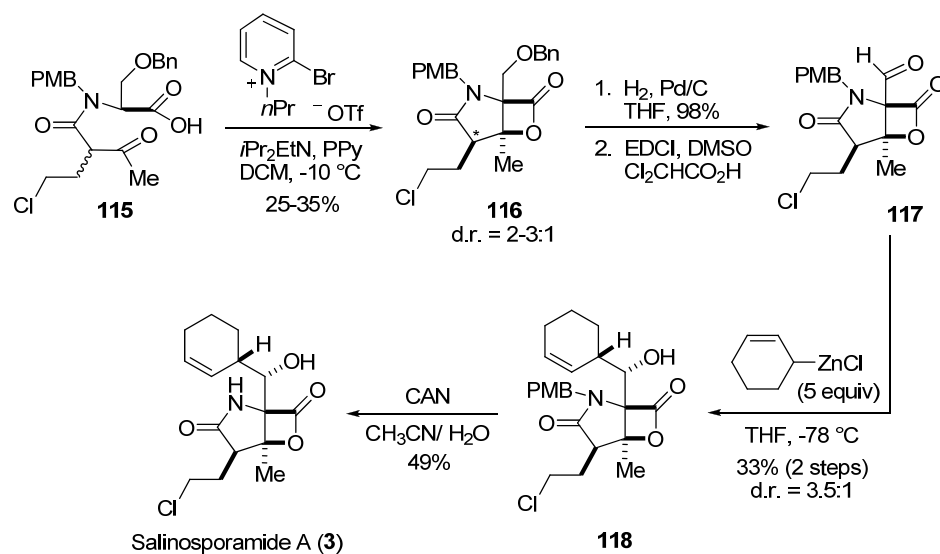
Scheme 2.1.2.4b Jacobsen's Total Synthesis of Lactacystin: Enantio- and Diastereoselective Conjugate Addition Strategy



Scheme 2.1.2.4c Potts's Total Synthesis of Salinosporamide A: Intramolecular Aldol Reaction Strategy

A third approach, developed by Potts, involves a novel intramolecular aldol reaction for the synthesis of the 2-alkylpyroglutamic acid core of salinosporamide A (**3**).²⁹ This enantioselective route is noteworthy because of the simultaneous generation of three stereocenters (C2, C3 and C4) during the aldol reaction. Specifically, enantiomerically pure oxazolidine- γ -lactam **110** was synthesized from β -ketoamide **107** where the C2 chirality, derived from D-serine, is maintained during the intramolecular aldol cyclization, and the C3 and C4 chiral centers are simultaneously constructed in a substrate-directed fashion (Scheme 2.1.2.4c). The resulting highly functionalized

intermediate **110** served as a key precursor for the enantioselective total synthesis of salinosporamide A (**3**).

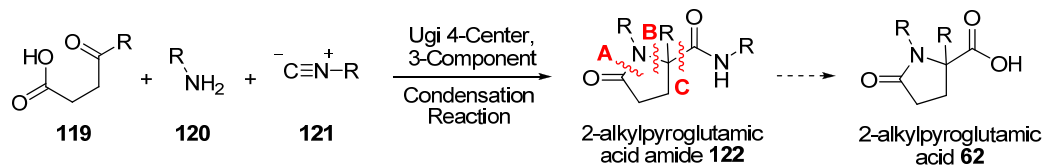


Scheme 2.1.2.4d Romo's Total Synthesis of Salinosporamide A: Intramolecular Bis-Cyclization Strategy

A fourth approach toward construction of the C2-C3 bond of 2-alkylpyroglutamic acids was introduced by Romo.³⁰ The unique strategy involves simultaneous generation of C-C and C-O bonds from a ketoacid precursor **115** to yield fused γ -lactam- β -lactone **116** via an intramolecular bis-cyclization process. This key reaction is thought to proceed by either a sequential aldol-lactonization sequence or possibly a [2+2] cycloaddition via a ketene intermediate. Eventually, **116** was elaborated through a short synthetic sequence into racemic salinosporamide A.

2.2 The Ugi Reaction

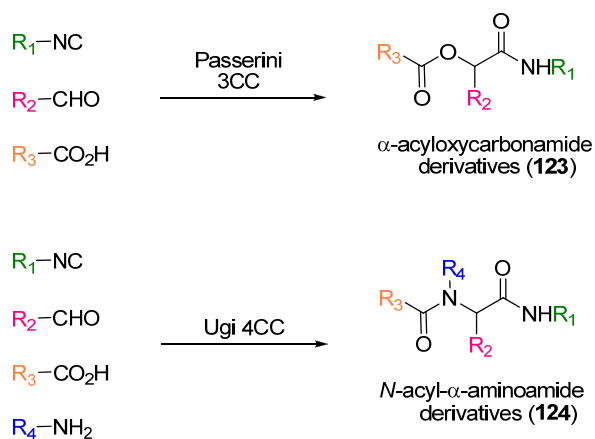
We sought the development of a novel route to 2-alkylpyroglutamic acid derivatives **62** via the Ugi 4-center 3-component condensation reaction (U-4C-3CCR) of γ -ketoacids **119**, amines **120**, and isocyanides **121** (Scheme 2.2). Initially, 2-alkylpyroglutamic acid amide **122** is generated via the U-4C-3CCR (see Section 2.2.1). If conversion of the C-terminal amide bond to a carboxylic acid could be achieved selectively, it would provide a unique approach to 2-alkylpyroglutamic acids. In addition, if a stereoselective Ugi reaction is achieved with a chiral γ -ketoacid, this strategy would be attractive for the synthesis of functionalized pyroglutamic acids including omuralide and salinosporamide A. This approach is distinctive due to the simultaneous generation of 3 bonds (labeled A, B, and C). The Ugi reaction of γ -ketoacids could be a general and efficient method to synthesize 2-alkylpyroglutamic acid derivatives due to the mild reaction conditions, generally high chemical yield, and convergent nature of the reaction.



Scheme 2.2 Strategy Towards 2-Alkylpyroglutamic Acid Synthesis

2.2.1 History of Multicomponent Reactions

Multicomponent reactions (MCRs) are one-step processes utilizing more than two starting materials that combine, with the majority of their atoms, directly into a new product. MCRs are widely considered powerful synthetic tools for the preparation of structurally diverse complex molecules as well as combinatorial libraries of compounds.^{31,32} A subclass of MCRs, incorporating isocyanides, are numerous and diverse and represent an especially effective way to synthesize novel scaffolds.^{33,34} The advantages of this convergent, diversity-oriented approach, are the rapid construction of complex carbon frameworks with operationally simple procedures and generally high overall yields.



Scheme 2.2.1 Passerini and Ugi Reaction

The chemistry of MCRs officially began around 1850 when Strecker introduced the general formation of α -aminocyanides from ammonia, carbonyl compounds, and hydrogen cyanide.³⁵ The chemistry of isocyanides began a short while afterward, in

1859, when Lieke formed allyl isocyanide from allyl iodide and silver cyanide.³⁶ However, the first MCR of isocyanides did not appear in the literature until much later, in 1921, when Passerini introduced the formation of α -acyloxycarbonamides (**123**, Scheme 2.2.1) from their reaction with carboxylic acids and carbonyl compounds.³⁷

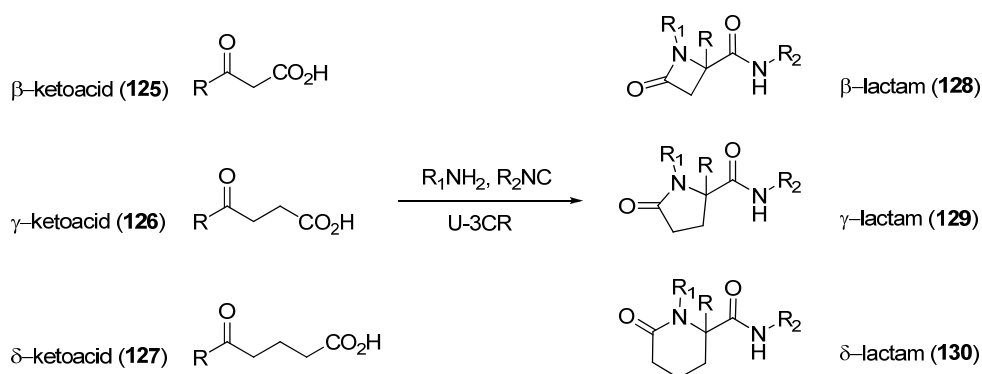
In 1959, Ugi introduced a novel and general one-pot four-component reaction, referred to as the Ugi reaction (U-4CR) since 1962, involving the addition of a carboxylic acid, amine, aldehyde or ketone, and isocyanide to give an *N*-acyl- α -aminoamide product (**124**).³⁸ The U-4CR has since then received considerable attention because the product was recognized as a protected amino acid, therefore, an application in the synthesis of natural and unnatural amino acids. Again, we are interested in a variation of the U-4CR, where the carbonyl and the carboxylic acid components are tethered into a γ -ketoacid, which allows for the synthesis of pyroglutamic acid amides via the U-4C-3CCR.

2.2.2 Ugi Reaction with γ -Ketoacids

The Ugi 4-component condensation reaction provides a linear, peptide like adduct. A conceptually simple approach to a cyclic structure is to tether two out of four of the components and perform an U-4C-3CCR. Indeed, various bifunctional components have been employed,³⁴ and lactams with different substitution patterns have been synthesized by using ω -oxo acids,^{39,40} ω -amino acids,⁴¹ and ω -amino aldehydes⁴² as components.

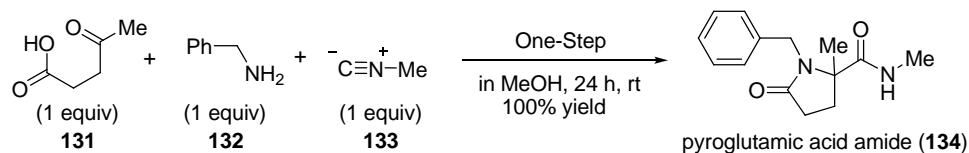
Tethering the carboxylic acid and carbonyl compound, into β -, γ -, or δ -ketoacids, **125-127**, generates the corresponding β -, γ -, and δ -lactam amides **128-130**, respectively,

via the U-4C-3CCR (Scheme 2.2.2a). Additionally, 7 and 8-membered rings have been formed via the U-4C-3CCR, although those reactions are typically lower yielding³⁹. The formation of the highly strained β -lactam ring is important biologically due to the well known therapeutic properties of β -lactam antibiotics.⁴³ In addition, the formation of 4-membered rings is typically challenging and their successful construction under mild reaction conditions is remarkable.



Scheme 2.2.2a Ketoacids in Ugi-4C-3CCR

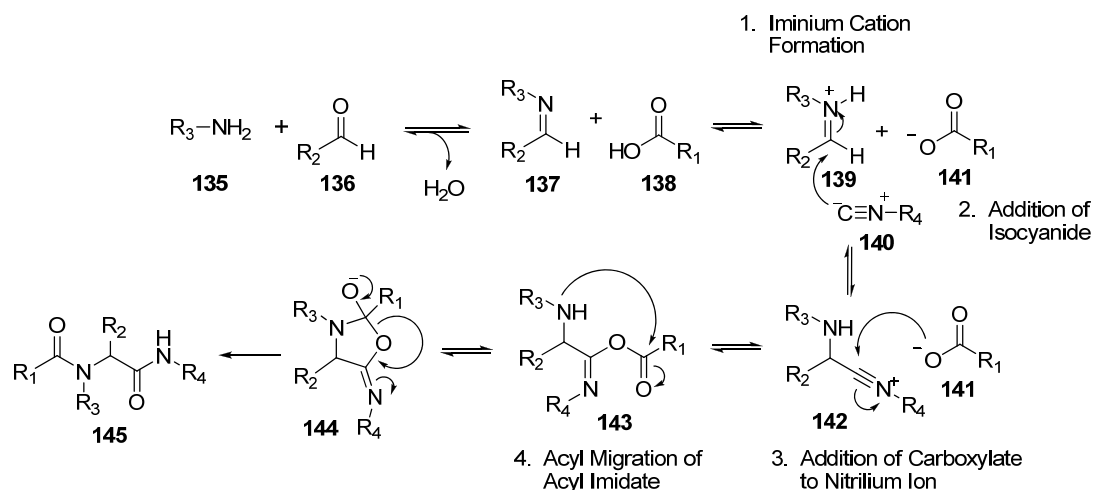
Ugi described the synthesis of pyroglutamic acid amide **134**³⁹ via the one-pot U-4C-3CCR of levulinic acid (**131**) with benzyl amine (**132**) and methyl isocyanide (**133**, Scheme 2.2.2b). The reaction was performed at room temperature, was complete in 24 hours, and a quantitative yield was obtained. Interestingly, although the Ugi reaction of ketones is typically sluggish, providing low yields even after extended reaction times and/or heating, the reaction of the tethered γ -ketoacid was very efficient.



Scheme 2.2.2b Ugi's Synthesis of Pyroglutamic Acid Amide

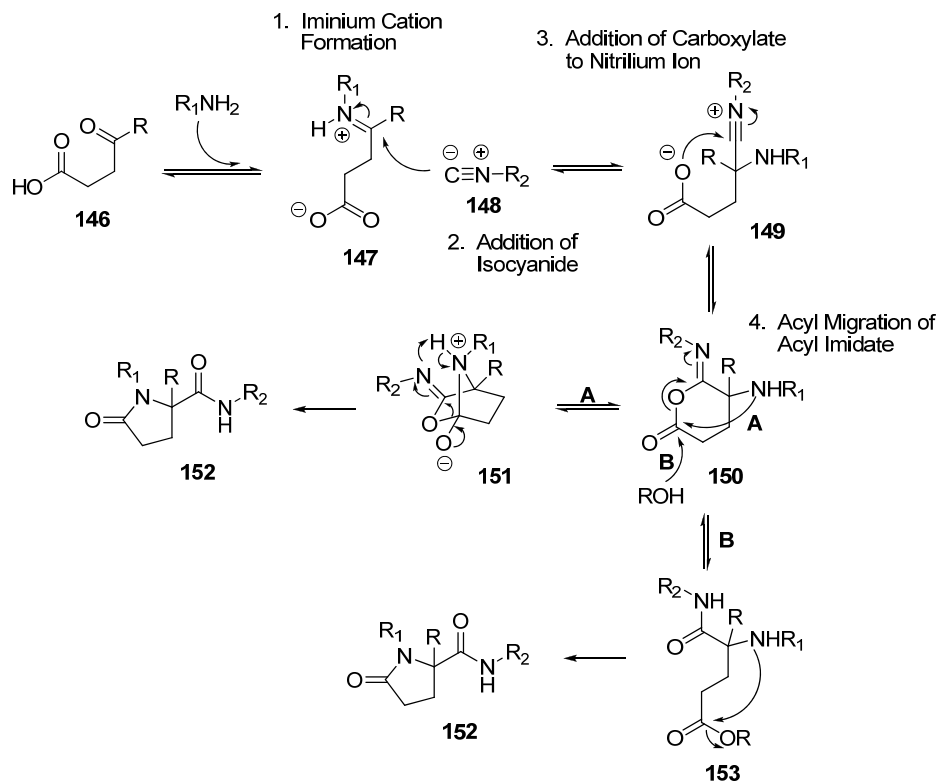
2.2.3 Mechanism

The proposed mechanism of the U-4CR^{44,45} (Scheme 2.2.3a) consists of equilibria between all intermediate steps until the final *trans*-acylation step where the product is in practice irreversibly formed. After imine **137** formation, from the amine **135** and carbonyl compound **136**, protonation of the imine by the carboxylic acid **138** generates an iminium cation **139**. Next, it was proposed that either direct addition of the isocyanide **140** to the iminium cation occurs (as shown), and the resulting electrophilic nitrilium ion **142** is captured by the carboxylate **141**, forming acylimidate **143**, or addition of the generated carboxylate gives a racemic α -amino α -acyloxy intermediate, which is then substituted by the isocyanide via an S_N2 reaction to yield acylimidate derivative **143**. The latter explanation is consistent with the fact that use of chiral isocyanides did not lead to any diastereoselectivity in the reaction (see section 2.2.4). Lastly, intramolecular acyl migration occurs from acylimidate **143** to yield the stable α -acylaminoamide **145** product.



Scheme 2.2.3a Mechanism of Ugi-4CCR

The mechanism of the Ugi reaction of γ -ketoacids is shown in Scheme 2.2.3b. The first step is imine formation, which presumably converts straight away to zwitterion **147**, via intramolecular proton transfer. Again, either direct addition of the isocyanide **148** to the iminium cation occurs, or addition of the intramolecular carboxylate occurs (not shown) followed by S_N2 substitution by the isocyanide, both resulting in electrophilic nitrilium ion **149** generation, which is then captured by the internal carboxylate forming acyl imidate **150**. The next step in this mechanism is also unclear and is thought to involve either intramolecular acyl migration (pathway A) to form intermediate bicycle **151**, which collapses to yield cyclic pyroglutamic acid amide **152**, or ring opening (pathway B) by addition of MeOH (commonly used as solvent) or H_2O (formed as byproduct in the first step) to the acyl center providing **153**, which is then quickly followed by lactam formation.

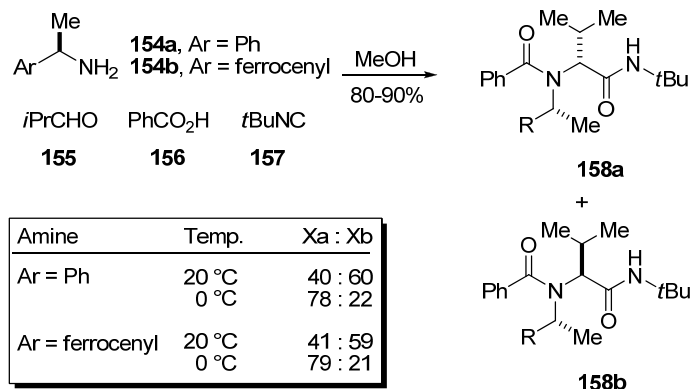


Scheme 2.2.3b Mechanism of Ugi-4C-3CCR

2.2.4 Stereochemical Aspects

During the Ugi reaction, a new stereocenter is formed, resulting in racemic products in the absence of stereoselection. An enantioselective variant of the Ugi reaction is still unknown, and as a result, the traditional approach to induce stereoselection in the Ugi MCR has been to use chiral starting materials. By a number of experiments, it was found that the best stereochemical induction was achieved by using chiral amines, whereas chiral aldehydes, isocyanides, and carboxylic acids gave poor or no induction.^{32,44} The ideal chiral amine would give high *de*'s and high chemical yields,

be universally applicable with all other starting materials, and be easy to cleave off under mild conditions to yield amino acid or peptide derivatives.

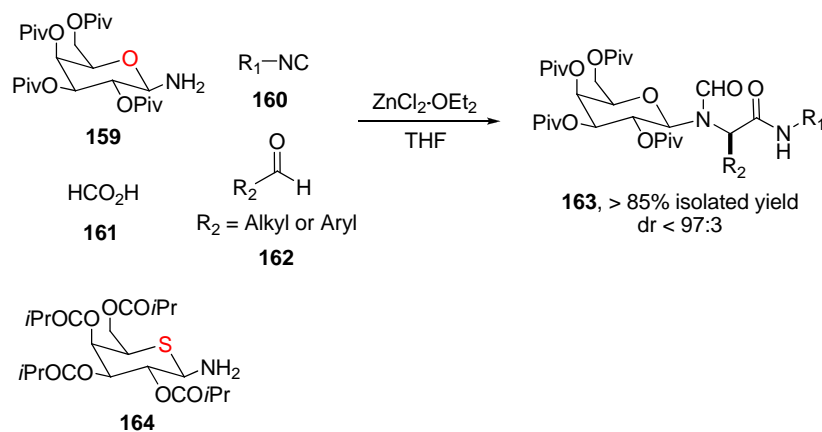


Scheme 2.2.4a Chiral Phenethylamines in the Ugi Reaction

The use of different aromatic amines, 1-Phenethylamines **154a**^{45,46} and α -aminoferrocenylamines **154b**⁴⁷, in the U-4CR with isobutyraldehyde (**155**), benzoic acid (**156**), and *t*-butyl isocyanide (**157**) at room temperature and 0 °C led to the formation of α -amino acid derivatives **158a**, **158b** in excellent yield with similar moderate diastereoselectivity, regardless of the amine used (Scheme 2.2.4a).

The use of galactoseylamine **159**⁴⁸ allowed the preparation of α -amino acid derivative **163** with excellent results (Scheme 2.2.4b), independent of the nature of both the aldehyde and the isocyanide. The reaction should be performed in the presence of 1 equiv of ZnCl₂ to obtain good diastereoselectivities. The role of the lewis acid seems to be to force the conformation of the initially formed galactosylimine by chelation with the nitrogen atom and the oxygen atom of the carbonyl group of the nearby pivaloyl ester. The chiral α -amino acid can be liberated by hydrolysis in two steps: The *N*-formal group

is first removed with HCl in MeOH, and the *N*-glycosidic bond is then cleaved by addition of water, with a 90-95% recovery of the corresponding *O*-pivaloyl galactose. The final hydrolysis of the amide moiety in aqueous HCl yields the free α -amino acid. The related 2,3,4-tri-*O*-pivaloyl- α -D-arabinosylamine was introduced successfully instead of chiral amine **159** to obtain amino acids with *S*-configuration.



Scheme 2.2.4b Chiral Sugar Derived Amines in the Ugi Reaction

In addition, Ugi recently presented a highly improved sugar derived auxiliary, a xylopyranose derived peracylated thiosugar **164**⁴⁹ containing the amine function in the anomeric position. Diastereoselectivities in the Ugi reaction with **164** were >90% in all cases and, moreover, the auxiliary could be cleaved off under very mild conditions with a soft electrophile, HgCl₂, at room temperature.

While these chiral amines effectively induce stereoselectivity in the U-4CR, they have not, as of yet, been applied to the U-4C-3CCR of γ -ketoacids. In our case, we hoped to induce stereoselectivity in the U-4C-3CCR by utilizing chiral γ -ketoacids.

2.2.5 Drug Discovery

By far, most of the applications of MCRs with isocyanides described until today arise from the area of drug discovery.⁵⁰ The emergence of combinatorial chemistry and high-speed parallel synthesis provided a resurgence in interest in MCRs for large chemical library production. Easily automated one-pot reactions, such as the Ugi reaction, are powerful tools for producing diverse arrays of compounds, often in one step and in high yield. Below an example of the utility of multicomponent reactions in the hit to lead discovery of new medicinal therapeutics is described.

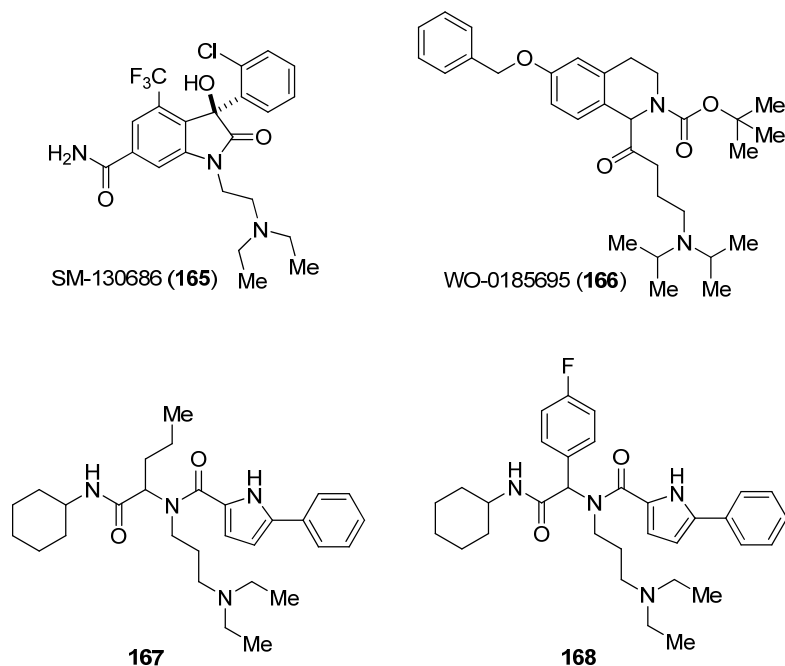


Figure 2.2.5 Compounds with GHS Agonist Activity

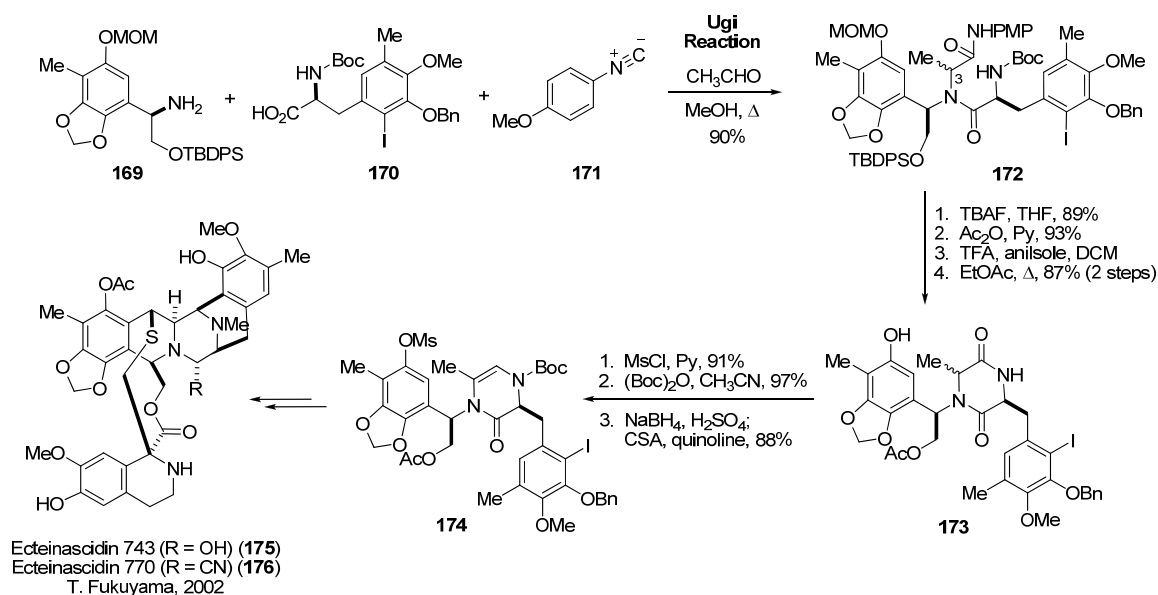
Asahi Kasei Pharma chemists chose two molecules with known growth hormone secretagogue (GHS) agonist activity, **165** and **166**, which were used as templates to computationally screen a large in house library (Figure 2.2.5).⁵¹ A total of 108 candidate compounds were selected out of the library, and five of them were found to be active in the low micromolar range in both cell based and direct binding assays. Among those, two were α -aminoacylamides, e.g. **167**, which are easily constructed via the U-4CR. A small directed library of analogs of those lead structures were then prepared. Forty compounds were prepared by the U-4CR and among those an inhibitor with a $K_i = 0.22 \mu\text{M}$, **168**, was discovered and an initial SAR could be established. These compounds were distinctly different structurally from the known GHS agonists. This approach clearly demonstrates the value of MCR chemistry in fast hit to lead conversion and eventually to the discovery of biologically useful compounds.

2.2.6 Natural Product Synthesis

Thus far, application of the Ugi reaction in natural product synthesis⁵² has been surprisingly scarce, given the mild, general, and convergent nature of the reaction, because of the major issue of stereocontrol of the newly formed stereocenter. However, the Ugi reaction has been applied in cases where the stereocenter formed in the reaction is later removed or the resultant diastereomeric mixture can be separated.

For example, Fukuyama described a total synthesis of the antitumor antibiotic ecteinascidine 743,⁵³ which is currently undergoing advanced clinical trials. A key reaction in this ambitious total synthesis is the convergent assembly of several parts of the

molecule via the Ugi reaction. Thus, the (R)-phenylglycinol derivative **169** and (S)-iodophenylalanine derivative **170** underwent the U-4CR with *p*-methoxyphenyl isocyanide **171** and acetaldehyde to give dipeptide **172** in 90% yield as a mixture of diastereomers⁵⁴ at C3 (Scheme 2.2.6). Efficient elaboration into diketopiperazine derivative **173** occurred after a simple exchange of protecting groups, Boc deprotection, and gentle heating. A four step sequence, including mesylation of the phenol, introduction of a Boc group onto the lactam nitrogen, partial reduction of the ring carbonyl with NaBH₄, and dehydration of the resultant hemiaminal derivative by treatment with CSA and quinoline, gave **174**. In this sequence, the racemic C3 stereocenter was essentially erased through conversion to a sp²-hybridized carbon atom. This intermediate was further elaborated into the ecteinascidin 743 (**175**).



Scheme 2.2.6 Fukuyama's Total Synthesis of Ecteinascidine 743

This sequence is one example that clearly shows the utility of the Ugi reaction in natural product synthesis. The convergent strategy is ideal for the construction of large and complex natural products and the conditions were mild enough to show compatibility with a variety of functional groups.

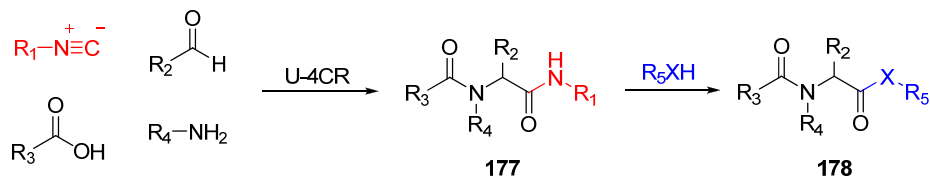
2.2 Convertible Isocyanides

In order to apply the U-4C-3CCR of γ -ketoacids to the synthesis of 2-alkylpyroglutamic acid derivatives, the resultant *C*-terminal amide bond must be selectively hydrolyzed. Standard reaction conditions for the hydrolysis of amides to carboxylic acids, *i.e.* heating with strong acid or base,⁵⁵ would likely result in the non-selective hydrolysis of both the *endo*- and *exo*- cyclic amides. Several convertible isocyanides have been developed specifically to allow for selective *C*-terminal amide bond cleavage.

2.3.1 Definition

An isocyanide that allows for conversion, post-condensation, of the resultant *C*-terminal amide bond (**177**, shown in red) of Ugi products into different functionalities (**178**, shown in blue) is termed a “Convertible Isocyanide” (Scheme 2.3.1). Several

convertible isocyanides have been developed and their application to post-condensation modification of Ugi products⁵⁶ will be introduced.

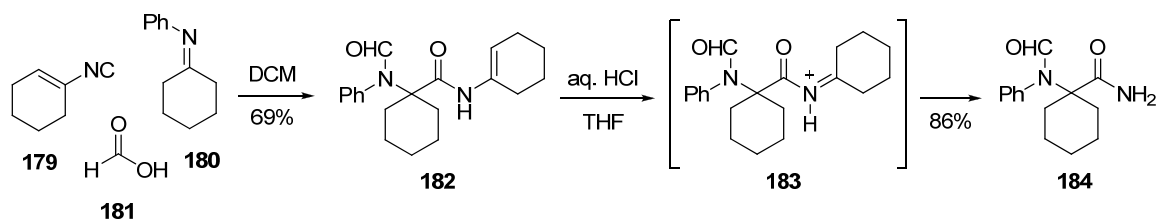


Scheme 2.3.1 Definition of Convertible Isocyanide

2.3.2 Known Convertible Isocyanides

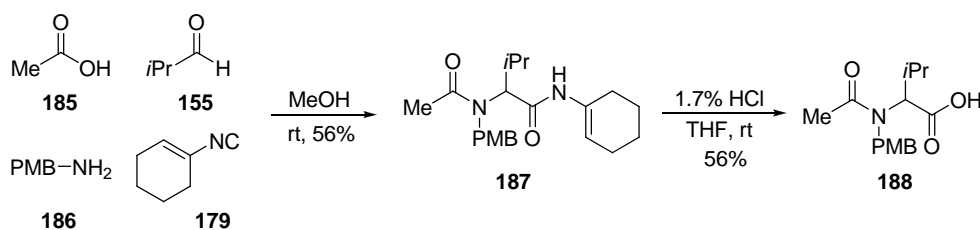
2.3.2.1 Armstrong's Universal Isocyanide

1-Cyclohexen-1-yl isocyanide (**179**) was first reported in 1963 by Ugi and Rosendahl as a synthetic equivalent of the unknown "hydrogen isocyanide".⁵⁷ The U-4CR between isocyanide **179**, cyclohexanone *N*-phenyl imine **180**, and formic acid (**181**) provided *N*-cyclohexen-1-yl amide **182** in 69% yield (Scheme 2.3.2.1a). The secondary amide was converted to primary α -acylamino amide **184** in 86% yield via acid catalyzed activation of the *N*-acyl enamide **182** to an *N*-acyl imminium ion **183**, which undergoes hydrolysis.



Scheme 2.3.2.1a Ugi's Application of 1-Cyclohexen-1-yl Isocyanide

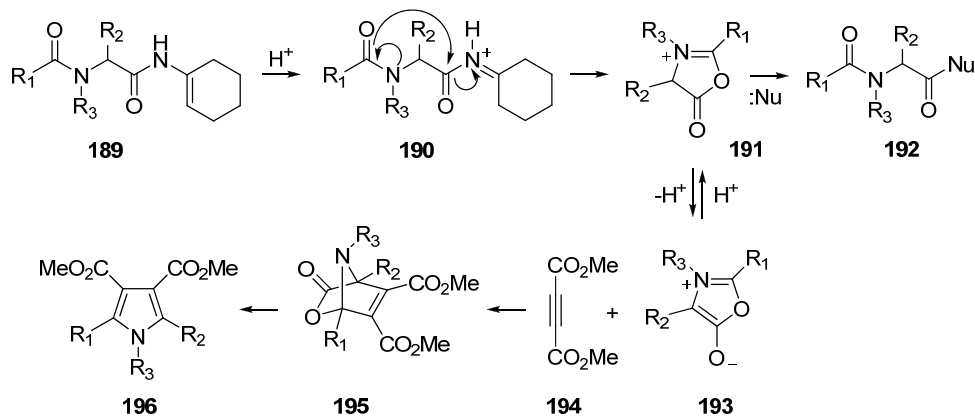
Armstrong reinvestigated isocyanide **179** in 1995 for a new synthetic purpose. He showed that U-4CR adduct **187**, obtained from reaction of **179** with isobutyraldehyde (**155**), *p*-methoxybenzylamine (**186**), and acetic acid (**185**), can be cleaved into the corresponding carboxylic acid **188** upon treatment with 1.7% HCl in THF at room temperature (Scheme 2.3.2.1b).⁵⁸



Scheme 2.3.2.1b Armstrong's Application of 1-Cyclohexen-1-yl Isocyanide

The reaction mechanism is thought to involve the formation of an activated azlactone/münchnone intermediate **191**, formed via protonation of *N*-acylenamide **189** to yield the *N*-acylimminium species **190**, which undergoes intramolecular cyclization (Scheme 2.3.2.1c). The acid and ester products can then arise from subsequent ring opening by water and alcohol, respectively. Evidence for the suggested mechanism was provided by trapping the azlactone intermediate via Diels-Alder reaction with dimethyl

acetylenedicarboxylate (**194**). The initial 1,3-dipolar cycloaddition product **195** eliminated CO₂ to give pyrrole **196**.⁵⁹



Scheme 2.3.2.1c Activated Azlactone/Münchnone Intermediate

The conversion, post-condensation, of Ugi product **189**, into the corresponding primary carboxamide or other carboxylic acid derivative depends on the structure of the Ugi product. An electron rich *N*-acyl moiety was required for azlactone formation, otherwise the primary amide was obtained.⁶⁰

The use of isocyanide **179** is further limited by its low stability, which prevents large scale preparation and storage. However, this problem can be circumvented by use of **197** or **198**, which are more stable derivatives of **179** (Figure 2.3.2.1).⁶¹

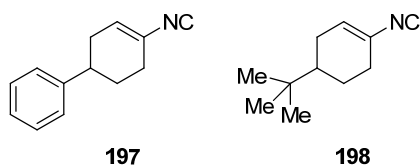
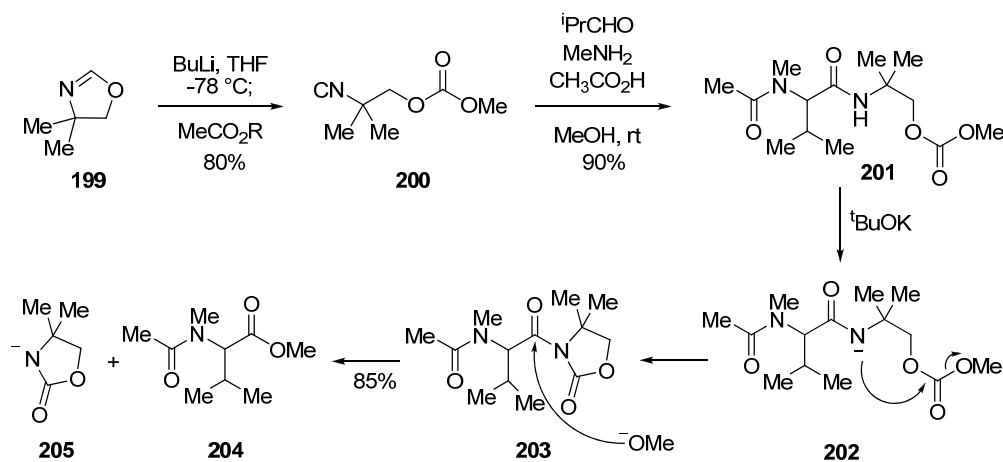


Figure 2.3.2.1 Stable Derivatives of 1-Cyclohexen-1-yl Isocyanide

2.3.2.2 Ugi's Isocyanide

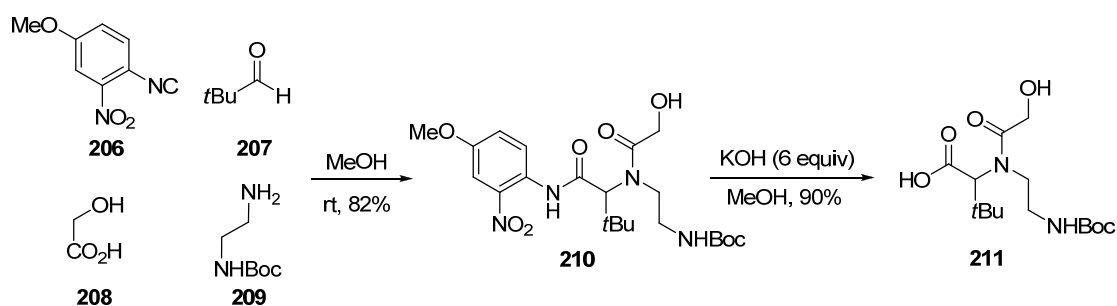
Ugi developed convertible isocyanide methyl 2-isocyano-2-methylpropyl carbonates **200**, prepared in one step from commercially available 4,4-dimethyl-2-oxazoline **199** (Scheme 2.3.2.2).⁶⁰ Deprotonation of **199** is achieved with *n*BuLi in THF at -78 °C and the resulting lithium alcoholate is captured with methyl chloroformate to provide isocyanide **200**. The U-4CR of **200** with isobutyraldehyde, methyl amine, and acetic acid afforded the expected Ugi product **201**, which could be converted into *N*-acyl α -aminoester **204**. The sequence involves base mediated *N*-acyloxazolidinone **203** formation by cyclization of the amide anion onto the carbonate of **202** followed by addition of methoxide and elimination of the oxazolidinone **205**.



Scheme 2.3.2.2 Ugi's Convertible Isocyanide

2.3.2.3 Marten's Isocyanide

Amide groups which are attached with an electron-withdrawing moiety are known to be easier to hydrolyze under alkaline conditions. Following this observation, Martens and co-workers developed 4-methoxy-2-nitrophenylisocyanide (**206**) as a convertible isocyanide.⁶² The U-4CR between isocyanide **206**, pivaldehyde (**207**), glycolic acid (**208**), and *mono*-Boc-ethylenediamine (**209**) afforded **210**, which when exposed to alkaline hydrolysis with methanolic potassium hydroxide, afforded acid **211** (Scheme 2.3.2.3).

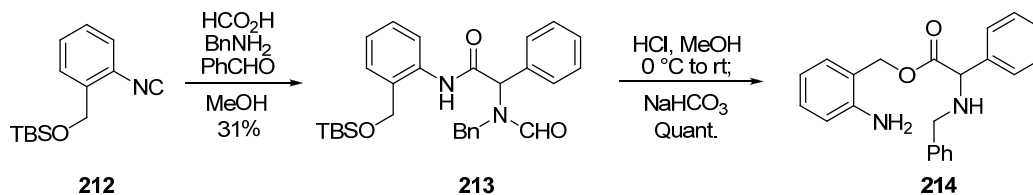


Scheme 2.3.2.3 Marten's Convertible Isocyanide

2.3.2.4 Linderman's Isocyanide

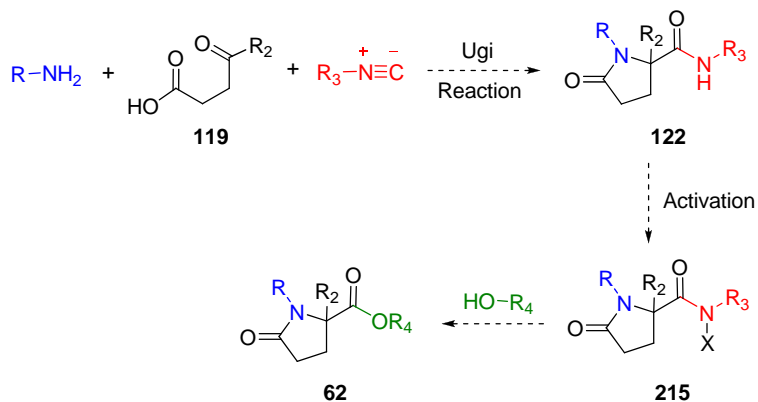
Another convertible isocyanide, 2-(*t*-butyldimethylsilyloxymethyl)-phenyl isocyanide **212**, was introduced by Linderman.^{55,63} U-4CR of isocyanide **212** with formic acid, benzylamine, and benzaldehyde gave Ugi adduct **213** (31%, 40% Passerini adduct was obtained), which, upon acid treatment followed by basification, underwent *O*-

desilylation and amide/ester exchange to afford the ester **214** in quantitative yield. (Scheme 2.3.2.4).



Scheme 2.3.2.4 Linderman's Convertible Isocyanide

2.3.3 Limitations of Existing Convertible Isocyanides

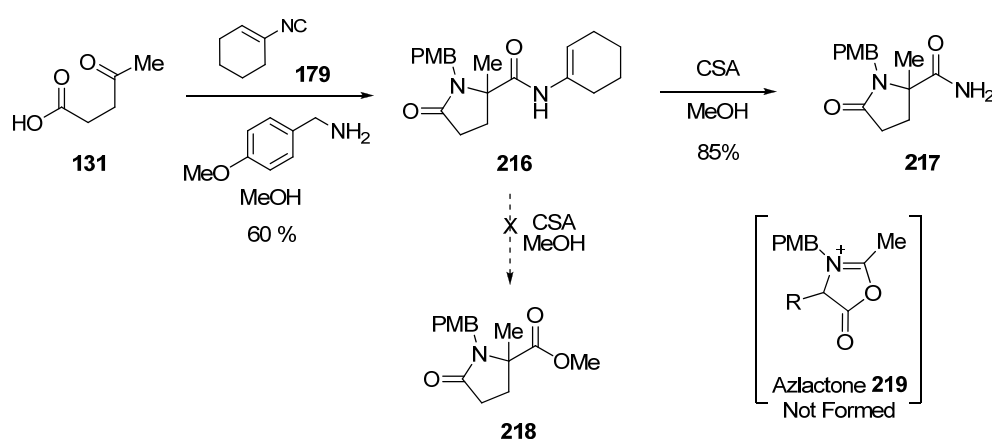


Scheme 2.3.3a Strategy for Application of Convertible Isocyanide to 2-Alkylpyroglutamic Acid Synthesis

We then set out to determine if we could apply one of the known convertible isocyanides to the synthesis of 2-alkylpyroglutamic acid derivatives **62** via the Ugi reaction of γ -ketoacids **119** (Scheme 2.3.3a). We sought a convertible isocyanide that

would facilitate the selective hydrolysis of the *C*-terminal amide bond (in red) of pyroglutamic acid amides **122**, via activation of that amide (see **215**), followed by hydrolysis to the corresponding pyroglutamic acid or ester **62**.

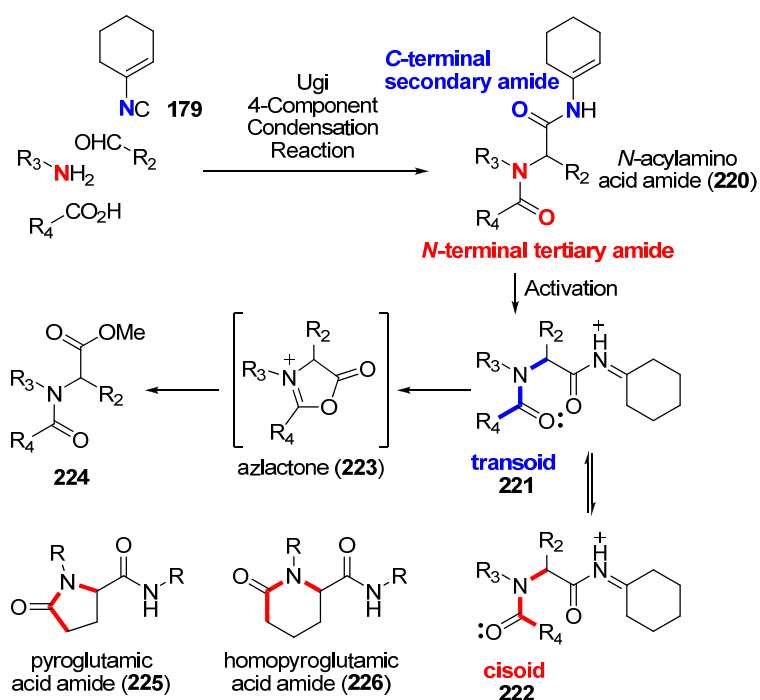
Ugi reaction of Armstrong's universal isocyanide **179** with levulinic acid (**131**) and *p*-methoxybenzylamine gave the corresponding pyroglutamic acid amide **216** (60%), which when subjected to CSA in methanol, provided the corresponding primary amide **217** instead of methyl ester **218** (Scheme 2.3.3b). This result indicated that the activated azlactone intermediate **219** was not formed (see section 2.3.2.1).



Scheme 2.3.3b Failed Application of Armstrong's Isocyanide

Failure in the formation of the azlactone intermediate can be explained upon investigation of the conformation of pyroglutamic acid amide Ugi products. The U-4CR, incorporating isocyanide **179**, furnishes a linear *N*-acylamino acid amide **220** product (Scheme 2.3.3c). The *N*-terminal tertiary amide (red atom label in **220**) created in the Ugi reaction is in equilibrium between the transoid and cisoid isomers (blue and red bold

bonds in **221** and **222**). When the C-terminal amide (blue atom label in **220**) is activated, only the transoid *N*-terminal amide **221** can participate in the formation of the azlactone intermediate **223**, which is readily hydrolyzed to give **224**. Pyroglutamic acid amides **225** and homopyroglutamic acid amides **226**, obtained from the Ugi reaction of γ -ketoacids and δ -ketoacids respectively, are conformationally locked as the cisoid isomer. This makes formation of the azlactone and therefore the subsequent hydrolysis not possible.



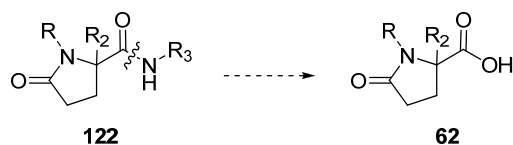
Scheme 2.3.3c Cisoid and Transoid Amide Rotamers

Thus, a convertible isocyanide not requiring participation of the γ -lactam amide in the activation mechanism will be required for the conversion of pyroglutamic amides

to pyroglutamic acids. The other aforementioned convertible isocyanides allow for hydrolysis of *C*-terminal amides via external activation, without an azlactone intermediate. However, using these isocyanides, we also failed to selectively hydrolyze pyroglutamic acid amides, likely due to the steric hindrance of the fully substituted α -carbon and the harsh hydrolytic conditions required.

2.3.4 New Convertible Isocyanide

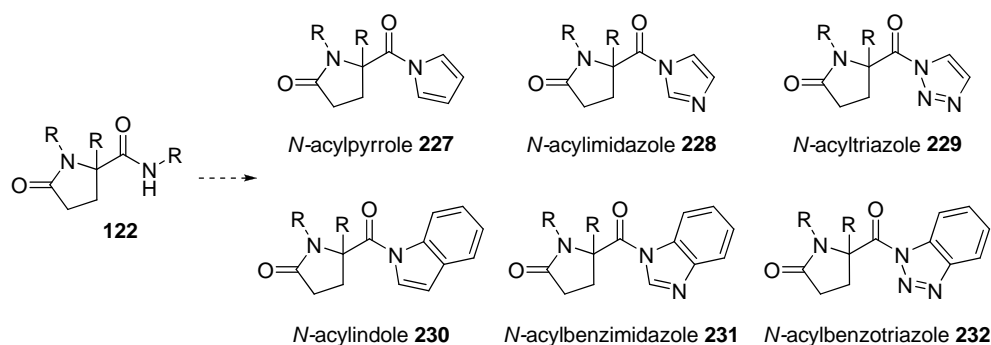
Unfortunately, the universal isocyanide **179**, as well as the other known convertible isocyanides, failed to hydrolyze the *C*-terminal amide of pyroglutamic acid amides. In view of that fact, we required an alternative convertible isocyanide which would allow, under mild conditions, for the selective activation and hydrolysis of the more hindered *C*-terminal amide of pyroglutamic acid amides **122** to the corresponding pyroglutamic acid **62** (Scheme 2.3.4).



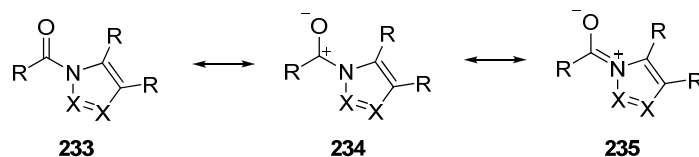
Scheme 2.3.4 Hydrolysis of *C*-Terminal Amide of Pyroglutamic Acid Amides

2.3.4.1 Activated Amides

A fundamental difference between the *C*- and *N*-terminal amides, of the pyroglutamic acid amide **122**, is that the former is a secondary amide while the latter is a tertiary amide. We hypothesized that selective activation of the secondary amide, in the presence of the tertiary amide, to an *N*-acyl- pyrrole (**227**),^{64,65} imidazole (**228**),^{66,67} triazole (**229**),⁶⁸ indoles (**230**),⁶⁴ benzimidazole (**231**),⁶⁷ or benzotriazole (**232**)⁶⁸ (Scheme 2.3.4.1a), which are known as activated tertiary amides, would allow for selective hydrolysis of the secondary amide bond under mildly basic conditions. Formation of the activated amides will be possible by designing a novel convertible isocyanide because the secondary amide is derived from the isocyanide. The activated amides **233** are unlike other tertiary amides in that there is less contribution from resonance forms of type **235** (Scheme 2.3.4.1b) to the overall structure and consequently the positive nature of the carbonyl carbon (see **234**) is retained, similar to a ketone. Most likely, an intramolecular reaction to form the activated heterocyclic amide will be necessary because an intermolecular reaction may be slow due to the steric hinderance surrounding the *C*-terminal pyroglutamic acid amide.



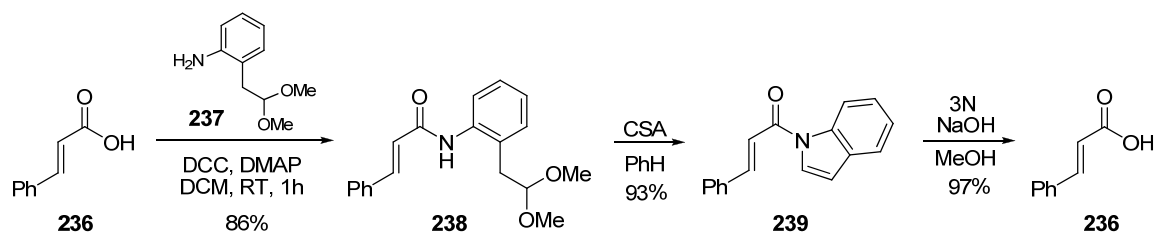
Scheme 2.3.4.1a Structure of Activated Amides



Scheme 2.3.4.1b Resonance Structures of Activated Amides

2.3.4.2 Activation of Anilide via *N*-Acylindole

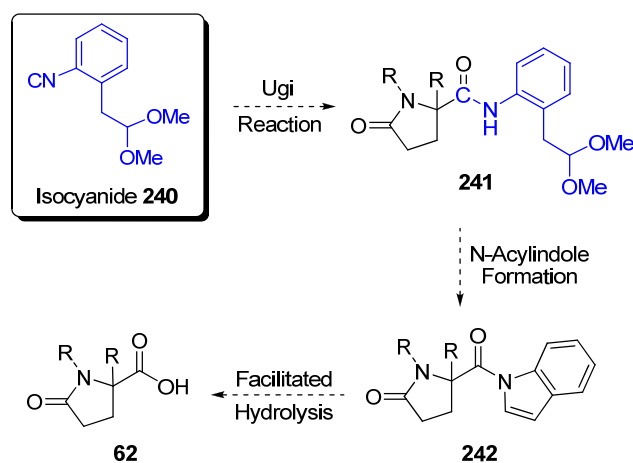
Initially, we took our inspiration from a report by Fukuyama, who had previously introduced 2-(2,2-dimethoxyethyl)aniline (**237**) as a protecting group for carboxylic acids.⁶⁹ Cinnamic acid (**236**) was protected as secondary *N*-acylanilide **238**, and regenerated by conversion of **238** into *N*-acylindole **239**, via treatment with CSA in benzene, followed by basic hydrolysis (Scheme 2.3.4.2). Formation of the aromatic *N*-Acylindole considerably alters the character of the amide by decreasing the double-bond character of the C-N amide bond which greatly weakens the bond. As a result, it is possible to selectively cleave this amide bond to the corresponding carboxylic acid under relatively mild basic conditions. In addition, it was demonstrated that *N*-acylindole **239** is a versatile intermediate that be converted to corresponding esters, thioesters, and amides, as well as to the carboxylic acid. Also, conversion of the anilide to the *N*-acylindole is an intramolecular reaction, which we believed an important factor for application to the much more sterically hindered pyroglutamic acid system.



Scheme 2.3.4.2 2,2-Dimethoxyethyl)aniline as a Carboxylic Acid Protecting Group

2.3.4.3 Strategy

We then hypothesized that the corresponding isocyanide, 1-isocyano-2-(2,2-dimethoxyethyl)benzene (**240**),⁷⁰ when utilized in the Ugi reaction of γ -ketoacids, would act as a convertible isocyanide for the synthesis of pyroglutamic acids. We surmised that a U-4C-3CCR incorporating isocyanide **240** and a γ -ketoacid would result in formation of *N*-acylanilide **241**, which upon conversion to *N*-acylindole **242** would be amenable to facile hydrolysis to yield 2-alkylpyroglutamic acid **62** (Scheme 2.3.4.3).



Scheme 2.3.4.3 Hypothesis of 1-Isocyano-2-(2,2-dimethoxyethyl)benzene

2.4 Conclusions

The 2-alkylpyroglutamic acid moiety is a relatively common substructure found in a number of natural products including lactacystin, salinosporamides A-B, and cinnabaramides A-C. As a result, we sought the development of a novel and general route to 2-alkylpyroglutamic acid derivatives via the Ugi 4-center 3-component condensation reaction (U-4C-3CCR) of γ -ketoacids. The advantages of the U-4C-3CCR are the exceptionally mild reaction conditions as well as the convergent nature of the reaction. In addition, the mild reaction conditions allow for a unified strategy towards derivative formation through the use of differentially functionalized linear γ -ketoacids. The disadvantages of the U-4C-3CCR are the lack of a general method to control the stereoselectivity in the reaction, the lack of a general procedure to access functionalized γ -ketoacids, and the lack of knowledge regarding the reaction mechanism.

It was known that 2-alkylpyroglutamic acid amides could be prepared via an U-4C-3CCR incorporating a tethered γ -ketoacid. In order to convert the pyroglutamic acid amide to a pyroglutamic acid, the C-terminal amide bond must be selectively hydrolyzed. Several convertible isocyanides have been developed specifically to allow for selective C-terminal amide bond cleavage. However, these isocyanides failed to cleave the C-terminal amide bond of the pyroglutamic acid amide. Based on the proven utility of 2-(2,2-dimethoxyethyl)aniline (**237**) as a protecting group for carboxylic acids, we

hypothesized that the corresponding isocyanide, 1-isocyano-2-(2,2-dimethoxyethyl)benzene (**240**), when utilized in the U-4C-3CCR of γ -ketoacids, would act as a convertible isocyanide for the synthesis of pyroglutamic acids.

2.5 Notes and References

- (1) Najera, C.; Yus, M. *Tetrahedron: Asymmetry* **1999**, *10*, 2245-2303.
- (2) Burgus, R.; Butcher, M.; Amoss, M.; Ling, N.; Monahan, M.; Rivier, J.; Fellows, R.; Blackwell, R.; Vale, W.; Guillemin, R. *Proc. Natl. Acad. Sci. U. S. A.* **1972**, *69*, 278-282; Matsuo, H.; Baba, Y.; Nair, R. M. G.; Arimura, A.; Schally, A. V. *Biochem. Biophys. Res. Commun.* **1971**, *43*, 1334-1339.
- (3) Li, W.; Moeller, K. D. *J. Am. Chem. Soc.* **1996**, *118*, 10106-10112; Olson, G. L.; Cheung, H.-C.; Chiang, E.; Madison, V. S.; Sepinwall, J.; Vincent, G. P.; Winokur, A.; Gary, K. A. *J. Med. Chem.* **1995**, *38*, 2866-2879.
- (4) Boulanger, A.; Abou-Mansour, E.; Badre, A.; Banaigs, B.; Combaut, G.; Francisco, C. *Tetrahedron Lett.* **1994**, *35*, 4345-4348.
- (5) Bhatnagar, P. K.; Alberts, D.; Callahan, J. F.; Heerding, D.; Huffman, W. F.; King, A. G.; LoCastro, S.; Pelus, L. M.; Takata, J. S. *J. Am. Chem. Soc.* **1996**, *118*, 12862-12863; Fushiya, S.; Watari, F.; Tashiro, T.; Kusano, G.; Nozoe, S. *Chem. Pharm. Bull. (Tokyo)* **1988**, *36*, 1366-1370.
- (6) Williamson, R. T.; Marquez, B. L.; Gerwick, W. H. *Tetrahedron* **1999**, *55*, 2881-2888; Yun, B.-S.; Ryoo, I.-J.; Lee, I.-K.; Yoo, I.-D. *Tetrahedron* **1998**, *54*, 15155-15160.
- (7) Omura, S.; Matsuzaki, K.; Fujimoto, T.; Kosuge, K.; Furuya, T.; Fujita, S.; Nakagawa, A. *J. Antibiot.* **1991**, *44*, 117-118; Omura, S.; Fujimoto, T.; Otaguro, K.; Matsuzaki, K.; Moriguchi, R.; Tanaka, H.; Sasaki, Y. *J. Antibiot.* **1991**, *44*, 113-116.

(8) Williams, P. G.; Buchanan, G. O.; Feling, R. H.; Kauffman, C. A.; Jensen, P. R.; Fenical, W. *J. Org. Chem.* **2005**, *70*, 6196-6203; Macherla, V. R.; Mitchell, S. S.; Manam, R. R.; Reed, K. A.; Chao, T.-H.; Nicholson, B.; Deyanat-Yazdi, G.; Mai, B.; Jensen, P. R.; Fenical, W. F.; Neuteboom, S. T. C.; Lam, K. S.; Palladino, M. A.; Potts, B. C. M. *J. Med. Chem.* **2005**, *48*, 3684-3687; Feling, R. H.; Buchanan, G. O.; Mincer, T. J.; Kauffman, C. A.; Jensen, P. R.; Fenical, W. *Angew. Chem. Int. Ed.* **2003**, *42*, 355-357.

(9) Stadler, M.; Bitzer, J.; Mayer-Bartschmid, A.; Mueller, H.; Benet-Buchholz, J.; Gantner, F.; Tichy, H.-V.; Reinemer, P.; Bacon, K. B. *J. Nat. Prod.* **2007**, *70*, 246-252.

(10) Sakai, R.; Oiwa, C.; Takaishi, K.; Kamiya, H.; Tagawa, M. *Tetrahedron Lett.* **1999**, *40*, 6941-6944.

(11) Morris, B. D.; Prinsep, M. R. *J. Nat. Prod.* **1999**, *62*, 688-693.

(12) Mori, T.; Takahashi, K.; Kashiwabara, M.; Uemura, D.; Katayama, C.; Iwadare, S.; Shizuri, Y.; Mitomo, R.; Nakano, F.; Matsuzaki, A. *Tetrahedron Lett.* **1985**, *26*, 1073-1076.

(13) Otani, T.; Yoshida, K.-I.; Kubota, H.; Kawai, S.; Ito, S.; Hori, H.; Ishiyama, T.; Oki, T. *J. Antibiot.* **2000**, *53*, 1397-1400.

(14) Takahashi, K.; Kawabata, M.; Uemura, D.; Iwadare, S.; Mitomo, R.; Nakano, F.; Matsuzaki, A. *Tetrahedron Lett.* **1985**, *26*, 1077-1078.

(15) Corey, E. J.; Li, W.; Reichard, G. A. *J. Am. Chem. Soc.* **1998**, *120*, 2330-2336; Corey, E. J.; Reichard, G. A. *J. Am. Chem. Soc.* **1992**, *114*, 10677-10678.

(16) Guillena, G.; Mico, I.; Najera, C.; Ezquerra, J.; Pedregal, C. *An. Quim. Int. Ed.* **1996**, *92*, 362-369.

(17) Brana, M. F.; Garranzo, M.; Perez-Castells, J. *Tetrahedron Lett.* **1998**, *39*, 6569-6572.

(18) Dikshit, D. K.; Maheshwari, A.; Panday, S. K. *Tetrahedron Lett.* **1995**, *36*, 6131-6134.

(19) Corey, E. J.; Li, W.; Nagamitsu, T. *Angew. Chem. Int. Ed.* **1998**, *37*, 1676-1679.

(20) Hamada, Y.; Kawai, A.; Kohno, Y.; Hara, O.; Shioiri, T. *J. Am. Chem. Soc.* **1989**, *111*, 1524-1525; Thottathil, J. K.; Moniot, J. L.; Mueller, R. H.; Wong, M. K. Y.; Kissick, T. P. *J. Org. Chem.* **1986**, *51*, 3140-3143.

(21) Uno, H.; Baldwin, J. E.; Russell, A. T. *J. Am. Chem. Soc.* **1994**, *116*, 2139-2140.

(22) Brennan, C. J.; Pattenden, G.; Rescourio, G. *Tetrahedron Lett.* **2003**, *44*, 8757-8760.

(23) Reddy, L. R.; Saravanan, P.; Corey, E. J. *J. Am. Chem. Soc.* **2004**, *126*, 6230-6231.

(24) Reddy, L. R.; Saravanan, P.; Fournier, J.-F.; Reddy, B. V. S.; Corey, E. J. *Org. Lett.* **2005**, *7*, 2703-2705; Reddy, L. R.; Fournier, J.-F.; Reddy, B. V. S.; Corey, E. J. *J. Am. Chem. Soc.* **2005**, *127*, 8974-8976; Reddy, L. R.; Fournier, J.-F.; Reddy, B. V. S.; Corey, E. J. *Org. Lett.* **2005**, *7*, 2699-2701.

(25) Kulinkovich, O. G. *Chem. Rev.* **2003**, *103*, 2597-2632.

(26) Hayes, C. J.; Sherlock, A. E.; Selby, M. D. *Org. Biomol. Chem.* **2006**, *4*, 193-195; Green, M. P.; Prodder, J. C.; Hayes, C. J. *Tetrahedron Lett.* **2002**, *43*, 6609-6611.

(27) Wardrop, D. J.; Bowen, E. G. *Chem. Commun. (Cambridge, U. K.)* **2005**, 5106-5108.

(28) Balskus, E. P.; Jacobsen, E. N. *J. Am. Chem. Soc.* **2006**, *128*, 6810-6812.

(29) Ling, T.; Macherla, V. R.; Manam, R. R.; McArthur, K. A.; Potts, B. C. *M. Org. Lett.* **2007**, *9*, 2289-2292.

(30) Ma, G.; Nguyen, H.; Romo, D. *Org. Lett.* **2007**, *9*, 2143-2146.

(31) Menendez, J. C. *Multicomponent Reactions Edited by J. Zhu and H. Bienayme*, 2006; Zhu, J.; Bienayme, H.; Editors *Multicomponent Reactions*, 2005; Nair, V. *Multicomponent reactions edited by Jieping Zhu and Hugues Bienayme*, 2005; Vol. 44; Marek, I. *Tetrahedron* **2005**, *61*, 11309; Ugi, I.; Ross, G.; Burdack, C. *Adv. Macromol. Supramol. Mater. Processes* **2003**, 239-250; Tuch, A.; Walle, S. *Handb. Comb. Chem.* **2002**, *2*, 685-705; Ugi, I. *Pure Appl. Chem.* **2001**, *73*, 187-191.

(32) Seayad, J.; List, B. *Multicompon. React.* **2005**, 277-299; Ramon Diego, J.; Yus, M. *Angewandte Chemie (International ed. in English)* **2005**, 44, 1602-1634.

(33) Veiderma, M. *Proc. Est. Acad. Sci., Chem.* **2007**, 56, 98-102; Ugi, I.; Werner, B. *Methods Reagents Green Chem.* **2007**, 3-22; Doemling, A. *Chem. Rev.* **2006**, 106, 17-89; Doemling, A. *Multicompon. React.* **2005**, 76-94; Banfi, L.; Riva, R. *Semin. Org. Synth., Summer Sch. "A. Corbella", 30th* **2005**, 15-38; Ugi, I.; Werner, B.; Doemling, A. *Molecules* **2003**, 8, 53-66; Domling, A. *Curr. Opin. Chem. Biol.* **2002**, 6, 306-313; Domling, A.; Ugi, I. *Angew. Chem. Int. Ed.* **2000**, 39, 3168-3210.

(34) Zhu, J. *Eur. J. Org. Chem.* **2003**, 1133-1144.

(35) Strecker, A. *Justus Liebigs Ann. Chem.* **1850**, 75, 27.

(36) Lieke, W. *Justus Liebigs Ann. Chem.* **1859**, 112, 316.

(37) Passerini, M.; Ragni, G.; Simone, L. *Gazz. Chim. Ital.* **1931**, 61, 964-969; Passerini, M. *Gazz. Chim. Ital.* **1921**, 51, 126-129.

(38) Ugi, I. *Angew. Chem.* **1962**, 74, 9-22.

(39) Hanusch-Kompa, C.; Ugi, I. *Tetrahedron Lett.* **1998**, 39, 2725-2728.

(40) Short, K. M.; Majalli, A. M. M. *Tetrahedron Lett.* **1997**, 38, 359-362; Harriman, G. C. B. *Tetrahedron Lett.* **1997**, 38, 5591-5594.

(41) Kim, Y. B.; Choi, E. H.; Keum, G.; Kang, S. B.; Lee, D. H.; Koh, H. Y.; Kim, Y. *Org. Lett.* **2001**, 3, 4149-4152; Park, S. J.; Keum, G.; Kang, S. B.; Koh, H. Y.; Kim, Y.; Lee, D. H. *Tetrahedron Lett.* **1998**, 39, 7109-7112; Ebert, B. M.; Ugi, I. K.; Grosche, M.; Herdtweck, E.; Herrmann, W. A. *Tetrahedron* **1998**, 54, 11887-11898; Pitlik, J.; Townsend, C. A. *Bioorg. Med. Chem. Lett.* **1997**, 7, 3129-3134; Doemling, A.; Starnecker, M.; Ugi, I. *Angew. Chem. Int. Ed.* **1995**, 34, 2238-2239.

(42) Maison, W. L., A.; Kosten, M.; Schlemminger, I.; Westerhoff, O.; Saak, W.; Martens, J. *J. Chem. Soc., Perkin Trans. 1* **2000**, 1867-1871.

(43) Hubschwerlen, C. *Compr. Med. Chem. II* **2006**, 7, 479-518; Neuhauser, M. M.; Danziger, L. H. *Drug Interact. Infect. Dis. (2nd Ed.)* **2005**, 255-287.

(44) Banfi, L.; Basso, A.; Guanti, G.; Riva, R. *Multicompon. React.* **2005**, 1-32.

(45) Ugi, I.; Offermann, K.; Herlinger, H.; Marquarding, D. *Justus Liebigs Ann. Chem.* **1967**, 709, 1-10; Ugi, I.; Kaufhold, G. *Justus Liebigs Ann. Chem.* **1967**, 709, 11-28.

(46) Kelly, C. L.; Lawrie, K. W. M.; Morgan, P.; Willis, C. L. *Tetrahedron Lett.* **2000**, 41, 8001-8005; Burger, K.; Mutze, K.; Hollweck, W.; Koksche, B. *Tetrahedron* **1998**, 54, 5915-5928; Ahmadian, H.; Nielsen, B.; Braeuner-Osborne, H.; Johansen, T. N.; Stensbol, T. B.; Slok, F. A.; Sekiyama, N.; Nakanishi, S.; Krogsgaard-Larsen, P.; Madsen, U. *J. Med. Chem.* **1997**, 40, 3700-3705; Madsen, U.; Frydenvang, K.; Ebert, B.; Johansen, T. N.; Brehm, L.; Krogsgaard-Larsen, P. *J. Med. Chem.* **1996**, 39, 183-190; Chen, S. Y.; Joullie, M. M. *J. Org. Chem.* **1984**, 49, 1769-1772; Divanfard, H. R.; Lysenko, Z.; Semple, J. E.; Wang, P. C.; Joullie, M. M.; Blount, J. F. *Heterocycles* **1981**, 16, 1975-1985; Semple, J. E.; Wang, P. C.; Lysenko, Z.; Joullie, M. M. *J. Am. Chem. Soc.* **1980**, 102, 7505-7510; Joullie, M. M.; Wang, P. C.; Semple, J. E. *J. Am. Chem. Soc.* **1980**, 102, 887-889.

(47) Siglmüller, F.; Herrmann, R.; Ugi, I. *Tetrahedron* **1986**, 42, 5931-5940; Herrmann, R.; Huebener, G.; Siglmüller, F.; Ugi, I. *Liebigs Ann. Chem.* **1986**, 251-268; Urban, R.; Ugi, I. *Angewandte Chemie (International ed. in English)* **1975**, 14, 61-62; Marquarding, D.; Hoffmann, P.; Heitzer, H.; Ugi, I. *J. Am. Chem. Soc.* **1970**, 92, 1969-1971.

(48) Kunz, H.; Pfrengle, W. *J. Am. Chem. Soc.* **1988**, 110, 651-652; Kunz, H.; Pfrengle, W. *Tetrahedron* **1988**, 44, 5487-5494.

(49) Ross, G.; Ugi, I. *Can. J. Chem.* **2001**, 79, 1934-1939.

(50) Musonda, C. C.; Little, S.; Yardley, V.; Chibale, K. *Bioorg. Med. Chem. Lett.* **2007**, 17, 4733-4736; Musonda, C. C.; Gut, J.; Rosenthal, P. J.; Yardley, V.; Carvalho de Souza, R. C.; Chibale, K. *Bioorg. Med. Chem.* **2006**, 14, 5605-5615; Hulme, C. *Multicompon. React.* **2005**, 311-341; Weber, L.; Doemling, A. *PharmaChem* **2004**, 3, 31-34; Guo, C.; Guo, Z. *Zhongguo Yaowu Huaxue Zazhi* **2003**, 13, 234-240.

(51) Shoda, M.; Harada, T.; Kogami, Y.; Tsujita, R.; Akashi, H.; Kouji, H.; Stahura, F. L.; Xue, L.; Bajorath, J. *J. Med. Chem.* **2004**, 47, 4286-4290.

(52) Zhao, C.; Cao, S.; Liu, N.; Shen, L.; Li, L.; Qian, X. *Huaxue Tongbao* **2006**, 69, 762-766; Toure, B. B.; Hall, D. G. *Multicompon. React.* **2005**, 342-397; Tietze, L. F.; Modi, A. *Med. Res. Rev.* **2000**, 20, 304-322.

(53) Endo, A.; Yanagisawa, A.; Abe, M.; Tohma, S.; Kan, T.; Fukuyama, T. *J. Am. Chem. Soc.* **2002**, 124, 6552-6554.

- (54) The ratio of diastereomers was not reported.
- (55) Linderman, R. J.; Binet, S.; Petrich, S. R. *J. Org. Chem.* **1999**, *64*, 8058.
- (56) Marcaccini, S.; Torroba, T. *Multicompon. React.* **2005**, 33-75.
- (57) Ugi, I.; Rosendahl, K. *Justus Liebigs Ann. Chem.* **1963**, 666, 65-67.
- (58) Keating, T. A.; Armstrong, R. W. *J. Am. Chem. Soc.* **1995**, *117*, 7842-7843.
- (59) Keating, T. A.; Armstrong, R. W. *J. Am. Chem. Soc.* **1996**, *118*, 2574-2583.
- (60) Rikimaru, K.; Yanagisawa, A.; Kan, T.; Fukuyama, T. *Synlett* **2004**, 41-44; Lindhorst, T.; Bock, H.; Ugi, I. *Tetrahedron* **1999**, *55*, 7411-7420.
- (61) Maison, W.; Schlemminger, I.; Westerhoff, O.; Martens, J. *Biorg. Med. Chem.* **2000**, *8*, 1343-1360.
- (62) Baldoli, C.; Maiorana, S.; Licandro, E.; Zinzalla, G.; Perdicchia, D. *Org. Lett.* **2002**, *4*, 4341-4344.
- (63) Linderman, R. J.; Binet, S.; Petrich, S. R. *J. Org. Chem.* **1999**, *64*, 336-337.
- (64) Linda, P.; Stener, A.; Cipiciani, A.; Savelli, G. *J. Heterocycl. Chem.* **1983**, *20*, 247-248.
- (65) Menger, F. M.; Donohue, J. A. *J. Am. Chem. Soc.* **1973**, *95*, 432-437.
- (66) Lee, J. P.; Bembi, R.; Fife, T. H. *J. Org. Chem.* **1997**, *62*, 2872-2876.
- (67) Fife, T. H. *Acc. Chem. Res.* **1993**, *26*, 325-331.
- (68) Katritzky, A. R.; Suzuki, K.; Wang, Z. *Synlett* **2005**, 1656-1665.

(69) Arai, E.; Tokuyama, H.; Linsell, M. S.; Fukuyama, T. *Tetrahedron Lett.* **1998**, *39*, 71-74.

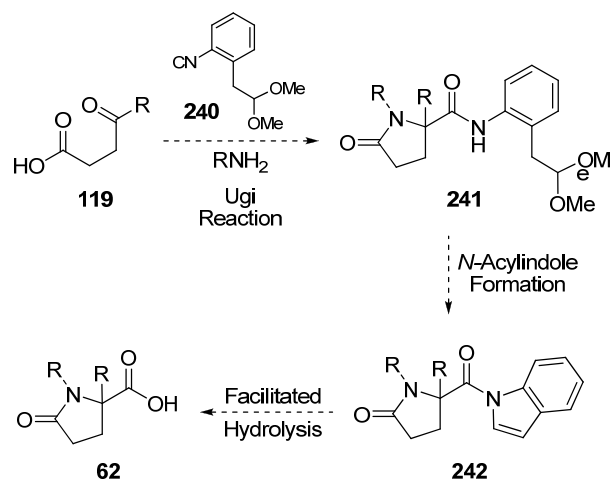
(70) Kobayashi, K.; Yoneda, K.; Mizumoto, T.; Umakoshi, H.; Morikawa, O.; Konishi, H. *Tetrahedron Lett.* **2003**, *44*, 4733-4736.

CHAPTER THREE

Synthesis of Proteasome Inhibitor Omuralide Featuring Stereocontrolled Ugi Reaction and Novel Convertible Isocyanide

3.1 1-Isocyano-2-(2,2-dimethoxyethyl)benzene

In the last chapter, we closed by hypothesizing that 1-isocyano-2-(2,2-dimethoxyethyl)benzene (**240**, Scheme 3.1), when utilized in the Ugi reaction of γ -ketoacids, would act as a convertible isocyanide for the synthesis of pyroglutamic acids. We proposed that a U-4C-3CCR incorporating isocyanide **240** and a γ -ketoacid **119** would result in formation of *N*-acylanilide **241**, which upon conversion to *N*-acylindole **242** would be amenable to facile hydrolysis to yield 2-alkylpyroglutamic acid **62** (Scheme 3.1). The factors we needed to address included the synthesis of isocyanide **240** from 2-(2,2-dimethoxyethyl)aniline (**237**, see section 2.3.4.2), the ability of isocyanide **240** to participate in Ugi reactions with γ -ketoacids, the capability of successfully converting the sterically hindered pyroglutamic acid anilide **241** to the corresponding *N*-acylindole **242**, and the ability to subsequently hydrolyze the hindered *N*-acylindole **242** under mild conditions.

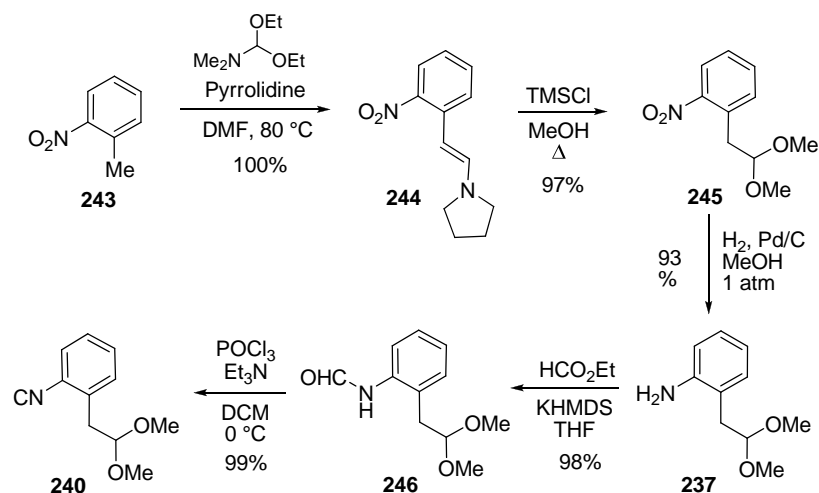


Scheme 3.1 Hypothesis of 1-Isocyanato-2-(2,2-dimethoxyethyl)benzene

3.1.1 Preparative Synthesis

Upon investigation, it was discovered that isocyanide **240** had been reported in the literature previously as a synthetic precursor to 3-methoxyquinolines.¹ Our preparative synthesis of isocyanide **240**² (Scheme 3.1.1), incorporated a modified synthesis that is a combination of procedures reported by K. Kobayashi¹ and Faul.³ Isocyanide **240** is prepared via a 5-step sequence starting from *o*-nitrotoluene (**243**), which is commercially available in large quantities and commonly used as an organic solvent. Leimgruber-Bacho enamine synthesis⁴ from *o*-nitrotoluene (**243**) provided pyrrolidine enamine **244** in quantitative yield. Hydrolysis of **244** to the methyl acetal **245** was successfully achieved with chlorotrimethylsilane (alternatively, acetyl chloride can be used) in refluxing methanol. Palladium catalyzed hydrogenolysis of the nitro group in

245 provided aniline **237** (an alternative synthesis of **237** was reported by Fukuyama in 1998),⁵ which was formylated with ethyl formate and KHMDS. Formamide **246** was successfully dehydrated to isocyanide **240** using POCl₃ and Et₃N. Conveniently, the reactions in this sequence are so efficient and high yielding that a single column chromatography, performed after the last step, was sufficient to yield 66% of pure isocyanide **240** over the entire 5-step sequence. Alternatively, by isolation of each intermediate (**X-X**), our overall yield increased to 88%. Isocyanide **240** is stable red-brown oil that can be stored at -20 °C for several months without decomposition. In addition, while many isocyanides are known for their foul smell, the odor of isocyanide **240** is reasonable.

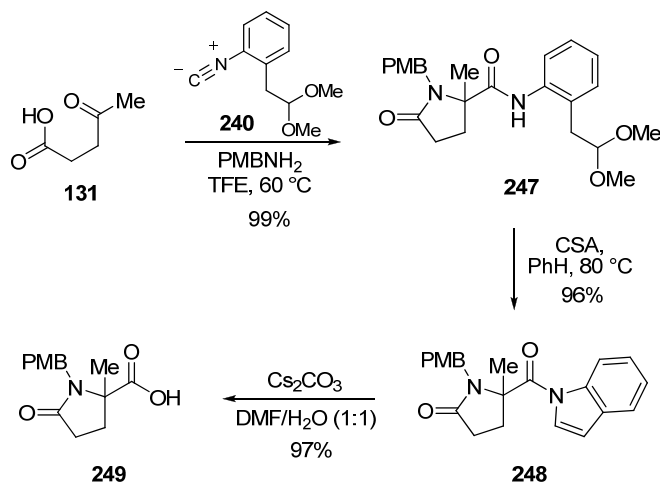


Scheme 3.1.1 Preparative Synthesis of Isocyanide **240**

3.1.2 Application as Convertible Isocyanide

3.1.2.1 Pyroglutamic Acid Synthesis

In order to quickly show the feasibility of using isocyanide (**240**), as a convertible isocyanide, for the preparation of pyroglutamic acids via the Ugi reaction, we sought to prepare pyroglutamic acid derivative **249** starting from commercially available levulinic acid (**131**, Scheme 3.1.2.1). The initial Ugi product anilide **247**, derived from levulinic acid (**131**), is readily converted to the corresponding pyroglutamic acid **249** via *N*-acylindole **248** under mild conditions. The *N*-acylindole **248** was formed by gentle heating (80 °C) of anilide **247** with CSA (0.5 equiv) in benzene, and hydrolyzed to pyroglutamic acid **249** under mildly basic conditions (Cs₂CO₃, DMF/H₂O, rt).

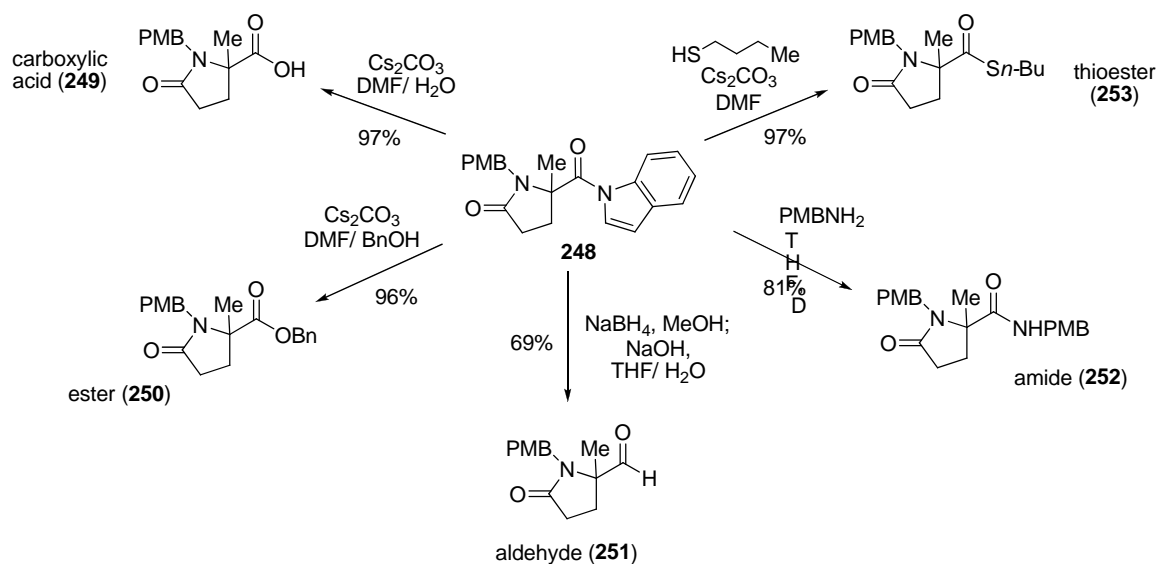


Scheme 3.1.2.1 Synthesis of Pyroglutamic Acid **249** with Convertible Isocyanide **240**

The privileged ability of the 2-(2,2-dimethoxyethyl)anilide **237**,⁵ originally demonstrated exclusively with unhindered substrates, had proven effective even with the hindered pyroglutamic acid amide. To our knowledge, this is the first demonstration of

the isocyanide in the Ugi reaction. The subsequent selective hydrolysis of the sterically more hindered *C*-terminal *exo*-amide proves the concept of **240** as a convertible isocyanide.

3.1.2.2 Pyroglutamic Acid Derivatives



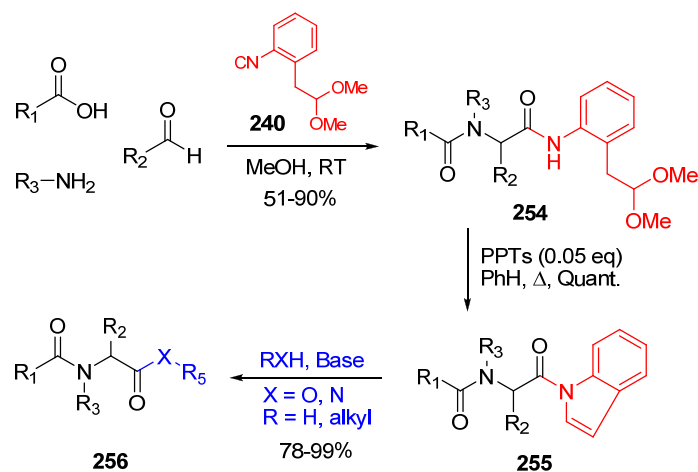
Scheme 3.1.2.2 Utility of *N*-Acylindole **248** as a Coupling Agent

By conversion of the pyroglutamic acid anilide to an *N*-acylindole, hydrolysis of the anilide was facilitated (see section 3.1.2.1). In addition, *N*-acylindole **248** may also be used as a coupling agent. Thus, the synthetic utility of the *N*-acylindole **248** was briefly explored. Conversion of **248** into the corresponding pyroglutamic acid (**249**, 97%), benzyl ester (**250**, 96%), aldehyde (**251**, 69%), *p*-methoxybenzyl amide (**252**, 81%), and *n*-butyl thioester (**253**, 97%) derivatives are described (Scheme 3.1.2.2).

Mildly basic conditions, Cs_2CO_3 combined with nucleophiles such as water, primary alcohols (1 equiv), and thiols (1 equiv), in DMF are enough to provide the corresponding carboxylic acid, ester, and thioester, respectively. An interesting two-step, one-pot, sequence converts the *N*-acylindole moiety directly into an aldehyde. Reduction of the *N*-acylindole with NaBH_4 provides an *N,O*-hemiacetal intermediate which is stable until treated with aqueous NaOH .⁵ Deprotonation to form the alkoxide of the hemiacetal hydroxyl group causes concurrent aldehyde formation and expulsion of indole. Overall a transamidation process, secondary amide formation occurred smoothly by heating *N*-acylindole **248** with a primary amine. Secondary alcohols (isopropanone) and amines (morpholine) failed to react presumably due to steric hindrance.

3.1.2.3 Linear Substrates

During the course of our studies, Wessjohann and co-workers published an extension of the utility of isocyanide **240**, expanding to the Ugi 4-component condensation reaction, Passerini reaction, and Ugi-Smiles reaction.⁶ Thus, isocyanide **240** underwent the U-4CR to afford linear Ugi adduct **254**, which was converted to *N*-acylindole **255** via activation with catalytic acid. Interestingly, *N*-acylindole **255** was stable and did not undergo azlactone formation (see section 2.3.2.1) which was possible under the acidic conditions employed. The *N*-acylindole **255** was then subject to base mediated hydrolysis to the corresponding carboxylic acid, ester, or amide (**256**, Scheme 3.1.2.3).



Scheme 3.1.2.3 Utility of Convertible Isocyanide **240** in the U-4CR by Wessjohann

3.2 Preliminary Studies

Having established isocyanide **240** as a convertible isocyanide, i.e. successful participation in the Ugi reaction of γ -ketoacids with a reasonable yield and the facile hydrolysis of the sterically hindered *exo*-amide, we chose to embark on a few preliminary studies to determine the feasibility of using β -hydroxy- γ -ketoacids in the Ugi reaction with isocyanide **240**.

Initially, we chose to synthesize β -hydroxy- γ -ketoacids **257-261** (Figure 3.2), in racemic form, to not only determine their general accessibility, but also their feasibility and resulting diastereoselectivity in the Ugi reaction with isocyanide **240**. β -Hydroxy- γ -ketoacids **257** and **261** were model studies for omuralide, whereas β -hydroxy- γ -ketoacids **258** and **260** were a model studies for α -methylomuralide (**58**) and *epi*-omuralide (see

section 3.4.1), respectively. Tertiary β -hydroxy- γ -ketoacid **259** represents a model study for salinosporamide A.

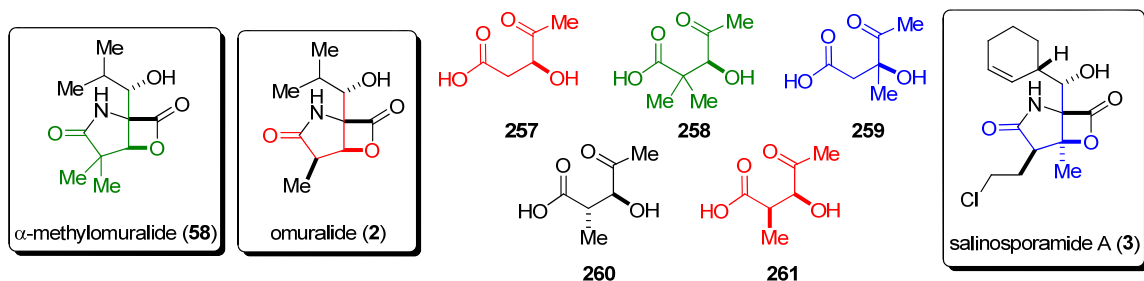
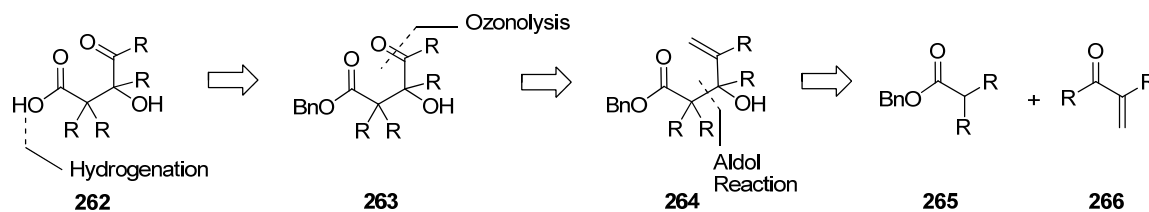


Figure 3.2 Structure of Model β -Hydroxy- γ -Ketoacids **257-261**

3.2.1 General Strategy Towards β -Hydroxy- γ -Ketoacids

We developed the following efficient and general strategy towards the synthesis of the β -hydroxy- γ -ketoacid motif **262** (Scheme 3.2.1). We planned to generate the carboxylic acid of **262** in the last step by hydrogenation of the corresponding benzyl ester **263**. Hydrogenolysis is known as both a mild and neutral reaction and as such the carboxylic acid could be generated without elimination of the hydroxyl group, as would be expected under common acidic or basic conditions. Next, we imagined the generation of the ketone in **263** by ozonolysis of the corresponding alkene in **264**. Lastly, we planned the construction of the carbon framework via an Aldol reaction between benzyl ester **265** and α,β -unsaturated aldehyde or ketone **266**. We synthesized β -hydroxy- γ -ketoacids **257-261** according to this general strategy. If desired, enantiomerically pure γ -

ketoacids could be generated via this strategy by employing a chiral auxillary in a stereoselective Aldol reaction.



Scheme 3.2.1 General Strategy towards the Synthesis of the β -Hydroxy- γ -Ketoacid Motif

3.2.2 Ugi Reaction of β -Hydroxy- γ -Ketoacids

With a convenient route to β -hydroxy- γ -ketoacids in hand, it was possible to investigate the key Ugi reaction with isocyanide **240**. Our concerns were a potential side reaction from the α -hydroxyimine, an intermediate in the Ugi reaction, known as Amadori rearrangement,⁷ in addition to the stereoselective outcome of the reaction.

The Ugi reaction of β -hydroxy- γ -ketoacid (**257a**), with isocyanide **240** and *p*-methoxybenzyl amine in 2,2,2-trifluoroethanol at rt, provided a 1:2 *syn/anti* diastereomeric mixture of Ugi product **B,C** in 65% yield (entry 1, Table 3.2.2). The assignment of the major and minor diastereomers, as *anti* and *syn* respectively, was done via ¹H-NMR spectroscopy through derivative formation.⁸ Although the resulting stereoselectivity in the Ugi reaction was modest and favoured the undesired stereoisomer,

we were encouraged to discover that unprotected β -hydroxy- γ -ketoacid **257a** did in fact provide the Ugi product in decent yield, which was unknown in the literature.

Table 3.2.2 The Ugi reaction of β -Hydroxy- γ -Ketoacids **257-261** with Convertible Isocyanide **240**

A $\xrightarrow[\text{TFE, rt}]{\text{PMBNH}_2}$ **B, Syn** + **C, Anti**

Entry	Substrates	syn:anti	Yield (%)		Entry	Substrates	syn:anti	Yield (%)
1		1:2	65%	4		-	-	0%
2		1:1	59%	5		1:3	74%	
3		3:2	73%	6		1:2	70%	

Protection of the hydroxyl group of **257a** as a bulky *tert*-butyldiphenylsilyl ether **257b** increased the amount of *syn*-isomer detected in the Ugi reaction, albeit only modestly, to 1:1 *syn/anti* (entry 2). Ugi reaction of α -dimethyl- β -hydroxy- γ -ketoacid **258** provided slightly more of the desired *syn*-isomer, affording a 3:2 *syn/anti* mixture (entry 3).

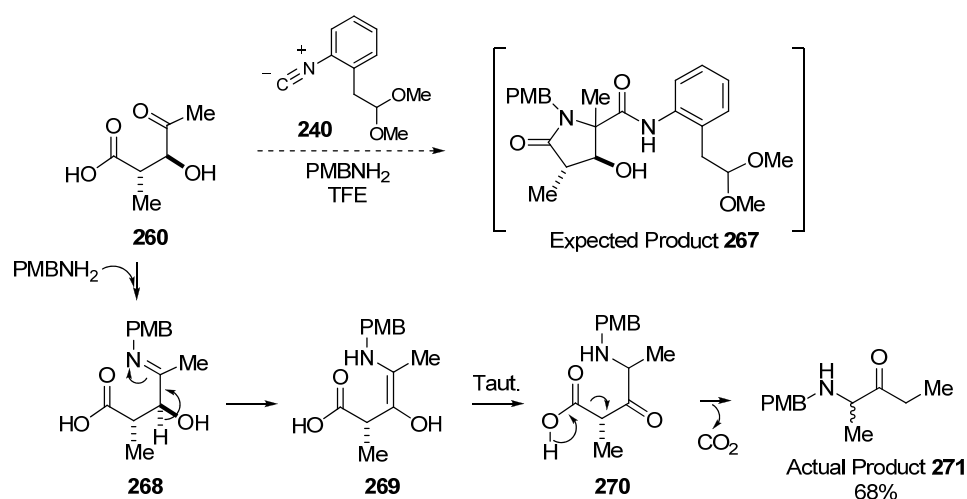
The results of the Ugi reaction of β -hydroxy- γ -ketoacids **260** and **261a**, which contain an additional and opposite chiral methyl substituent, provided an unexpected result. While γ -ketoacid **260** did not provide the Ugi product, and instead gave a side product without consumption of the isocyanide (entry 4, see section 3.2.2.1), its epimer **261a**, in stark contrast, provided a 1:3 *syn/anti* diastereomeric mixture of Ugi product **B,C** in 74% yield (entry 5). Again we attempted protection of the hydroxyl group of **261a**, in order to enhance the resulting diastereoselectivity of the Ugi reaction to favour the *syn* isomer. We synthesized MOM ether **261b**, and while we found an increase in the amount of *syn*-isomer detected in the Ugi reaction, unfortunately, the ratio shift was again only modest, giving a 1:2 *syn/anti* mixture (entry 6). In summary, the Ugi reaction of β -hydroxy- γ -ketoacids was generally feasible, proving good yields of the Ugi product. On the other hand, the stereoselectivity induced by chiral ketoacids was only modest.

3.2.2.1 The Amadori Rearrangement

β -Hydroxy- γ -ketoacid **260** when reacted with isocyanide **240** and *p*-methoxybenzyl amine in TFE at rt, unexpectedly, provided 2-(4-methoxybenzylamino)pentan-3-one (**271**) in 68% yield (Scheme 3.2.2.1). This product is the result of an Amadori rearrangement,⁷ which is known to take place from α -hydroxyimines, an intermediate in the Ugi reaction. Presumably, these two reactions compete, and interestingly, the Amadori rearrangement proved faster than the Ugi reaction on this substrate alone. Potentially any α -hydroxyimine might participate in the

Amadori rearrangement under the Ugi reaction conditions. The outcome probably depends on the conformation of the imine intermediate.

The mechanism of the Amadori rearrangement is thought to begin with imine **268** formation, followed by deprotonation to enamine **269** (presumably catalyzed by the internal acid), tautomerization to the α -aminoketone **270**, and lastly, decarboxylation affords **271**.



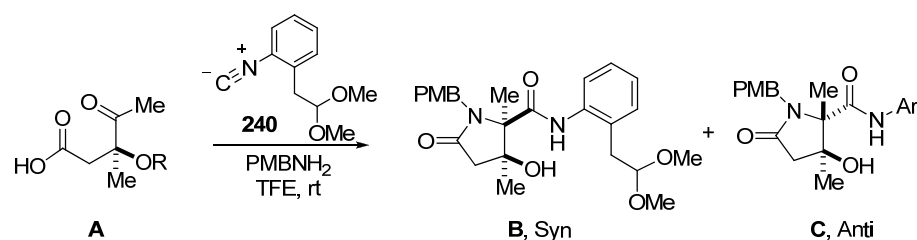
Scheme 3.2.2.1 The Amadori Rearrangement of β -Hydroxy- γ -Ketoacid **260**

3.2.3 Ugi Reaction of β -Hydroxy- β -Methyl- γ -Ketoacids

As a model study for salinosporamide A, the Ugi reaction of β -hydroxy- β -methyl- γ -ketoacid **259a** was investigated. The stereoselectivity of the Ugi reaction could be expected to change dramatically by addition of the β -methyl substituent. Reaction of **259a** with isocyanide **240** and *p*-methoxybenzyl amine in 2,2,2-trifluoroethanol, provided

a 1:2 *syn/anti* diastereomeric mixture of Ugi products **B,C** in 79% yield (entry 1, Table 3.2.3). Protection of the tertiary alcohol in **259a** as MOM ether **259b**, resulted in a slight increase in the amount of *syn*-isomer detected, providing a 1:1 *syn/anti* mixture (entry 2). Interestingly, protection as MTM ether **259c**, resulted in another slight increase in the amount of *syn*-isomer detected, giving a 2:1 *syn/anti* mixture (entry 3). We believe it likely that the improved *syn* selectivity, from entries 1 to 3, is the result of a greater facial bias, during the addition of the isocyanide, due to increased steric interactions and/or precoordination to the oxygen and sulfur atom of **259b** and **259c**, respectively.

Table 3.2.3 Ugi Reaction of β -Hydroxy- β -Methyl- γ -Ketoacids **259a-c** with Convertible Isocyanide **240**



Entry	Substrates	syn:anti	Yield (%)
1	 259a	1:2	79%
2	 259b	1:1	51%
3	 259c	2:1	47%

3.3 Stereocontrolled Formal Synthesis of Proteasome Inhibitor

Omuralide

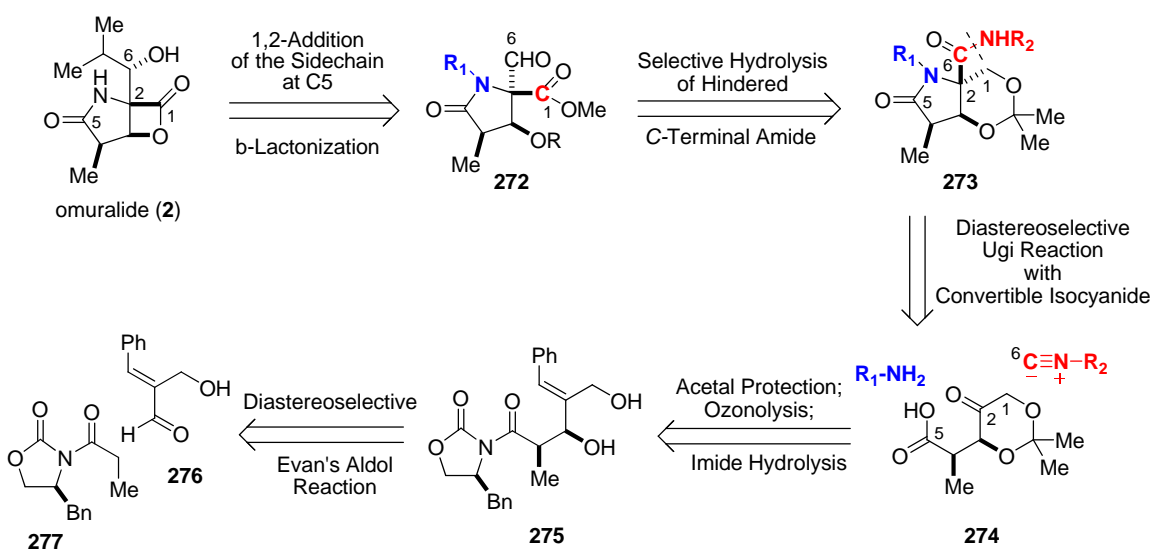
Having established the general viability of using isocyanide **240** in the Ugi reaction with simple β -hydroxy- γ -ketoacids, we undertook our original goal of applying **240** in a stereocontrolled synthesis of omuralide (**2**). The major remaining concern was the issue of stereocontrol in the Ugi reaction.

3.3.1 Retrosynthetic Analysis

Scheme 3.3.1 outlines our retrosynthetic plan for the stereocontrolled synthesis of omuralide (**2**). We imagined, in the late stage, 1,2-addition of the isopropyl side chain to an aldehyde intermediate **272** as well as the formation of the β -lactone ring.⁹ The pyroglutamic ester derivative **272** could then be obtained from the selective activation and methanolysis of the *exo*-amide in **273**. We envisioned utilizing the Ugi multi-component condensation reaction to diastereoselectively form the pyroglutamic acid amide ring of **273** from a densely functionalized cyclic γ -ketoacid **274** (see section 3.3.1.1). The design of the γ -ketoacid is crucial for a successful stereocontrolled Ugi reaction. Our strategy is described in the following section.

To obtain **274**, we again employed our general strategy towards the synthesis of β -hydroxy- γ -ketoacids, consisting of an Aldol condensation with an unsaturated

aldehyde, followed by ozonolysis. The unsaturated aldehyde is required for easy installation of the ketone moiety of the ketoacid via ozonolysis after the Aldol reaction. A modified version of a magnesium-catalyzed diastereoselective Evan's Aldol reaction¹⁰ would be used to access diol **275**. We chose to incorporate unprotected (*E*)-2-(hydroxymethyl)cinnamaldehyde (**276**) in the Aldol reaction in order to prevent possible δ -lactonization from **275**, which could occur under the acidic or basic conditions required for a deprotection step.

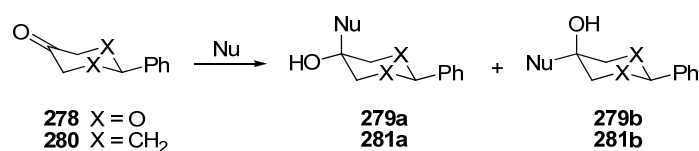


Scheme 3.3.1 Retrosynthetic Analysis for the Stereocontrolled Synthesis of Omuralide (**2**).

3.3.1.1 Nucleophilic Additions to 1,3-Dioxan-5-ones

Nucleophilic additions to 1,3-dioxan-5-ones, the heterocyclic system of γ -ketoacid **274**, had been previously investigated.¹¹ Jochims *et al* studied the reaction of 2-

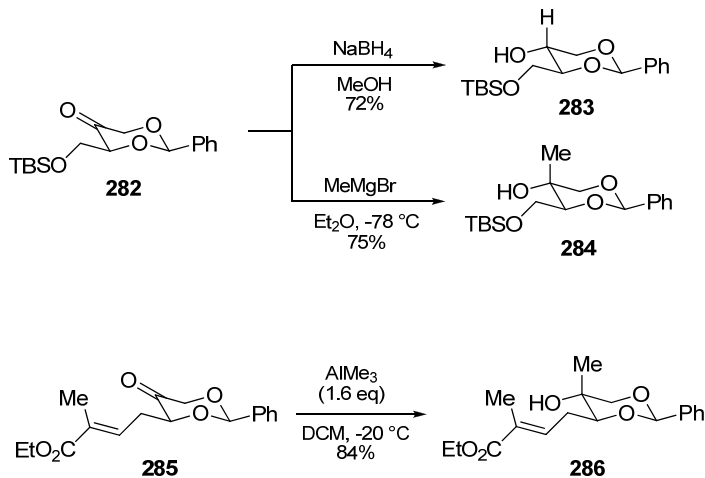
phenyl-1,3-dioxan-5-one (**278**) with LiAlH_4 and various Grignard reagents (Scheme 3.3.1.1a).¹² They found that acetal **278** underwent nucleophilic additions to the carbonyl group almost exclusively from the axial orientation, allowing the formation of equatorial alcohols **279a**. In contrast, it is noteworthy that nucleophilic addition to 4-phenylcyclohexanone (**280**), the carbocyclic analogue of **278**, showed much poorer selectivity, favoring axial attack with smaller nucleophiles and equatorial attack with larger nucleophiles. The authors explained these results on the basis of a competition between the steric hinderance to axial attack, imposed mainly by the axial substituents in the β -position (steric approach control), and the stereoelectronic barrier to the equatorial approach, due to the development of a torsional strain between the forming C-Nu bond and the C-H and C-C bonds proximal to the carbonyl group. For dioxanone **278**, axial attack is practically unhindered because of the absence of substituents in the β -position. Since the aforementioned torsional barrier is still present, this explains why **278** reacts with nucleophiles predominantly via axial attack.



Scheme 3.3.1.1a Nucleophilic Additions to 2-Phenyl-1,3-dioxan-5-one (**278**) and 4-Phenylcyclohexanone (**280**)

In agreement with this precedent, reduction of 1,3-dioxan-5-one **282** with NaBH_4 in MeOH yielded exclusively equatorial alcohol **283** (Scheme 3.3.1.1b). In like manner,

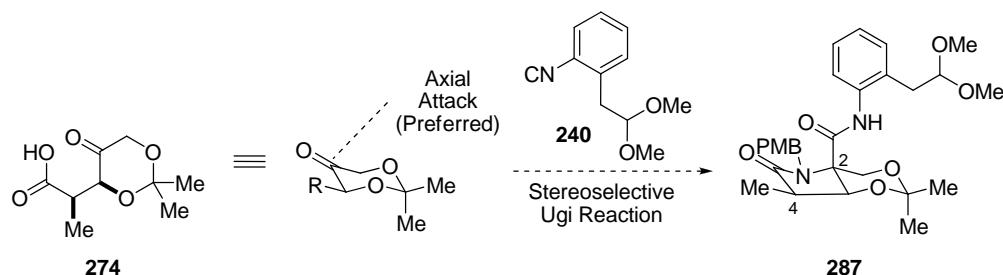
Grignard addition (MeMgBr , Et_2O , $-78\text{ }^\circ\text{C}$) to 1,3-dioxan-5-one **282** provided tertiary alcohol **284** in $>20:1$ selectivity.¹³ The chair conformation of the mono-substituted dioxanone is defined, because the substituent will prefer to reside in the equatorial position. Even though the addition of a α -hydroxymethyl substituent might have introduced a chelation point, the result is still consistent with favored axial attack. In addition, during his studies toward the synthesis of brevotoxin B, Nicolaou and coworkers reported a similar finding. They noted exclusive formation of tertiary alcohol **285** via axial directed methyl addition to 1,3-dioxan-5-one **286** with trimethylaluminum.¹⁴



Scheme 3.3.1.1b Nucleophilic Additions to Substituted 1,3-dioxan-5-ones **282** and **285**

Based on this precedent, we chose chiral γ -ketoacid **274** as the key ketoacid precursor to the Ugi reaction. We expected to observe selective axial attack of

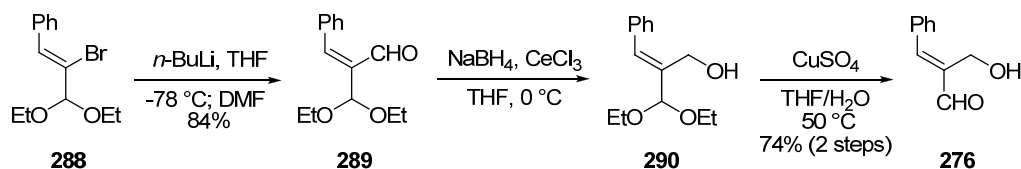
isocyanide **240** providing Ugi product **287** which contains the desired stereochemistry at C2 of proteasome inhibitor omuralide.



Scheme 3.3.1.1c Expected Stereochemical Outcome in the Ugi Reaction of γ -Ketoacid **274** with Convertible Isocyanide **240**

3.3.2 Synthesis of (*E*)-2-hydroxymethylcinnamaldehyde (**276**)

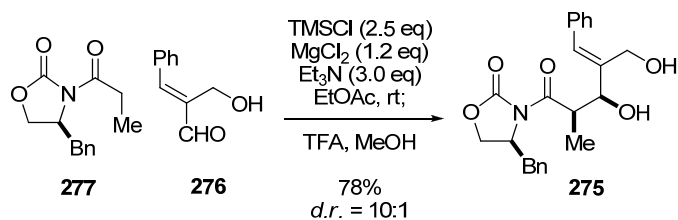
We targeted γ -ketoacid **274** as a key precursor for a stereocontrolled Ugi reaction generating the γ -lactam ring of omuralide (**2**). The first challenge was the synthesis of (*E*)-2-(hydroxymethyl)cinnamaldehyde (**276**) which was unknown in the literature. Thus, acetal **288**¹⁵ was subjected to lithium-halogen exchange with *n*-BuLi and then quenched with DMF to yield aldehyde **289** in 84% yield (Scheme 3.3.2). Reduction of the aldehyde occurred with NaBH₄ to give **290** under Luche conditions. Lastly, the mild Lewis acid mediated acetal deprotection of **290** provided aldehyde **276** in 74% over two steps. It should be noted that aldehyde **276** is a stable yellow solid that is amenable to storage at 0 °C without noticeable decomposition over at least several months.



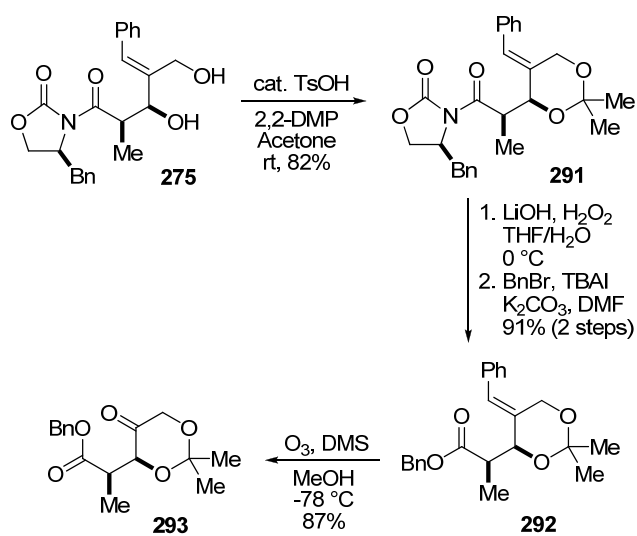
Scheme 3.3.2 Synthesis of (*E*)-2-(Hydroxymethyl)cinnamaldehyde (**276**)

3.3.3 Synthesis of γ -Ketoacid **274**

With the synthesis of (*E*)-2-(hydroxymethyl)cinnamaldehyde (**276**) complete, we set our attention to the synthesis of γ -ketoacid **274**. Due to the mild conditions of the Evans aldol reaction of acyloxazolidinones **277**,¹⁰ we believed it possible to use (*E*)-2-(hydroxymethyl)cinnamaldehyde (**276**) directly in the aldol reaction without protection of the primary alcohol in advance. By modifying the original reaction conditions to include an extra equivalent of TMSCl and Et₃N to protect the free alcohol of the unsaturated aldehyde *in situ*, as well as including an additional equivalent of MgCl₂, the aldol reaction proceeded smoothly to afford the resulting 1,3-diol adduct **275** in 78% yield as a 10:1 diastereomixture (Scheme 3.3.3a). The stereochemistry of the minor isomer is unknown. As we expected, δ -lactonization was prevented under the reaction conditions. The diol was protected as the acetonide to give **291** isolated in 82% yield as a single diastereomer (Scheme 3.3.3b). It was unambiguously assigned as the required aldol product **291** by X-ray crystallography (Figure 3.3.3), which is consistent with the literature.¹⁰ Lithium peroxide mediated hydrolysis of the chiral auxiliary and benzyl protection of the resultant carboxylic acid gave **292** in 91% yield. Ozonolysis of the *exo*-olefin provided γ -ketoester **293** in 87% yield.



Scheme 3.3.3a Evans Aldol Reaction incorporating (*E*)-2-(hydroxymethyl)cinnamaldehyde (**276**)



Scheme 3.3.3b Synthesis of γ -Ketoester **291**

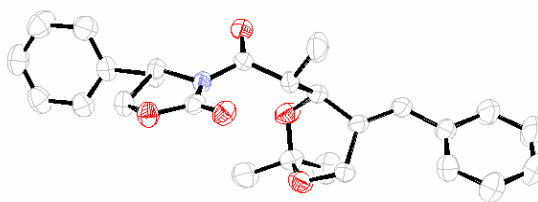
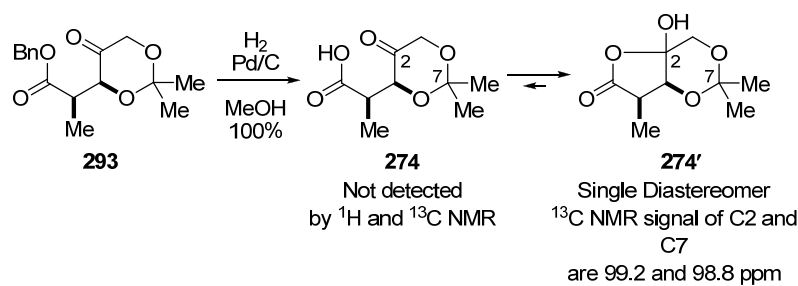


Figure 3.3.3 X-ray Crystal Structure of **291**

Hydrogenolysis of γ -ketoester **293** provided the Ugi precursor γ -ketoacid **274**, which was then subjected to the Ugi reaction with isocyanide **240** without purification. It should be noted that γ -ketoacid **274** exists as a single diastereomer of a hemiketal at C2 (**274'**). The ^{13}C NMR chemical shift of C2 clearly indicated the hemiketal carbon instead of an intact carbonyl group (Scheme 3.3.3c). Nevertheless, this γ -ketoacid could participate in the Ugi reaction due to the equilibrium between the keto- and hemiketal-form (see below).

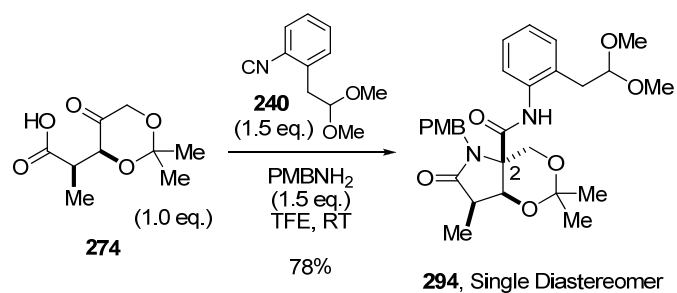


Scheme 3.3.3c Synthesis and Observed Structure of γ -Ketoacid **294**

3.3.4 Stereoselective Ugi Reaction of γ -Ketoacid **274**

Much to our delight, the Ugi reaction of ketoacid **274** with isocyanide **240** and *p*-methoxybenzylamine in 2,2,2-trifluoroethanol furnished γ -lactam **294** in 78% yield as a single diastereomer (Scheme 3.3.4). As expected, the product resulting from axial attack of the isocyanide was obtained. The relative stereochemistry of the resulting stereocenter, C2 of the Ugi product **294**, was unambiguously assigned by X-ray crystallography (Figure 3.3.4). Interestingly, the crystal structure revealed that the N-H

bond of the anilide is hydrogen bonded to one of the acetal oxygen atoms, corresponding to the primary alcohol. Unexpectedly, this hydrogen bond significantly weakened the stability of the acetal protecting group, leading to steady decomposition of **294** over time (monitored by ^1H NMR spectroscopy) to the corresponding free diol when dissolved and allowed to sit in deuterated chloroform at room temperature.



Scheme 3.3.4 Stereoselective Ugi Reaction of γ -Ketoacid **274** with Convertible Isocyanide **240**

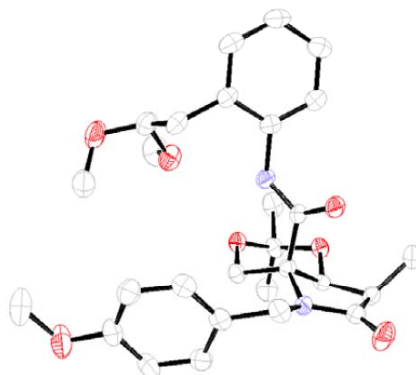


Figure 3.3.4 X-Ray Crystal Structure of **294**

3.3.4.1 Proposed Explanation of Diastereoselectivity

As we expected, the diastereoselectivity of the Ugi reaction of γ -ketoacid **274** with isocyanide **240** is consistent with the preference of nucleophiles to approach the carbonyl group of 1,3-dioxan-5-ones exclusively from the axial orientation. The chair conformation of the mono-substituted dioxanone imminium ion **295** is defined, because the substituent will prefer to reside in the equatorial position. Again, axial attack is almost completely unhindered, because of the absence of substituents in the β -position, whereas equatorial attack encounters torsional strain, due to the presence of the axial C-H bonds (Figure 3.3.4.1).

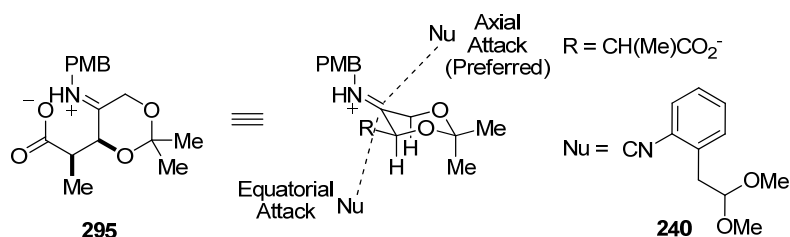
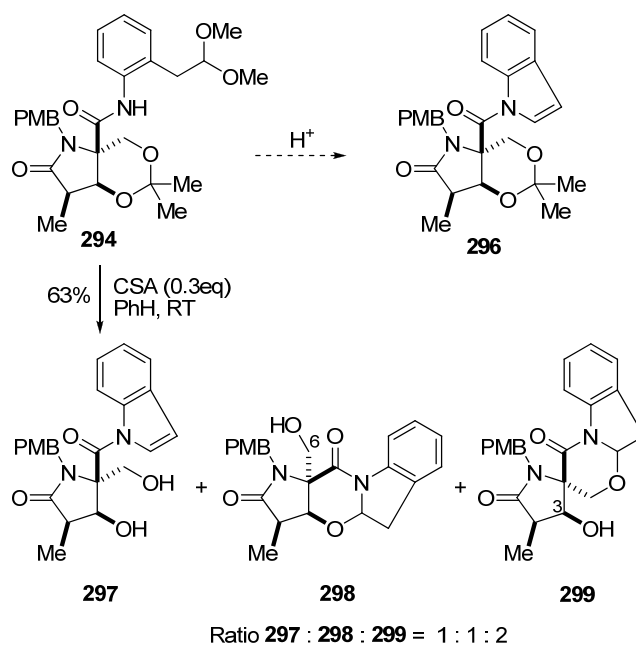


Figure 3.3.4.1 Explanation of Diastereoselectivity in the Ugi reaction of γ -ketoacid **274** with Convertible Isocyanide **240**

3.3.5 Failure of Indole Formation

Having established a synthesis of the γ -lactam ring of omuralide (**2**), with all three stereocenters of the ring set, we set out to selectively hydrolyze the *C*-terminal *exo*-amide bond of **294** via activation under acidic conditions to *N*-acylindole **296** (Scheme 3.3.5).

Unfortunately, deprotection of the acetonide protecting group proved much faster than *N*-acylindole formation. Treatment of **294** with a catalytic amount of CSA in benzene did not provide *N*-acylindole **296** as expected, but gave a 1:1:2 mixture of *N*-acylindole **297**, and *N,O*-acetals **298** and **299** as single diastereomers. *N,O*-Acetals **298** and **299** were assigned by ¹H-NMR spectroscopy based on the chemical shift of the C6 and C3 protons, after acetylation of the hydroxyl groups, which were 4.57 ppm and 5.08 ppm, respectively. The configuration of the newly formed *N,O*-acetal stereocenter in **298** and **299** was not determined, although they were single diastereomers.

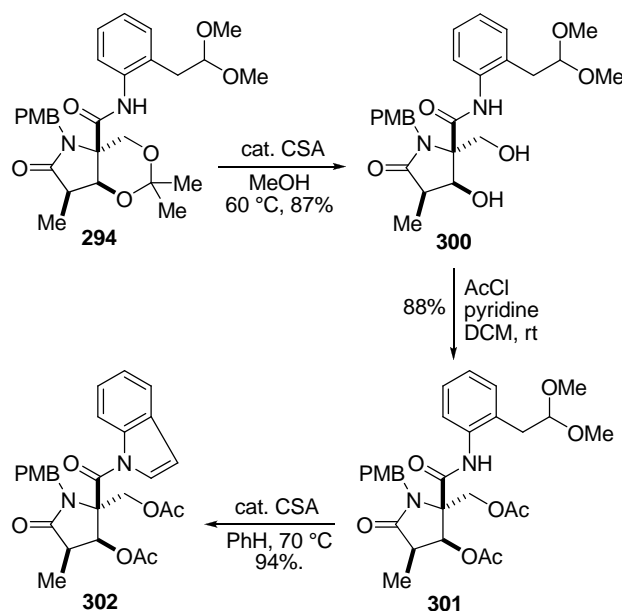


Scheme 3.3.5 Failure of *N*-Acylindole Formation from Ugi Anilide **294**

In addition, we could not find any conditions which would convert *N*-acylindole **297** into the corresponding β -lactone (with concurrent expulsion of indole) or to convert

N,O-acetals **298** and **299** back to *N*-acylindole **297**. It seems possible that the fused- and spiro-ring systems provide enhanced stability to the *N,O*-acetals.

3.3.6 Formation of *N*-Acylindole **302**

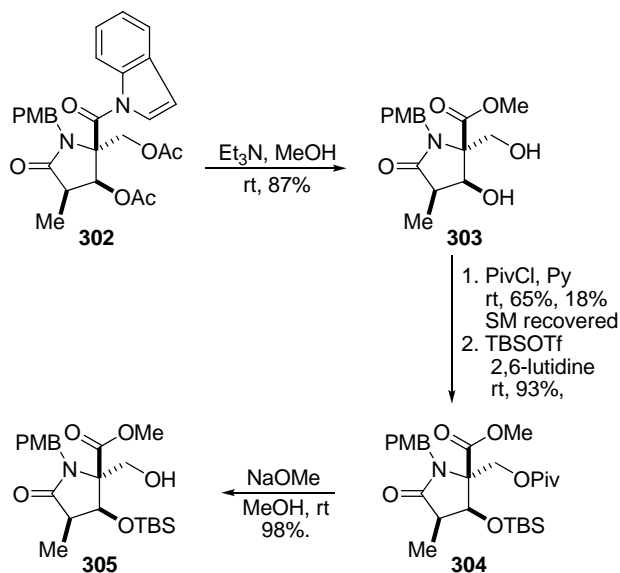


Scheme 3.3.6 Synthesis of *N*-Acylindole **302**

In order to circumvent undesired *N,O*-acetal formation, we decided to selectively remove the acetonide protecting group before forming the indole ring. Treatment of Ugi product **294** with a catalytic amount of CSA in MeOH furnished free diol **300** without deprotection of the methyl acetal or formation of the *N*-acylindole (Scheme 3.3.6). We chose MeOH as solvent for the reaction specifically to preserve the methyl acetal and thus prevent indole formation at this moment. Diol **300** was then protected as diacetate

301, which was stable under the acid catalyzed indole formation conditions that afforded the desired *N*-acylindole **302** without formation of side products.

3.3.7 Completion of Formal Synthesis of Omuralide



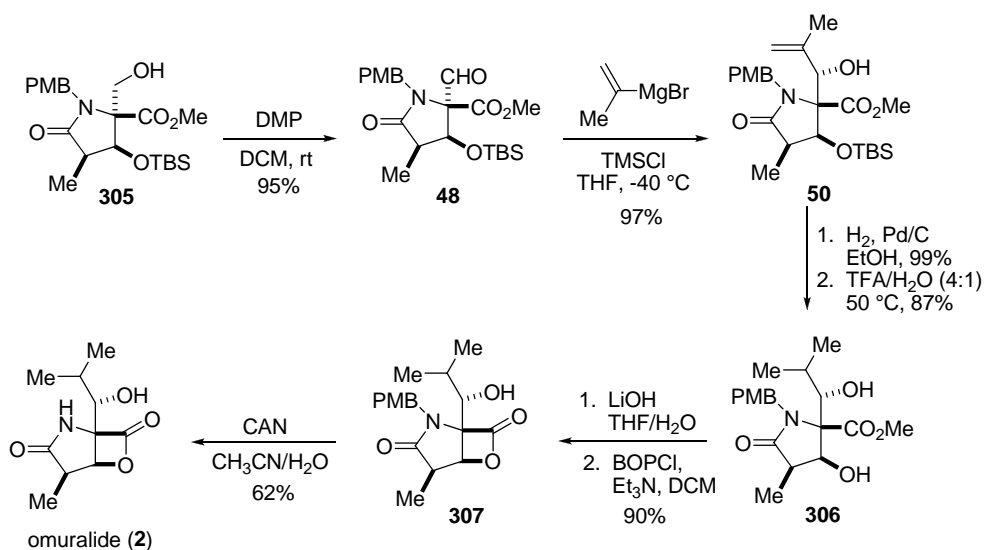
Scheme 3.3.7 Completion of the Formal Total Synthesis of Omuralide (2)

Direct conversion to the methyl ester diol **303**, via the methanolysis of the *N*-acylindole moiety and deprotection of both acetate esters, occurred in 87% yield by stirring in a 10:1 MeOH/Et₃N mixture overnight at room temperature (Scheme 3.3.7). The following sequence led to the completion of the formal total synthesis of omuralide: selective pivaloate formation of the primary alcohol of **303**, using excess pivoyl chloride and a catalytic amount of pyridine, subsequent TBS protection of the remaining secondary alcohol to form **304**, and NaOMe mediated removal of the pivaloate providing

305, which is an intermediate in Corey's total synthesis of omuralide (**2**, see section 1.4.2).⁹

In summary, our formal total synthesis of omuralide was 9.1% overall yield (15 steps) starting with known acetal (**288**). The key features of the synthesis include the development of 1-isocyano-2-(2,2-dimethoxyethyl)benzene (**240**) as a novel convertible isocyanide and its application in a stereocontrolled Ugi reaction.

3.3.8 Corey's Endgame



Scheme 3.3.8 Conversion of Common Intermediate **305** to Omuralide (**2**) reported by Corey

The conversion of common intermediate **305** to omuralide (**2**), reported by Corey,⁹ begins with an DMP oxidation to aldehyde **48** (95%) followed by addition of isopropenyl magnesium bromide, in the presence of TMSCl as a trapping reagent, to

yield adduct **50** (97%) as a single diastereomer (Scheme 3.3.8). Hydrogenolysis, followed by acid catalyzed desilylation, provided **306** in good yield. Saponification of methyl ester **306**, followed by treatment with BOPCl, provided β -lactone **307** in 90% yield. Lastly, CAN mediated oxidative deprotection of the PMB group (62%) provided omuralide (**2**).

3.4 Expanded Stereoselective Ugi Reaction of γ -Ketoacids

3.4.1 Objective

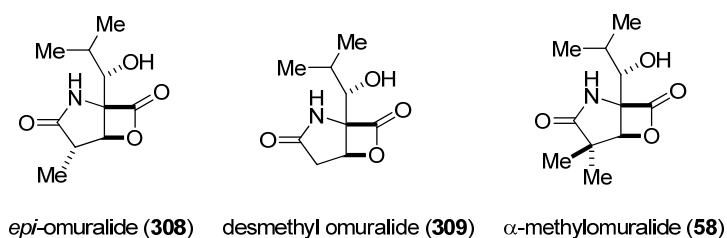


Figure 3.4.1a Structures of *epi*-Omuralide (**308**), desmethyl-Omuralide (**309**), and α -Methyl-Omuralide (**58**)

We now turned our attention to the stereocontrolled formal synthesis of *epi*-omuralide (**308**), desmethylomuralide (**309**), and α -methylomuralide (**58**, Figure 3.4.1a). In order to achieve this goal, we undertook the synthesis of γ -ketoacids **310-312** (Figure 3.4.1). We expected the formation of Ugi products **313-315**, respectively, because the

conformation of the dioxanone ring should be defined. Thus, the stereochemical output of the Ugi reaction should be unaffected by substituents in the α -position (on the side chain attached to the dioxanone ring system).

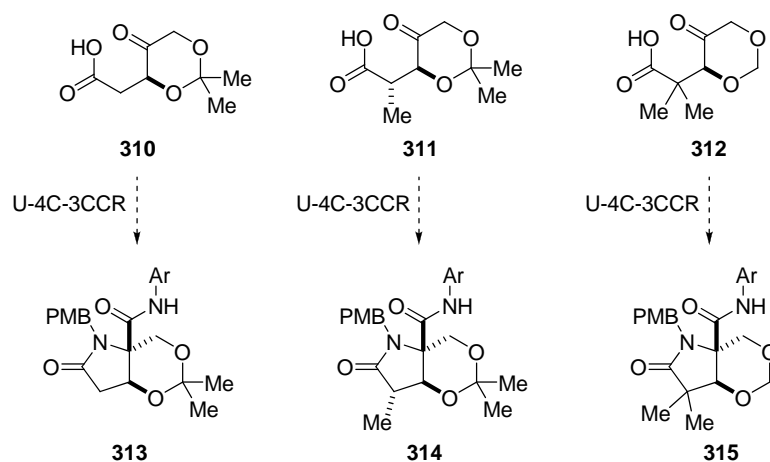
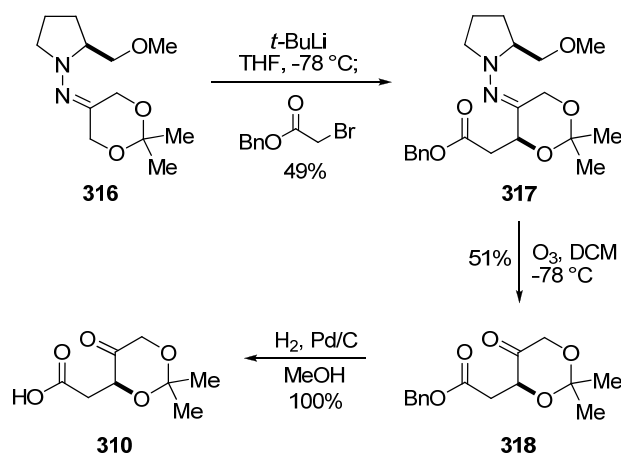


Figure 3.4.1 Structures of Targeted γ -Ketoacids **310-312** and Expected Stereochemical Output via U-4C-3CCR

3.4.2 Enantioselective Synthesis of γ -ketoacid **310**

We began with the enantioselective synthesis of γ -ketoacid **310**. Although the methyl, ethyl, and *tert*-butyl esters of carboxylic acid **310** were known in the literature,^{16,17} the conversion of those esters to **310** was unknown. In addition, our attempted base mediated hydrolysis of the methyl ester of **310** was unsuccessful, providing a complex mixture of products. Based on our previous results, we surmised that formation of the carboxylic acid in **310** would occur most efficiently from benzyl ester **318** due to the mild and neutral conditions of hydrogenolysis. In targeting γ -

ketoester **318**, we decided to utilize Evan's SAMP-hydrazone asymmetric alkylation protocol.^{16,18} Asymmetric α -alkylation of 2,2-dimethyl-1,3-dioxan-5-one-SAMP-hydrazone **316** with benzyl bromoacetate occurred via the aza-enolate, generated by deprotonation of **316** with *tert*-butyllithium at low temperature (Scheme 3.4.2). Hydrazone **317** was isolated as a single diastereomer. Oxidative cleavage of the C-N double bond of **317** with ozone¹⁹ provided γ -ketoester **318** which was then subjected to palladium mediated hydrogenolysis to yield γ -ketoacid **310**.

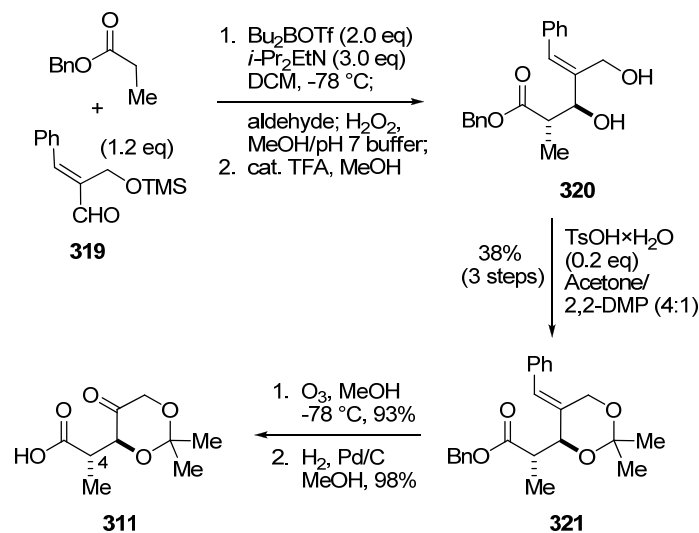


Scheme 3.4.2 Enantioselective Synthesis of γ -Ketoacid **310**

3.4.3 Racemic Synthesis of γ -ketoacid **311**

Next, we tackled the racemic synthesis of γ -ketoacid **311**, formally an epimer of γ -ketoacid **274** at C4. Our synthesis commenced with the boron-mediated *syn*-aldol reaction²⁰ of benzyl propionate and aldehyde **319** (Scheme 3.4.3). After deprotection of the TMS group, the resulting 1,3-diol was protected as an acetonide to give **321**.

Ozonolysis provided the corresponding β -hydroxy- γ -ketoester (not shown), and then γ -ketoacid **311** was formed via hydrogenolysis.

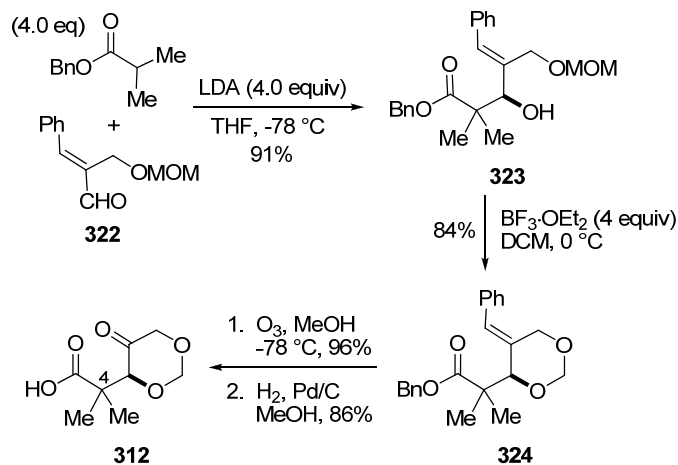


Scheme 3.4.3 Racemic Synthesis of γ -Ketoacid **311**

3.4.4 Racemic Synthesis of γ -ketoacid **312**

Lastly, the racemic synthesis of γ -ketoacid **312**, containing a *gem*-dimethyl substituent at C4, was also undertaken. Aldol reaction between benzyl isobutyrate and aldehyde **322** provided adduct **323** in 91% yield (Scheme 3.4.4). An excess of the enolate was required in the reaction to ensure a good yield. Due to the tendency of hindered aldol adducts containing *gem*-dimethyl substituents to undergo the facile retro-aldol reaction, the protection of the resultant secondary alcohol in **323** was performed immediately without unnecessary handling or storage. Acetal **324** was generated by intramolecular trapping of an oxonium ion, generated from the MOM-protected primary

alcohol, by the secondary alcohol of **323**, via a 6-*endo*-trig cyclization. This sequence, originally reported by Rychnovsky,²¹ was most successful when run very dilute with $\text{BF}_3 \cdot \text{OEt}_2$ as the lewis acid. Again, ozonolysis provided the corresponding β -hydroxy- γ -ketoester (not shown), and then the γ -ketoacid **312** was formed via hydrogenolysis.



Scheme 3.4.4 Racemic Synthesis of γ -Ketoacid **312**

3.4.5 Stereoselectivity in the Ugi Reaction

We then explored the Ugi reaction of cyclic β, δ -dihydroxy- γ -ketoacids **310-312** with isocyanide **240** and *p*-methoxybenzylamine in 2,2,2-trifluoroethanol at room temperature. (Table 3.4.5). In all cases, the Ugi products were obtained in good yield (72-80%) and with excellent diastereoselectivity (>10:1).

Table 3.4.5 Stereoselective Ugi reaction of β,δ -Dihydroxy- γ -Ketoacids **310-312**

Entry	Substrates	Products	dr	Yield (%)
1			>20 : 1	78
2			>20 : 1	80
3			10 : 1	72
4			>20 : 1	76

The relative stereochemistry of the Ugi product **314** obtained from cyclic β,δ -dihydroxy- γ -ketoacids **311** (entry 3) was unambiguously determined by X-ray crystallography (Figure 3.4.5). The relative stereochemistry of the new fully-substituted stereocenter (C2) remained the same, with respect to the C3, as mentioned previously (entry 1) suggesting that substituents at C4 do not affect the stereochemical output of the Ugi reaction. This result was expected because the presence or absence of a C4

substituent, in any orientation, should not affect the conformation of the dioxanone ring. The relative stereochemistry of Ugi products (**313** and **315**, entries 2,4) resulting from cyclic β,δ -dihydroxy- γ -ketoacids **310** and **312**, containing hydrogen and *gem*-dimethyl C4 substituents, respectively, was not determined, but was assumed based on comparison.

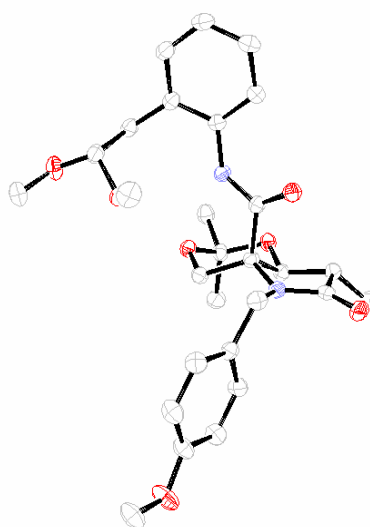


Figure 3.4.5 X-Ray Crystal Structure of **314**

3.5 Conclusions

In conclusion, a general and practical route to 2-alkylpyroglutamic acids via the U-4C-3CCR of γ -ketoacids was developed. 1-Isocyano-2-(2,2-dimethoxyethyl)benzene (**240**) was developed and applied as a novel convertible isocyanide that readily affords

pyroglutamic acid derivatives from pyroglutamic acid amides via selective C-terminal amide cleavage. The resultant Ugi product anilide, derived from the Ugi reaction of γ -ketoacids and isocyanide **240**, was converted to an activated *N*-acylindole, via treatment with catalytic acid, and then hydrolyzed under mildly basic conditions. The synthetic utility of the *N*-acylindole was extended to the synthesis of a pyroglutamic ester, thioester, aldehyde, and amide.

Having established isocyanide **240** as a convertible isocyanide, we chose to embark on a few preliminary studies to determine the general accessibility of β -hydroxy- γ -ketoacids, as well as their feasibility and resulting diastereoselectivity in the Ugi reaction with isocyanide **240**. Although the resulting stereoselectivity in the Ugi reaction was modest and typically favored the undesired *anti* stereoisomer, we were encouraged to discover that the majority of the unprotected β -hydroxy- γ -ketoacids did in fact provide the Ugi product in decent yield, which was unknown in the literature.

Then, having established the general viability of using isocyanide **240** in the Ugi reaction with simple β -hydroxy- γ -ketoacids, we undertook our original goal of applying **240** in a stereocontrolled synthesis of omuralide (**2**). The key step was a stereoselective Ugi reaction of a cyclic 1,3-dioxan-5-one containing γ -ketoacid with isocyanide **240**. Additionally, three related cyclic γ -ketoacids, variably substituted at C4, were synthesized and subjected to the Ugi reaction. The results showed that substitution at C4 does not affect the stereochemical output of the Ugi reaction and the Ugi product was universally obtained in good yield and excellent stereoselectivity.

Despite our successful development and incorporation of a stereoselective Ugi reaction in the formal total synthesis of omuralide (**2**), we still had several issues to

overcome in our synthesis. Those issues were incompatibility of the unprotected hydroxyl groups during *N*-acylindole formation and the unsuccessful β -lactone formation from the activated *N*-acylindole in the presence of the unprotected hydroxyl group.

3.6 Acknowledgments

CHAPTER THREE, in part, is a reprint of the material as it appears in (1) Gilley, C. B.; Buller, M. J.; Kobayashi, Y. "New Entry to Convertible Isocyanides for the Ugi Reaction and its Application to the Stereocontrolled Formal Total Synthesis of the Proteasome Inhibitor Omuralide" *Organic Letters* **2007**, *9*, 3631-3634. (2) Buller, M. J.; Gilley, C. B.; Nguyen, B.; Olshansky, L.; Fraga, B.; Kobayashi, Y. "Synthesis of Functionalized Pyroglutamic Acids. Part 1: The Synthetic Utility of *N*-Acylindole and the Ugi Reaction with a Chiral Levulinic Acid" *Synlett* (Manuscript in Revision) and (3) Gilley, C. B.; Buller, M. J.; Kobayashi, Y. "Synthesis of Functionalized Pyroglutamic Acids. Part 2: The Stereoselective Condensation of Multi-Functional Groups with Chiral Levulinic Acids" *Synlett* (Manuscript in Revision). The dissertation author was the primary or secondary investigator and author of this paper.

3.7 Experimental

3.7.1 Materials and Methods

All reagents were commercially obtained (Aldrich, Fisher) at highest commercial quality and used without further purification except where noted. Organic solutions were concentrated by rotary evaporation below 45 °C at approximately 20 mmHg. Tetrahydrofuran (THF), methanol (MeOH), chloroform (CHCl₃), dichloromethane (DCM), ethyl acetate (EtOAc), 2,2,2-trifluoroethanol (TFE), and acetone were reagent grade and used without further purification. Yields refer to chromatographically and spectroscopically (¹H NMR, ¹³C NMR) homogeneous materials, unless otherwise stated. Reactions were monitored by thin-layer chromatography (TLC) carried out on 0.25 mm E. Merck silica gel plates (60F-254) using UV light and cerium molybdate solution with heat as visualizing agents. E. Merck silica gel (60, particle size 0.040-0.063 mm) was used for flash chromatography. Preparative thin-layer chromatography separations were carried out on 0.50 mm E. Merck silica gel plates (60F-254). NMR spectra were recorded on Varian Mercury 300, 400 and/or Unity 500 MHz instruments and calibrated using the residual undeuterated solvent as an internal reference. Chemical shifts (δ) are reported in parts per million (ppm) and coupling constants (J) are reported in hertz (Hz). The following abbreviations were used to designate multiplicities: s= singlet, d= doublet, t= triplet, q= quartet, quint.= quintet, sp = septet, m= multiplet, br= broad. High resolution mass spectra (HRMS) were recorded on a Finnigan LCQDECA mass spectrometer under electrospray ionization (ESI) or atmospheric pressure chemical ionization (APCI) conditions, or on a Thermofinnigan Mat900XL mass spectrometer under electron impact (EI), chemical ionization (CI), or fast atom bombardment (FAB) conditions. X-ray data were recorded on a Bruker SMART APEX CCD X-ray

diffractometer. Specific optical rotations were recorded on a Jasco P-1010 polarimeter and the specific rotations were calculated based on the equation $[\alpha]_D^{25} = (100 \cdot \alpha) / (l \cdot c)$, where the concentration c is in g/100 mL and the path length l is in decimeters.

3.7.2 Preparative Procedures

(244). A solution of 2-nitrotoluene (**243**) (10.0 g, 73.0 mmol, 1.0 equiv), dimethylformamide diethylacetal (12.4 mL, 87.4 mmol, 1.2 equiv) and pyrrolidine (7.40 mL, 87.8 mmol, 1.2 equiv) in DMF (80 mL) was heated to 80 °C. After 24 h, H₂O (800 mL) was added and the mixture was extracted with EtOAc (5 x 200 mL), dried over Na₂SO₄, filtered, and concentrated *in vacuo*. The crude dark-red oil (**244**) was taken to the next reaction without further purification. R_f (20% EtOAc/ Hexanes) = 0.4. ¹H NMR (400 MHz, CDCl₃) δ : 7.82 (d, J = 8.4 Hz, 1H), 7.44 (d, J = 8.0 Hz, 1H), 7.29 (t, J = 6.8 Hz, 1H), 7.23 (d, J = 13.6 Hz, 1H), 6.92 (t, J = 7.2 Hz, 1H), 5.82 (d, J = 13.6 Hz, 1H), 3.31 (t, J = 6.8 Hz, 4H), 1.94 (t, J = 6.4 Hz, 4H). ¹³C NMR (100 MHz, CDCl₃) δ : 144.9, 140.7, 136.4, 132.6, 125.7, 124.2, 122.1, 91.4, 49.4, 25.5. HRMS (EI) m/z calcd for C₁₂H₁₄O₂N₂ (M⁺) 218.1050, found 218.1053.

(245). To a solution of **244** (15.9 g, 73.0 mmol, 1.0 equiv) in MeOH (150 mL) was added chlorotrimethylsilane (14.3 mL, 110 mmol, 1.5 equiv) over 5 min. The mixture was heated at reflux for 36 h, at which time it was concentrated *in vacuo*. The crude material was diluted with 5% aqueous citric acid (200 mL) and extracted with EtOAc (3 x 200 mL). The organic layer was then washed with saturated NaHCO₃, brine, dried over

Na₂SO₄, filtered, and concentrated *in vacuo* to yield **245** (14.8 g, 70.2 mmol, 96% over 2 steps) as a red oil. R_f (20% EtOAc/ Hexanes) = 0.5. ¹H NMR (400 MHz, CDCl₃) δ: 7.88 (d, J = 8.4 Hz, 1H), 7.52 (t, J = 8.0 Hz, 1H), 7.38 (m, 2H), 4.56 (t, J = 5.6 Hz, 1H), 3.34 (s, 6H), 3.21 (d, J = 5.6 Hz, 2H). ¹³C NMR (100 MHz, CDCl₃) δ: 150.2, 133.9, 133.0, 132.8, 131.9, 127.8, 124.7, 104.8, 54.5, 37.1. HRMS (EI) m/z calcd for C₁₀H₁₂O₄N₁ (M⁺) 210.0761, found 210.0765.

(237). To a solution of **245** (13.8 g, 65.3 mmol, 1.0 equiv) in MeOH (100 mL) was added Pd/C (3.47 g, 3.26 mmol, 0.05 equiv). A balloon of H₂ was applied for 2 d, then the mixture was filtered through celite and concentrated *in vacuo* to yield **237** (11.0 g, 60.8 mmol, 93%) as a yellow oil. R_f (20% EtOAc/ Hexanes) = 0.4. ¹H NMR (400 MHz, CDCl₃) δ: 7.04 (d, J = 7.6 Hz, 2H), 6.73 (t, J = 7.6 Hz, 1H), 6.68 (d, J = 8.0 Hz, 1H), 4.50 (t, J = 5.6 Hz, 1H), 3.37 (s, 6H), 2.87 (d, J = 5.2 Hz, 2H). ¹³C NMR (100 MHz, CDCl₃) δ: 146.2, 131.5, 127.9, 122.6, 118.9, 116.5, 106.8, 54.2, 36.7. HRMS (EI) m/z calcd for C₁₀H₁₅O₂N₁ (M⁺) 181.1097, found 181.1100.

(246). To a solution of **237** (11.3 g, 62.5 mmol, 1.0 equiv) and ethyl formate (7.80 mL, 93.7 mmol, 1.5 equiv) in THF (75 mL) at 0 °C was added 1 M LHMDS in PhMe (114 mL, 114 mmol, 1.8 equiv) . The mixture was warmed to 23 °C and stirred for 12 h at which time it was heated to reflux. After stirring at reflux for 18 h, saturated NH₄Cl was added and it was extracted with EtOAc (3 x 100 mL). The organic layer was dried over Na₂SO₄, filtered, and concentrated *in vacuo*. The resultant oil was purified by flash chromatography (EtOAc/ hexanes 20-50%) to yield **246** (12.4 g, 59.5 mmol, 95%) as a yellow oil. R_f (30% EtOAc/ Hexanes) = 0.3. ¹H NMR (400 MHz, CDCl₃) 8.71-8.75 (m,

1H), 8.41-8.49 (m, 1H), 7.09-7.29 (m, 4H), 4.46 (dd, $J = 10.8, 5.2$ Hz, 1H), 3.42 (s, 3H), 3.39 (s, 3H), 2.94 (d, $J = 5.6$ Hz, 1H), 2.92 (d, $J = 5.6$ Hz, 1H). ^{13}C NMR (100 MHz, CDCl_3) δ : 163.2, 159.5, 136.7, 132.1, 131.4, 129.1, 128.4, 127.9, 126.1, 125.5, 124.2, 121.5, 107.2, 106.4, 54.8, 54.3, 37.2, 36.7. HRMS (EI) m/z calcd for $\text{C}_{11}\text{H}_{15}\text{O}_3\text{N}_1$ (M^+) 209.1046, found 209.1050.

(Isocyanide, 240). To a solution of **246** (12.4 g, 59.5 mmol, 1.0 equiv) in DCM (150 mL) at 0 °C was added Et_3N (42.5 mL, 303 mmol, 5.1 equiv) followed by phosphorus oxychloride (8.60 mL, 91.1 mmol, 1.5 equiv). The mixture was warmed to 23 °C and stirred for 2 h, at which time it was poured into saturated NaHCO_3 (500 mL) and extracted with DCM (3 x 200 mL). The organic layer was dried over Na_2SO_4 , filtered, and concentrated *in vacuo*. The resultant oil was purified by flash chromatography (1:1 hexanes/DCM) to yield **240** (11.0 g, 57.3 mmol, 96%) as a red-brown oil. R_f (30% EtOAc/ Hexanes) = 0.8. ^1H NMR (400 MHz, CDCl_3) δ : 7.24-7.37 (m, 4H), 4.60 (t, $J = 5.2$ Hz, 1H), 3.37 (s, 6H), 3.07 (d, $J = 5.6$ Hz, 2H), ^{13}C NMR (100 MHz, CDCl_3) δ : 166.4, 133.8, 131.6, 129.5, 127.7, 127.0, 104.0, 54.2, 36.3. HRMS (EI) m/z calcd for $\text{C}_{11}\text{H}_{12}\text{O}_2\text{N}_1$ (M^+) 190.0863, found 191.0941, (M^+-H) 190.0863, found 191.0937.

(247). To a solution of levulinic acid (**131**) (133 mg, 1.15 mmol, 1.1 equiv) in TFE (3 mL) was added *p*-methoxybenzylamine (0.155 mL, 1.16 mmol, 1.1 equiv.) and isocyanide **240** (199 mg, 1.04 mmol, 1.0 equiv.). The reaction mixture was stirred at 60 °C for 5 h. The volatiles were removed *in vacuo* and the crude oil was purified by flash chromatography (EtOAc/ hexanes 40-100%) to yield Ugi product **247** (438 mg, 99%) as a pale yellow oil. R_f (50% EtOAc/ Hexanes) = 0.2. ^1H NMR (400 MHz, CDCl_3) δ : 8.90

(s, 1H), 7.62 (d, $J = 8.4$ Hz, 1H), 7.26-7.22 (m, 3H), 7.16 (d, $J = 6.8$ Hz, 1H), 7.09 (t, $J = 6.8$ Hz, 1H), 6.78 (d, $J = 8.4$ Hz, 2H), 4.96 (d, $J = 15.2$ Hz, 1H), 4.43 (t, $J = 5.2$ Hz, 1H), 4.08 (d, $J = 15.2$ Hz, 1H), 3.73 (s, 3H), 3.38 (s, 3H), 3.37 (s, 3H), 2.81 (d, $J = 5.6$ Hz, 2H), 2.67-2.60 (m, 1H), 2.57-2.49 (m, 1H), 2.45-2.39 (m, 1H), 2.03-1.95 (m, 1H), 1.42 (s, 3H); ^{13}C NMR (100 MHz, CDCl_3) δ : 175.8, 172.2, 159.1, 136.3, 131.3, 130.2, 129.7 (2C), 128.6, 127.7, 125.6, 124.7, 114.1, 106.8, 68.1, 55.4, 54.6, 54.5, 44.7, 37.1, 33.5, 29.8, 24.0; HRMS (EI) m/z calcd for $\text{C}_{24}\text{H}_{30}\text{O}_5\text{N}_2$ (M^+) 426.2149, found 426.2144.

(248). To a solution of **247** (563 mg, 1.32 mmol, 1.0 equiv) in benzene (5 mL) was added *dl*-camphorsulphonic acid (156 mg, 0.658 mmol, 0.5 equiv). The reaction mixture was stirred at 80 °C for 4 h, then allowed to cool and quenched with sat. NaHCO_3 (10 mL) and extracted with EtOAc (3 x 20 mL). The organic layer was dried over Na_2SO_4 , filtered, and concentrated *in vacuo*. The resultant oil was purified by flash chromatography (EtOAc/ hexanes 50%) to yield **248** (460 mg, 96%) as an off-white solid. R_f (50% EtOAc/ Hexanes) = 0.4. Mp = 100-102 °C. ^1H NMR (400 MHz, CDCl_3) δ : 8.40 (d, $J = 8.0$ Hz, 1H), 7.51 (d, $J = 7.2$ Hz, 1H), 7.35 (t, $J = 7.2$ Hz, 1H), 7.27 (t, $J = 7.6$ Hz, 1H), 7.21 (d, $J = 3.6$ Hz, 1H), 7.08 (d, $J = 8.4$ Hz, 1H), 6.54 (d, $J = 8.4$ Hz, 2H), 6.49 (d, $J = 4.0$ Hz, 1H), 4.59 (d, $J = 15.2$, 1H), 4.27 (d, $J = 15.6$ Hz, 1H), 3.59 (s, 3H), 2.73-2.66 (m, 3H), 2.21-2.16 (m, 1H), 1.60 (s, 3H); ^{13}C NMR (100 MHz, CDCl_3) δ : 174.9, 171.5, 159.1, 136.8, 130.2 (2C), 129.6, 128.7, 125.8, 124.5, 124.4, 120.9, 117.5, 113.9, 110.3, 69.2, 55.4, 45.1, 31.6, 29.2, 25.3; HRMS (EI) m/z calcd for $\text{C}_{22}\text{H}_{22}\text{O}_3\text{N}_2$ (M^+) 362.1625, found 362.1631.

(Pyroglutamic Acid, 249). To a solution of **248** (20 mg, 0.056 mmol, 1.0 equiv) in DMF (0.5 mL) and H₂O (0.5 mL) was added Cs₂CO₃ (18 mg, 0.056 mmol, 1.0 equiv). The reaction mixture was stirred at 23 °C for 5.5 h, then diluted with H₂O (5 mL), made basic with 1M NaOH, and extracted with EtOAc (2 x 10 mL). The aqueous layer was then made acidic with 1M HCl and extracted with EtOAc (2 x 10 mL). The combined organic layers were dried over Na₂SO₄, filtered, and concentrated *in vacuo* to yield pure **249** (14 mg, 97%) as a white solid. R_f (50% EtOAc/ Hexanes) = 0.05. Mp = 194-196 °C. ¹H NMR (400 MHz, (CD₃)₂SO) δ: 7.19 (d, J = 8.8 Hz, 2H), 6.83 (d, J = 8.8 Hz, 2H), 4.58 (d, J = 15.2 Hz, 1H), 3.95 (d, J = 15.2 Hz, 2H), 3.71 (s, 3H), 2.34-2.30 (m, 2H), 2.26-2.19 (m, 1H), 1.90-1.82, (m, 1H), 1.27 (s, 3H); ¹³C NMR (100 MHz, (CD₃)₂SO) δ: 176.1, 159.2, 131.6, 129.9, 114.6, 67.0, 56.0, 44.5, 32.8, 30.2, 24.1; HRMS (EI) m/z calcd for C₁₄H₁₇O₄N₁ (M⁺) 263.1152, found 263.1150.

(250). To a solution of **248** (100 mg, 0.276 mmol, 1.0 equiv.) in DMF (5.5 mL) was added benzyl alcohol (0.034 mL, 0.331 mmol, 1.2 equiv.) and Cs₂CO₃ (126 mg, 0.386 mmol, 1.4 equiv.). The reaction mixture was stirred at room temperature for 75 min, and then diluted with a saturated aqueous NH₄Cl solution and extracted with EtOAc. The combined organic layers were washed with brine, dried over Na₂SO₄, filtered, and concentrated *in vacuo*. The crude mixture was purified by flash column chromatography (1:2 Hex/EtOAc) to yield **250** as clear oil (94 mg, 96%). R_f (2:1 EtOAc/ Hexanes) = 0.53; ¹H NMR (300 MHz, CDCl₃) δ: 7.38-7.21 (m, 5H), 7.17 (d, J = 8.7 Hz, 2H), 6.77 (d, J = 9.0 Hz, 2H), 4.97 (d, J = 12.3 Hz, 1H), 4.73 (d, J = 12.3 Hz, 1H), 4.46 (d, J = 15.3, 1H), 4.31 (d, J = 15.6, 1H), 3.75 (s, 3H), 2.61-2.36 (m, 2H), 2.31-2.23 (m, 1H), 1.91-1.80

(m, 1H), 1.43 (s, 3H); ^{13}C (75 MHz, CDCl_3) δ : 176.0, 173.5, 159.1, 135.4, 129.9, 129.6, 128.9, 128.7, 128.2, 113.9, 67.4, 66.2, 55.5, 44.0, 32.3, 30.0, 23.4; HRMS (EI) m/z calcd for $\text{C}_{21}\text{H}_{23}\text{N}_1\text{O}_4$ (M^+) 353.1622, found 353.1618.

(251). To a solution of **248** (18 mg, 0.049 mmol, 1.0 equiv.) in MeOH (1 mL) was added sodium borohydride (2 mg, 0.049 mmol, 1.0 equiv.). The reaction mixture was stirred for 1 h, then quenched with acetone (1 mL) and concentrated *in vacuo*. The crude mixture was then dissolved in 1:1 THF/ H_2O (1 mL) and 1 M NaOH (0.050 mL, 0.050 mmol, 1.0 equiv.) was added. The mixture was stirred for 1 h, then diluted with H_2O and extracted with EtOAc. The combined organic layers were dried over Na_2SO_4 , filtered, and concentrated *in vacuo*. The crude mixture was purified by preparative thin-layer chromatography (1:5 Hex/EtOAc) to provide **251** as a clear oil (8 mg, 69%). R_f (2:1 EtOAc/Hexanes) = 0.17; ^1H NMR (300 MHz, CDCl_3) δ : 9.04, (s, 1H), 7.14 (d, J = 8.4 Hz, 2H), 6.78 (d, J = 8.7 Hz, 2H), 4.60 (d, J = 15 Hz, 1H), 4.13 (d, J = 14.7 Hz, 1H), 3.74 (s, 3H), 2.47 (t, J = 7.5 Hz, 2H), 2.16-2.07 (m, 1H), 1.77 (dt, J = 13.8, 8.7 Hz, 1H), 1.31 (s, 3H); ^{13}C (75 MHz, CDCl_3) δ : 199.4, 175.5, 159.4, 130.1, 129.4, 114.3, 69.7, 55.4, 43.6, 29.4, 28.3, 19.1; HRMS (EI) m/z calcd for $\text{C}_{14}\text{H}_{17}\text{N}_1\text{O}_3$ (M^+) 247.1203, found 247.1204.

(252). To a solution of **248** (18 mg, 0.050 mmol, 1.0 equiv.) in THF (3 mL) was added *p*-methoxybenzylamine (0.068 mL, 0.510 mmol, 10 equiv.). The reaction was heated to reflux and stirred for 15 h, and then concentrated *in vacuo*. The crude mixture was purified by preparative thin-layer chromatography (1:3 Hex/EtOAc) to furnish **252** as a

clear oil (15 mg, 81%). R_f (3:1 EtOAc/ Hexanes) = 0.22; ^1H NMR (300 MHz, CDCl_3) δ : 7.18 (d, J = 8.7 Hz, 2H), 6.99 (d, J = 8.4 Hz, 2H), 6.86-6.74 (m, 4H), 6.05 (bs, 1H), 4.36 (q, J = 13.8, 2H), 4.26 (dd, J = 14.4, 6.3 Hz, 1H), 3.91 (dd, J = 14.4, 5.1 Hz, 1H), 3.78 (s, 3H), 3.76 (s, 3H), 2.45-2.26 (m, 3H), 2.04-1.84 (m, 1H), 1.44 (s, 3H); ^{13}C (75 MHz, CDCl_3) δ : 176.5, 173.4, 159.2, 130.0, 129.8, 129.3, 114.4, 114.2, 67.9, 55.5, 55.4, 44.2, 43.6, 33.9, 29.7, 23.2; HRMS (EI) m/z calcd for $\text{C}_{22}\text{H}_{26}\text{N}_2\text{O}_4$ (M^+) 382.1887, found 382.1892.

(253). To a solution of **248** (100 mg, 0.276 mmol, 1.0 equiv.) in DMF (2 mL) was added 1-butanethiol (0.045 mL, 0.414 mmol, 1.5 equiv.) and Cs_2CO_3 (140 mg, 0.414 mmol, 1.5 equiv.). The reaction was stirred for 20 min, then diluted with saturated aqueous NH_4Cl and extracted with EtOAc. The combined organic layers were washed with brine, dried over Na_2SO_4 , filtered, and concentrated *in vacuo*. The crude mixture was purified by flash column chromatography (1:2 Hex/EtOAc) to afford **253** as clear oil (90 mg, 97%). R_f (3:1 EtOAc/ Hexanes) = 0.88; ^1H NMR (300 MHz, CDCl_3) δ : 7.20 (d, J = 8.4 Hz, 2H), 6.81 (d, J = 8.4 Hz, 2H), 4.96 (d, J = 15.3 Hz, 1H), 3.86 (d, J = 15.6 Hz, 1H), 3.77 (s, 3H), 2.85 (t, J = 6.6 Hz, 2H), 2.65-2.41 (m, 2H), 2.29-2.21 (m, 1H), 1.94-1.83 (m, 1H), 1.53 (p, J = 7.8 Hz, 2H), 1.39 (p, J = 7.2 Hz, 2H), 1.36 (s, 3H), 0.92 (t, J = 7.5 Hz, 3H); ^{13}C (75 MHz, CDCl_3) δ : 203.8, 176.4, 159.0, 130.4, 129.4, 114.0, 73.1, 55.5, 45.0, 33.2, 31.5, 29.6, 29.2, 23.7, 22.2, 13.8; HRMS (EI) m/z calcd for $\text{C}_{18}\text{H}_{25}\text{N}_1\text{O}_3\text{S}_1$ (M^+) 335.1550, found 335.1553.

(289)^X. To a solution of **288** (17.4 g, 60.9 mmol, 1.0 equiv.) in hexanes (170 mL) at -78 °C was added *n*-BuLi (67 mL, 1.0 M, 1.1 equiv.). The reaction mixture was stirred at -78 °C for 1h then warmed to -50 °C for 0.5h. After the mixture was recooled to -78 °C, DMF (8.9 g, 122 mmol, 2.0 equiv.) was added as a THF (30 mL) solution. After 0.5h of stirring, the reaction was quenched with sat. NH₄Cl and extracted with Et₂O. The organic layer was washed with brine, dried over Na₂SO₄, filtered, and concentrated in vacuo. The resultant oil was purified by flash chromatography (EtOAc/ hexanes 5-10%) to yield **289** as a light yellow oil (12.0 g, 84%). *R_f*(10% EtOAc/ Hexanes) = 0.5. ¹H NMR (500 MHz, CDCl₃) δ: 9.90 (s, 1H), 7.95 (s, 1H), 7.36-7.41 (m, 5H), 5.45 (s, 1H), 3.73 (quint., *J* = 7.2 Hz, 2H), 3.61 (quint., *J* = 6.8 Hz, 2H), 1.25 (t, 7.2 Hz, 6H). ¹³C NMR (100 MHz, CDCl₃) δ: 191.8, 146.4, 138.1, 133.6, 130.4, 129.9, 128.7, 97.8, 63.4, 15.5. HRMS (EI) *m/z* calcd for C₁₄H₁₈O₃ (M⁺) 234.1250, found 234.1253.

(290). To a solution of **289** (12.0 g, 51.2 mmol, 1.0 equiv.) in EtOH (180 mL) was added cerium trichloride heptahydrate (19.1 g, 51.3 mmol, 1.0 equiv.). Once the mixture reached homogeneity, the reaction mixture was cooled to 0 °C and sodium borohydride (1.94 g, 51.3 mmol, 1.0 equiv.) was added portionwise. The reaction temperature was kept below 10 °C during the addition. Once the reaction was complete by TLC, the reaction mixture was diluted with Et₂O and H₂O was carefully added to quench the reaction. The aqueous layer was extracted with Et₂O and washed with brine. The organic layer was dried over Na₂SO₄, filtered, and concentrated to yield a crude yellow oil (**290**) which was taken to the next step without further purification. *R_f*(20% EtOAc/

Hexanes) = 0.3. ^1H NMR (500 MHz, CDCl_3) δ : 7.28-7.42 (m, 5H), 6.74 (s, 1H), 4.95 (s, 1H), 4.30 (d, $J = 5.2$ Hz, 2H), 3.74 (quint., $J = 7.2$ Hz, 2H), 3.57 (quint., $J = 7.2$ Hz, 2H), 2.67 (t, $J = 5.6$ Hz, 1H), 1.27 (t, $J = 6.8$ Hz, 6H). ^{13}C NMR (100 MHz, CDCl_3) δ : 136.9, 135.9, 131.9, 129.3, 128.5, 127.9, 106.1, 63.0, 58.3, 15.4. HRMS (EI) m/z calcd for $\text{C}_{14}\text{H}_{20}\text{O}_3$ (M^+) 236.1407, found 236.1405.

(α -(hydroxymethyl)cinnamaldehyde, 276). To a solution of **290** (12.1 g, 51.0 mmol, 1.0 equiv.) in MeOH (100 mL) and H_2O (20 mL) was added copper sulfate pentahydrate (6.37 g, 25.5 mmol, 0.5 equiv.). The mixture was heated to 50 °C for 2h. The reaction mixture was diluted with Et_2O and washed with H_2O and then brine. The organic layer was dried over Na_2SO_4 , filtered, and concentrated to a yellow oil. The crude mixture was purified by flash chromatography (20-30% EtOAc/ Hexanes) to yield 6.10 g (74%, 2 steps) of **276** as a yellow solid. R_f (50% EtOAc/ Hexanes) = 0.4. Mp = 53-56 °C. ^1H NMR (500 MHz, CDCl_3) δ : 9.61 (s, 1H), 7.57-7.58 (m 2H), 7.45-7.48 (m, 4H), 4.55 (d, $J = 5.0$ Hz, 2H), 2.76 (t, $J = 6.0$ Hz, 1H). ^{13}C NMR (100 MHz, CDCl_3) δ : 196.0, 153.0, 140.3, 134.1, 130.7, 130.3, 129.1, 55.8. HRMS calcd for $\text{C}_{10}\text{H}_{10}\text{O}_2$ (M^+) 162.0675, found 162.0673.

(275). To a solution of propionamide **277^X** (6.24 g, 26.8 mmol, 1.0 equiv.) in EtOAc (125 mL) was added aldehyde **276** (4.91 g, 30.3 mmol, 1.13 equiv.), MgCl_2 (3.06 g, 32.1 mmol, 1.2 equiv.), Et_3N (11.2 mL, 80.4 mmol, 3.0 equiv.), and TMSCl (8.5 mL, 67.2 mmol, 2.5 equiv.). After being stirred at 23 °C overnight, the mixture was pushed through a plug of SiO_2 with Et_2O . Removal of the volatiles *in vacuo* provided an oil

which was diluted with MeOH (50 mL). Trifluoroacetic acid (5 drops) was added and the reaction mixture was stirred for 10 min. The volatiles were evaporated and the crude residue was purified by flash chromatography (EtOAc/ hexanes 30 to 75%) to yield 8.27 g (78%) of **275** (10:1 mixture of inseparable diastereomers) as a clear viscous oil. Major Diastereomer: $R_f(30\% \text{ EtOAc/ Hexanes}) = 0.3$. $^1\text{H NMR}$ (500 MHz, CDCl_3) δ : 7.23-7.39 (m, 10H), 6.72 (s, 1H), 4.71-4.74 (m, 1H), 4.41-4.54 (m, 4H), 4.15-4.22 (m, 2H), 3.35 (dd, $J = 2.5, 13.0$ Hz, 1H), 2.75 (dd, $J = 9.5, 13.5$ Hz, 1H), 1.20 (d, $J = 7.0$ Hz, 3H). $^{13}\text{C NMR}$ (100 MHz, CDCl_3) δ : 176.7, 154.0, 138.7, 136.0, 135.6, 132.8, 129.7, 129.2, 128.6, 127.8, 127.5, 81.1, 66.3, 59.2, 56.0, 41.5, 37.9, 15.2. HRMS calcd for $\text{C}_{23}\text{H}_{25}\text{O}_5\text{N}_1$ (M^+) 395.1727, found 395.1734. $[\alpha]_D^{25} +5.95$ ($c = 0.021$ g/mL, CHCl_3).

(291). To a solution of aldol adduct **275** (252 mg, 0.640 mmol, 1.0 equiv.) in acetone (8 mL) and DMP (1 mL) at 23 °C was added a catalytic amount of *p*-toluenesulfonic acid monohydrate. After the reaction was complete by TLC, the residue was diluted with EtOAc and washed with saturated NaHCO_3 and brine. The organic layer was dried over Na_2SO_4 , filtered, and concentrated to yield a pale yellow oil. Flash chromatography (EtOAc/ Hexanes 10-20%) gave 229 mg (82%) of pure **291** as a white solid which was a single diastereomer. $R_f(30\% \text{ EtOAc/ Hexanes}) = 0.6$. Mp = 121-122 °C. $^1\text{H NMR}$ (500 MHz, CDCl_3) δ : 7.25-7.38 (m, 8H), 7.17 (d, $J = 7.5$ Hz, 2H), 6.48 (s, 1H), 4.68-4.79 (m, 4H), 4.54-4.60 (m, 1H), 4.14-4.21 (m, 2H), 3.39 (dd, $J = 2.5, 13.0$ Hz, 1H), 2.67 (dd, $J = 10.5, 13.5$ Hz, 1H), 1.39 (s, 3H), 1.37 (s, 3H), 1.21 (d, $J = 7.0$ Hz, 3H). $^{13}\text{C NMR}$ (100 MHz, CDCl_3) δ : 176.0, 153.4, 135.9, 135.7, 135.6, 129.7, 129.2, 129.1, 128.7, 127.6,

127.5, 126.3, 99.8, 78.3, 66.1, 61.6, 55.7, 42.1, 38.2, 28.9, 24.5, 15.0. HRMS calcd for $C_{26}H_{29}O_5N_1$ (M^+) 435.2040, found 435.2025. $[\alpha]_D^{25} +60.4$ ($c = 0.022$ g/mL, $CHCl_3$).

(292). To a solution of **291** (157.2 mg, 0.361 mmol, 1.0 equiv.) in THF/ H_2O (4:1, 7 mL) at 0 °C was added 30% H_2O_2 solution in H_2O (0.33 mL, 2.91 mmol, 8.0 equiv.) and then $LiOH \cdot H_2O$ (30 mg, 0.715 mmol, 2.0 equiv.). After 30 min., the reaction mixture was warmed to 23 °C and stirred for 3h. The THF was removed *in vacuo* and the H_2O was removed on the freeze pump overnight. The foamy lithium salt was dissolved in DMF (2 mL) and benzyl bromide (0.052 mL, 0.437 mmol, 1.2 equiv.), catalytic tetrabutylammonium iodide as well as excess K_2CO_3 were added. After stirring at 23 °C for 2h, the reaction mixture was diluted with EtOAc and washed with H_2O , and brine. The organic layer was dried over Na_2SO_4 , filtered and concentrated to yield a pale yellow oil. Flash chromatography (EtOAc/ hexanes 5%) gave 120 mg (91%) of pure **292** as a clear oil which crystallized slowly at room temperature. R_f (30% EtOAc/ Hexanes) = 0.8. $M_p = 45-47$ °C. 1H NMR (500 MHz, $CDCl_3$) δ : 7.23-7.38 (m, 8H), 7.07 (d, $J = 7.0$ Hz, 2H), 6.36 (s, 1H), 5.24 (d, $J = 12.0$ Hz, 1H), 5.14 (d, $J = 12.5$ Hz, 1H), 4.63 (s, 2H), 4.55 (d, $J = 7.5$ Hz, 1H), 3.15 (sp, $J = 8.0$ Hz, 1H), 1.36 (s, 3H), 1.30 (s, 3H), 1.22 (d, $J = 7.0$ Hz, 3H). ^{13}C NMR (100 MHz, $CDCl_3$) δ : 174.8, 136.3, 136.0, 135.9, 129.0, 128.7, 128.6, 128.5, 128.4, 127.5, 125.7, 99.9, 77.6, 66.5, 61.6, 45.0, 28.2, 24.5, 14.5. HRMS calcd for $C_{23}H_{26}O_4$ (M^+) 366.1826, found 366.1823. $[\alpha]_D^{25} +61.2$ ($c = 0.029$ g/mL, $CHCl_3$).

(293). To a solution of benzylidene **292** (448 mg, 1.22 mmol, 1.0 equiv.) in MeOH (30 mL) was added a small amount of Sudan III indicator. The reaction mixture was cooled to -78 °C, and ozone was bubbled in until the pink color disappeared. The reaction mixture was flushed with N₂ gas and methyl sulfide (0.45 mL, 6.13 mmol, 5.0 equiv.) was added. After allowing the reaction to warm to 23 °C, the volatiles were removed *in vacuo*. The crude mixture was subjected directly to flash chromatography (EtOAc/hexanes 10%) to yield 310 mg (87%) of **293** as a clear oil. $R_f(30\% \text{ EtOAc/ Hexanes}) = 0.7$. ¹H NMR (400 MHz, CDCl₃) δ: 7.32-7.36 (m, 5H), 5.21 (d, $J = 12.8$ Hz, 1H), 5.04 (d, $J = 12.0$ Hz, 1H), 4.30 (dd, $J = 1.6, 4.8$ Hz, 1H), 4.11 (dd, $J = 1.2, 16.4$ Hz, 1H), 3.90 (d, $J = 16.8$ Hz, 1H), 3.17 (dq, $J = 4.8, 7.2$ Hz, 1H), 1.37 (s, 3H), 1.32 (d, $J = 6.8$ Hz, 3H), 1.32 (s, 3H). ¹³C NMR (100 MHz, CDCl₃) δ: 207.6, 172.3, 135.8, 128.7, 128.5, 128.4, 101.1, 76.5, 67.0, 66.9, 40.5, 24.4, 23.6, 13.6. HRMS calcd for C₁₆H₂₀O₅ (M⁺) 292.1305, found 292.1309. $[\alpha]_D^{25} -106.1$ ($c = 0.023$ g/mL, CHCl₃).

(274). To a solution of ketoester **293** (307 mg, 1.05 mmol, 1.0 equiv.) in MeOH (20 mL) was added ~10% by weight activated Pd/C. A balloon of H₂ was applied for 5h. After flushing the solution with N₂, the reaction mixture was filtered over celite and concentrated to yield 224 mg (100%) of pure ketoacid **274** as a white solid which was used without further purification. $R_f(30\% \text{ EtOAc/ Hexanes}) = 0.05$. Mp = 129-130 °C. ¹H NMR (300 MHz, CDCl₃) δ: 4.20 (d, $J = 4.5$ Hz, 1H), 4.02 (d, $J = 12.5$ Hz, 1H), 3.93 (d, $J = 12.9$ Hz, 1H), 3.11 (dq, $J = 4.5, 6.5$ Hz, 1H), 1.47 (s, 3H), 1.35 (s, 3H), 1.16 (d, $J = 7.2$ Hz, 3H). ¹³C NMR (100 MHz, CDCl₃) δ: 179.6, 99.2, 98.8, 72.9, 64.5, 39.0, 27.4,

20.2, 7.4 HRMS calcd for $C_9H_{13}O_5$ (M-H)⁺ = 201.0758, found 201.0753. $[\alpha]_D^{25}$ -1.71 (c = 0.025 g/mL, $CHCl_3$).

(294). To a solution of ketoacid **274** (313 mg, 1.55 mmol, 1.0 equiv.) in TFE (5 mL) was added *p*-methoxybenzylamine (320 mg, 2.33 mmol, 1.5 equiv.) and isocyanide **240** (440 mg, 2.30 mmol, 1.5 equiv.). After stirring at 23 °C overnight, the volatiles were removed *in vacuo*. Flash chromatography (EtOAc/ hexanes 30-50%) gave 618 mg (78%) of γ -lactam **294** as a foamy white solid which was a single diastereomer. R_f (50% EtOAc/ Hexanes) = 0.3. Mp = 148-150 °C. ¹H NMR (500 MHz, $CDCl_3$) δ : 9.34 (s, 1H), 7.65 (d, J = 8.0 Hz, 1H), 7.26 (m, 2H), 7.17 (m, 3H), 6.83 (d, J = 8.0 Hz, 2H), 5.08 (d, J = 14.5 Hz, 1H), 4.48 (t, J = 5.0 Hz, 1H), 4.42 (d, J = 8.5 Hz, 1H), 3.81 (d, J = 8.0 Hz, 1H), 3.79 (s, 3H), 3.77 (d, J = 4.2 Hz, 1H), 3.63 (d, J = 11.5 Hz, 1H), 3.31 (s, 3H), 3.29 (s, 3H), 2.90 (d, J = 6.0 Hz, 2H), 2.82 (sp, J = 8.0 Hz, 1H), 1.53 (s, 5H), 1.30 (d, J = 8.0 Hz, 3H). ¹³C NMR (100 MHz, $CDCl_3$) δ : 177.6, 169.7, 159.5, 136.3, 131.0, 130.4, 130.4, 129.7, 127.6, 126.3, 126.0, 114.3, 105.8, 103.2, 76.0, 69.6, 64.9, 55.5, 54.5, 53.8, 45.5, 38.9, 36.0, 29.5, 19.6, 9.9. HRMS calcd for $C_{28}H_{36}O_7N_2$ (M⁺) 512.2517, found 512.2521. $[\alpha]_D^{25}$ +40.5 (c = 0.013 g/mL, $CHCl_3$).

(300). To a solution of **294** (596 mg, 1.16 mmol, 1.0 equiv.) in MeOH (12 mL) was added *dl*-camphorsulphonic acid (27mg, 0.116 mmol, 0.1 equiv.). The reaction mixture was heated to 60 °C for 3h, then diluted with EtOAc and washed with saturated $NaHCO_3$ and brine. The organic layer was dried over Na_2SO_4 , filtered, and concentrated to an oil. Flash chromatography (EtOAc/ hexanes 50-75%) afforded 480 mg (87%) of pure **300** as

a foamy white solid. R_f (75% EtOAc/ Hexanes) = 0.3. Mp = 55-58 °C. ^1H NMR (500 MHz, CDCl_3) δ : 9.22 (s, 1H), 7.69 (d, J = 8.0 Hz, 1H), 7.28 (m, 3H), 7.19 (d, J = 7.0 Hz, 1H), 7.15 (t, J = 7.5 Hz, 1H), 6.82 (d, J = 8.5 Hz, 2H), 5.33 (d, J = 14.5 Hz, 1H), 4.60 (d, J = 7.5 Hz, 1H), 4.45 (t, J = 5.5 Hz, 1H), 3.95 (d, J = 15.0 Hz, 1H), 3.83 (d, J = 12.5 Hz, 1H), 3.78 (s, 3H), 3.73 (s, 3H), 3.34 (s, 3H), 3.31 (d, J = 12.5 Hz, 1H), 3.01 (dd, J = 5.5, 14.0 Hz, 1H), 2.80 (sp, J = 7.0 Hz, 1H), 2.77 (d, J = 5.5, 14.5 Hz, 1H), 1.24 (d, J = 7.0 Hz, 3H). ^{13}C NMR (100 MHz, CDCl_3) δ : 178.0, 170.0, 159.5, 135.9, 131.6, 130.1, 130.0, 129.4, 127.6, 126.0, 124.7, 114.5, 106.1, 75.2, 71.2, 64.3, 55.5, 54.8, 53.6, 45.4, 40.5, 36.5, 9.2 HRMS calcd for $\text{C}_{25}\text{H}_{32}\text{O}_7\text{N}_2$ (M^+) 472.2204, found 472.2201. $[\alpha]_D^{25} +5.30$ (c = 0.027 g/mL, CHCl_3).

(301). Diol **300** (437 mg, 0.925 mmol, 1.0 equiv.) was dissolved in pyridine (5 mL) and acetic anhydride (2 mL). The reaction mixture was stirred at 23 °C for 1h. After the volatiles were removed *in vacuo*, the crude product was then diluted with EtOAc and washed with sat. NH_4Cl , sat. NaHCO_3 , and brine. The organic layer was dried over Na_2SO_4 , filtered and concentrated to an oil. Flash chromatography (EtOAc/ hexanes 75%) afforded 452 mg (88%) of diacetate **301** as a clear viscous oil. R_f (75% EtOAc/ Hexanes) = 0.6. ^1H NMR (500 MHz, CDCl_3) δ : 9.23 (s, 1H), 7.78 (d, J = 8.0 Hz, 1H), 7.30 (t, J = 8.0 Hz, 1H), 7.26 (d, J = 8.0 Hz, 2H), 7.22 (d, J = 8.0 Hz, 1H), 7.15 (t, J = 7.5 Hz, 1H), 6.77 (d, J = 8.5 Hz, 2H), 5.64 (d, J = 8.0 Hz, 1H), 5.41 (d, J = 15.0 Hz, 1H), 4.51 (d, J = 12.0 Hz, 1H), 4.48 (d, J = 5.0 Hz, 1H), 4.20 (d, J = 12.5 Hz, 1H), 3.98 (d, J = 14.5 Hz, 1H), 3.76 (s, 3H), 3.43 (s, 3H), 3.40 (s, 3H), 2.99 (sp, J = 8.0 Hz, 1H), 2.96 (d, J = 5.5 Hz, 1H), 1.99 (s, 3H), 1.71 (s, 3H), 1.22 (d, J = 7.0 Hz, 3H). ^{13}C NMR (100

MHz, CDCl₃) δ : 177.1, 169.7, 169.5, 165.8, 159.5, 136.1, 131.6, 130.1, 129.2, 128.5, 128.0, 125.9, 124.1, 114.1, 106.7, 73.1, 72.8, 64.9, 55.5, 54.9, 54.4, 45.9, 39.7, 37.1, 20.8, 20.6, 9.9 HRMS calcd for C₂₉H₃₆O₉N₂ (M⁺) 556.2415, found 556.2409. $[\alpha]_D^{25} +30.8$ ($c = 0.024$ g/mL, CHCl₃).

(302). To a solution of diacetate **301** (445 mg, 0.799 mmol, 1.0 equiv.) in benzene (15 mL) was added *dl*-camphorsulphonic acid (37 mg, 0.159 mmol, 0.2 equiv.) at 23 °C. The reaction mixture was heated to 70 °C for 2h. When the reaction was complete by TLC, the solution was then concentrated and the crude product was purified by flash chromatography (EtOAc/ hexanes 75%) to afford 370 mg (94%) of *N*-acylindole **302** as a foamy white solid. R_f (75% EtOAc/ Hexanes) = 0.7. Mp = 62-65 °C. ¹H NMR (500 MHz, CDCl₃) δ : 8.40 (d, $J = 8.5$ Hz, 1H), 7.55 (d, $J = 8.0$ Hz, 1H), 7.38 (t, $J = 8.0$ Hz, 1H), 7.32 (t, $J = 7.5$ Hz, 1H), 7.28 (d, $J = 4.0$ Hz, 1H), 7.08 (br d, $J = 5.5$ Hz, 2H), 6.65 (br d, $J = 6.5$ Hz, 2H), 6.57 (s, 1H), 5.73 (br d, $J = 5.5$ Hz, 1H), 4.90 (br d, $J = 13.5$ Hz, 1H), 4.64 (d, $J = 12.5$ Hz, 1H), 4.34 (d, $J = 12.0$ Hz, 1H), 3.67 (s, 3H), 3.08 (sp, $J = 7.5$ Hz, 1H), 1.85 (s, 3H), 1.61 (br s, 3H), 1.28 (d, $J = 7.0$ Hz, 1H). ¹³C NMR (100 MHz, CDCl₃) δ : 176.7, 169.4, 169.4, 166.8, 159.5, 136.6, 130.3, 129.6, 127.7, 125.9, 125.7, 124.9, 121.1, 117.2, 114.0, 110.4, 73.7, 65.8, 55.4, 45.8, 39.8, 20.8, 20.2, 9.5 HRMS calcd for C₂₇H₂₈O₇N₂ (M⁺) 492.1891, found 492.1897. $[\alpha]_D^{25} -23.2$ ($c = 0.029$ g/mL, CHCl₃).

(303). A solution of *N*-acylindole **302** (367 mg, 0.742 mmol, 1.0 equiv.) in MeOH (15 mL) and triethylamine (1.5 mL) was stirred at 23 °C overnight. The reaction mixture was

then concentrated and the crude product was purified by flash chromatography (EtOAc 100%) to afford 209 mg (87%) of diol **303** as a clear oil. $R_f(75\% \text{ EtOAc/ Hexanes}) = 0.1$. $^1\text{H NMR}$ (500 MHz, CDCl_3) δ : 7.25 (d, $J = 8.5$ Hz, 2H), 6.82 (d, $J = 8.5$ Hz, 2H), 4.99 (d, $J = 15.0$ Hz, 1H), 4.50 (d, $J = 8.0$ Hz, 1H), 4.04 (d, $J = 15.5$ Hz, 1H), 3.88 (d, $J = 12.0$ Hz, 1H), 3.78 (s, 3H), 3.70 (s, 3H), 3.53 (d, $J = 12.5$ Hz, 1H), 2.83 (sp, $J = 7.5$ Hz, 1H), 1.23 (d, $J = 8.0$ Hz, 3H). $^{13}\text{C NMR}$ (100 MHz, CDCl_3) δ : 178.3, 170.9, 159.3, 129.9, 129.6, 114.4, 75.7, 71.4, 63.1, 55.5, 52.6, 44.6, 40.7, 9.7. HRMS calcd for $\text{C}_{16}\text{H}_{21}\text{O}_6\text{N}_1$ (M^+) 323.1363, found 323.1361. $[\alpha]_D^{25} -19.7$ ($c = 0.067$ g/mL, CHCl_3).

(303a). A solution of diol **303** (201 mg, 0.622 mmol, 1.0 equiv.) was dissolved in trimethylacetyl chloride (3 mL) and pyridine (0.1 mL). After being stirred at 23 °C overnight, the reaction mixture was diluted with EtOAc and filtered through a cotton plug. After concentration, the crude product was purified by flash chromatography (EtOAc/ hexanes 50-75%) to afford 164 mg (65%) of pivoylate **303a** (not shown in text) as a clear oil. $R_f(75\% \text{ EtOAc/ Hexanes}) = 0.8$. $^1\text{H NMR}$ (500 MHz, CDCl_3) δ : 7.19 (d, $J = 8.5$ Hz, 2H), 6.78 (d, $J = 8.5$ Hz, 2H), 4.57 (d, $J = 15.5$ Hz, 1H), 4.41 (m, 3H), 4.29 (d, $J = 12.5$ Hz, 1H), 3.76 (s, 3H), 3.60 (s, 3H), 2.80 (sp, $J = 7.5$ Hz, 1H), 1.26 (d, $J = 7.5$ Hz, 3H), 1.09 (s, 9H). $^{13}\text{C NMR}$ (100 MHz, CDCl_3) δ : 177.8, 177.4, 169.5, 159.1, 130.0, 129.0, 114.0, 74.0, 71.5, 63.7, 55.4, 52.7, 44.9, 40.5, 38.9, 27.2, 9.7. HRMS calcd for $\text{C}_{21}\text{H}_{29}\text{O}_7\text{N}_1$ (M^+) 407.1939, found 407.1942. $[\alpha]_D^{25} +1.73$ ($c = 0.022$ g/mL, CHCl_3).

(304). A solution of pivoylate **303a** (159 mg, 0.390 mmol, 1.0 equiv.) was dissolved in TBSOTf (3 mL) and 2,6-lutidine (0.4 mL). After being stirred at 23 °C for 2 h, the

reaction mixture was diluted with EtOAc and washed with sat. NH₄Cl, sat. NaHCO₃, and brine. The organic layer was dried over Na₂SO₄, filtered, and concentrated. The crude product was then purified by flash chromatography (EtOAc/ hexanes 30%) to afford 189 mg (93%) of **304** as a clear oil. R_f (50% EtOAc/ Hexanes) = 0.7. ¹H NMR (500 MHz, CDCl₃) δ : 7.20 (d, J = 9.0 Hz, 2H), 6.77 (d, J = 8.5 Hz, 2H), 4.52 (d, J = 13.0 Hz, 1H), 4.48 (d, J = 9.5 Hz, 1H), 4.45 (d, J = 15.5 Hz, 1H), 4.41 (d, J = 13.0 Hz, 1H), 4.25 (d, J = 15.0 Hz, 1H), 3.75 (s, 3H), 3.42 (s, 3H), 2.68 (sp, J = 8.5 Hz, 1H), 1.22 (d, J = 8.0 Hz, 3H), 1.09 (s, 9H), 0.85 (s, 9H), 0.05 (s, 3H), 0.04 (s, 3H). ¹³C NMR (100 MHz, CDCl₃) δ : 177.7, 177.5, 169.4, 159.2, 130.5, 128.7, 113.9, 73.3, 70.3, 61.1, 55.4, 52.2, 44.3, 40.8, 39.0, 27.2, 25.8, 18.1, 11.4, -4.6, -5.0 HRMS calcd for C₂₇H₄₃O₇N₁Si₁ (M⁺) 521.2803, found 521.2812. $[\alpha]_D^{25}$ +34.4 (c = 0.028 g/mL, CHCl₃).

(305). To a solution of **304** (181 mg, 0.346 mmol, 1.0 equiv.) in MeOH (4 mL) at 23 °C was added NaOMe (187 mg, 3.46 mmol, 10 equiv.) portionwise until reaction was complete by TLC. The reaction mixture was then diluted with EtOAc and washed with sat. NH₄Cl and brine. The organic layer was dried over Na₂SO₄, filtered, and concentrated. The crude product was then purified by flash chromatography (EtOAc/ hexanes 30-50%) to afford 148 mg (98%) of **305** as a clear oil. R_f (50% EtOAc/ Hexanes) = 0.5. ¹H NMR (500 MHz, CDCl₃) δ : 7.28 (d, J = 9.0 Hz, 2H), 6.84 (d, J = 8.5 Hz, 2H), 5.00 (d, J = 15.0 Hz, 1H), 4.55 (d, J = 9.0 Hz, 1H), 3.83 (d, J = 13.0 Hz, 1H), 3.88 (d, J = 15.0 Hz, 1H), 3.88 (s, 3H), 3.73 (d, J = 12.0 Hz, 1H), 3.63 (s, 3H), 2.70 (sp, J = 8.5 Hz, 1H), 1.22 (d, J = 8.0 Hz, 3H), 0.87 (s, 9H), 0.07 (s, 3H), 0.06 (s, 3H). ¹³C NMR (100 MHz, CDCl₃) δ : 178.3, 170.6, 159.4, 129.9, 129.7, 114.5, 75.7, 70.0,

61.5, 55.5, 52.3, 44.4, 40.9, 25.9, 18.1, 11.4, -4.6, -4.9. HRMS calcd for C₂₂H₃₅O₆N₁Si₁ (M⁺) 437.2228, found 437.2234. [α]_D²⁵ -4.43 (*c* = 0.028 g/mL, CHCl₃).

(317). To a solution of (S)-1-(2,2-dimethyl-1,3-dioxan-5-ylideneamino)-2-methoxymethylpyrrolidine **316** (278 mg, 1.15 mmol, 1.0 equiv., **SI-7**) in THF (4 mL) at -78 °C under N₂ was added *tert*-butyllithium (1.5M solution in pentane, 1.0 mL, 1.3 equiv.) dropwise. The solution was stirred at -78 °C for 2h and then benzyl bromoacetate (0.29 mL, 1.82 mmol, 1.6 equiv.) was added in one portion and stirring was continued at -78 °C for 1h. After warming to room temperature slowly over 3h, the solution was partitioned between Et₂O (30 mL) and a pH-7 phosphate buffer (10 mL). The organic layer was further washed with brine, dried over Na₂SO₄, filtered, and concentrated *in vacuo* to yield a crude oil which existed as a mixture of the *E* and *Z* isomers of the hydrazone. The mixture was then isomerized to yield the *E* hydrazone exclusively by heating the crude oil neat at 50 °C for 10 min. Flash column chromatography with SiO₂ (20-30% EtOAc/ pentane) provided 220 mg (49%) of **317** as a clear oil isolated as a single diastereomer. R_f(30% EtOAc/ Hexanes) = 0.47; ¹H NMR (500 MHz, CDCl₃) δ: 7.30-7.38 (m, 5H), 5.16 (d, *J* = 12.5 Hz, 1H), 5.13 (d, *J* = 12.0 Hz, 1H), 4.86-4.88 (m, 1H), 4.70 (d, *J* = 6.0 Hz, 2H), 4.45 (d, *J* = 15.5 Hz, 1H), 4.17 (dd, *J* = 1.0 Hz, *J* = 15.5 Hz, 1H), 3.33 (s, 3H), 3.19-3.27 (m, 1H), 3.01-3.06 (m, 2H), 2.56 (dd, *J* = 9.0 Hz, *J* = 17.0 Hz, 1H), 2.38(dd, *J* = 9.0 Hz, *J* = 16.5 Hz, 1H), 1.93-1.98 (m, 1H), 1.78-1.84 (m, 2H), 1.61-1.67 (m, 1H), 1.36 (s, 6H). ¹³C (100 MHz, CDCl₃) δ: 171.3, 160.0, 141.2, 136.2, 128.8, 128.7, 128.5, 128.4, 127.8, 127.2, 101.0, 75.7, 67.8, 67.0,

66.5, 65.5, 60.0, 59.4, 55.7, 37.7, 26.9, 24.1, 24.0, 23.0. HRMS (EI) m/z calcd for $C_{21}H_{30}N_2O_5$ (M^+) 390.2149, found 390.2151.

(318). Ozone was bubbled in to a solution of **317** (150 mg, 0.384 mmol, 1.0 equiv.) in DCM (8 mL) at -78 °C until a blue color appeared in the solution. The solution was then flushed with N_2 and warmed to room temperature. The mixture was concentrated *in vacuo* to yield a crude oil which was purified by flash column chromatography with SiO_2 (10-20% EtOAc/ hexanes) to yield 55 mg (51%) of **318** as a clear oil. R_f (30% EtOAc/ Hexanes) = 0.55; 1H NMR (500 MHz, $CDCl_3$) δ : 7.26-7.37 (m, 5H), 5.16 (d, $J = 12.5$ Hz, 1H), 5.14 (d, $J = 12.5$ Hz, 1H), 4.72 (ddd, $J = 1.5$ Hz, $J = 4.0$ Hz, $J = 8.0$ Hz, 1H), 4.30 (dd, $J = 1.5$ Hz, $J = 17.0$ Hz, 1H), 4.03 14 (d, $J = 17.0$ Hz, 1H), 2.94 (dd, $J = 3.5$ Hz, $J = 16.5$ Hz, 1H), 2.66 (dd, $J = 7.5$ Hz, $J = 16.5$ Hz, 1H), 1.44 (s, 3H), 1.40 (s, 3H). ^{13}C (100 MHz, $CDCl_3$) δ : 208.3, 170.3, 135.8, 128.8, 128.6, 128.5, 101.4, 71.8, 66.9, 66.7, 34.5, 23.9, 23.7. HRMS (EI) m/z calcd for $C_{15}H_{18}O_5$ (M^+) 278.1149, found 278.1152.

(310). To a solution of **318** (42.0 mg, 0.151 mmol, 1.0 equiv) in methanol (5 mL) was added a catalytic amount of Palladium 10 wt.% on activated carbon and reaction mixture was stirred under a balloon of H_2 for 1h. The reaction mixture was then filtered through celite and concentrated *in vacuo* to yield **310** (28.3 mg, 100%) as a viscous white foam. The crude material was used in the next reaction without further purification. R_f (30% EtOAc/ Hexanes) = 0.07; 1H NMR (500 MHz, $CDCl_3$) δ : 5.37 (br s, 1H), 4.53 (br s, 1H), 4.17 (d, $J = 15.0$ Hz, 1H), 3.98 (d, $J = 15.0$ Hz, 1H), 2.77 (dd, $J = 5.0$ Hz, $J = 17.0$ Hz,

1H), 1.48 (s, 3H), 1.39 (s, 3H). HRMS (EI) m/z calcd for $C_8H_{12}O_5$ (M^+) 188.0679, found 188.0682.

(313). To a solution of **310** (117 mg, 0.622 mmol, 1.0 equiv) in TFE (3 mL) was added *p*-methoxybenzylamine (130 mg, 0.948 mmol, 1.5 equiv.) and 1-isocyano-2-(2,2-dimethoxyethyl)benzene (**240**, 180 mg, 0.941 mmol, 1.5 equiv.). The reaction mixture was stirred at room temperature overnight and then concentrated *in vacuo* to yield a crude yellow oil which was purified by flash column chromatography with SiO_2 (30-50% EtOAc/ hexanes) to yield 249 mg (80%) of **313** as a clear viscous oil. R_f (50% EtOAc/ Hexanes) = 0.45; 1H NMR (500 MHz, $CDCl_3$) δ : 9.32 (s, 1H), 7.74 (d, $J = 8.5$ Hz, 1H), 7.27 (t, $J = 8.0$ Hz, 1H), 7.23 (d, $J = 7.5$ Hz, 1H), 7.20 (d, $J = 8.5$ Hz, 2H), 7.15 (t, $J = 7.5$ Hz, 1H), 6.83 (d, $J = 8.0$ Hz, 2H), 5.00 (d, $J = 15.0$ Hz, 1H), 4.45 (t, $J = 5.5$ Hz, 1H), 4.39 (dd, $J = 8.0$ Hz, $J = 13.0$ Hz, 1H), 3.94 (d, $J = 10.5$ Hz, 1H), 3.89 (d, $J = 14.5$ Hz, 1H), 3.78 (s, 3H), 3.57 (d, $J = 11.0$ Hz, 1H), 3.33 (s, 3H), 3.31 (s, 3H), 3.08 (dd, $J = 13.0$ Hz, $J = 15.5$ Hz, 1H), 2.91 (dd, $J = 5.5$ Hz, $J = 13.5$ Hz, 1H), 2.89 (dd, $J = 4.5$ Hz, $J = 18.0$ Hz, 1H), 2.60 (dd, $J = 7.5$ Hz, $J = 15.5$ Hz, 1H), 1.51 (s, 3H), 1.45 (s, 3H). ^{13}C (100 MHz, $CDCl_3$) δ : 173.4, 168.0, 159.5, 136.3, 131.1, 130.3, 129.8, 129.4, 127.6, 126.1, 125.8, 114.2, 106.3, 102.9, 73.6, 68.6, 65.0, 55.5, 54.3, 54.1, 44.9, 36.6, 34.4, 29.5, 19.6.

(319). To a solution of α -(hydroxymethyl)cinnamaldehyde (**276**, 900 mg, 5.55 mmol, 1.0 equiv.) in THF (40 mL) was added triethylamine (2.3 mL, 16.5 mmol, 3.0 equiv.) and chlorotrimethylsilane (1.75 mL, 13.8 mmol, 2.5 equiv.) at room temperature. The mixture was stirred vigorously for 30 min and then filtered through a small plug of SiO_2

and eluted with Et₂O. The Et₂O solution was then concentrated *in vacuo* to yield 1.20 g (92%) of **319** as a light yellow oil. R_f (20% EtOAc/ Hexanes) = 0.85. ¹H NMR (400 MHz, CDCl₃) δ : 9.60 (s, 1H), 7.72-7.74 (m, 2H), 7.42-7.46 (m, 4H), 4.46 (s, 2H), 0.17 (s, 9H). ¹³C (75 MHz, CDCl₃) δ : 194.5, 153.8, 140.1, 134.4, 130.8, 130.6, 129.0, 54.1, -0.12. HRMS (EI) m/z calcd for C₁₃H₁₇O₂Si₁ (M⁺-H) 233.0992, found 233.0983.

(320). To a solution of benzyl propionate (272 mg, 1.66 mmol, 1.0 equiv.) in DCM (25 mL) at -78 °C under N₂ was added dibutylboron triflate (solution in DCM, 1.0 M, 3.3 mL, 2.0 equiv.) and diisopropylethylamine (0.8 mL, 4.90 mmol, 3.0 equiv.) dropwise. The solution was stirred at -78 °C for 1h and then a DCM (1 mL) solution of **319** (485 mg, 2.07 mmol, 1.2 equiv.) was added dropwise and stirring was continued at -78 °C for 1h. After warming to 0 °C slowly over 1h, the solution was quenched with a 1:1 mixture of pH-7 phosphate buffer/ MeOH (4mL). After 5 min of vigorous stirring, MeOH was added until the mixture was homogenous. A 30% H₂O₂ solution (2 mL) was added, slowly at first, and the mixture was stirred at room temperature for 2h. The solution was partitioned between DCM (50 mL) and brine (30 mL). The organic layer was dried over Na₂SO₄, filtered, and concentrated *in vacuo* to yield a crude oil which was diluted with MeOH (30 mL). Trifluoroacetic acid (3 drops) was added and the mixture was stirred for 5 min and then concentrated *in vacuo*. The crude oil was purified by flash column chromatography with SiO₂ (30-50% EtOAc/ hexanes) to yield 321 mg (59% crude) of **320** which was taken to the next reaction as a mixture with an inseparable impurity. R_f (50% EtOAc/ Hexanes) = 0.43. HRMS (EI) m/z calcd for C₂₀H₂₂O₄ (M⁺) 326.1513, found 326.1518.

(321). To the crude mixture (see above) of **320** (321 mg, 0.983 mmol, 1.0 equiv.) in acetone (8 mL) and 2,2-DMP (2 mL) was added *p*-tolenesulfonic acid monohydrate (37 mg, 0.195 mmol, 0.2 equiv.) at room temperature. The reaction mixture was stirred for 30 min and then diluted with EtOAc (40 mL) and washed with a saturated NaHCO₃ solution (20 mL). The organic layer was further washed with brine, dried over Na₂SO₄, filtered, and concentrated *in vacuo* to yield a crude oil which was purified by flash column chromatography with SiO₂ (5% EtOAc/ hexanes) to yield 233 mg (38% crude, 3 steps) of **321** as a clear oil. R_f (20% EtOAc/ Hexanes) = 0.49. ¹H NMR (400 MHz, CDCl₃) δ: 7.25-7.37 (m, 8H), 7.08 (d, *J* = 6.8 Hz, 2H), 6.29 (s, 1H), 5.20 (d, *J* = 12.0 Hz, 1H), 5.16 (d, *J* = 12.4 Hz, 1H), 4.89 (d, *J* = 4.8 Hz, 1H), 4.62 (dt, *J* = 1.3 Hz, *J* = 14.8 Hz, 1H), 4.57 (dd, *J* = 1.6 Hz, *J* = 14.4 Hz, 1H), 3.11 (m, 1H), 1.41 (s, 3H), 1.36 (d, *J* = 6.8 Hz, 3H), 1.33 (s, 3H). ¹³C (100 MHz, CDCl₃) δ: 174.3, 138.7, 136.2, 136.1, 129.0, 128.8, 128.6, 128.6, 128.5, 127.4, 123.3, 100.2, 73.6, 66.7, 61.1, 43.7, 26.4, 24.0, 11.3. HRMS (EI) *m/z* calcd for C₂₃H₂₆O₄ (M⁺) 366.1826, found 366.1826.

(321a). Ozone was bubbled in to a solution of **321** (215 mg, 0.587 mmol, 1.0 equiv.) in MeOH (20 mL) at -78 °C containing a catalytic amount of Sudan III indicator until the pink color in the solution disappeared. The solution was then flushed with N₂ and methyl sulfide (0.2 mL, 2.72 mmol, 5.0 equiv.) was added. The solution was then warmed to room temperature and concentrated *in vacuo* to yield a crude oil which was purified by flash column chromatography with SiO₂ (5-10% Et₂O/ hexanes) to yield 160 mg (93%) of ketoester **321a** (not shown in text) as a clear oil. R_f (20% EtOAc/ Hexanes) = 0.41. ¹H

NMR (500 MHz, CDCl₃) δ : 7.34-7.36 (m, 5H), 5.20 (d, J = 12.0 Hz, 1H), 5.13 (d, J = 12.0 Hz, 1H), 4.67 (dd, J = 1.5 Hz, J = 5.5 Hz, 1H), 4.23 (dd, J = 1.5 Hz, J = 17.0 Hz, 1H), 4.00 (d, J = 17.0 Hz, 1H), 3.01 (dq, J = 5.5 Hz, J = 7.0 Hz, 1H), 1.40 (s, 3H), 1.37 (s, 3H), 1.21 (d, J = 6.5 Hz, 3H). ¹³C (75 MHz, CDCl₃) δ : 208.5, 173.6, 136.0, 128.9, 128.5, 128.5, 101.3, 77.5, 67.0, 66.9, 39.4, 23.9, 23.6, 11.8. HRMS (EI) m/z calcd for C₁₆H₂₀O₅ (M⁺) 292.1305, found 292.1302.

(311). To a solution of ketoester **321a** (157 mg, 0.537 mmol, 1.0 equiv) in methanol (20 mL) was added a catalytic amount of Palladium 10 wt.% on activated carbon and reaction mixture was stirred under a balloon of H₂ for 1h. The reaction mixture was then filtered through Celite and concentrated *in vacuo* to yield **311** (107 mg, 98%) as a clear viscous oil. R_f(50% EtOAc/ Hexanes) = 0.50. Mp = 117-118 °C. ¹H NMR (400 MHz, CDCl₃) δ : 6.93 (br s, 1H), 4.22 (br s, 1H), 4.06 (d, J = 14.4 Hz, 1H), 3.93 (d, J = 14.4 Hz, 1H), 2.65-2.67 (m, 1H), 1.45 (s, 3H), 1.36 (s, 3H), 1.32 (d, J = 7.2 Hz, 3H). ¹³C (100 MHz, CDCl₃) δ : 180.1, 100.3, 77.5, 76.3, 42.3, 25.6, 22.1, 14.2.

(314). To a solution of **311** (43 mg, 0.213 mmol, 1.0 equiv) in TFE (1 mL) was added *p*-methoxybenzylamine (32 mg, 0.233 mmol, 1.1 equiv.) and 1-isocyano-2-(2,2-dimethoxyethyl)benzene (**240**, 53 mg, 0.277 mmol, 1.3 equiv.). The reaction mixture was stirred at room temperature overnight and then concentrated *in vacuo* to yield a crude yellow oil which was purified by flash column chromatography with SiO₂ (30-50% EtOAc/ hexanes) to yield 78 mg (72%) as an inseperable 10:1 diastereomixture of **314** (major diastereomer pictured) as a clear viscous oil. R_f(50% EtOAc/ Hexanes) = 0.48.

(Major Diastereomer) ^1H NMR (500 MHz, CDCl_3) δ : 9.30 (s, 1H), 7.72 (d, $J = 7.5$ Hz, 1H), 7.14-7.29 (m, 5H), 6.83 (d, $J = 8.5$ Hz, 2H), 5.02 (d, $J = 15.0$ Hz, 1H), 4.46 (t, $J = 5.0$ Hz, 1H), 3.98 (d, $J = 8.0$ Hz, 1H), 3.95 (d, $J = 4.5$ Hz, 1H), 3.90 (d, $J = 11.5$ Hz, 1H), 3.79 (s, 3H), 3.49 (d, $J = 10.5$ Hz, 1H), 3.34 (d, $J = 10.0$ Hz, 1H), 3.33 (s, 3H), 3.31 (s, 3H), 3.13 (quint., $J = 6.5$ Hz, 1H), 2.92 (dd, $J = 5.5$ Hz, $J = 13.5$ Hz, 1H), 2.87 (dd, $J = 5.5$ Hz, $J = 13.5$ Hz, 1H), 1.50 (s, 3H), 1.46 (s, 3H), 1.30 (d, $J = 7.0$ Hz, 3H). (Minor Diastereomer, distinguishable diagnostic peaks) ^1H NMR (500 MHz, CDCl_3) δ : 9.15 (s, 1H), 5.14 (d, $J = 15.5$ Hz, 1H), 1.35 (d, $J = 8.5$ Hz, 3H). (Major Diastereomer) ^{13}C (75 MHz, CDCl_3) δ : 175.8, 168.3, 159.4, 136.3, 131.2, 130.3, 130.0, 129.8, 129.7, 127.6, 126.1, 125.9, 114.2, 106.1, 102.8, 80.4, 77.5, 68.9, 63.4, 55.5, 54.1, 53.9, 45.0, 38.8, 36.6, 29.5, 19.6, 13.3. (Minor Diastereomer, distinguishable diagnostic peaks) ^{13}C (75 MHz, CDCl_3) δ : 177.8, 170.1, 159.3, 131.2, 124.8, 114.1, 106.5, 75.4, 62.7, 54.8, 45.2, 43.7, 29.9, 25.7, 22.6, 15.4. HRMS (EI) m/z calcd for $\text{C}_{28}\text{H}_{36}\text{N}_2\text{O}_7$ (M^+) 512.2517, found 512.2509.

(322). To a solution of α -(hydroxymethyl)cinnamaldehyde (**276**, 194 mg, 1.20 mmol, 1.0 equiv.)² in DCM (3 mL) was added diisopropylethylamine (0.52 mL, 2.99 mmol, 2.5 equiv.) and chloromethyl methyl ether, tech. (0.18 mL, 2.37 mmol, 2.0 equiv.) at room temperature. The mixture was stirred for 2h and then diluted with Et_2O (40 mL), washed with a saturated NH_4Cl solution (10 mL), and brine (10 mL). The Et_2O solution was dried over Na_2SO_4 , filtered, and concentrated *in vacuo* to yield 238 mg (97%) of **322** as a light yellow oil. R_f (20% EtOAc / Hexanes) = 0.40. ^1H NMR (400 MHz, CDCl_3) δ : 9.63 (s, 1H), 7.67-7.70 (m, 2H), 7.50 (s, 1H), 7.44-7.47 (m, 3H), 4.75 (s, 2H), 4.41 (s, 2H),

3.42 (s, 3H). ^{13}C NMR (75 MHz, CDCl_3) δ : 194.4, 154.2, 138.0, 134.2, 130.8, 129.5, 129.1, 97.1, 59.2, 55.9. HRMS (EI) m/z calcd for $\text{C}_{12}\text{H}_{14}\text{O}_3$ (M^+) 206.0937, found 206.0939.

(323). A solution of lithium diisopropylamine (4.0 equiv) is prepared in THF (35 mL) from diisopropylamine (0.55mL) and *n*-butyllithium (2.89 M solution in *n*-hexane, 0.34mL) under N_2 at -78°C . To this solution was added a THF (5 mL) solution of benzyl isobutyrate (690mg, 3.88 mmol, 4.0 equiv) over 5 minutes. Stirring at -78°C is continued for 30 minutes and a THF (2 mL) solution of **322** (200 mg, 0.97mmol, 1.0 equiv) is added. The mixture is stirred for 40 min. and then quenched by addition of a NH_4Cl solution (5mL). The resulting solution is poured in Et_2O (350mL) and washed with water (100 mL). The organic layer was dried over Na_2SO_4 , filtered and concentrated *in vacuo*. The resultant viscous oil was purified by flash chromatography on silica gel (5:95 \rightarrow 3:7 ethyl acetate/hexane) to yield **323** as a colorless viscous oil (50 mg, 91%). R_f (20% EtOAc/ Hexanes) = 0.31. ^1H NMR (400 MHz, CDCl_3) δ : 7.29-7.40 (m, 10H), 6.72 (s, 1H), 5.19 (d, $J = 12.4$ Hz, 1H), 5.13 (d, $J = 12.4$ Hz, 1H), 4.62 (d, $J = 6.8$ Hz, 1H), 4.60 (d, $J = 6.4$ Hz, 1H), 4.55 (d, $J = 4.4$ Hz, 1H), 4.26 (d, $J = 11.6$ Hz, 1H), 4.21 (d, $J = 11.2$ Hz, 1H), 3.72 (d, $J = 5.2$ Hz, 1H) 3.34 (s, 3H), 1.31 (s, 3H), 1.29 (s, 3H). ^{13}C NMR (100 MHz, CDCl_3) δ : 177.4, 137.0, 136.2, 134.7, 129.2, 128.8, 128.5, 128.4, 128.1, 127.7, 97.0, 81.2, 66.7, 64.8, 56.0, 48.0, 23.6, 21.0 HRMS (EI) m/z calcd for $\text{C}_{23}\text{H}_{28}\text{O}_5$ (M^+) 384.1931, found 384.1936, ($\text{M}^+ - \text{OH}$) 367.1904, found 367.1908.

(324). A solution of **323** (158 mg, 0.411 mmol, 1.0 equiv) in anhydrous DCM (120 mL) was cooled in ice bath at 0 °C under N₂. A solution of boron fluoride-ether (0.20 mL, 1.59 mmol, 3.9 equiv.) in DCM (2 mL) was added dropwise over 20 min. at the same temperature. The mixture was stirred at 0 °C for 0.5 h, then quenched with Et₂O (200mL), washed with saturated aqueous NaHCO₃ and brine. The Et₂O solution was dried over Na₂SO₄, filtered, and concentrated *in vacuo* and purified by flash chromatography on silica gel (5% EtOAc /hexanes) to yield 122 mg (84%) of **324** as a clear oil. R_f(20% EtOAc/ Hexanes) = 0.57. ¹H NMR (400 MHz, CDCl₃) δ: 7.04-7.39 (m, 8H), 7.05 (d, *J* = 7.2 Hz, 2H), 6.43 (s, 1H), 5.17 (s, 2H), 4.96 (d, *J* = 6.0 Hz, 1H), 4.88 (d, *J* = 5.2 Hz, 1H), 4.81 (d, *J* = 13.2 Hz, 1H), 4.77 (s, 1H), 4.64 (d, *J* = 13.2 Hz, 1H), 1.42 (s, 3H), 1.38 (s, 3H). ¹³C NMR (75 MHz, CDCl₃) δ: 176.3, 136.3, 135.4, 132.3, 129.8, 129.4, 128.8, 128.6, 128.4, 128.3, 127.9, 90.3, 84.3, 66.8, 66.4, 48.3, 22.7, 21.2. HRMS (EI) m/z calcd for C₂₂H₂₄O₄ (M⁺) 352.1669, found 352.1664.

(324a). Ozone was bubbled in to a solution of **324** (93 mg, 0.264 mmol, 1.0 equiv.) in DCM (25 mL) at -78 °C containing a catalytic amount of Sudan III indicator until the pink color in the solution disappeared. The solution was then flushed with N₂ and methyl sulfide (0.2 mL, 2.72 mmol, 10.0 equiv.) was added. The solution was then warmed to room temperature and concentrated *in vacuo* to yield a crude oil which was purified by flash column chromatography with SiO₂ (5-10% Et₂O/ hexanes) to yield 70 mg (96%) of ketoester **324a** as a clear oil. R_f(20% EtOAc/ Hexanes) = 0.43. ¹H NMR (300 MHz, CDCl₃) δ: 7.29-7.37 (m, 5H), 5.20 (d, *J* = 12.3 Hz, 1H), 5.12 (d, *J* = 5.4 Hz, 1H), 5.10 (d, *J* = 12.3 Hz, 1H), 4.92 (d, *J* = 6.3 Hz, 1H), 4.45 (s, 1H), 4.29 (d, *J* = 17.4 Hz, 1H), 4.19

(d, $J = 17.1$ Hz, 1H), 1.35 (s, 3H), 1.29 (s, 3H). ^{13}C NMR (75 MHz, CDCl_3) δ : 204.5, 175.2, 136.1, 128.8, 128.4, 128.3, 91.8, 86.2, 73.4, 70.0, 46.1, 23.2, 20.2 HRMS (EI) m/z calcd for $\text{C}_{15}\text{H}_{18}\text{O}_5$ (M^+) 278.1149, found 278.1146.

(312). To a solution of ketoester **324a** (55 mg, 0.198 mmol, 1.0 equiv) in MeOH (10 mL) was added a catalytic amount of Palladium 10 wt.% on activated carbon and reaction mixture was stirred under a balloon of H_2 for 1h. The reaction mixture was then filtered through Celite, concentrated *in vacuo*, and purified by flash column chromatography with SiO_2 (30-50% EtOAc/ hexanes) to yield **312** (32 mg, 86%) as a clear viscous oil. R_f (50% EtOAc/ Hexanes) = 0.49. ^1H NMR (300 MHz, CDCl_3) δ : 5.09 (br s, 1H), 5.00 (d, $J = 6.4$ Hz, 1H), 4.63 (d, $J = 6.0$ Hz, 1H), 4.23 (d, $J = 12.4$ Hz, 1H), 3.92 (s, 1H), 3.74 (d, $J = 12.4$ Hz, 1H), 1.50 (s, 3H), 1.26 (s, 3H). ^{13}C NMR (75 MHz, CDCl_3) δ : 183.0, 97.1, 91.4, 82.2, 70.2, 46.3, 24.9, 19.0. HRMS (EI) m/z calcd for $\text{C}_8\text{H}_{12}\text{O}_5$ (M^+) 188.0679, found 188.0678.

(315). To a solution of **312** (30 mg, 0.159 mmol, 1.0 equiv) in TFE (2 mL) was added *p*-methoxybenzylamine (24 mg, 0.175 mmol, 1.1 equiv.) and 1-isocyano-2-(2,2-dimethoxyethyl)benzene (**240**, 40 mg, 0.209 mmol, 1.3 equiv.). The reaction mixture was stirred at room temperature overnight and then concentrated *in vacuo* to yield a crude yellow oil which was purified by flash column chromatography with SiO_2 (30-50% EtOAc/ hexanes) to yield 60 mg (76%) as a >20:1 diastereomixture of **315** (major diastereomer pictured) as a clear viscous oil. R_f (50% EtOAc/ Hexanes) = 0.51; ^1H NMR (400 MHz, CDCl_3) δ : 9.43 (s, 1H), 7.78 (d, $J = 4.0$ Hz, 1H), 7.12-7.30 (m, 5H), 6.82-6.85

(m, 2H), 5.44 (d, $J = 5.6$ Hz, 1H), 5.22 (d, $J = 14.8$ Hz, 1H), 4.85 (d, $J = 5.6$ Hz, 1H), 4.39 (dd, $J = 2.8, 4.8$ Hz, 1H), 4.24 (d, $J = 14.8$ Hz, 1H), 3.98 (d, $J = 10.8$ Hz, 1H), 3.79 (s, 3H), 3.63 (s, 1H), 3.32 (s, 6H), 2.97 (dd, $J = 6.4, 13.6$ Hz, 1H), 2.90 (dd, $J = 5.2, 13.6$ Hz, 1H), 1.35 (s, 3H), 1.15 (s, 3H); ^{13}C NMR (75 MHz, CDCl_3) δ : 177.6, 169.8, 159.4, 136.6, 131.0, 130.4, 130.1, 129.6, 127.4, 125.7, 125.2, 114.3, 107.3, 96.1, 90.2, 74.2, 62.1, 55.5, 55.1, 54.5, 45.6, 42.3, 36.6, 25.8, 16.8; HRMS (EI) m/z calcd for $\text{C}_{27}\text{H}_{34}\text{N}_2\text{O}_7$ (M^+) 498.2361, found 498.2365.

3.8 Notes and References

(1) Kobayashi, K.; Yoneda, K.; Mizumoto, T.; Umakoshi, H.; Morikawa, O.; Konishi, H. *Tetrahedron Lett.* **2003**, *44*, 4733-4736.

(2) Gilley, C. B.; Buller, M. J.; Kobayashi, Y. *Org. Lett.* **2007**, *9*, 3631-3634.

(3) Faul, M. M.; Grutsch, J. L.; Kobierski, M. E.; Kopach, M. E.; Krumrich, C. A.; Staszak, M. A.; Udodong, U.; Vicenzi, J. T.; Sullivan, K. A. *Tetrahedron* **2003**, *59*, 7215-7229.

(4) Coe, J. W.; Vetelino, M. G.; Bradlee, M. J. *Tetrahedron Lett.* **1996**, *37*, 6045-6048.

(5) Arai, E.; Tokuyama, H.; Linsell, M. S.; Fukuyama, T. *Tetrahedron Lett.* **1998**, *39*, 71-74.

(6) Kreye, O.; Westermann, B.; Wessjohann, L. A. *Synlett* **2007**, 3188-3192.

(7) Hodge, J. E. *Adv. Carb. Chem.* **1955**, *10*, 169-205.

(8) A ¹H-NMR spectra of the syn methyl ester derived from Ugi product X was obtained by conversion of Ugi product X to the corresponding γ-lactam-β-lactone bicycle and subsequent methanolysis. This spectra was compared to a spectra containing the 1:2 mixture of methyl ester diastereomers, obtained from methanolysis of the N-acylindole derived from Ugi product X. We determined by spectral comparison that the anti diastereomer was major.

(9) Corey, E. J.; Li, W.; Nagamitsu, T. *Angew. Chem. Int. Ed.* **1998**, *37*, 1676-1679.

(10) Evans, D. A.; Tedrow, J. S.; Shaw, J. T.; Downey, C. W. *J. Am. Chem. Soc.* **2002**, *124*, 392-393.

(11) Kaneno, D.; Zhang, J.; Iwaoka, M.; Tomoda, S. *Heteroat. Chem* **2001**, *12*, 358-368; Senda, Y.; Sakurai, H.; Itoh, H. *Bull. Chem. Soc. Jpn.* **1999**, *72*, 285-288; Carda, M.; Casabo, P.; Gonzalez, F.; Rodriguez, S.; Domingo, L. R.; Marco, J. A. *Tetrahedron: Asymmetry* **1997**, *8*, 559-577; Wu, Y. D.; Houk, K. N. *J. Am. Chem. Soc.* **1987**, *109*, 908-910; Kobayashi, Y. M.; Lambrecht, J.; Jochims, J. C.; Burkert, U. *Chem. Ber.* **1978**, *111*, 3442-3459.

(12) Jochims, J. C.; Kobayashi, Y.; Skrzewski, E. *Tetrahedron Lett.* **1974**, 571-574.

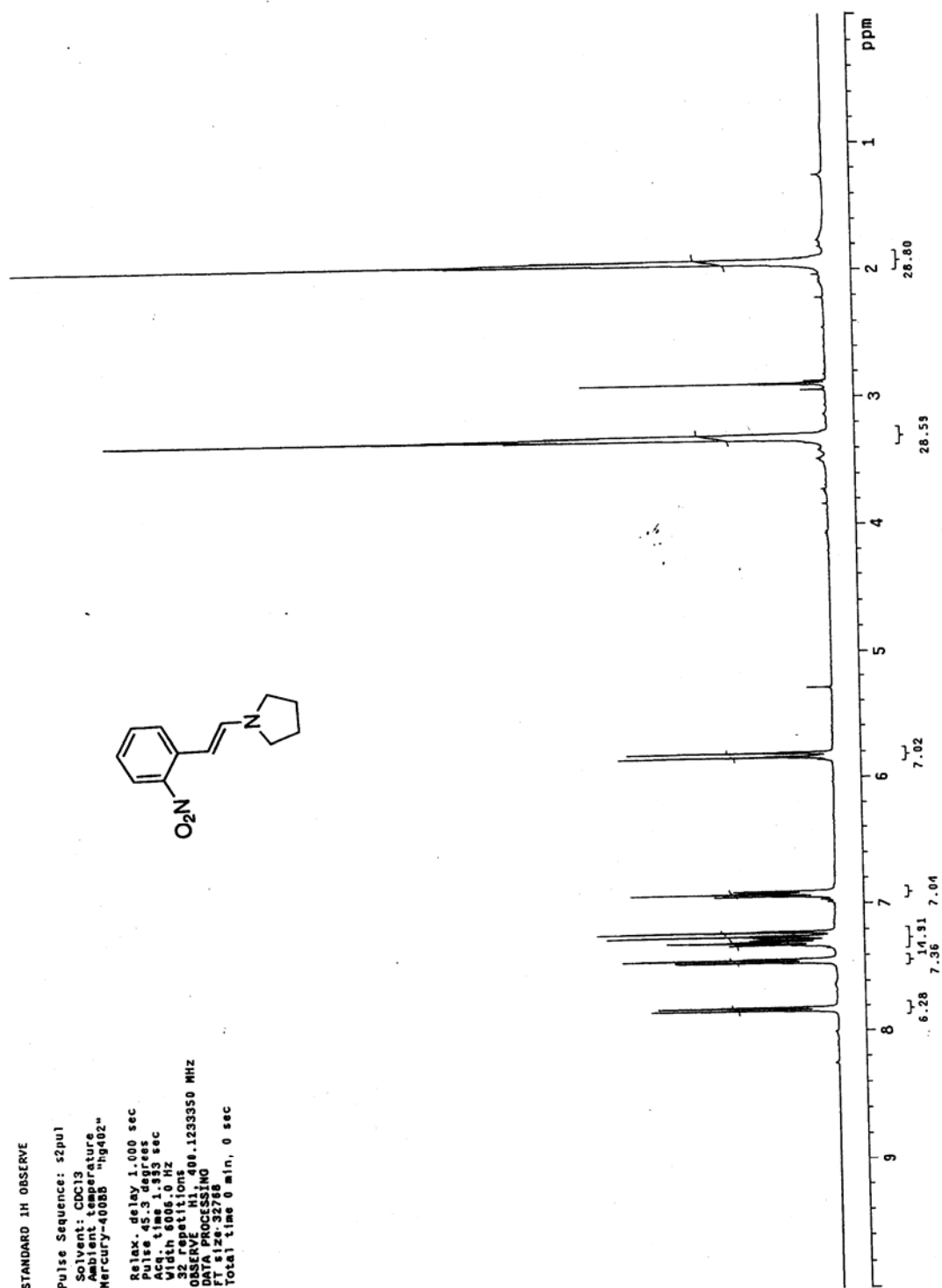
(13) Lagisetti, C.; Urbansky, M.; Coates, R. M. *J. Org. Chem.* **2007**, *72*, 9886-9895; Urbansky, M.; Davis, C. E.; Surjan, J. D.; Coates, R. M. *Org. Lett.* **2004**, *6*, 135-138.

(14) Nicolaou, K. C.; Nugiel, D. A.; Couladouros, E.; Hwang, C. K. *Tetrahedron* **1990**, *46*, 4517-4552.

(15) Dockendorff, C.; Sahli, S.; Olsen, M.; Milhau, L.; Lautens, M. *J. Am. Chem. Soc.* **2005**, *127*, 15028-15029; Doi, T.; Nagamiya, H.; Kokubo, M.; Hirabayashi, K.; Takahashi, T. *Tetrahedron* **2002**, *58*, 2957-2963; Doi, T.; Hirabayashi, K.; Kokubo, M.; Komagata, T.; Yamamoto, K.; Takahashi, T. *J. Org. Chem.* **1996**, *61*, 8360-8361; Cowles, R. S.; Miller, J. R.; Hollingworth, R. M.; Abdel-Aal, M. T.; Szurdoki, F.; Bauer, K.; Matolcsy, G. *J. Chem. Ecol.* **1990**, *16*, 2401-2428.

(16) Enders, D.; Bockstiegel, B. *Synthesis* **1989**, 493-496; Enders, D.; Voith, M.; Ince, S. J. *Synthesis* **2002**, 1775-1779.

- (17) Enders, D.; Hieronymi, A.; Ridder, A. *Synlett* **2005**, 2391-2393; Galletti, E.; Avramova, S. I.; Renzulli, M. L.; Corelli, F.; Botta, M. *Tetrahedron Lett.* **2007**, *48*, 751-754.
- (18) Enders, D.; Bettray, W. *Asymmetric Synth. Chem. Biol. Methods* **2007**, 38-75; Enders, D.; Bettray, W. *Asymmetric Synth.* **2007**, 21-26; Job, A.; Janeck, C. F.; Bettray, W.; Peters, R.; Enders, D. *Tetrahedron* **2002**, *58*, 2253-2329.
- (19) Enders, D.; Gatzweiler, W.; Jegelka, U. *Synthesis* **1991**, 1137-1141.
- (20) Abiko, A. *Acc. Chem. Res.* **2004**, *37*, 387-395; Abiko, A.; Liu, J.-F.; Buske, D. C.; Moriyama, S.; Masamune, S. *J. Am. Chem. Soc.* **1999**, *121*, 7168-7169; Abiko, A.; Liu, J.-F.; Masamune, S. *J. Org. Chem.* **1996**, *61*, 2590-2591; Inoue, T.; Liu, J.-F.; Buske, D. C.; Abiko, A. *J. Org. Chem.* **2002**, *67*, 5250-5256; Liu, J.-F.; Abiko, A.; Pei, Z.; Buske, D. C.; Masamune, S. *Tetrahedron Lett.* **1998**, *39*, 1873-1876.
- (21) Dalgard, J. E.; Rychnovsky, S. D. *Org. Lett.* **2005**, *7*, 1589-1591.

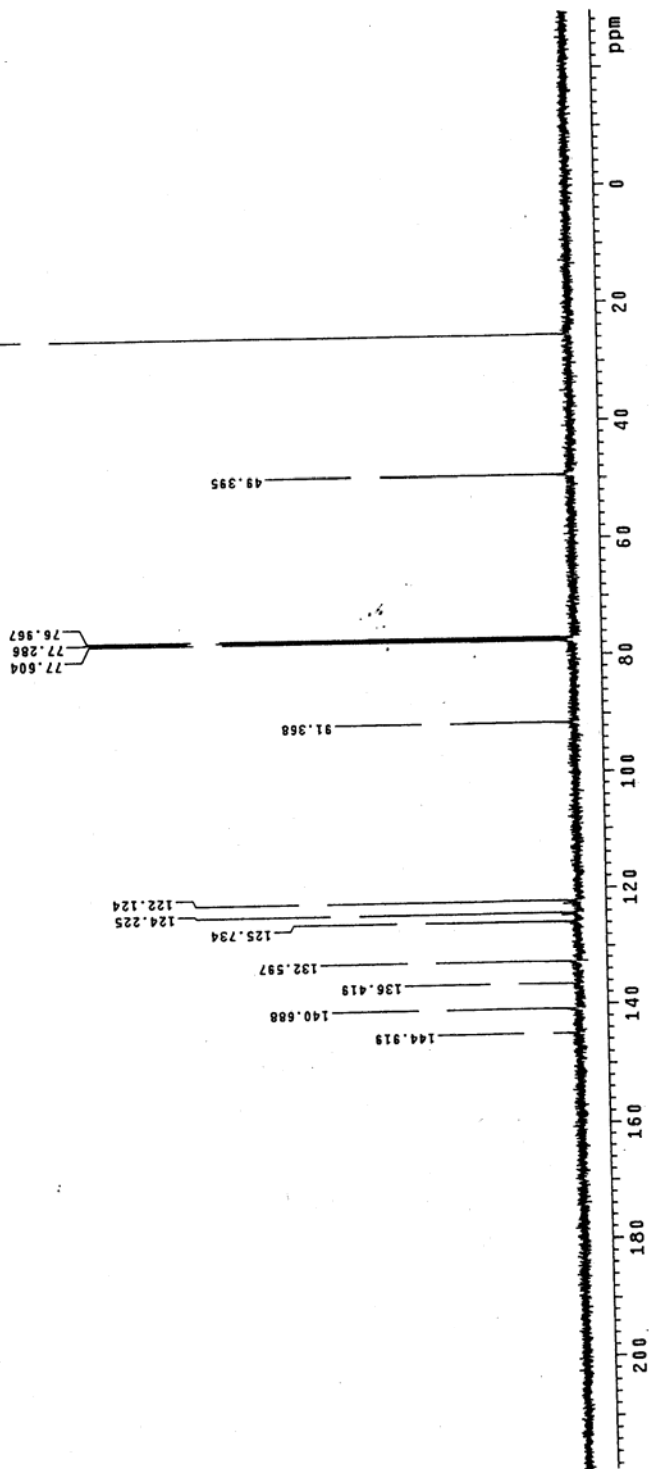
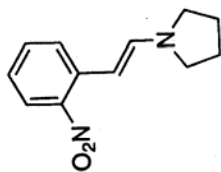
^1H NMR spectrum of compound 244

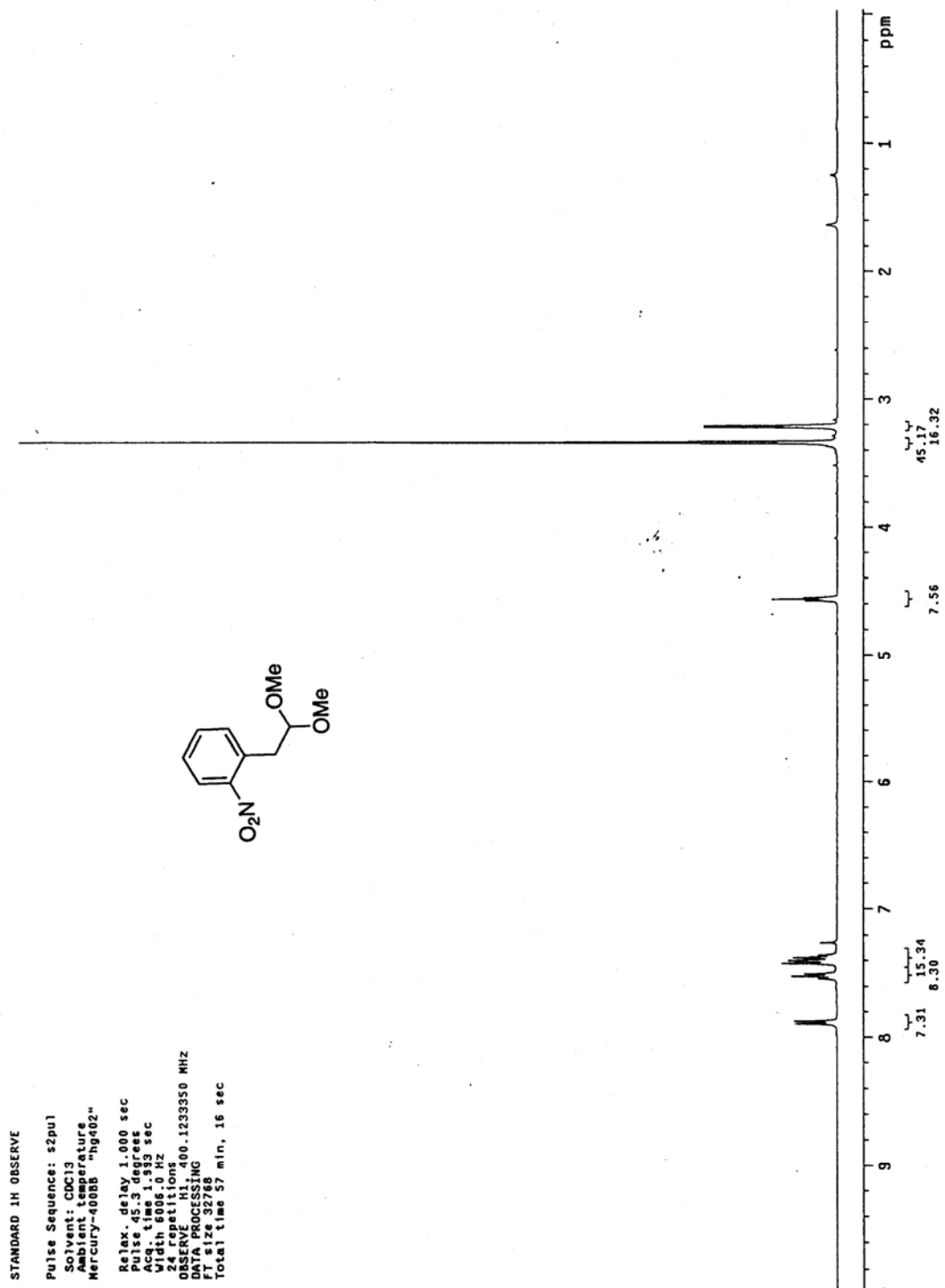
¹³C NMR spectrum of compound 244

EXP 000113
13C OBSERVE

Pulse Sequence: szpul
Solvent: CDC13
Ambient temperature
Mercury-400BB "hg402"

Relax. delay 4.000 sec
Pulse 13.4 degrees
Acq. time 1.189 sec
Width 25000.0 Hz
132 repetitions
132 repetition rate
DECUPLE H1, 400.6110686 MHZ
DECUPLE H1, 400.1253602 MHZ
Power 38 dB,
continuously on
WALTZ-16 modulated
DATA PROCESSING
Line processing 1.0 Hz
111.823 sec
Total time 1 hr, 42 min, 55 sec



^1H NMR spectrum of compound 245

^{13}C NMR spectrum of compound 245

13C OBSERVE

Pulse Sequence: s2pul

Solvent: CDCl3

Ambient temperature

Mercury-40005B "hg402"

Pulse 53.4 degrees

Acq. time 1.199 sec

Width 25000.0 Hz

1976 repetitions

OBSERVE C13, 100.6110686 MHz

DECOUPLE H1, 400.1253602 MHz

continuously on

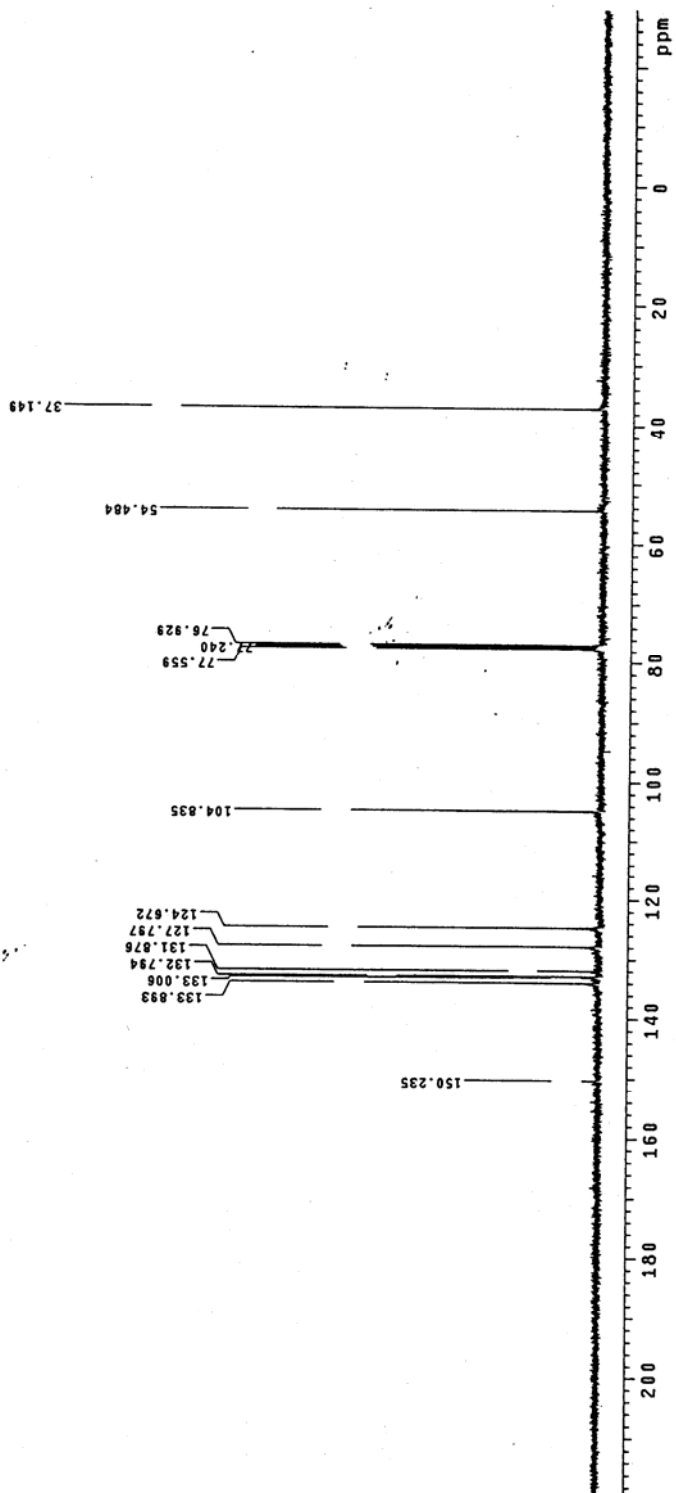
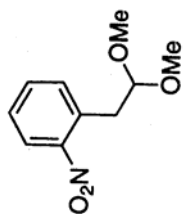
WALTZ-16 modulated

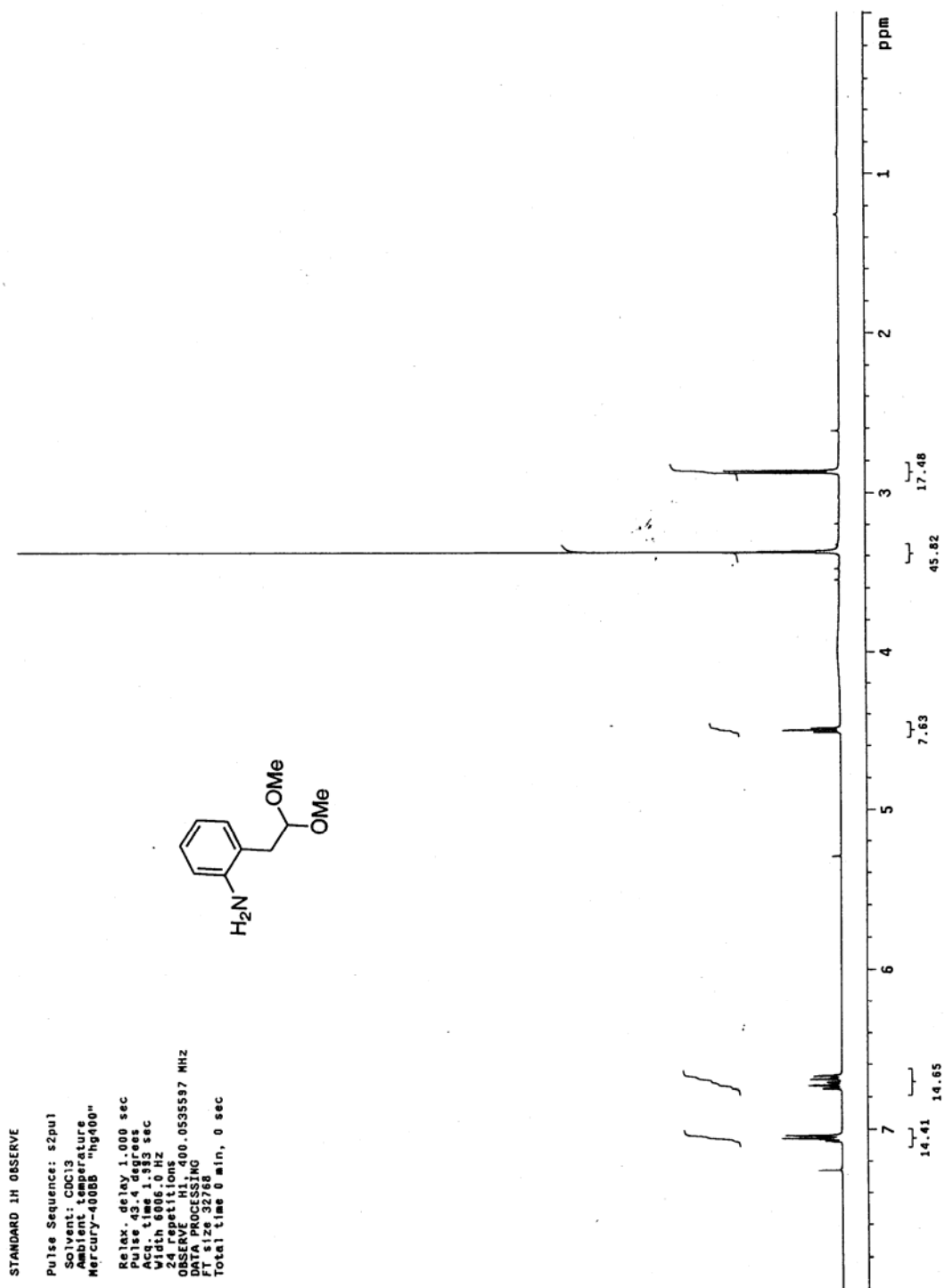
DATA PROCESSING

Line broadening 1.0 Hz

FT size 65536

Total time 1 hr, 12 min, 30 sec



¹H NMR spectrum of compound 237

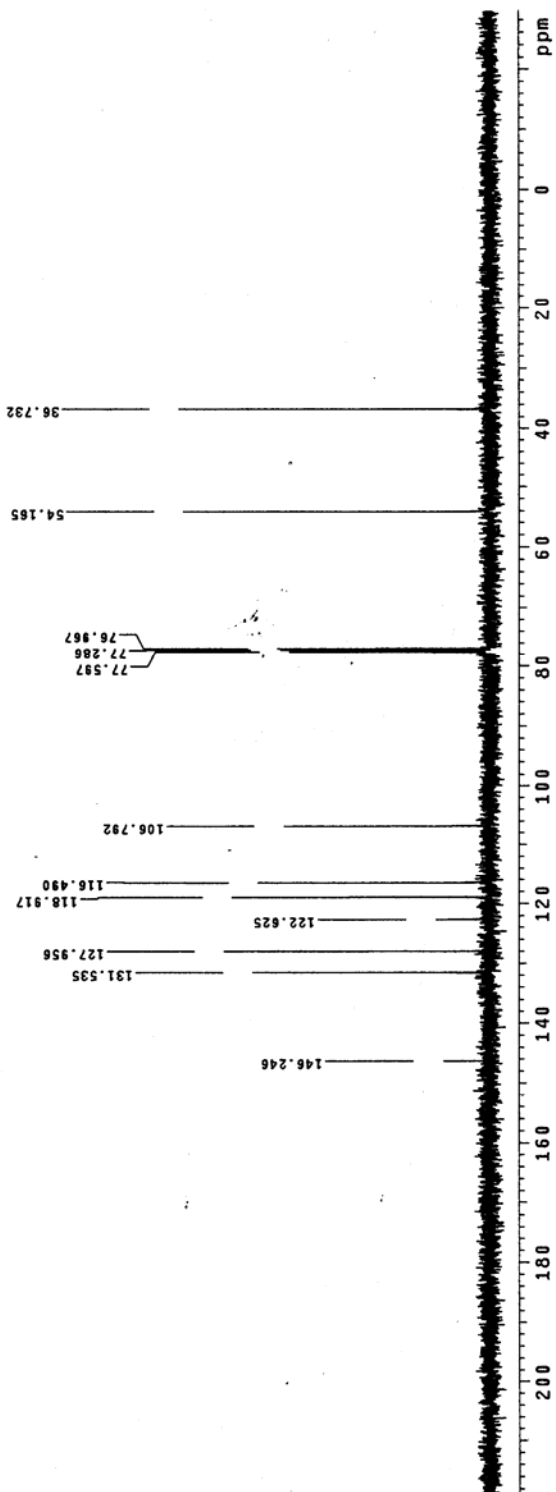
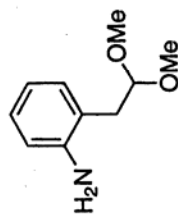
^{13}C NMR spectrum of compound **237**

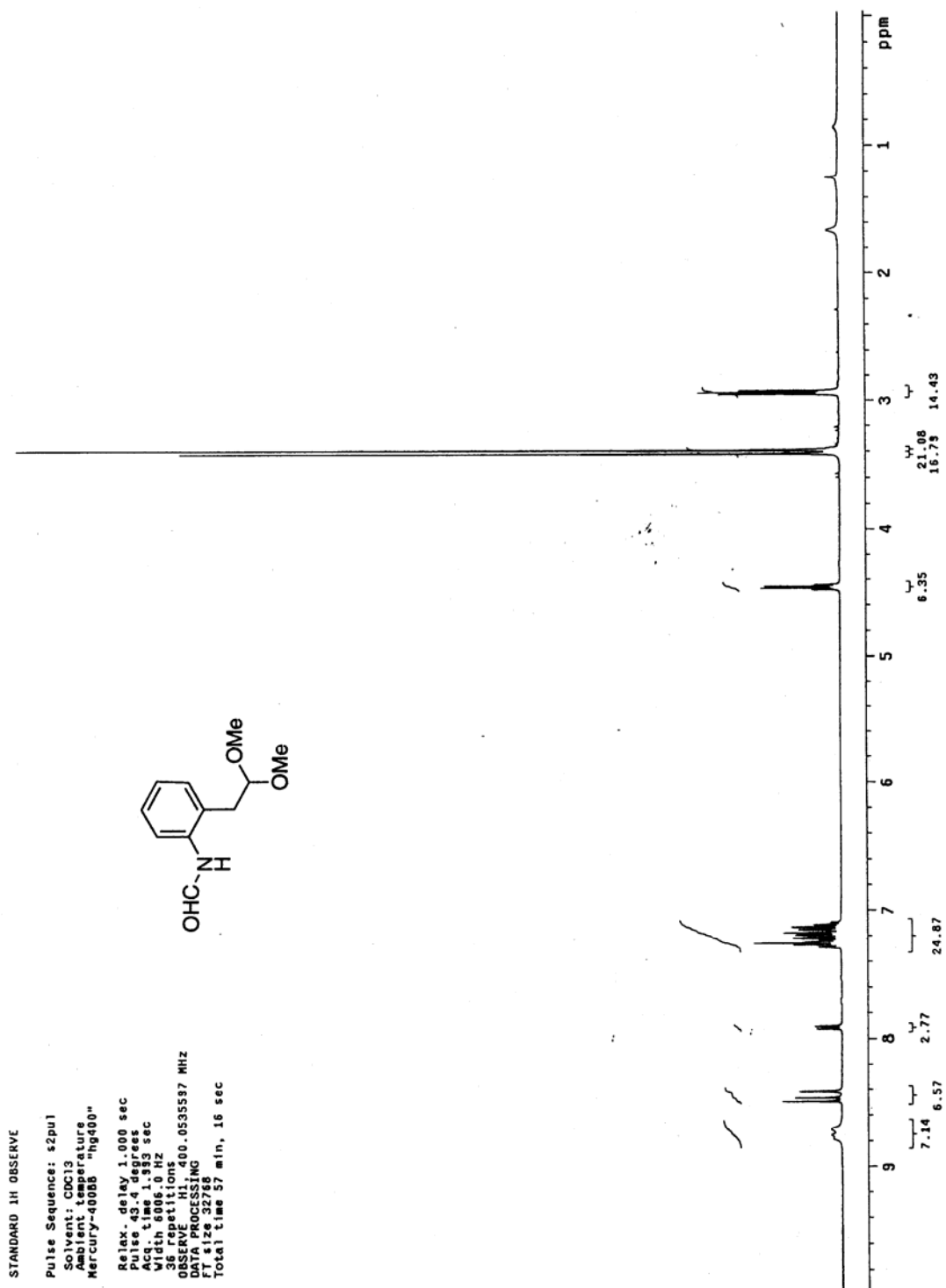
Qhlmq

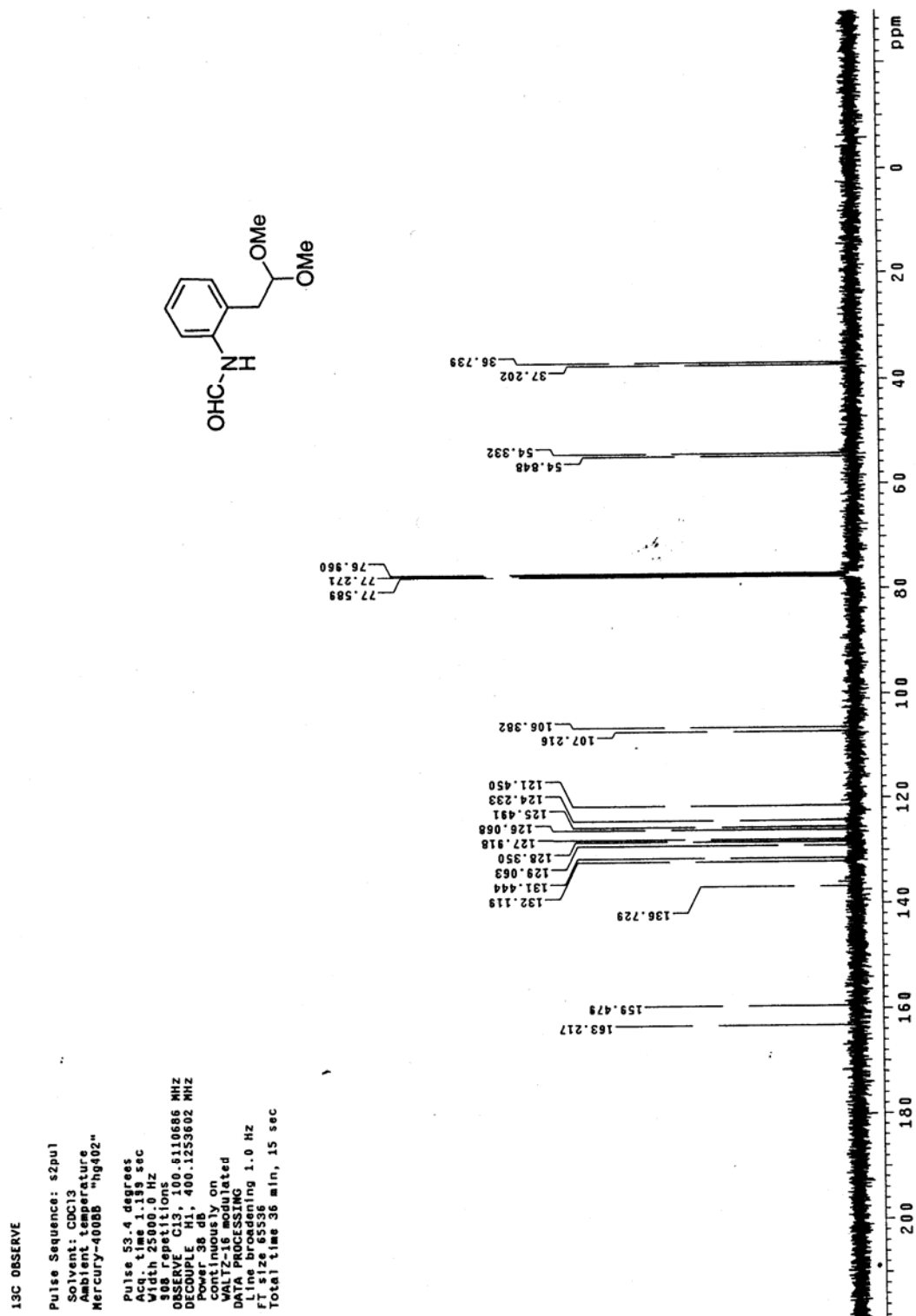
 ^{13}C OBSERVE

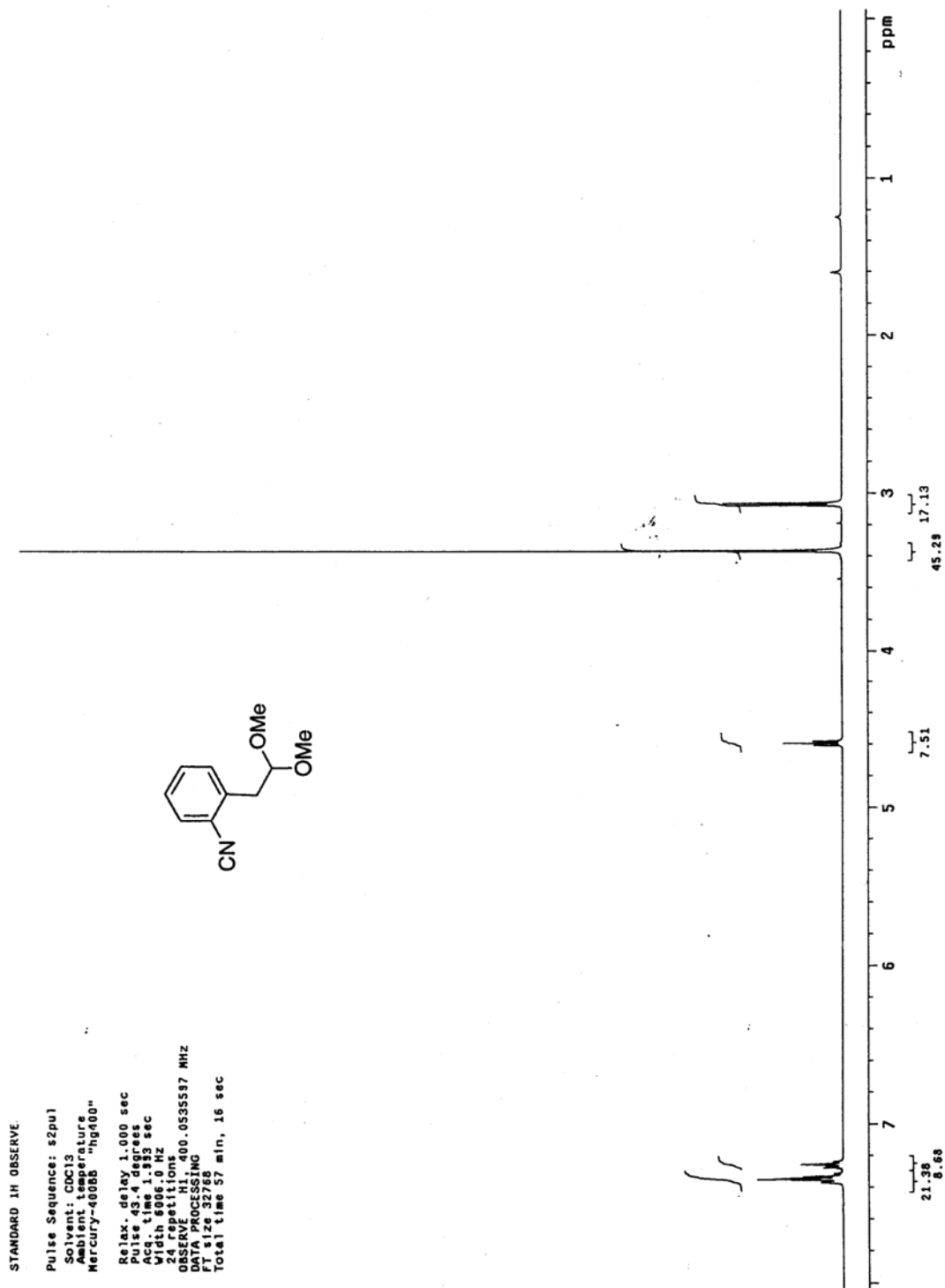
Pulse Sequence: s2pul
 Solvent: CDCl₃
 Acq. temperature
 Mercury-400BB "hg402"

Pulse 52.4 degrees
 Acq. time 1.19 sec
 Width 25000.0 Hz
 364 repetitions
 OBSERVE C13, 100.6110686 MHZ
 DECOUPLE H1, 400.1253602 MHZ
 Power 38 db
 Continuously on
 WALTZ16 pulsed
 DATA PROCESSING
 Line broadening 1.0 Hz
 FT size 65536
 Total time 1 hr, 12 min, 30 sec



¹H NMR spectrum of compound 246

¹³C NMR spectrum of compound 246

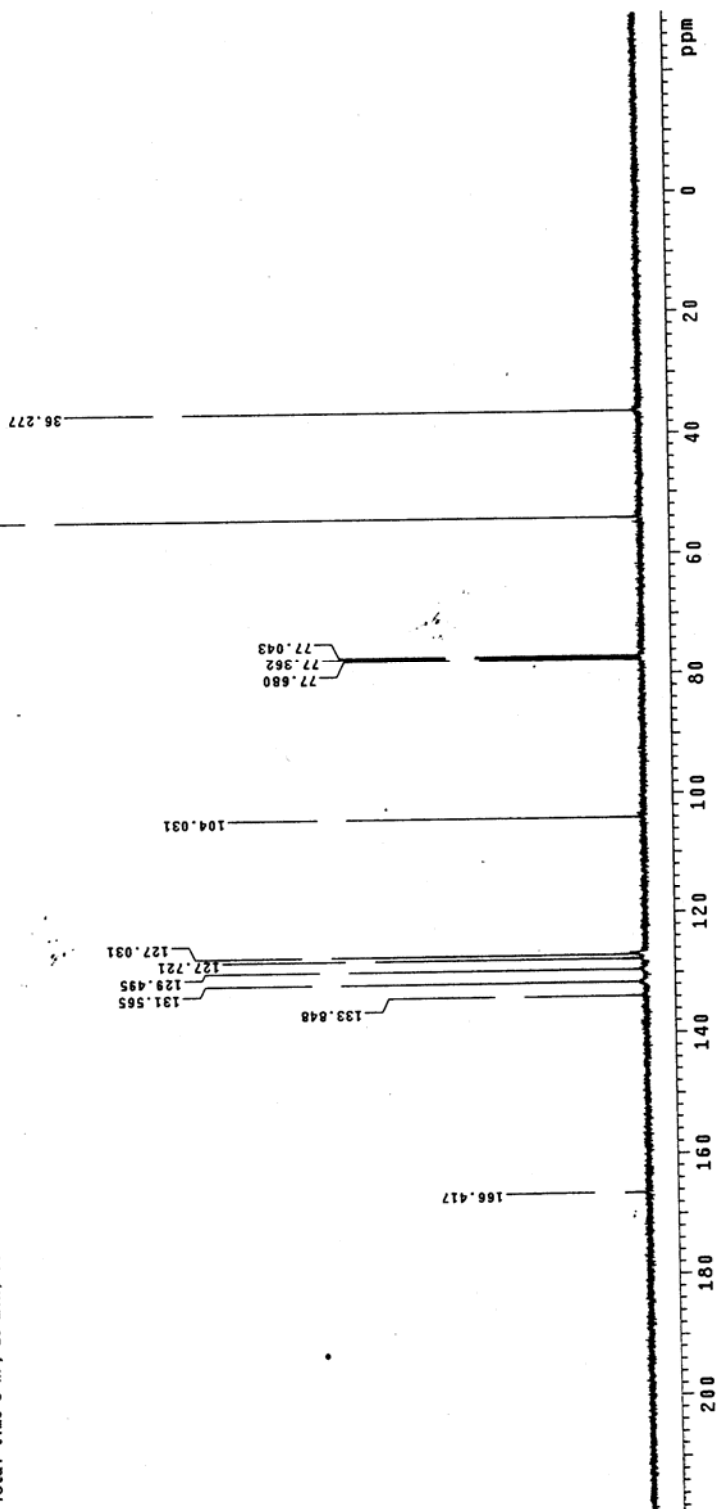
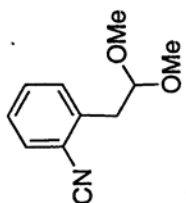
¹H NMR spectrum of compound 240

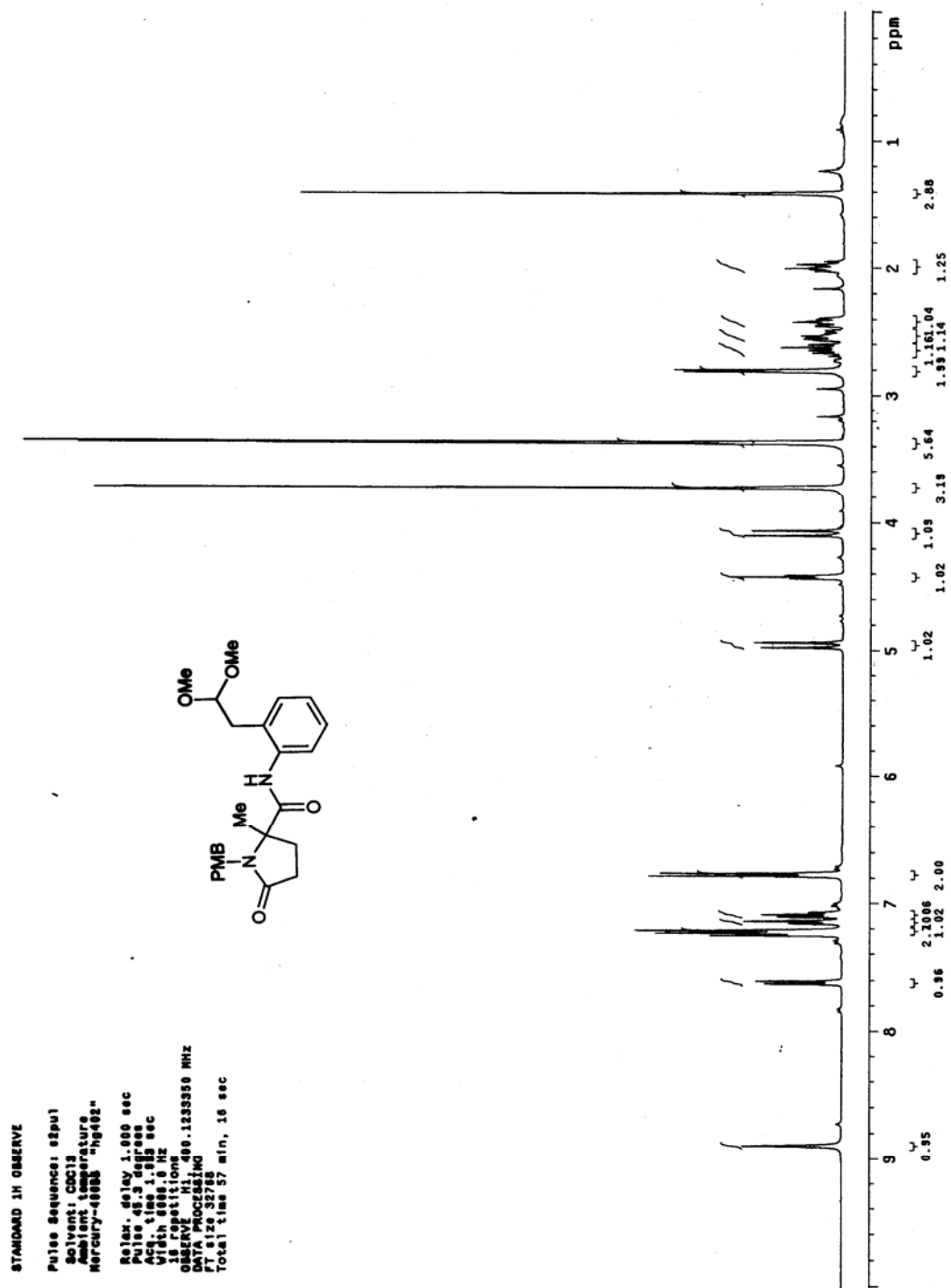
¹³C NMR spectrum of compound 240

15-min file
13C OBSERVE

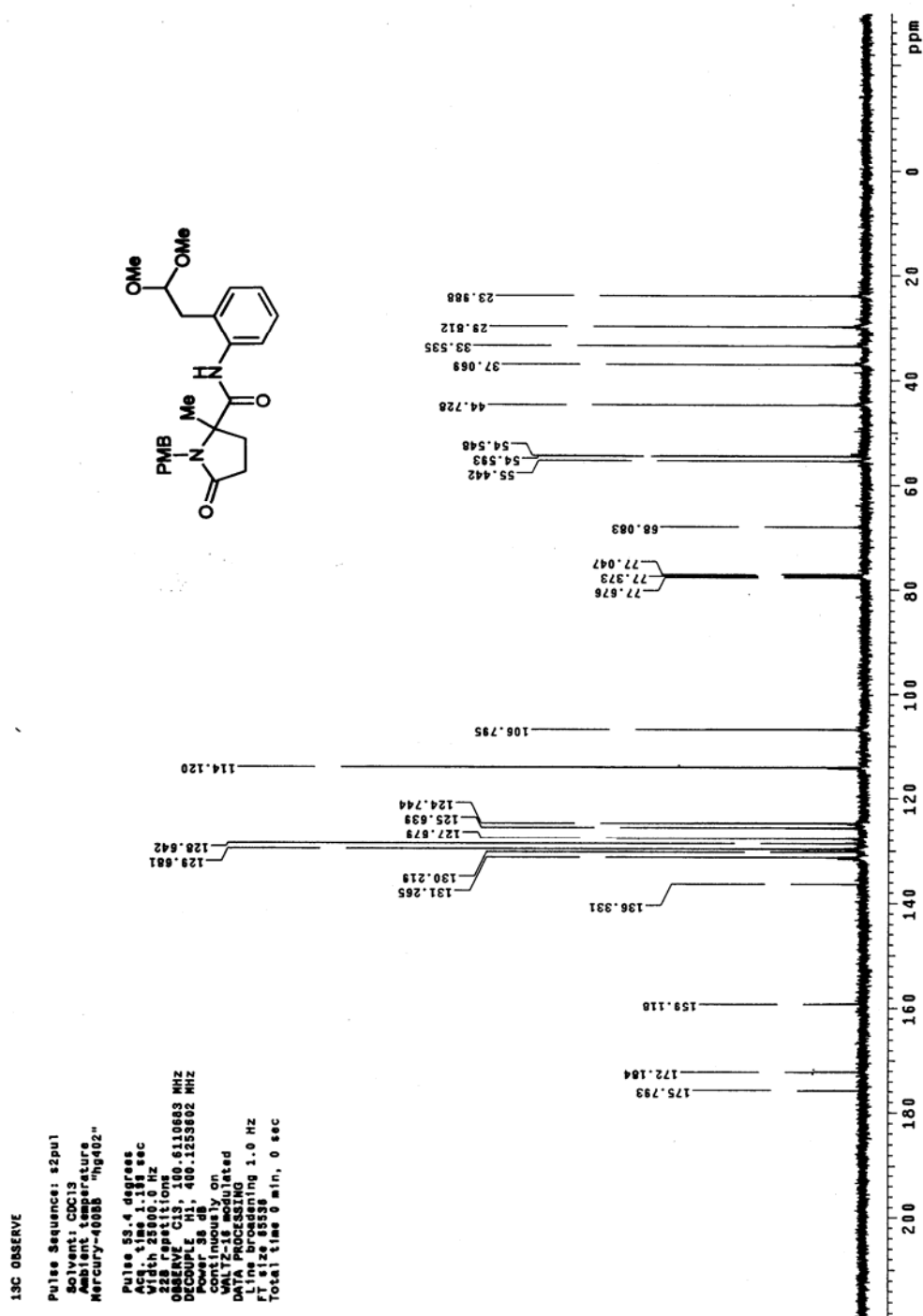
Pulse Sequence: s2pu1
Solvent: CDCl3
Ambient temperature
Mercury-4000B "hg402"

Relax. delay 4.000 sec
Pulse 53.4 degrees
Acq. time 1.199 sec
Width 25000.0 Hz
Offset 100.625000 MHz
O2 offset 100.6110686 MHz
DECOUPLE C13, 100.6110686 MHz
DECOUPLE H1, 400.1253602 MHz
Power 38 dB
continuously on
WALTZ-16 modulated
DATA PROCESSING
Line broadening 1.0 Hz
F1 size 63536
Total time 3 hr, 25 min, 50 sec

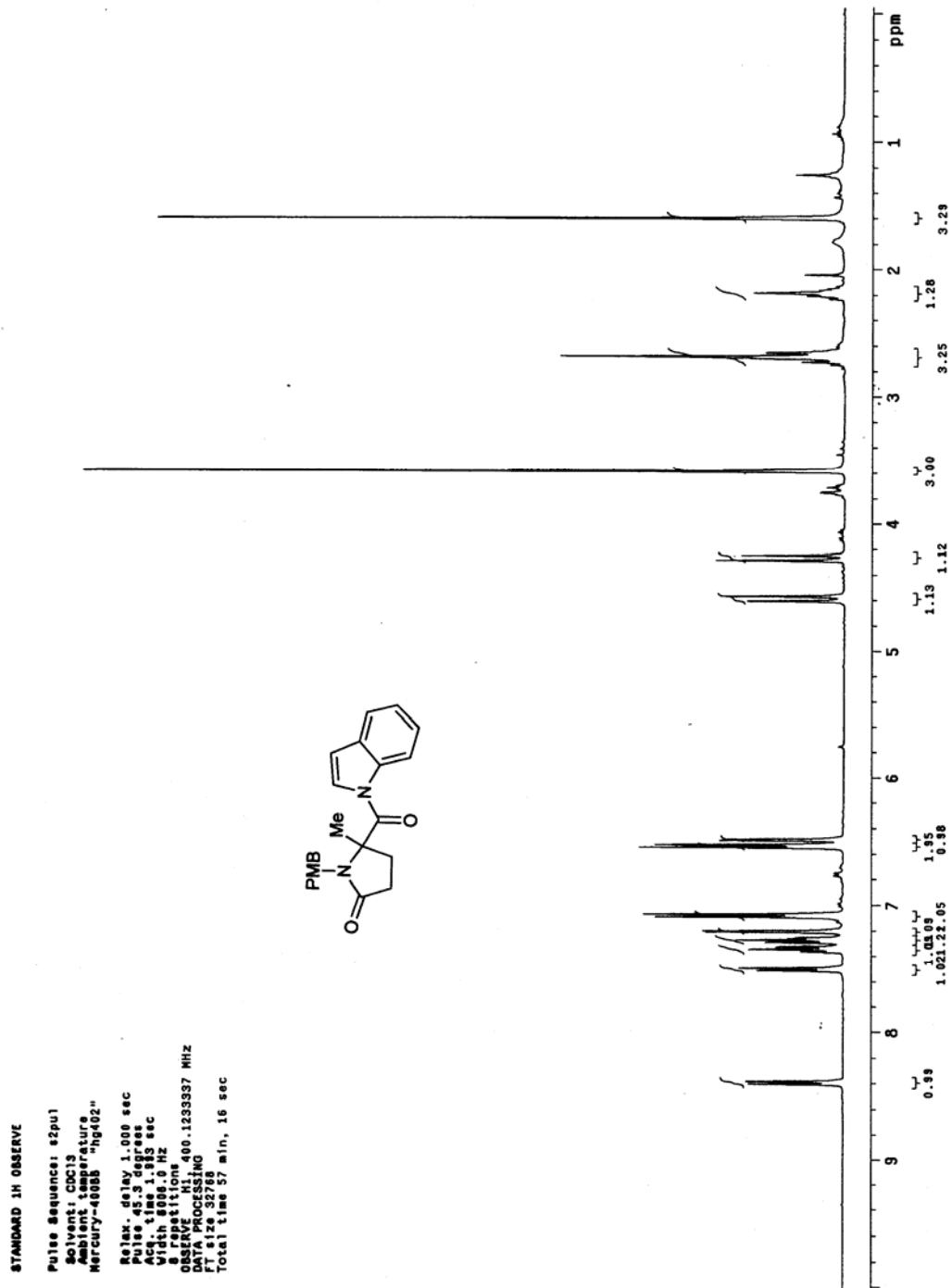


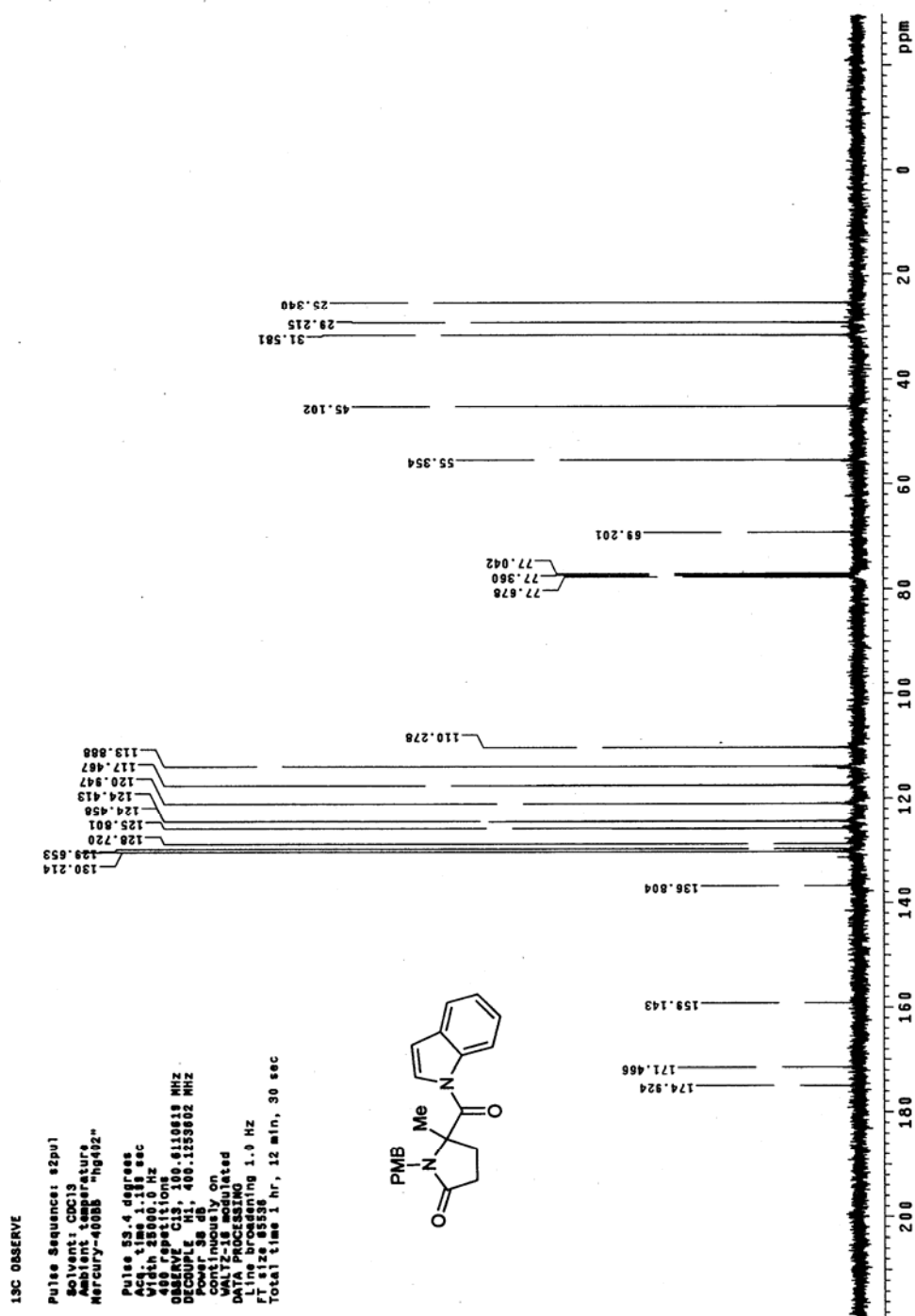
¹H NMR spectrum of compound 247

M414

^{13}C NMR spectrum of compound **247**

7E1-1142W

¹H NMR spectrum of compound 248

¹³C NMR spectrum of compound 248

¹H NMR spectrum of compound 249

STANDARD 1H OBSERVE

Pulse Sequence: s2pu1

Solvent: DMSO

Ambient temperature

Mercury-400BB "hg402"

Relax. delay: 1.000 sec

Pulse: 42.5 degrees

Acq. time: 1.000 sec

Width: 8006.0 Hz

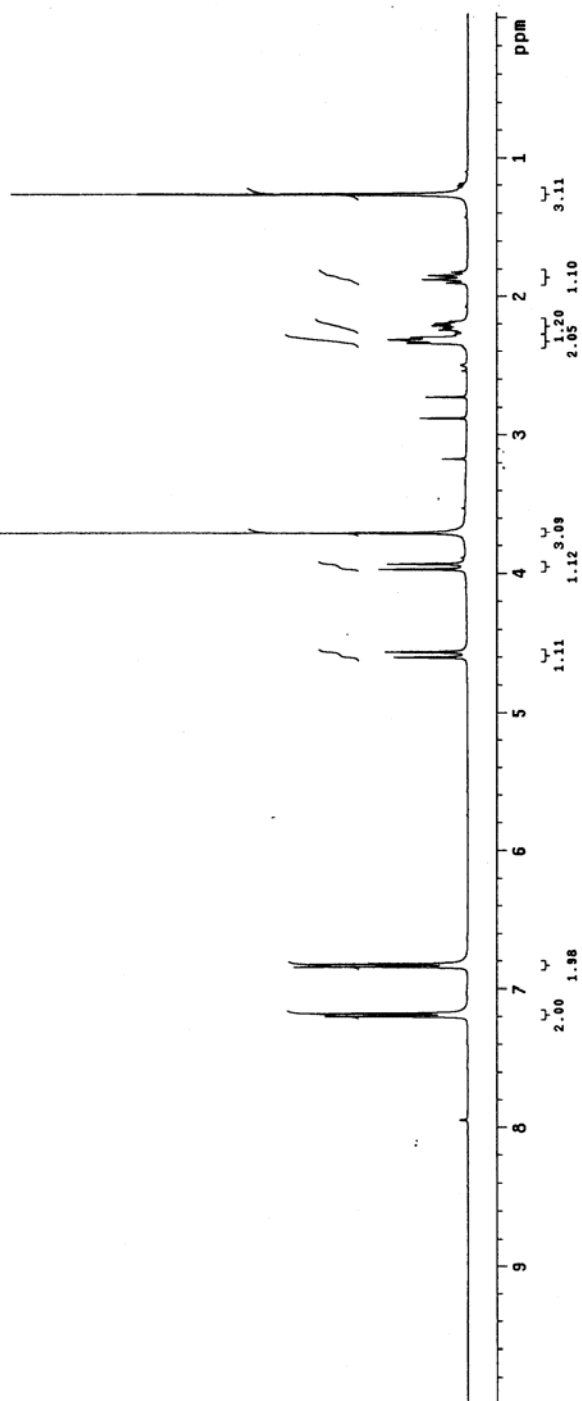
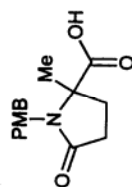
16 repetitions

OBSERVE HI: 400.1252283 MHz

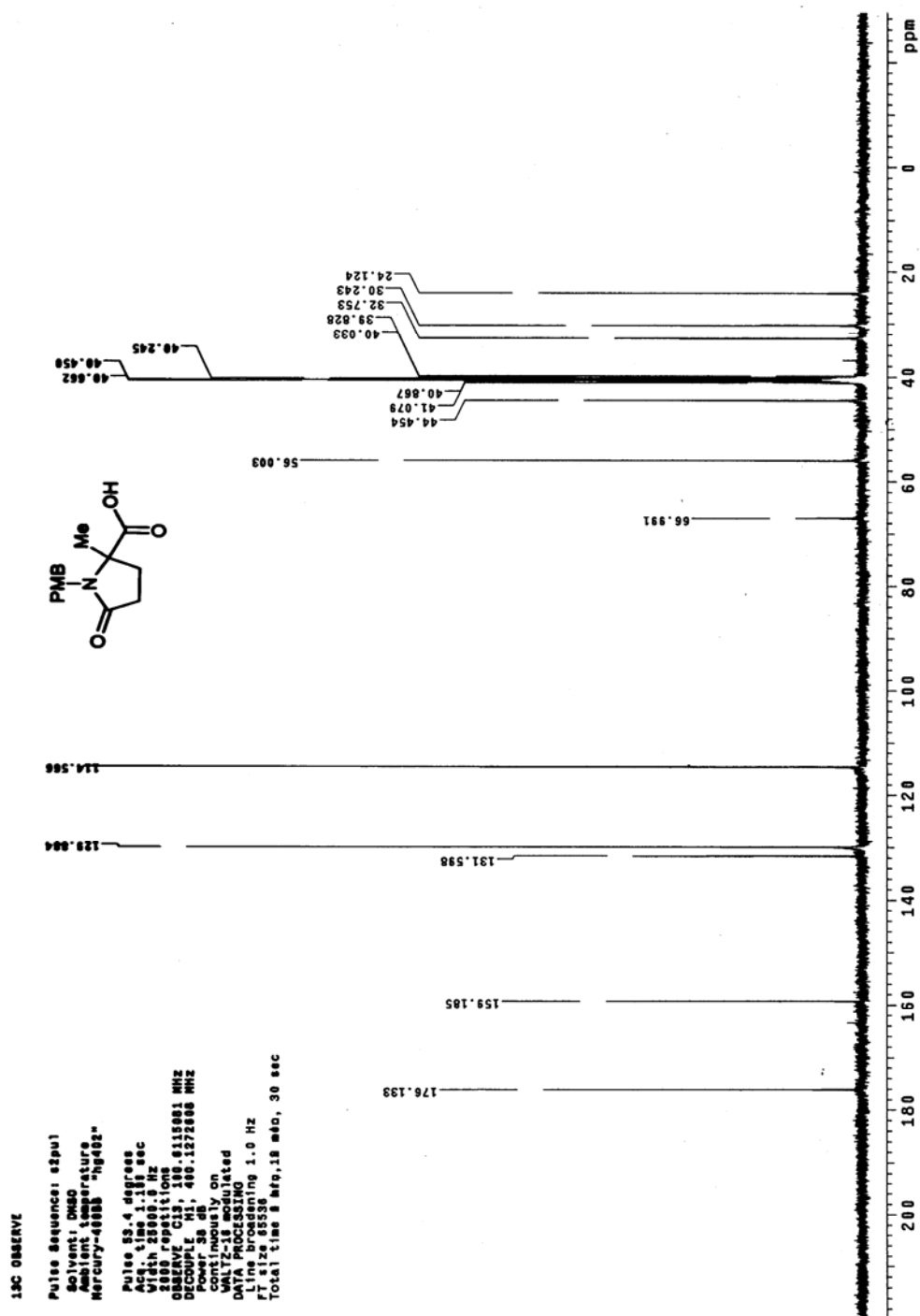
DATA PROCESSING

P1: 0.000 sec

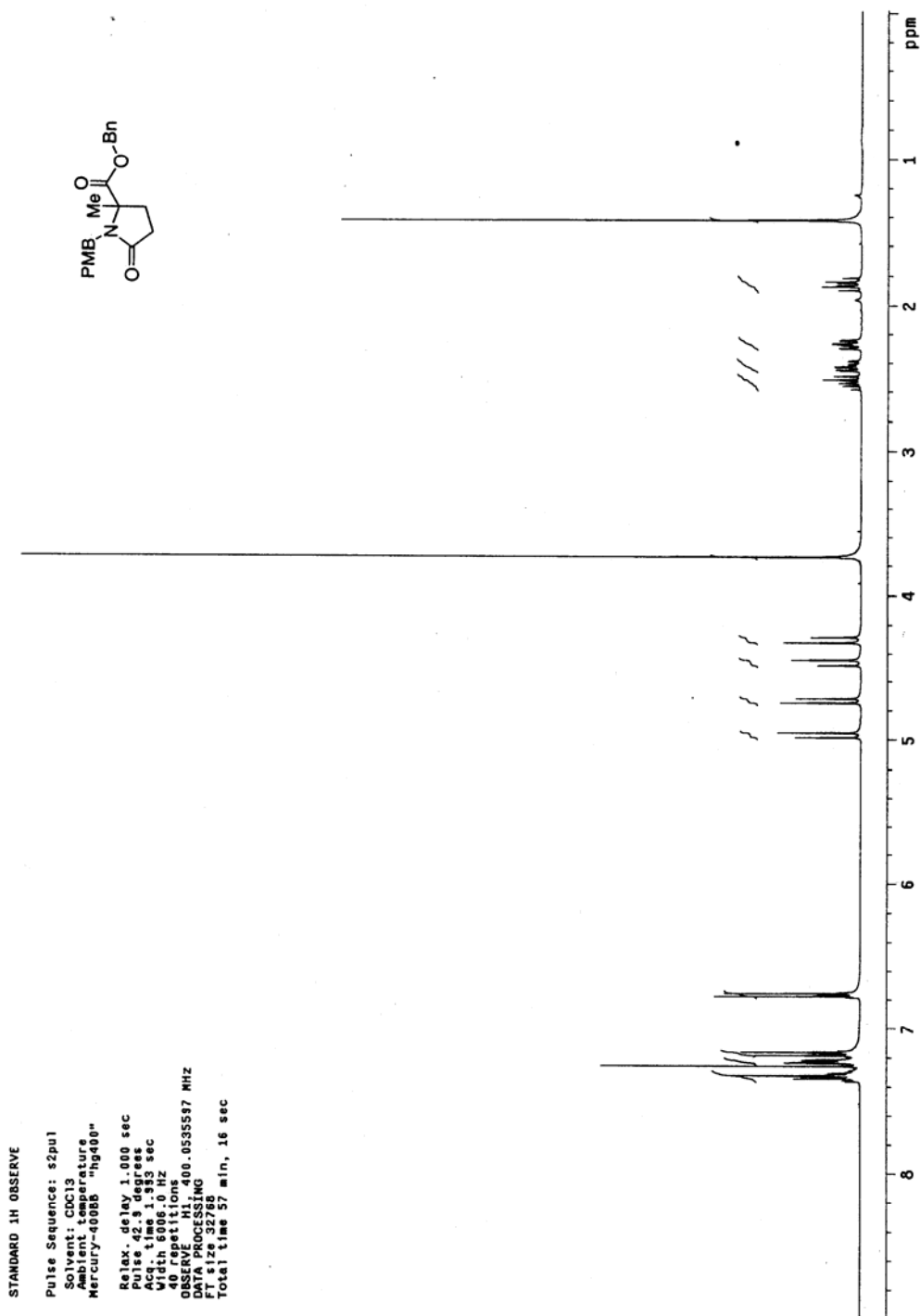
Total time: 0 min, 0 sec

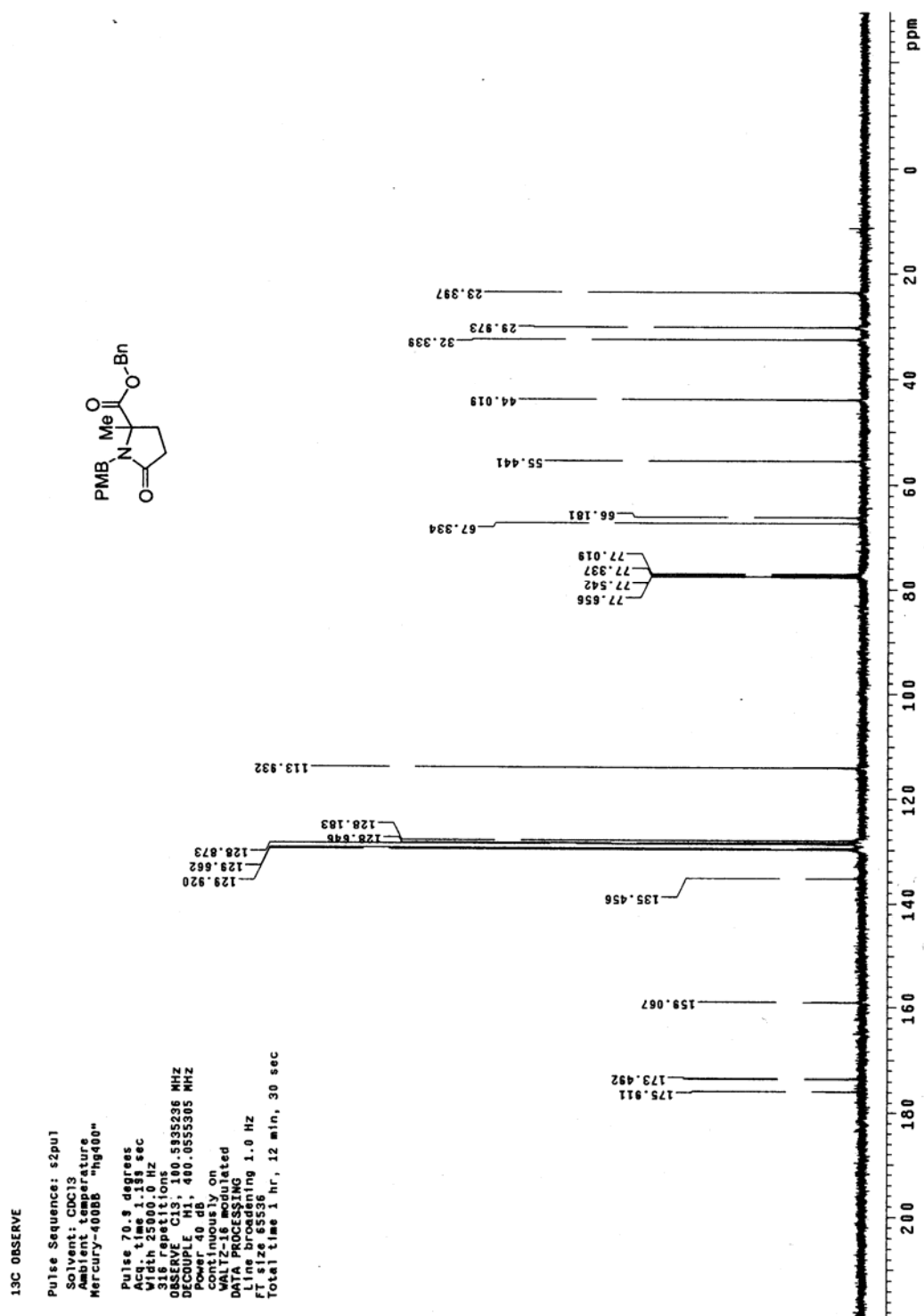


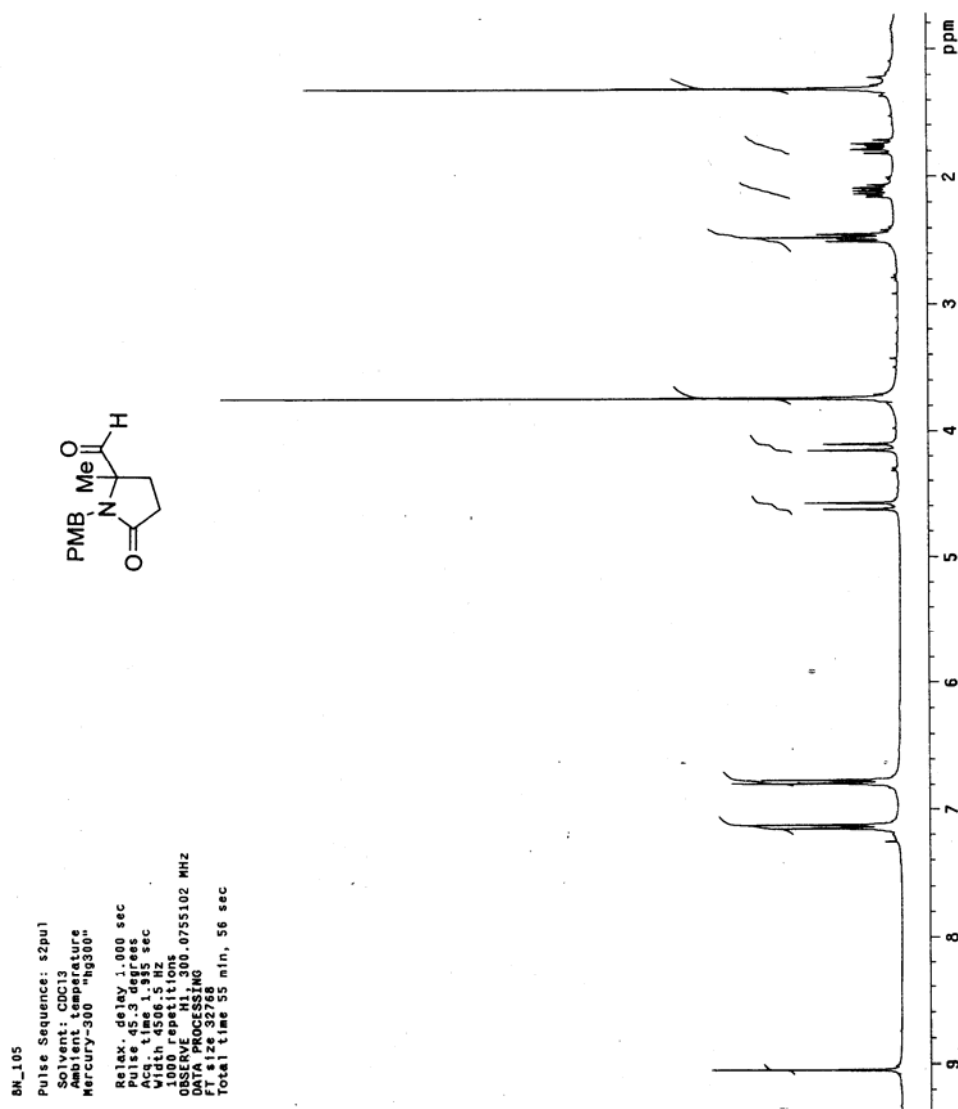
MB417

^{13}C NMR spectrum of compound 249

M8417-12-1

¹H NMR spectrum of compound **250**

^{13}C NMR spectrum of compound **250**

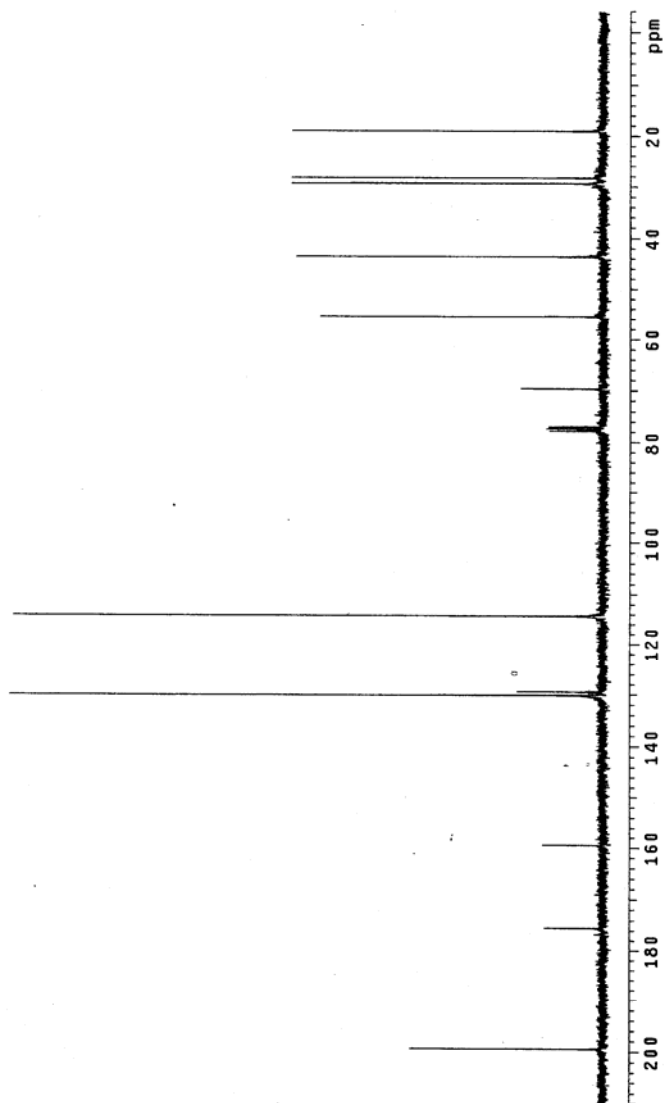
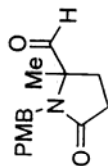
¹H NMR spectrum of compound **251**

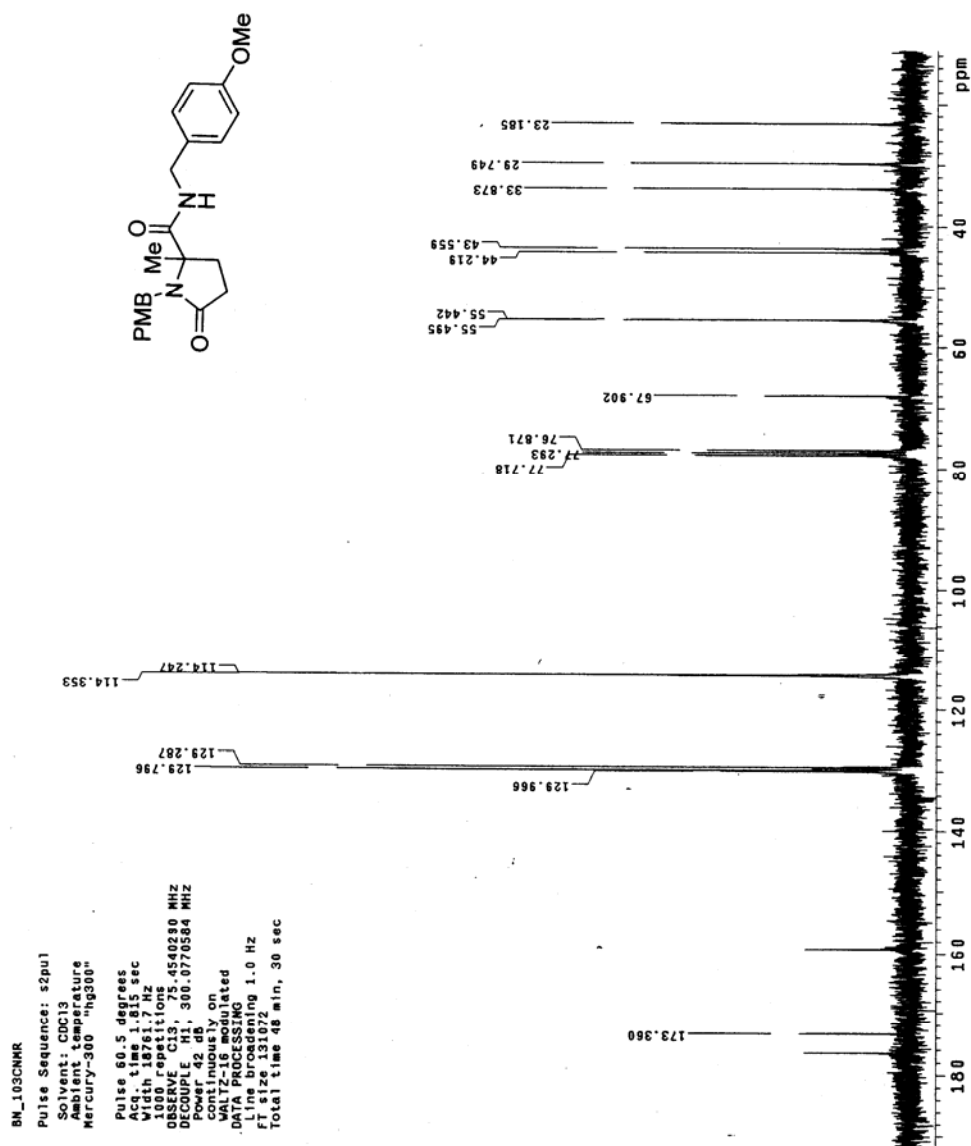
^{13}C NMR spectrum of compound **251**

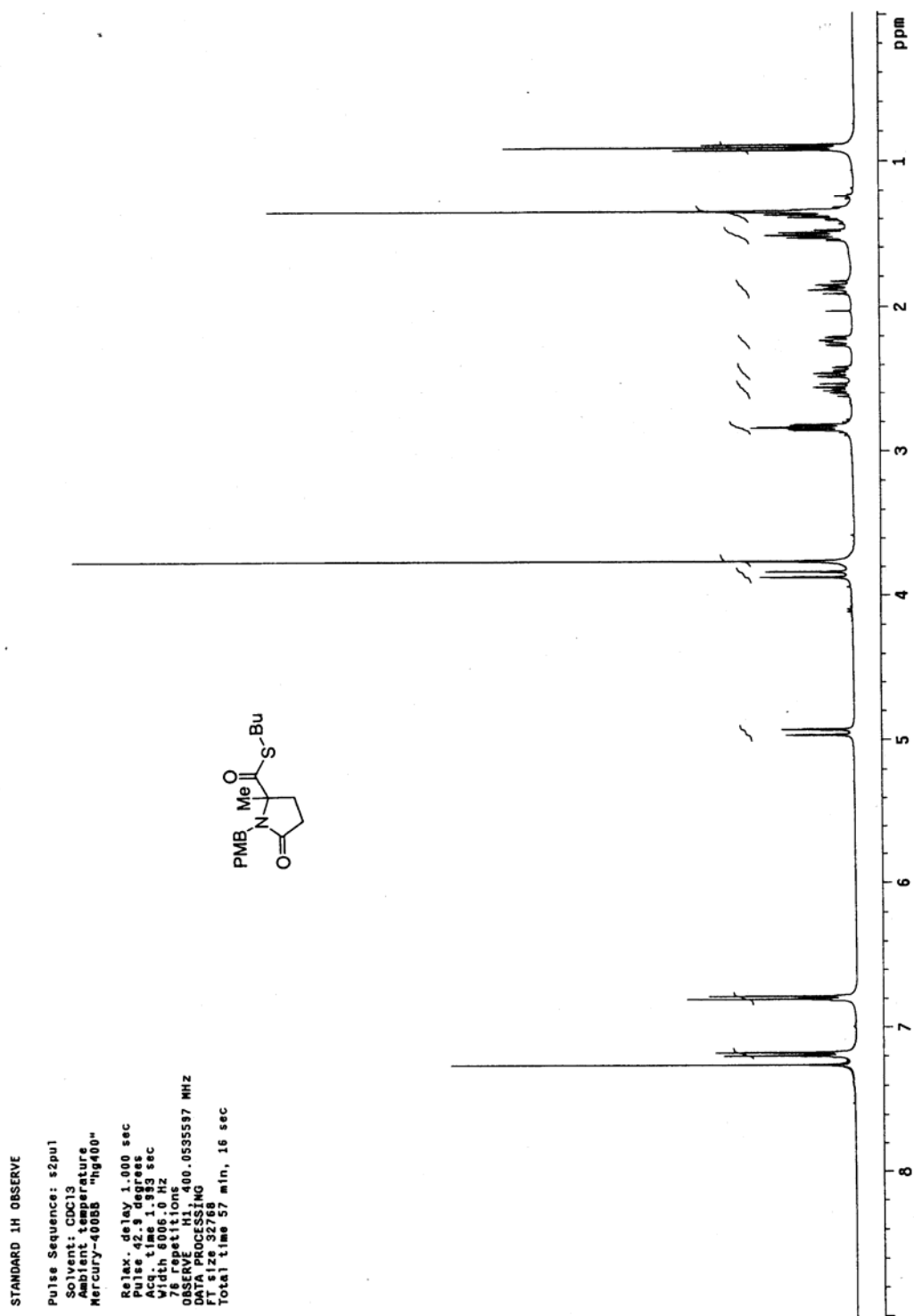
BN_105CMR

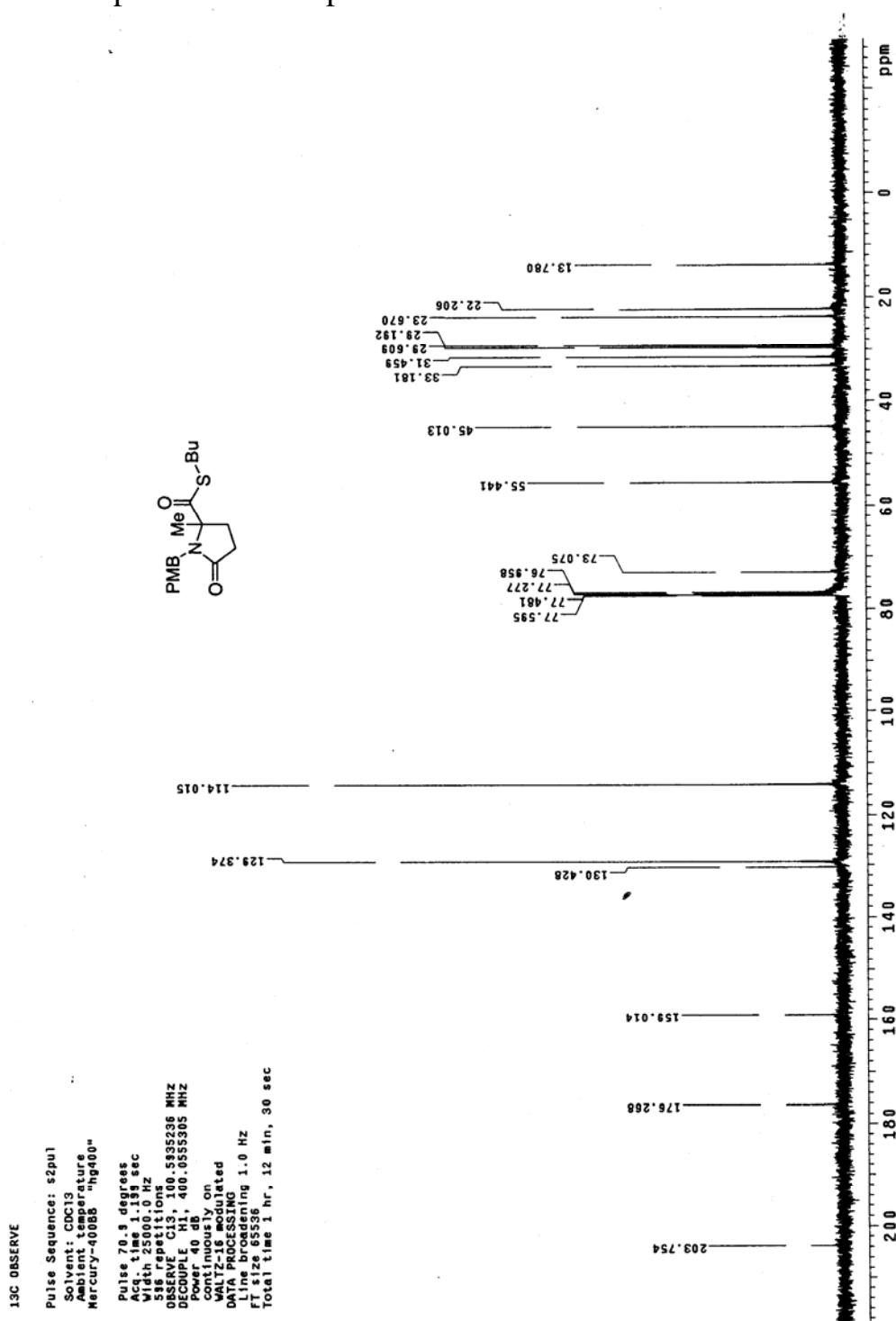
Pulse Sequence: s2pul
Solvent: CDCl₃
Ambient temperature
Mercury-300 "hg300"

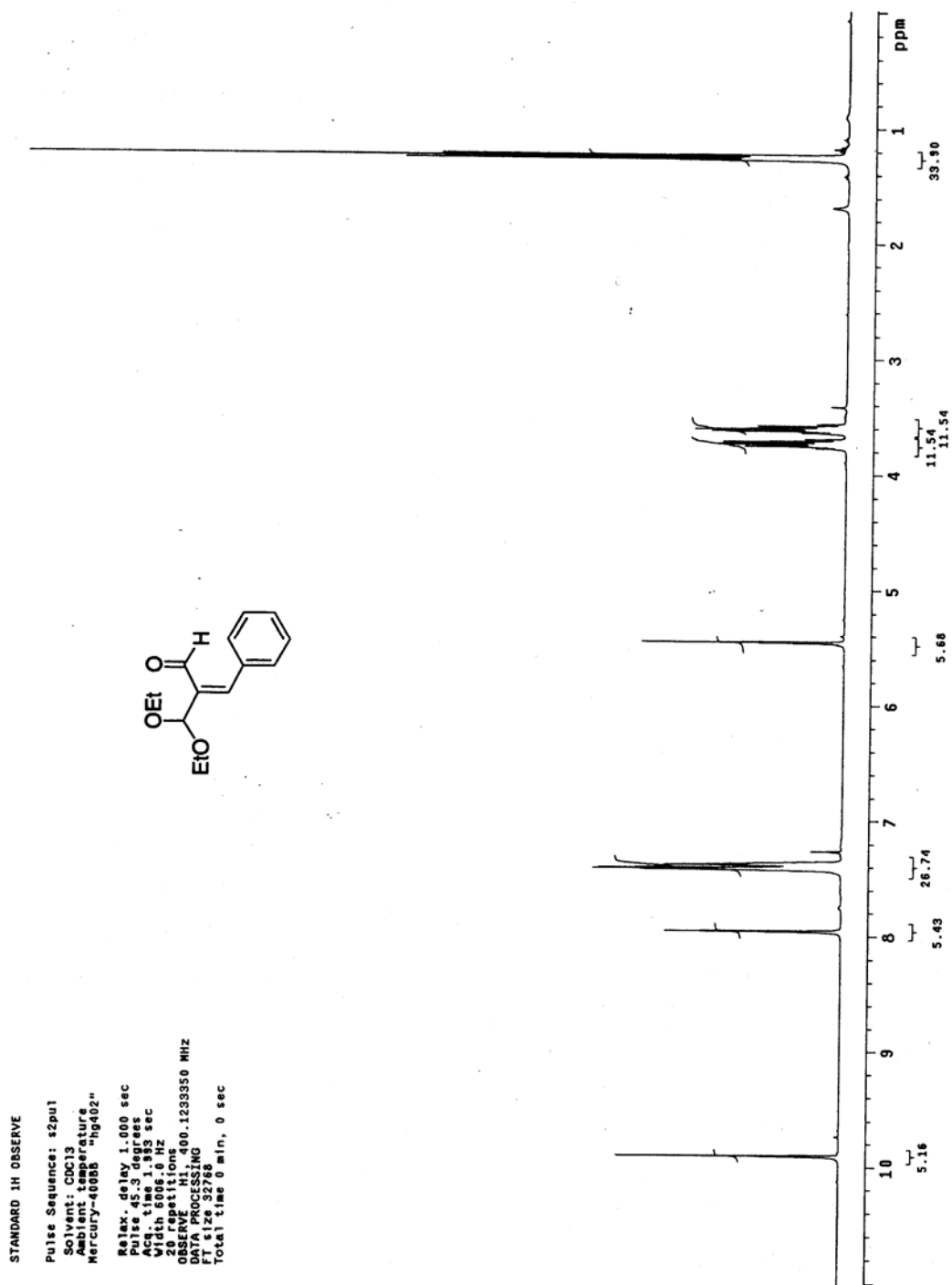
Pulse 60.5 degrees
Acq. time 1.515 sec
Date_ 11-11-82
280 repetitions
OBSERVE C13, 75.4540290 MHZ
DECOUPLE H1, 300.0770584 MHZ
Power 42 db
Gate: On
WALTZ-16 modulated
DATA PROCESSING
Line broadening 1.0 Hz
F1 size 131072
Total time 0 min, 0 sec

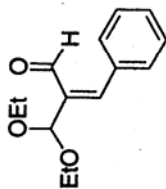


^{13}C NMR spectrum of compound **252**

¹H NMR spectrum of compound 253

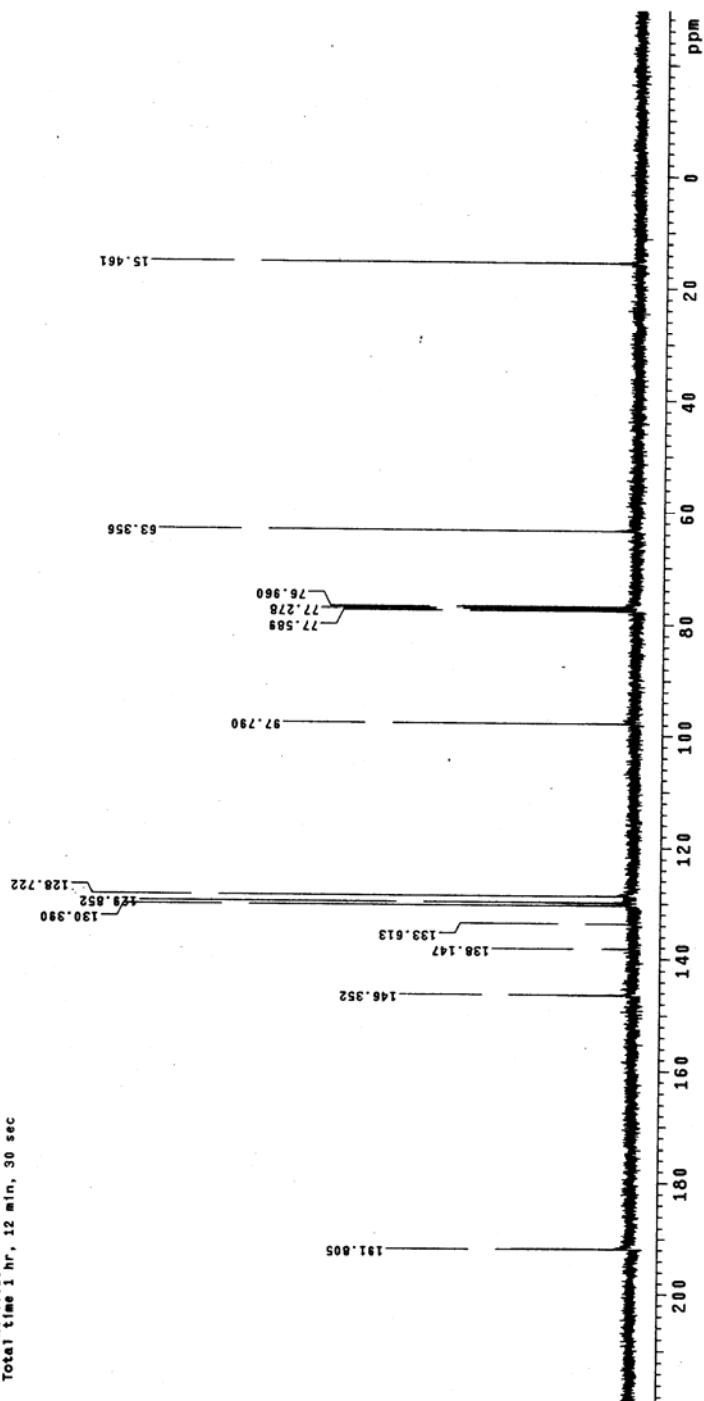
¹³C NMR spectrum of compound 253

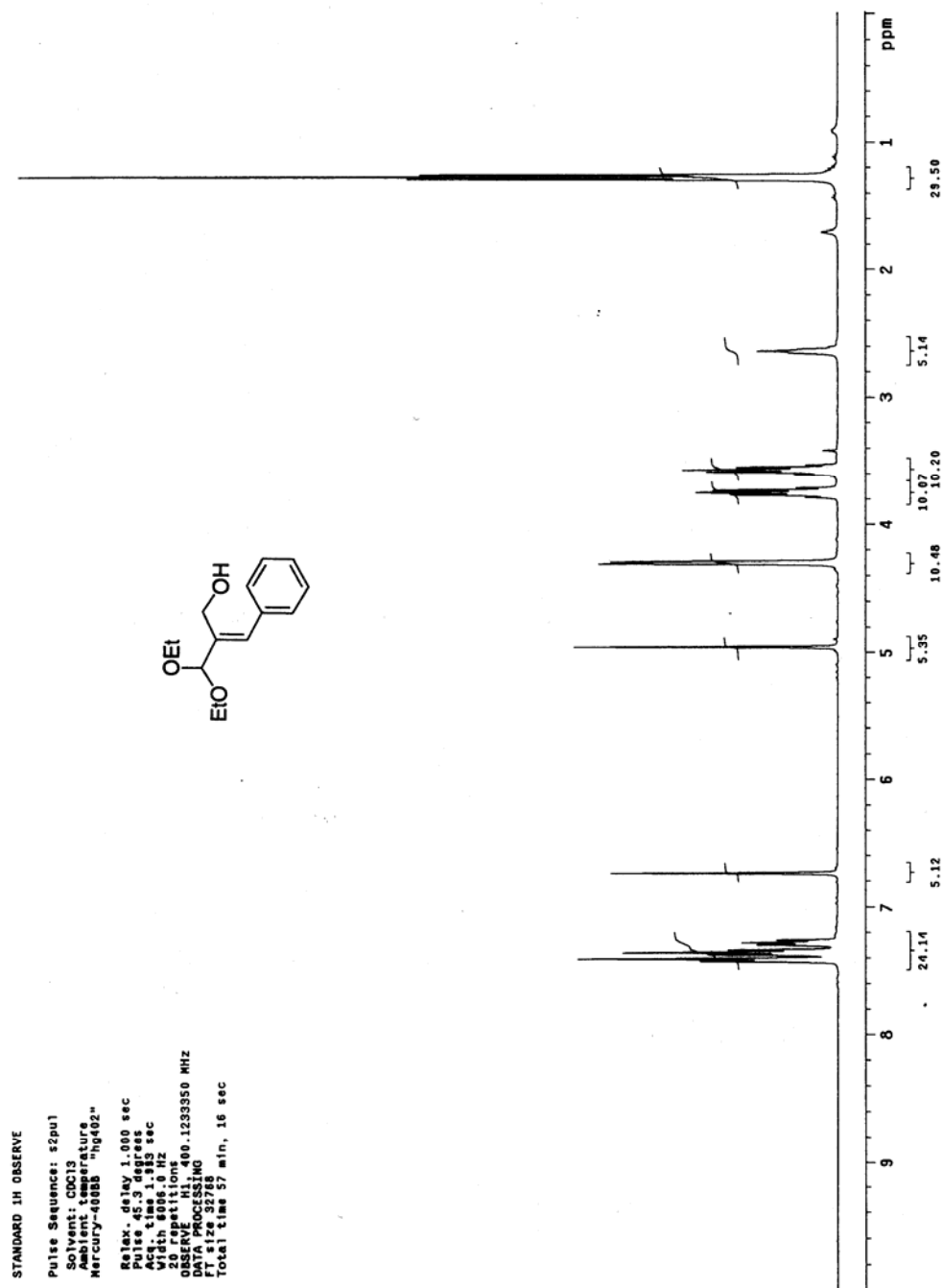
¹H NMR spectrum of compound 289

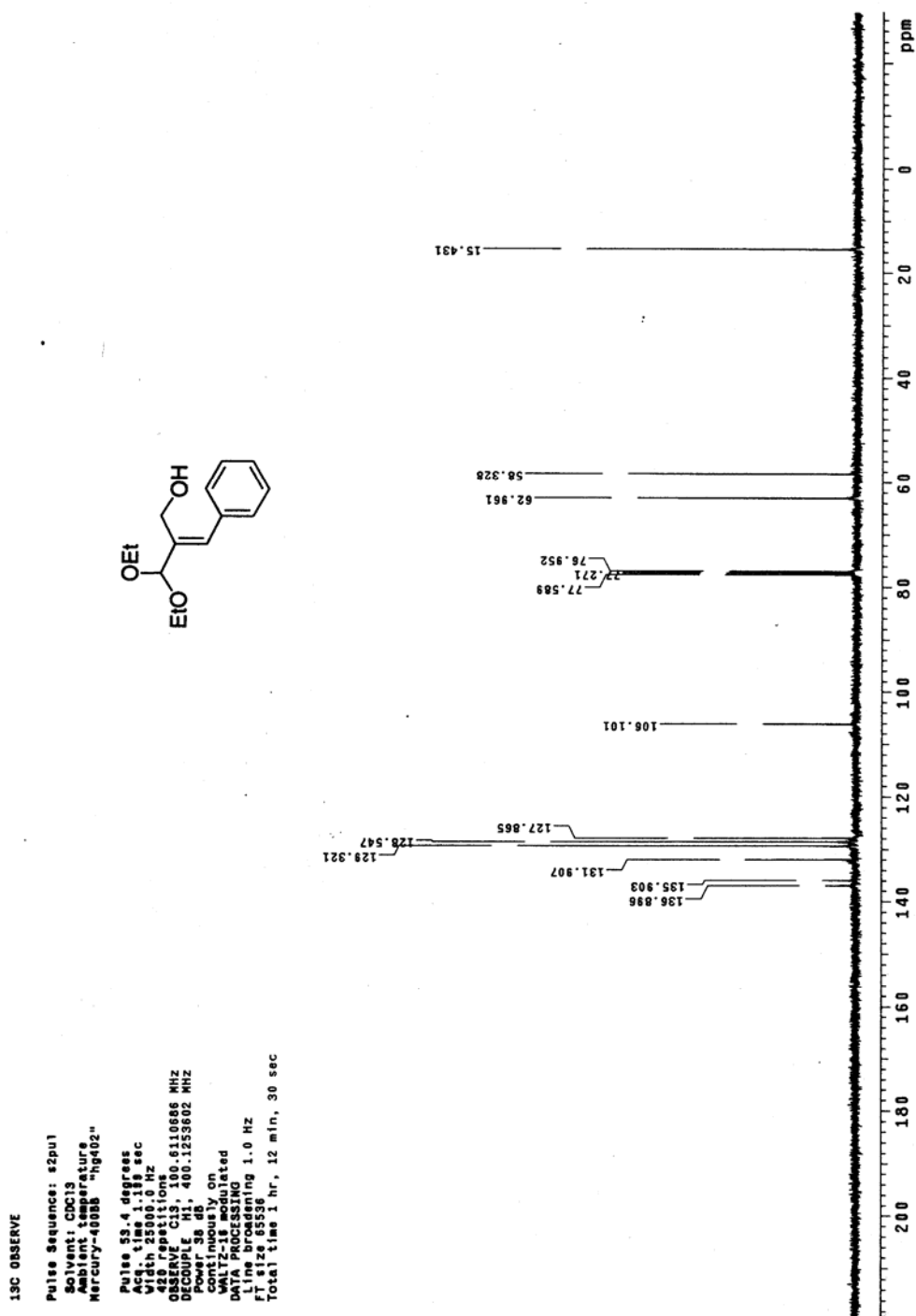
^{13}C NMR spectrum of compound 289

^{13}C OBSERVE

Pulse Sequence: s2pu1
 Solvent: CDCl3
 Ambient temperature
 Mercury-40085 "hg402"
 Pulse 53.4 degrees
 Wdth 1.10 sec
 Wdth 1.10 sec
 378 repetitions
 OBSERVE C13, 100.6110886 MHZ
 DECOUPLE H1, 400.1253802 MHZ
 Power 38. dB
 Continually On
 WAIT 15.000 sec
 DATA PROCESSING
 Line broadening 1.0 Hz
 FT size 65536
 Total time 1 hr, 12 min, 30 sec



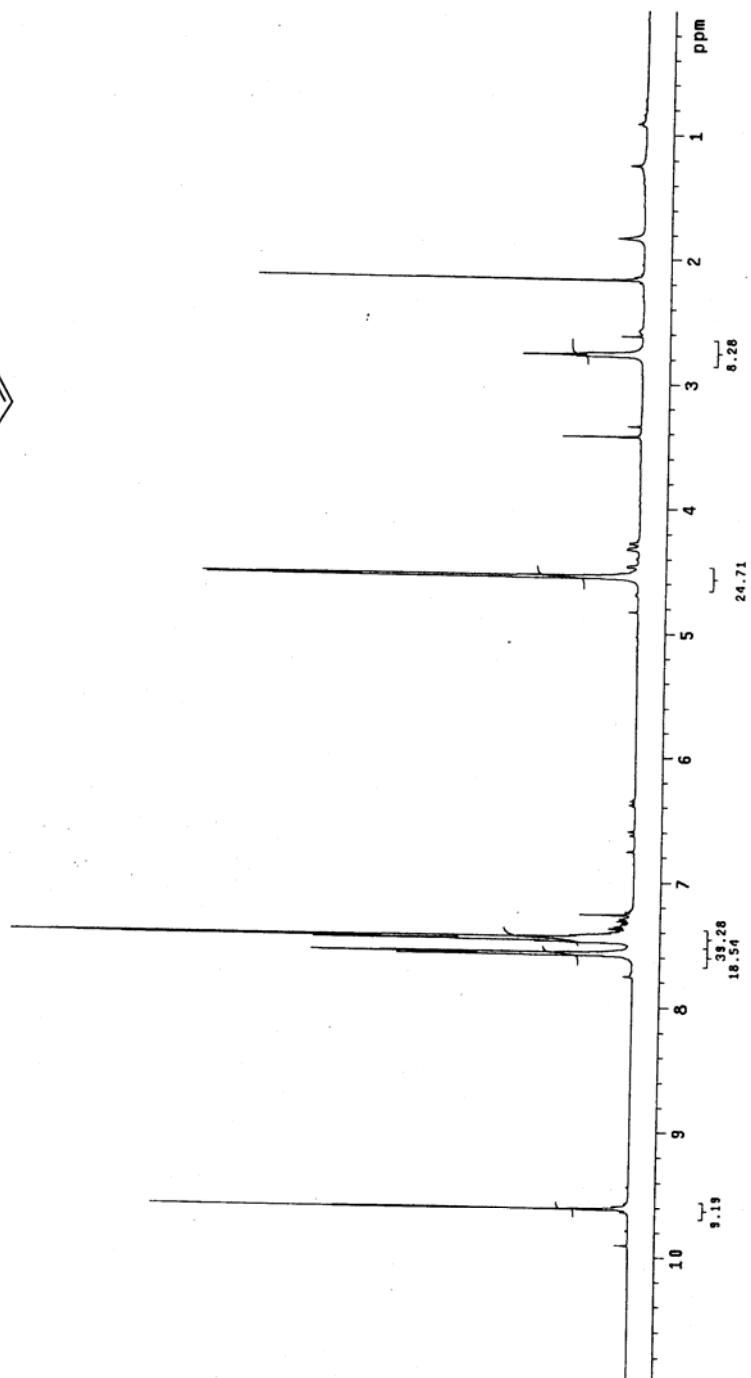
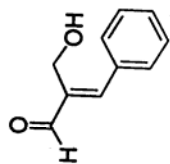
¹H NMR spectrum of compound **290**

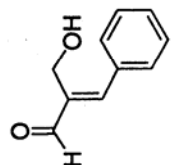
¹³C NMR spectrum of compound **290**

¹H NMR spectrum of compound 276

STANDARD PROTON PARAMETERS
Pulse Sequence: s2pul
Solvent: CDCl3
Temp: 25.0 C / 298.1 K
UNITY-500 "un500"

Pulse 51.5 degrees
Acq. time 1.892 sec
SFO 300.135000 MHz
38 channels
OBSERVE H1 500.3087850 MHz
DATA PROCESSING
Line broadening 0.3 Hz
F2 size 32736
Total time 31 min, 42 sec

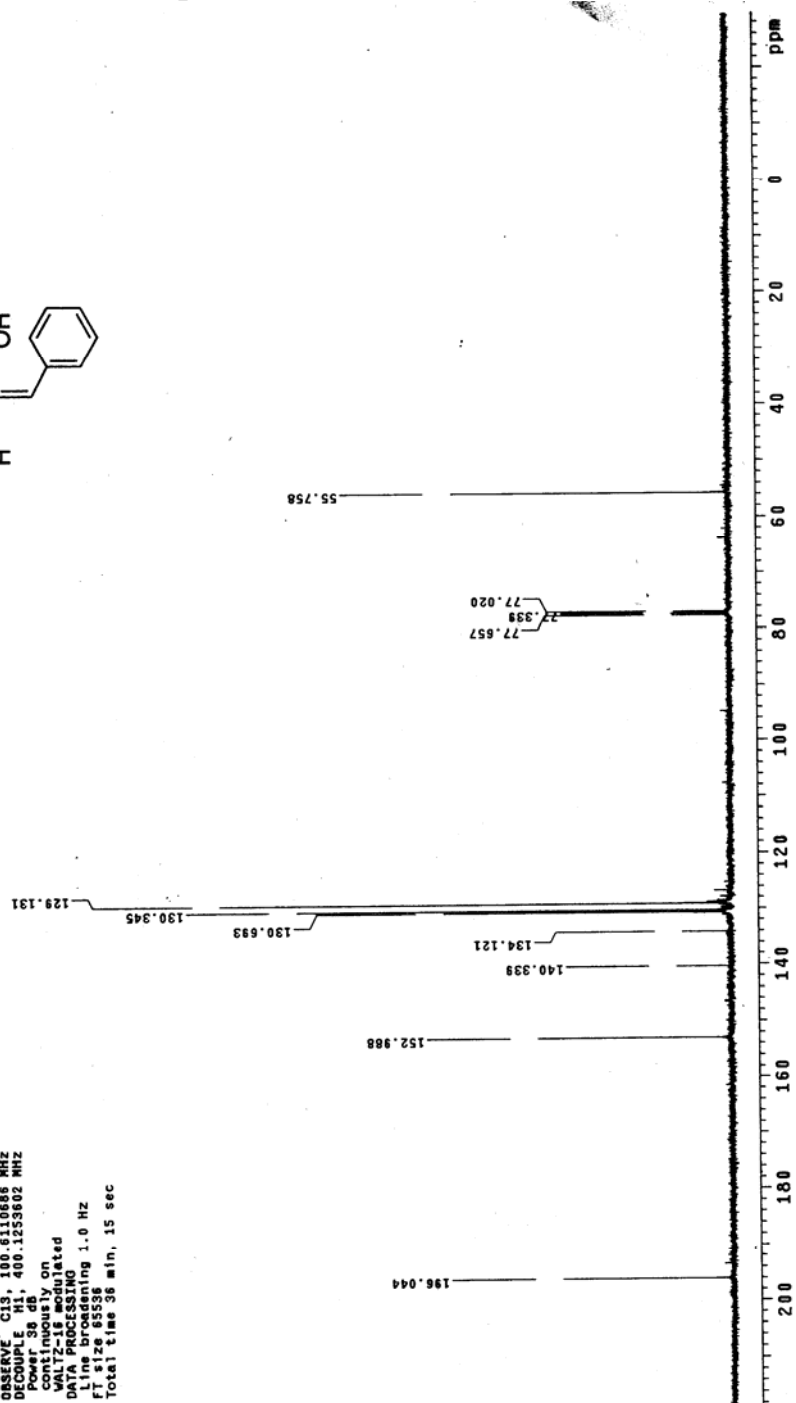


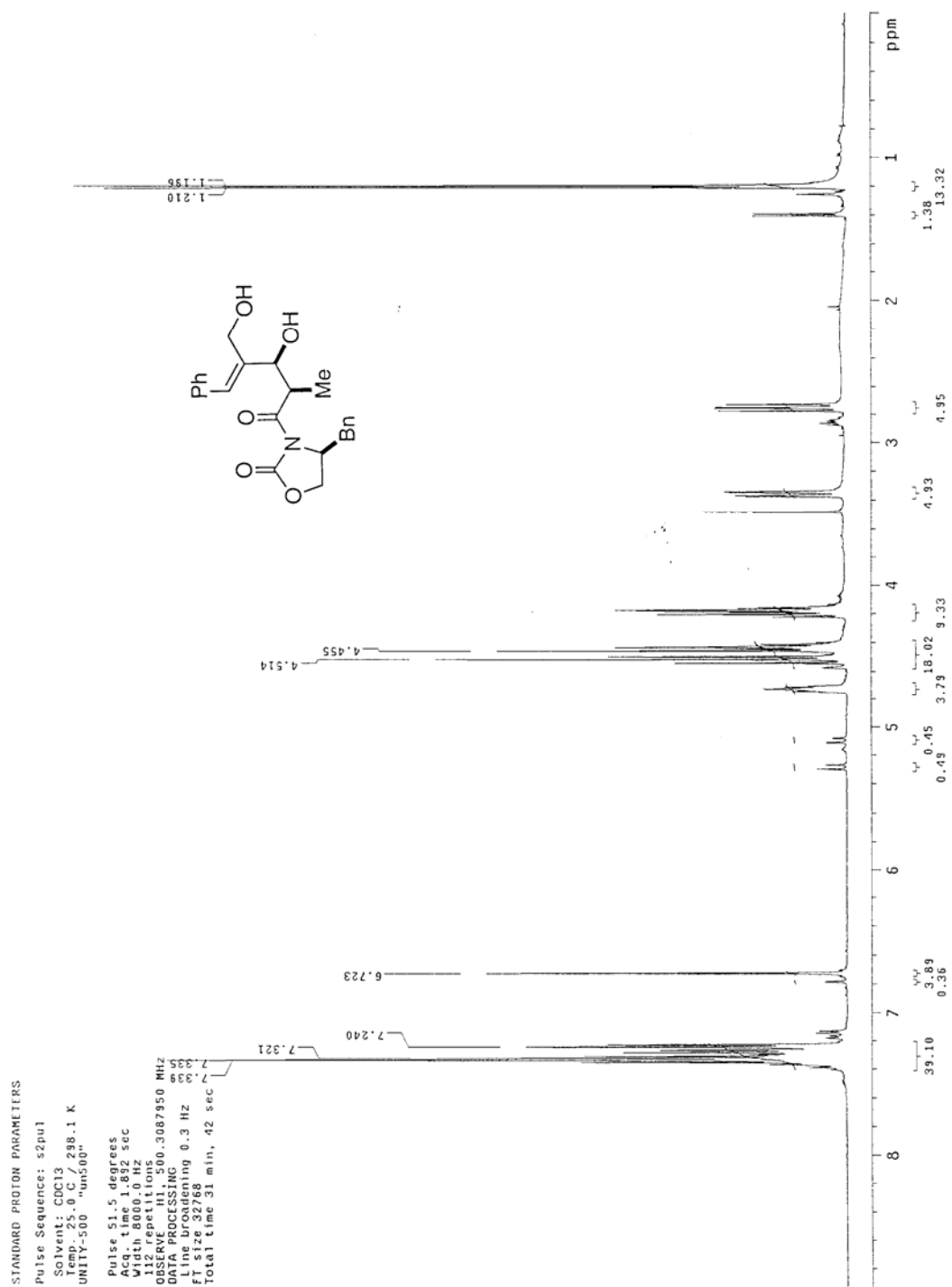
¹³C NMR spectrum of compound 276

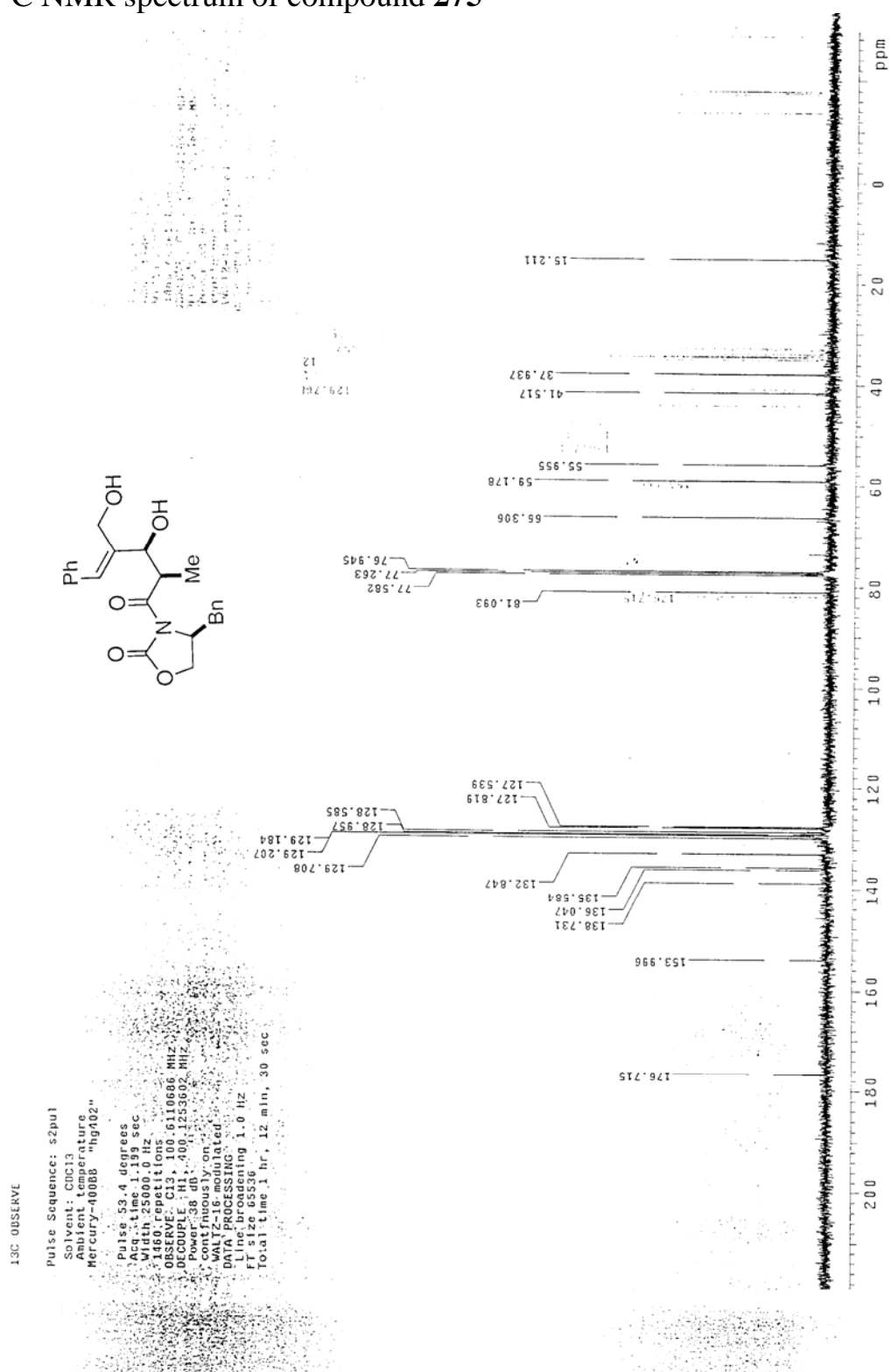
¹³C OBSERVE

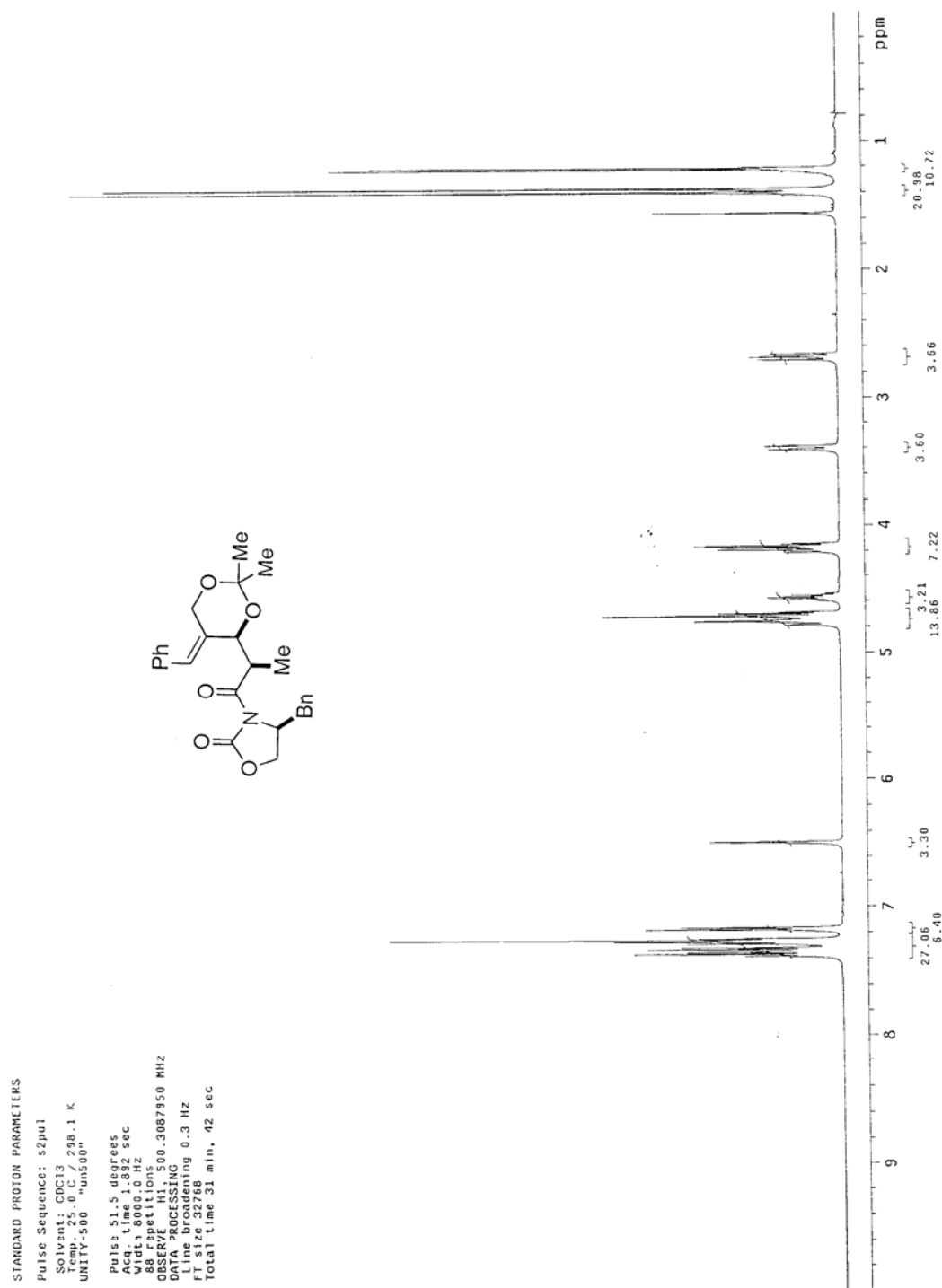
Pulse Sequence: s2pu1
 Solvent: CDCl3
 Ambient temperature
 Mercury-4000B "hg402"

Pulse 53.4 degrees
 Width 2500.0 Hz
 152 repetitions
 OBSERVE C13, 100.6110686 MHz
 DECOUPLE H1, 400.1253602 MHz
 Continuously on
 WALTZ-16 modulated
 DATA PROCESSING
 Line broadening 1.0 Hz
 FI size 6558
 Total time 38 min, 15 sec



¹H NMR spectrum of compound **275**

^{13}C NMR spectrum of compound **275**

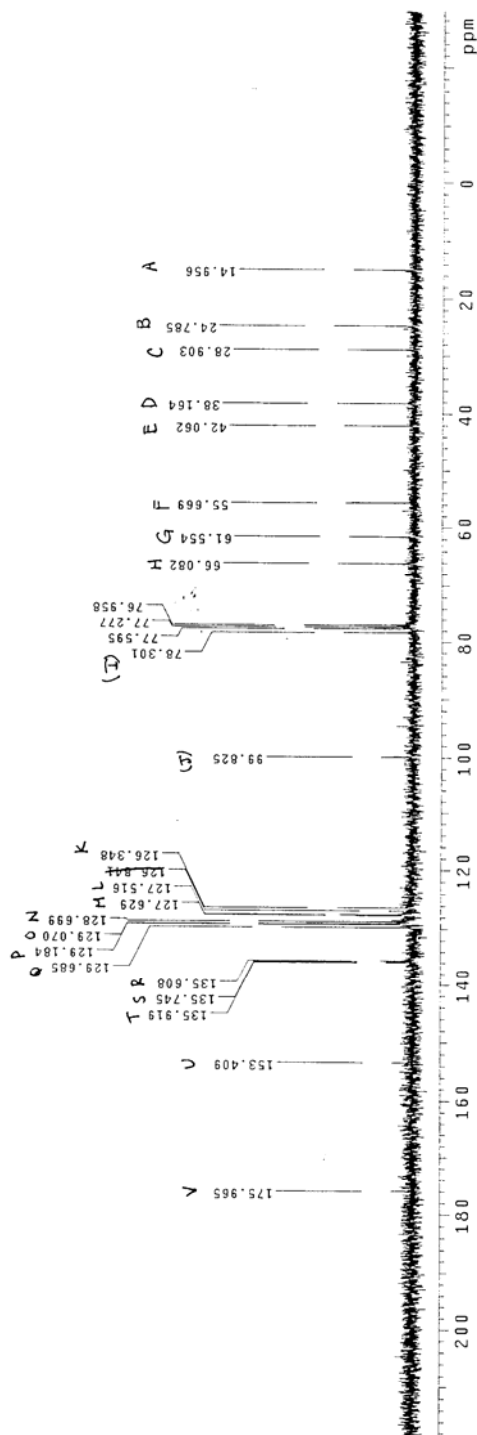
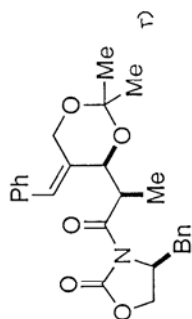
^1H NMR spectrum of compound **291**

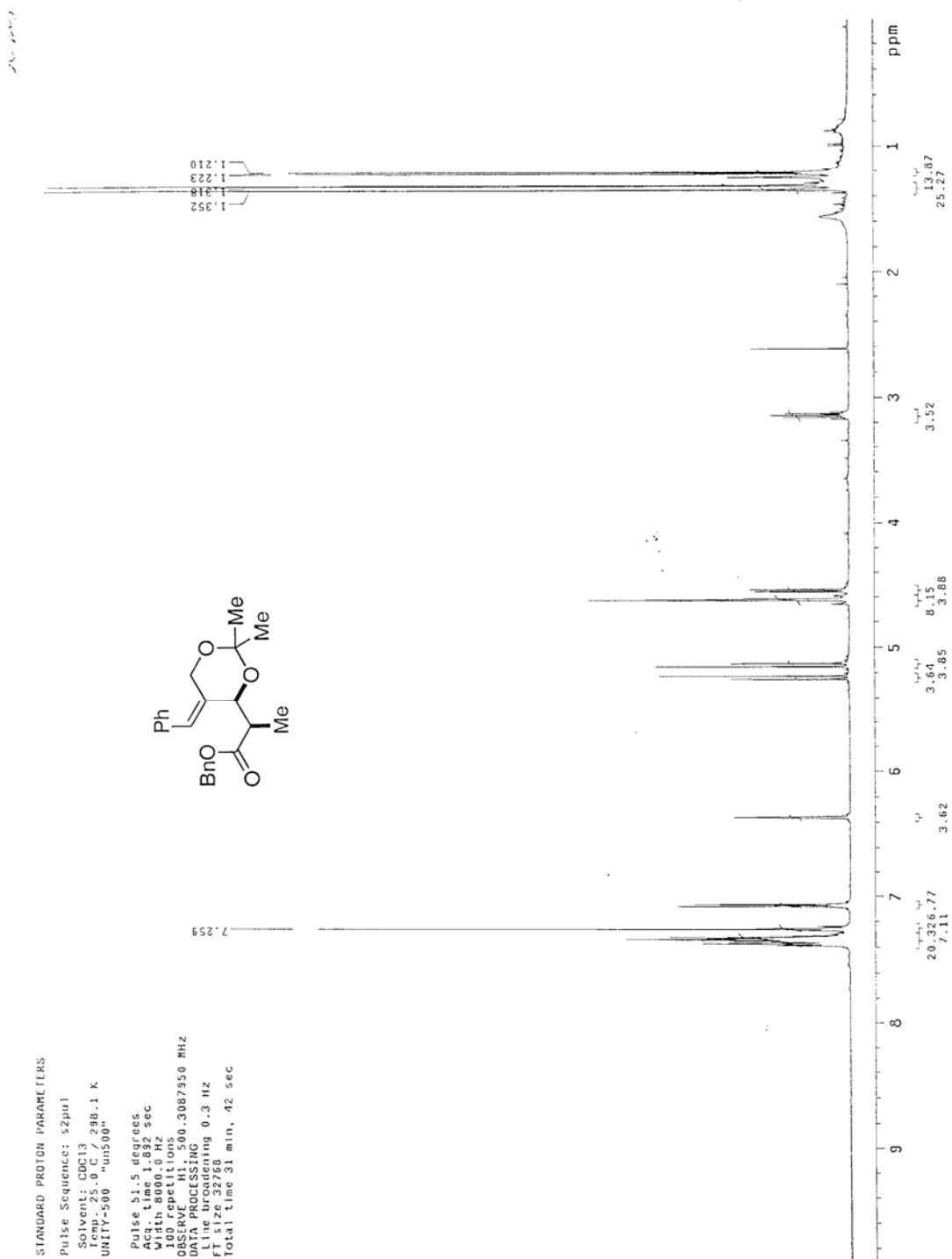
^{13}C NMR spectrum of compound **291**

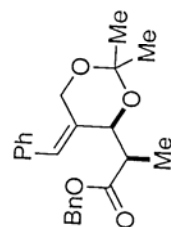
^{13}C OBSERVE

Pulse Sequence: s2pu1
 Solvent: CDCl3
 Ambient Temperature
 Mercury-400B5 "hg400"

Pulse 53.4 degrees
 Acc. time 1.199 sec
 Width 25000.0 Hz
 Frequency 101.626 MHz
 OBSERVE CH 13
 DECOUPLE H1 400.0555305 MHz
 Power 42 dB
 continuously on
 WALTZ-16 modulated
 DATA PROCESSING
 F1 size 65536
 F2 size 65536
 Total time 1 hr, 12 min, 30 sec

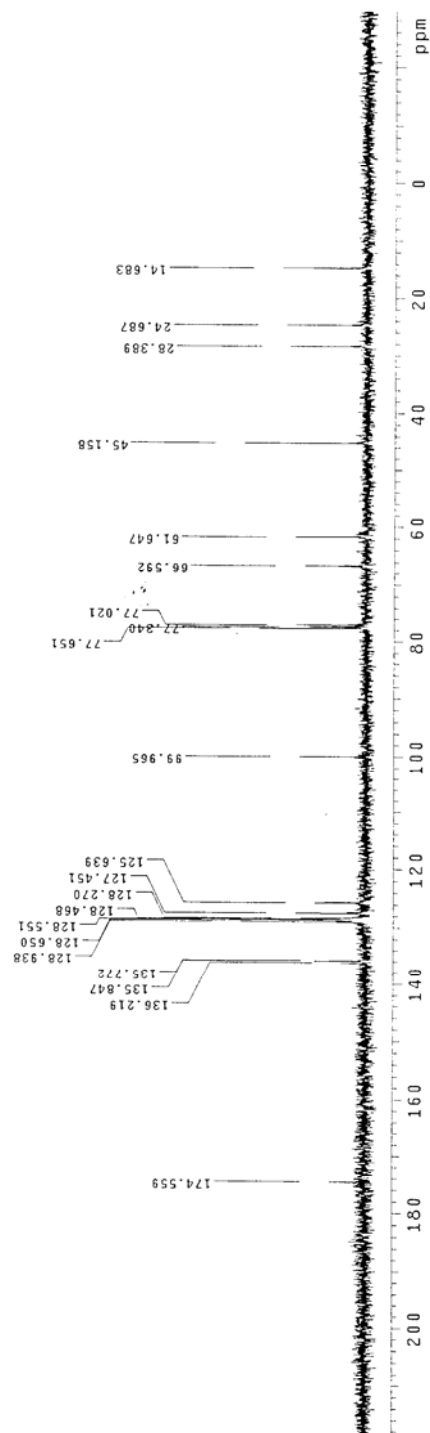


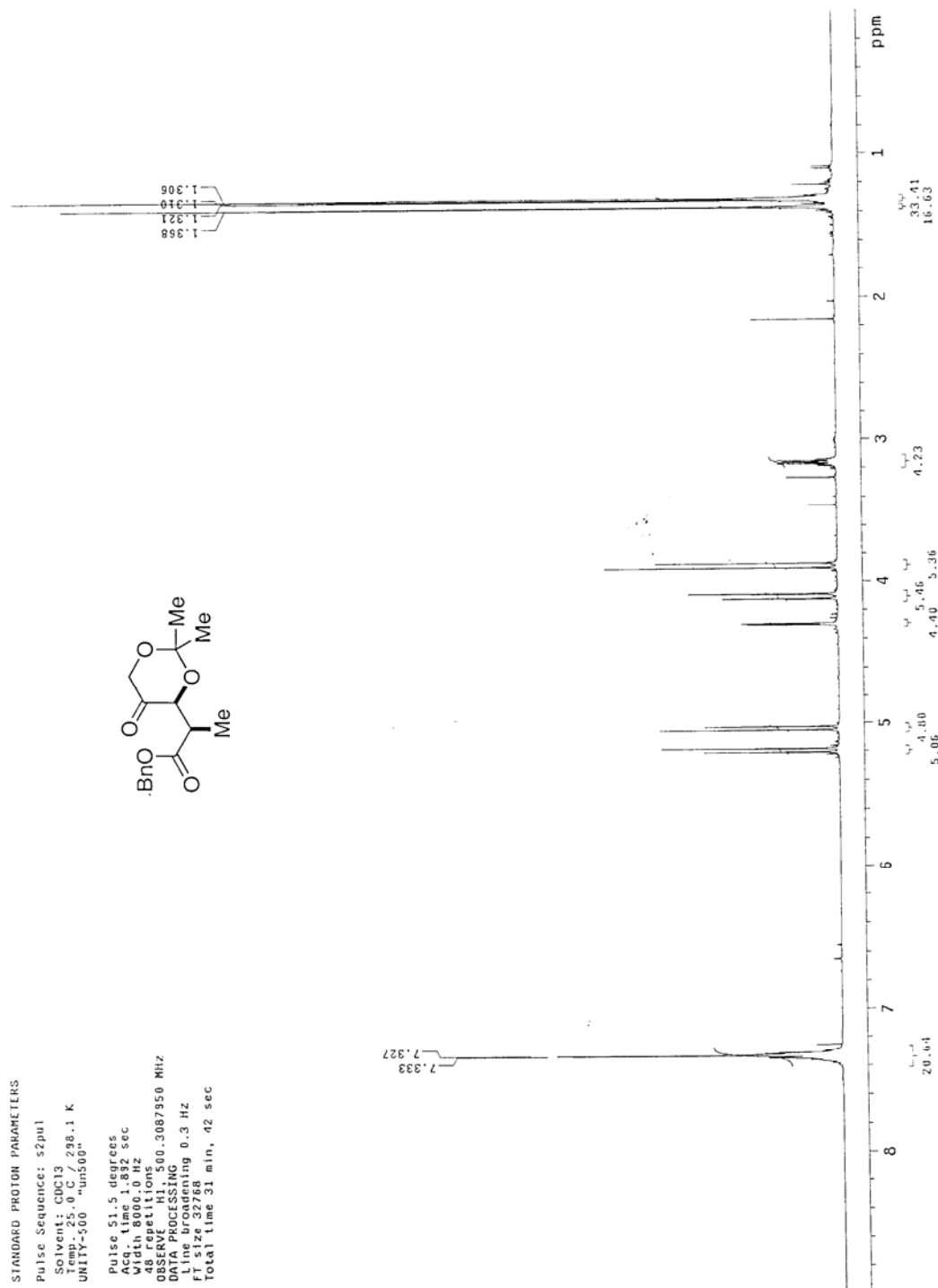
¹H NMR spectrum of compound **292**

¹³C NMR spectrum of compound 292

¹³C OBSERVE

Pulse Sequence: s2pul
 Solvent: CDCl3
 Ambient temperature
 Mercury-40000 "hg400"
 PULSE SEQUENCE
 Pulse 63.6 degrees
 Acq. time 1.199 sec
 Width 25000.0 Hz
 48 repetitions
 4800000000 Hz
 DECOUPLE H1, 400.0555302 MHz
 Power 39 dB
 continuously on
 WALTZ-16 modulated
 DATA PROCESSING
 FT sz 65556
 Total time 35 min, 15 sec

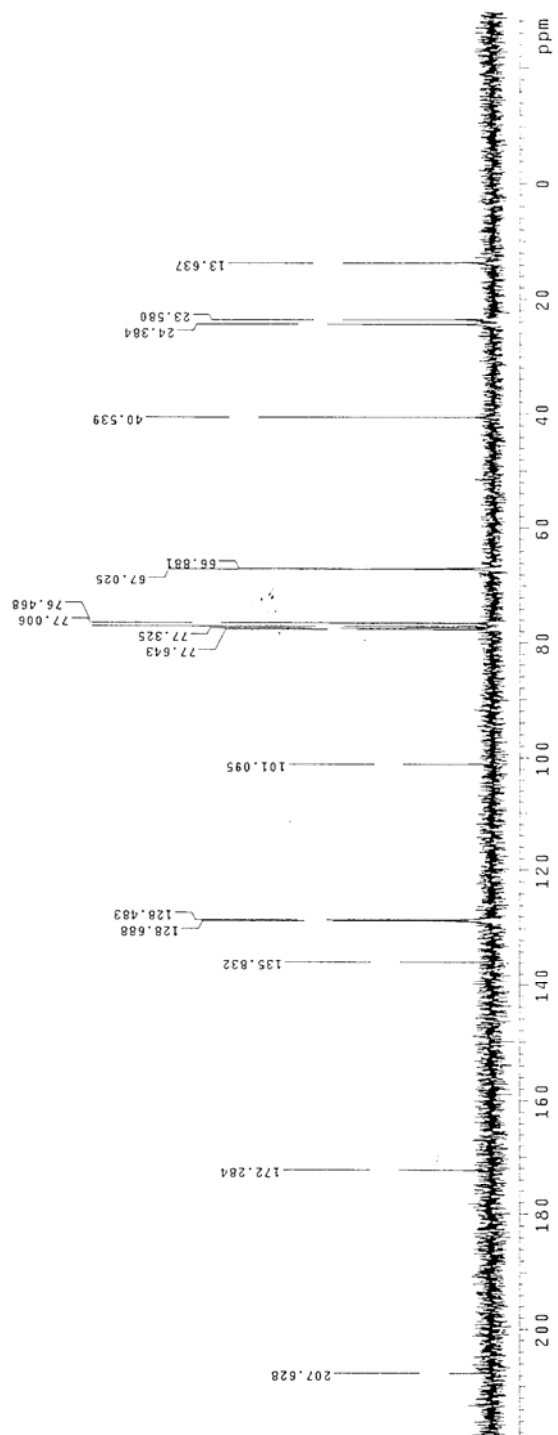
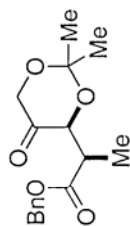


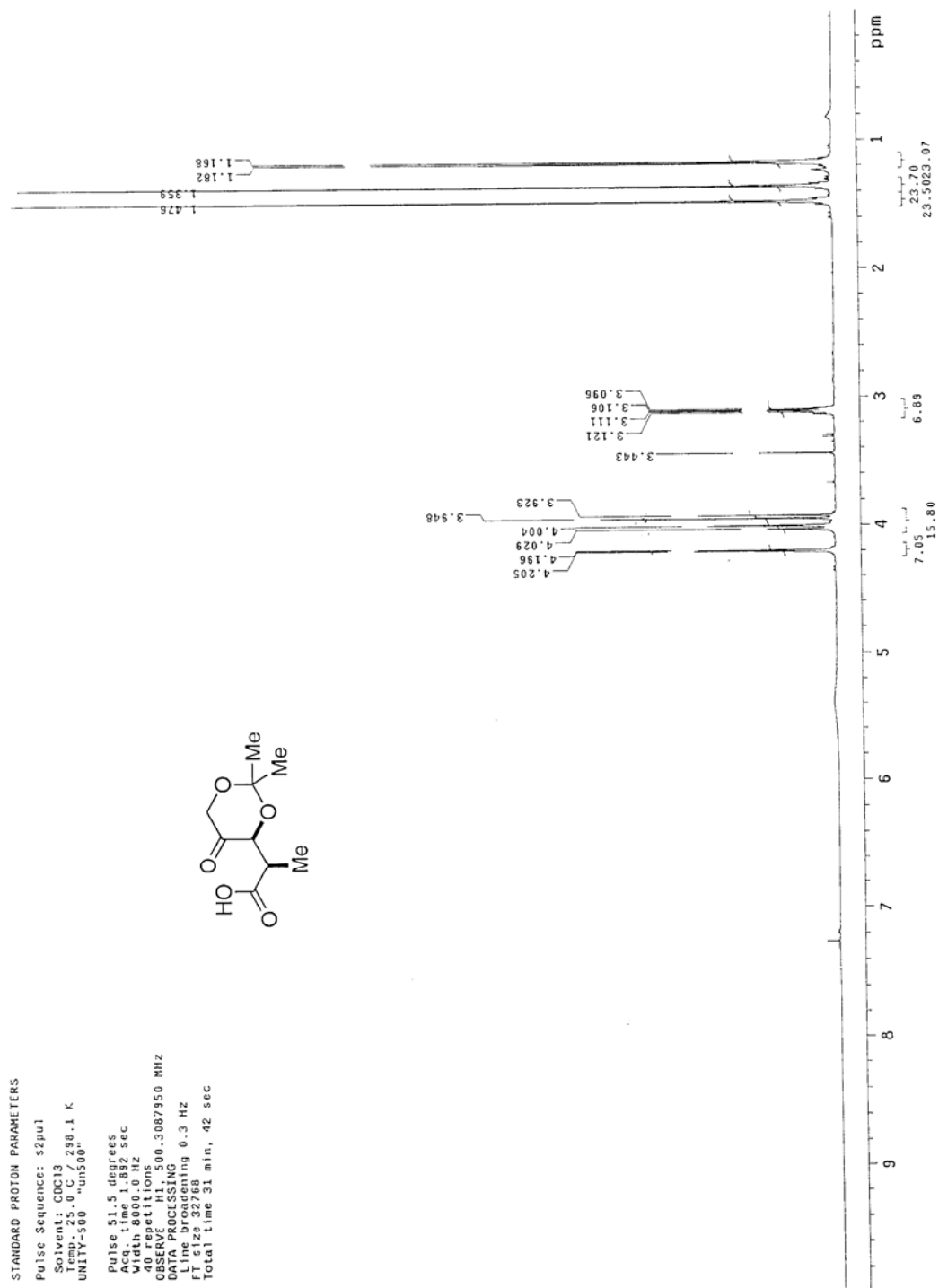
¹H NMR spectrum of compound 293

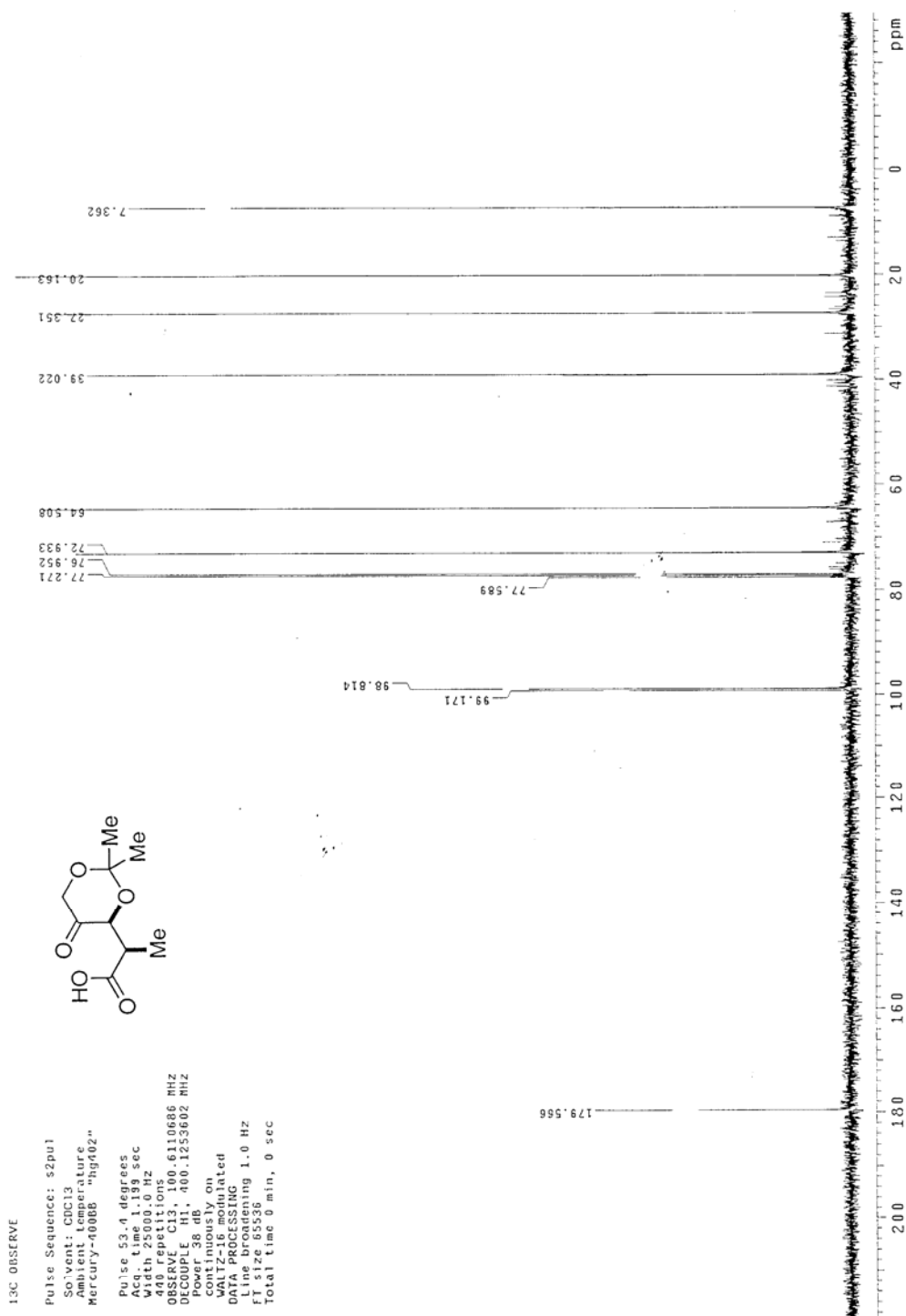
^{13}C NMR spectrum of compound **293**

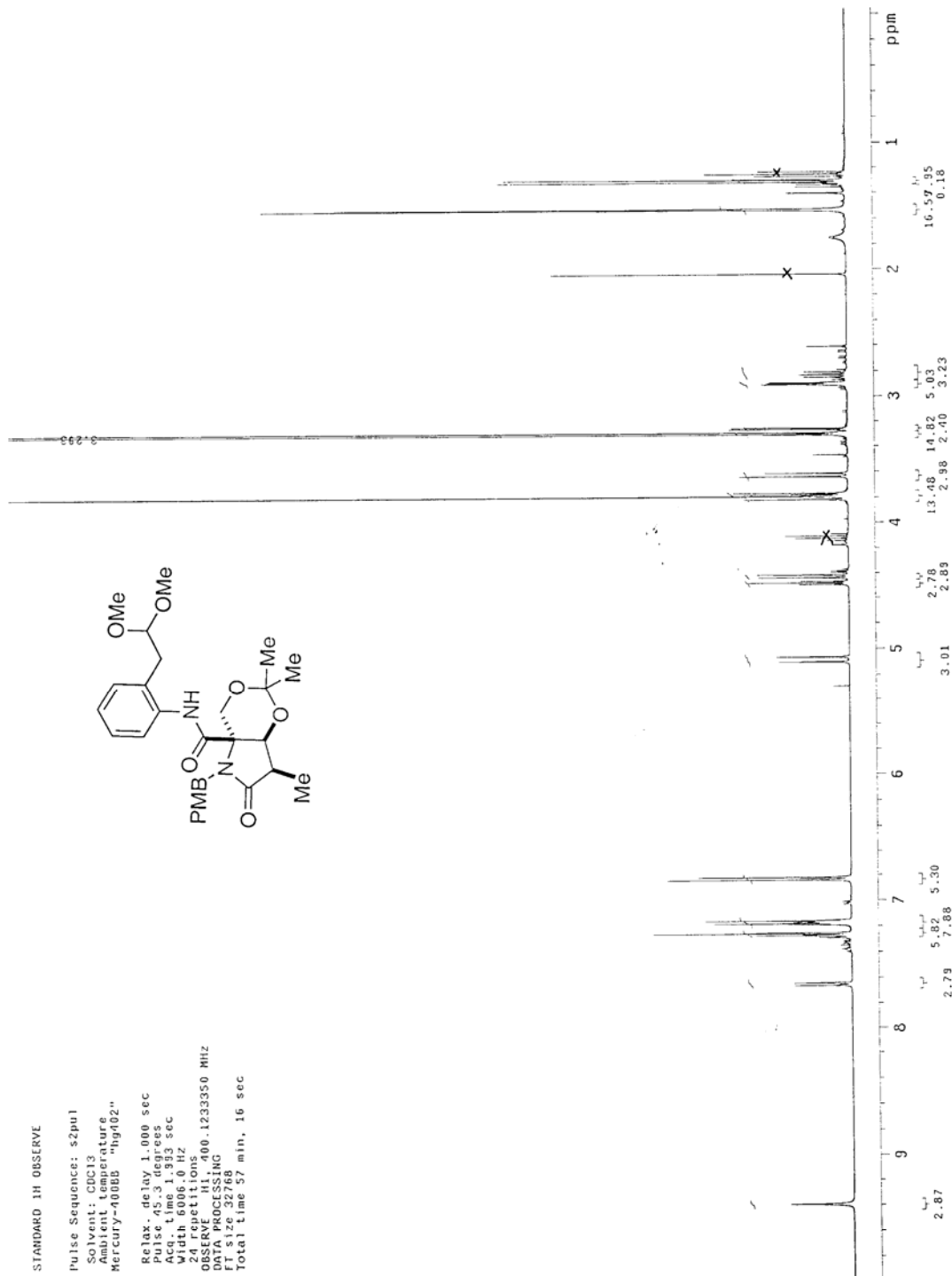
^{13}C OBSERVE

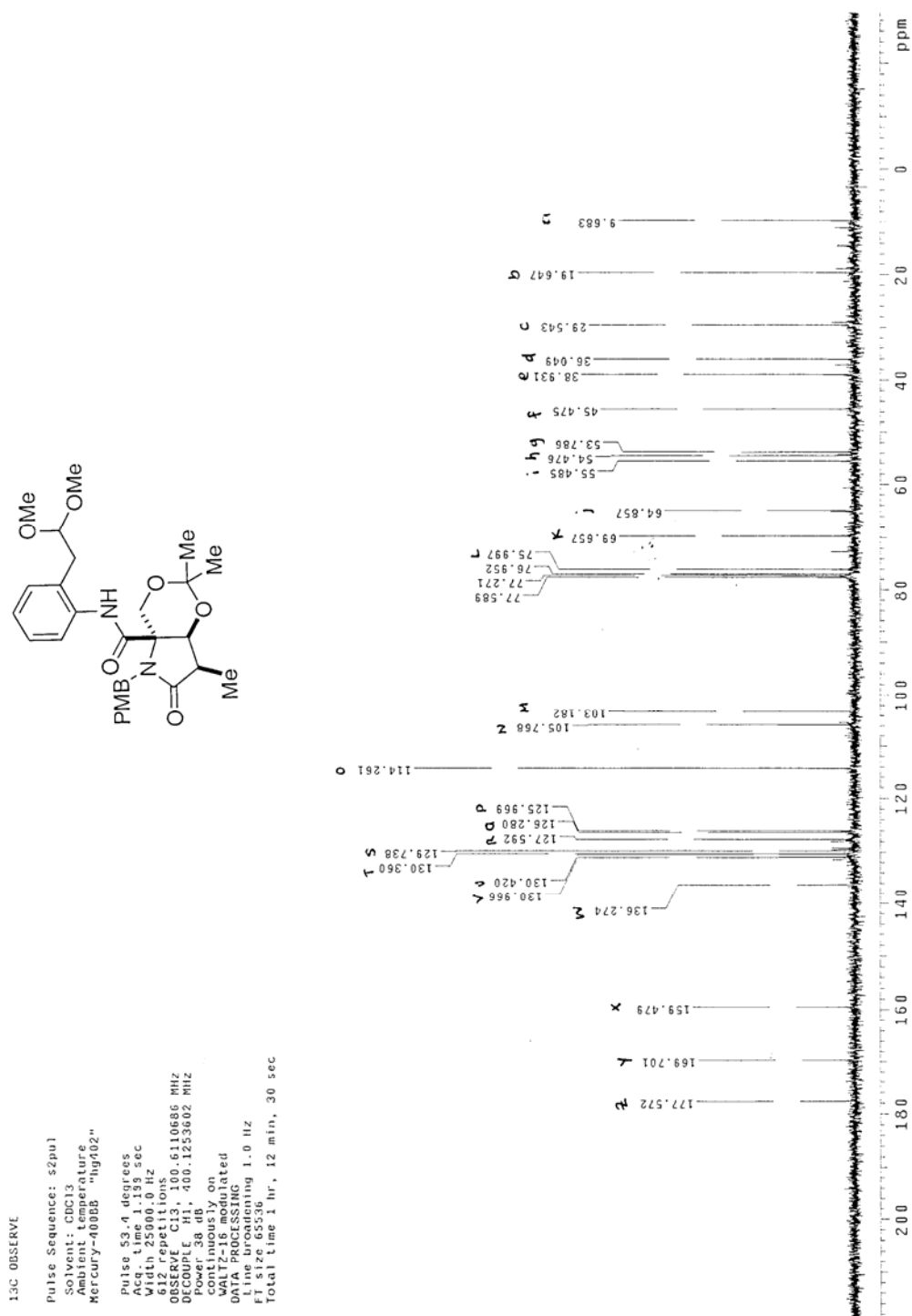
Pulse Sequence: s2pu1
 Solvent: CDCl_3
 Ambient Temperature
 Mercury-400BB "hg400"
 PULSE SEQUENCE
 pulse 69.6 degrees
 Acq. time 1.199 sec
 Width 25000.0 Hz
 OBSERV. CH1, 400.555502 MHz
 DECOUPLE H1, 400.555502 MHz
 Power 39 dB
 continuously on
 WALTZ-16 modulated
 DATA PROCESSING
 Acquisition time 1.0 Hz
 FT size 65536
 Total time 36 min, 15 sec



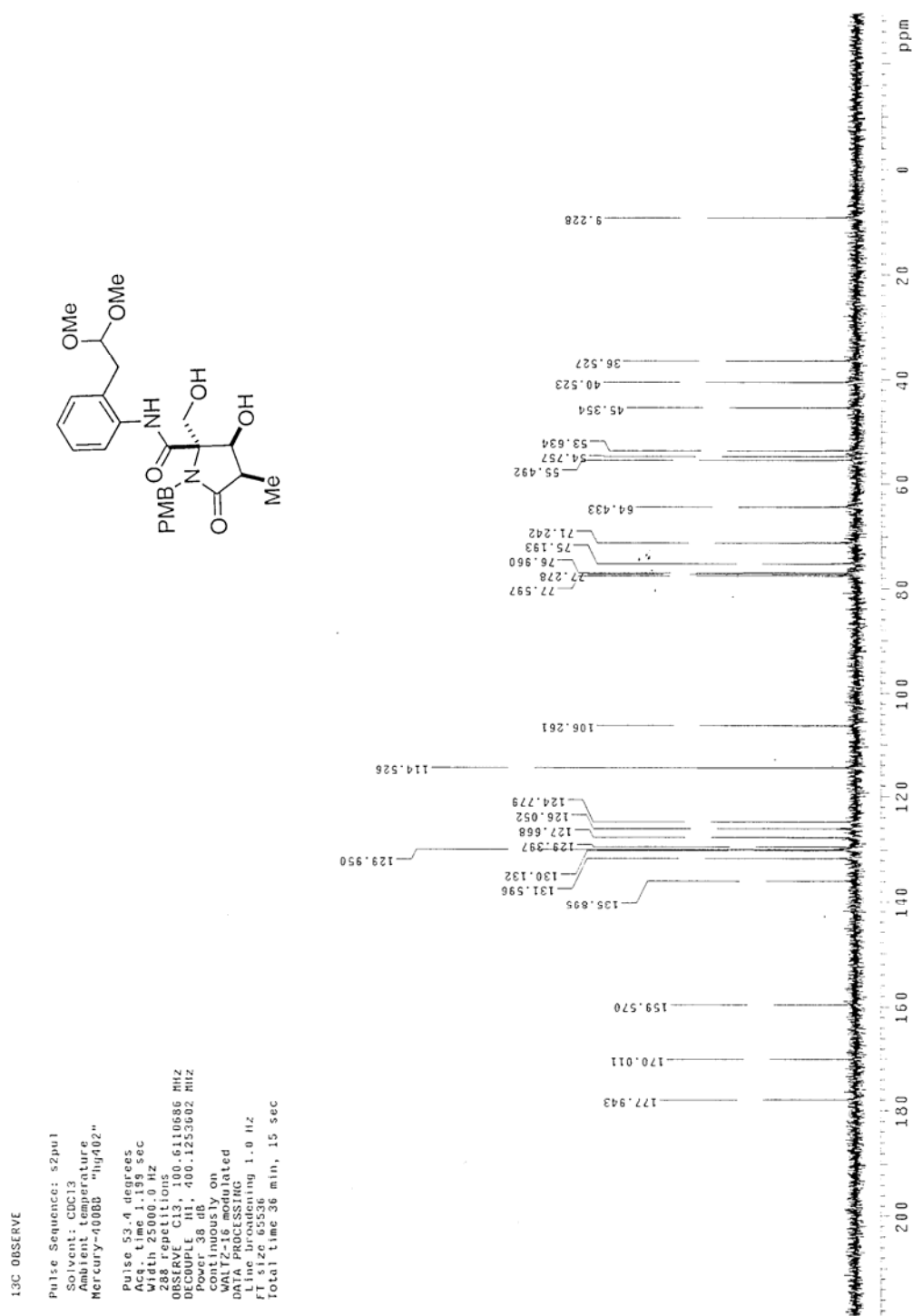
¹H NMR spectrum of compound 274

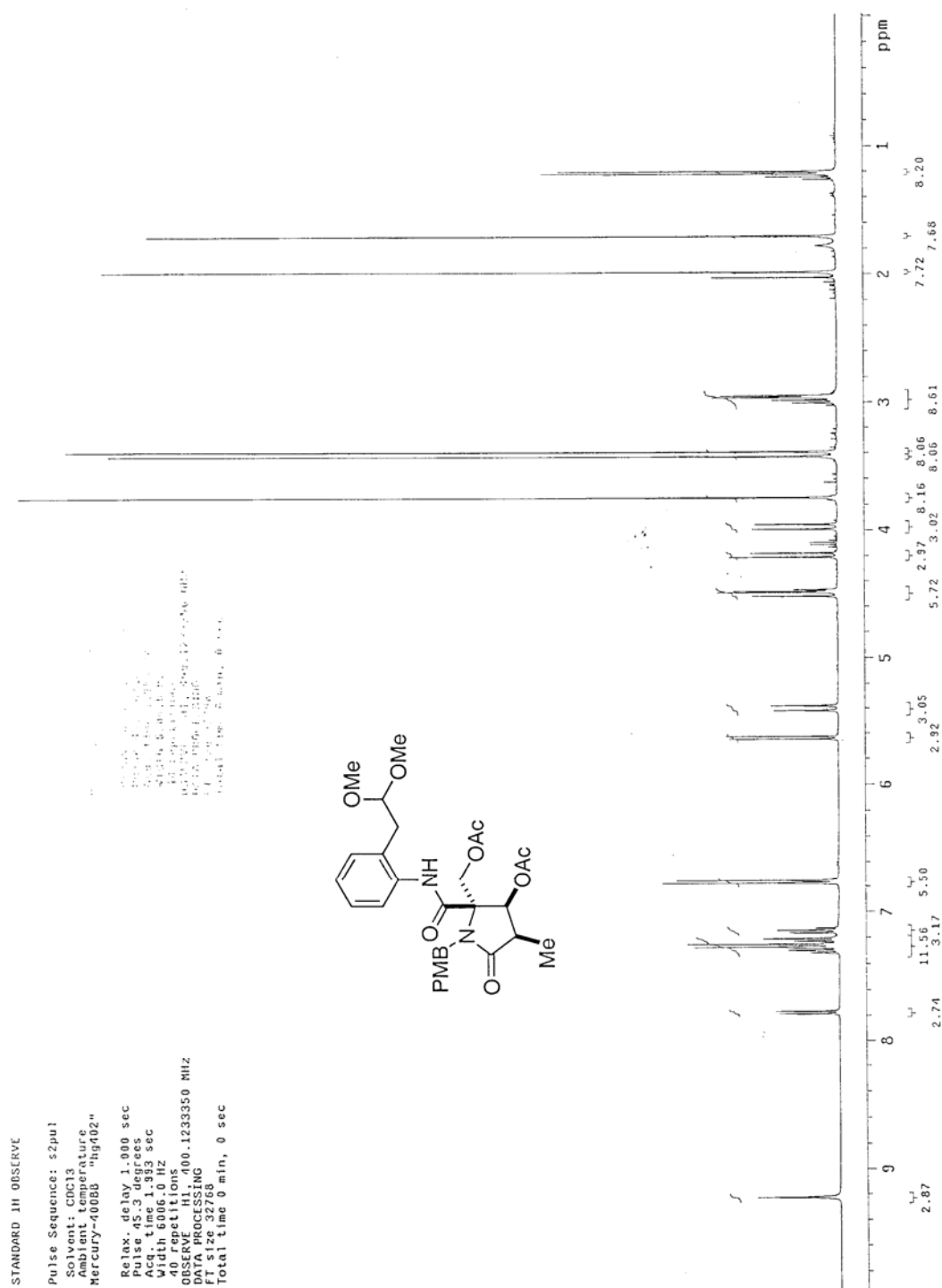
¹³C NMR spectrum of compound 274

¹H NMR spectrum of compound 294

^{13}C NMR spectrum of compound **294**

^1H NMR spectrum of compound **300**

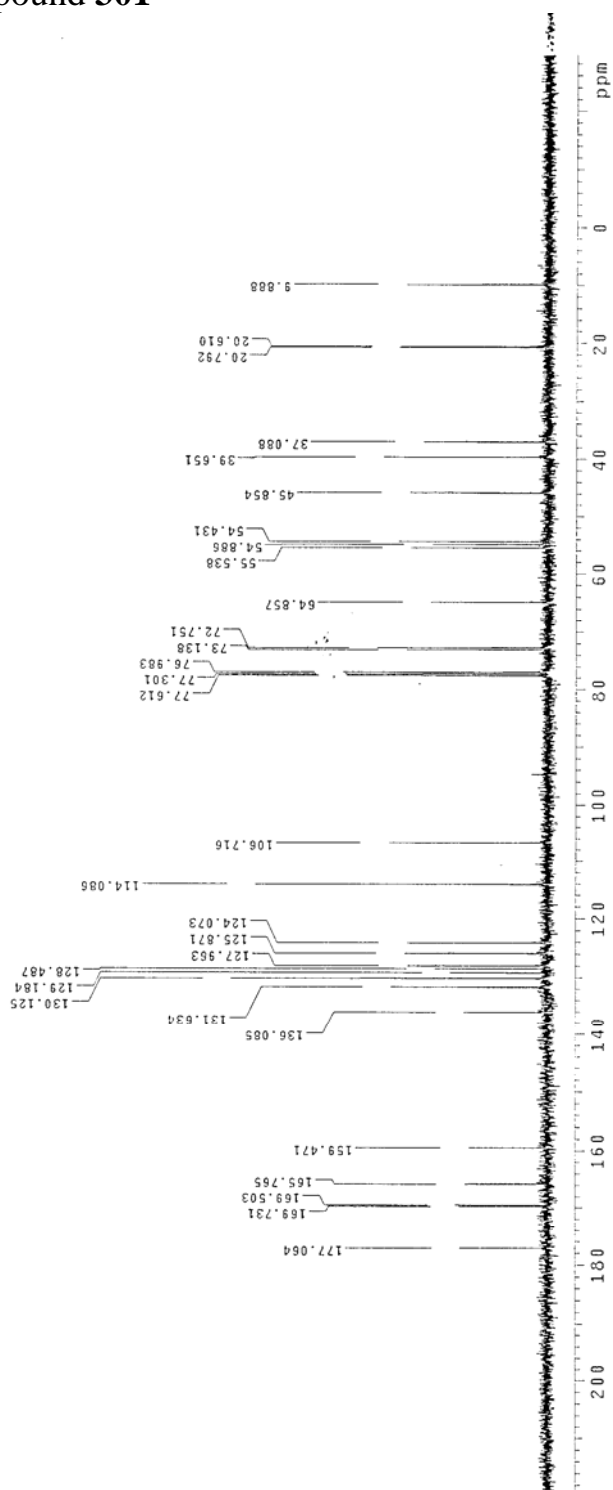
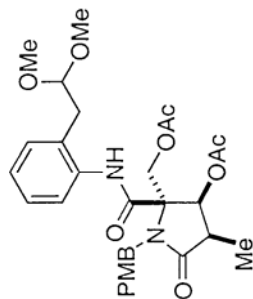
^{13}C NMR spectrum of compound **300**

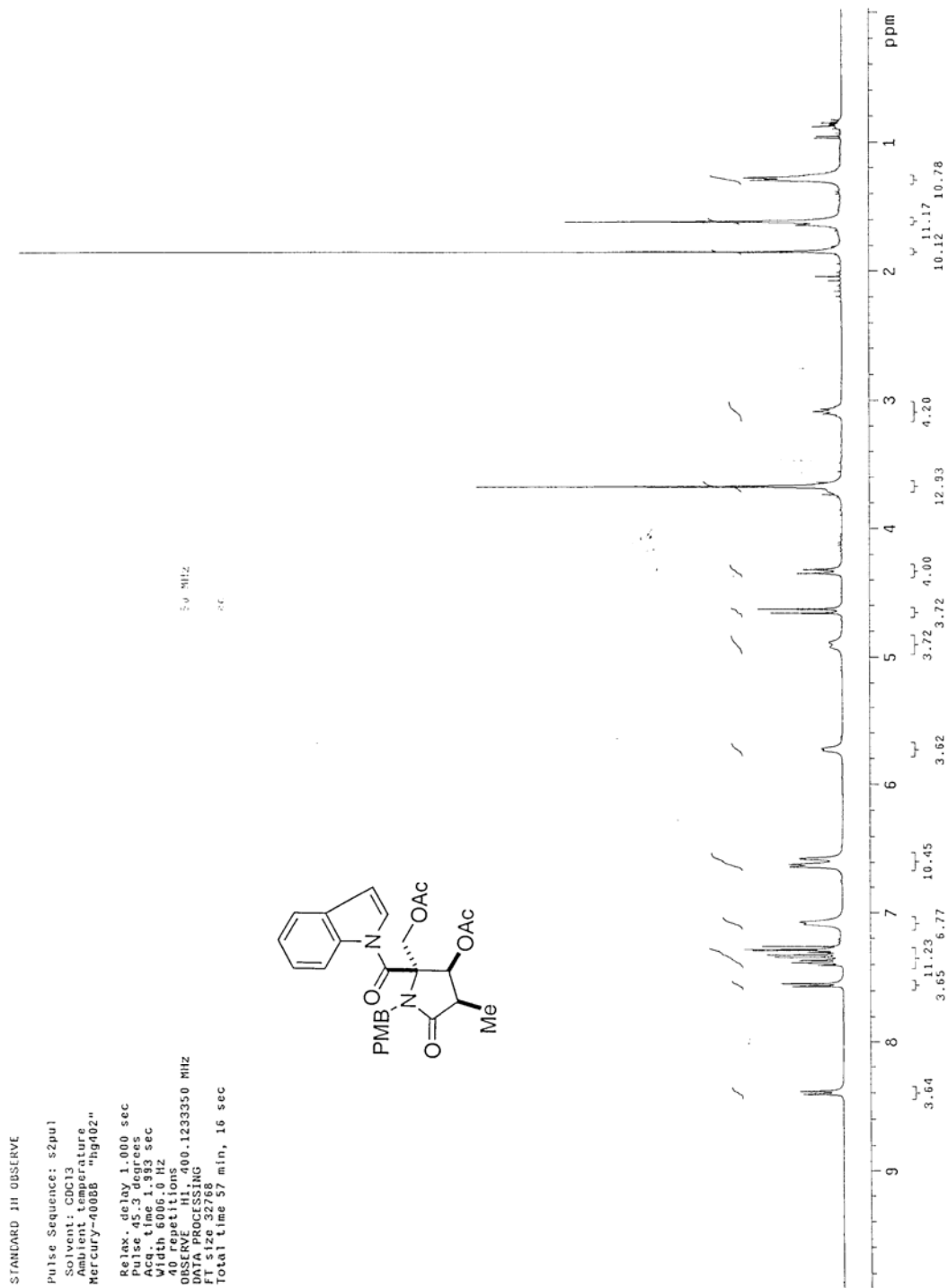
¹H NMR spectrum of compound 301

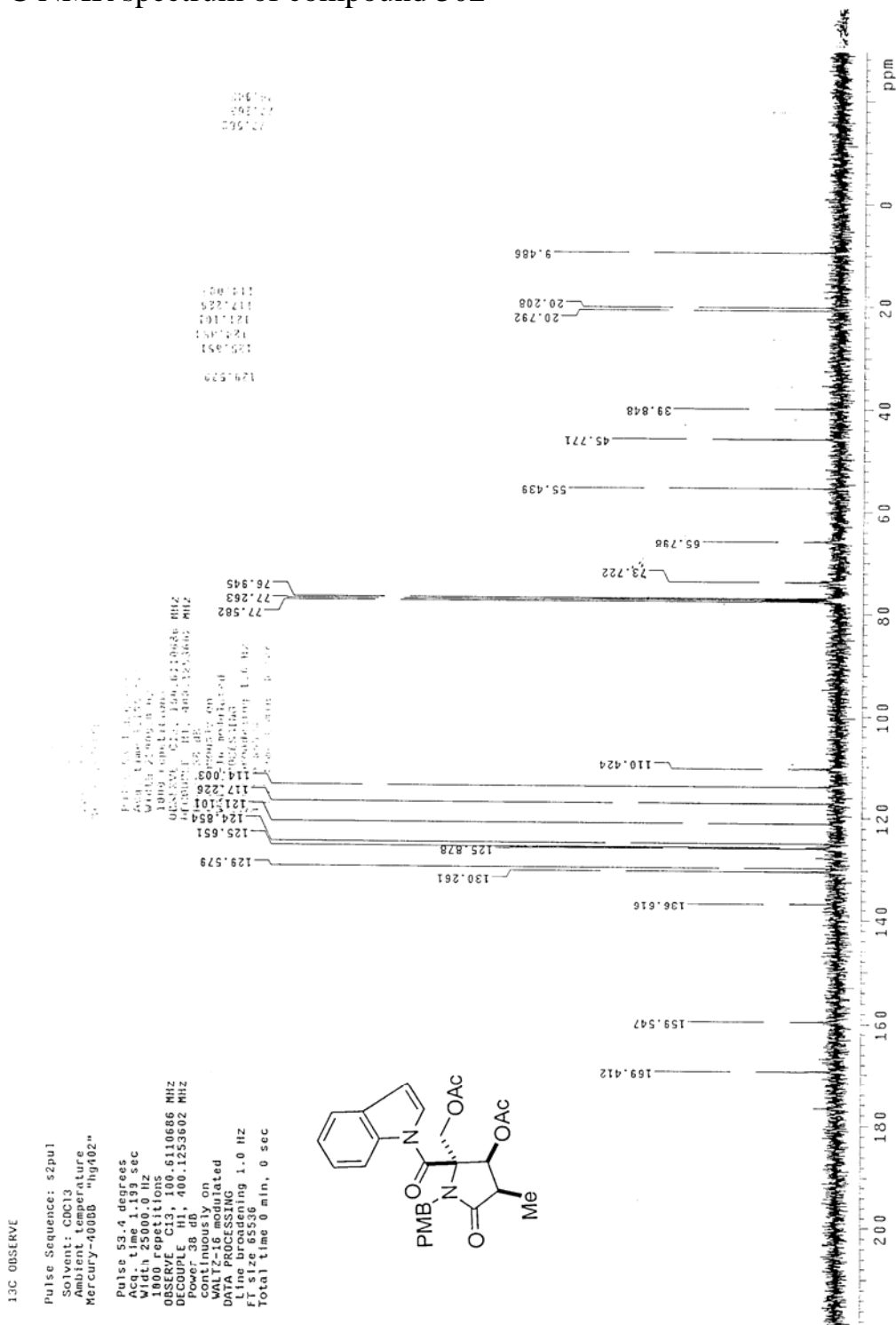
^{13}C NMR spectrum of compound **301**

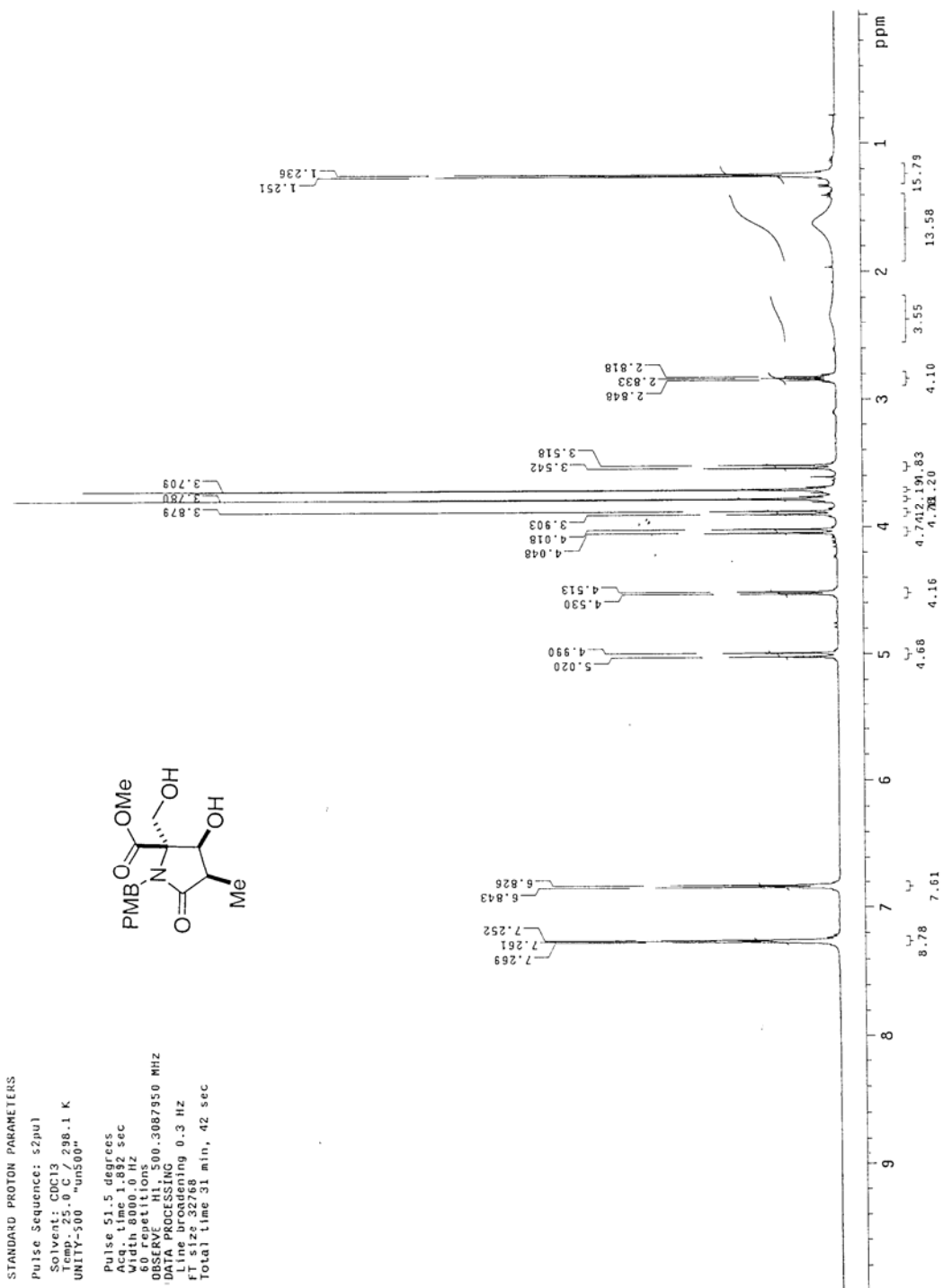
^{13}C OBSERVE

Pulse Sequence: s2pul1
 Solvent: CDCl3
 Ambient temperature
 Mercury-40000 "hg402"
 Pulse 53.4 degrees
 Acq. time 1.19 sec
 Width 25000.0 Hz
 256 repetitions
 Frequency CH3, 100.6110666 MHz
 DECOUPLE H1, 400.1253692 MHz
 Power 38 dB, continuously on
 WALTZ-16 modulated
 DATA PROCESSING
 File: 055889
 F1: 655889
 Total time 36 min, 15 sec



¹H NMR spectrum of compound 302

^{13}C NMR spectrum of compound **302**

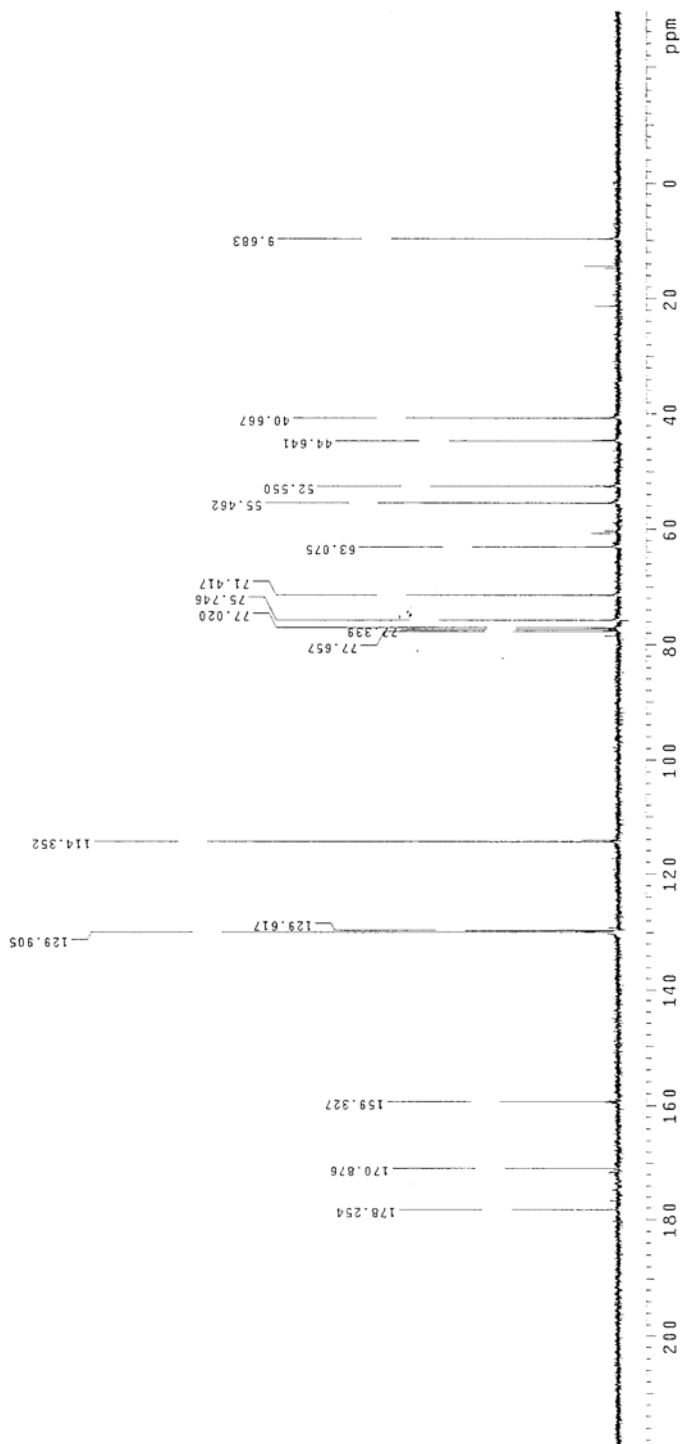
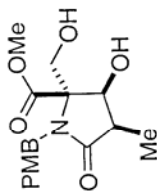
¹H NMR spectrum of compound 303

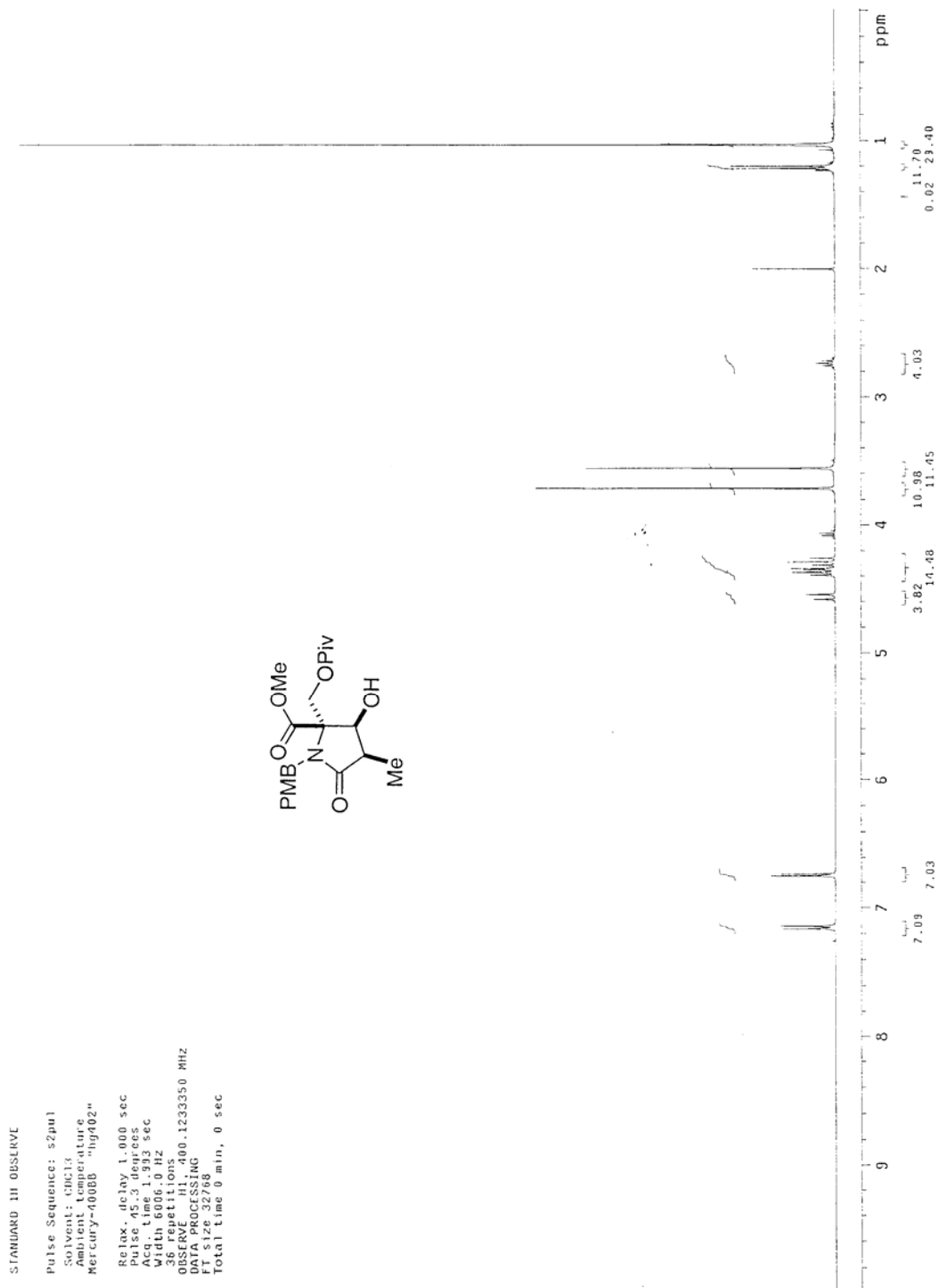
^{13}C NMR spectrum of compound **303**

^{13}C OBSERVE

Pulse Sequence: s2pul
 Solvent: CDCl₃
 Ambient temperature
 Mercury-000BB "hgr02"

Pulse 53.4 degrees
 Acquisition 1.0 sec
 Width 25000.0 Hz
 184 repetitions
 OBSERVE C13, 100.6119686 MHz
 DECOUPLE H1, 400.1253602 MHz
 Power 38 dB
 Gain 18.00
 WAIT-16 modulated
 DATA PROCESSING
 Line broadening 1.0 Hz
 FT size 65536
 Total time 0 min, 0 sec



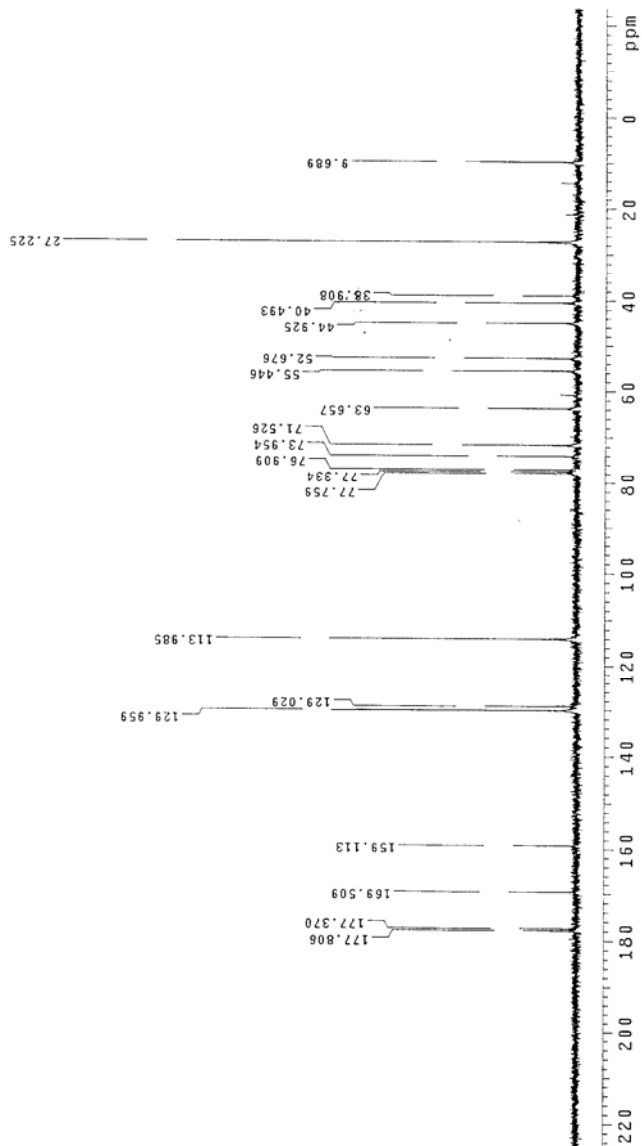
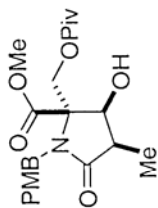
¹H NMR spectrum of compound **303a**

¹³C NMR spectrum of compound **303a**

¹³C OBSERVE

Pulse Sequence: s2pul
 Solvent: CDCl₃
 Ambient Temperature
 Mercury-300 "Hg300"

Pulse 60.5 degrees
 Acq. time 1.615 sec
 Width 18761.7 Hz
 140 repetitions
 OBSERVE C13, 75.4540290 MHz
 PULSE C13, 300.0770584 MHz
 Power 42 dB, 300.0770584 MHz
 continuously on
 WALTZ-16 modulated
 DATA PROCESSING
 Line Acquisition 1.0 Hz
 F1 Acquisition 1.0 Hz
 Total time 0 min, 0 sec



¹H NMR spectrum of compound 304

STANDARD PROTON PARAMETERS

Pulse Sequence: s2hu1

Solvent: CDCl₃

Temp.: 25.0 C / 298.1 K

UNITY-500 "um500"

Pulse 51.5 degrees

Acq. time 1.092 sec

Pulsed 0.0002

40 repetitions

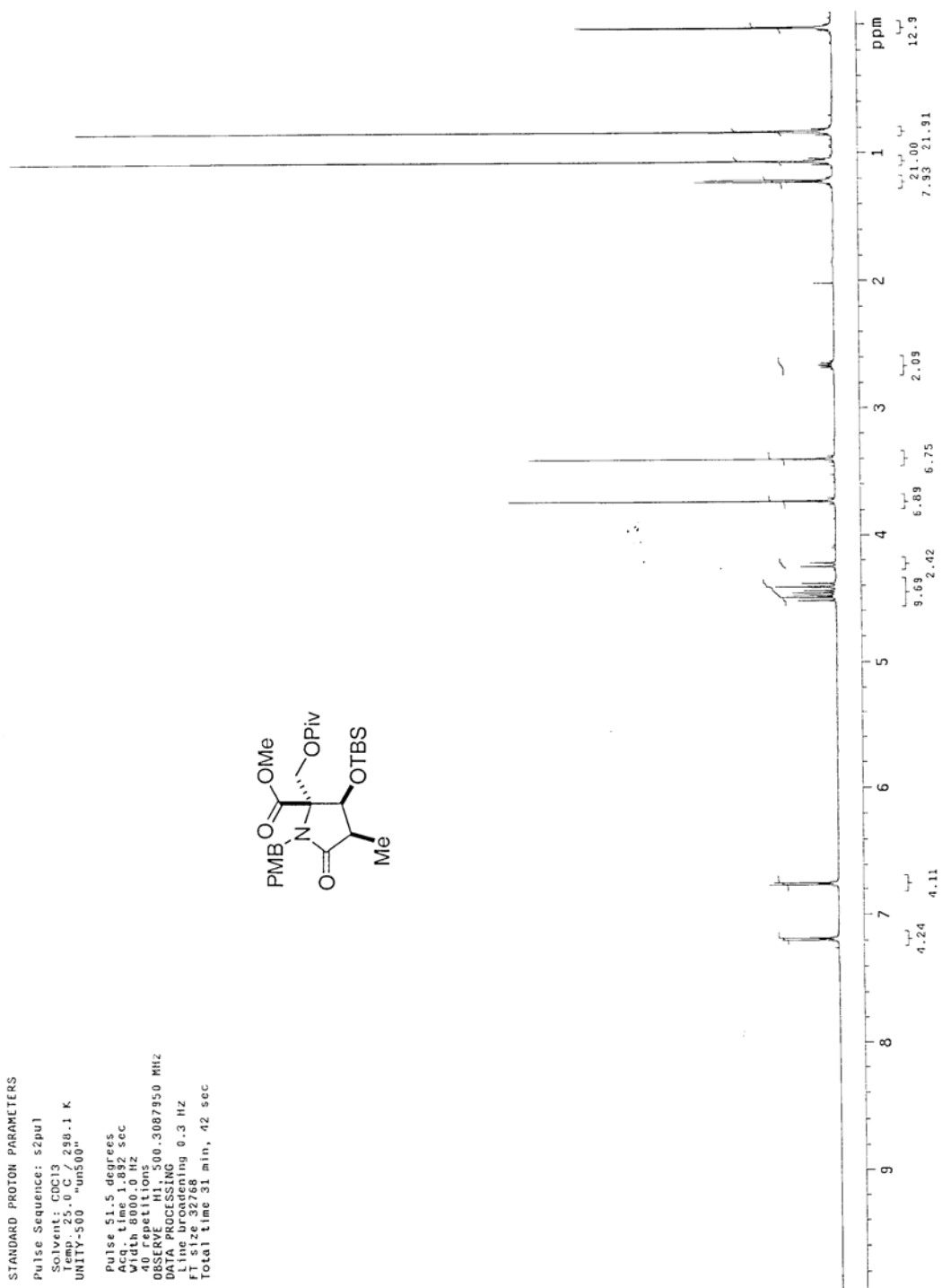
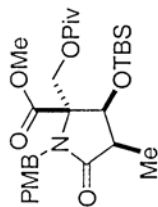
OBSERVE H1, 500.3087950 MHz

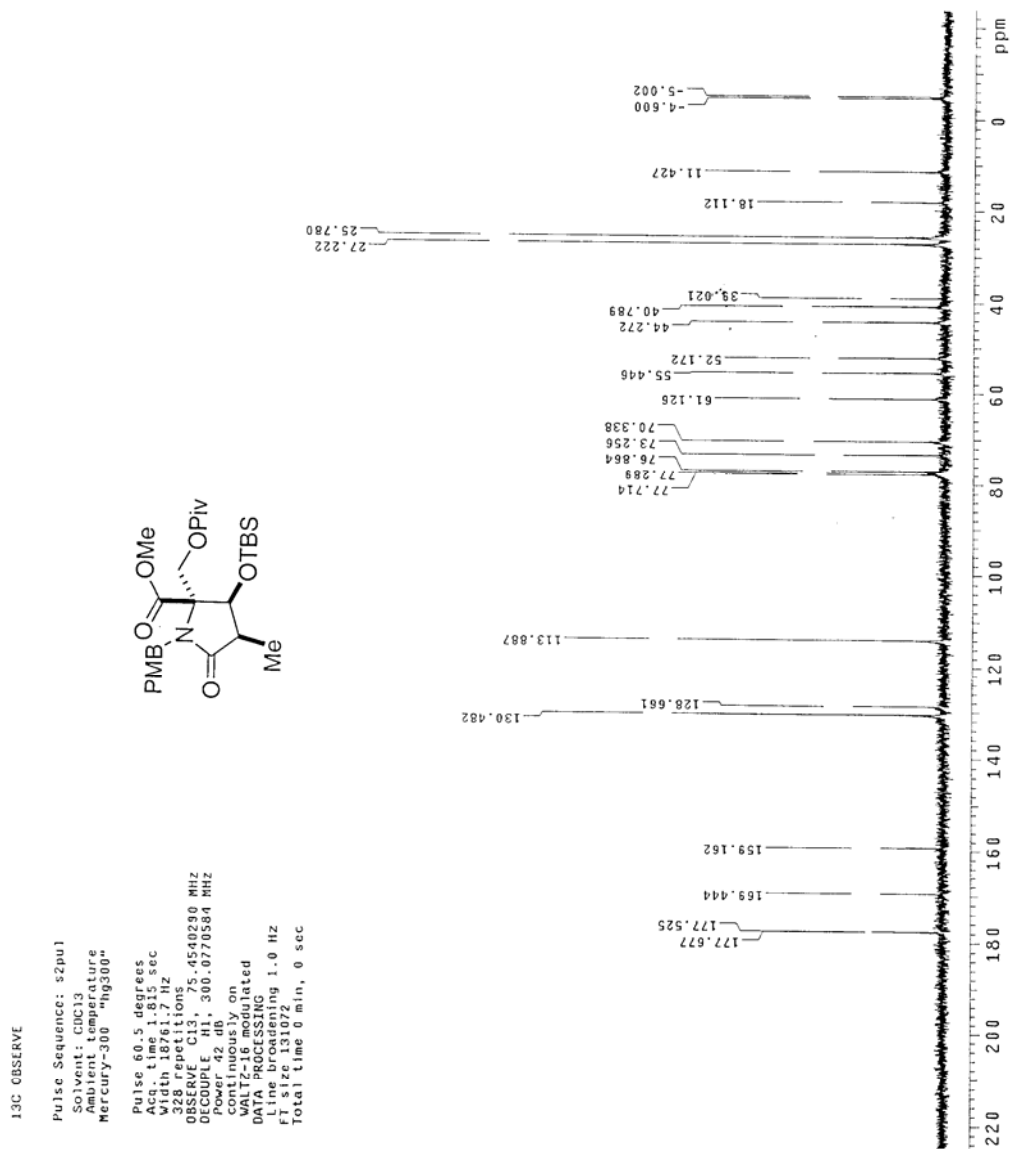
DATA PROCESSING

Line broadening 0.3 Hz

FT size 32768

Total time 31 min, 42 sec

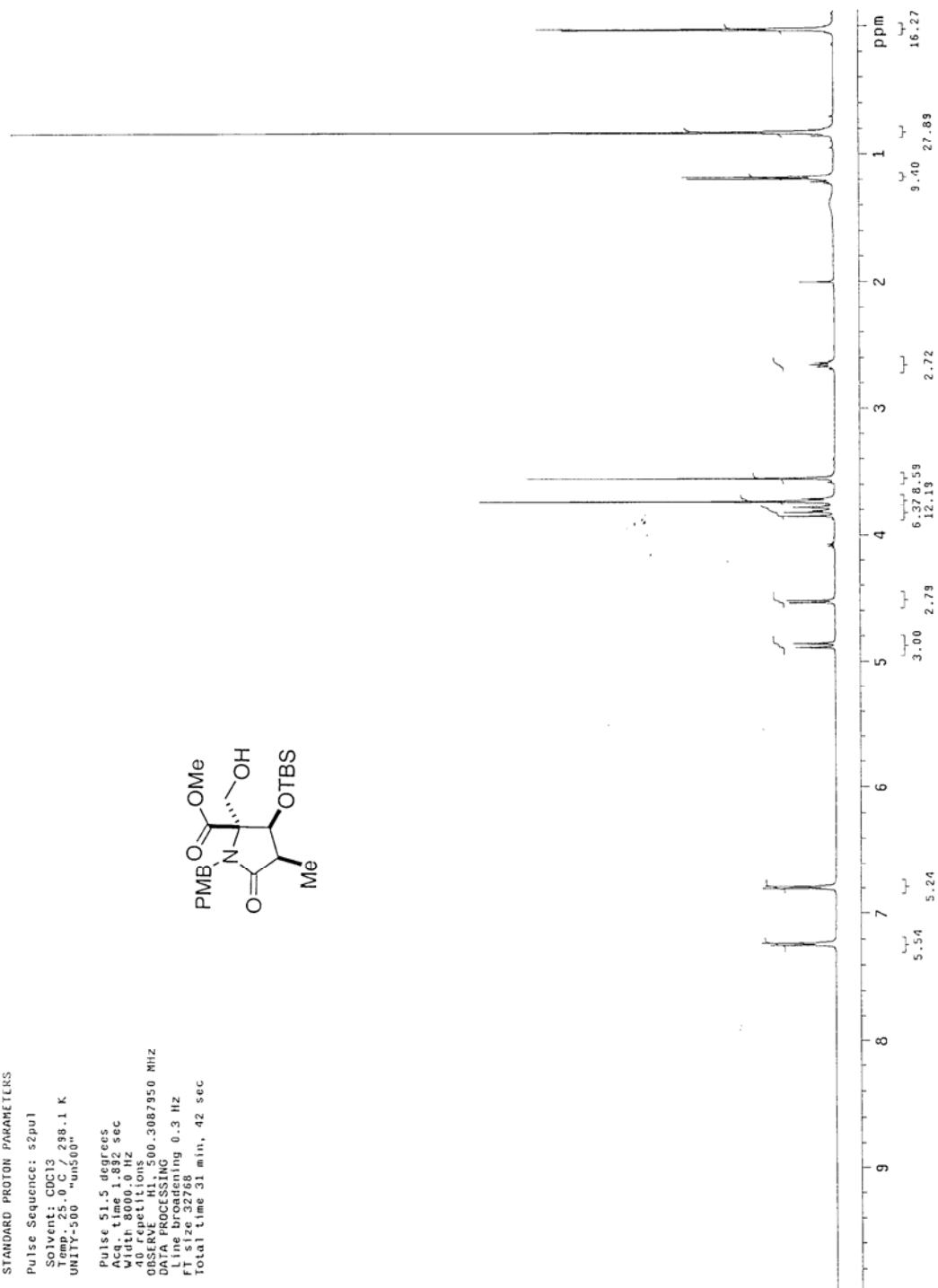
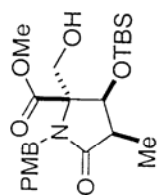


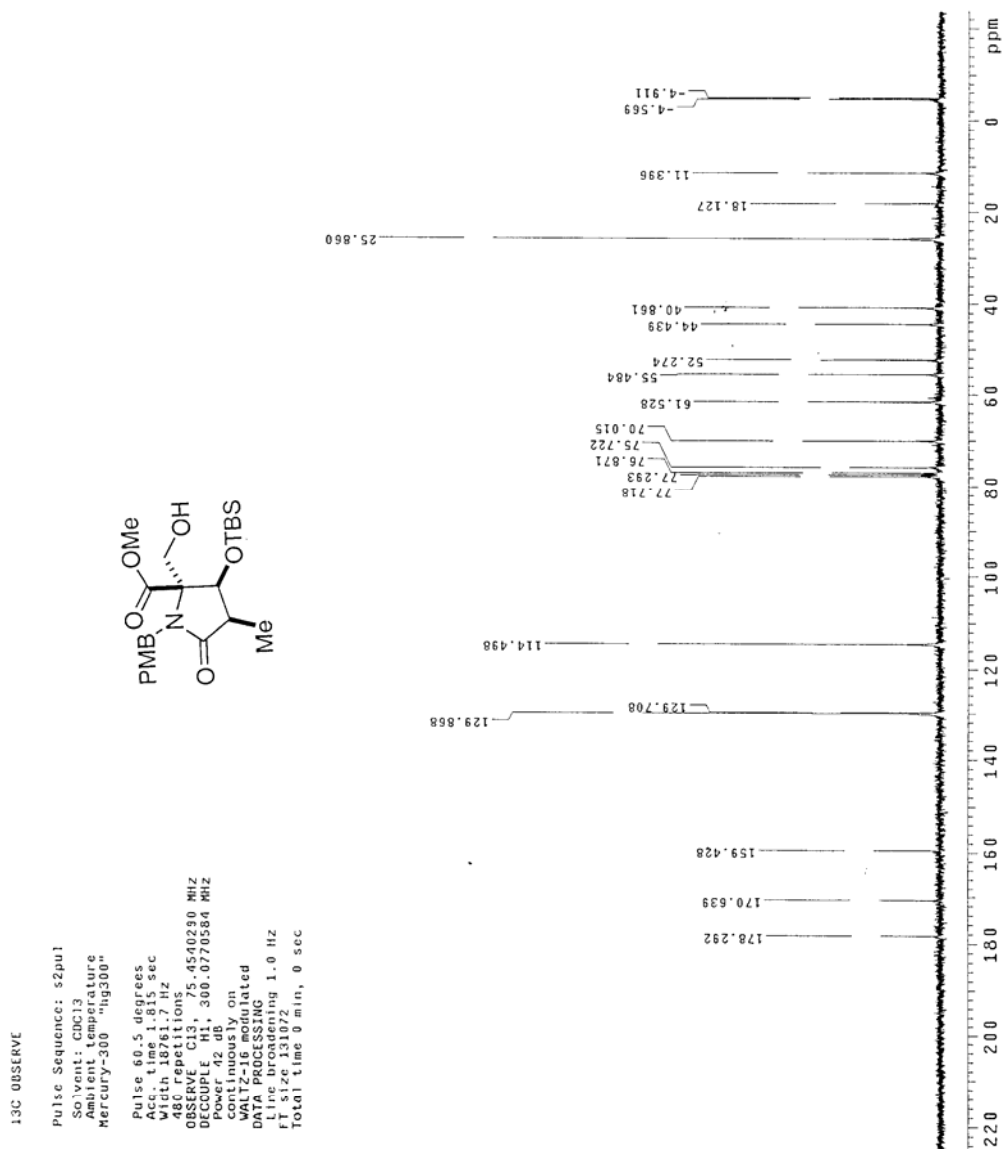
^{13}C NMR spectrum of compound **304**

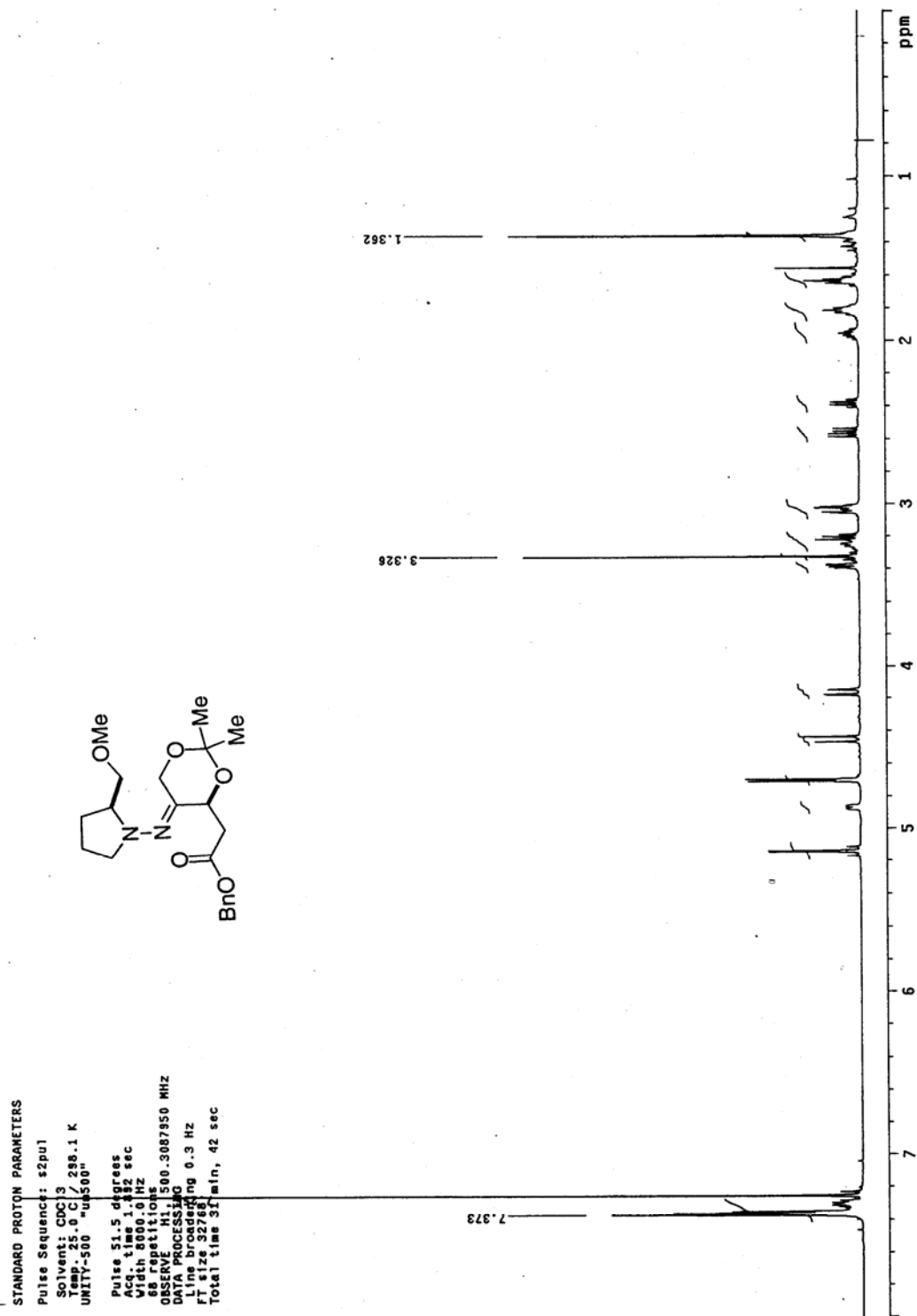
¹H NMR spectrum of compound **305**

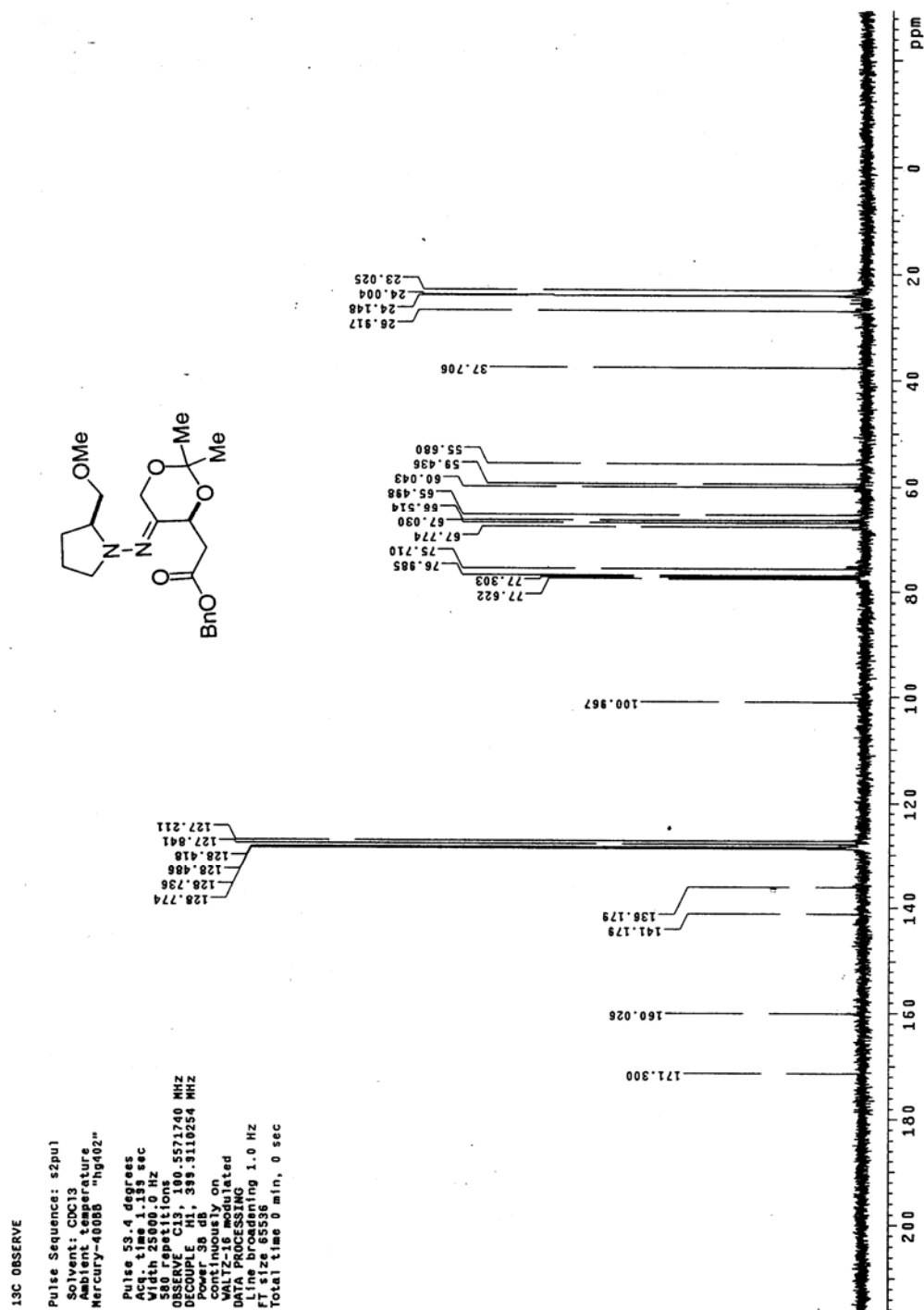
STANDARD PROTON PARAMETERS

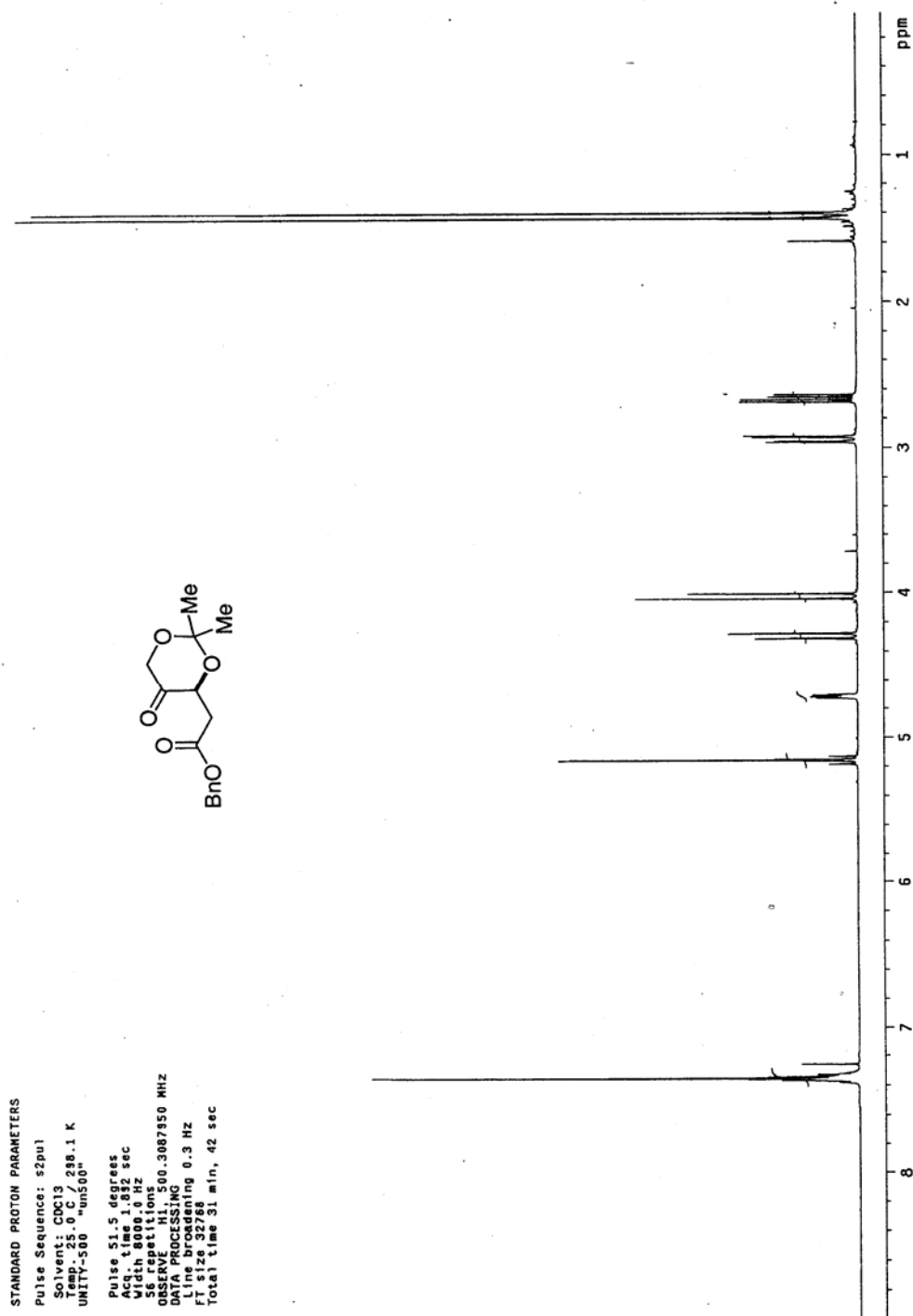
Pulse Sequence: s2pu1
Solvent: CDCl3
Temp.: 25.0 C / 298.1 K
UNITY-500 "un500"
Pulse 51.5 degrees
Acq. time 1.892 sec
Width 8000.0 Hz
Sweep 60000.0 Hz
OS 16 repetitions
OS 16 repetitions
DATA PROCESSING 00.3087950 MHZ
Line broadening 0.3 Hz
FT size 32768
Total time 31 min, 42 sec

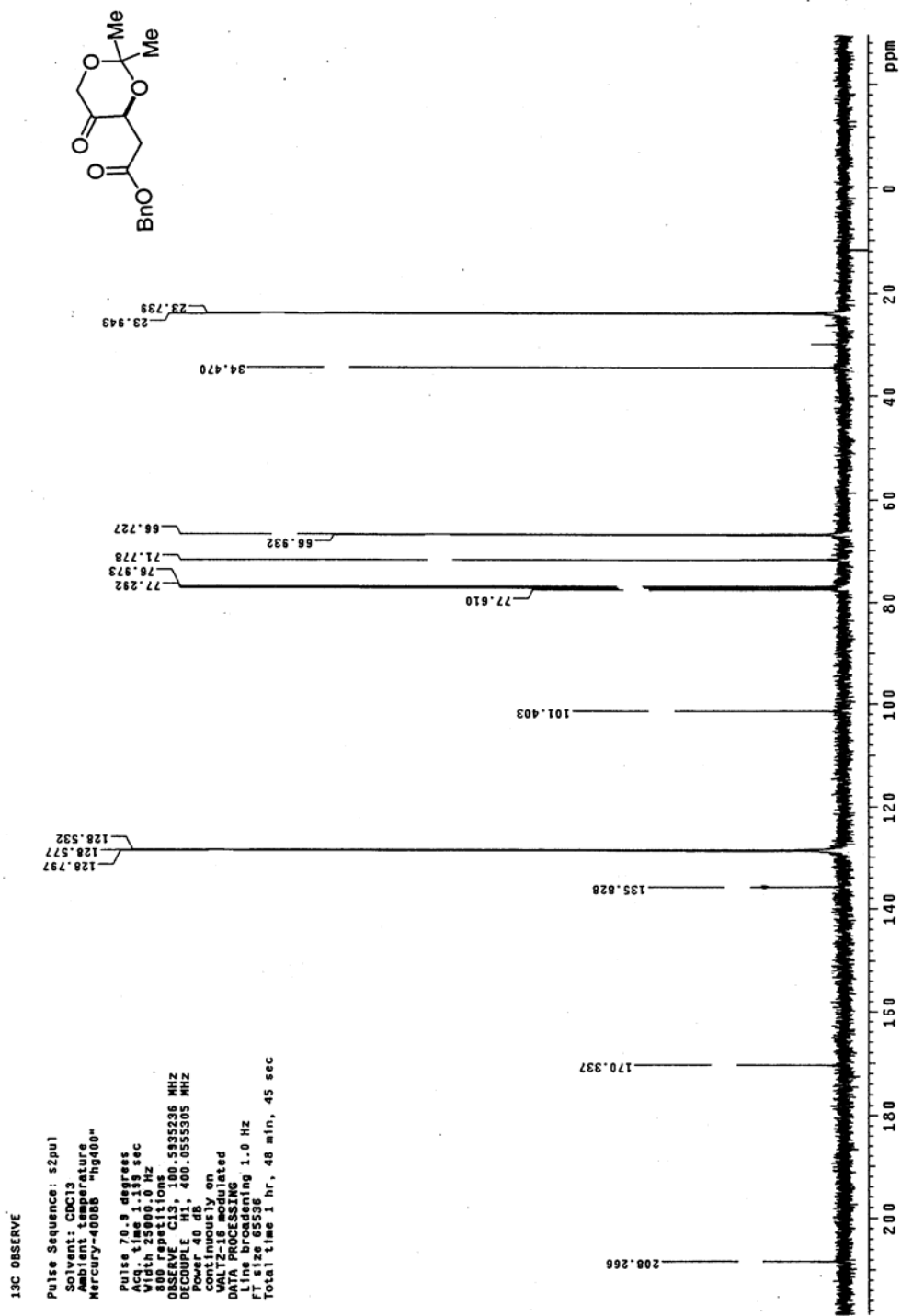


¹³C NMR spectrum of compound **305**

¹H NMR spectrum of compound 317

^{13}C NMR spectrum of compound 317

¹H NMR spectrum of compound 318

¹³C NMR spectrum of compound 318

¹H NMR spectrum of compound 310

STANDARD PROTON PARAMETERS

Pulse Sequence: s2pu1

Solvent: CDCl₃

Temp: 25.0 C / 298.1 K

UNITY-500 -uns00"

Pulse 51.5 degrees

Acq 1.12 sec

Width 2000.0 Hz

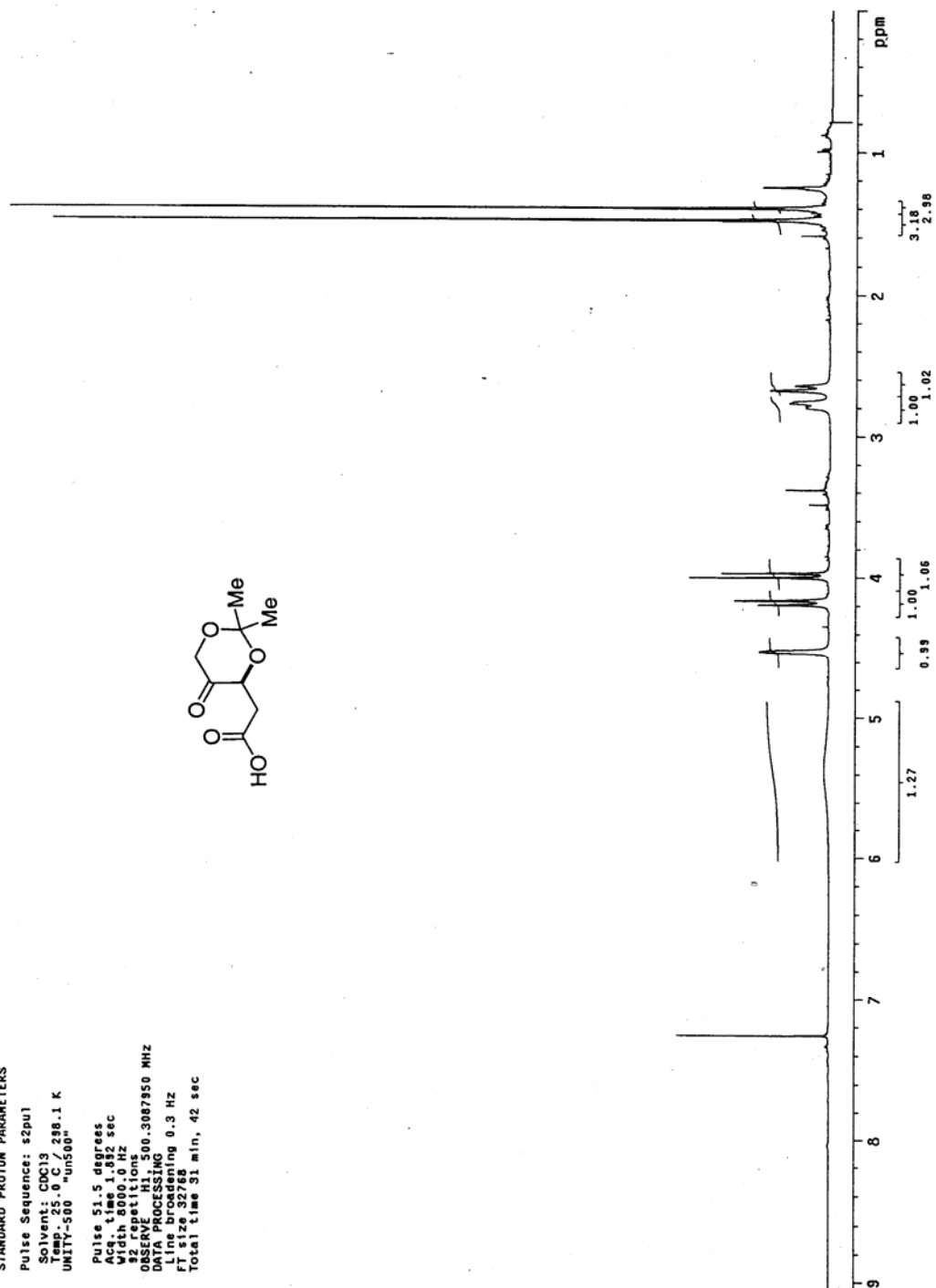
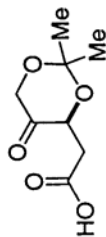
92 repetitions

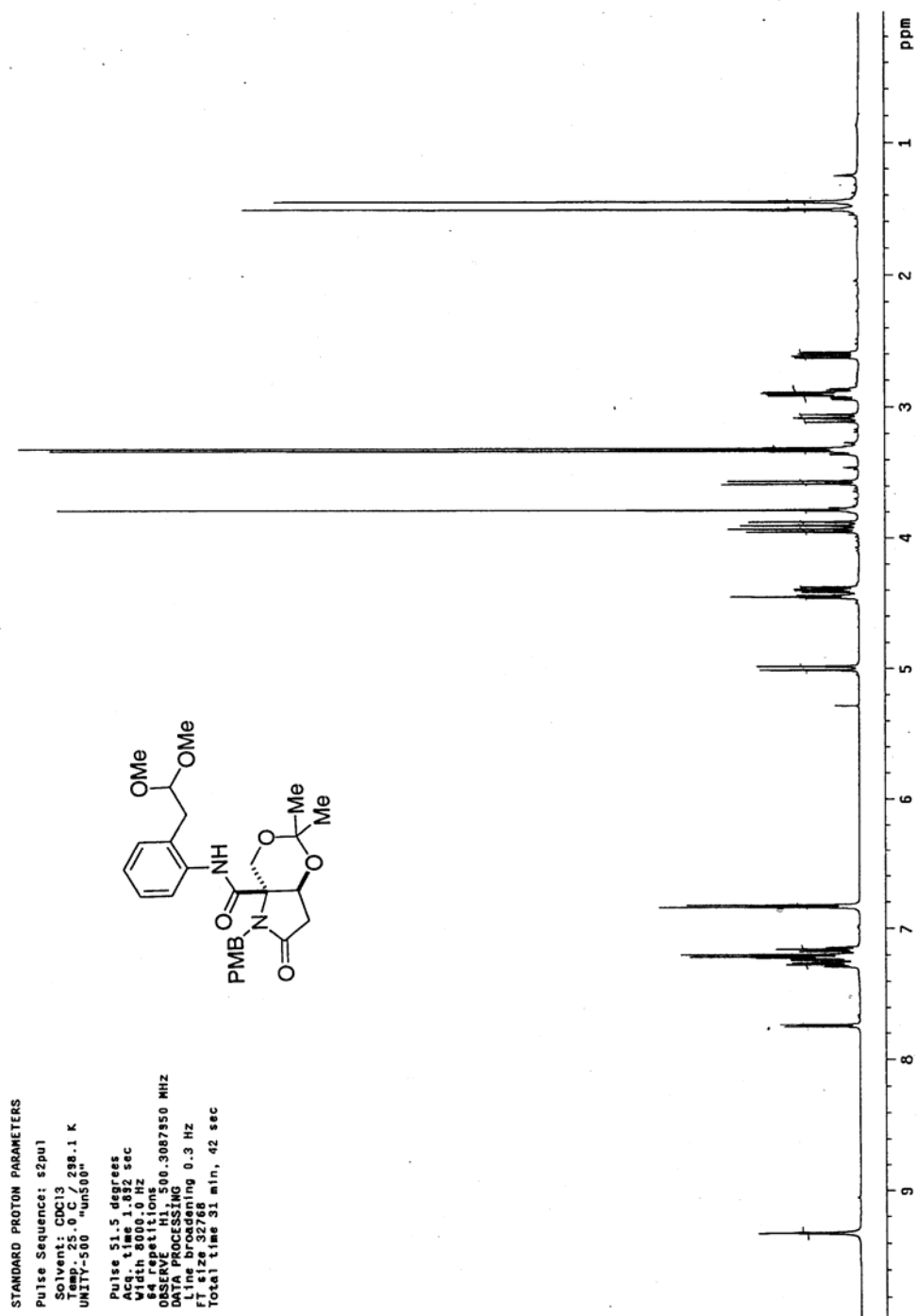
OBSERVE H1, 500.3087950 MHz

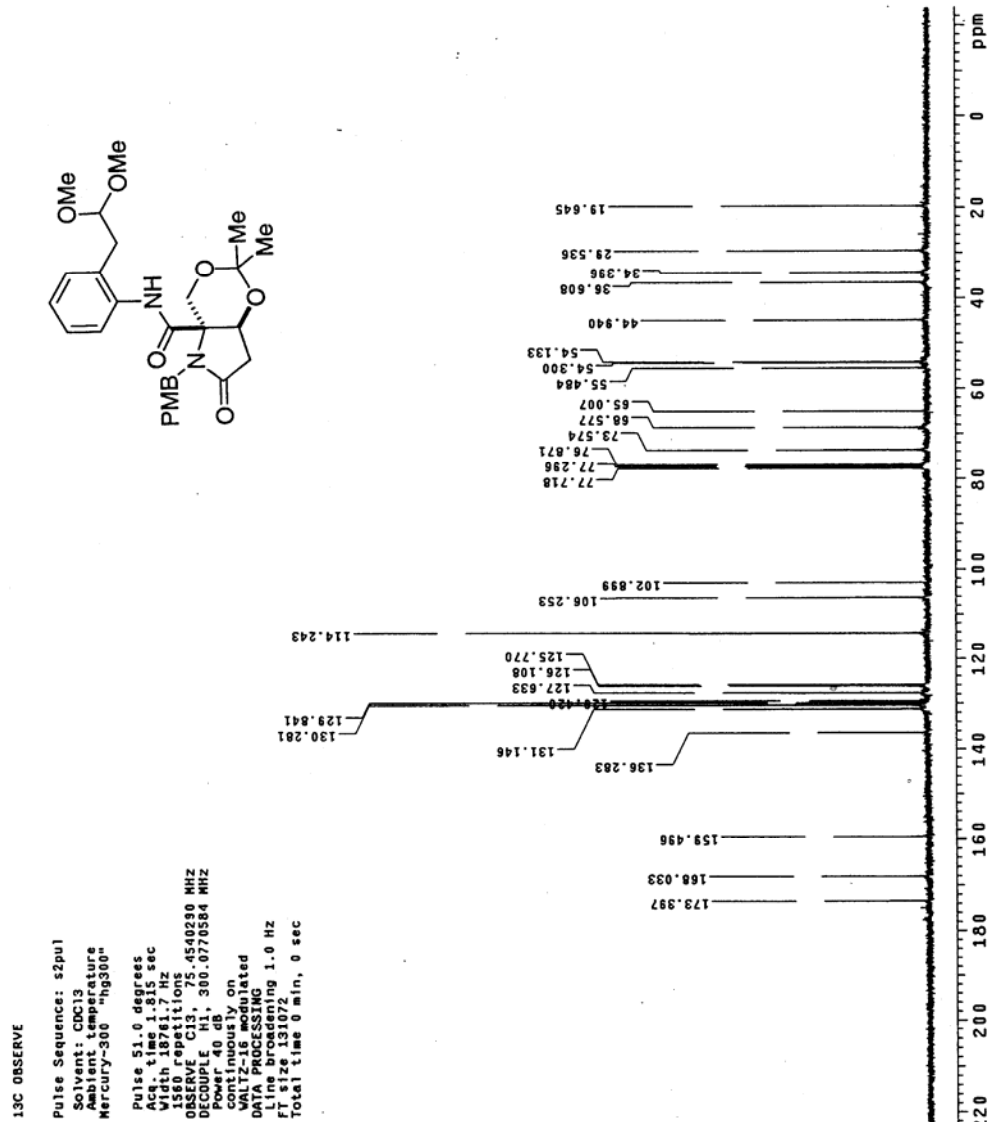
DATA PROCESSING

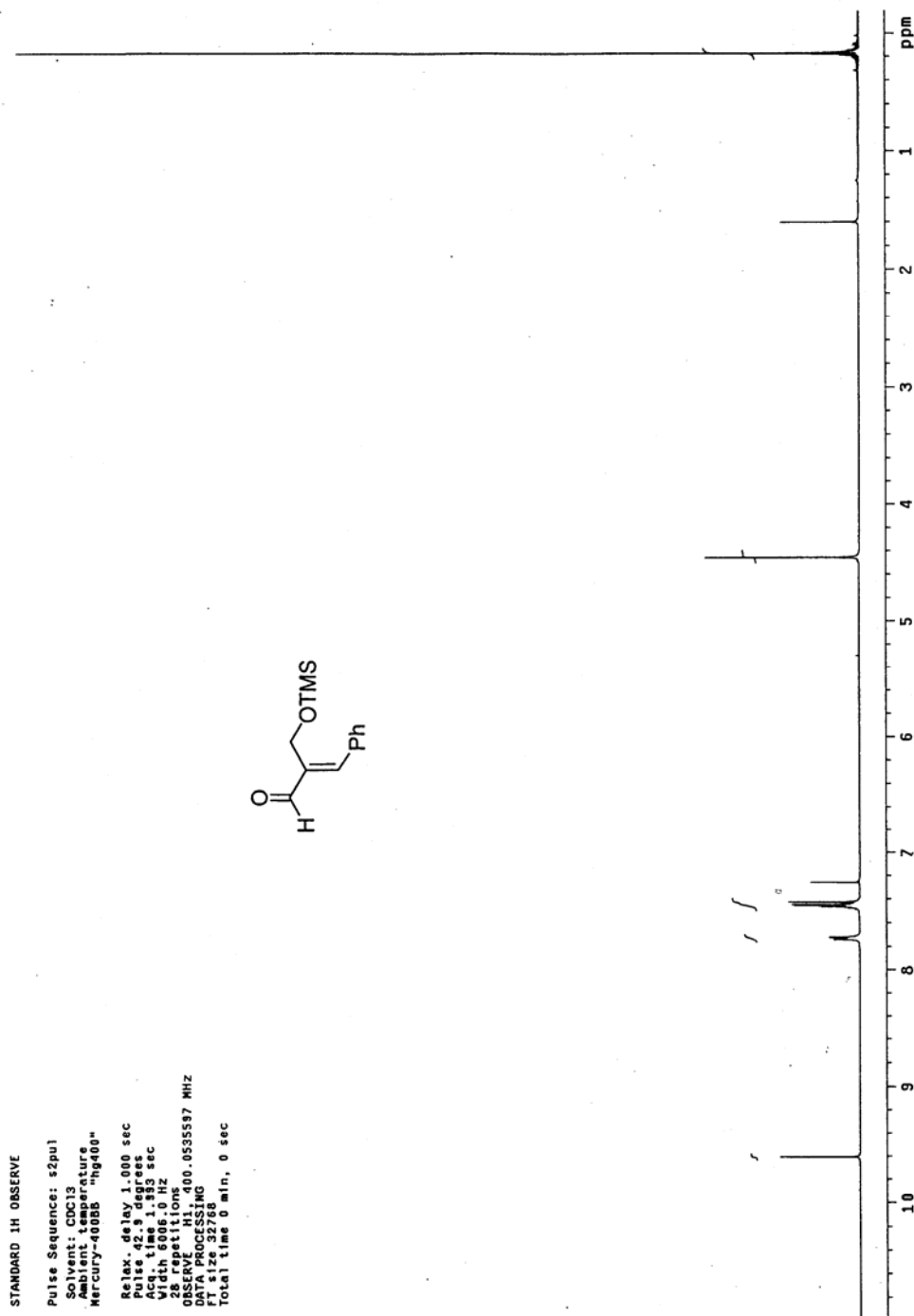
F1 us 30780

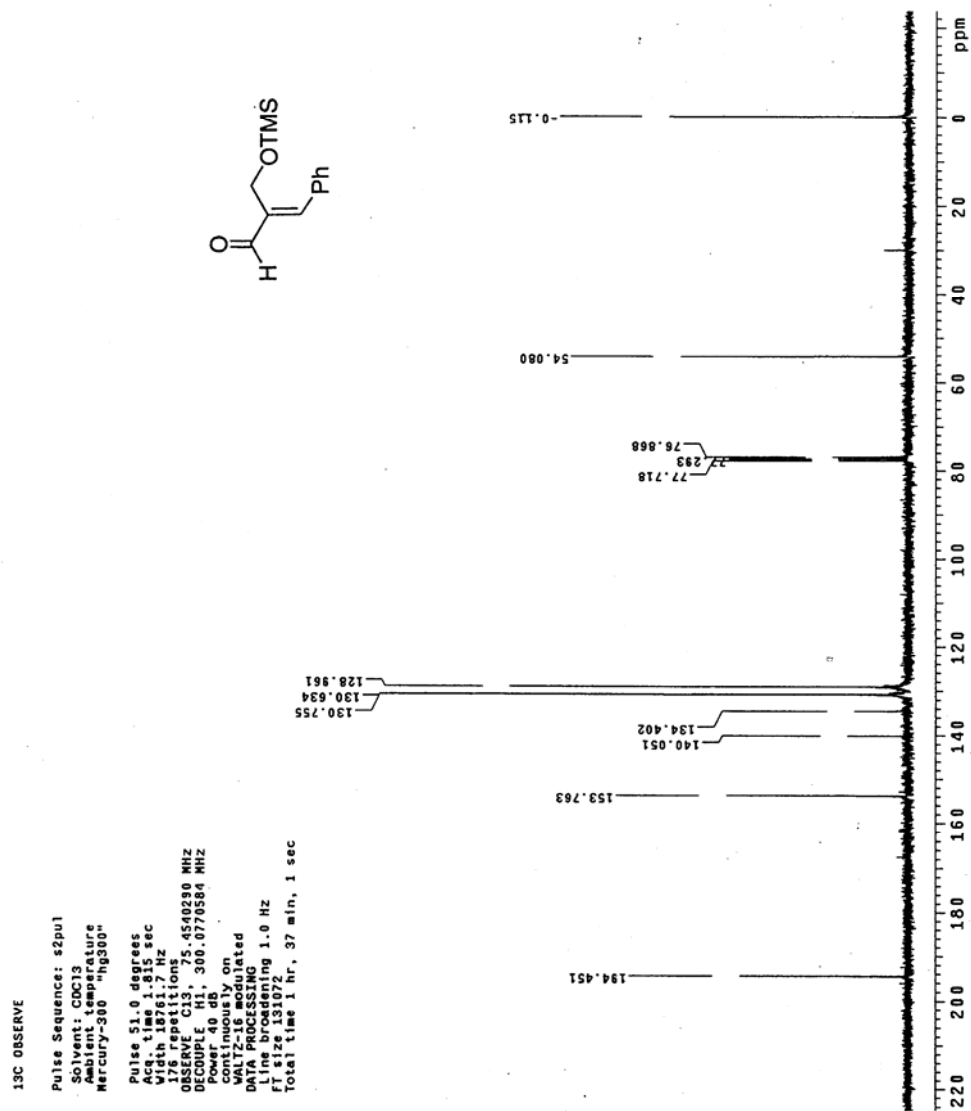
Total time 31 min, 42 sec

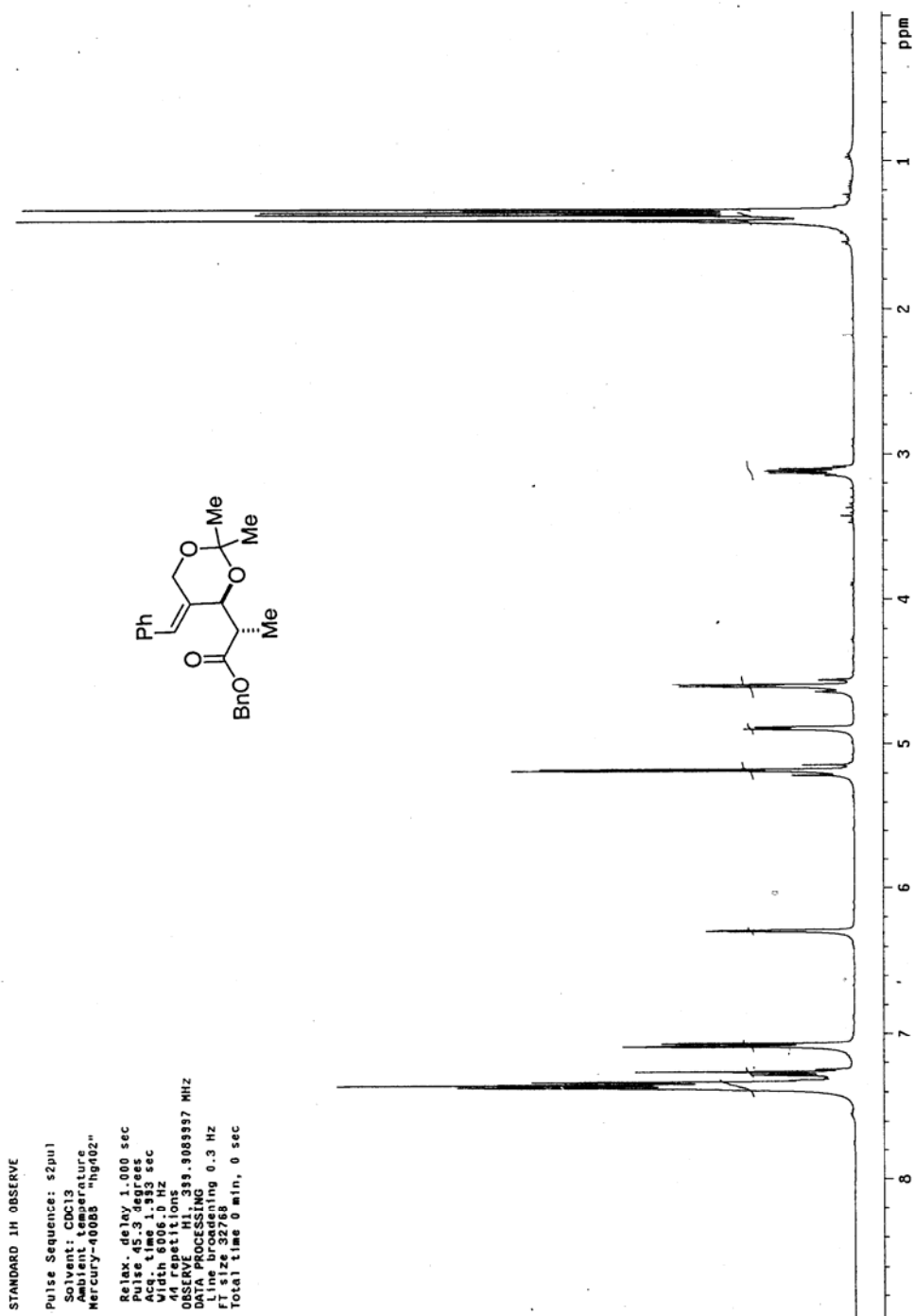


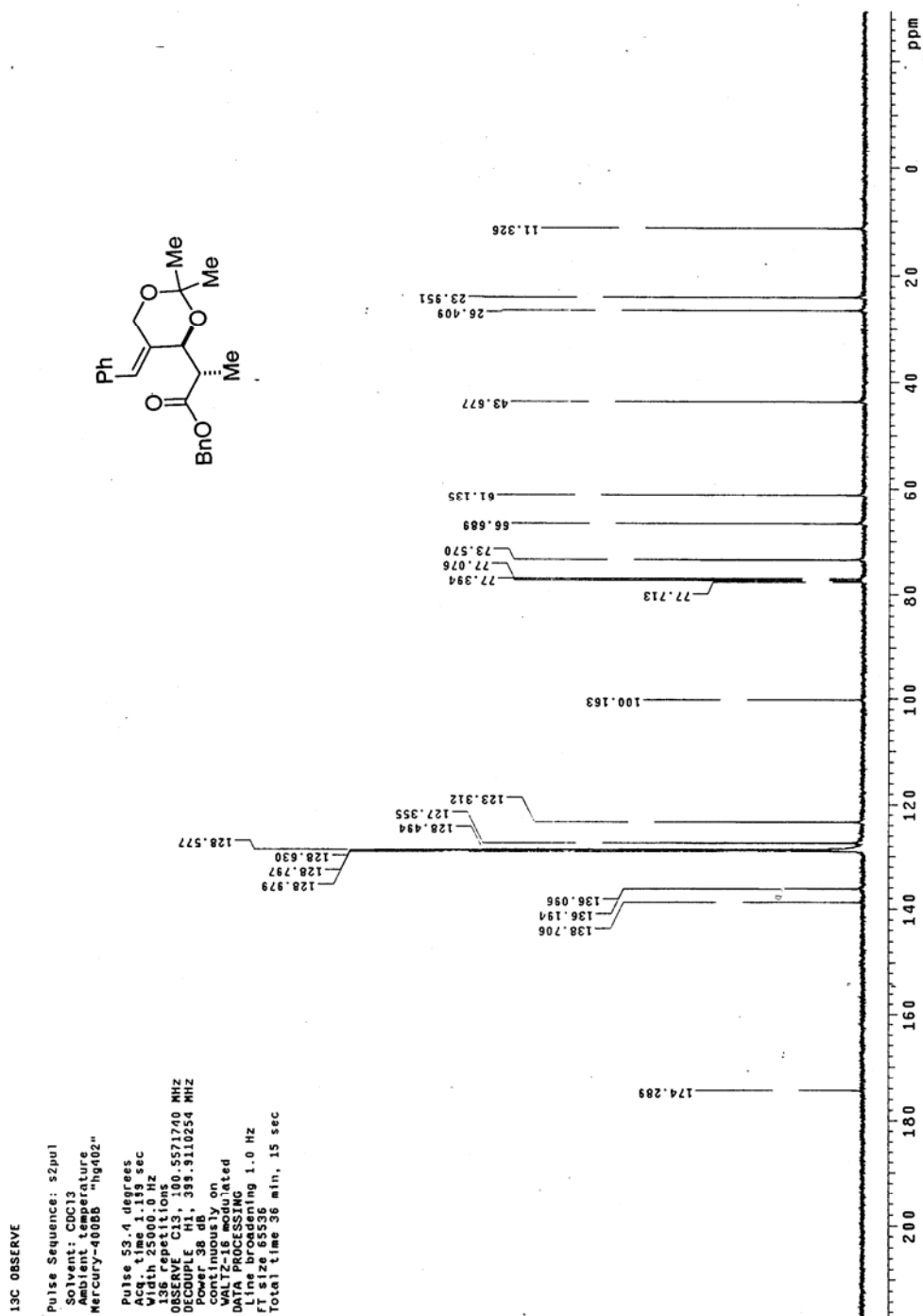
¹H NMR spectrum of compound 313

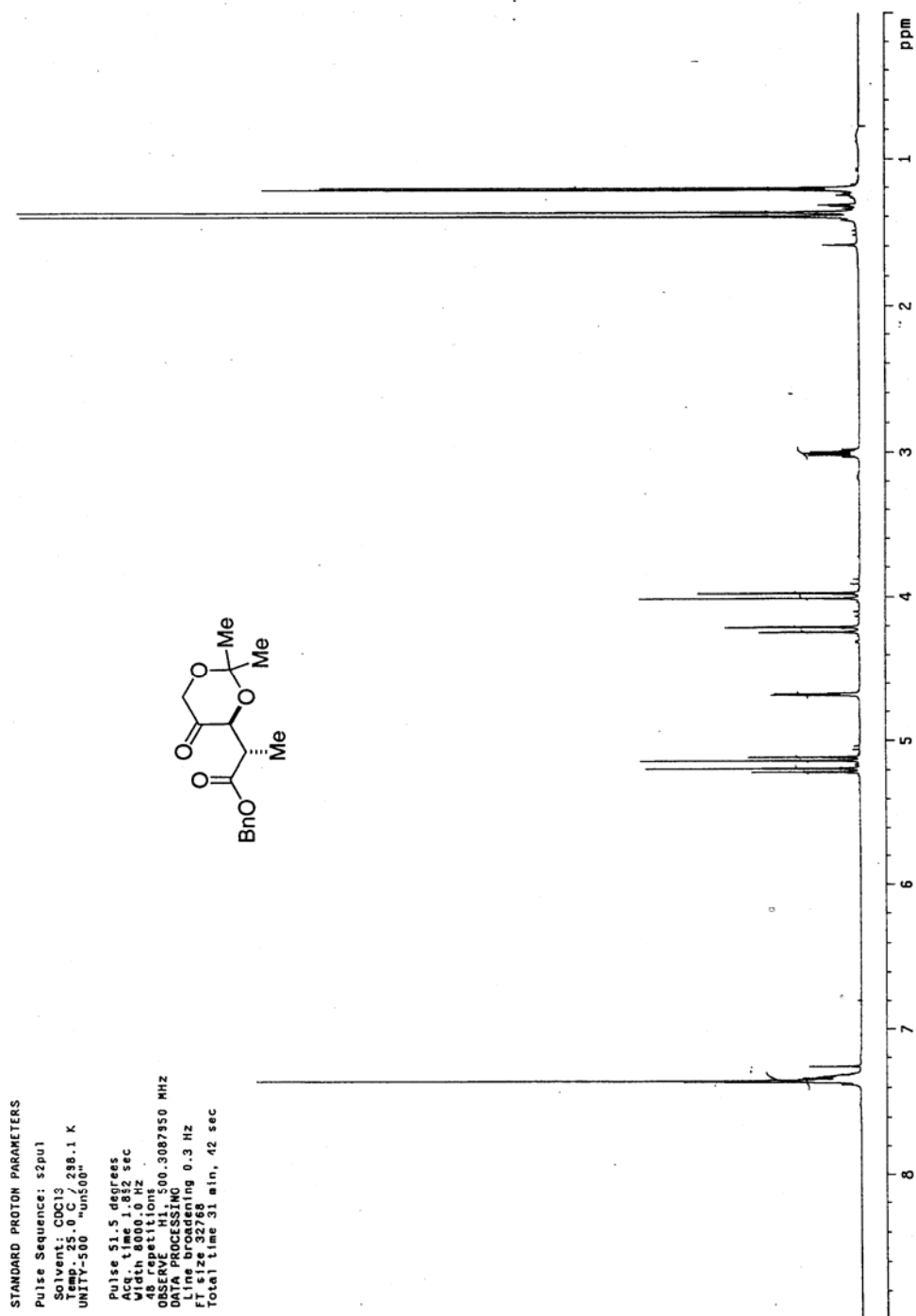
¹³C NMR spectrum of compound 313

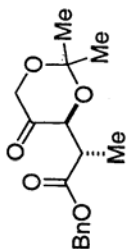
¹H NMR spectrum of compound 319

¹³C NMR spectrum of compound 319

¹H NMR spectrum of compound 321

^{13}C NMR spectrum of compound **321**

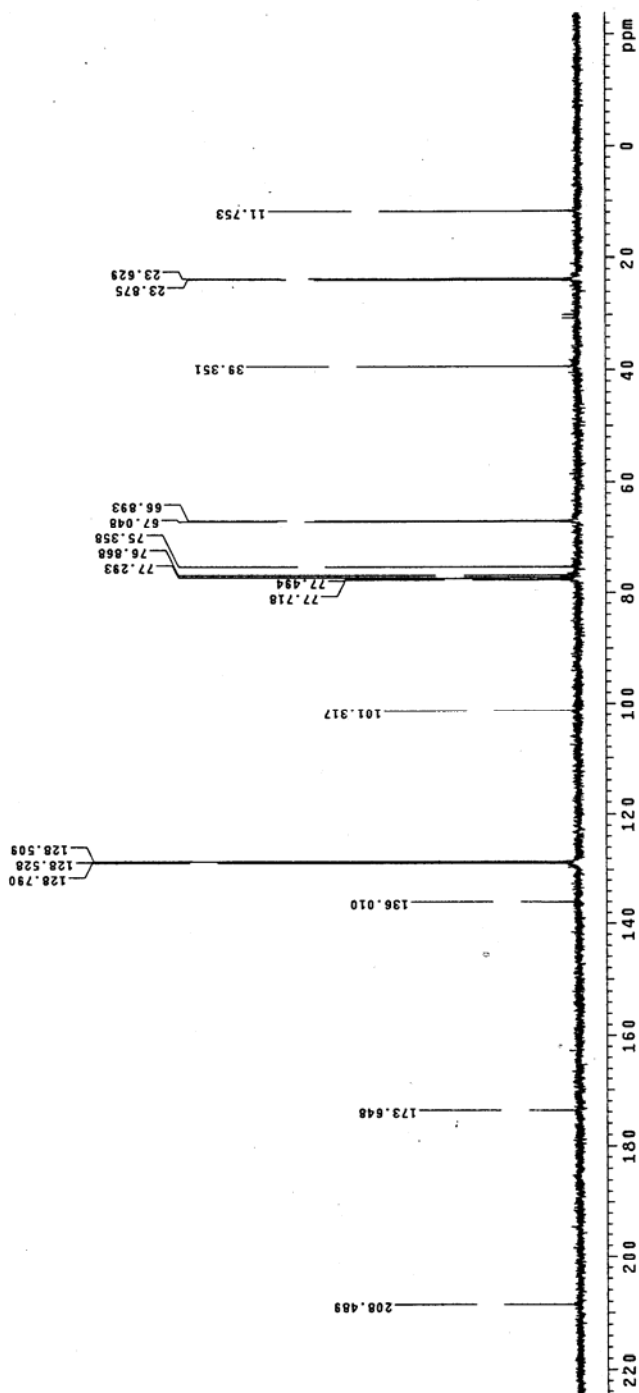
¹H NMR spectrum of compound **321a**

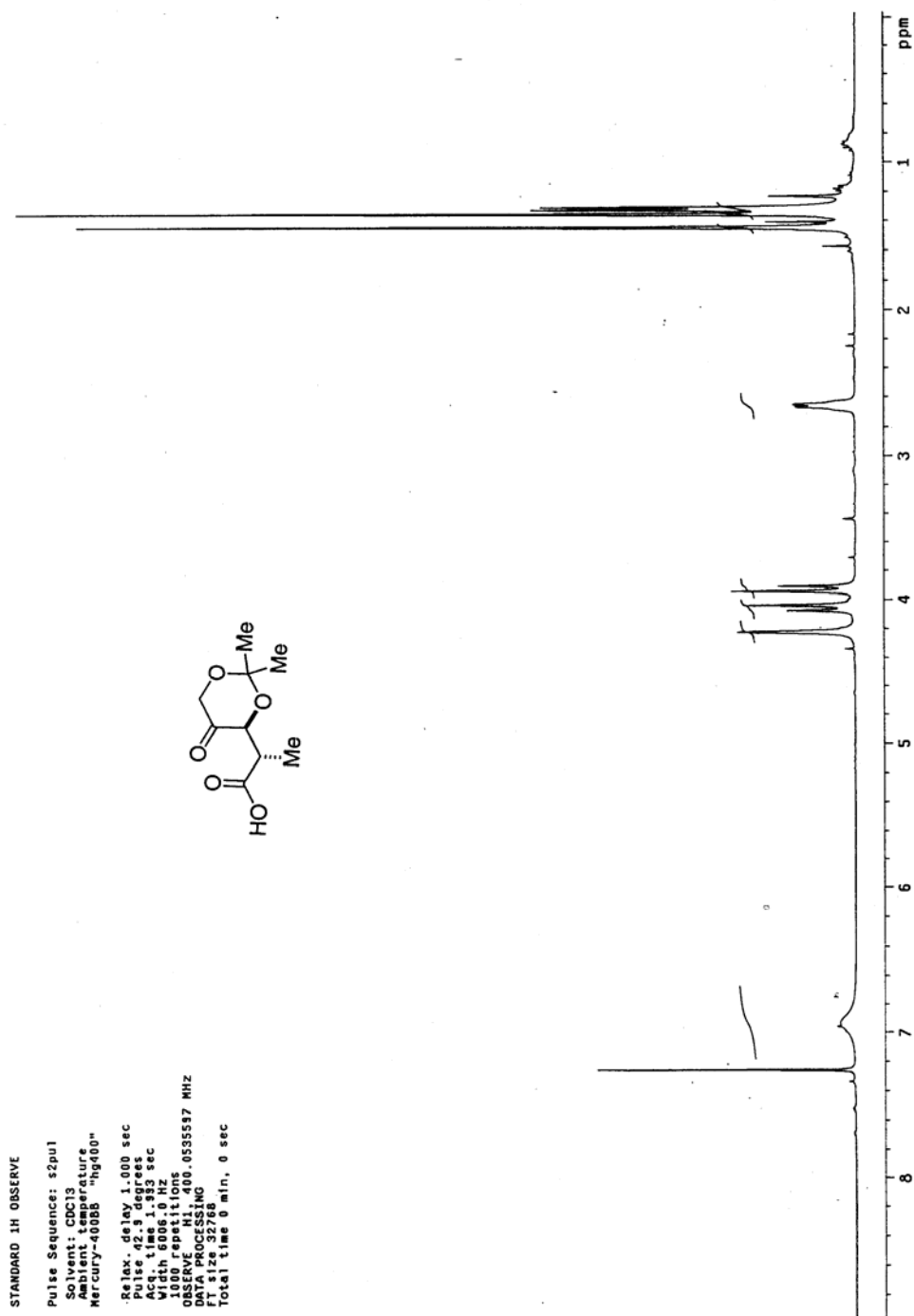
¹³C NMR spectrum of compound **321a**

¹³C OBSERVE

Pulse Sequence: s2pul
Solvent: CDCl₃
Ambient temperature
Mercury-300 "hg300"

Pulse 51.0 degrees
Acq. time 1.915 sec
1000 repetitions
OBSERVE C13, 75.4540290 MHZ
DECOUPLE H1, 300.0770564 MHZ
Power 40 db
Continuously on
WAIT=15 seconds
DATA PROCESSING
Line broadening 1.0 Hz
FT size 131072
Total time 0 min, 0 sec



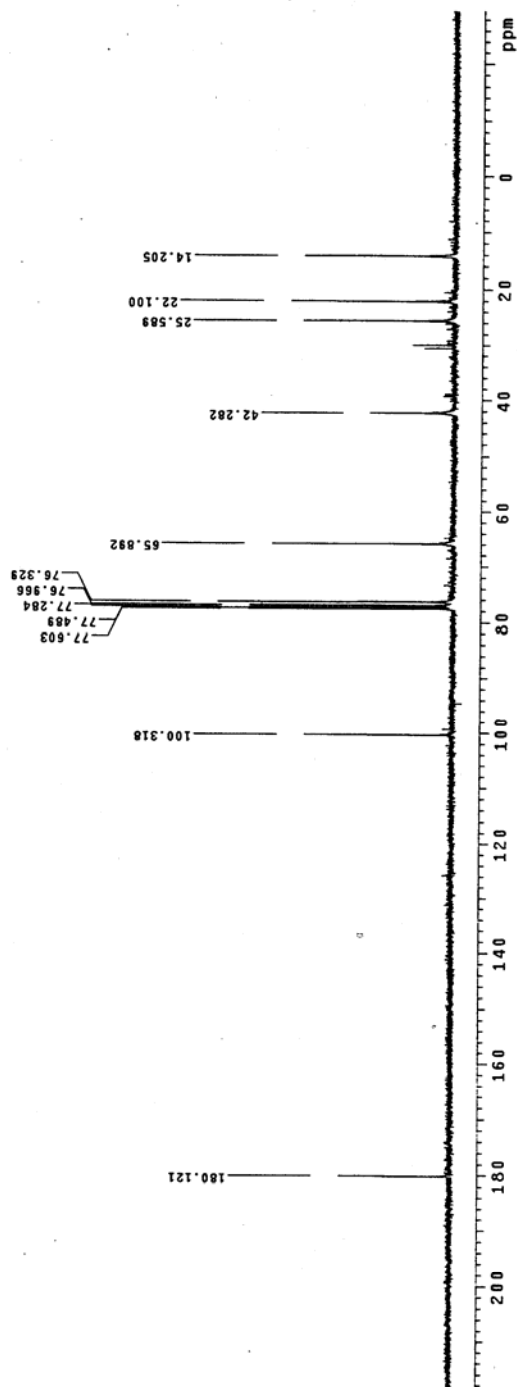
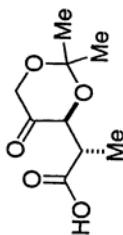
^1H NMR spectrum of compound **311**

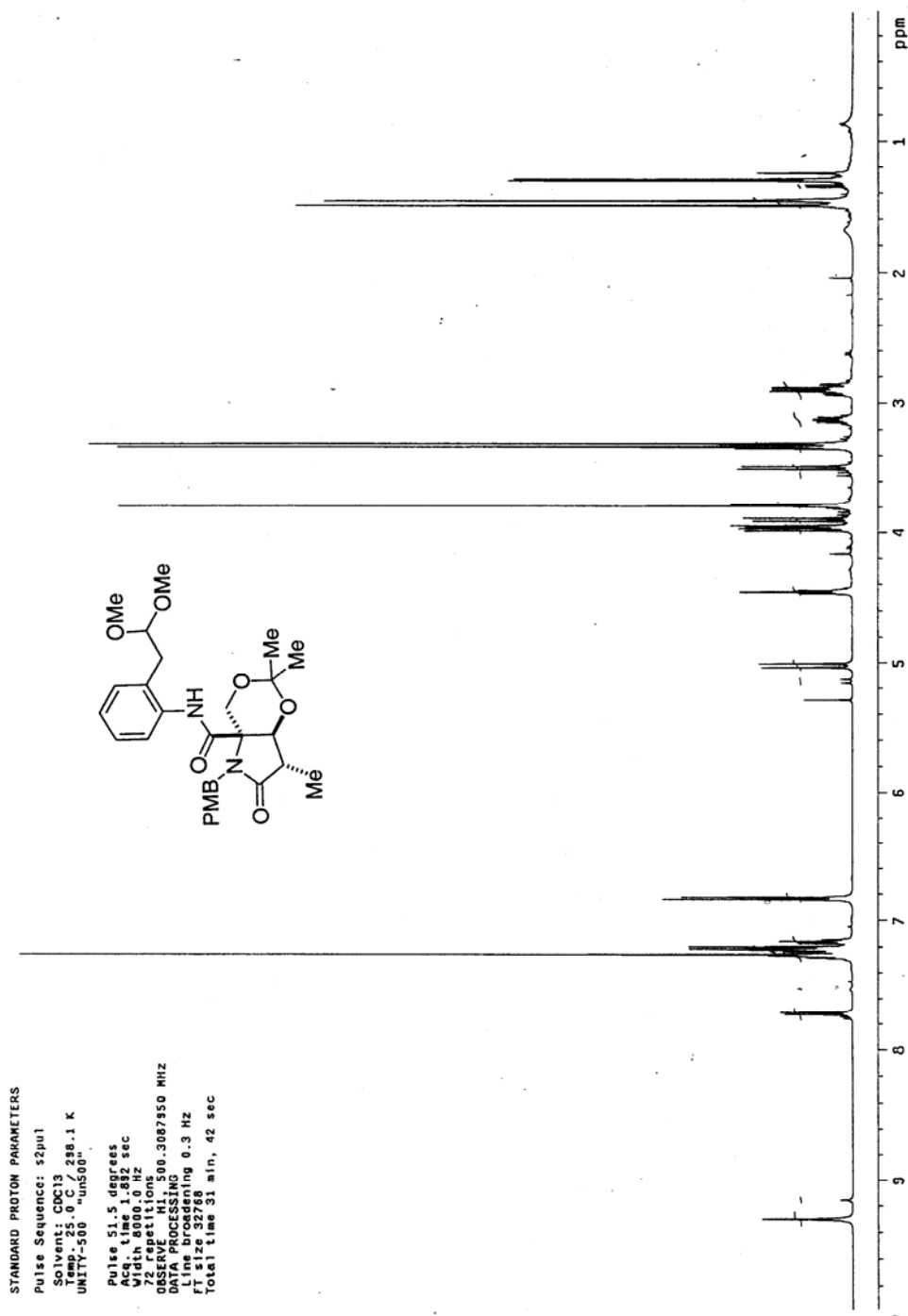
¹³C NMR spectrum of compound **311**

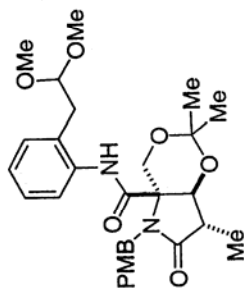
¹³C OBSERVE

Pulse Sequence: s2pul
Solvent: CDCl₃
Ambient temperature
Mercury-400BB "hg400"

Pulse 70.9 degrees
Acq. time 0.33 sec
2000 repetitions
OBSERVE C13, 100.535236 MHz
DECOUPLE H1, 400.0555305 MHz
Power 40 db
SOLVENT DECOUPLING on
WALTZ-16 modulated
DATA PROCESSING
Line broadening 1.0 Hz
FT size 65536
Total time 1 hr, 12 min, 30 sec



¹H NMR spectrum of compound 314

^{13}C NMR spectrum of compound 314

^{13}C OBSERVE

Pulse Sequence: s2pul

Solvent: CDCl₃

Ambient temperature

Mercury-300 "hg300"

Pulse 51.0 degrees

Acq. time 1.915 sec

2000 repetitions

2000 repetitions

OBSERVE C13, 75.4540290 MHz

DECOUPLE H1, 300.0770584 MHz

Power 40 db

Continuously on

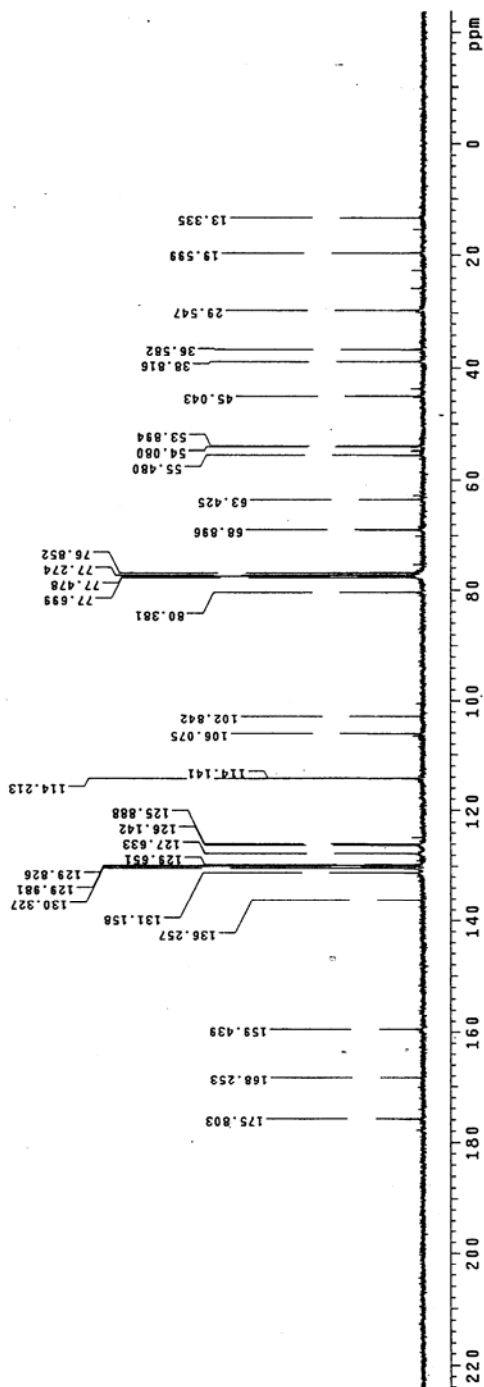
Waltz16 Modulated

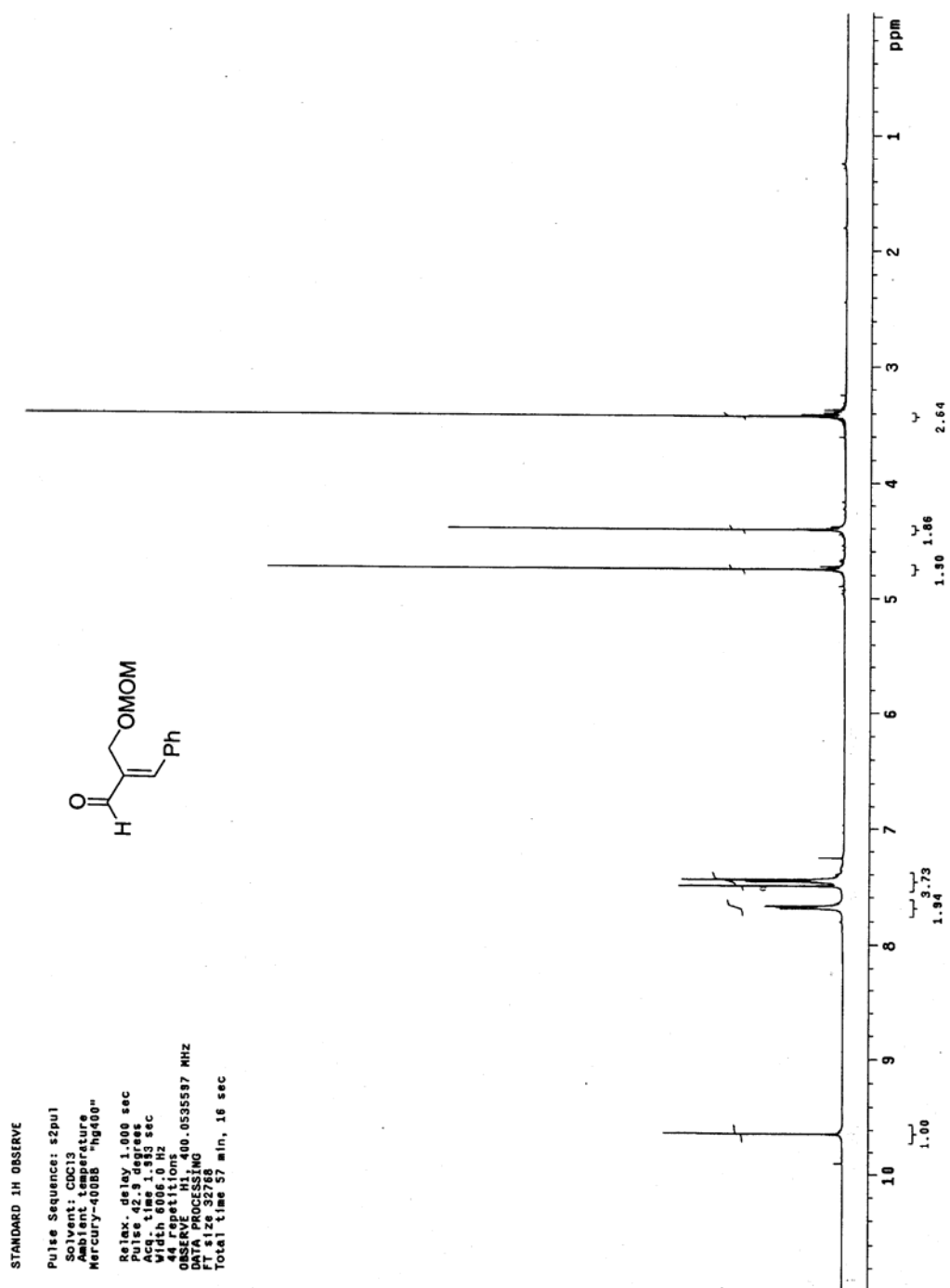
DATA PROCESSING

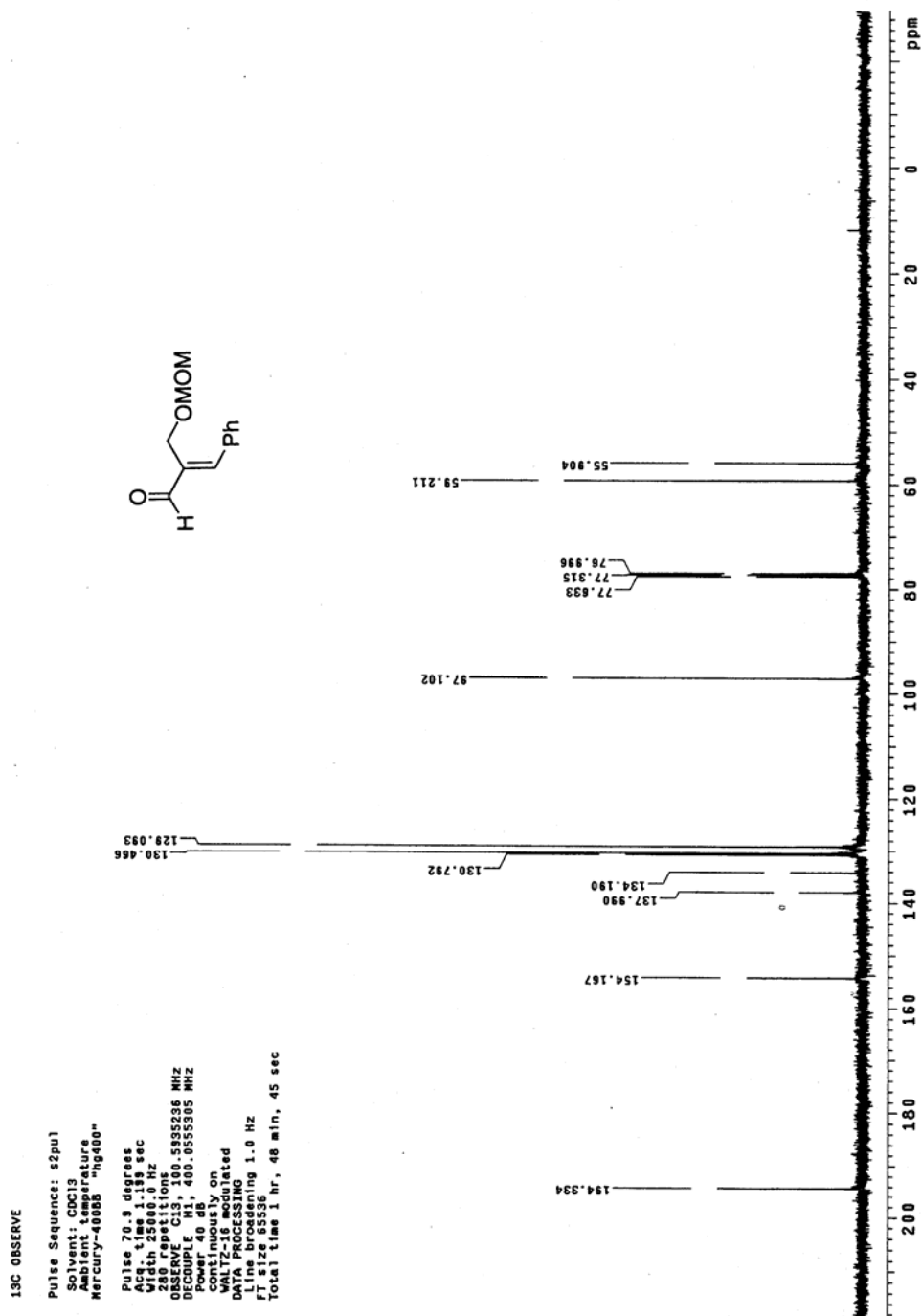
Line broadening 1.0 Hz

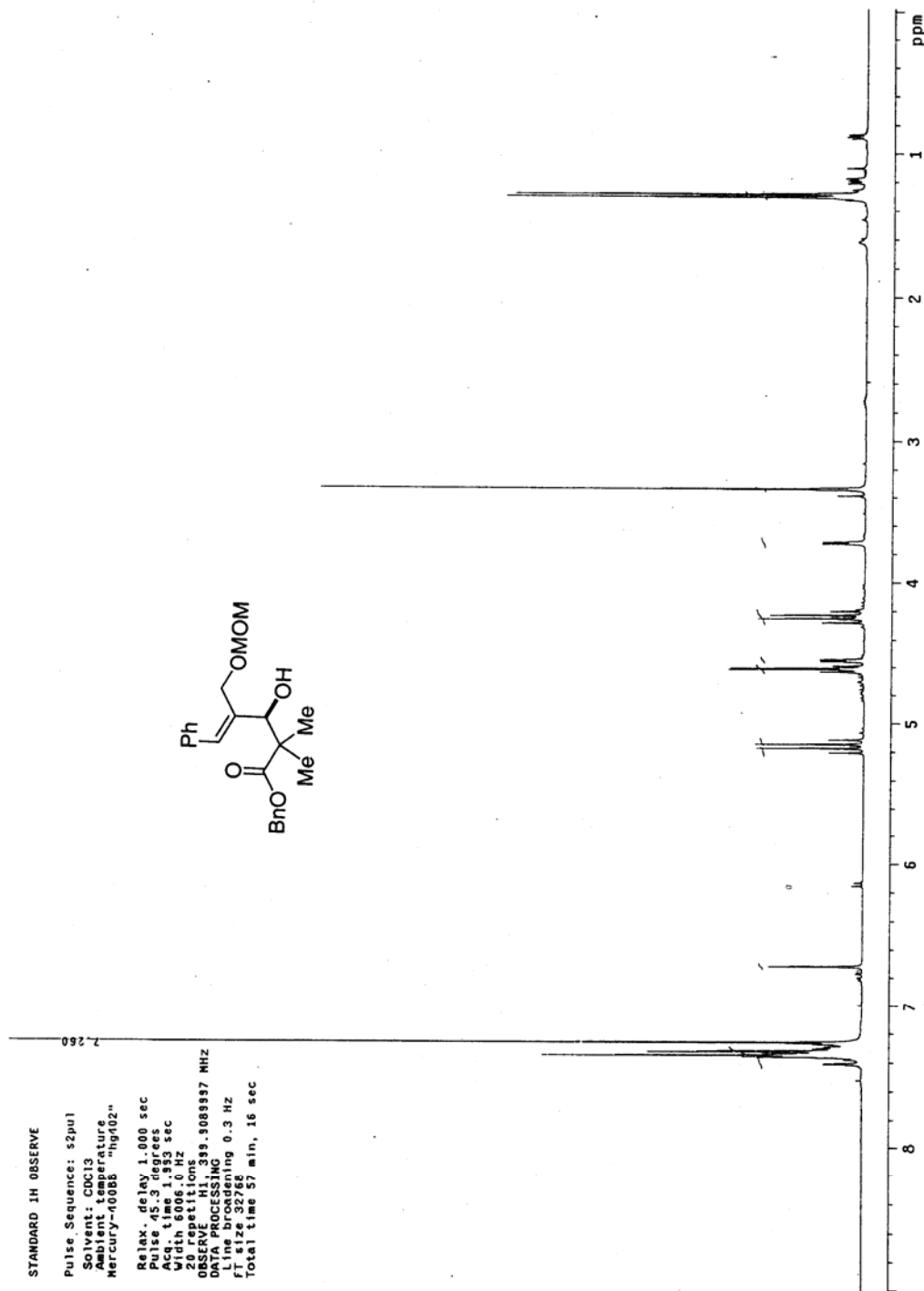
FT size 131072

Total time 1 hr, 37 min, 1 sec



^1H NMR spectrum of compound 322

¹³C NMR spectrum of compound 322

¹H NMR spectrum of compound 323

^{13}C NMR spectrum of compound **323**

^{13}C OBSERVE

Pulse Sequence: s2pul

Solvent: CDCl₃

Temperature:

Mercury-400BB "hg402"

Pulse 53.4 degrees

Acq. time 1.195 sec

Width 25000.0 Hz

569 repetitions

Observed C13, 100.5571740 MHz

Computed C13, 393.316254 MHz

Power 38 dB

continuously on

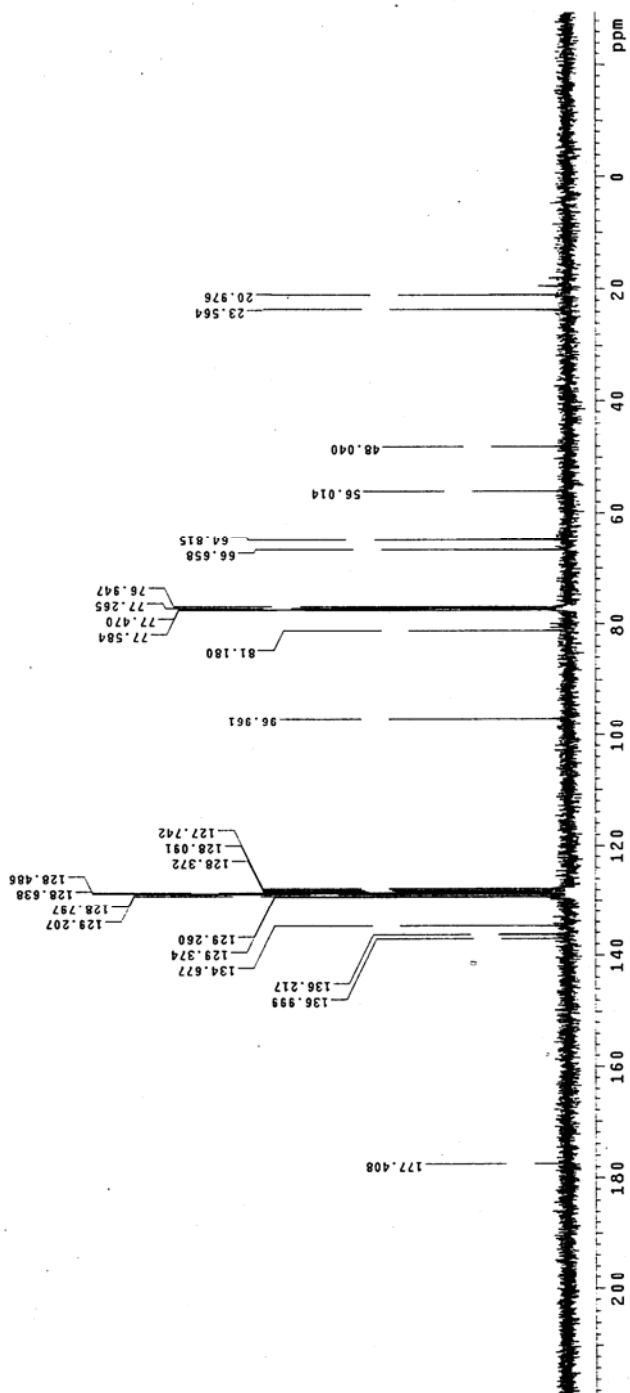
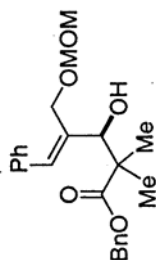
WALTZ-16 modulated

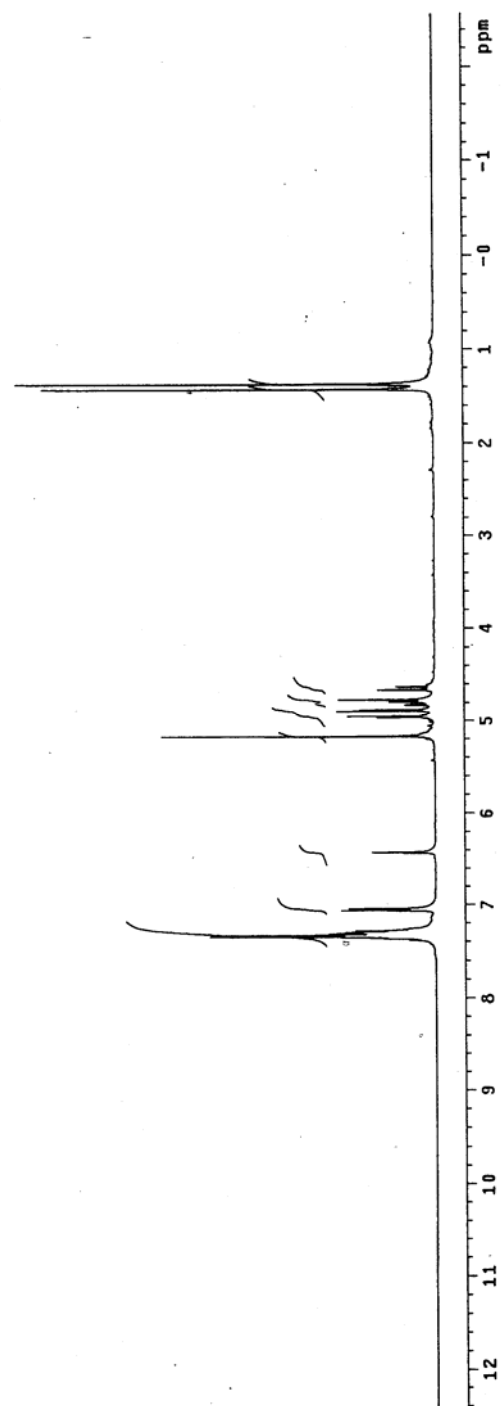
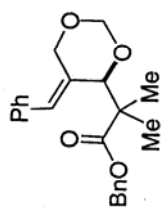
DATA PROCESSING

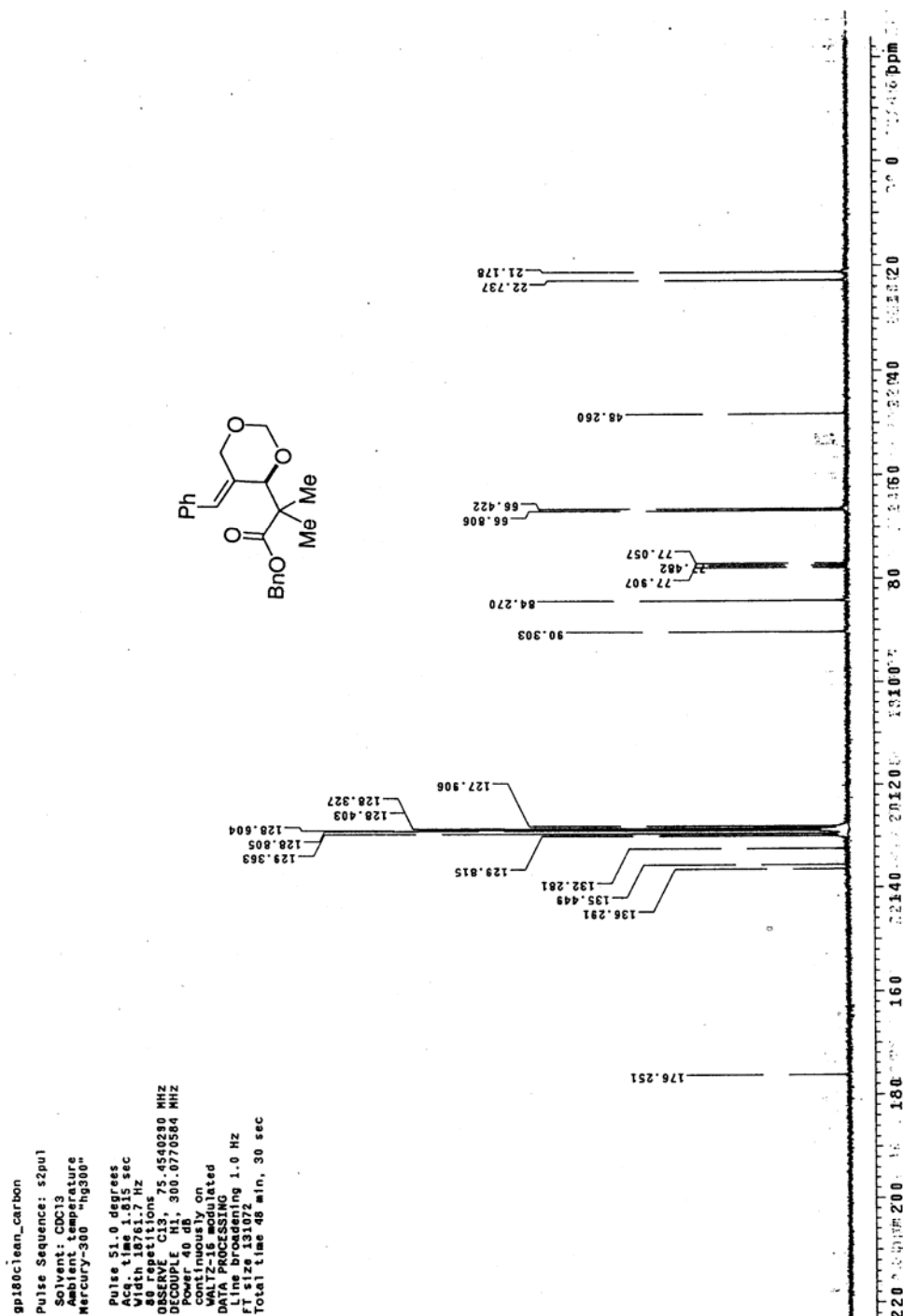
FT size 65556

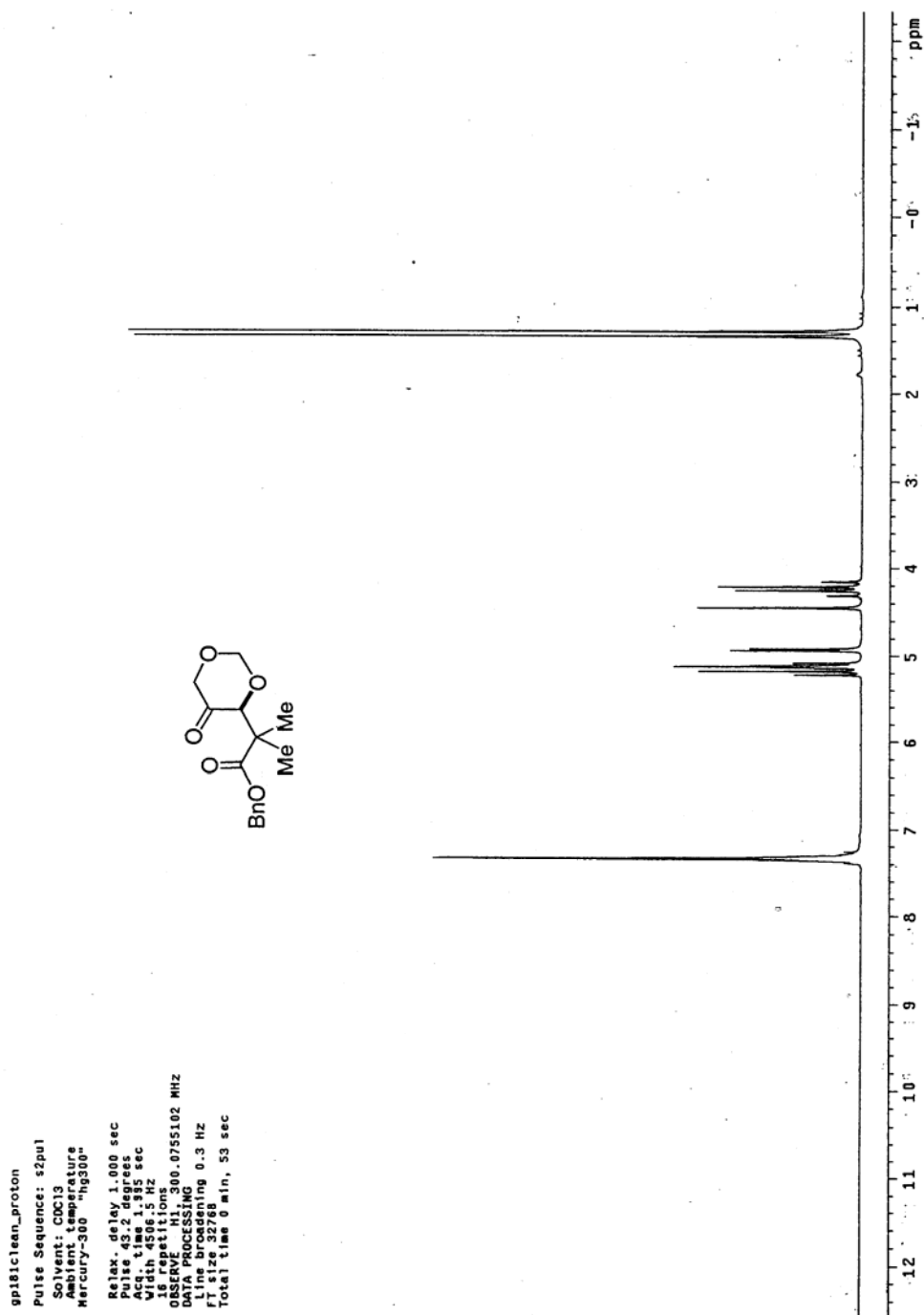
FT size 65556

Total time 36 min, 15 sec



¹H NMR spectrum of compound 324

¹³C NMR spectrum of compound 324

¹H NMR spectrum of compound 324a

¹³C NMR spectrum of compound 324a

¹³C OBSERVE

Pulse Sequence: s2pu1

Solvent: CDCl₃

Ambient temperature

Mercury-300 "hg300"

Pulse 51.0 degree

Acq 1.15 sec

Width 18761.7 Hz

492 repetitions

OBSERVE C13, 75.4540290 MHz

DECOUPLE H1, 300.0770564 MHz

continuously on

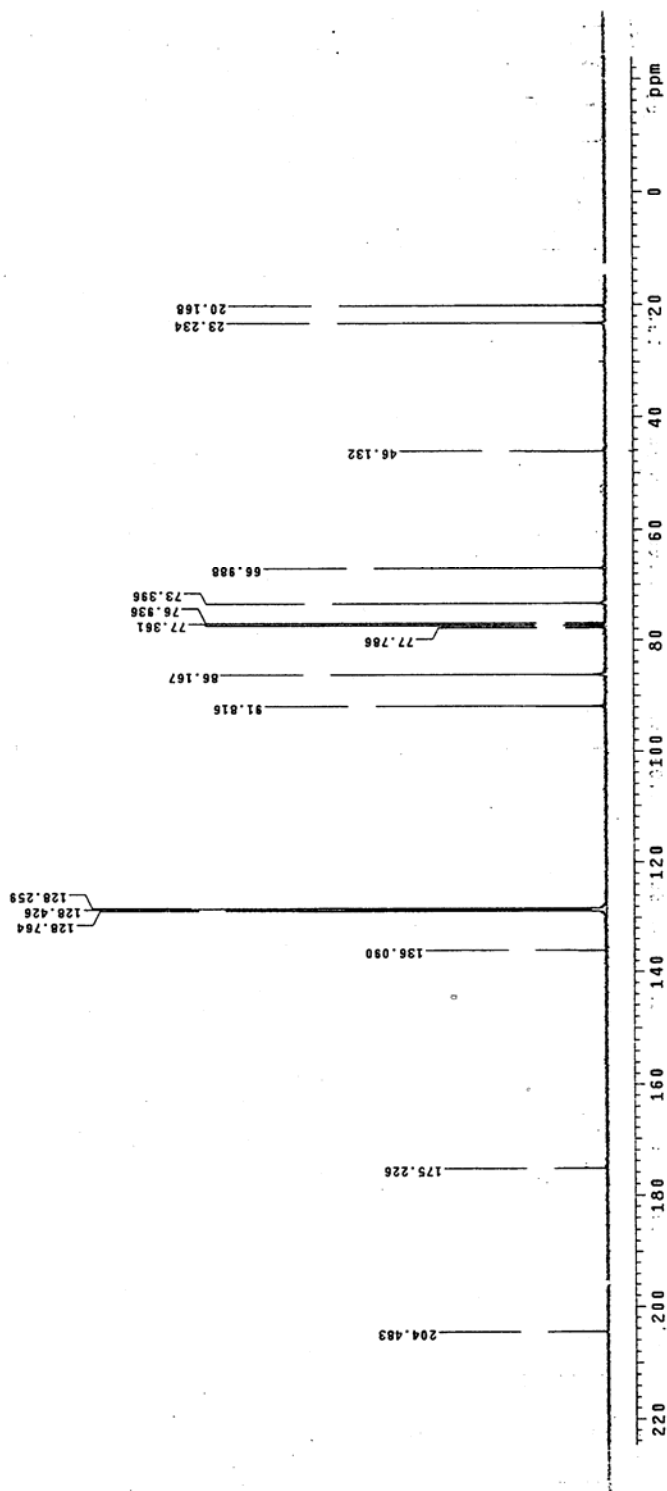
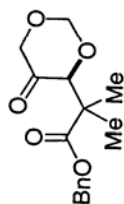
WALTZ-16 modulated

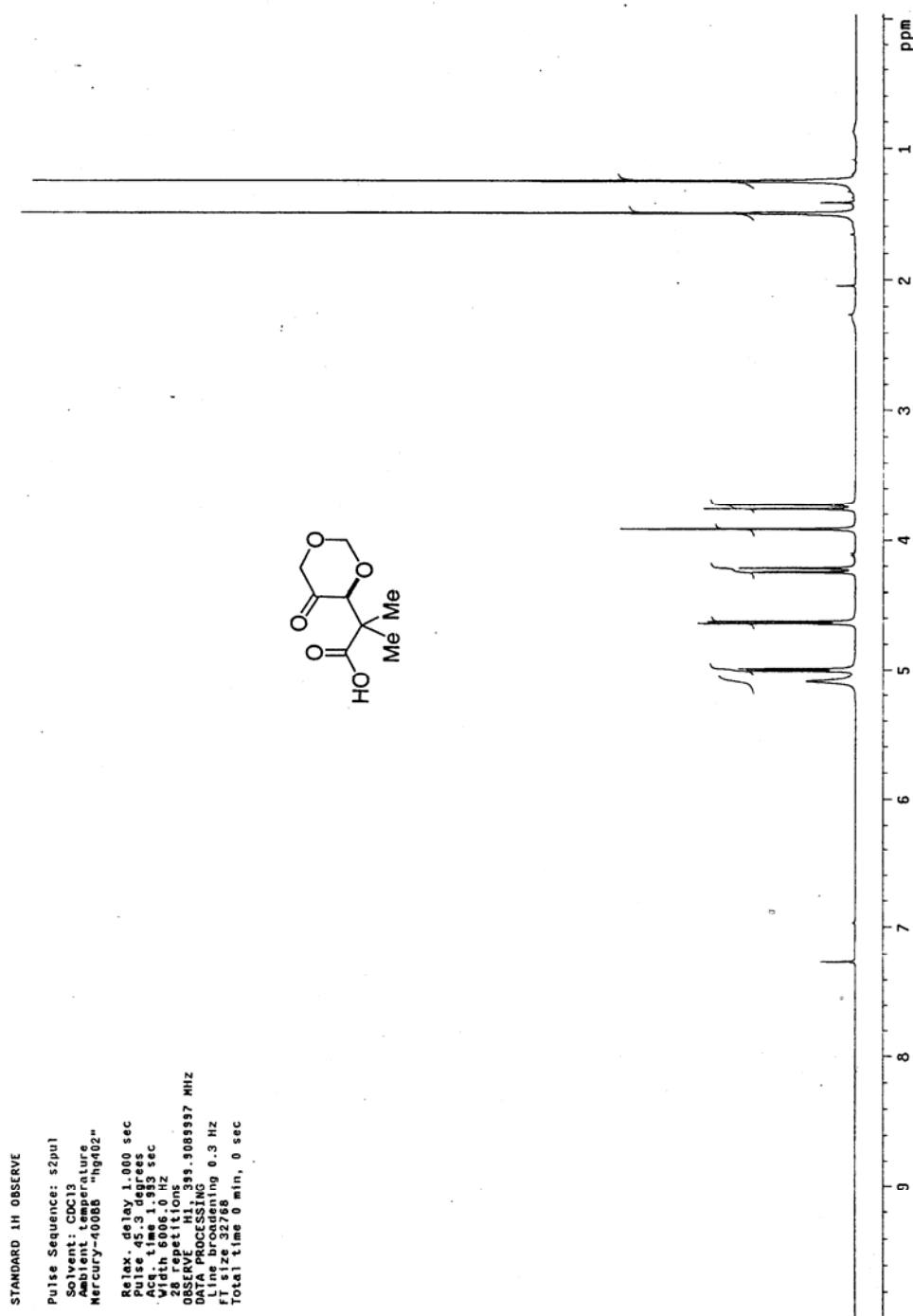
DATA PROCESSING

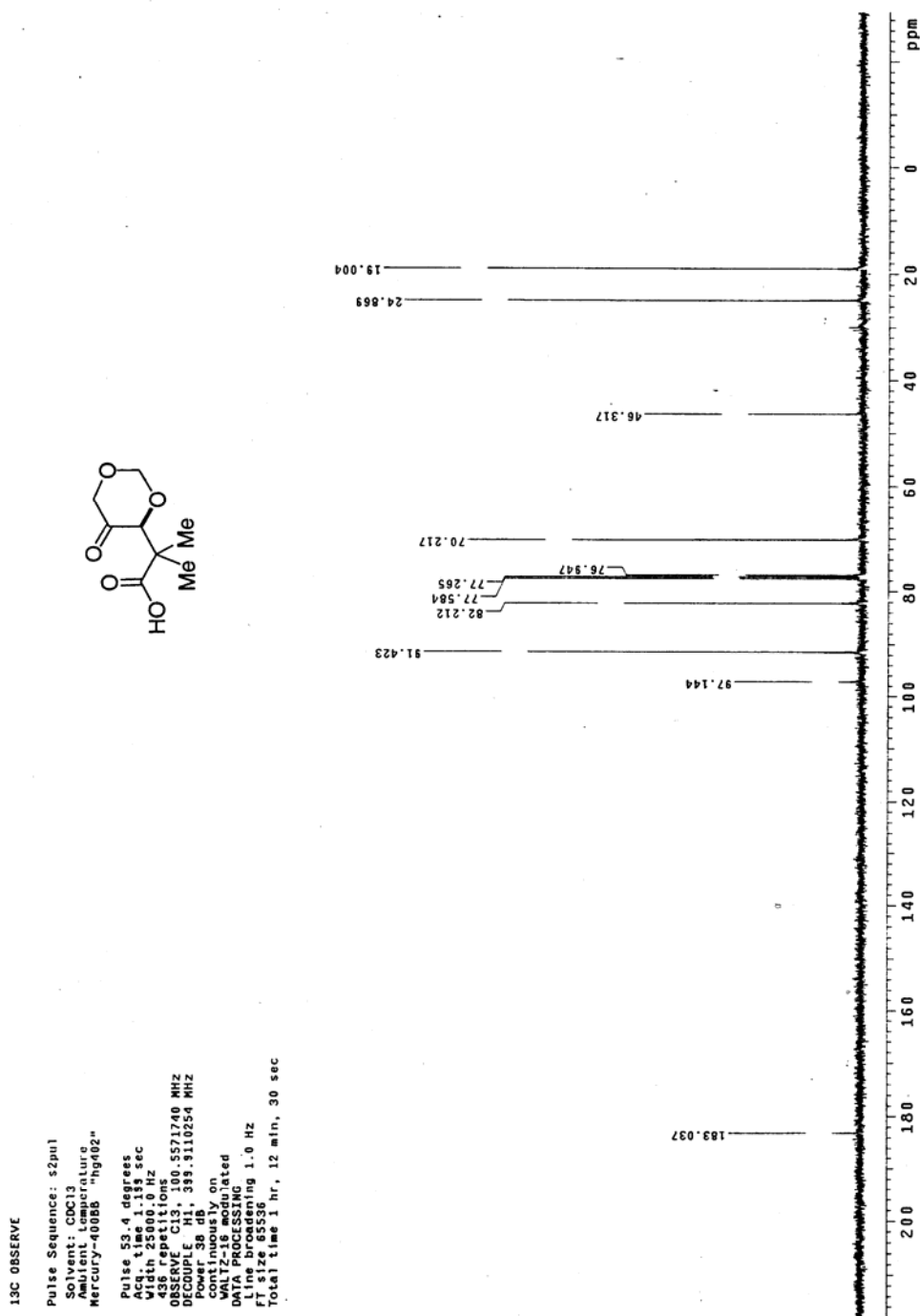
Line broadening 1.0 Hz

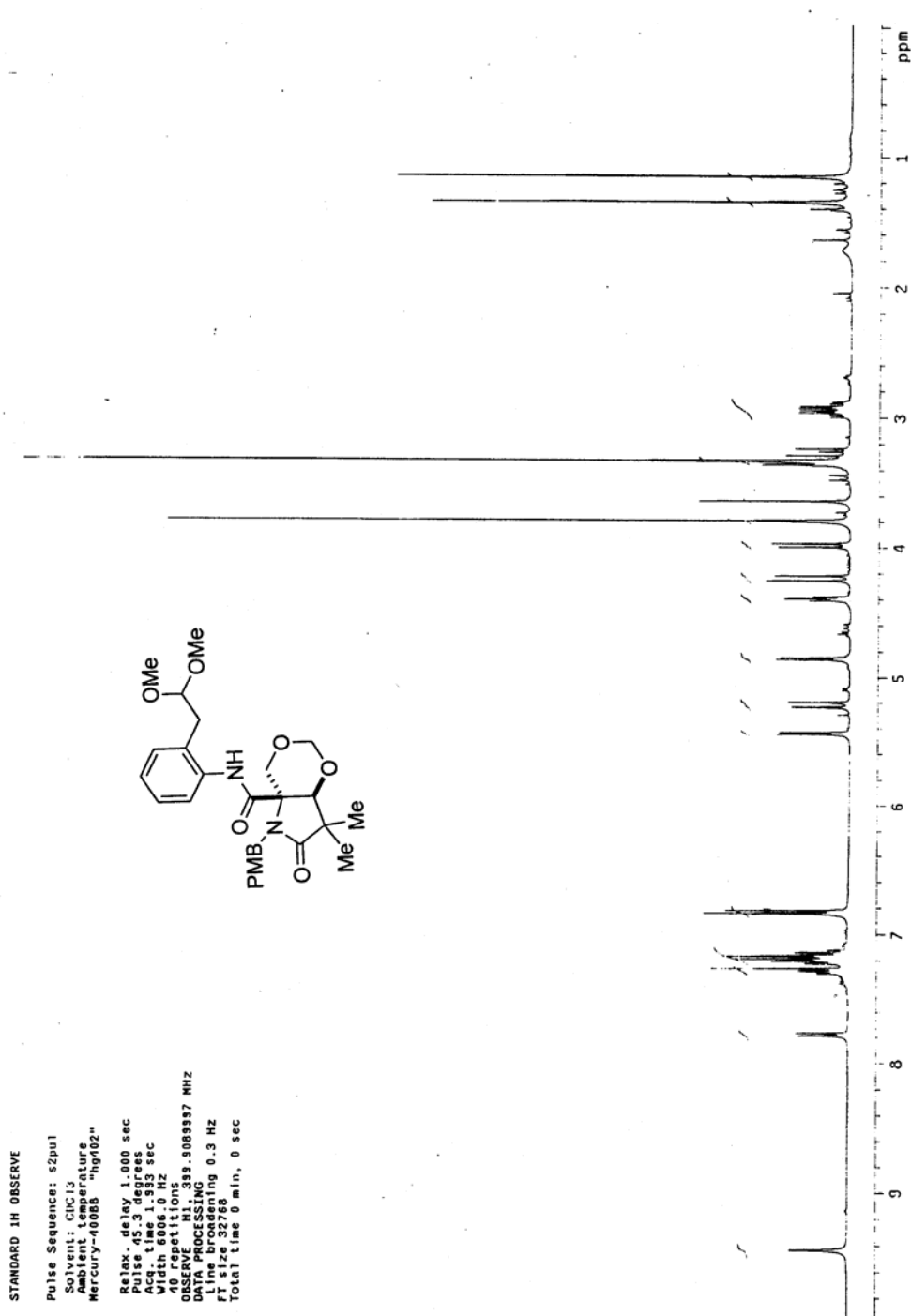
Fr 12.317

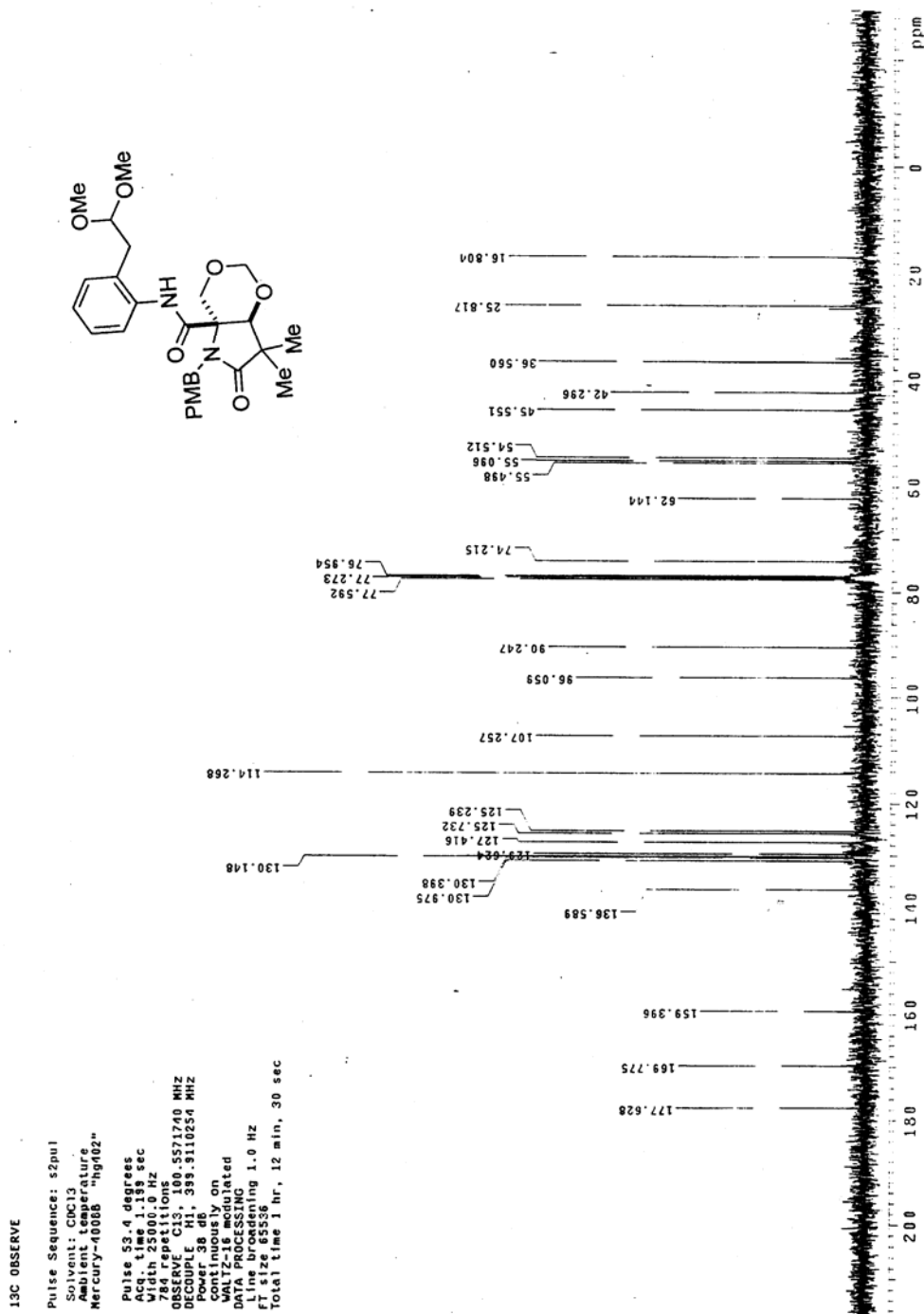
Total time 16 min, 30 sec

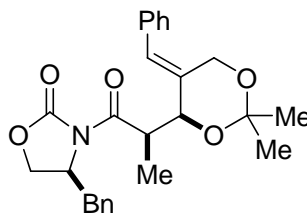


¹H NMR spectrum of compound 312

¹³C NMR spectrum of compound 312

¹H NMR spectrum of compound 315

^{13}C NMR spectrum of compound **315**

X-ray Crystal Structure Report of Aldol Adduct **291****291**

A colorless rod 0.25 x 0.10 x 0.08 mm in size was mounted on a Cryoloop with Paratone oil. Data were collected in a nitrogen gas stream at 208(2) K using phi and omega scans. Crystal-to-detector distance was 60 mm and exposure time was 10 seconds per frame using a scan width of 0.3°. Data collection was 99.9% complete to 25.00° in θ . A total of 8401 reflections were collected covering the indices, $-44 \leq h \leq 46$, $-3 \leq k \leq 8$, $-15 \leq l \leq 14$. 3633 reflections were found to be symmetry independent, with an R_{int} of 0.0238. Indexing and unit cell refinement indicated a C centered, monoclinic lattice. The space group was found to be C2 (No. 5). The data were integrated using the Bruker SAINT software program and scaled using the SADABS software program. Solution by direct methods (SIR-2004) produced a complete heavy-atom phasing model consistent with the proposed structure. All non-hydrogen atoms were refined anisotropically by full-matrix least-squares (SHELXL-97). All hydrogen atoms were placed using a riding model. Their positions were constrained relative to their parent atom using the appropriate HFIX command in SHELXL-97.

Table 1. Crystal data and structure refinement for kob07.

X-ray ID	kob07	
Sample/notebook ID	KOB07	
Empirical formula	C ₂₆ H ₂₉ N O ₅	
Formula weight	435.50	
Temperature	208(2) K	
Wavelength	0.71073 Å	
Crystal system	Monoclinic	
Space group	C2	
Unit cell dimensions	a = 35.160(3) Å	α = 90°.
	b = 6.0221(5) Å	β = 106.5180(10)°.
	c = 11.5890(10) Å	γ = 90°.
Volume	2352.6(3) Å ³	
Z	4	
Density (calculated)	1.230 Mg/m ³	
Absorption coefficient	0.085 mm ⁻¹	
F(000)	928	
Crystal size	0.25 x 0.10 x 0.08 mm ³	
Crystal color/habit	colorless rod	
Theta range for data collection	2.42 to 28.26°.	
Index ranges	-44 ≤ h ≤ 46, -3 ≤ k ≤ 8, -15 ≤ l ≤ 14	
Reflections collected	8401	
Independent reflections	3633 [R(int) = 0.0238]	
Completeness to theta = 25.00°	99.9 %	
Absorption correction	Semi-empirical from equivalents	
Max. and min. transmission	0.9932 and 0.9791	
Refinement method	Full-matrix least-squares on F ²	
Data / restraints / parameters	3633 / 1 / 292	
Goodness-of-fit on F ²	1.041	
Final R indices [I > 2σ(I)]	R1 = 0.0419, wR2 = 0.1105	
R indices (all data)	R1 = 0.0485, wR2 = 0.1148	
Absolute structure parameter	-0.1(11)	
Largest diff. peak and hole	0.412 and -0.183 e.Å ⁻³	

Table 2. Atomic coordinates ($\times 10^4$) and equivalent isotropic displacement parameters ($\text{\AA}^2 \times 10^3$) for kob07. $U(\text{eq})$ is defined as one third of the trace of the orthogonalized U^{ij} tensor.

	x	y	z	$U(\text{eq})$
C(1)	8051(1)	9565(5)	-3504(2)	56(1)
C(2)	7945(1)	8915(6)	-4697(2)	68(1)
C(3)	8066(1)	6926(6)	-5038(2)	65(1)
C(4)	8305(1)	5579(5)	-4171(2)	60(1)
C(5)	8413(1)	6205(5)	-2978(2)	49(1)
C(6)	8289(1)	8217(4)	-2628(2)	42(1)
C(7)	8402(1)	8896(5)	-1326(2)	46(1)
C(8)	8040(1)	8796(4)	-849(2)	35(1)
C(9)	7853(1)	6494(4)	-1001(2)	43(1)
C(10)	7882(1)	7664(4)	891(2)	37(1)
C(11)	8335(1)	10875(4)	1065(2)	38(1)
C(12)	8477(1)	10793(4)	2427(2)	40(1)
C(13)	8266(1)	12575(6)	2940(2)	72(1)
C(14)	8927(1)	11169(4)	2824(2)	41(1)
C(15)	9089(1)	10576(4)	4140(2)	38(1)
C(16)	9121(1)	8124(4)	4366(2)	41(1)
C(17)	9324(1)	8011(4)	2558(2)	47(1)
C(18)	9299(1)	6440(6)	1522(2)	65(1)
C(19)	9748(1)	8586(7)	3229(3)	80(1)
C(20)	9176(1)	12149(4)	4989(2)	45(1)
C(21)	9293(1)	11914(4)	6305(2)	45(1)
C(22)	9198(1)	10099(5)	6903(2)	49(1)
C(23)	9309(1)	10021(6)	8147(2)	59(1)
C(24)	9516(1)	11726(7)	8821(2)	68(1)
C(25)	9613(1)	13547(6)	8242(2)	79(1)
C(26)	9501(1)	13650(5)	7005(2)	69(1)
N(1)	8132(1)	9030(3)	466(1)	35(1)
O(1)	7696(1)	6259(3)	14(1)	44(1)
O(2)	7822(1)	7667(3)	1858(1)	45(1)
O(3)	8403(1)	12422(3)	493(1)	52(1)

O(4)	9124(1)	6934(3)	3313(1)	53(1)
O(5)	9106(1)	9929(3)	2066(1)	53(1)

Table 3. Bond lengths [\AA] and angles [$^\circ$] for kob07.

C(1)-C(6)	1.380(3)	C(13)-H(13C)	0.9700
C(1)-C(2)	1.383(4)	C(14)-O(5)	1.428(3)
C(1)-H(1)	0.9400	C(14)-C(15)	1.511(3)
C(2)-C(3)	1.367(5)	C(14)-H(14)	0.9900
C(2)-H(2)	0.9400	C(15)-C(20)	1.337(3)
C(3)-C(4)	1.375(4)	C(15)-C(16)	1.499(3)
C(3)-H(3)	0.9400	C(16)-O(4)	1.418(3)
C(4)-C(5)	1.379(3)	C(16)-H(16A)	0.9800
C(4)-H(4)	0.9400	C(16)-H(16B)	0.9800
C(5)-C(6)	1.388(4)	C(17)-O(5)	1.412(3)
C(5)-H(5)	0.9400	C(17)-O(4)	1.423(3)
C(6)-C(7)	1.504(3)	C(17)-C(18)	1.511(4)
C(7)-C(8)	1.524(3)	C(17)-C(19)	1.514(4)
C(7)-H(7A)	0.9800	C(18)-H(18A)	0.9700
C(7)-H(7B)	0.9800	C(18)-H(18B)	0.9700
C(8)-N(1)	1.472(2)	C(18)-H(18C)	0.9700
C(8)-C(9)	1.523(3)	C(19)-H(19A)	0.9700
C(8)-H(8)	0.9900	C(19)-H(19B)	0.9700
C(9)-O(1)	1.443(2)	C(19)-H(19C)	0.9700
C(9)-H(9A)	0.9800	C(20)-C(21)	1.469(3)
C(9)-H(9B)	0.9800	C(20)-H(20)	0.9400
C(10)-O(2)	1.198(2)	C(21)-C(22)	1.386(4)
C(10)-O(1)	1.342(2)	C(21)-C(26)	1.396(4)
C(10)-N(1)	1.391(3)	C(22)-C(23)	1.383(3)
C(11)-O(3)	1.207(3)	C(22)-H(22)	0.9400
C(11)-N(1)	1.394(3)	C(23)-C(24)	1.367(4)
C(11)-C(12)	1.515(3)	C(23)-H(23)	0.9400
C(12)-C(13)	1.519(3)	C(24)-C(25)	1.379(5)
C(12)-C(14)	1.535(3)	C(24)-H(24)	0.9400
C(12)-H(12)	0.9900	C(25)-C(26)	1.375(4)
C(13)-H(13A)	0.9700	C(25)-H(25)	0.9400
C(13)-H(13B)	0.9700	C(26)-H(26)	0.9400

C(6)-C(1)-C(2)	120.3(3)	O(2)-C(10)-O(1)	122.05(19)
C(6)-C(1)-H(1)	119.8	O(2)-C(10)-N(1)	128.9(2)
C(2)-C(1)-H(1)	119.8	O(1)-C(10)-N(1)	109.08(16)
C(3)-C(2)-C(1)	121.3(3)	O(3)-C(11)-N(1)	119.73(17)
C(3)-C(2)-H(2)	119.4	O(3)-C(11)-C(12)	122.60(19)
C(1)-C(2)-H(2)	119.4	N(1)-C(11)-C(12)	117.60(19)
C(2)-C(3)-C(4)	118.8(2)	C(11)-C(12)-C(13)	109.34(18)
C(2)-C(3)-H(3)	120.6	C(11)-C(12)-C(14)	108.33(17)
C(4)-C(3)-H(3)	120.6	C(13)-C(12)-C(14)	110.85(19)
C(3)-C(4)-C(5)	120.6(3)	C(11)-C(12)-H(12)	109.4
C(3)-C(4)-H(4)	119.7	C(13)-C(12)-H(12)	109.4
C(5)-C(4)-H(4)	119.7	C(14)-C(12)-H(12)	109.4
C(4)-C(5)-C(6)	120.7(2)	C(12)-C(13)-H(13A)	109.5
C(4)-C(5)-H(5)	119.6	C(12)-C(13)-H(13B)	109.5
C(6)-C(5)-H(5)	119.6	H(13A)-C(13)-H(13B)	109.5
C(1)-C(6)-C(5)	118.3(2)	C(12)-C(13)-H(13C)	109.5
C(1)-C(6)-C(7)	120.7(2)	H(13A)-C(13)-H(13C)	109.5
C(5)-C(6)-C(7)	121.0(2)	H(13B)-C(13)-H(13C)	109.5
C(6)-C(7)-C(8)	110.09(16)	O(5)-C(14)-C(15)	113.15(17)
C(6)-C(7)-H(7A)	109.6	O(5)-C(14)-C(12)	109.61(17)
C(8)-C(7)-H(7A)	109.6	C(15)-C(14)-C(12)	109.04(17)
C(6)-C(7)-H(7B)	109.6	O(5)-C(14)-H(14)	108.3
C(8)-C(7)-H(7B)	109.6	C(15)-C(14)-H(14)	108.3
H(7A)-C(7)-H(7B)	108.2	C(12)-C(14)-H(14)	108.3
N(1)-C(8)-C(9)	99.61(16)	C(20)-C(15)-C(16)	125.4(2)
N(1)-C(8)-C(7)	114.28(16)	C(20)-C(15)-C(14)	121.2(2)
C(9)-C(8)-C(7)	111.74(18)	C(16)-C(15)-C(14)	113.43(18)
N(1)-C(8)-H(8)	110.3	O(4)-C(16)-C(15)	111.47(18)
C(9)-C(8)-H(8)	110.3	O(4)-C(16)-H(16A)	109.3
C(7)-C(8)-H(8)	110.3	C(15)-C(16)-H(16A)	109.3
O(1)-C(9)-C(8)	104.37(16)	O(4)-C(16)-H(16B)	109.3
O(1)-C(9)-H(9A)	110.9	C(15)-C(16)-H(16B)	109.3
C(8)-C(9)-H(9A)	110.9	H(16A)-C(16)-H(16B)	108.0
O(1)-C(9)-H(9B)	110.9	O(5)-C(17)-O(4)	108.45(17)
C(8)-C(9)-H(9B)	110.9	O(5)-C(17)-C(18)	106.8(2)
H(9A)-C(9)-H(9B)	108.9	O(4)-C(17)-C(18)	106.0(2)

O(5)-C(17)-C(19)	111.2(2)	C(10)-N(1)-C(11)	125.45(17)
O(4)-C(17)-C(19)	111.9(2)	C(10)-N(1)-C(8)	109.61(16)
C(18)-C(17)-C(19)	112.2(2)	C(11)-N(1)-C(8)	121.46(17)
C(17)-C(18)-H(18A)	109.5	C(10)-O(1)-C(9)	109.68(15)
C(17)-C(18)-H(18B)	109.5	C(16)-O(4)-C(17)	115.13(18)
H(18A)-C(18)-H(18B)	109.5	C(17)-O(5)-C(14)	117.48(16)
C(17)-C(18)-H(18C)	109.5		
H(18A)-C(18)-H(18C)	109.5		
H(18B)-C(18)-H(18C)	109.5		
C(17)-C(19)-H(19A)	109.5		
C(17)-C(19)-H(19B)	109.5		
H(19A)-C(19)-H(19B)	109.5		
C(17)-C(19)-H(19C)	109.5		
H(19A)-C(19)-H(19C)	109.5		
H(19B)-C(19)-H(19C)	109.5		
C(15)-C(20)-C(21)	129.3(2)		
C(15)-C(20)-H(20)	115.3		
C(21)-C(20)-H(20)	115.3		
C(22)-C(21)-C(26)	117.5(2)		
C(22)-C(21)-C(20)	124.0(2)		
C(26)-C(21)-C(20)	118.5(2)		
C(23)-C(22)-C(21)	120.7(2)		
C(23)-C(22)-H(22)	119.6		
C(21)-C(22)-H(22)	119.6		
C(24)-C(23)-C(22)	121.1(3)		
C(24)-C(23)-H(23)	119.5		
C(22)-C(23)-H(23)	119.5		
C(23)-C(24)-C(25)	119.0(2)		
C(23)-C(24)-H(24)	120.5		
C(25)-C(24)-H(24)	120.5		
C(26)-C(25)-C(24)	120.4(3)		
C(26)-C(25)-H(25)	119.8		
C(24)-C(25)-H(25)	119.8		
C(25)-C(26)-C(21)	121.3(3)		
C(25)-C(26)-H(26)	119.4		
C(21)-C(26)-H(26)	119.4		

Symmetry transformations used to generate equivalent atoms:

Table 4. Anisotropic displacement parameters ($\text{\AA}^2 \times 10^3$) for kob07. The anisotropic displacement factor exponent takes the form: $-2\pi^2 [h^2 a^{*2} U^{11} + \dots + 2 h k a^* b^* U^{12}]$

U ¹¹	U ²²	U ³³	U ²³	U ¹³	U ¹²
C(1)69(2)	57(2)	46(1)	3(1)	24(1)	2(1)
C(2)76(2)	89(2)	44(1)	15(2)	22(1)	7(2)
C(3)70(2)	89(2)	39(1)	-14(2)	19(1)	-12(2)
C(4)76(2)	58(2)	55(2)	-16(1)	32(1)	-8(1)
C(5)52(1)	53(1)	46(1)	-4(1)	21(1)	-4(1)
C(6)41(1)	51(1)	38(1)	-7(1)	18(1)	-10(1)
C(7)39(1)	60(2)	42(1)	-12(1)	14(1)	-9(1)
C(8)36(1)	38(1)	29(1)	-3(1)	7(1)	-1(1)
C(9)44(1)	50(1)	35(1)	-6(1)	12(1)	-10(1)
C(10)33(1)	42(1)	35(1)	2(1)	8(1)	5(1)
C(11)41(1)	34(1)	35(1)	-4(1)	5(1)	7(1)
C(12)44(1)	40(1)	33(1)	-7(1)	6(1)	3(1)
C(13)64(2)	91(2)	49(1)	-27(2)	-2(1)	29(2)
C(14)48(1)	30(1)	41(1)	3(1)	5(1)	0(1)
C(15)40(1)	32(1)	38(1)	5(1)	4(1)	-1(1)
C(16)49(1)	33(1)	38(1)	2(1)	10(1)	-4(1)
C(17)46(1)	49(1)	47(1)	7(1)	14(1)	7(1)
C(18)80(2)	65(2)	57(1)	-2(1)	30(1)	14(2)
C(19)44(1)	109(3)	83(2)	-8(2)	13(1)	6(2)
C(20)50(1)	32(1)	45(1)	2(1)	-2(1)	-4(1)
C(21)38(1)	43(1)	45(1)	-3(1)	-2(1)	1(1)
C(22)42(1)	57(2)	47(1)	-7(1)	14(1)	-10(1)
C(23)51(1)	79(2)	48(1)	3(1)	17(1)	-11(1)
C(24)59(2)	95(2)	41(1)	1(2)	0(1)	-10(2)
C(25)90(2)	75(2)	50(2)	-8(2)	-16(1)	-22(2)
C(26)85(2)	53(2)	53(2)	2(1)	-7(1)	-17(2)
N(1)36(1)	39(1)	28(1)	-2(1)	7(1)	2(1)
O(1)43(1)	49(1)	41(1)	-5(1)	14(1)	-11(1)
O(2)49(1)	53(1)	36(1)	3(1)	16(1)	1(1)
O(3)67(1)	37(1)	44(1)	2(1)	4(1)	-5(1)
O(4)78(1)	36(1)	49(1)	-1(1)	22(1)	-1(1)

O(5)60(1)

56(1)

44(1)

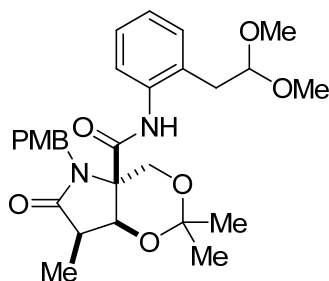
10(1)

17(1)

13(1)

Table 5. Hydrogen coordinates ($\times 10^4$) and isotropic displacement parameters ($\text{\AA}^2 \times 10^3$) for kob07.

	x	y	z	U(eq)
H(1)	7961	10930	-3288	67
H(2)	7786	9860	-5285	82
H(3)	7987	6486	-5850	78
H(4)	8394	4220	-4395	72
H(5)	8574	5258	-2394	59
H(7A)	8508	10410	-1242	56
H(7B)	8608	7901	-853	56
H(8)	7842	9921	-1257	42
H(9A)	7642	6386	-1761	51
H(9B)	8052	5349	-988	51
H(12)	8417	9316	2707	48
H(13A)	7982	12320	2668	107
H(13B)	8325	14023	2668	107
H(13C)	8356	12520	3812	107
H(14)	8978	12766	2728	49
H(16A)	9366	7807	5004	49
H(16B)	8897	7624	4644	49
H(18A)	9385	7199	903	98
H(18B)	9027	5948	1191	98
H(18C)	9468	5166	1808	98
H(19A)	9750	9612	3876	120
H(19B)	9876	9271	2679	120
H(19C)	9890	7244	3561	120
H(20)	9161	13616	4702	55
H(22)	9056	8907	6458	58
H(23)	9242	8774	8536	71
H(24)	9590	11657	9666	82
H(25)	9757	14726	8695	94
H(26)	9566	14913	6624	83

X-ray Crystal Structure Report of Ugi Adduct **294****294**

A colorless needle 0.35 x 0.10 x 0.10 mm in size was mounted on a Cryoloop with Paratone oil. Data were collected in a nitrogen gas stream at 208(2) K using phi and omega scans. Crystal-to-detector distance was 60 mm and exposure time was 40 seconds per frame using a scan width of 0.3°. Data collection was 99.9% complete to 25.00° in θ . A total of 15122 reflections were collected covering the indices, $-10 \leq h \leq 9$, $-14 \leq k \leq 14$, $-29 \leq l \leq 29$. 4580 reflections were found to be symmetry independent, with an R_{int} of 0.0390. Indexing and unit cell refinement indicated a primitive, orthorhombic lattice. The space group was found to be P2(1)2(1)2(1) (No. 19). The data were integrated using the Bruker SAINT software program and scaled using the SADABS software program. Solution by direct methods (SIR-2004) produced a complete heavy-atom phasing model consistent with the proposed structure. All non-hydrogen atoms were refined anisotropically by full-matrix least-squares (SHELXL-97). All hydrogen atoms were placed using a riding model. Their positions were constrained relative to their parent atom using the appropriate HFIX command in SHELXL-97.

Table 1. Crystal data and structure refinement for kob02.

X-ray ID	kob02	
Sample/notebook ID	CG-712	
Empirical formula	C ₂₈ H ₃₆ N ₂ O ₇	
Formula weight	512.59	
Temperature	208(2) K	
Wavelength	0.71073 Å	
Crystal system	Orthorhombic	
Space group	P2(1)2(1)2(1)	
Unit cell dimensions	a = 8.5250(9) Å	α = 90°.
	b = 12.0770(14) Å	β = 90°.
	c = 25.174(3) Å	γ = 90°.
Volume	2591.8(5) Å ³	
Z	4	
Density (calculated)	1.314 Mg/m ³	
Absorption coefficient	0.094 mm ⁻¹	
F(000)	1096	
Crystal size	0.35 x 0.10 x 0.10 mm ³	
Crystal color/habit	colorless needle	
Theta range for data collection	2.34 to 25.03°.	
Index ranges	-10 ≤ h ≤ 9, -14 ≤ k ≤ 14, -29 ≤ l ≤ 29	
Reflections collected	15122	
Independent reflections	4580 [R(int) = 0.0390]	
Completeness to theta = 25.00°	99.9 %	
Absorption correction	Semi-empirical from equivalents	
Max. and min. transmission	0.9906 and 0.9677	
Refinement method	Full-matrix least-squares on F ²	
Data / restraints / parameters	4580 / 0 / 340	
Goodness-of-fit on F ²	1.090	
Final R indices [I > 2σ(I)]	R1 = 0.0427, wR2 = 0.0899	
R indices (all data)	R1 = 0.0506, wR2 = 0.0928	
Absolute structure parameter	0.3(10)	
Largest diff. peak and hole	0.146 and -0.161 e.Å ⁻³	

Table 2. Atomic coordinates ($\times 10^4$) and equivalent isotropic displacement parameters ($\text{\AA}^2 \times 10^3$) for kob02. $U(\text{eq})$ is defined as one third of the trace of the orthogonalized U^{ij} tensor.

	x	y	z	$U(\text{eq})$
C(1)	1925(2)	5181(2)	7149(1)	26(1)
C(2)	1765(2)	5885(2)	7576(1)	30(1)
C(3)	908(3)	5557(2)	8017(1)	38(1)
C(4)	230(3)	4518(2)	8029(1)	40(1)
C(5)	372(3)	3829(2)	7595(1)	36(1)
C(6)	1196(2)	4148(2)	7144(1)	28(1)
C(7)	1315(2)	3381(2)	6678(1)	34(1)
C(8)	2660(3)	2578(2)	6748(1)	41(1)
C(9)	2645(3)	1905(2)	5858(1)	54(1)
C(10)	5390(3)	2617(2)	6894(1)	57(1)
C(11)	2904(2)	6457(2)	6464(1)	23(1)
C(12)	4144(2)	6642(2)	6018(1)	24(1)
C(13)	5023(3)	5588(2)	5855(1)	26(1)
C(14)	6981(2)	6023(2)	6546(1)	30(1)
C(15)	7351(3)	5547(2)	7082(1)	42(1)
C(16)	8441(2)	6175(2)	6210(1)	41(1)
C(17)	5479(2)	7435(2)	6178(1)	25(1)
C(18)	4802(2)	8591(2)	6160(1)	29(1)
C(19)	4279(3)	9111(2)	6682(1)	36(1)
C(20)	3514(2)	8429(2)	5745(1)	29(1)
C(21)	2069(2)	6947(2)	5301(1)	33(1)
C(22)	2368(2)	5865(2)	5018(1)	30(1)
C(23)	1394(3)	4972(2)	5094(1)	35(1)
C(24)	1672(3)	3961(2)	4849(1)	41(1)
C(25)	2969(3)	3843(2)	4526(1)	40(1)
C(26)	3948(3)	4736(2)	4442(1)	38(1)
C(27)	3639(3)	5738(2)	4680(1)	34(1)
C(28)	2456(4)	1928(2)	4358(1)	68(1)
N(1)	2927(2)	5478(1)	6715(1)	27(1)
N(2)	3429(2)	7322(1)	5605(1)	26(1)
O(1)	2623(2)	1657(1)	6411(1)	51(1)

O(2)	4054(2)	3186(1)	6689(1)	40(1)
O(3)	1947(2)	7177(1)	6552(1)	31(1)
O(4)	5927(2)	5242(1)	6304(1)	27(1)
O(5)	6204(2)	7058(1)	6647(1)	27(1)
O(6)	2716(2)	9144(1)	5542(1)	45(1)
O(7)	3387(2)	2886(2)	4273(1)	57(1)

Table 3. Bond lengths [\AA] and angles [$^\circ$] for kob02.

C(1)-C(2)	1.377(3)	C(13)-H(13B)	0.9800
C(1)-C(6)	1.394(3)	C(14)-O(5)	1.436(3)
C(1)-N(1)	1.433(3)	C(14)-O(4)	1.438(3)
C(2)-C(3)	1.386(3)	C(14)-C(15)	1.500(3)
C(2)-H(2)	0.9400	C(14)-C(16)	1.515(3)
C(3)-C(4)	1.382(3)	C(15)-H(15A)	0.9700
C(3)-H(3)	0.9400	C(15)-H(15B)	0.9700
C(4)-C(5)	1.377(4)	C(15)-H(15C)	0.9700
C(4)-H(4)	0.9400	C(16)-H(16A)	0.9700
C(5)-C(6)	1.391(3)	C(16)-H(16B)	0.9700
C(5)-H(5)	0.9400	C(16)-H(16C)	0.9700
C(6)-C(7)	1.498(3)	C(17)-O(5)	1.407(2)
C(7)-C(8)	1.512(3)	C(17)-C(18)	1.512(3)
C(7)-H(7A)	0.9800	C(17)-H(17)	0.9900
C(7)-H(7B)	0.9800	C(18)-C(19)	1.524(3)
C(8)-O(1)	1.400(3)	C(18)-C(20)	1.527(3)
C(8)-O(2)	1.405(3)	C(18)-H(18)	0.9900
C(8)-H(8)	0.9900	C(19)-H(19A)	0.9700
C(9)-O(1)	1.425(3)	C(19)-H(19B)	0.9700
C(9)-H(9A)	0.9700	C(19)-H(19C)	0.9700
C(9)-H(9B)	0.9700	C(20)-O(6)	1.213(2)
C(9)-H(9C)	0.9700	C(20)-N(2)	1.385(3)
C(10)-O(2)	1.426(3)	C(21)-N(2)	1.462(3)
C(10)-H(10A)	0.9700	C(21)-C(22)	1.511(3)
C(10)-H(10B)	0.9700	C(21)-H(21A)	0.9800
C(10)-H(10C)	0.9700	C(21)-H(21B)	0.9800
C(11)-O(3)	1.213(2)	C(22)-C(23)	1.374(3)
C(11)-N(1)	1.341(3)	C(22)-C(27)	1.386(3)
C(11)-C(12)	1.558(3)	C(23)-C(24)	1.388(3)
C(12)-N(2)	1.458(3)	C(23)-H(23)	0.9400
C(12)-C(13)	1.533(3)	C(24)-C(25)	1.380(3)
C(12)-C(17)	1.541(3)	C(24)-H(24)	0.9400
C(13)-O(4)	1.431(2)	C(25)-O(7)	1.368(3)
C(13)-H(13A)	0.9800	C(25)-C(26)	1.380(3)

C(26)-C(27)	1.376(3)	C(28)-H(28A)	0.9700
C(26)-H(26)	0.9400	C(28)-H(28B)	0.9700
C(27)-H(27)	0.9400	C(28)-H(28C)	0.9700
C(28)-O(7)	1.418(3)	N(1)-H(1)	0.8700
C(2)-C(1)-C(6)	121.1(2)	O(1)-C(9)-H(9B)	109.5
C(2)-C(1)-N(1)	119.9(2)	H(9A)-C(9)-H(9B)	109.5
C(6)-C(1)-N(1)	118.85(19)	O(1)-C(9)-H(9C)	109.5
C(1)-C(2)-C(3)	120.0(2)	H(9A)-C(9)-H(9C)	109.5
C(1)-C(2)-H(2)	120.0	H(9B)-C(9)-H(9C)	109.5
C(3)-C(2)-H(2)	120.0	O(2)-C(10)-H(10A)	109.5
C(4)-C(3)-C(2)	119.8(2)	O(2)-C(10)-H(10B)	109.5
C(4)-C(3)-H(3)	120.1	H(10A)-C(10)-H(10B)	109.5
C(2)-C(3)-H(3)	120.1	O(2)-C(10)-H(10C)	109.5
C(5)-C(4)-C(3)	119.7(2)	H(10A)-C(10)-H(10C)	109.5
C(5)-C(4)-H(4)	120.2	H(10B)-C(10)-H(10C)	109.5
C(3)-C(4)-H(4)	120.2	O(3)-C(11)-N(1)	123.72(19)
C(4)-C(5)-C(6)	121.6(2)	O(3)-C(11)-C(12)	119.11(18)
C(4)-C(5)-H(5)	119.2	N(1)-C(11)-C(12)	117.12(17)
C(6)-C(5)-H(5)	119.2	N(2)-C(12)-C(13)	118.75(17)
C(5)-C(6)-C(1)	117.7(2)	N(2)-C(12)-C(17)	98.32(16)
C(5)-C(6)-C(7)	120.2(2)	C(13)-C(12)-C(17)	103.02(16)
C(1)-C(6)-C(7)	122.10(19)	N(2)-C(12)-C(11)	108.07(15)
C(6)-C(7)-C(8)	110.84(19)	C(13)-C(12)-C(11)	113.97(16)
C(6)-C(7)-H(7A)	109.5	C(17)-C(12)-C(11)	113.68(16)
C(8)-C(7)-H(7A)	109.5	O(4)-C(13)-C(12)	107.08(16)
C(6)-C(7)-H(7B)	109.5	O(4)-C(13)-H(13A)	110.3
C(8)-C(7)-H(7B)	109.5	C(12)-C(13)-H(13A)	110.3
H(7A)-C(7)-H(7B)	108.1	O(4)-C(13)-H(13B)	110.3
O(1)-C(8)-O(2)	111.7(2)	C(12)-C(13)-H(13B)	110.3
O(1)-C(8)-C(7)	114.9(2)	H(13A)-C(13)-H(13B)	108.6
O(2)-C(8)-C(7)	107.13(17)	O(5)-C(14)-O(4)	110.93(15)
O(1)-C(8)-H(8)	107.6	O(5)-C(14)-C(15)	105.76(17)
O(2)-C(8)-H(8)	107.6	O(4)-C(14)-C(15)	105.10(19)
C(7)-C(8)-H(8)	107.6	O(5)-C(14)-C(16)	111.86(19)
O(1)-C(9)-H(9A)	109.5	O(4)-C(14)-C(16)	110.87(18)

C(15)-C(14)-C(16)	112.02(19)	C(22)-C(21)-H(21A)	109.1
C(14)-C(15)-H(15A)	109.5	N(2)-C(21)-H(21B)	109.1
C(14)-C(15)-H(15B)	109.5	C(22)-C(21)-H(21B)	109.1
H(15A)-C(15)-H(15B)	109.5	H(21A)-C(21)-H(21B)	107.9
C(14)-C(15)-H(15C)	109.5	C(23)-C(22)-C(27)	118.1(2)
H(15A)-C(15)-H(15C)	109.5	C(23)-C(22)-C(21)	120.8(2)
H(15B)-C(15)-H(15C)	109.5	C(27)-C(22)-C(21)	121.1(2)
C(14)-C(16)-H(16A)	109.5	C(22)-C(23)-C(24)	121.7(2)
C(14)-C(16)-H(16B)	109.5	C(22)-C(23)-H(23)	119.1
H(16A)-C(16)-H(16B)	109.5	C(24)-C(23)-H(23)	119.1
C(14)-C(16)-H(16C)	109.5	C(25)-C(24)-C(23)	119.2(2)
H(16A)-C(16)-H(16C)	109.5	C(25)-C(24)-H(24)	120.4
H(16B)-C(16)-H(16C)	109.5	C(23)-C(24)-H(24)	120.4
O(5)-C(17)-C(18)	119.48(17)	O(7)-C(25)-C(24)	124.8(2)
O(5)-C(17)-C(12)	110.01(16)	O(7)-C(25)-C(26)	115.5(2)
C(18)-C(17)-C(12)	106.51(16)	C(24)-C(25)-C(26)	119.7(2)
O(5)-C(17)-H(17)	106.7	C(27)-C(26)-C(25)	120.3(2)
C(18)-C(17)-H(17)	106.7	C(27)-C(26)-H(26)	119.9
C(12)-C(17)-H(17)	106.7	C(25)-C(26)-H(26)	119.9
C(17)-C(18)-C(19)	117.76(18)	C(26)-C(27)-C(22)	121.0(2)
C(17)-C(18)-C(20)	100.19(16)	C(26)-C(27)-H(27)	119.5
C(19)-C(18)-C(20)	115.62(18)	C(22)-C(27)-H(27)	119.5
C(17)-C(18)-H(18)	107.5	O(7)-C(28)-H(28A)	109.5
C(19)-C(18)-H(18)	107.5	O(7)-C(28)-H(28B)	109.5
C(20)-C(18)-H(18)	107.5	H(28A)-C(28)-H(28B)	109.5
C(18)-C(19)-H(19A)	109.5	O(7)-C(28)-H(28C)	109.5
C(18)-C(19)-H(19B)	109.5	H(28A)-C(28)-H(28C)	109.5
H(19A)-C(19)-H(19B)	109.5	H(28B)-C(28)-H(28C)	109.5
C(18)-C(19)-H(19C)	109.5	C(11)-N(1)-C(1)	124.89(18)
H(19A)-C(19)-H(19C)	109.5	C(11)-N(1)-H(1)	117.6
H(19B)-C(19)-H(19C)	109.5	C(1)-N(1)-H(1)	117.6
O(6)-C(20)-N(2)	123.4(2)	C(20)-N(2)-C(12)	109.95(17)
O(6)-C(20)-C(18)	126.9(2)	C(20)-N(2)-C(21)	118.28(17)
N(2)-C(20)-C(18)	109.57(18)	C(12)-N(2)-C(21)	122.02(17)
N(2)-C(21)-C(22)	112.41(17)	C(8)-O(1)-C(9)	115.21(18)
N(2)-C(21)-H(21A)	109.1	C(8)-O(2)-C(10)	112.67(18)

C(13)-O(4)-C(14)	118.64(16)	C(25)-O(7)-C(28)	118.2(2)
C(17)-O(5)-C(14)	109.63(15)		

Symmetry transformations used to generate equivalent atoms:

Table 4. Anisotropic displacement parameters ($\text{\AA}^2 \times 10^3$) for kob02. The anisotropic displacement factor exponent takes the form: $-2\pi^2 [h^2 a^{*2} U^{11} + \dots + 2 h k a^* b^* U^{12}]$

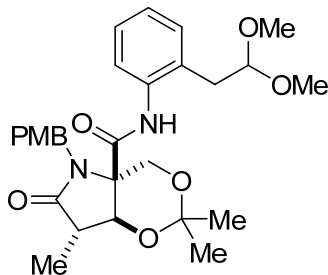
	U ¹¹	U ²²	U ³³	U ²³	U ¹³	U ¹²
C(1)	20(1)	30(1)	29(1)	7(1)	-2(1)	4(1)
C(2)	28(1)	30(1)	32(1)	4(1)	-6(1)	-2(1)
C(3)	39(1)	46(2)	30(1)	3(1)	2(1)	4(1)
C(4)	36(1)	46(2)	37(1)	14(1)	9(1)	3(1)
C(5)	28(1)	35(2)	45(2)	13(1)	2(1)	-2(1)
C(6)	22(1)	26(1)	37(1)	6(1)	-2(1)	4(1)
C(7)	32(1)	28(1)	43(1)	6(1)	0(1)	-5(1)
C(8)	47(1)	29(1)	45(2)	6(1)	5(1)	4(1)
C(9)	60(2)	42(2)	59(2)	-10(1)	5(2)	-4(1)
C(10)	48(2)	56(2)	67(2)	-3(2)	-10(1)	21(2)
C(11)	19(1)	22(1)	28(1)	-2(1)	-2(1)	-1(1)
C(12)	25(1)	22(1)	24(1)	2(1)	-3(1)	1(1)
C(13)	27(1)	28(1)	25(1)	-4(1)	-3(1)	3(1)
C(14)	24(1)	33(1)	32(1)	-5(1)	-1(1)	7(1)
C(15)	44(1)	42(1)	40(1)	-6(1)	-12(1)	13(1)
C(16)	24(1)	44(2)	55(2)	-6(1)	1(1)	3(1)
C(17)	23(1)	29(1)	23(1)	-1(1)	1(1)	-1(1)
C(18)	31(1)	22(1)	33(1)	0(1)	4(1)	-4(1)
C(19)	40(1)	27(1)	40(1)	-6(1)	-2(1)	3(1)
C(20)	31(1)	28(1)	29(1)	2(1)	5(1)	2(1)
C(21)	30(1)	38(1)	29(1)	-1(1)	-8(1)	7(1)
C(22)	29(1)	36(1)	24(1)	0(1)	-10(1)	3(1)
C(23)	29(1)	43(1)	34(1)	-1(1)	-3(1)	0(1)
C(24)	35(1)	37(1)	50(2)	-2(1)	-4(1)	-9(1)
C(25)	43(1)	38(1)	39(1)	-12(1)	-6(1)	-1(1)
C(26)	35(1)	47(2)	30(1)	-12(1)	2(1)	-2(1)
C(27)	33(1)	39(1)	30(1)	-1(1)	-3(1)	-9(1)
C(28)	80(2)	41(2)	83(2)	-21(2)	-6(2)	-6(2)
N(1)	24(1)	23(1)	34(1)	3(1)	5(1)	3(1)
N(2)	30(1)	23(1)	25(1)	1(1)	-1(1)	3(1)

O(1)	63(1)	23(1)	66(1)	0(1)	11(1)	4(1)
O(2)	36(1)	32(1)	53(1)	3(1)	-3(1)	8(1)
O(3)	29(1)	25(1)	39(1)	3(1)	6(1)	7(1)
O(4)	26(1)	25(1)	30(1)	-1(1)	-4(1)	3(1)
O(5)	25(1)	29(1)	28(1)	-5(1)	-4(1)	2(1)
O(6)	53(1)	28(1)	54(1)	6(1)	-13(1)	10(1)
O(7)	58(1)	43(1)	68(1)	-25(1)	6(1)	-6(1)

Table 5. Hydrogen coordinates ($\times 10^4$) and isotropic displacement parameters ($\text{\AA}^2 \times 10^3$) for kob02.

	x	y	z	U(eq)
H(2)	2236	6589	7568	36
H(3)	789	6039	8307	46
H(4)	-326	4283	8331	48
H(5)	-100	3125	7605	43
H(7A)	1476	3813	6353	41
H(7B)	332	2967	6640	41
H(8)	2623	2302	7118	49
H(9A)	3421	2474	5788	80
H(9B)	1619	2167	5749	80
H(9C)	2909	1242	5659	80
H(10A)	5552	1939	6694	85
H(10B)	5218	2439	7265	85
H(10C)	6309	3085	6861	85
H(13A)	4278	5008	5753	32
H(13B)	5712	5739	5552	32
H(15A)	6405	5526	7295	63
H(15B)	8131	6006	7256	63
H(15C)	7758	4802	7040	63
H(16A)	9041	6798	6344	62
H(16B)	8140	6315	5845	62
H(16C)	9075	5509	6227	62
H(17)	6279	7393	5894	30
H(18)	5607	9083	6003	34
H(19A)	5187	9237	6906	53
H(19B)	3557	8615	6862	53
H(19C)	3760	9810	6611	53
H(21A)	1791	7514	5039	39
H(21B)	1175	6857	5542	39
H(23)	517	5048	5317	42

H(24)	984	3363	4903	49
H(26)	4829	4660	4220	45
H(27)	4300	6345	4613	41
H(28A)	1385	2077	4248	102
H(28B)	2473	1736	4732	102
H(28C)	2873	1318	4151	102
H(1)	3601	4987	6606	32

X-ray Crystal Structure Report for Ugi Adduct **314****314**

A colorless block 0.12 x 0.10 x 0.04 mm in size was mounted on a Cryoloop with Paratone oil. Data were collected in a nitrogen gas stream at 100(2) K using phi and omega scans. Crystal-to-detector distance was 60 mm and exposure time was 10 seconds per frame using a scan width of 0.3°. Data collection was 99.3% complete to 25.00° in θ . A total of 16263 reflections were collected covering the indices, $-13 \leq h \leq 13$, $-38 \leq k \leq 32$, $-11 \leq l \leq 6$. 4596 reflections were found to be symmetry independent, with an R_{int} of 0.0363. Indexing and unit cell refinement indicated a primitive, orthorhombic lattice. The space group was found to be Pna2(1) (No. 33). The data were integrated using the Bruker SAINT software program and scaled using the SADABS software program. Solution by direct methods (SIR-2004) produced a complete heavy-atom phasing model consistent with the proposed structure. All non-hydrogen atoms were refined anisotropically by full-matrix least-squares (SHELXL-97). All hydrogen atoms were placed using a riding model. Their positions were constrained relative to their parent atom using the appropriate HFIX command in SHELXL-97.

Table 1. Crystal data and structure refinement for kob10.

X-ray ID	kob10	
Sample/notebook ID	CG-1068	
Empirical formula	C ₂₈ H ₃₆ N ₂ O ₇	
Formula weight	512.59	
Temperature	100(2) K	
Wavelength	0.71073 Å	
Crystal system	Orthorhombic	
Space group	Pna2(1)	
Unit cell dimensions	a = 10.435(2) Å	α = 90°.
	b = 29.115(6) Å	β = 90°.
	c = 8.6581(18) Å	γ = 90°.
Volume	2630.4(9) Å ³	
Z	4	
Density (calculated)	1.294 Mg/m ³	
Absorption coefficient	0.093 mm ⁻¹	
F(000)	1096	
Crystal size	0.12 x 0.10 x 0.04 mm ³	
Crystal color/habit	colorless block	
Theta range for data collection	1.40 to 28.22°.	
Index ranges	-13 ≤ h ≤ 13, -38 ≤ k ≤ 32, -11 ≤ l ≤ 6	
Reflections collected	16263	
Independent reflections	4596 [R(int) = 0.0363]	
Completeness to theta = 25.00°	99.3 %	
Absorption correction	Semi-empirical from equivalents	
Max. and min. transmission	0.9963 and 0.9889	
Refinement method	Full-matrix least-squares on F ²	
Data / restraints / parameters	4596 / 1 / 340	
Goodness-of-fit on F ²	1.077	
Final R indices [I > 2σ(I)]	R1 = 0.0371, wR2 = 0.0877	
R indices (all data)	R1 = 0.0464, wR2 = 0.0909	
Largest diff. peak and hole	0.223 and -0.177 e.Å ⁻³	

Table 2. Atomic coordinates ($\times 10^4$) and equivalent isotropic displacement parameters ($\text{\AA}^2 \times 10^3$) for kob10. $U(\text{eq})$ is defined as one third of the trace of the orthogonalized U^{ij} tensor.

	x	y	z	$U(\text{eq})$
C(1)	3407(2)	914(1)	2504(2)	22(1)
C(2)	2472(2)	867(1)	1161(2)	23(1)
C(3)	4070(2)	1261(1)	-479(2)	24(1)
C(4)	4735(2)	876(1)	1754(2)	22(1)
C(5)	5620(2)	777(1)	3100(2)	25(1)
C(6)	4727(2)	477(1)	4088(3)	26(1)
C(7)	3253(2)	1362(1)	3489(2)	22(1)
C(8)	2340(2)	2152(1)	3490(2)	22(1)
C(9)	2894(2)	2300(1)	4859(2)	24(1)
C(10)	2503(2)	2710(1)	5536(3)	30(1)
C(11)	1561(2)	2974(1)	4847(3)	32(1)
C(12)	1045(2)	2831(1)	3458(3)	29(1)
C(13)	1415(2)	2423(1)	2733(2)	24(1)
C(14)	811(2)	2300(1)	1207(3)	26(1)
C(15)	-372(2)	1994(1)	1352(3)	27(1)
C(16)	-441(2)	1407(1)	3269(3)	41(1)
C(17)	-2092(2)	1706(1)	-129(3)	36(1)
C(18)	4150(2)	1729(1)	-1221(3)	30(1)
C(19)	4363(2)	880(1)	-1625(3)	31(1)
C(20)	6863(2)	527(1)	2677(3)	34(1)
C(21)	2389(2)	350(1)	4394(2)	27(1)
C(22)	1803(2)	-65(1)	3627(2)	24(1)
C(23)	2482(2)	-323(1)	2555(2)	26(1)
C(24)	1982(2)	-723(1)	1934(3)	30(1)
C(25)	763(2)	-875(1)	2368(2)	29(1)
C(26)	53(2)	-613(1)	3397(3)	33(1)
C(27)	571(2)	-213(1)	4012(3)	31(1)
C(28)	-825(2)	-1463(1)	2208(3)	40(1)
N(1)	3494(1)	532(1)	3569(2)	23(1)
N(2)	2692(1)	1726(1)	2798(2)	22(1)

O(1)	2768(1)	1229(1)	86(2)	23(1)
O(2)	4966(1)	1264(1)	800(2)	24(1)
O(3)	3641(1)	1361(1)	4821(2)	29(1)
O(4)	-11(1)	1543(1)	1781(2)	28(1)
O(5)	-960(1)	1985(1)	-102(2)	34(1)
O(6)	5049(1)	220(1)	5126(2)	32(1)
O(7)	389(1)	-1281(1)	1732(2)	40(1)

-

Table 3. Bond lengths [\AA] and angles [$^\circ$] for kob10.

C(1)-N(1)	1.448(2)	C(14)-C(15)	1.527(3)
C(1)-C(2)	1.524(3)	C(14)-H(14A)	0.9900
C(1)-C(4)	1.534(2)	C(14)-H(14B)	0.9900
C(1)-C(7)	1.566(3)	C(15)-O(5)	1.401(3)
C(2)-O(1)	1.440(2)	C(15)-O(4)	1.417(2)
C(2)-H(2A)	0.9900	C(15)-H(15)	1.0000
C(2)-H(2B)	0.9900	C(16)-O(4)	1.420(3)
C(3)-O(1)	1.447(2)	C(16)-H(16A)	0.9800
C(3)-O(2)	1.449(2)	C(16)-H(16B)	0.9800
C(3)-C(18)	1.507(3)	C(16)-H(16C)	0.9800
C(3)-C(19)	1.521(3)	C(17)-O(5)	1.434(2)
C(4)-O(2)	1.419(2)	C(17)-H(17A)	0.9800
C(4)-C(5)	1.515(3)	C(17)-H(17B)	0.9800
C(4)-H(4)	1.0000	C(17)-H(17C)	0.9800
C(5)-C(20)	1.531(3)	C(18)-H(18A)	0.9800
C(5)-C(6)	1.537(3)	C(18)-H(18B)	0.9800
C(5)-H(5)	1.0000	C(18)-H(18C)	0.9800
C(6)-O(6)	1.217(2)	C(19)-H(19A)	0.9800
C(6)-N(1)	1.372(2)	C(19)-H(19B)	0.9800
C(7)-O(3)	1.222(2)	C(19)-H(19C)	0.9800
C(7)-N(2)	1.350(2)	C(20)-H(20A)	0.9800
C(8)-C(9)	1.388(3)	C(20)-H(20B)	0.9800
C(8)-C(13)	1.409(3)	C(20)-H(20C)	0.9800
C(8)-N(2)	1.424(2)	C(21)-N(1)	1.456(2)
C(9)-C(10)	1.391(3)	C(21)-C(22)	1.508(3)
C(9)-H(9)	0.9500	C(21)-H(21A)	0.9900
C(10)-C(11)	1.383(3)	C(21)-H(21B)	0.9900
C(10)-H(10)	0.9500	C(22)-C(23)	1.390(3)
C(11)-C(12)	1.382(3)	C(22)-C(27)	1.396(3)
C(11)-H(11)	0.9500	C(23)-C(24)	1.383(3)
C(12)-C(13)	1.399(3)	C(23)-H(23)	0.9500
C(12)-H(12)	0.9500	C(24)-C(25)	1.398(3)
C(13)-C(14)	1.507(3)	C(24)-H(24)	0.9500

C(25)-O(7)	1.362(2)	C(28)-O(7)	1.434(2)
C(25)-C(26)	1.386(3)	C(28)-H(28A)	0.9800
C(26)-C(27)	1.391(3)	C(28)-H(28B)	0.9800
C(26)-H(26)	0.9500	C(28)-H(28C)	0.9800
C(27)-H(27)	0.9500	N(2)-H(2)	0.8800
N(1)-C(1)-C(2)	117.13(15)	O(6)-C(6)-N(1)	125.01(19)
N(1)-C(1)-C(4)	99.05(14)	O(6)-C(6)-C(5)	126.35(17)
C(2)-C(1)-C(4)	104.40(15)	N(1)-C(6)-C(5)	108.60(17)
N(1)-C(1)-C(7)	107.36(15)	O(3)-C(7)-N(2)	124.26(18)
C(2)-C(1)-C(7)	115.23(15)	O(3)-C(7)-C(1)	118.59(16)
C(4)-C(1)-C(7)	112.55(14)	N(2)-C(7)-C(1)	117.15(16)
O(1)-C(2)-C(1)	106.77(14)	C(9)-C(8)-C(13)	120.53(17)
O(1)-C(2)-H(2A)	110.4	C(9)-C(8)-N(2)	121.50(16)
C(1)-C(2)-H(2A)	110.4	C(13)-C(8)-N(2)	117.98(18)
O(1)-C(2)-H(2B)	110.4	C(8)-C(9)-C(10)	120.32(18)
C(1)-C(2)-H(2B)	110.4	C(8)-C(9)-H(9)	119.8
H(2A)-C(2)-H(2B)	108.6	C(10)-C(9)-H(9)	119.8
O(1)-C(3)-O(2)	110.32(15)	C(11)-C(10)-C(9)	120.2(2)
O(1)-C(3)-C(18)	104.80(14)	C(11)-C(10)-H(10)	119.9
O(2)-C(3)-C(18)	106.60(15)	C(9)-C(10)-H(10)	119.9
O(1)-C(3)-C(19)	111.20(15)	C(10)-C(11)-C(12)	119.02(19)
O(2)-C(3)-C(19)	111.85(15)	C(10)-C(11)-H(11)	120.5
C(18)-C(3)-C(19)	111.75(17)	C(12)-C(11)-H(11)	120.5
O(2)-C(4)-C(5)	119.76(15)	C(11)-C(12)-C(13)	122.57(18)
O(2)-C(4)-C(1)	110.00(14)	C(11)-C(12)-H(12)	118.7
C(5)-C(4)-C(1)	103.82(16)	C(13)-C(12)-H(12)	118.7
O(2)-C(4)-H(4)	107.6	C(12)-C(13)-C(8)	117.22(19)
C(5)-C(4)-H(4)	107.6	C(12)-C(13)-C(14)	118.62(17)
C(1)-C(4)-H(4)	107.6	C(8)-C(13)-C(14)	124.15(18)
C(4)-C(5)-C(20)	115.03(17)	C(13)-C(14)-C(15)	113.85(17)
C(4)-C(5)-C(6)	99.63(14)	C(13)-C(14)-H(14A)	108.8
C(20)-C(5)-C(6)	112.18(16)	C(15)-C(14)-H(14A)	108.8
C(4)-C(5)-H(5)	109.9	C(13)-C(14)-H(14B)	108.8
C(20)-C(5)-H(5)	109.9	C(15)-C(14)-H(14B)	108.8
C(6)-C(5)-H(5)	109.9	H(14A)-C(14)-H(14B)	107.7

O(5)-C(15)-O(4)	109.52(16)	N(1)-C(21)-C(22)	113.42(16)
O(5)-C(15)-C(14)	106.93(17)	N(1)-C(21)-H(21A)	108.9
O(4)-C(15)-C(14)	110.35(15)	C(22)-C(21)-H(21A)	108.9
O(5)-C(15)-H(15)	110.0	N(1)-C(21)-H(21B)	108.9
O(4)-C(15)-H(15)	110.0	C(22)-C(21)-H(21B)	108.9
C(14)-C(15)-H(15)	110.0	H(21A)-C(21)-H(21B)	107.7
O(4)-C(16)-H(16A)	109.5	C(23)-C(22)-C(27)	117.48(18)
O(4)-C(16)-H(16B)	109.5	C(23)-C(22)-C(21)	121.40(16)
H(16A)-C(16)-H(16B)	109.5	C(27)-C(22)-C(21)	121.09(18)
O(4)-C(16)-H(16C)	109.5	C(24)-C(23)-C(22)	121.52(17)
H(16A)-C(16)-H(16C)	109.5	C(24)-C(23)-H(23)	119.2
H(16B)-C(16)-H(16C)	109.5	C(22)-C(23)-H(23)	119.2
O(5)-C(17)-H(17A)	109.5	C(23)-C(24)-C(25)	120.31(19)
O(5)-C(17)-H(17B)	109.5	C(23)-C(24)-H(24)	119.8
H(17A)-C(17)-H(17B)	109.5	C(25)-C(24)-H(24)	119.8
O(5)-C(17)-H(17C)	109.5	O(7)-C(25)-C(26)	125.68(17)
H(17A)-C(17)-H(17C)	109.5	O(7)-C(25)-C(24)	115.27(18)
H(17B)-C(17)-H(17C)	109.5	C(26)-C(25)-C(24)	119.04(19)
C(3)-C(18)-H(18A)	109.5	C(25)-C(26)-C(27)	119.88(18)
C(3)-C(18)-H(18B)	109.5	C(25)-C(26)-H(26)	120.1
H(18A)-C(18)-H(18B)	109.5	C(27)-C(26)-H(26)	120.1
C(3)-C(18)-H(18C)	109.5	C(26)-C(27)-C(22)	121.70(19)
H(18A)-C(18)-H(18C)	109.5	C(26)-C(27)-H(27)	119.1
H(18B)-C(18)-H(18C)	109.5	C(22)-C(27)-H(27)	119.1
C(3)-C(19)-H(19A)	109.5	O(7)-C(28)-H(28A)	109.5
C(3)-C(19)-H(19B)	109.5	O(7)-C(28)-H(28B)	109.5
H(19A)-C(19)-H(19B)	109.5	H(28A)-C(28)-H(28B)	109.5
C(3)-C(19)-H(19C)	109.5	O(7)-C(28)-H(28C)	109.5
H(19A)-C(19)-H(19C)	109.5	H(28A)-C(28)-H(28C)	109.5
H(19B)-C(19)-H(19C)	109.5	H(28B)-C(28)-H(28C)	109.5
C(5)-C(20)-H(20A)	109.5	C(6)-N(1)-C(1)	111.00(15)
C(5)-C(20)-H(20B)	109.5	C(6)-N(1)-C(21)	122.56(17)
H(20A)-C(20)-H(20B)	109.5	C(1)-N(1)-C(21)	122.90(15)
C(5)-C(20)-H(20C)	109.5	C(7)-N(2)-C(8)	127.47(17)
H(20A)-C(20)-H(20C)	109.5	C(7)-N(2)-H(2)	116.3
H(20B)-C(20)-H(20C)	109.5	C(8)-N(2)-H(2)	116.3

C(2)-O(1)-C(3)	117.91(13)	C(15)-O(5)-C(17)	112.72(16)
C(4)-O(2)-C(3)	109.35(13)	C(25)-O(7)-C(28)	117.28(17)
C(15)-O(4)-C(16)	114.30(17)		

Symmetry transformations used to generate equivalent atoms:

Table 4. Anisotropic displacement parameters ($\text{\AA}^2 \times 10^3$) for kob10. The anisotropic displacement factor exponent takes the form: $-2\pi^2 [h^2 a^{*2} U^{11} + \dots + 2 h k a^* b^* U^{12}]$

U ¹¹	U ²²	U ³³	U ²³	U ¹³	U ¹²
C(1)25(1)	19(1)	20(1)	1(1)	-1(1)	2(1)
C(2)28(1)	21(1)	21(1)	2(1)	-2(1)	-1(1)
C(3)24(1)	28(1)	21(1)	0(1)	-2(1)	2(1)
C(4)24(1)	23(1)	20(1)	-2(1)	0(1)	1(1)
C(5)26(1)	26(1)	24(1)	-2(1)	-4(1)	3(1)
C(6)31(1)	21(1)	25(1)	-7(1)	-5(1)	3(1)
C(7)19(1)	23(1)	22(1)	1(1)	1(1)	0(1)
C(8)22(1)	21(1)	23(1)	1(1)	3(1)	-1(1)
C(9)25(1)	25(1)	23(1)	1(1)	1(1)	-1(1)
C(10)38(1)	26(1)	26(1)	-3(1)	3(1)	-5(1)
C(11)33(1)	23(1)	39(1)	-4(1)	8(1)	1(1)
C(12)25(1)	24(1)	38(1)	3(1)	2(1)	2(1)
C(13)20(1)	23(1)	29(1)	4(1)	3(1)	0(1)
C(14)26(1)	25(1)	29(1)	5(1)	-2(1)	4(1)
C(15)25(1)	27(1)	29(1)	1(1)	-2(1)	4(1)
C(16)40(1)	44(1)	40(1)	12(1)	7(1)	-3(1)
C(17)28(1)	46(1)	34(1)	2(1)	-6(1)	-5(1)
C(18)30(1)	34(1)	25(1)	4(1)	-3(1)	-1(1)
C(19)36(1)	33(1)	24(1)	-6(1)	-1(1)	5(1)
C(20)30(1)	38(1)	34(1)	-4(1)	-6(1)	9(1)
C(21)33(1)	26(1)	23(1)	3(1)	3(1)	1(1)
C(22)26(1)	24(1)	22(1)	5(1)	0(1)	1(1)
C(23)24(1)	26(1)	29(1)	0(1)	4(1)	-2(1)
C(24)27(1)	35(1)	27(1)	-3(1)	6(1)	-1(1)
C(25)31(1)	34(1)	23(1)	-1(1)	1(1)	-9(1)
C(26)24(1)	45(1)	31(1)	-3(1)	7(1)	-8(1)
C(27)31(1)	36(1)	27(1)	-4(1)	6(1)	2(1)
C(28)34(1)	49(1)	37(1)	-3(1)	2(1)	-20(1)
N(1)26(1)	19(1)	24(1)	2(1)	-3(1)	0(1)
N(2)27(1)	22(1)	18(1)	-1(1)	-2(1)	4(1)
O(1)26(1)	23(1)	21(1)	2(1)	-2(1)	1(1)

O(2)24(1)	28(1)	19(1)	1(1)	-2(1)	0(1)
O(3)39(1)	27(1)	20(1)	1(1)	-6(1)	4(1)
O(4)28(1)	29(1)	28(1)	4(1)	0(1)	2(1)
O(5)28(1)	42(1)	31(1)	7(1)	-8(1)	-3(1)
O(6)38(1)	28(1)	28(1)	4(1)	-8(1)	6(1)
O(7)38(1)	50(1)	34(1)	-13(1)	10(1)	-22(1)

Table 5. Hydrogen coordinates ($\times 10^4$) and isotropic displacement parameters ($\text{\AA}^2 \times 10^3$) for kob10.

	x	y	z	U(eq)
H(2A)	2572	563	660	28
H(2B)	1578	896	1531	28
H(4)	4729	598	1074	27
H(5)	5822	1068	3661	30
H(9)	3543	2120	5337	29
H(10)	2885	2809	6475	36
H(11)	1273	3250	5322	38
H(12)	414	3018	2976	34
H(14A)	1455	2141	562	32
H(14B)	566	2587	667	32
H(15)	-974	2125	2136	33
H(16A)	-56	1607	4052	62
H(16B)	-187	1088	3463	62
H(16C)	-1377	1433	3318	62
H(17A)	-1856	1384	32	54
H(17B)	-2519	1739	-1131	54
H(17C)	-2675	1805	694	54
H(18A)	3552	1744	-2093	45
H(18B)	5025	1782	-1592	45
H(18C)	3924	1965	-461	45
H(19A)	4178	582	-1149	46
H(19B)	5270	893	-1916	46
H(19C)	3830	918	-2548	46
H(20A)	6660	248	2091	51
H(20B)	7325	444	3622	51
H(20C)	7401	730	2046	51
H(21A)	1731	594	4478	33
H(21B)	2655	266	5455	33
H(23)	3308	-223	2240	32
H(24)	2469	-894	1209	36

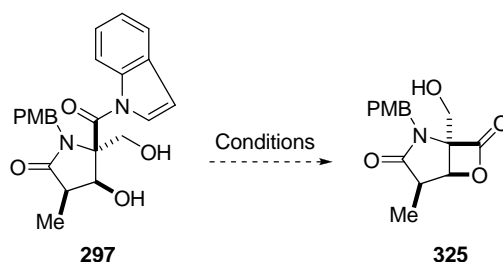
H(26)	-786	-708	3682	40
H(27)	74	-36	4713	38
H(28A)	-841	-1492	3336	60
H(28B)	-952	-1766	1740	60
H(28C)	-1511	-1256	1875	60
H(2)	2525	1697	1807	27

CHAPTER FOUR

2-Nitrophenyl Isocyanide as a Versatile Convertible Isocyanide: Rapid Access to the Fused γ -Lactam- β -lactone Bicycle of Omuralide

4.1 New Convertible Isocyanide

In the last chapter, we described a formal total synthesis of proteasome inhibitor omuralide (**2**) employing a stereocontrolled Ugi reaction as the key step. We reported the development of a convertible isocyanide, 1-isocyano-2-(2,2-dimethoxyethyl)benzene (**240**) for its utility in the Ugi reaction and demonstrated the selective cleavage of the resultant *C*-terminal amide bond of pyroglutamic acid amide Ugi products derived from the isocyanide. The sterically hindered *exo*-anilide was successfully converted to a methyl ester via methanolysis after conversion to the corresponding *N*-acylindole. However, the direct intramolecular conversion of the activated *N*-acylindole intermediate **297** to the β -lactone **325** (and concurrent expulsion of indole) was never realized (Scheme 4.1). In addition, the acidic conditions required to form the *N*-acylindole intermediate were not compatible with the adjacent unprotected alcohols causing unwanted side products (see section 3.3.5).



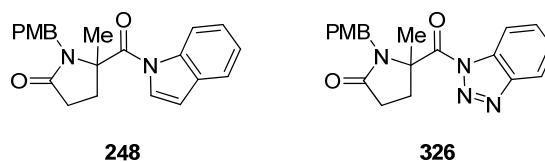
Scheme 4.1 Failed Intramolecular Conversion of the Activated *N*-Acylindole Intermediate **297** to β -lactone **325**

We then sought an alternative convertible isocyanide which would allow for the conversion of the Ugi product amide to the corresponding β -lactone via its appropriate activation. It should satisfy the following requirements: (a) quick and easy preparation from an inexpensive commercially available material, (b) mild activation conditions that are compatible with unprotected hydroxyl groups, (c) enhanced activation of the carbonyl group, and (d) spontaneous formation of the β -lactone when the activated carbonyl group is generated.

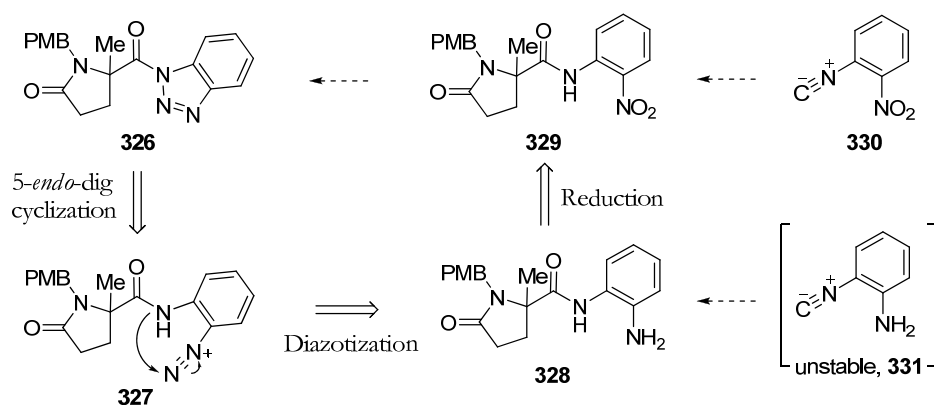
4.1.1 Strategy

Our strategy was to target *N*-acylbenzotriazole (*N*-acylBt) **326** instead of *N*-acylindole **248** (Scheme 4.1.1a). The presence of two additional electronegative nitrogen atoms in benzotriazole, compared with the carbon atoms in indole, should make it a better leaving group. Indeed, the proton on the nitrogen atom of benzotriazole (pKa 11.9 in

DMSO) is more acidic than that of indole (pKa 20.95).¹ Therefore, we expected direct β -lactonization from an *N*-acylBt generated in the presence of a β -hydroxyl group to generate the fused γ -lactam- β -lactone bicycle.



Scheme 4.1.1a Structures of *N*-acylindole **248** and *N*-acylbenzotriazole **326**



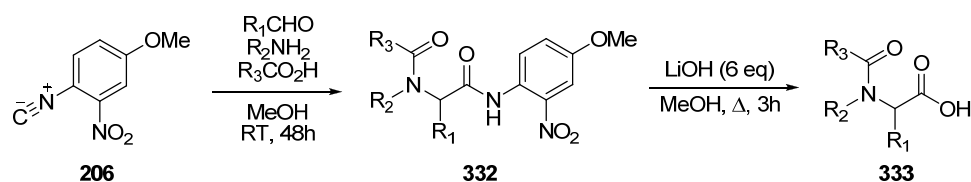
Scheme 4.1.1b Retrosynthetic Strategy Towards Synthesis of *N*-Acylbenzotriazole **326**

Retrosynthetically, we envisioned that *N*-acylBt **326** could be prepared *in situ* from the diazotization of *ortho*-aminoanilide **328** followed by subsequent *5-endo-dig* cyclization of the amide nitrogen (Scheme 4.1.1b).² Because 2-isocyanobenzylidene diazonium ion (**331**) is an unstable compound, which if generated would spontaneously cyclize to benzimidazole,³ we thought to generate *ortho*-aminoanilide **328** by reduction of *ortho*-

nitroanilide **329**, which could be the result of an Ugi reaction incorporating 2-nitrophenyl isocyanide (**330**).

4.1.2 4-Methoxy-2-Nitrophenyl Isocyanide

As was previously mentioned (see section 2.3.2.3), a similar isocyanide, 4-methoxy-2-nitrophenyl isocyanide (**206**),⁴ was introduced as a hydrolyzable isocyanide in the Ugi 4-component condensation reaction (Scheme 4.1.2). Due to the activation of the amide bond of the resulting Ugi product anilide **332**, via the electron withdrawing *ortho*-nitro group, direct hydrolysis to carboxylic acid **333** was achieved without additional activation. However, rather harsh basic conditions (6 equiv LiOH in refluxing MeOH, 3 h) were required for the hydrolysis of the anilide. In addition, the hydrolysis of sterically hindered Ugi products could be difficult.



Scheme 4.1.2 4-Methoxy-2-Nitrophenyl Isocyanide (**206**) as Convertible Isocyanide in the Ugi Reaction

4.2 N-Acylbenzotriazoles

N-Acylbenzotriazoles are known as stable, non-moisture sensitive, acid chloride equivalents.⁵ Thus, they are useful acylating agents, especially when the corresponding acid chlorides are unstable, difficult to synthesize, or unknown. Reactions with *N*-acylbenzotriazoles offer efficient transformations under mild conditions, and provide an alternative convenient procedure for *N*-, *C*-, *S*-, and *O*-acylation.

4.2.1 Preparation

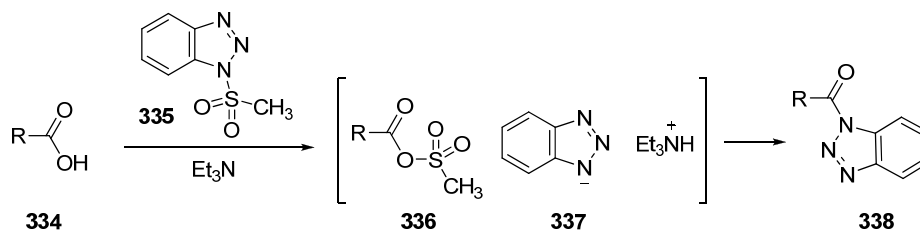
N-acylbenzotriazoles are typically prepared by three routes: (a) heating benzotriazole with an acid chloride;⁶ (b) reaction of 1-(methanesulfonyl)benzotriazole with a carboxylic acid salt;^{6,7} and (c) reaction of a carboxylic acid with benzotriazole in the presence of thionyl chloride.⁸ Less commonly, *N*-acylbenzotriazoles have been prepared by *5-endo-dig* cyclization of an anilide to an *ortho*-diazonium salt as described above.²

4.2.1.1 Coupling of Benzotriazole with Acid Chlorides

In most cases, *N*-acylbenzotriazoles can be prepared in good yield directly from the reaction of benzotriazole with acid chlorides.⁶ The reaction can be performed without solvent and typically requires heating from 80-100 °C. However, this approach is not useful for the many carboxylic acids of which the corresponding acid chlorides are unstable or difficult to obtain.

4.2.1.2 Reaction with 1-(Methanesulfonyl)benzotriazole

1-(Methanesulfonyl)benzotriazole (**335**)^{6,7} is a useful reagent for the conversion of carboxylic acids **334** directly into their corresponding *N*-acylBt **338**, eliminating the necessity of handling acid chlorides (Scheme 4.2.1.2). This sequence probably goes through intermediate formation of the mixed carboxylic sulfonic anhydride **336** and benzotriazole anion **337**, which is then acylated by the mixed anhydride. This procedure is particularly valuable for carboxylic acids whose corresponding acid chloride is unstable, and while it generally provides *N*-acylbenzotriazoles in one step from carboxylic acids in good yields, some problems were encountered with base-sensitive, olefinic, acetylenic, and dicarboxylic acids.

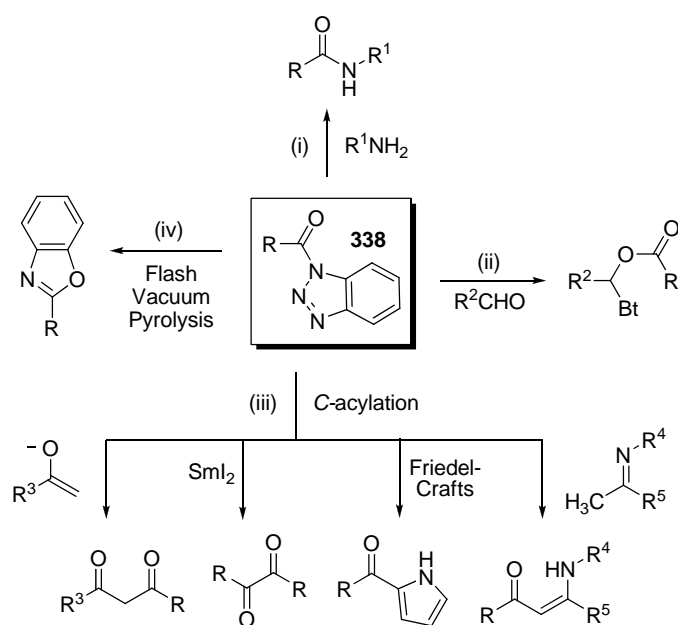


Scheme 4.2.1.2 Synthesis of *N*-Acylbenzotriazoles via Reaction of 1-(Methanesulfonyl)benzotriazole (**335**)

4.2.1.3 Reaction with Thionyl Chloride

Later it was found that room temperature treatment of carboxylic acids with thionyl chloride in the presence of excess benzotriazole could, in many cases more conveniently, provide *N*-acylbenzotriazoles in good yield.⁸ It is unclear whether the corresponding acid chloride is an intermediate in the reaction. In any case, the reaction is generally mild and success was met with a wide range of carboxylic acids demonstrating the general applicability of this procedure.

4.2.2 Utility



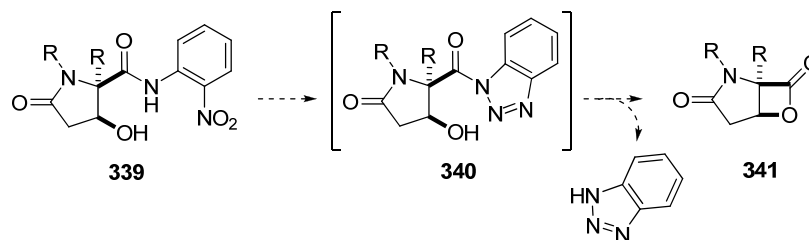
Scheme 4.2.2a Synthetic Applications of *N*-acylbenzotriazoles

N-Acylbenzotriazoles (**338**, Scheme 4.2.2a) have numerous synthetic applications including use as a (i) neutral *N*-acylation agents for the preparation of primary,

secondary, and tertiary amides,⁹ acyl azides,¹⁰ and peptides;¹¹ including *N*-formylation¹² and *N*-trifluoroacylation;¹³ (ii) for *O*-acylation in additions to aldehydes to give esters;¹⁴ (iii) for *C*-acylation reagents for the synthesis of 1,3-⁹ and 1,2-diketones,¹⁵ for the conversion of imines into enaminones,¹⁶ and for the regiospecific acylation of pyrroles and indoles;¹⁷ and (iv) in the preparation of benzoxazoles by flash vacuum pyrolysis.¹⁸

In addition to the many synthetic applications of *N*-acylbenzotriazoles, they often offer great synthetic advantages over conventional acid chlorides due to their stability towards hydrolysis, their chemoselectivity, and their crystalline nature. Also, benzotriazole is a convenient byproduct because the relatively low pK_a allows for simple removal from the crude reaction mixture by extraction with an aqueous alkaline solution (1N NaOH).

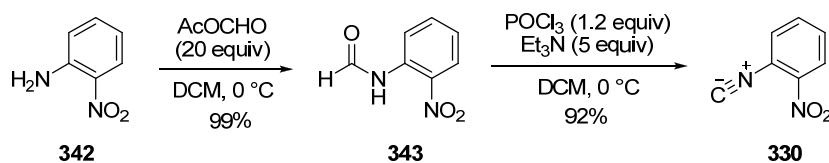
Again, we speculated the enhanced activation of the carbonyl group of *N*-acylbenzotriazoles would allow for direct β -lactone **341** formation, when *N*-acylbenzotriazole **340** is generated from Ugi product **339** in the presence of a hydroxyl group at the β -position (Scheme 4.2.2b).



Scheme 4.4.2b Hypothesis of Direct β -Lactone formation via Activated *N*-acylbenzotriazole

4.3 Preparation of 2-Nitrophenyl Isocyanide

Upon investigation, it was found that 2-nitrophenyl isocyanide (**330**) is a readily available solid which can be prepared in two steps (87%) from 2-nitroaniline (**342**, Scheme 4.3) and has been reported as a ligand of a metal complex previously.³ Interestingly, isocyanide **330** had not been utilized previously as a convertible isocyanide in a multicomponent condensation reaction. 2-Nitrophenyl formamide (**343**) can be prepared by formylation of 2-nitroaniline (**342**) via treatment with an excess of acetic-formic anhydride (formed from the gentle heating of acetic anhydride in the presence of formic acid). Dehydration of formamide **343**, to isocyanide **330**, was accomplished with POCl₃ and Et₃N. Isocyanide **330** is a stable solid that can be purified by column chromatography on neutral alumina and can be stored for several months in a -20 °C freezer.

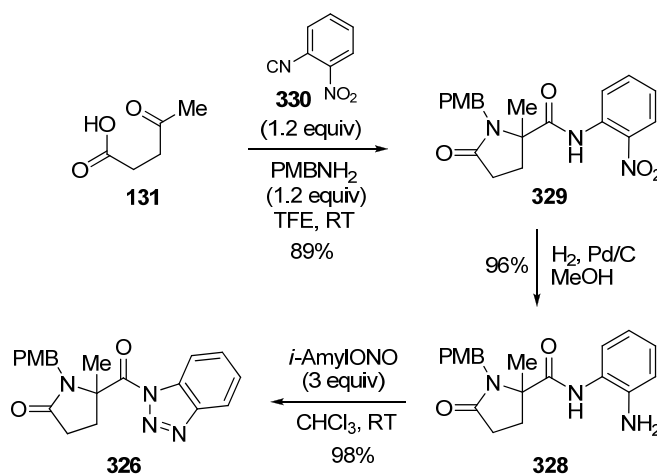


Scheme 4.3 Synthesis of 2-Nitrophenyl Isocyanide (**330**)

4.4 2-Nitrophenyl Isocyanide as a Convertible Isocyanide

4.4.1 *N*-Acylbenzotriazole

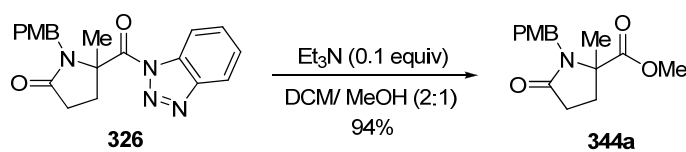
In order to quickly ascertain whether 2-nitrophenyl isocyanide (**330**) would be an effective convertible isocyanide, allowing for the synthesis of a series of pyroglutamic acid derivatives, we sought to prepare *N*-acylBt **326** starting from commercially available levulinic acid (**131**) (Scheme 4.4.1a). The initial *o*-nitroanilide **329**, derived from the Ugi reaction of levulinic acid (**131**) with *p*-methoxybenzylamine and isocyanide **330**, is readily converted to the corresponding *N*-acylBt **326** through hydrogenolysis of the nitro group to the aniline **328** and subsequent diazotization of the amino group followed by 5-*endo-dig* cyclization of the anilide toward the diazonium salt. The formation of *N*-acylBt **326** occurred spontaneously, while the diazonium salt was not observed.



Scheme 4.4.1a Synthesis of *N*-Acylbenzotriazole **326**

N-acylBt **326** is a stable isolable solid, which can be purified by SiO₂ column chromatography. Interestingly, the resulting isoamyl alcohol did not react with the *N*-acylBt to afford the corresponding isoamyl ester during the reaction, probably due to the steric hindrance of **326** and also the so-called Newman's "rule of six"¹⁹ (regarding isoamyl alcohol) which describes steric crowding during the hydrolysis of carboxylic esters. According to the "rule of six", the greater the number of atoms at the six position, the greater the steric effect. Nevertheless, facile β -lactonization could still be expected, because the process is an intramolecular reaction.

As we expected, the sterically hindered *N*-acylBt possessed the expected reactivity. Methanolysis of *N*-acylBt **326** occurred with a catalytic amount of Et₃N in DCM/MeOH (2:1) at room temperature in 10 minutes. The corresponding pure methyl ester (**344a**, Scheme 4.4.1b) was obtained in 94% yield after basic aqueous extraction (1N NaOH) of benzotriazole without the need for further purification.



Scheme 4.4.1b Methanolysis of *N*-Acylbenzotriazole **326**

4.4.2 Synthetic Utility

Table 4.4.2 Synthetic Utility of *N*-Acylbenzotriazole **326**

Entry	Nucleophile	Product	Yield	Entry	Nucleophile	Product	Yield
1	MeOH		94% ^{a,f}	5	EtNH ₂		97% ^c
2	HO-CH ₂ -CH=CH ₂		90% ^b	6	ClMg-CH ₂ -SiMe ₃		97% ^{d,e}
3	BnOH		84% ^b	7	NaBH ₄		79% ^{e,f}
4	BuSH		99% ^b				

^a. 0.1 eq Et₃N; rt ^b. 1.1 eq nucleophile; 0.1 eq Et₃N; DCM, rt ^c. 1.1 eq EtNH₂; DCM, rt ^d. 3.0 eq. nucleophile; THF ^e. 0 °C to rt ^f. DCM/ MeOH (2:1)

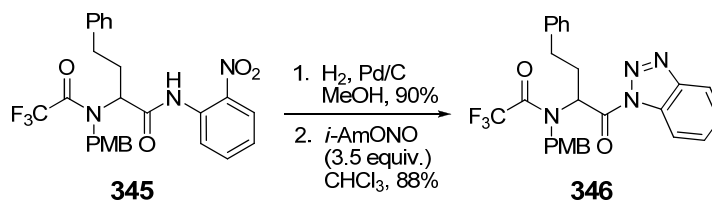
Table 4.4.2 shows the synthetic utility of the *N*-acylbenzotriazole **326**. Conversion of **326** into 2-methylpyrrolidonic acid esters **344a-c** (entry 1-3), thioester **344d** (entry 4), amide **344e** (entry 5) and ketone **344f** (entry 6) derivatives as well as the reduction to its hydroxymethyl derivative **344g** (entry 7) are described. In general, primary oxo-, thio- and amine containing nucleophiles (1.1 equiv) displace benzotriazole with catalytic amount of triethylamine (0.1 equiv) in dichloromethane at room temperature. The reactions were complete within 10 minutes and excellent yields of the corresponding adducts were obtained (84-99%). In addition, when employing volatile nucleophiles (entries 1, 4-6) the products were obtained in pure form without SiO₂

column chromatography, because the resulting benzotriazole could be extracted by wash with aqueous alkaline solution.

The nucleophilic addition of secondary alcohols and amines to *N*-acylBt **326** failed presumably due to the steric hindrance of the substrate. On the other hand, trimethylsilylmethylmagnesium chloride was efficiently added to *N*-acylBt **326** yielding the corresponding α -silyloxyketone in 97% yield. However, the addition of other Grignard and alkyllithium species to **326** resulted predominantly in formation of the corresponding tertiary alcohol by addition of 2 equiv. of the reagent, which is in contrast to previously reported results using similar, but less hindered, substrates.²⁰ Allylmagnesium bromide, lithium phenylacetylide, and 2-lithiothiophene gave the corresponding tertiary alcohol in 78%, 65%, and 78% respectively. It may be that the steric congestion at the neighboring fully substituted carbon causes the collapse of the proposed tetrahedral intermediate (similar to the case with Weinreb amides) which normally allows for preferential formation of ketones over tertiary alcohols.

Reduction of *N*-acylBt **326** with NaBH₄ (3 equiv) provided the completely reduced hydroxymethyl derivative. However, reduction of the corresponding *N*-acylindole (also with NaBH₄) provided the corresponding aldehyde via intermediate formation of an *N,O*-acetal (see section 3.1.2.2). This *N,O*-acetal derived from the *N*-acylindole is a stable intermediate, only collapsing and releasing indole when further treated with NaOH. On the other hand, the *N,O*-acetal derived from the *N*-acylBt did not prove as stable, presumably because benzotriazole is a better leaving group when compared to indole. This table indicates the reactivity and versatility of *N*-acylbenzotriazoles, which is effective even to the hindered pyroglutamic amides.

4.4.3 Synthesis of Amino Acid



Scheme 4.4.3 Synthesis of Linear *N*-Acylbenzotriazole **346**

We further explored the utility of this methodology to extend to linear Ugi products. The conformational flexibility of the linear system provided the possibility of azlactone/ müchnone formation, similar to that reported by Armstrong with the “universal isocyanide”.²¹ Anilide **345**, derived from the Ugi reaction of hydrocinnamaldehyde with 2-nitrophenyl isocyanide **330**, *p*-methoxybenzylamine, and trifluoroacetic acid (65% yield) was converted to *N*-acylBt **346** by hydrogenolysis and subsequent benzotriazole formation (Scheme 4.4.3). Interestingly, the formation of an azlactone intermediate and subsequent hydrolysis was not observed. Instead, the *N*-acylBt **346** was isolable and stable to flash column chromatography. Most likely, the suppression of the azlactone formation was possible due to the neutral conditions employed to generate the *N*-acylbenzotriazole and the poor nucleophilicity of the carbonyl group of the trifluoroacetamide. Acidic conditions and an electron-rich *N*-acyl group are required for azlactone formation with Armstrong’s universal isocyanide (see section 2.3.2.1).²² The

synthetic utility of *N*-acylbenzotriazole species of this type, including direct peptide coupling, was discussed earlier (see section 4.4.2).^{11,23}

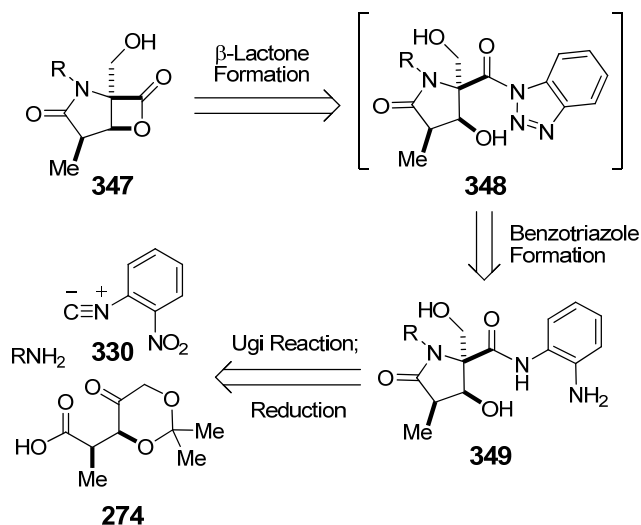
4.5 Synthesis of the Fused γ -Lactam- β -lactone Bicycle

Having established 2-nitrophenyl isocyanide (**330**) as a convertible isocyanide, we undertook our original goal of the stereocontrolled synthesis of the common fused γ -lactam- β -lactone bicyclic ring structure among proteasome inhibitors omuralide (**2**), salinosporamides A,B **3-4**, and cinnabaramides A-C **5-7**. Our goal was to establish a shortened synthetic route towards the common fused bicycle that includes direct β -lactone formation from the activated *N*-acylBt intermediate.

4.5.1 Retrosynthetic Analysis

Scheme 4.5.1 outlines our retrosynthetic plan for the synthesis of the common core bicycle **347**. We chose **347** as a probe to evaluate the feasibility and applicability of isocyanide **330** in natural product synthesis. A number of synthetic routes show the introduction of the isopropyl or cyclohex-2-enylcarbinol side chains of omuralide and salinosporamide A, respectively, in the late stage via an aldehyde intermediate. In addition, Romo recently reported a diastereocontrolled 1,2-addition of a cyclohexenyl zinc reagent even in the presence of the preformed β -lactone.²⁴ With methodology

already established to introduce those side chains in the late stage, we sought the rapid construction of the common core fused γ -lactam- β -lactone bicyclic ring system **347** starting from a linear precursor through two consecutive ring formation steps.

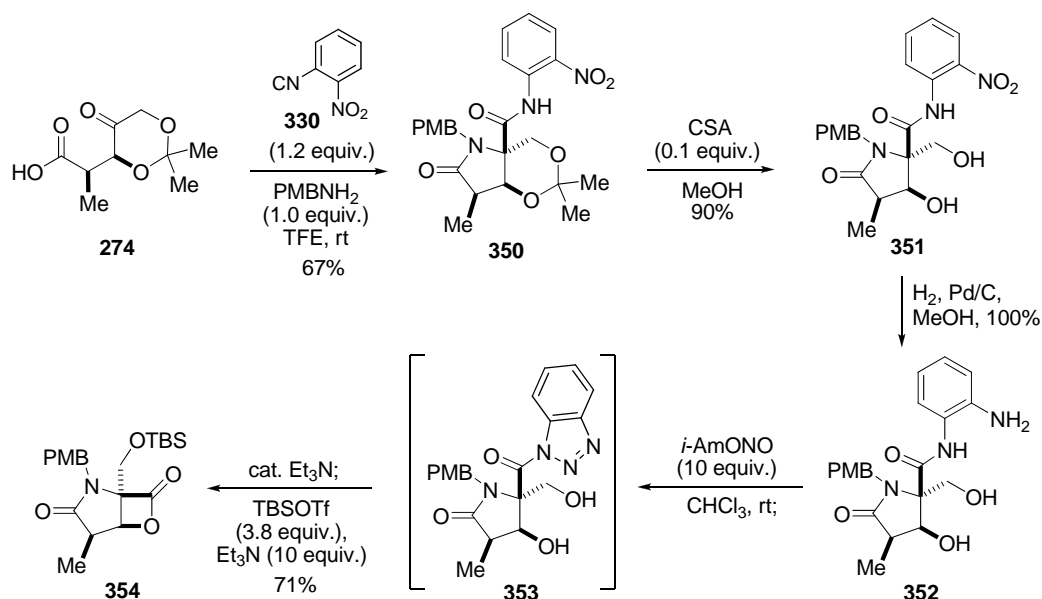


Scheme 4.5.1 Retrosynthetic Analysis of the Stereocontrolled Synthesis of Fused γ -Lactam- β -Lactone Bicycle **347**

We planned the *in situ* generation of *N*-acylBt **348** from the diazotization of *o*-aminoanilide **349** followed by *5-endo-dig* cyclization of the amide nitrogen. *o*-Aminoanilide **349** could have derived from the diastereoselective Ugi reaction of γ -ketoacid **274** with 2-nitrophenyl isocyanide (**330**) and *p*-methoxybenzylamine.

4.5.2 Enantioselective Synthesis of Fused γ -Lactam- β -Lactone **354**

The remaining challenges were (1) the stereoselective formation of the fully substituted carbon (C4 of omuralide) during the Ugi reaction with isocyanide **330**, (2) the compatibility of unprotected functional groups during the conversion of the nitroanilide to an *N*-acylBt, and (3) the intramolecular β -lactone formation with the activated *N*-acylBt. The enantioselective preparation of **274** was previously described (see section 3.3.3).



Scheme 4.5.2 Stereocontrolled Synthesis of Fused γ -Lactam- β -Lactone Bicycle **354**

The Ugi 4C-3CC reaction of functionalized chiral γ -ketoacid **274** with isocyanide **330** furnished γ -lactam **350** in 67% yield as a single diastereomer (Scheme 4.5.2). The relative stereochemistry of the resulting stereocenter of Ugi product **350** was unambiguously assigned by X-ray crystallography (Figure 4.5.2). As expected, axial attack of the isocyanide toward the iminium intermediate exclusively furnished the

desired isomer **350**. Attempted hydrolysis of the *o*-nitroanilide under basic conditions did not provide the corresponding carboxylic acid presumably due to steric hindrance.

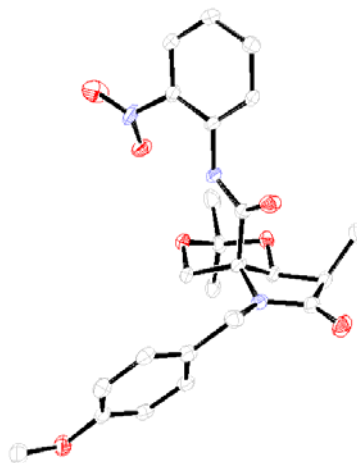


Figure 4.5.2 X-Ray Crystal Structure of **350**

Treatment of Ugi adduct **350** with catalytic amount of CSA smoothly deprotected the acetonide moiety to give the free 1,3-diol **351** in 90% yield. Fortunately, the transfer of the nitrobenzene functionality onto the resulting alcohols via a Meisenheimer complex, known as the Smiles rearrangement,²⁵ did not occur (although it could readily happen under basic conditions). Hydrogenolysis of the nitro group provided *o*-aminoanilide **352** as a precursor of the *N*-acylBt in quantitative yield. Alternative conditions for the reduction of nitro group are: SnCl₂ HCl, EtOH, heat. These conditions are compatible with the presence of unsaturated bonds as well as other functionality not compatible with

hydrogenolysis. In addition, we are aware that aminoanilide **352** could be a precursor to form an *N*-acylbenzimidazole²⁶ (pKa 16.4, between an indole and a benzotriazole).

Diazotization of the aniline **352** and subsequent benzotriazole formation **353** by 5-*endo-dig* cyclization of amide at the *ortho* position occurred smoothly under the neutral conditions mediated by isoamyl nitrite in chloroform at room temperature. The mild nature of the reaction allowed efficient conversion even in the presence of the unprotected alcohols without any side reactions. The formation of the *N*-acylBt **353** was indicated by TLC without β -lactone formation at that moment. Again, the isoamyl alcohol formed during nitrosonation of the aniline **352** did not react with the resulting *N*-acylBt **353** *in situ* to afford the corresponding isoamyl ester.

As we designed, fused γ -lactam- β -lactone formation occurred *in situ* with the addition of a catalytic amount of triethylamine (0.1 equiv). Spiro- γ -lactam- β -lactone formation was not detected. The remaining primary alcohol of the fused γ -lactam- β -lactone bicycle and the resulting isoamyl alcohol were protected as a TBS ether, then the core fused γ -lactam- β -lactone bicycle **354** was isolated in 71 % yield in one pot (3 steps from **352**).

4.6 Conclusions

In this chapter, we introduced 2-nitrophenyl isocyanide (**330**) as a convertible isocyanide and demonstrated its feasibility and applicability in an efficient synthesis of

the fused γ -lactam- β -lactone bicycle of omuralide (**2**). To our knowledge, this is the first demonstration of the isocyanide as a convertible isocyanide in the Ugi reaction. The resulting sterically hindered anilide can be converted under mild neutral conditions to an *N*-acylbenzotriazole, which is known as a stable acid chloride equivalent. Starting from a linear γ -ketoacid precursor, the fused γ -lactam- β -lactone bicycle was prepared only in four steps by a sequential biscyclization strategy; a stereocontrolled Ugi reaction and the concomitant direct β -lactonization following the formation of an *N*-acylbenzotriazole intermediate. In addition, the conditions required to generate the *N*-acylBt were mild and compatible with unprotected alcohols.

Due to the superior activation of the carbonyl group provided by the *N*-acylBt, when compared to the *N*-acylindole, the *N*-acylBt is amenable to intra- or intermolecular attack from a variety of nucleophiles with a catalytic amount of base to form the coupling products of the pyroglutamic acid derivatives. Conveniently, after the coupling reaction, the resulting benzotriazole can be readily removed from the reaction mixture by extraction with 1N NaOH. Owing to the mild nature of the reaction conditions, as well as the high compatibility with other functional groups, the applicability of this methodology will be extended to the synthesis of other natural products, which contain a fused γ -lactam- β -lactone bicycle as the core structure. Application to total synthesis of salinosporamide A (**3**) will be possible by a similar strategy.

4.7 Acknowledgments

CHAPTER FOUR, in part, is a reprint of the material as it appears in Gilley, C. B.; Kobayashi, Y. "2-Nitrophenyl Isocyanide as a Versatile Convertible Isocyanide: Rapid Access to a Fused γ -Lactam- β -lactone Bicycle" *J. Org. Chem.* **2008**, *73*, 4198-4204. The dissertation author was the primary investigator and author of this paper.

4.8 Experimental

4.8.1 Materials and Methods

All reagents were commercially obtained at highest commercial quality and used without further purification except where noted. Organic solutions were concentrated by rotary evaporation below 45 °C at approximately 20 mmHg. Tetrahydrofuran (THF), methanol (MeOH), chloroform (CHCl₃), dichloromethane (DCM), ethyl acetate (EtOAc), 2,2,2-trifluoroethanol (TFE), and acetone were reagent grade and used without further purification. Yields refer to chromatographically and spectroscopically (¹H NMR, ¹³C NMR) homogeneous materials, unless otherwise stated. Reactions were monitored by thin-layer chromatography (TLC) carried out on 0.25 mm silica gel plates using UV light and cerium molybdate solution with heat as visualizing agents. Silica gel (60, particle size 0.040-0.063 mm) was used for flash chromatography. Preparative thin-layer chromatography separations were carried out on 0.50 mm silica gel plates. NMR spectra were recorded on Varian Mercury 300, 400 and/or Unity 500 MHz instruments and

calibrated using the residual undeuterated solvent as an internal reference. Chemical shifts (δ) are reported in parts per million (ppm) and coupling constants (J) are reported in hertz (Hz). The following abbreviations were used to designate multiplicities: s= singlet, d= doublet, t= triplet, q= quartet, quint.= quintet, sp = septet, m= multiplet, br= broad. High resolution mass spectra (HRMS) were recorded on a Finnigan LCQDECA mass spectrometer under electrospray ionization (ESI) or atmospheric pressure chemical ionization (APCI) conditions, or on a Thermofinnigan Mat900XL mass spectrometer under electron impact (EI), chemical ionization (CI), or fast atom bombardment (FAB) conditions. X-ray data were recorded on a Bruker SMART APEX CCD X-ray diffractometer. Specific optical rotations were recorded on a Jasco P-1010 polarimeter and the specific rotations were calculated based on the equation $[\alpha]_D^{25} = (100 \cdot \alpha)/(l \cdot c)$, where the concentration c is in g/100 mL and the path length l is in decimeters.

4.8.2 Preparative Procedures

(329). To a solution of levulinic acid (**131**) (152 mg, 1.31 mmol, 1.0 equiv.) in TFE (5 mL) was added *p*-methoxybenzylamine (216 mg, 1.58 mmol, 1.2 equiv.) and isocyanide **330** (243 mg, 1.64 mmol, 1.2 equiv.) at room temperature. The reaction mixture was stirred overnight and then concentrated *in vacuo*. The crude mixture was applied directly to flash chromatography (30-75% EtOAc/ Hexanes) to yield 445 mg (89%) of **329** as a viscous orange oil. R_f (75% EtOAc/ Hexanes) = 0.53; HRMS (EI) m/z calcd for $C_{20}H_{21}N_4O_5$ (M^+) 383.1476, found 383.1474; 1H NMR (400 MHz, $CDCl_3$, ppm) δ : 10.47

(s, 1H), 8.50 (d, $J = 8.4$ Hz, 1H), 8.10 (d, $J = 8.4$ Hz, 1H), 7.55 (t, $J = 8.8$ Hz, 1H), 7.11-7.15 (m, 3H), 6.56 (d, $J = 8.4$ Hz, 2H), 4.53 (d, $J = 14.8$ Hz, 1H), 4.37 (d, $J = 15.2$, Hz, 1H), 3.55 (s, 3H), 2.64-2.73 (m, 1H), 2.48-2.56 (m, 1H), 2.32-2.39 (m, 1H), 1.96-2.07 (m, 1H), 1.56 (s, 3H); ^{13}C NMR (100 MHz, CDCl_3 , ppm) δ : 175.6, 172.9, 159.0, 136.5, 136.0, 134.3, 130.1, 129.1, 125.9, 123.8, 121.8, 113.9, 67.8, 55.2, 44.1, 33.0, 29.5, 22.8; IR (film, cm^{-1}) 2937, 1693, 1608, 1581, 1499, 1398, 1250, 1173, 1037, 742.

(328). To a solution of **329** (445 mg, 1.16 mmol, 1.0 equiv.) in MeOH (30 mL) was added ~10% by weight Pd/C at room temperature. A balloon of H_2 was applied and the reaction mixture was stirred for 2h. The mixture was then filtered through celite and washed with methanol. Concentration *in vacuo* yielded 394 mg (96%) of **328** as a white solid which was used without further purification. R_f (75% EtOAc/ Hexanes) = 0.18; Mp = 47-52 °C; HRMS (EI) m/z calcd for $\text{C}_{20}\text{H}_{23}\text{N}_3\text{O}_3$ (M^+) 353.1734, found 353.1730; ^1H NMR (400 MHz, CDCl_3 , ppm) δ : 7.97 (s, 1H), 7.24 (d, $J = 9.4$ Hz, 2H), 7.00 (t, $J = 7.6$ Hz, 1H), 6.78-6.81 (m, 3H), 6.67-6.72 (m, 2H), 4.62 (d, $J = 15.2$, 1H), 4.36 (d, $J = 15.2$, 1H), 3.74 (s, 3H), 3.64 (s, 2H), 2.54-2.63 (m, 1H), 2.41-2.50 (m, 2H), 1.96-2.03 (m, 1H), 1.50 (s, 3H); ^{13}C NMR (100 MHz, CDCl_3 , ppm) δ : 176.5, 172.3, 159.4, 140.9, 129.9, 129.9, 127.4, 125.3, 124.1, 119.6, 118.7, 114.5, 68.3, 55.5, 44.5, 34.1, 29.8, 23.4; IR (film, cm^{-1}) 2969, 2060, 1667, 1501, 1449, 1404, 1248, 1186, 1029, 750.

(326). To a solution of anilide **328** (363 mg, 1.03 mmol, 1.0 equiv.) in CHCl_3 (10 mL) was added isoamyl nitrite (0.4 mL, 2.99 mmol, 3.0 equiv.) at room temperature. The reaction mixture was stirred overnight and then concentrated *in vacuo*. The crude

mixture was applied directly to flash chromatography (50-75% EtOAc/ Hexanes) to yield 365 mg (98%) of *N*-acylbenzotriazole **326** as a yellow solid. R_f (75% EtOAc/ Hexanes) = 0.50; Mp = 136-139 °C; HRMS (EI) m/z calcd for $C_{20}H_{20}N_4O_3$ (M^+) 364.1530, found 364.1535; 1H NMR (400 MHz, $CDCl_3$, ppm) δ : 8.02 (d, J = 8.4 Hz, 1H), 7.90 (d, J = 8.4 Hz, 1H), 7.53 (t, J = 8.0 Hz, 1H), 7.44 (t, J = 8.4 Hz, 1H), 6.90 (d, J = 8.4 Hz, 2H), 6.27 (d, J = 8.8 Hz, 2H), 4.80 (d, J = 14.8 Hz, 1H), 4.15 (d, J = 14.8 Hz, 1H), 3.41 (s, 3H), 2.85-2.98 (m, 2H), 2.59-2.68 (m, 1H), 2.17-2.26 (m, 1H), 1.83 (s, 3H); ^{13}C NMR (100 MHz, $CDCl_3$, ppm) δ : 175.9, 172.5, 158.6, 130.4, 129.9, 127.8, 126.3, 120.0, 114.8, 113.4, 68.1, 55.0, 43.7, 31.3, 29.7, 25.0; IR (film, cm^{-1}) 2995, 2943, 1724, 1689, 1522, 1398, 1363, 1239, 1033, 959, 757.

(344a). To a solution of *N*-acylbenzotriazole **326** (182 mg, 0.499 mmol, 1.0 equiv.) in DCM/ MeOH (2/1, 3mL) was added triethylamine (0.01 mL, 0.07 mmol, 0.1 equiv.) at room temperature. The reaction mixture was stirred for 10 min then concentrated *in vacuo*. The crude oil was diluted with EtOAc and washed with 1N NaOH and brine. The solution was dried over Na_2SO_4 and concentrated *in vacuo* to yield 130 mg (94%) of methyl ester **344a** as a clear oil. No further purification was necessary. R_f (50% EtOAc/ Hexanes) = 0.29; HRMS (EI) m/z calcd for $C_{15}H_{19}N_1O_4$ (M^+) 277.1309, found 277.1312; 1H NMR (400 MHz, $CDCl_3$, ppm) δ : 7.18 (d, J = 8.4 Hz, 2H), 6.79 (d, J = 8.8 Hz, 2H), 4.42 (d, J = 15.6 Hz, 1H), 4.35 (d, J = 14.8 Hz, 1H), 3.76 (s, 3H), 3.44 (s, 3H), 2.52-2.60 (m, 1H), 2.40-2.47 (m, 1H), 2.25-2.31(m, 1H), 1.82-1.90 (m, 1H), 1.42 (s, 3H); ^{13}C NMR (100 MHz, $CDCl_3$, ppm) δ : 175.9, 174.2, 159.1, 129.9, 129.6, 113.9, 66.0,

55.5, 52.6, 43.9, 32.4, 29.9, 23.4; IR (film, cm^{-1}) 2995, 2943, 1740, 1693, 1608, 1503, 1398, 1247, 1169, 1115, 1021, 812.

General Procedure: To a solution of *N*-acylbenzotriazole **326** (182 mg, 0.499 mmol, 1.0 equiv.) in DCM (1 mL) was added alcohol (1.1 equiv.) and triethylamine (0.01 mL, 0.07 mmol, 0.1 equiv.) at room temperature. The reaction mixture was stirred for 30 min then concentrated *in vacuo*. The crude oil was diluted with EtOAc and washed with 1N NaOH and brine. The solution was dried over Na_2SO_4 and concentrated *in vacuo*. The crude products were then either purified by flash chromatography (30-75% EtOAc/Hexanes) to yield the pure esters **344b**, **344c** or obtained in very pure form without further purification for **344d**.

(344b). 137 mg, 90% R_f (50% EtOAc/ Hexanes) = 0.37; HRMS (EI) m/z calcd for $\text{C}_{17}\text{H}_{21}\text{N}_1\text{O}_4$ (M^+) 303.1465, found 303.1461; ^1H NMR (400 MHz, CDCl_3 , ppm) δ : 7.15 (d, $J = 8.4$ Hz, 2H), 6.75 (d, $J = 8.4$ Hz, 2H), 5.67-5.77 (m, 1H), 5.15-5.22 (m, 2H), 4.43 (d, $J = 15.6$ Hz, 1H), 4.37 (dd, $J = 5.6$ Hz, 13.2, 1H), 4.31 (d, $J = 15.2$ Hz, 1H), 4.17 (dd, $J = 5.6$ Hz, 13.2, 1H), 3.72 (s, 3H), 2.49-2.59 (m, 1H), 2.37-2.44 (m, 1H), 2.24-2.30 (m, 1H), 2.80-2.88 (m, 1H), 1.39 (s, 3H); ^{13}C NMR (100 MHz, CDCl_3 , ppm) δ : 175.9, 173.3, 159.0, 131.6, 129.9, 129.6, 119.0, 113.9, 66.2, 66.1, 55.4, 44.0, 32.4, 30.0, 23.3; IR (film, cm^{-1}) 2986, 2943, 1740, 1693, 1511, 1394, 1247, 1165, 1099, 1033.

(344c). 149 mg, 84% R_f (50% EtOAc/ Hexanes) = 0.39; HRMS (EI) m/z calcd for $\text{C}_{21}\text{H}_{23}\text{N}_1\text{O}_4$ (M^+) 353.1622, found 353.1622; ^1H NMR (400 MHz, CDCl_3 , ppm) δ : 7.31-

7.34 (m, 3H), 7.21-7.24 (m, 2H), 7.17 (d, $J = 8.8$ Hz, 2H), 6.77 (d, $J = 8.8$ Hz, 2H), 4.97 (d, $J = 12.4$ Hz, 1H), 4.74 (d, $J = 12.4$ Hz, 1H), 4.47 (d, $J = 15.6$ Hz, 1H), 4.31 (d, $J = 15.2$ Hz, 1H), 3.74 (s, 3H), 2.49-2.58 (m, 1H), 2.38-2.46 (m, 1H), 2.24-2.30 (m, 1H), 2.81-2.90 (m, 1H), 1.43 (s, 3H); ^{13}C NMR (100 MHz, CDCl_3 , ppm) δ : 175.9, 173.5, 159.1, 135.5, 129.9, 129.7, 128.9, 128.6, 128.2, 113.9, 67.3, 66.2, 55.4, 44.0, 32.3, 30.0, 23.4; IR (film, cm^{-1}) 2986, 2925, 1736, 1685, 1515, 1398, 1243, 1165, 1107, 1033.

(344d). 166 mg, 99% R_f (50% EtOAc/ Hexanes) = 0.55; HRMS (EI) m/z calcd for $\text{C}_{18}\text{H}_{25}\text{N}_1\text{O}_3\text{S}_1$ (M^+) 335.1550, found 335.1546; ^1H NMR (400 MHz, CDCl_3 , ppm) δ : 7.18 (d, $J = 8.4$ Hz, 2H), 6.79 (d, $J = 8.4$ Hz, 2H), 4.95 (d, $J = 15.6$ Hz, 1H), 3.86 (d, $J = 15.6$ Hz, 1H), 3.76 (s, 3H), 2.82-2.86 (m, 2H), 2.53-2.60 (m, 1H), 2.41-2.48 (m, 1H), 2.20-2.27 (m, 1H), 1.83-1.92 (m, 1H), 1.48-1.55 (m, 2H), 1.32-1.41 (m, 2H), 1.34 (s, 3H), 0.91 (t, $J = 7.6$ Hz, 3H); ^{13}C NMR (100 MHz, CDCl_3 , ppm) δ : 203.8, 176.3, 159.0, 130.4, 129.4, 114.0, 73.1, 55.4, 45.0, 33.2, 31.5, 29.6, 29.2, 23.7, 22.2, 13.8; IR (film, cm^{-1}) 2960, 2934, 1693, 1612, 1522, 1383, 1247, 1177, 1037, 979, 812.

(344e). To a solution of *N*-acylbenzotriazole **326** (182 mg, 0.499 mmol, 1.0 equiv.) in DCM (1 mL) was added ethylamine (2.0 M, 0.27 mL, 0.540 mmol, 1.1 equiv.) as a THF solution. The reaction mixture was stirred for 30 min then concentrated *in vacuo*. The crude oil was diluted with EtOAc and washed with 1H HCl, 1N NaOH, and brine. The solution was dried over Na_2SO_4 and concentrated *in vacuo* to yield 140 mg (97%) of amide **344e** as a yellow solid. No further purification was necessary. R_f (75% EtOAc/ Hexanes) = 0.15; Mp = 125-127 °C; HRMS (EI) m/z calcd for $\text{C}_{16}\text{H}_{22}\text{N}_2\text{O}_3$ (M^+)

290.1625, found 290.1626; ^1H NMR (400 MHz, CDCl_3 , ppm) δ : 7.22 (d, $J = 8.4$ Hz, 2H), 6.80 (d, $J = 8.4$ Hz, 2H), 5.86 (br s, 1H), 4.42 (d, $J = 14.8$ Hz, 1H), 4.33 (d, $J = 15.2$ Hz, 1H), 3.75 (s, 3H), 3.05-3.11 (m, 1H), 2.93-2.99 (m, 1H), 2.40-2.49 (m, 2H), 2.26-2.32 (m, 1H), 1.85-1.93 (m, 1H), 1.41 (s, 3H), 0.86 (t, $J = 7.2$ Hz, 3H); ^{13}C NMR (100 MHz, CDCl_3 , ppm) δ : 176.5, 173.3, 159.3, 130.2, 129.8, 114.3, 67.9, 55.5, 44.2, 34.8, 33.8, 29.8, 23.3, 14.5; IR (film, cm^{-1}) 2986, 2925, 1658, 1515, 1410, 1247, 1169, 1037, 812.

(344f). To a solution of *N*-acylbenzotriazole **326** (91 mg, 0.250 mmol, 1.0 equiv.) in THF (2 mL) under N_2 atmosphere at -78 °C was added trimethylsilylmethylmagnesium chloride (1M in Et_2O , 0.75 mL, 3.0 equiv.) dropwise. The reaction mixture was stirred at -78 °C for 30 min then warmed to room temperature and stirred for an additional 1 hr. Saturated NH_4Cl was added to quench and the mixture was extracted with EtOAc. The resultant organic layer was washed successively with 1N NaOH, and brine. The solution was then dried over Na_2SO_4 and concentrated *in vacuo* to yield 80.8 mg (97%) of **344f**. The crude product required no further purification. R_f (30% EtOAc/ Hexanes) = 0.46; HRMS (EI) m/z calcd for $\text{C}_{18}\text{H}_{27}\text{NO}_3\text{Si}_1$ (M^+) 333.1715, found 333.1748; ^1H NMR (400 MHz, CDCl_3 , ppm) δ : 7.16 (d, $J = 8.0$ Hz, 2H), 6.77 (d, $J = 8.0$ Hz, 2H), 4.58 (d, $J = 15.6$ Hz, 1H), 4.12 (d, $J = 14.8$ Hz, 1H), 3.74 (s, 3H), 3.69 (d, $J = 14.4$ Hz, 1H), 3.46 (d, $J = 14.4$ Hz, 1H), 2.43-2.51 (m, 2H), 2.23-2.29 (m, 1H), 1.82-1.89 (m, 1H), 1.37 (s, 3H), 0.04 (s, 9H); ^{13}C NMR (100 MHz, CDCl_3 , ppm) δ : 175.9, 174.5, 159.0, 130.0, 129.7, 113.9, 66.6, 59.1, 55.4, 44.2, 32.5, 30.0, 23.8, -2.8; IR (film, cm^{-1}) 2945, 2840, 1723, 1607, 1510, 1388, 1248, 1165, 1097, 1029, 859, 757.

(344g). To a solution of *N*-acylbenzotriazole **326** (91 mg, 0.250 mmol, 1.0 equiv.) in DCM/MeOH (2/1, 3 mL) at 0 °C was added sodium borohydride (28 mg, 0.740 mmol, 3 equiv.). The reaction mixture was stirred at 0 °C for 30 min then warmed to room temperature and stirred for an additional 1 hr. Acetone was added to quench and the mixture was diluted with EtOAc. The resultant organic layer was washed successively with 1N NaOH, and brine. The solution was then dried over Na₂SO₄ and concentrated *in vacuo* to yield 49.4 mg (79%) of **344g**. The crude product required no further purification. R_f (75% EtOAc/ Hexanes) = 0.25; HRMS (EI) m/z calcd for C₁₄H₁₉NO₃ (M⁺) 249.1359, found 249.1362; ¹H NMR (300 MHz, CDCl₃, ppm) δ : 7.23 (d, J = 8.7 Hz, 2H), 6.81 (d, J = 8.4 Hz, 2H), 4.49 (d, J = 15.0 Hz, 1H), 4.20 (d, J = 15.3 Hz, 1H), 3.75 (s, 3H), 3.44 (d, J = 12.0 Hz, 1H), 3.20 (d, J = 12.0 Hz, 1H), 2.33-2.60 (m, 3H), 2.13-2.22 (m, 1H), 1.63-1.73 (m, 1H), 1.07 (s, 3H); ¹³C NMR (100 MHz, CDCl₃, ppm) δ : 176.5, 169.1, 131.0, 129.2, 114.4, 67.2, 65.2, 55.5, 42.4, 30.3, 29.7, 22.4; IR (film, cm⁻¹) 3437, 2951, 1660, 1515, 1408, 1238, 1170, 1029.

(345). To a solution of hydrocinnamaldehyde, 90% (300 mg, 2.01 mmol, 1.0 equiv.) in TFE (10 mL) was added *p*-methoxybenzylamine (338 mg, 2.46 mmol, 1.2 equiv.) and trifluoroacetic acid (0.19 mL, 2.47 mmol, 1.2 equiv.). The mixture was stirred with 4 Å molecular sieves at room temperature for 20 min and then isocyanide **330** (365 mg, 2.46 mmol, 1.2 equiv.) was added. The reaction mixture was stirred overnight and then concentrated to yield a brown oil. The mixture was purified by flash chromatography (10-30% EtOAc/ Hexanes) to yield 750 mg (65%) of **345** as a yellow solid. R_f (20% EtOAc/ Hexanes) = 0.50; Mp = 95-97 °C; HRMS (EI) m/z calcd for C₂₆H₂₄N₃O₅F₃ (M⁺)

515.1663, found 515.1672; The title compound exists at room temperature as a 2.2/1 mixture of rotamers. When peaks corresponding to the same proton(s) from each rotamer can be identified, they are listed separately as major and minor. ^1H NMR (400 MHz, CDCl_3 , ppm) Major: δ : 10.4 (br s, 1H), 8.45 (d, $J = 8.4$ Hz, 1H), 8.16 (d, $J = 8.4$ Hz, 1H), 7.56 (t, $J = 8.8$ Hz, 1H), 7.14-7.31 (m, 7H), 7.04 (d, $J = 8.4$ Hz, 2H), 6.73 (d, $J = 8.4$ Hz, 2H), 4.65 (d, $J = 16.0$ Hz, 1H), 4.50 (d, $J = 15.6$ Hz, 1H), 4.34 (d, $J = 6.8$ Hz, 1H), 3.71 (s, 3H), 2.64-2.74 (m, 3H), 2.10-2.15 (m, 1H); Minor: δ : 10.6 (br s, 1H), 8.51 (d, $J = 8.4$ Hz, 1H), 8.13 (d, $J = 8.4$ Hz, 1H), 7.58 (t, $J = 8.8$ Hz, 1H), 7.09 (d, $J = 8.4$ Hz, 2H), 6.54 (d, $J = 8.4$ Hz, 2H), 4.90 (d, $J = 16.0$ Hz, 1H), 4.64 (d, $J = 15.6$ Hz, 1H), 4.37 (d, $J = 8.0$ Hz, 1H), 3.60 (s, 3H), 2.48-2.59 (m, 3H), 1.94-2.05 (m, 1H); ^{13}C NMR (100 MHz, CDCl_3 , ppm) δ : 168.0, 167.0, 160.1, 157.9, 140.4, 140.1, 136.9, 135.8, 134.3, 130.5, 130.3, 129.0, 128.9, 128.8, 128.6, 126.7, 125.8, 125.4, 124.0, 123.8, 122.8, 122.1, 118.1, 115.2, 114.5, 113.8, 61.4, 60.4, 55.4, 55.2, 50.8, 47.4, 32.9, 32.5, 31.5, 29.9; IR (film, cm^{-1}) 3350, 2942, 1694, 1607, 1587, 1500, 1456, 1432, 1335, 1272, 1199, 1150, 1029, 748.

(345a). To a solution of **345** (600 mg, 1.16 mmol, 1.0 equiv.) in MeOH (20 mL) was added ~ 10% by weight activated palladium on carbon. The flask was fitted with a rubber septum and a balloon of H_2 gas was introduced at room temperature with stirring. After 30 min, N_2 gas was flushed through the reaction mixture and the palladium was removed by filtration through Celite. The light yellow solution was concentrated to yield 509 mg of **345a** (90%, not shown) as a light yellow foamy solid which was used without further purification. R_f (20% EtOAc/Hexanes) = 0.24; Mp = 45-49 °C; HRMS (EI) m/z calcd for $\text{C}_{26}\text{H}_{26}\text{N}_3\text{O}_3\text{F}_3$ (M^+) 485.1921, found 485.1925; ^1H NMR (500 MHz, CDCl_3 ,

ppm) δ : 7.40 (br s, 1H), 7.23-7.33 (m, 3H), 7.14 (d, $J = 7.5$ Hz, 2H), 7.00-7.05 (m, 3H), 6.84-6.89 (m, 3H), 6.68-6.78 (m, 2H), 4.76 (d, $J = 15.5$ Hz, 1H), 4.36 (d, $J = 15.5$ Hz, 1H), 4.14 (d, $J = 7.5$ Hz, 1H), 3.80 (s, 3H), 3.73 (br s, 2H), 2.62-2.68 (m, 3H), 2.13-2.15 (m, 1H); ^{13}C NMR (100 MHz, CDCl_3 , ppm) δ : 167.2, 160.2, 141.1, 140.4, 130.3, 129.9, 129.0, 128.7, 128.6, 127.6, 126.7, 126.1, 125.5, 123.1, 119.0, 117.5, 114.9, 61.1, 55.6, 51.9, 32.6, 29.7; IR (film, cm^{-1}) 3369, 3039, 2981, 1684, 1617, 1515, 1447, 1248, 1199, 1146, 1034, 820, 743.

(346). To a solution of **345a** (21.0 mg, 0.0443 mmol, 1.0 equiv.) in CHCl_3 (1 mL) was added isoamyl nitrite (0.02 mL, 0.150 mmol, 3.5 equiv.). The reaction mixture was stirred for 10 min at room temperature and then concentrated to yield a yellow oil. The mixture was purified by preparative thin-layer chromatography (20% EtOAc/ Hexanes) to yield 19.0 mg (88%) of **346** as a clear oil. R_f (20% EtOAc/ Hexanes) = 0.53; HRMS (EI) m/z calcd for $[\text{C}_{26}\text{H}_{23}\text{N}_4\text{O}_3\text{F}_3 (\text{M}^+)]$ 496.1717, found 496.1714; The title compound exists at room temperature as a 3.7/1 mixture of rotamers. When peaks corresponding to the same proton(s) from each rotamer can be identified, they are listed separately as major and minor. ^1H NMR (400 MHz, CDCl_3 , ppm) Major, δ : 8.13 (d, $J = 8.0$ Hz, 1H), 8.10 (d, $J = 8.0$ Hz, 1H), 7.63 (t, $J = 7.0$ Hz, 1H), 7.51 (t, $J = 7.5$ Hz, 1H), 7.08-7.25 (m, 5H), 7.00 (d, $J = 7.0$ Hz, 2H), 6.72 (d, $J = 9.0$ Hz, 2H), 5.24 (dd, $J = 5.0, 8.0$ Hz, 1H), 3.70 (s, 3H), 2.66-2.75 (m, 2H), 2.47-2.55 (m, 1H), 1.87-1.94 (m, 1H); Minor, δ : 8.04 (d, $J = 8.0$ Hz, 1H), 8.03 (d, $J = 8.0$ Hz, 1H), 6.92 (d, $J = 7.0$ Hz, 2H), 6.57 (d, $J = 9.0$ Hz, 2H), 6.10 (t, $J = 6.5$ Hz, 1H), 4.89 (d, $J = 4.5$ Hz, 1H), 3.60 (s, 3H); ^{13}C NMR (100 MHz, CDCl_3 , ppm) δ : 167.8, 160.0, 146.1, 140.5, 131.3, 130.9, 130.8, 130.5, 129.3, 128.8,

128.6, 128.5, 126.9, 126.7, 126.5, 125.5, 120.5, 120.3, 114.6, 114.4, 114.0, 60.6, 55.4, 55.3, 52.0, 48.8, 33.0, 32.8, 32.7, 31.0; IR (film, cm^{-1}) 2942, 1738, 1684, 1612, 1505, 1447, 1379, 1257, 1209, 1180, 1150, 1029, 961, 835, 743.

(350). To a solution of γ -ketoacid **274** (98.0 mg, 0.485 mmol, 1.0 equiv.) in TFE (2 mL) was added *p*-methoxybenzylamine (66.5 mg, 0.485 mmol, 1.0 equiv.) and isocyanide **330** (86.0 mg, 0.581 mmol, 1.2 equiv.) at room temperature. The reaction mixture was stirred overnight and then concentrated to yield a red-brown oil. The mixture was purified by flash chromatography (30-50% EtOAc/ Hexanes) to yield 153 mg (67%) of anilide **350** as a yellow solid which was a single diastereomer. R_f (50% EtOAc/ Hexanes) = 0.40; Mp = 68-71 °C; $[\alpha]_D^{25} = +15$ ($c = 0.020$, CHCl_3); HRMS (EI) m/z calcd for $\text{C}_{24}\text{H}_{27}\text{N}_3\text{O}_7$ (M^+) 469.1844, found 469.1836; ^1H NMR (500 MHz, CDCl_3 , ppm) δ : 11.46 (s, 1H), 8.63 (d, $J = 9.0$ Hz, 1H), 8.17 (d, $J = 8.0$ Hz, 1H), 7.67 (t, $J = 7.5$ Hz, 1H), 7.26 (m, 1H), 7.16 (d, $J = 8.0$ Hz, 2H), 6.82 (d, $J = 8.0$, Hz 2H), 5.11 (d, $J = 14.5$ Hz, 1H), 4.45 (d, $J = 8.5$ Hz, 1H), 3.84 (m, 2H), 3.80 (s, 3H), 3.64 (d, $J = 11.5$ Hz, 1H), 2.86 (quint., $J = 8.5$ Hz, 1H), 1.55 (s, 3H), 1.54 (s, 3H), 1.26 (d, $J = 7.5$ Hz, 3H); ^{13}C NMR (100 MHz, CDCl_3 , ppm) δ : 177.0, 171.0, 159.6, 135.4, 133.4, 130.3, 129.4, 125.9, 124.5, 124.3, 114.3, 103.7, 76.1, 69.3, 65.3, 55.5, 45.3, 38.8, 29.3, 19.5, 9.8; IR (film, cm^{-1}) 2998, 2942, 2917, 2886, 1711, 1608, 1583, 1513, 1434, 1345, 1274, 1250, 1180, 738.

(351). To a solution of **350** (130.5 mg, 0.278 mmol, 1.0 equiv.) in MeOH (3 mL) was added camphorsulfonic acid (7 mg, 0.03 mmol, 0.1 equiv.). The reaction mixture was heated to 70 °C with stirring for 1h. After cooling to room temperature, the mixture

concentrated and purified directly by flash chromatography (50-75% EtOAc/ Hexanes) to yield 107 mg (90%) of diol **351** as a yellow solid. $R_f(75\% \text{ EtOAc/ Hexanes}) = 0.15$; Mp = 72-75 °C; $[\alpha]_D^{25} = +28$ ($c = 0.014$, CHCl_3 , ppm); HRMS (EI) m/z calcd for $\text{C}_{21}\text{H}_{23}\text{N}_3\text{O}_7$ (M^+) 429.1531, found 429.1526; ^1H NMR (400 MHz, CDCl_3) δ : 10.88 (s, 1H), 8.63 (d, $J = 8.8$ Hz, 1H), 8.17 (d, $J = 8.4$ Hz, 1H), 7.65 (t, $J = 7.2$ Hz, 1H), 7.24 (m, 2H), 6.72 (d, $J = 8.4$ Hz, 2H), 5.01 (d, $J = 15.2$ Hz, 1H), 4.71 (dd, $J = 5.6, 8.0$ Hz, 1H), 4.18 (d, $J = 15.2$ Hz, 1H), 3.71 (s, 3H), 3.58 (dd, $J = 6.8, 12.0$ Hz, 1H), 2.86 (quint., $J = 7.6$ Hz, 1H), 2.50 (d, $J = 5.2$ Hz, 1H), 2.25 (t, $J = 6.0$ Hz, 1H), 1.29 (d, $J = 7.2$ Hz, 3H); ^{13}C NMR (100 MHz, CDCl_3 , ppm) δ : 178.3, 170.1, 159.3, 137.5, 135.8, 133.6, 130.0, 129.7, 125.9, 129.7, 125.9, 124.2, 122.8, 114.3, 75.3, 71.4, 64.0, 55.4, 45.2, 40.6, 9.6; IR (film, cm^{-1}) 3340, 2942, 1670, 1607, 1583, 1505, 1437, 1340, 1272, 1233, 1175, 1029, 738.

(352). To a solution of diol **351** (95.1 mg, 0.221 mmol, 1.0 equiv.) in MeOH (6 mL) was added ~ 10% by weight activated palladium on carbon. The flask was fitted with a rubber septum and a balloon of H_2 gas was introduced at room temperature with stirring. After 30 min, N_2 gas was flushed through the reaction mixture and the palladium was removed by filtration through Celite. The clear solution was concentrated to yield 88.4 mg of *o*-aminoanilide **352** (100%) as a clear oil which was used without further purification. $R_f(100\% \text{ EtOAc}) = 0.18$; $[\alpha]_D^{25} = +8.3$ ($c = 0.021$, CHCl_3); HRMS (EI) m/z calcd for $\text{C}_{21}\text{H}_{25}\text{N}_3\text{O}_5$ (M^+) 399.1789, found 399.1792; ^1H NMR (400 MHz, CDCl_3 , ppm) δ : 8.15 (s, 1H), 7.22 (d, $J = 6.8$ Hz, 2H), 7.03 (t, $J = 5.6$ Hz, 1H), 6.79 (d, $J = 7.4$ Hz, 2H), 6.72 (t, $J = 6.0$ Hz, 1H), 6.66 (d, $J = 6.0$ Hz, 1H), 4.83 (d, $J = 15.2$ Hz, 1H),

4.49 (d, $J = 7.2$ Hz, 1H), 4.17 (d, $J = 14.8$ Hz, 1H), 3.80-3.67 (m, 6H), 3.44 (d, $J = 12.0$ Hz, 1H), 2.72 (quint., $J = 8.0$ Hz, 1H), 1.17 (d, $J = 7.6$ Hz, 3H); ^{13}C NMR (100 MHz, CDCl_3 , ppm) δ : 178.7, 170.2, 159.3, 140.8, 129.9, 129.7, 128.4, 127.3, 122.9, 119.8, 117.9, 114.4, 74.9, 71.1, 64.0, 55.5, 45.4, 40.5, 9.6; IR (film, cm^{-1}) 3369, 3010, 2932, 2825, 1670, 1612, 1510, 1456, 1408, 1296, 1238, 1175, 1029, 748.

(354). To a solution of *o*-aminoanilide **352** (9.1 mg, 0.023 mmol, 1.0 equiv.) in CHCl_3 (1 mL) was added isoamyl nitrite (0.03 mL, 0.22 mmol, 10 equiv.) at room temperature. The reaction mixture was stirred for 5 min, and after detection of *N*-acylbenzotriazole **353** by TLC analysis, triethylamine (0.01 mL) was added to form β -lactone. The reaction mixture was stirred an additional 5 min, and *tert*-butyldimethylsilyl trifluoromethanesulfonate (0.02 mL, 0.087 mmol, 3.8 equiv.) and additional triethylamine (0.02 mL, 0.22 mmol, 10 equiv. total) were added. The reaction mixture was stirred for 1h and then diluted with ethyl acetate (5 mL) and washed with brine (2 x 5 mL). After drying with sodium sulfate, the solution was concentrated and purified by preparative thin-layer chromatography (30% EtOAc/ Hexanes) to yield 6.5 mg (71%) of β -lactone **354** as a clear oil. R_f (30% EtOAc/ Hexanes) = 0.39; $[\alpha]_D^{25} = -31$ ($c = 0.016$, CHCl_3); HRMS (EI) m/z calcd for $\text{C}_{21}\text{H}_{31}\text{N}_1\text{O}_5\text{Si}_1$ (M^+) 405.1966, found 405.1973; ^1H NMR (400 MHz, CDCl_3 , ppm) δ : 7.19 (d, $J = 8.4$ Hz, 2H), 6.83 (d, $J = 8.4$ Hz, 2H), 5.03 (d, $J = 6.0$ Hz, 1H), 4.85 (d, $J = 15.2$ Hz, 1H), 4.22 (d, $J = 15.2$ Hz, 1H), 3.90 (d, $J = 10.8$ Hz, 1H), 3.79 (s, 3H), 3.43 (d, $J = 10.8$ Hz, 1H), 2.77 (quint., $J = 7.2$ Hz, 1H), 1.37 (d, $J = 7.6$ Hz, 3H), 0.82 (s, 9H), -0.01 (s, 3H), -0.04 (s, 3H); ^{13}C NMR (100 MHz, CDCl_3 , ppm) δ : 175.2, 167.8, 159.6, 129.5, 129.1, 114.3, 81.0, 74.4, 58.5, 55.5, 44.8, 38.6, 25.8,

18.3, 8.6, -5.5, -5.5; IR (film, cm^{-1}) 2932, 2854, 1835, 1709, 1510, 1461, 1393, 1248, 1117, 835, 767.

4.9 Notes and References

- (1) Bordwell, F. G. *Acc. Chem. Res.* **1988**, *21*, 456-463.
- (2) Katritzky, A. R.; Ji, F. B.; Fan, W. Q.; Beretta, P.; Bertoldi, M. *J. Heterocycl. Chem.* **1992**, *29*, 1519-1523; Plummer, B. F.; Russell, S. R.; Reese, W. G.; Watson, W. H.; Krawiec, M. *J. Org. Chem.* **1991**, *56*, 3219-3223; Hart, H.; Ok, D. *J. Org. Chem.* **1986**, *51*, 979-986.
- (3) Hahn, F. E.; Plumed, C. G.; Muender, M.; Luegger, T. *Chem. Eur. J.* **2004**, *10*, 6285-6293.
- (4) Baldoli, C.; Maiorana, S.; Licandro, E.; Zinzalla, G.; Perdicchia, D. *Org. Lett.* **2002**, *4*, 4341-4344.
- (5) Katritzky, A. R.; Suzuki, K.; Wang, Z. *Synlett* **2005**, 1656-1665.
- (6) Katritzky, A. R.; Shobana, N.; Pernak, J.; Afridi, A. S.; Fan, W. Q. *Tetrahedron* **1992**, *48*, 7817-7822.
- (7) Katritzky, A. R.; He, H.-Y.; Suzuki, K. *J. Org. Chem.* **2000**, *65*, 8210-8213.
- (8) Katritzky, A. R.; Zhang, Y.; Singh, S. K. *Synthesis* **2003**, 2795-2798.
- (9) Katritzky, A. R.; Pastor, A. *J. Org. Chem.* **2000**, *65*, 3679-3682.

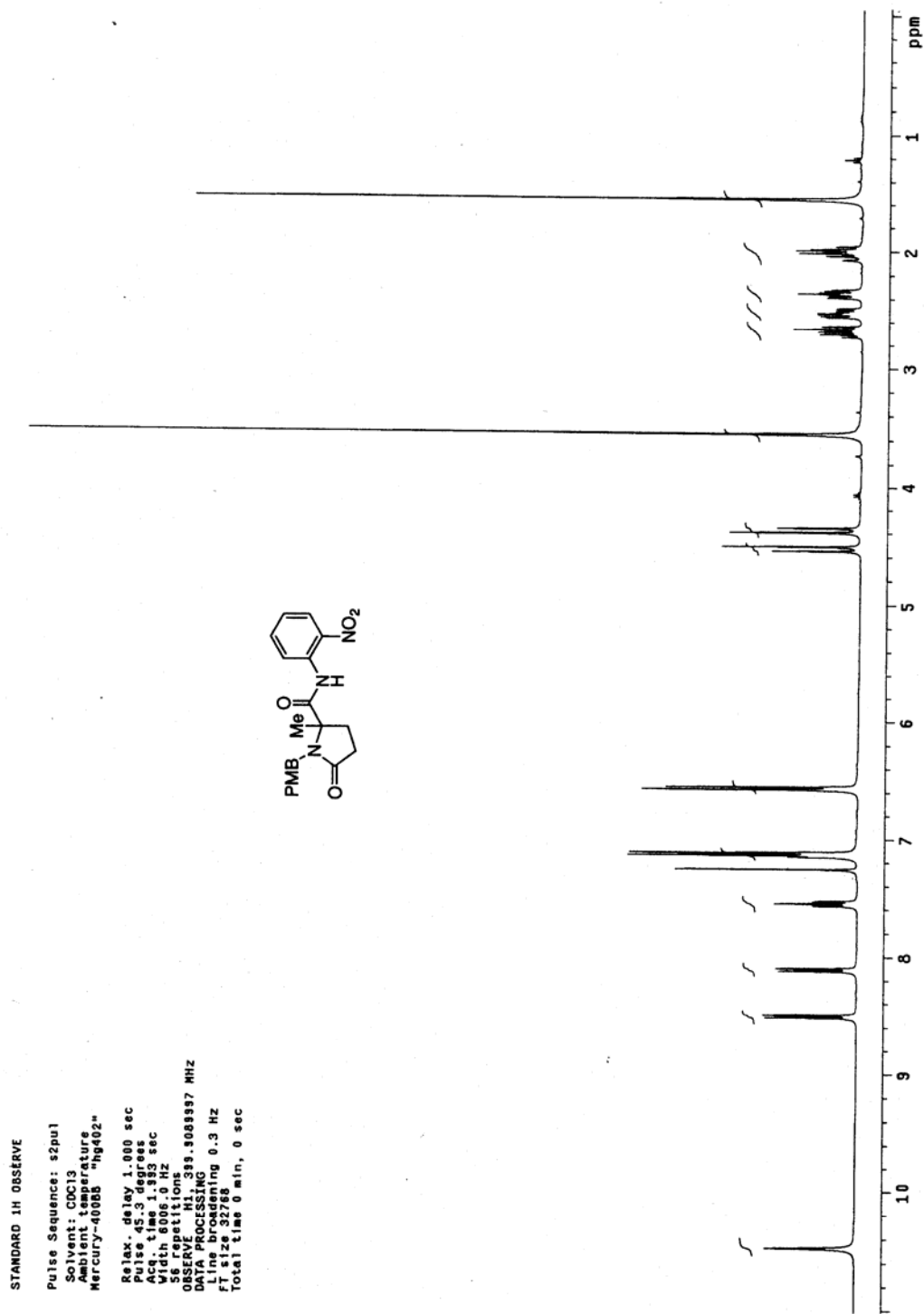
- (10) Katritzky, A. R.; Widyan, K.; Kirichenko, K. *J. Org. Chem.* **2007**, *72*, 5802-5804.
- (11) Katritzky, A. R.; Meher, G.; Angrish, P. *Chem. Biol. Drug Des.* **2006**, *68*, 326-333.
- (12) Katritzky, A. R.; Chang, H. X.; Yang, B. *Synthesis* **1995**, 503-505.
- (13) Katritzky, A. R.; Yang, B.; Semenzin, D. *J. Org. Chem.* **1997**, *62*, 726-728.
- (14) Katritzky, A. R.; Pastor, A.; Voronkov, M. V. *J. Heterocycl. Chem.* **1999**, *36*, 777-781.
- (15) Wang, X.; Zhang, Y. *Tetrahedron Lett.* **2002**, *43*, 5431-5433.
- (16) Katritzky, A. R.; Fang, Y.; Donkor, A.; Xu, J. *Synthesis* **2000**, 2029-2032.
- (17) Katritzky, A. R.; Suzuki, K.; Singh, S. K.; He, H.-Y. *J. Org. Chem.* **2003**, *68*, 5720-5723.
- (18) Baradarani, M. M.; Khalafy, J.; Prager, R. H. *Aust. J. Chem.* **1999**, *52*, 775-780.
- (19) Newman, M. S. *J. Am. Chem. Soc.* **1950**, *72*, 4783-4786.
- (20) Katritzky, A. R.; Le, K. N. B.; Khelashvili, L.; Mohapatra, P. P. *J. Org. Chem.* **2006**, *71*, 9861-9864.
- (21) Keating, T. A.; Armstrong, R. W. *J. Am. Chem. Soc.* **1996**, *118*, 2574-2583.
- (22) Rikimaru, K.; Yanagisawa, A.; Kan, T.; Fukuyama, T. *Synlett* **2004**, 41-44; Lindhorst, T.; Bock, H.; Ugi, I. *Tetrahedron* **1999**, *55*, 7411-7420.

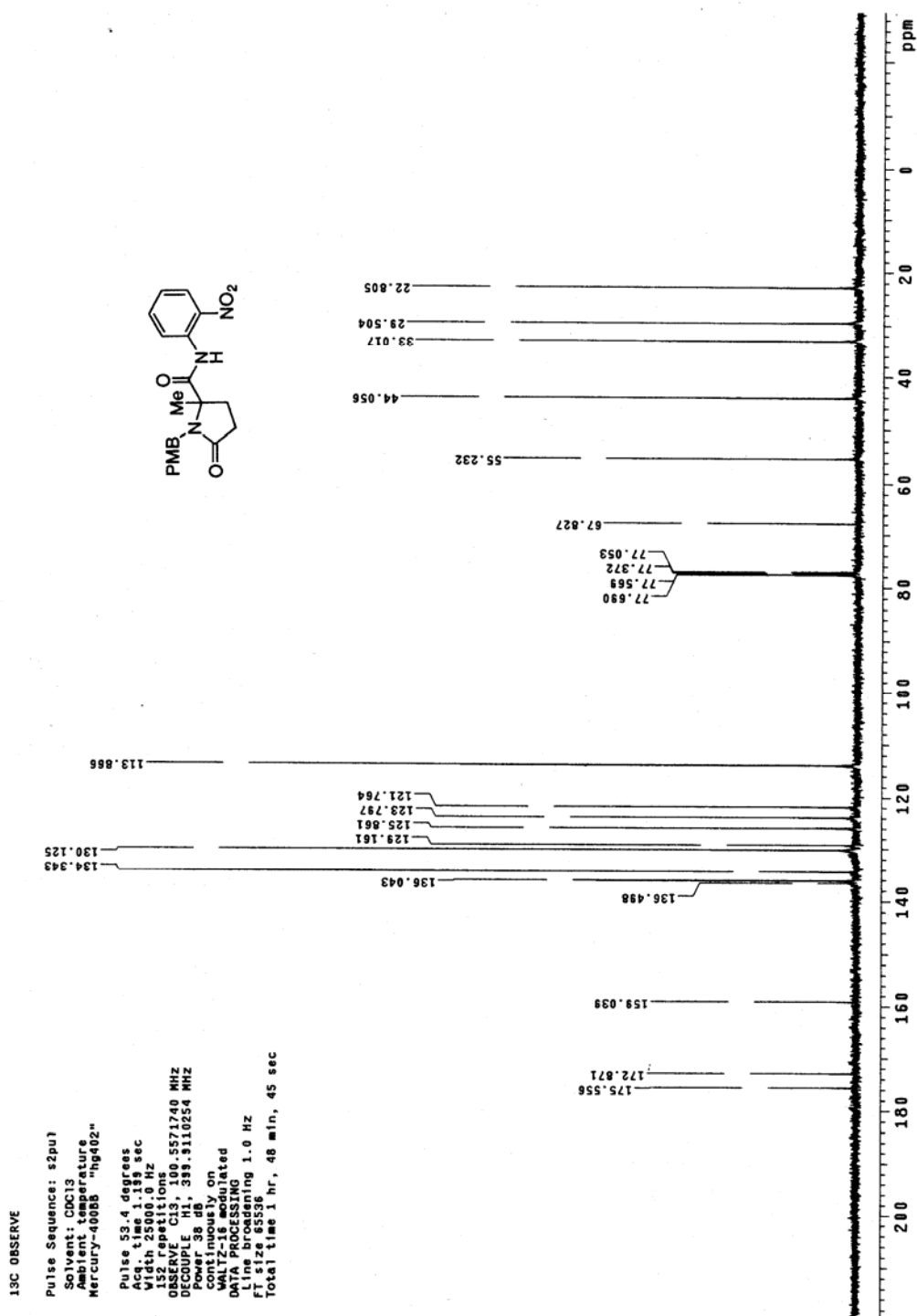
(23) Katritzky, A. R.; Abdel-Fattah, A. A. A.; Gromova, A. V.; Witek, R.; Steel, P. J. *J. Org. Chem.* **2005**, *70*, 9211-9214; Katritzky, A. R.; Abdel-Fattah, A. A. A.; Vakulenko, A. V.; Tao, H. *J. Org. Chem.* **2005**, *70*, 9191-9197; Katritzky, A. R.; Angrish, P. *Synthesis* **2006**, 4135-4142; Katritzky, A. R.; Angrish, P.; Huer, D.; Suzuki, K. *Synthesis* **2005**, 397-402; Katritzky, A. R.; Angrish, P.; Suzuki, K. *Synthesis* **2006**, 411-424; Katritzky, A. R.; Jiang, R.; Suzuki, K. *J. Org. Chem.* **2005**, *70*, 4993-5000; Katritzky, A. R.; Shestopalov, A. A.; Suzuki, K. *Synthesis* **2004**, 1806-1813; Katritzky, A. R.; Suzuki, K.; Singh, S. K. *Synthesis* **2004**, 2645-2652; Katritzky, A. R.; Todadze, E.; Cusido, J.; Angrish, P.; Shestopalov, A. A. *Chem. Biol. Drug Des.* **2006**, *68*, 37-41; Katritzky, A. R.; Todadze, E.; Shestopalov, A. A.; Cusido, J.; Angrish, P. *Chem. Biol. Drug Des.* **2006**, *68*, 42-47.

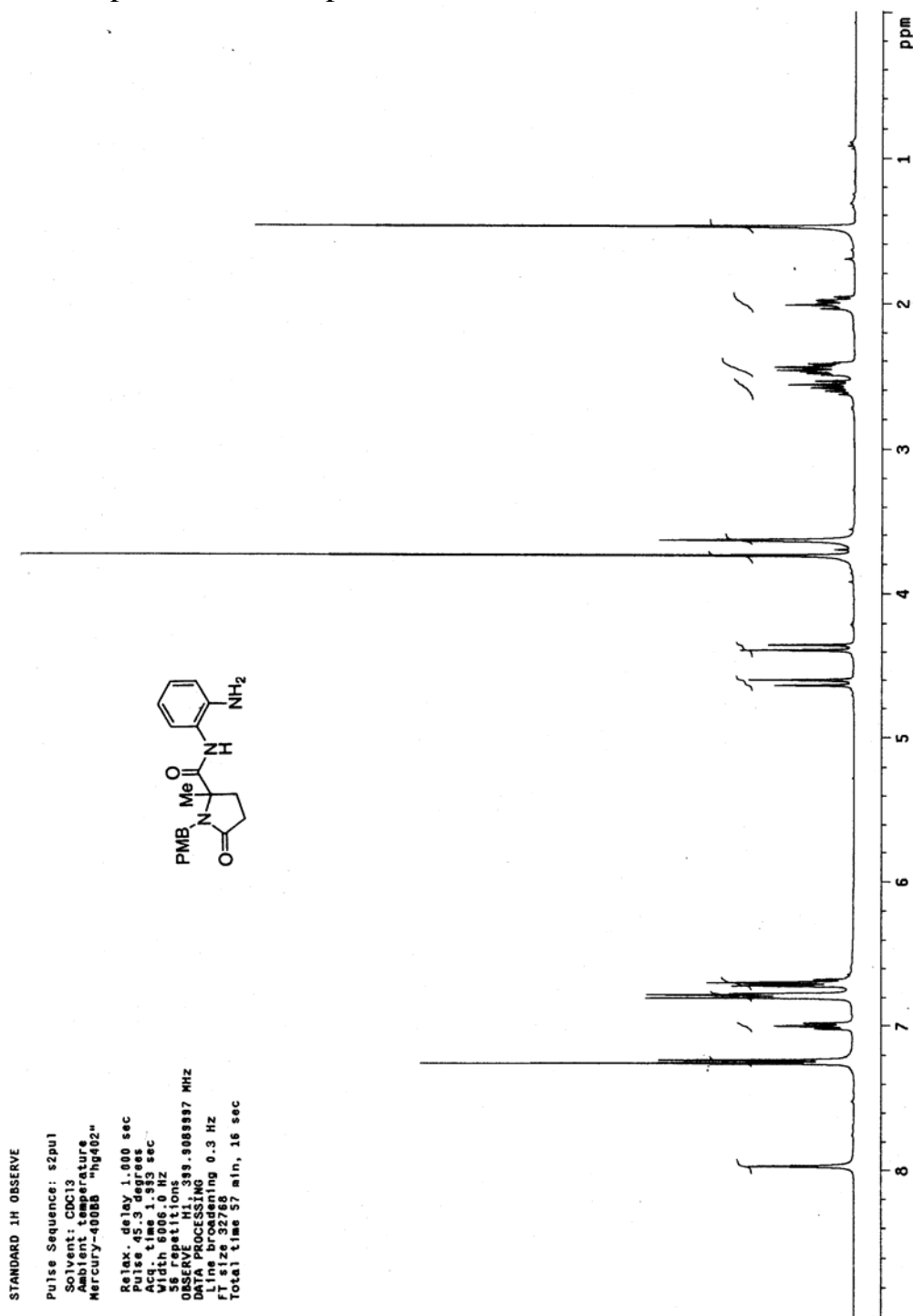
(24) Ma, G.; Nguyen, H.; Romo, D. *Org. Lett.* **2007**, *9*, 2143-2146.

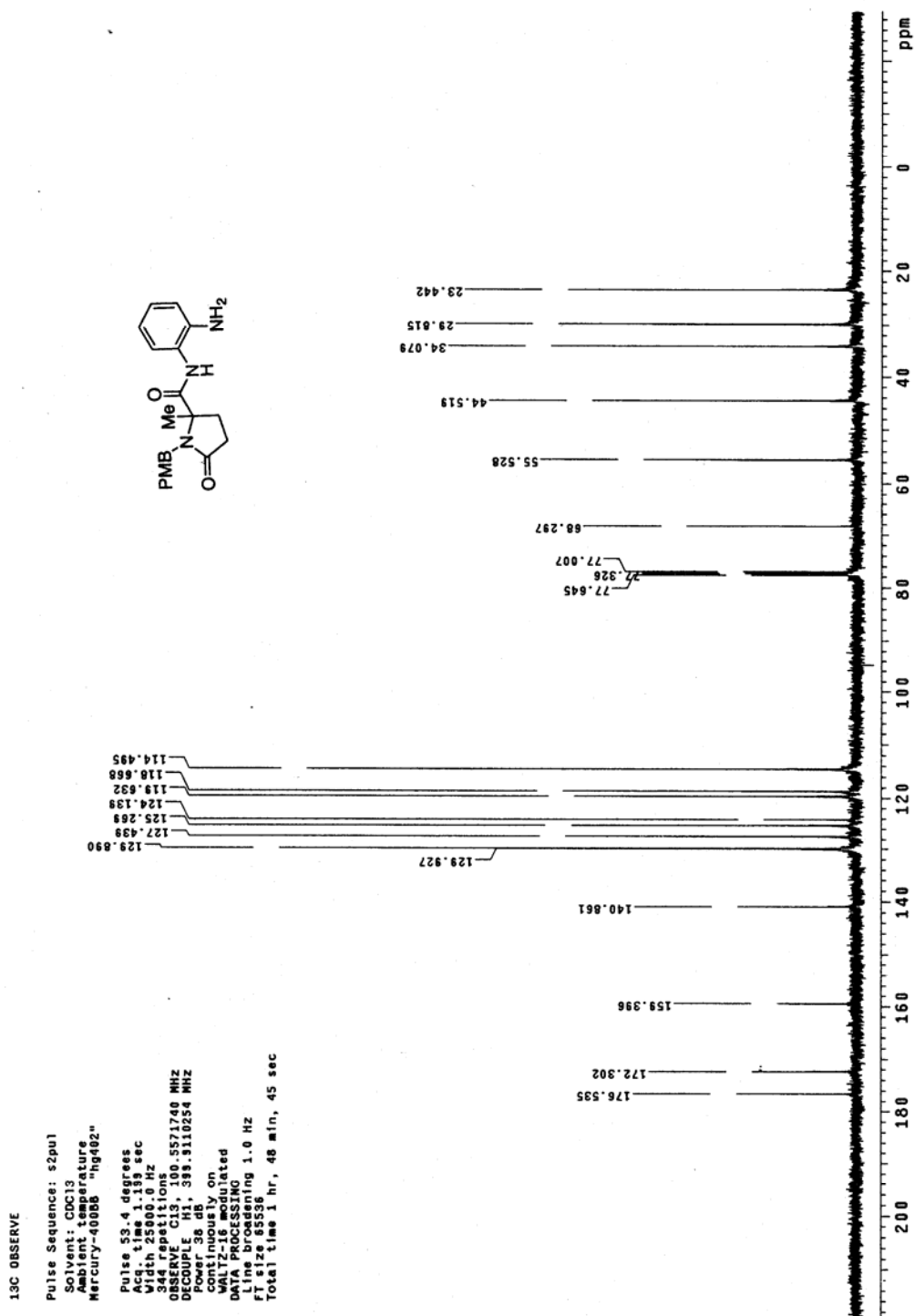
(25) El Kaiem, L.; Gizolme, M.; Grimaud, L.; Oble, J. *J. Org. Chem.* **2007**, *72*, 4169-4180; El Kaim, L.; Gizolme, M.; Grimaud, L.; Oble, J. *Org. Lett.* **2006**, *8*, 4019-4021; El Kaim, L.; Grimaud, L.; Oble, J. *Angew. Chem. Int. Ed.* **2005**, *44*, 7961-7964.

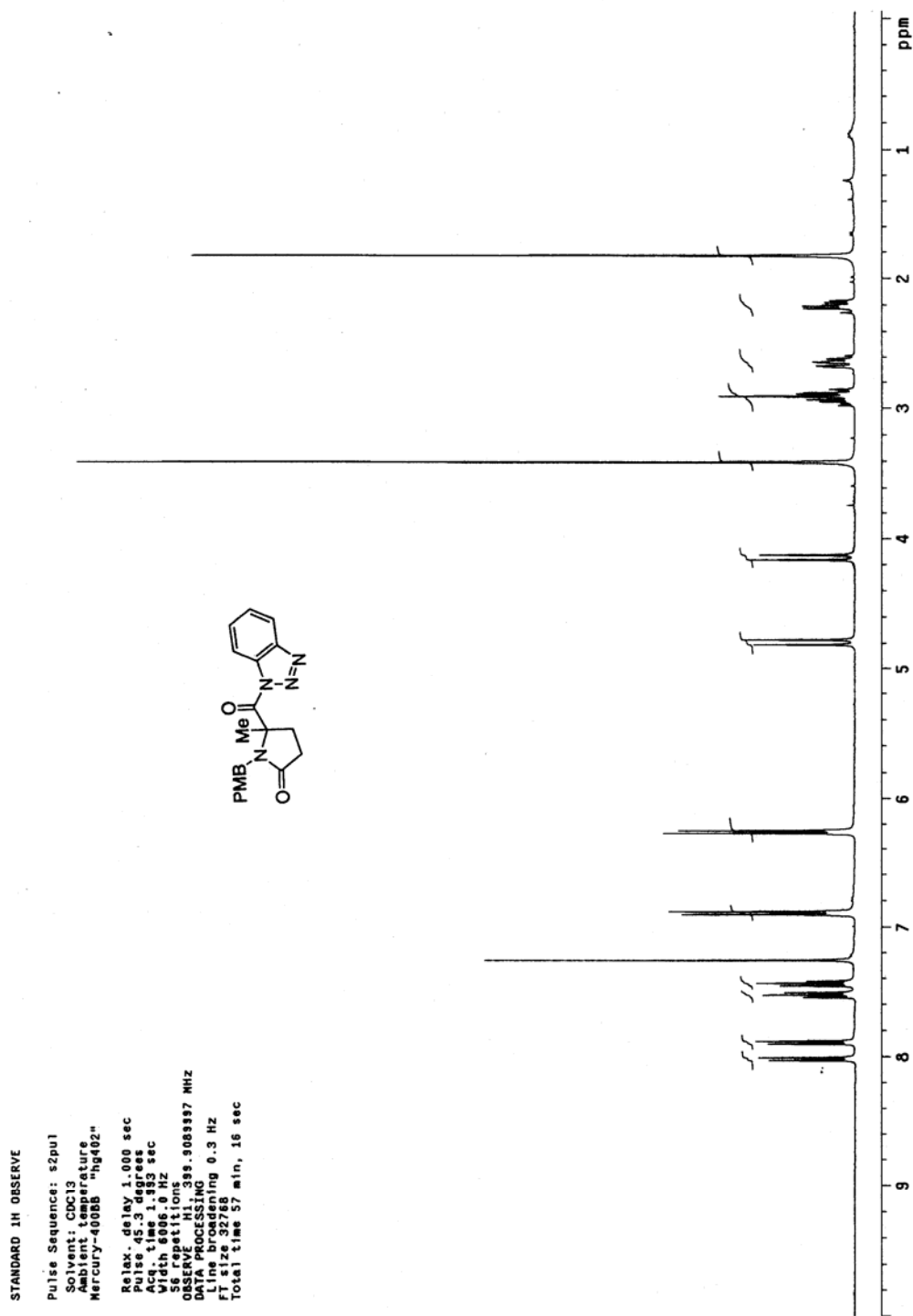
(26) Tanaka, K.; Shimazak, M.; Murakami, Y. *Chem. Pharm. Bull. (Tokyo)* **1982**, *30*, 2714-2722.

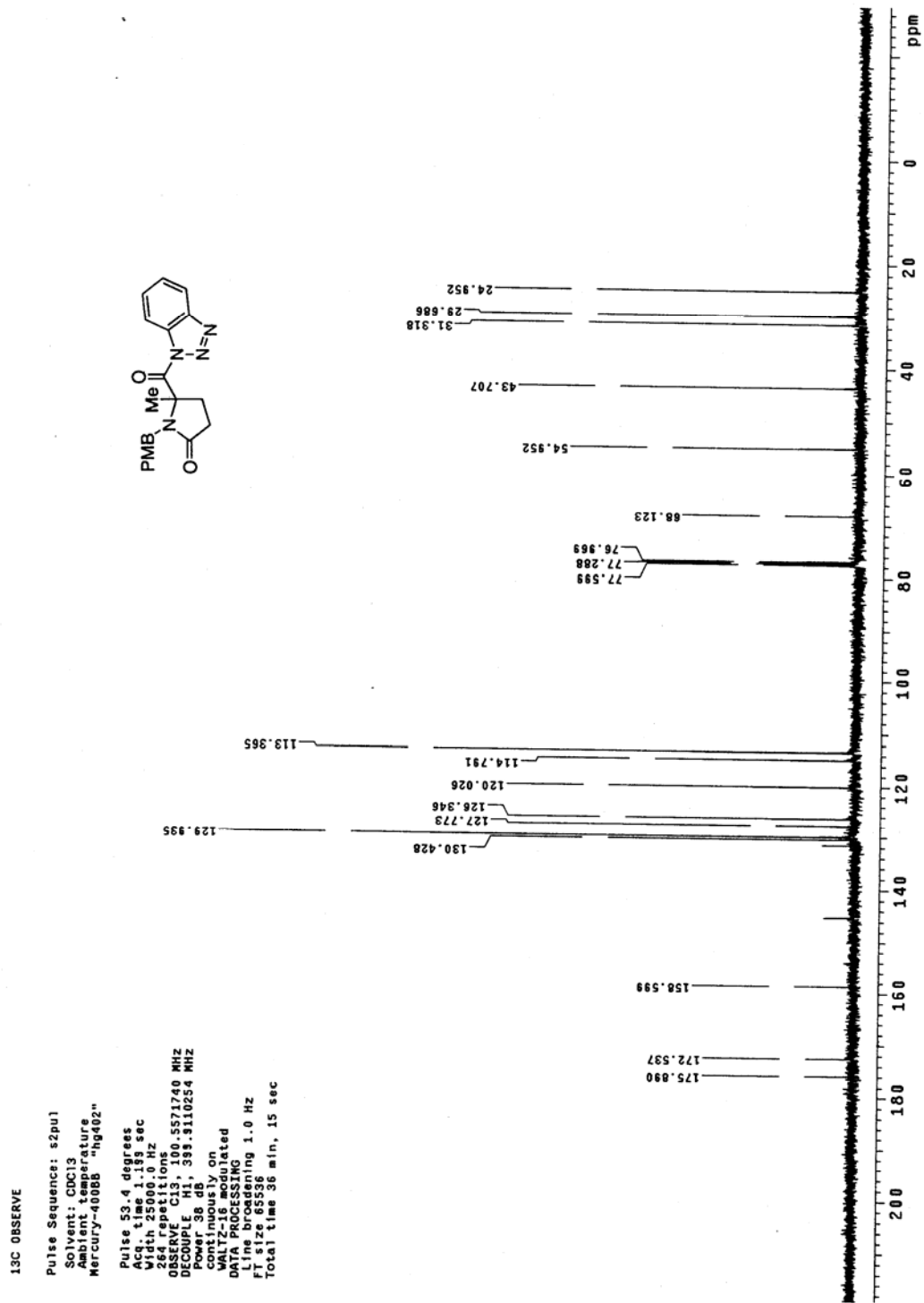
¹H NMR spectrum of compound 329

^{13}C NMR spectrum of compound **329**

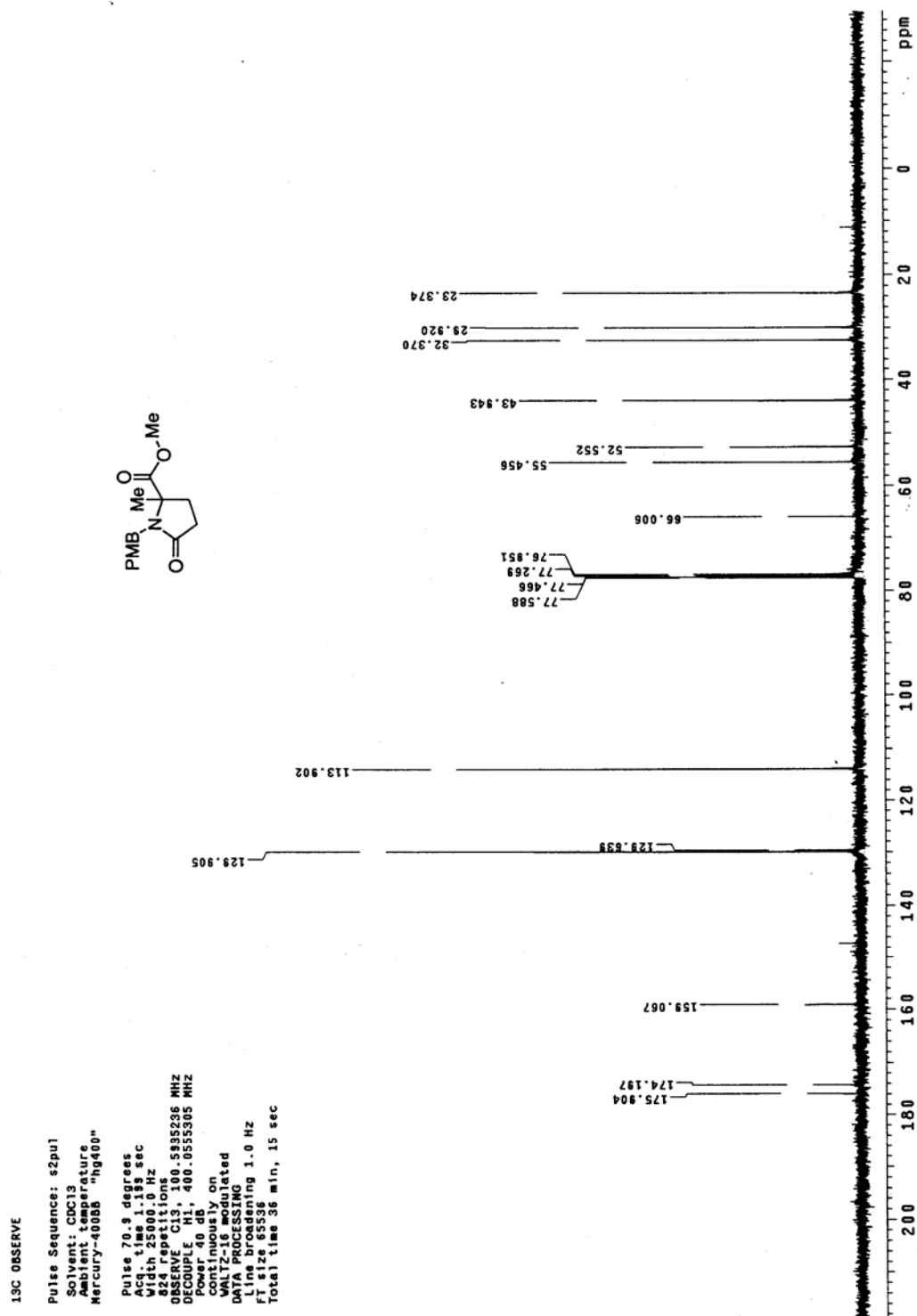
¹H NMR spectrum of compound 328

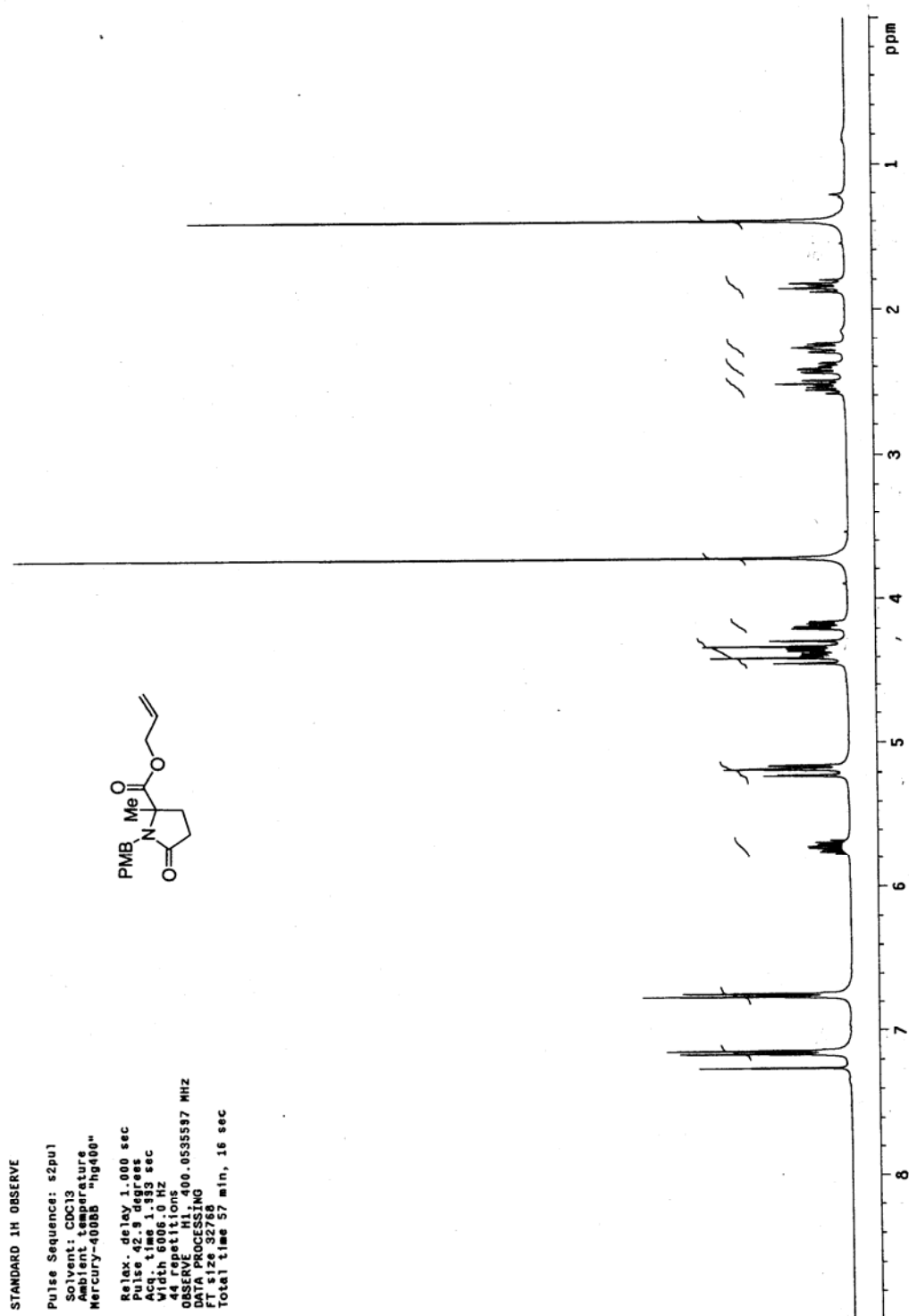
^{13}C NMR spectrum of compound 328

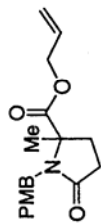
¹H NMR spectrum of compound 326

^{13}C NMR spectrum of compound **326**

¹H NMR spectrum of compound 344a

^{13}C NMR spectrum of compound **344a**

¹H NMR spectrum of compound 344b

^{13}C NMR spectrum of compound **344b**

^{13}C OBSERVE

Pulse Sequence: s2pul

Solvent: CDCl₃

Ambient temperature

Mercury-400BB "hg400"

Pulse 70.9 degrees

Acq. time 1.189 sec

Width 25000.0 Hz

Observer: J. J. J.

OBSERVE PC13, 400.5935236 MHz

DECOUPLE H1, 400.0555395 MHz

Power 40 dB,

continuously on

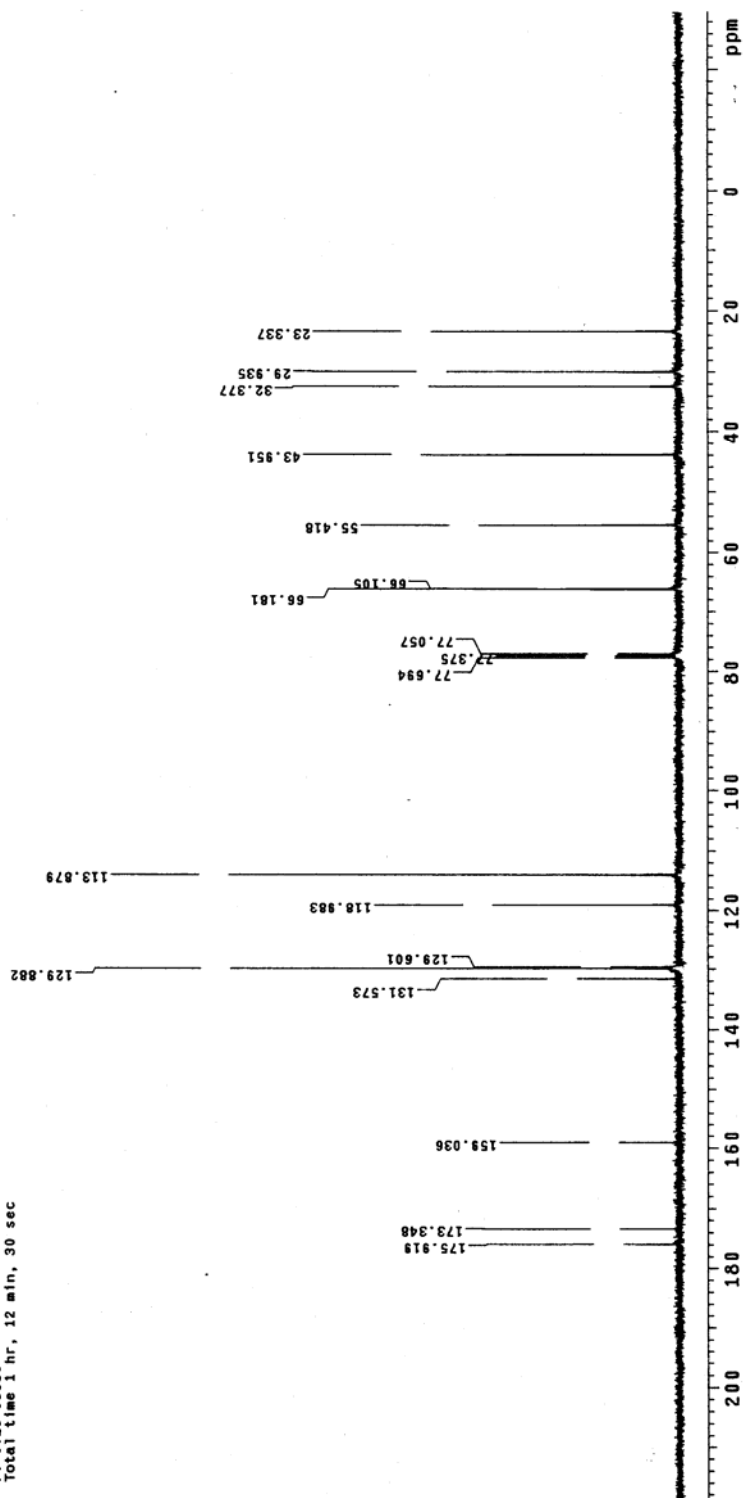
WALTZ-16 modulated

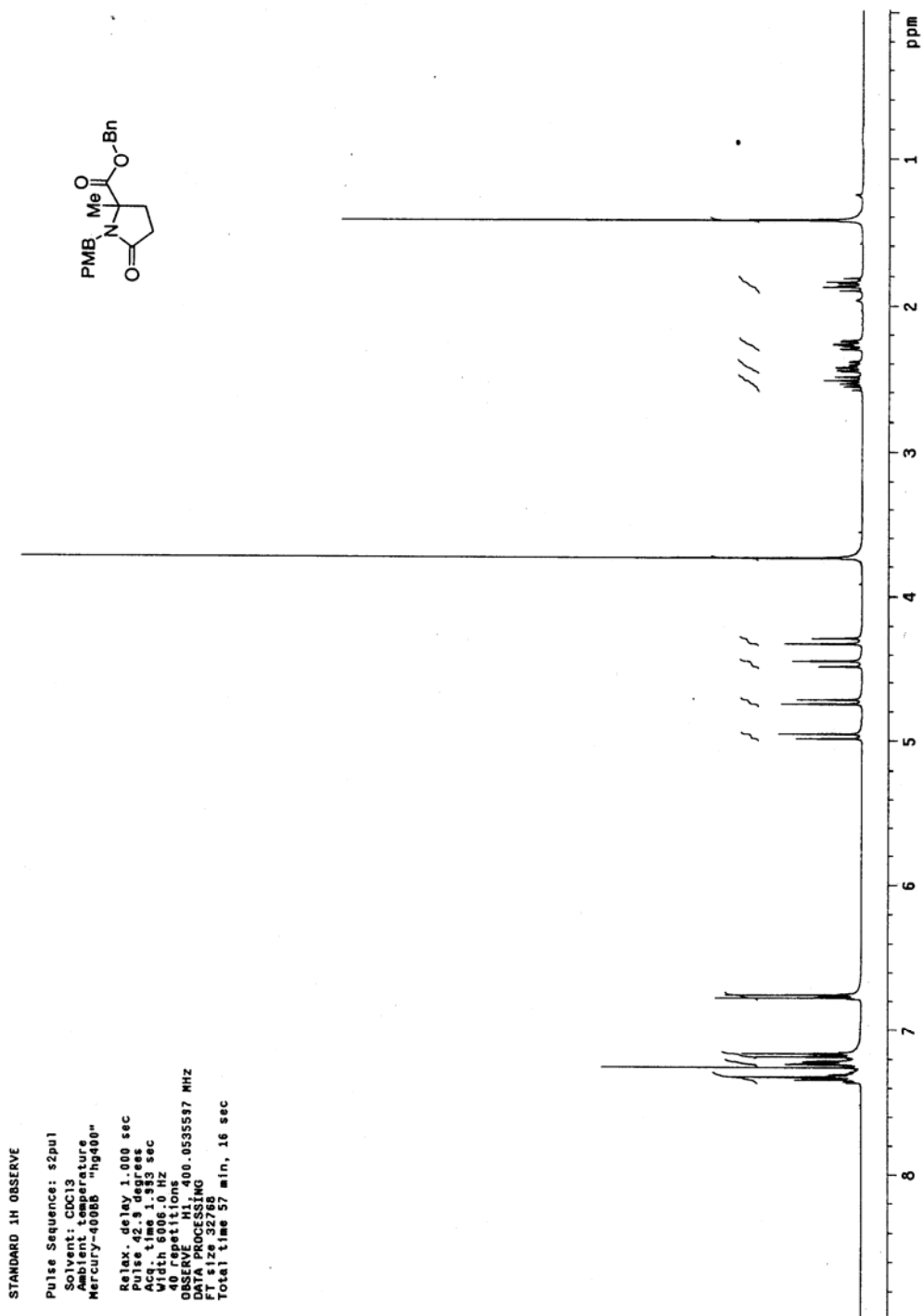
DATA PROCESSING

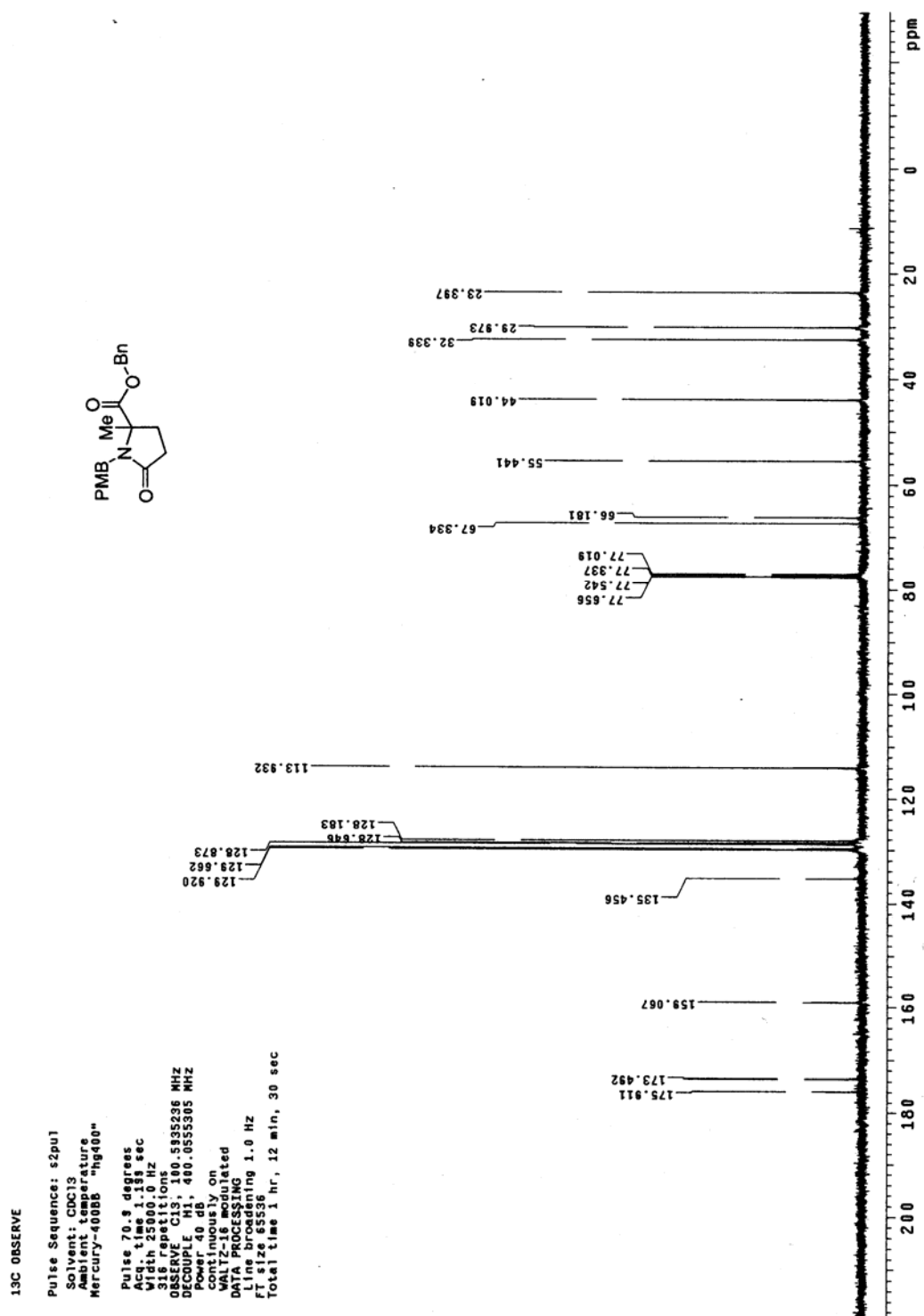
File processing 1.0 Hz

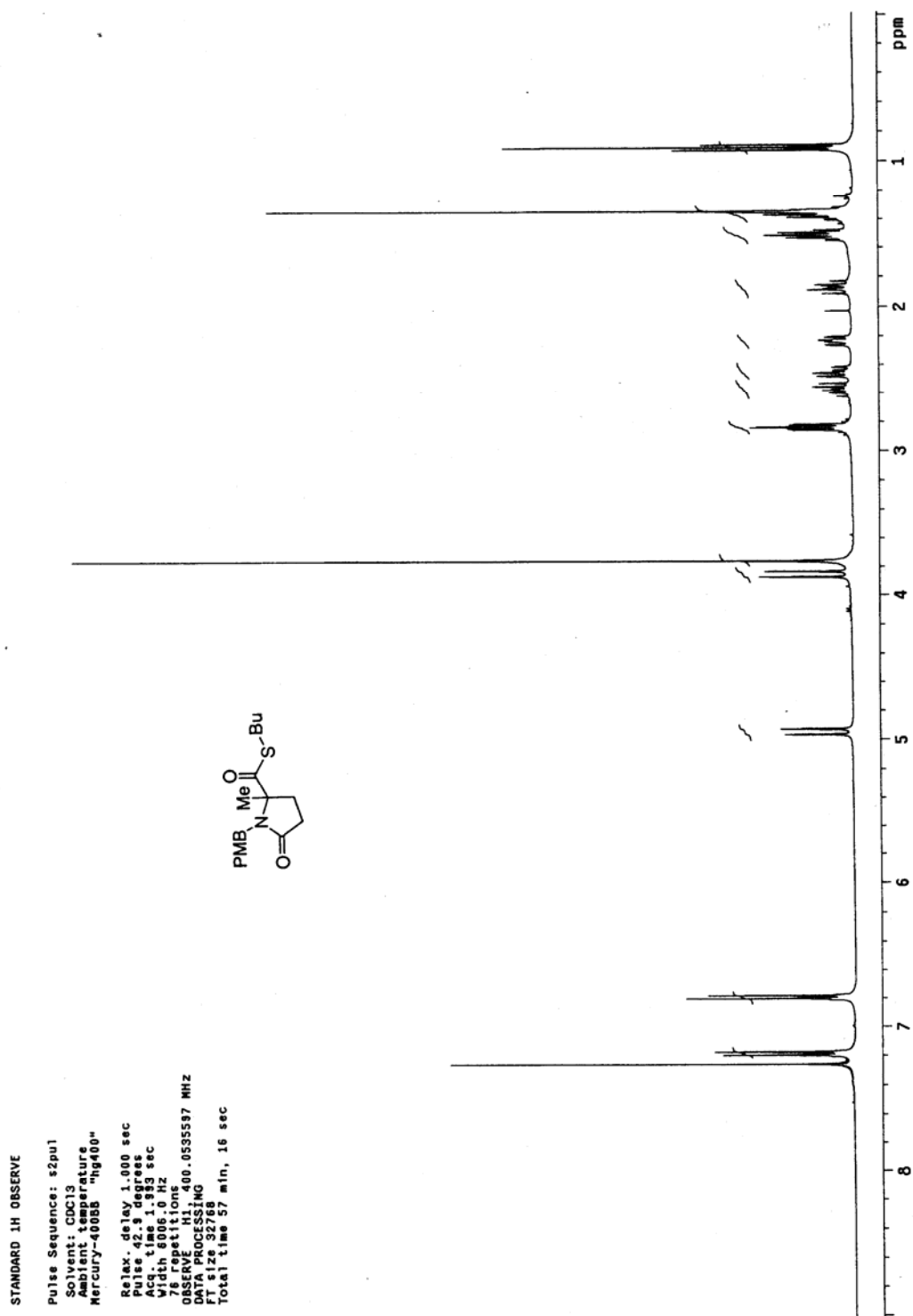
File size 17.353 Mb

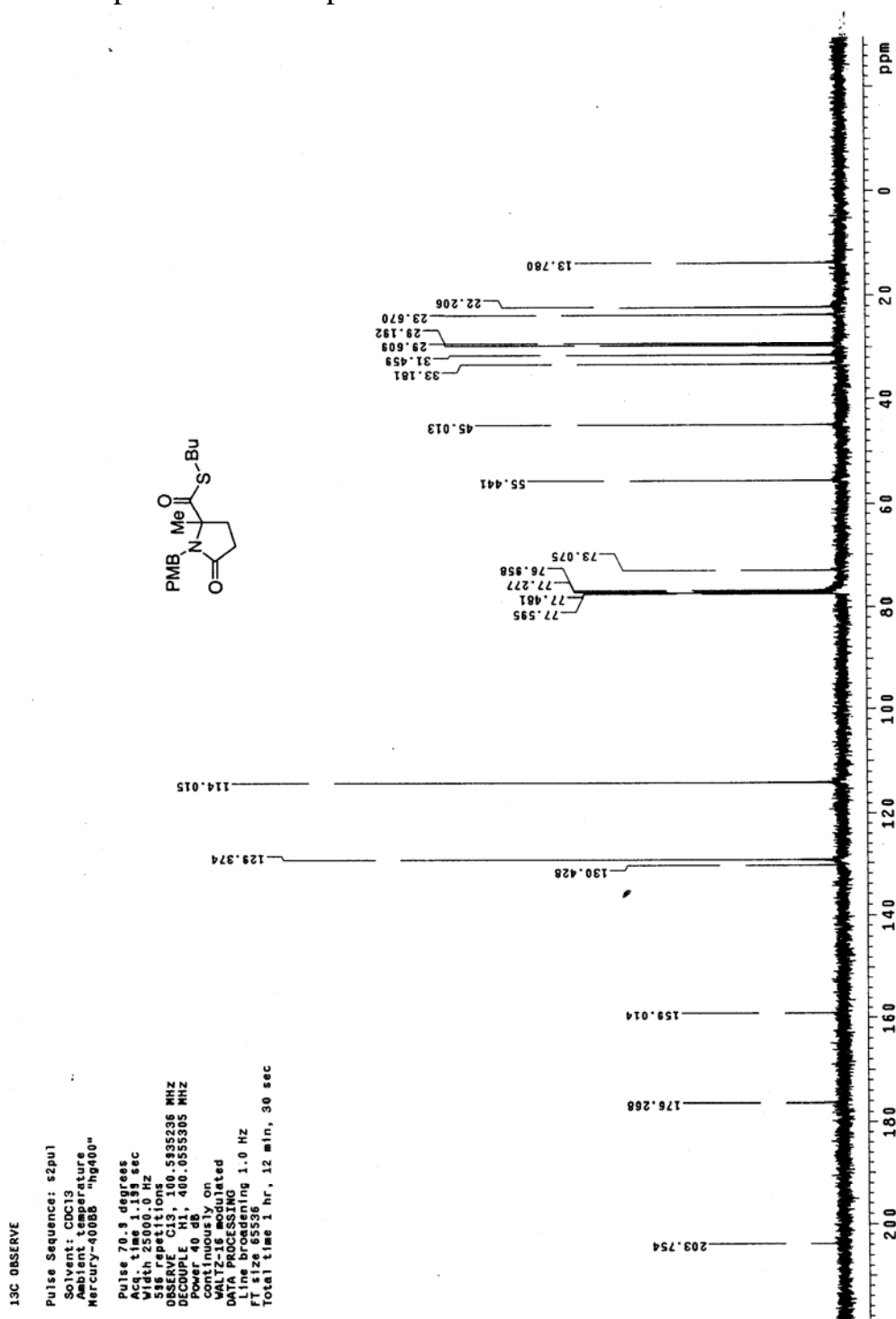
Total time 1 hr, 12 min, 30 sec

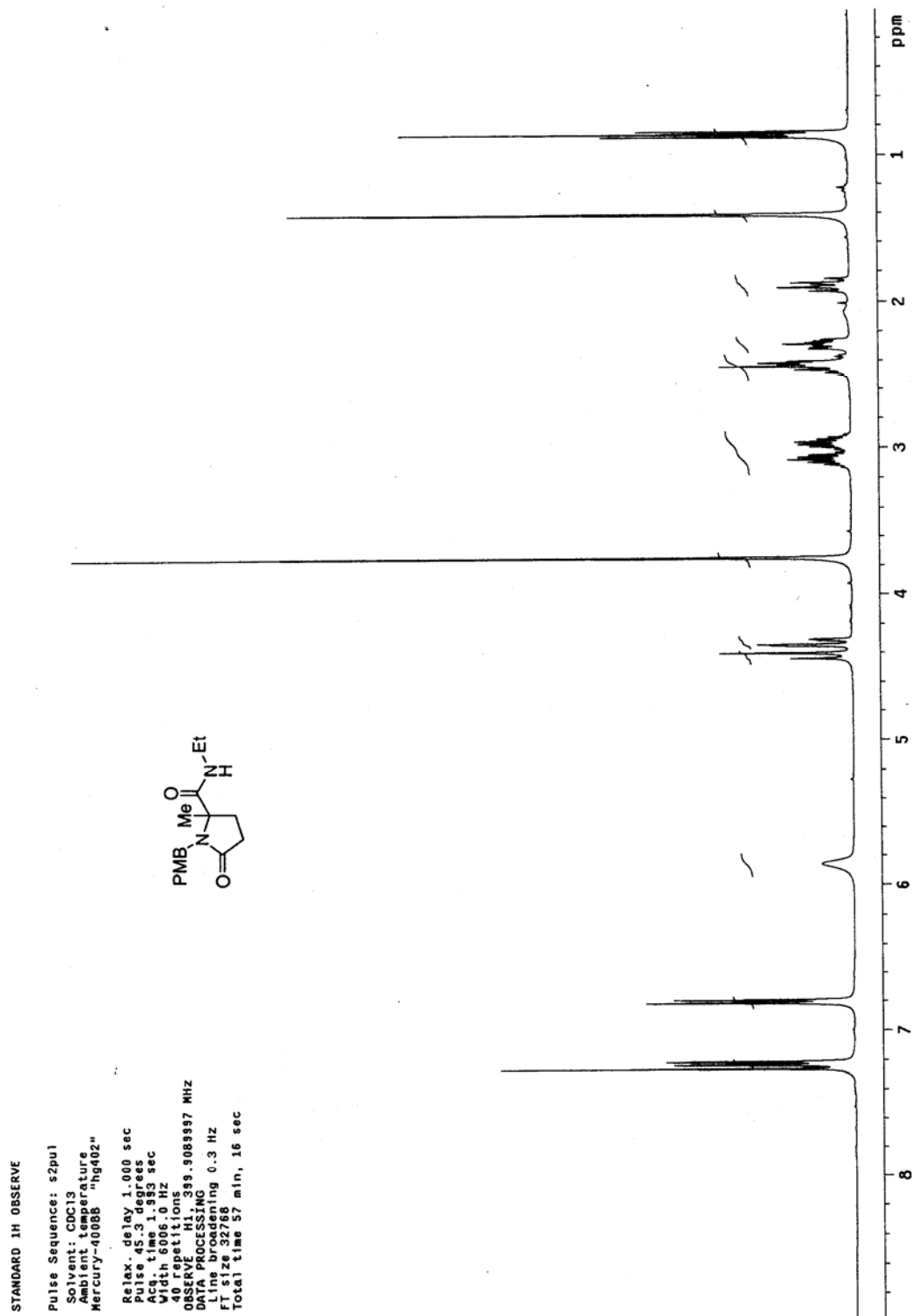


¹H NMR spectrum of compound **344c**

^{13}C NMR spectrum of compound **344c**

¹H NMR spectrum of compound 344d

¹³C NMR spectrum of compound 344d

¹H NMR spectrum of compound 344e

^{13}C NMR spectrum of compound **344e**

^{13}C OBSERVE

Pulse Sequence: s2pul

Solvent: CDCl₃

Ambient temperature

Mercury-40055 "hg400"

Pulse 70.3 degrees

Acq. time 1.189 sec

Width 25000.0 Hz

232 repetitions

OBSERVE C13, 100.582286 MHz

POWER 40 dB, 400.055555 MHz

continuously on

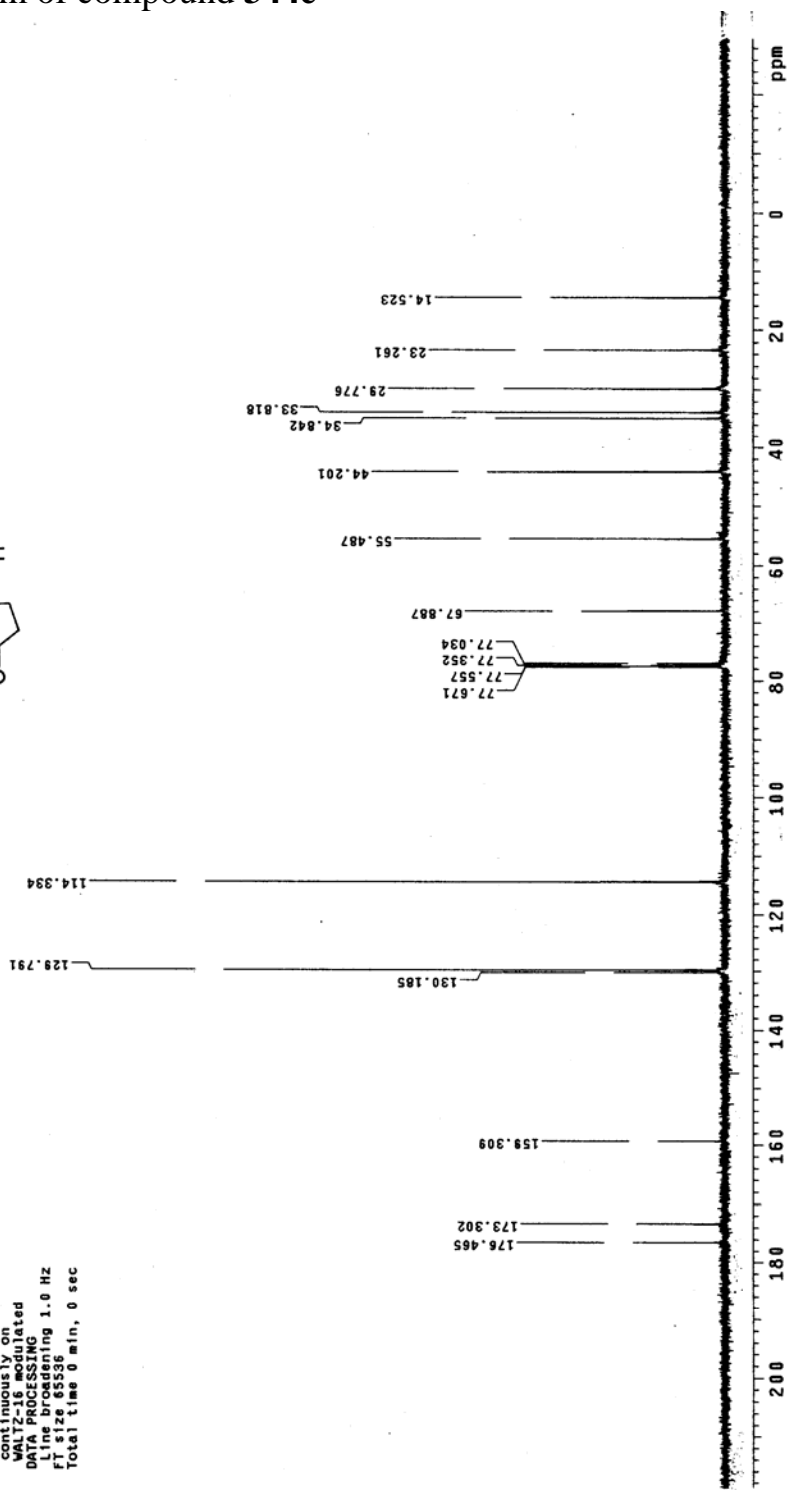
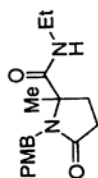
WALTZ-16 modulated

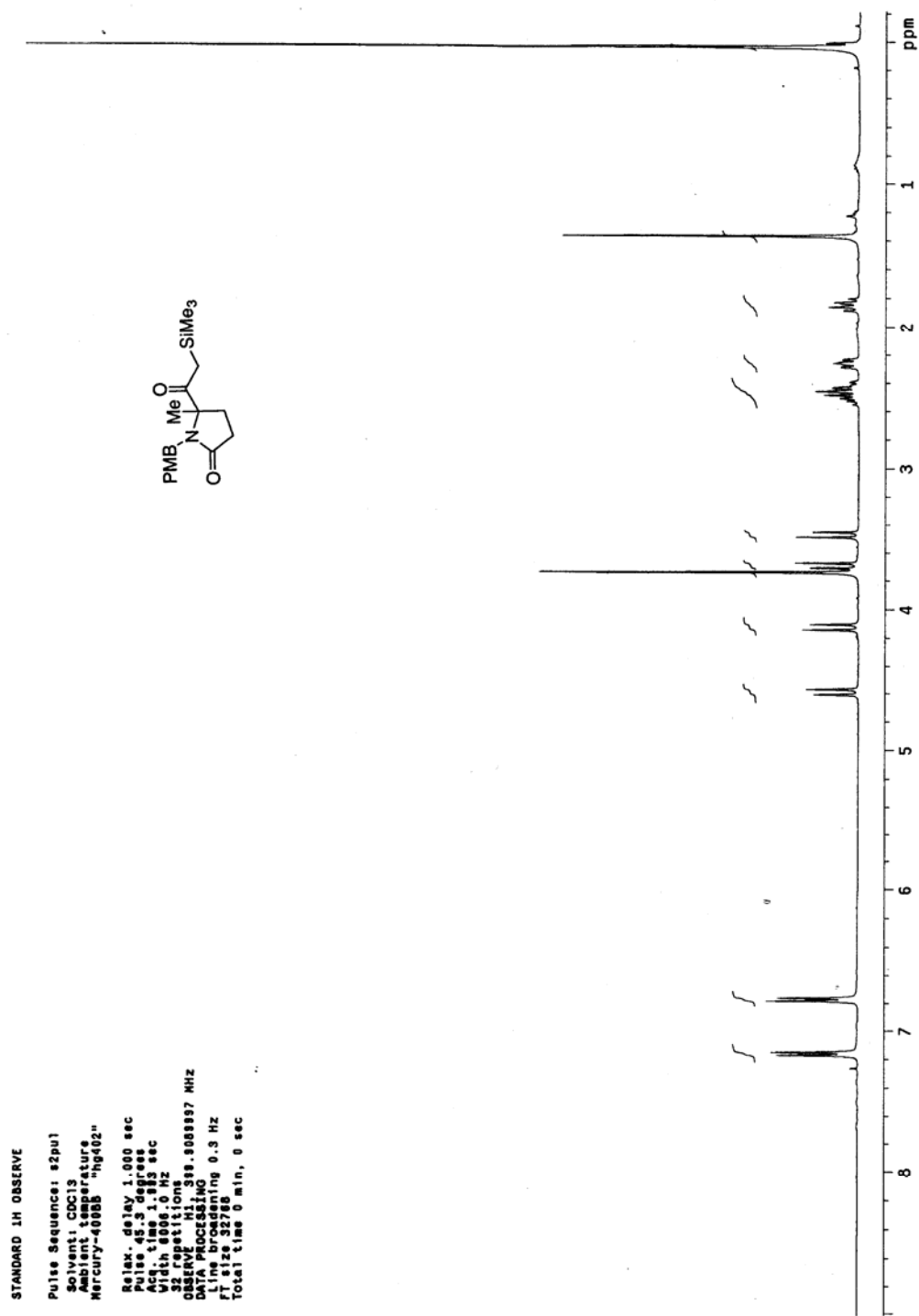
DATA PROCESSING

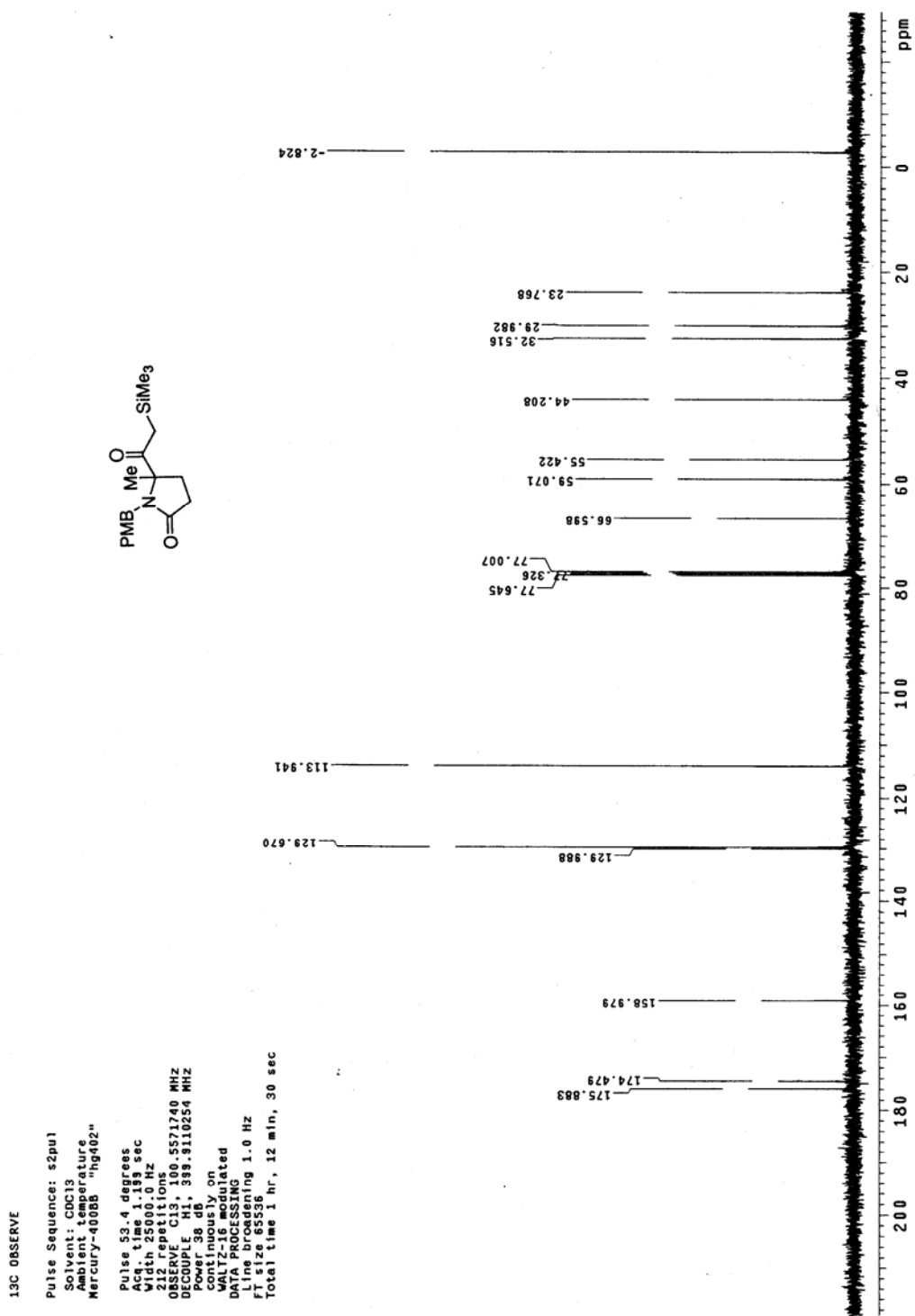
Line broadening 1.0 Hz

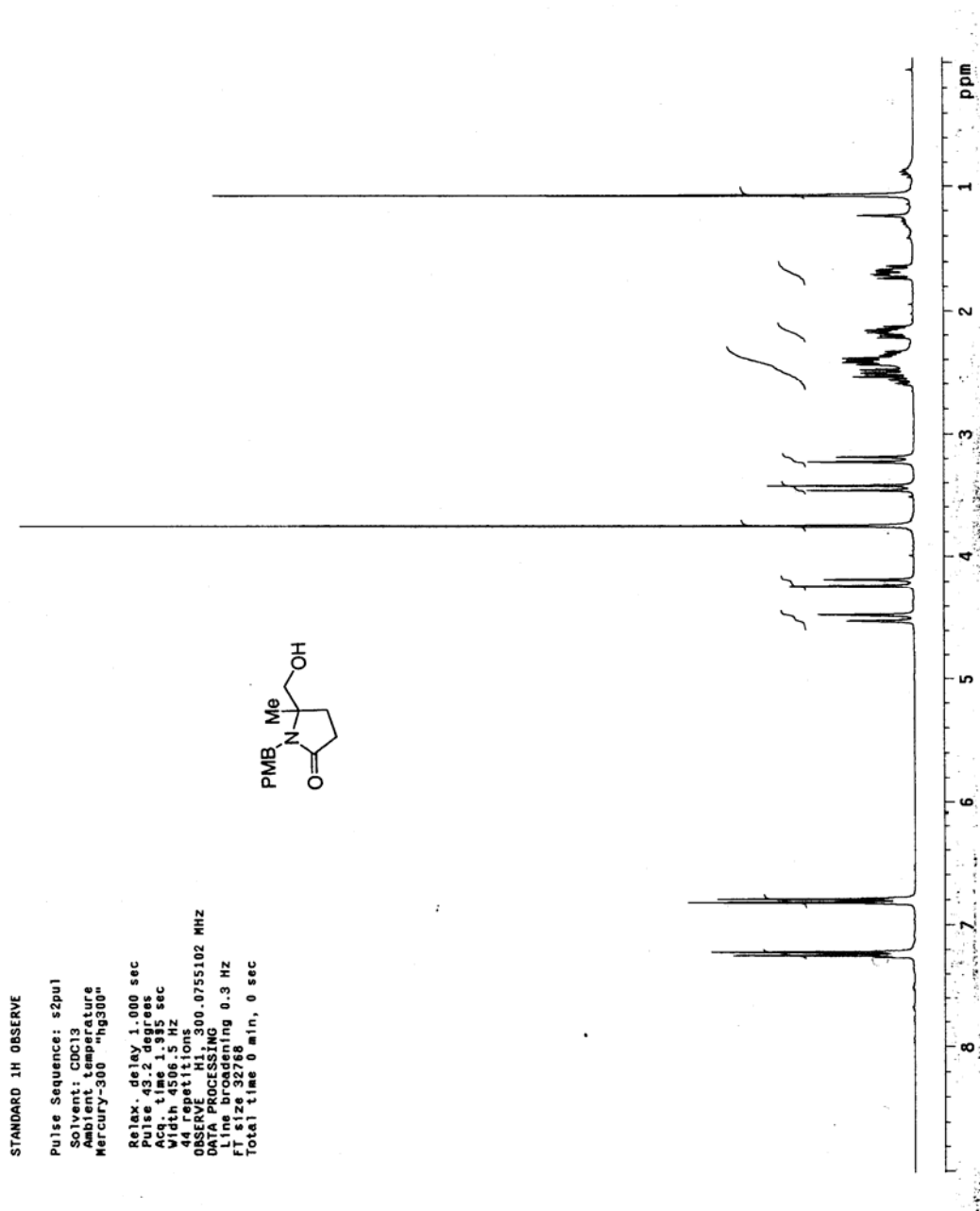
F1 size 32768

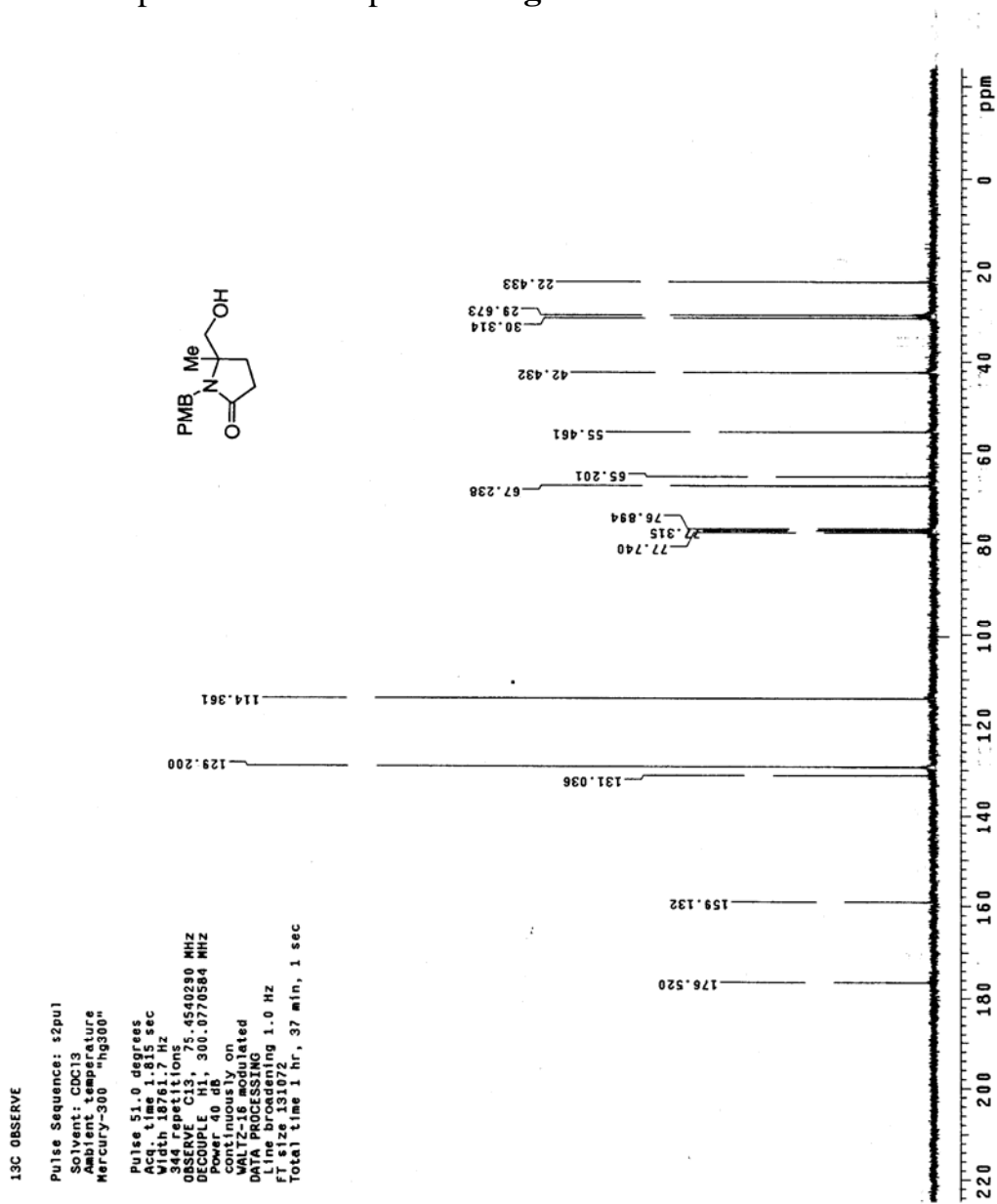
Total time 0 min, 0 sec



¹H NMR spectrum of compound 344f

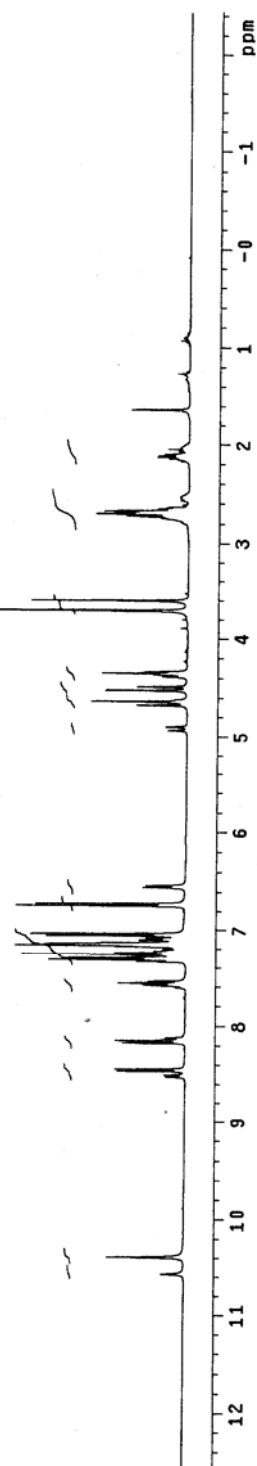
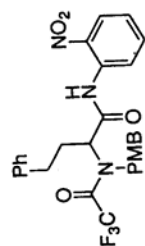
^{13}C NMR spectrum of compound 344f

¹H NMR spectrum of compound 344g

¹³C NMR spectrum of compound 344g

¹H NMR spectrum of compound 345

STANDARD 1H OBSERVE

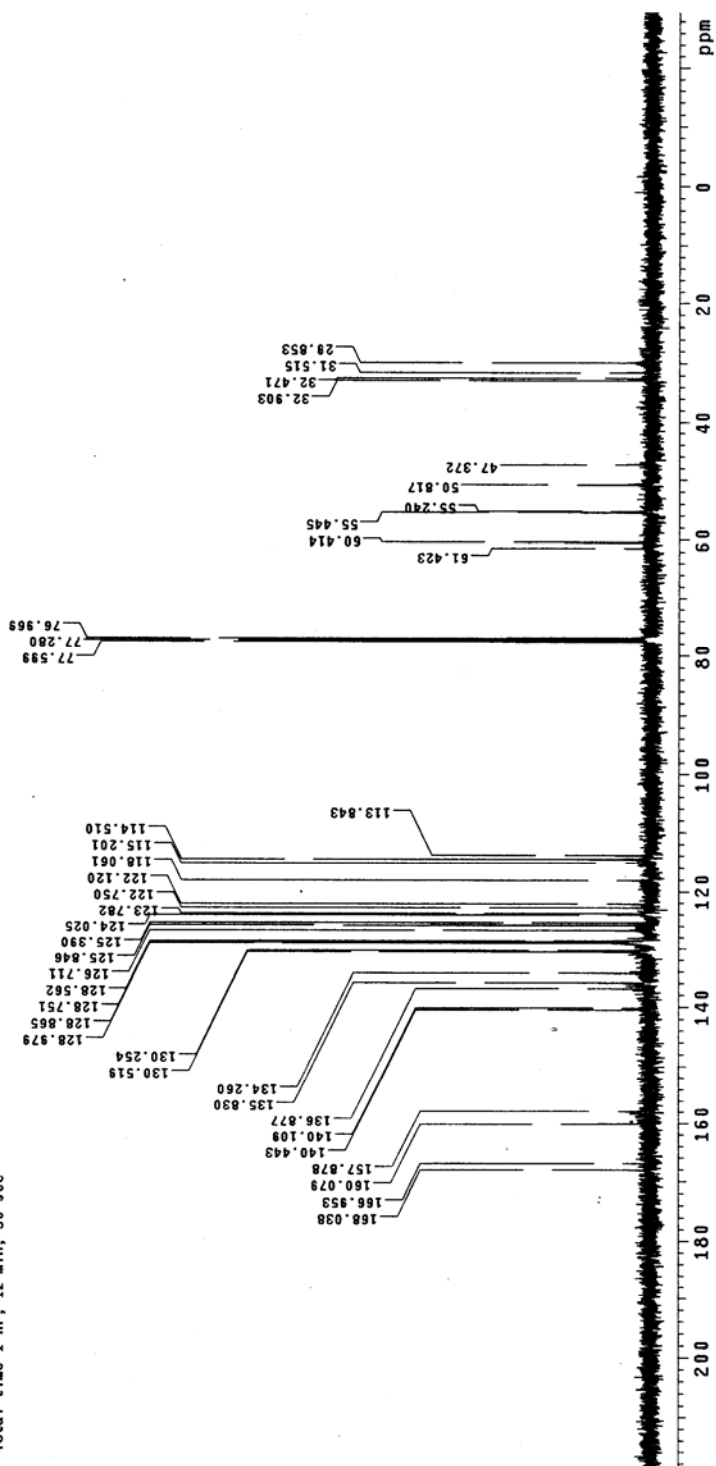
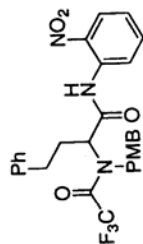
Pulse Sequence: s2pu1
Solvent: CDCl3
Temperature: 25.000000
Mercury-400SS "hg402"Relax. delay: 1.000 sec
Pulse: 45.3 degree
Acq. time: 1.993 sec
Width: 6006.0 Hz
40 repetitionsOBSERVE HI: 399.3089997 MHz
DATA PROCESSING
FT size: 32768
Averaging: 0.3 Hz
Total time: 0 min, 0 sec

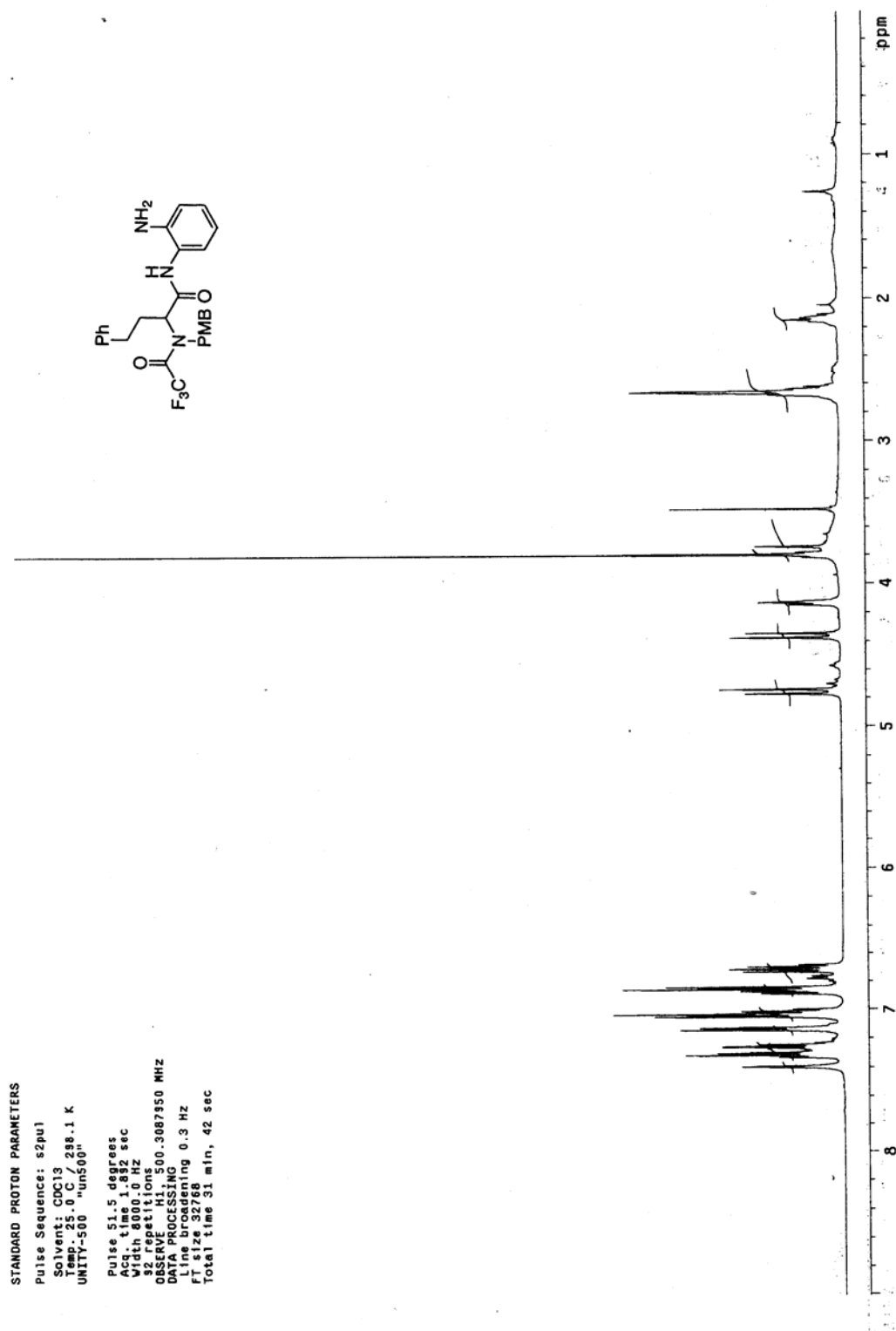
^{13}C NMR spectrum of compound **345**

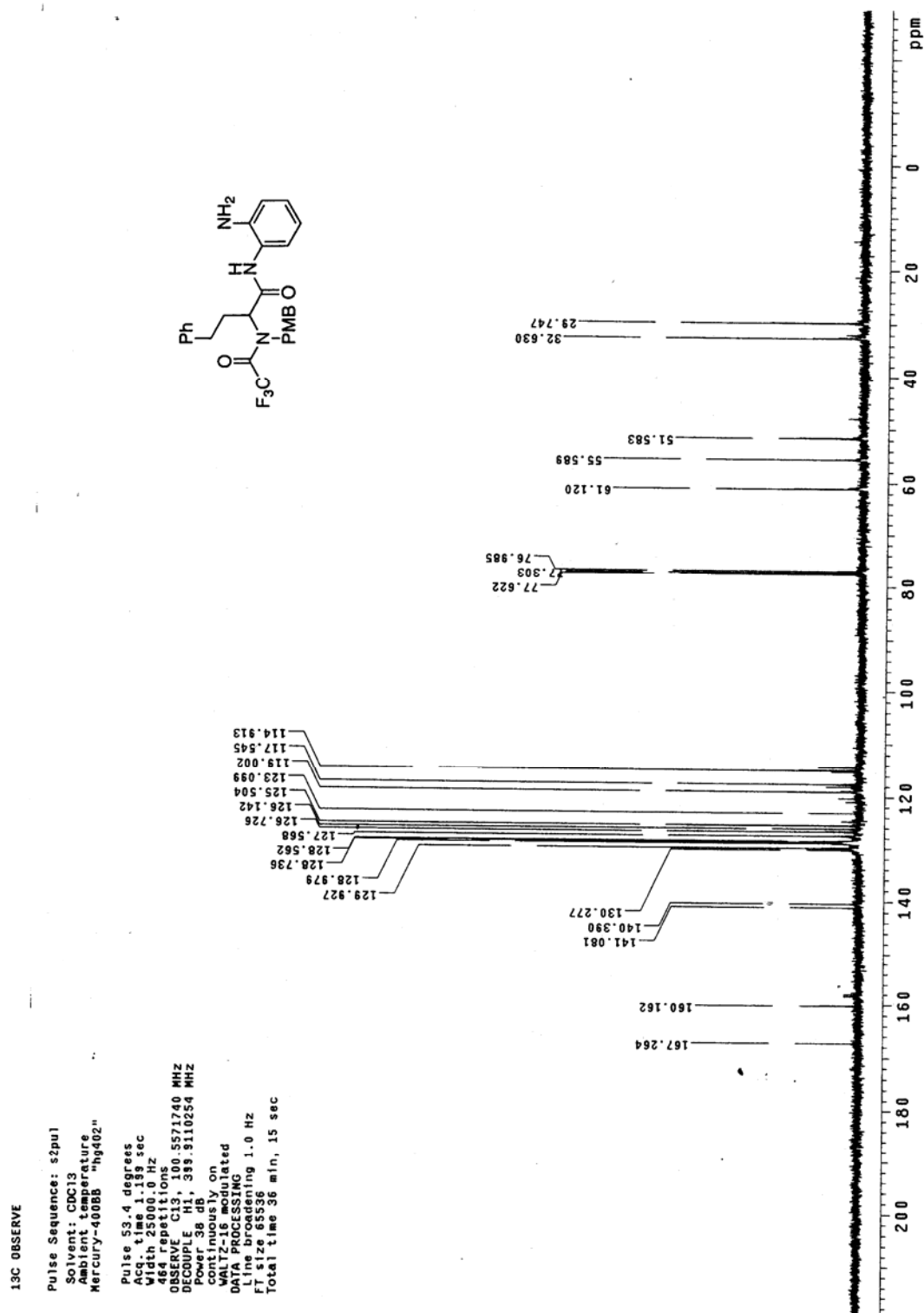
^{13}C OBSERVE

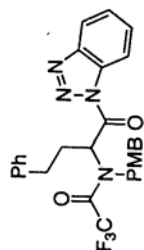
Pulse Sequence: s2pu1
 Solvent: CDCl3
 Ambient temperature
 Mercury-400BB "hg402"

Pulse 53.4 degrees
 Width 1.0000 sec
 Width 25000.0 Hz
 656 repetitions
 OBSERVE C13, 100.5571740 MHZ
 DECOUPLE H1, 399.3110254 MHZ
 Power 38 dB
 Continuously on
 Continuously on
 DATA PROCESSING
 Line broadening 1.0 Hz
 FT size 65536
 Total time 1 hr, 12 min, 30 sec



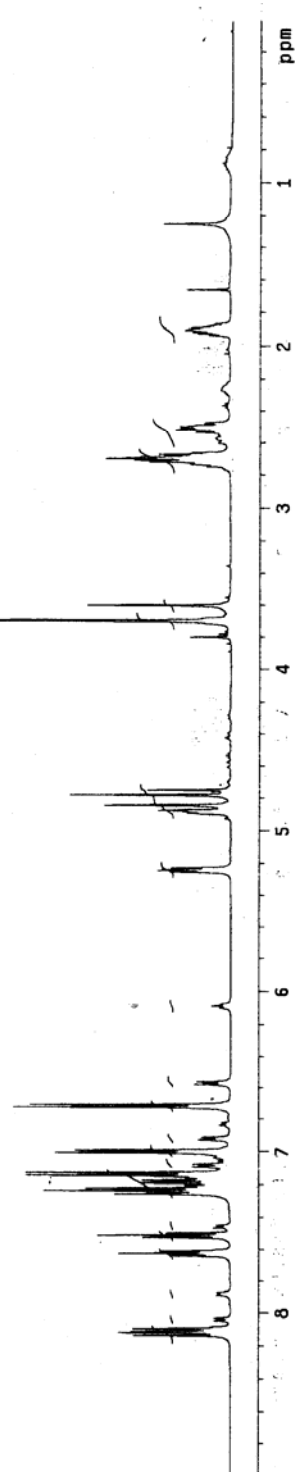
¹H NMR spectrum of compound 345a

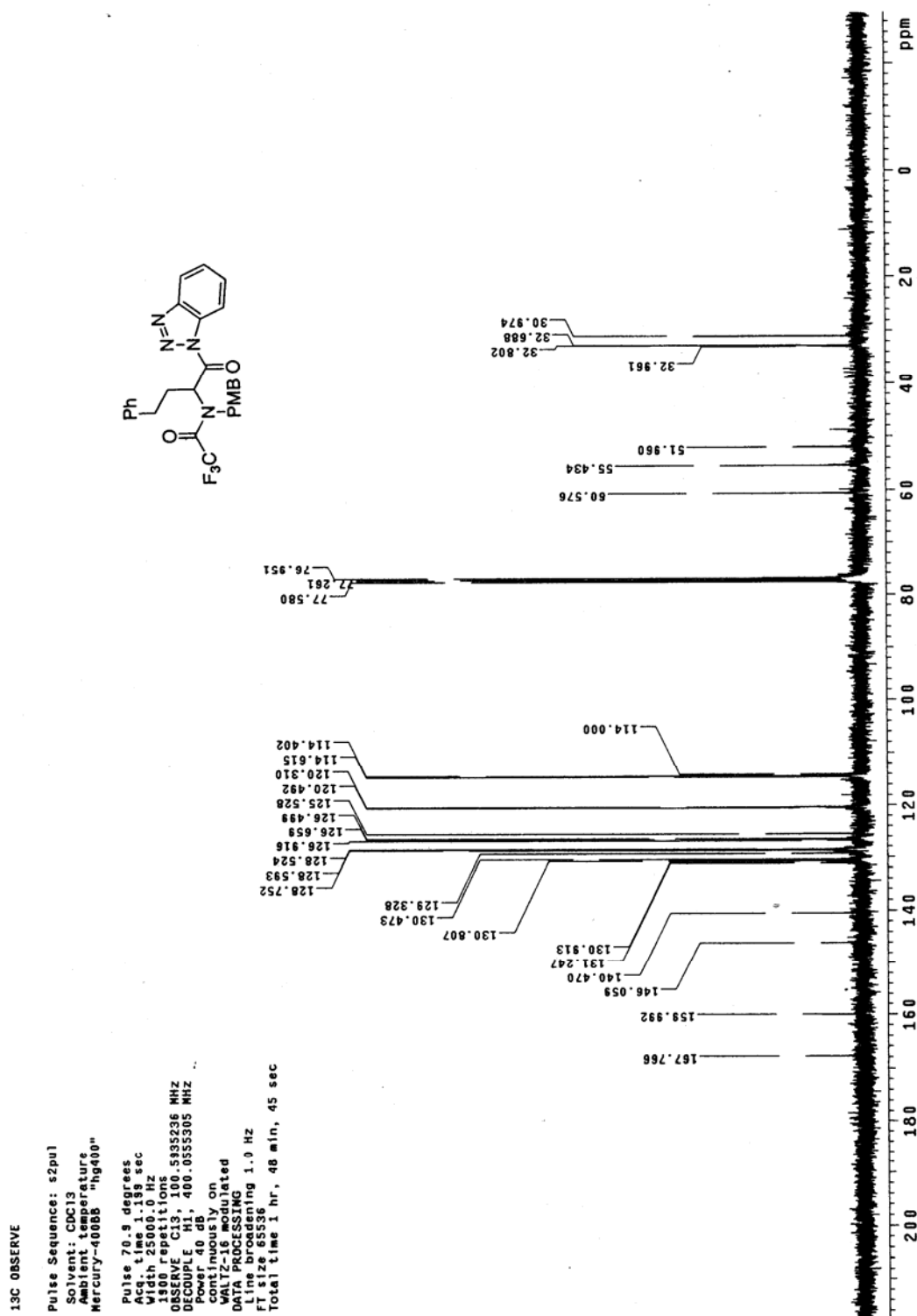
¹³C NMR spectrum of compound 345a

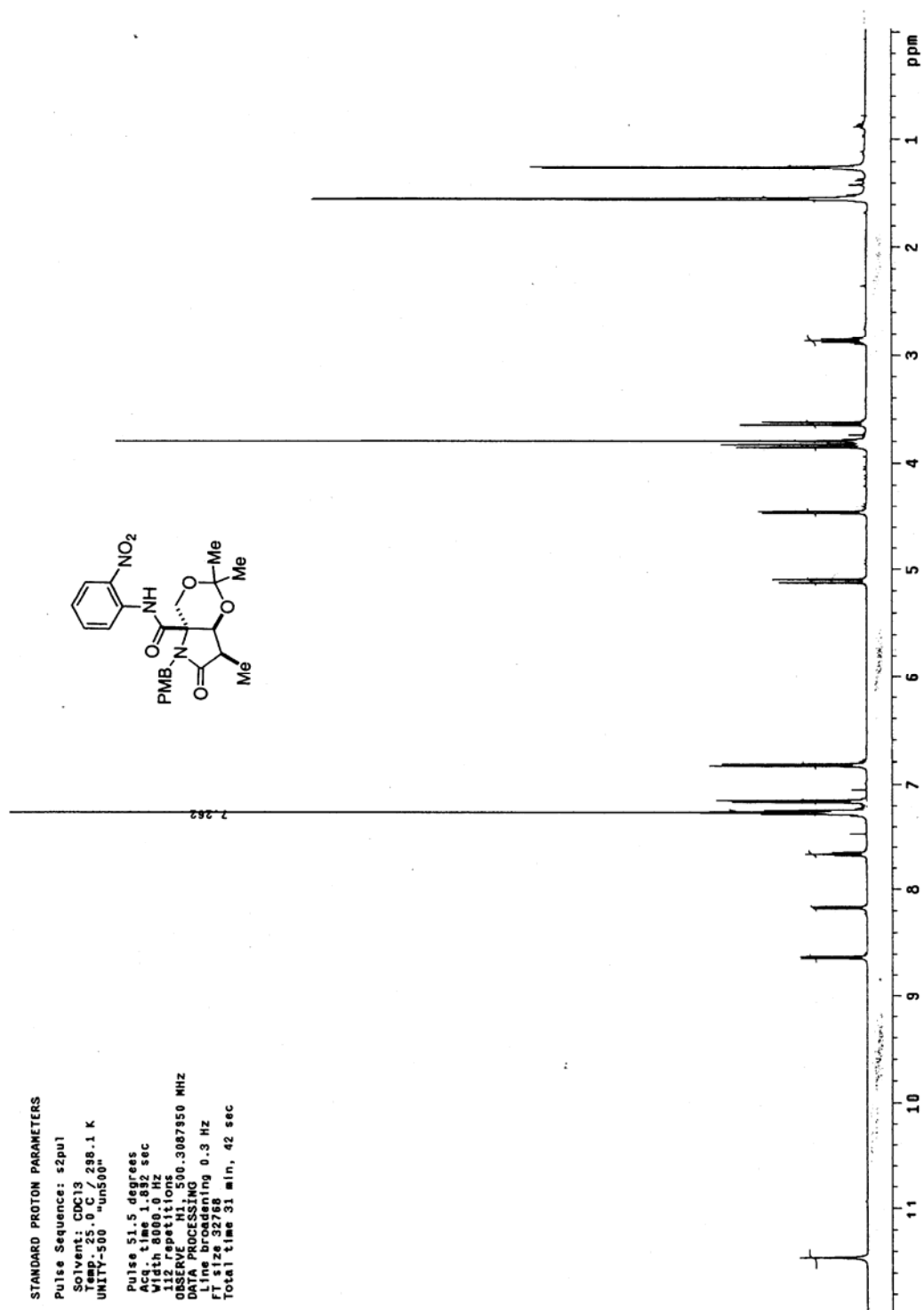
¹H NMR spectrum of compound 346

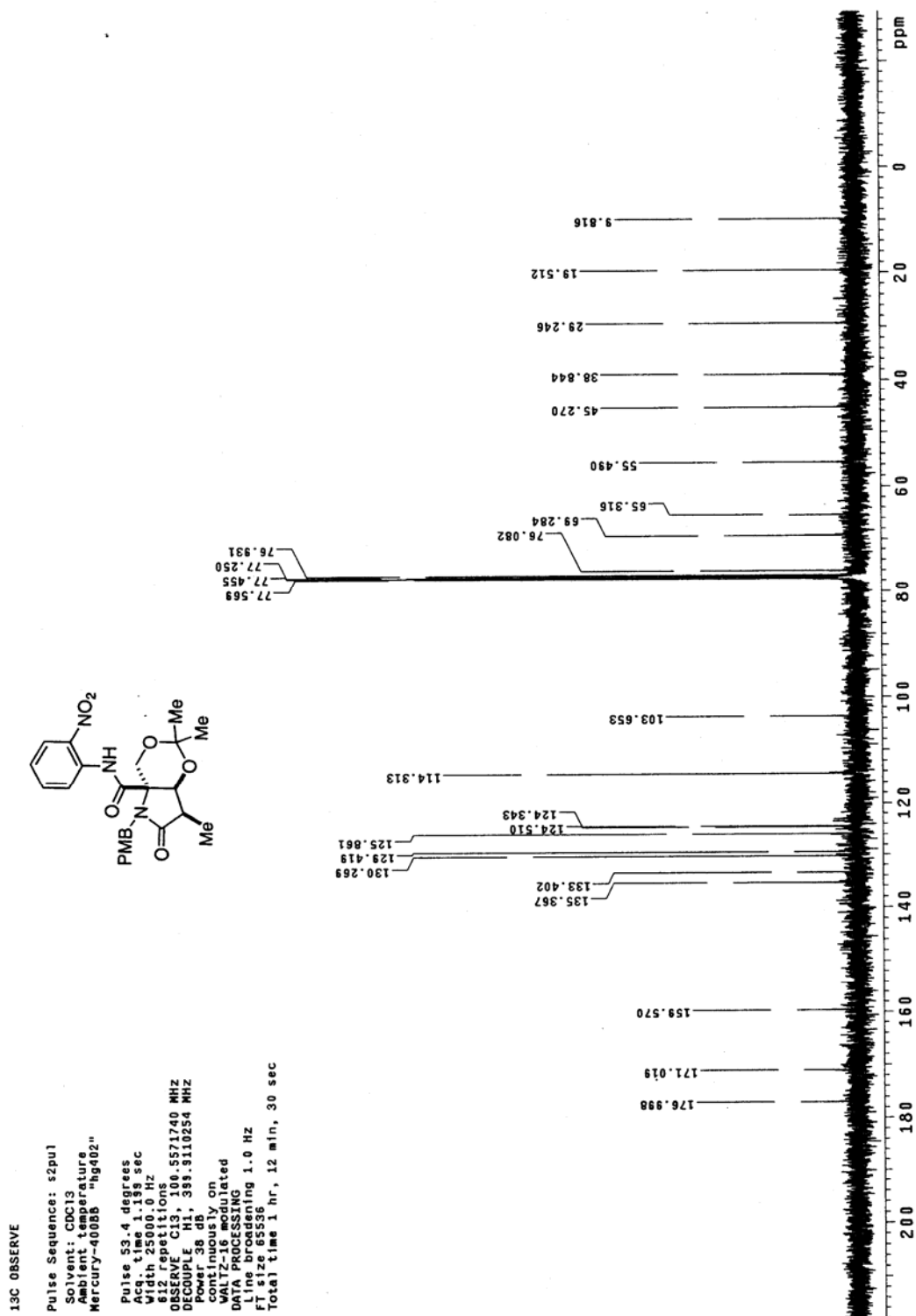
STANDARD PROTON PARAMETERS

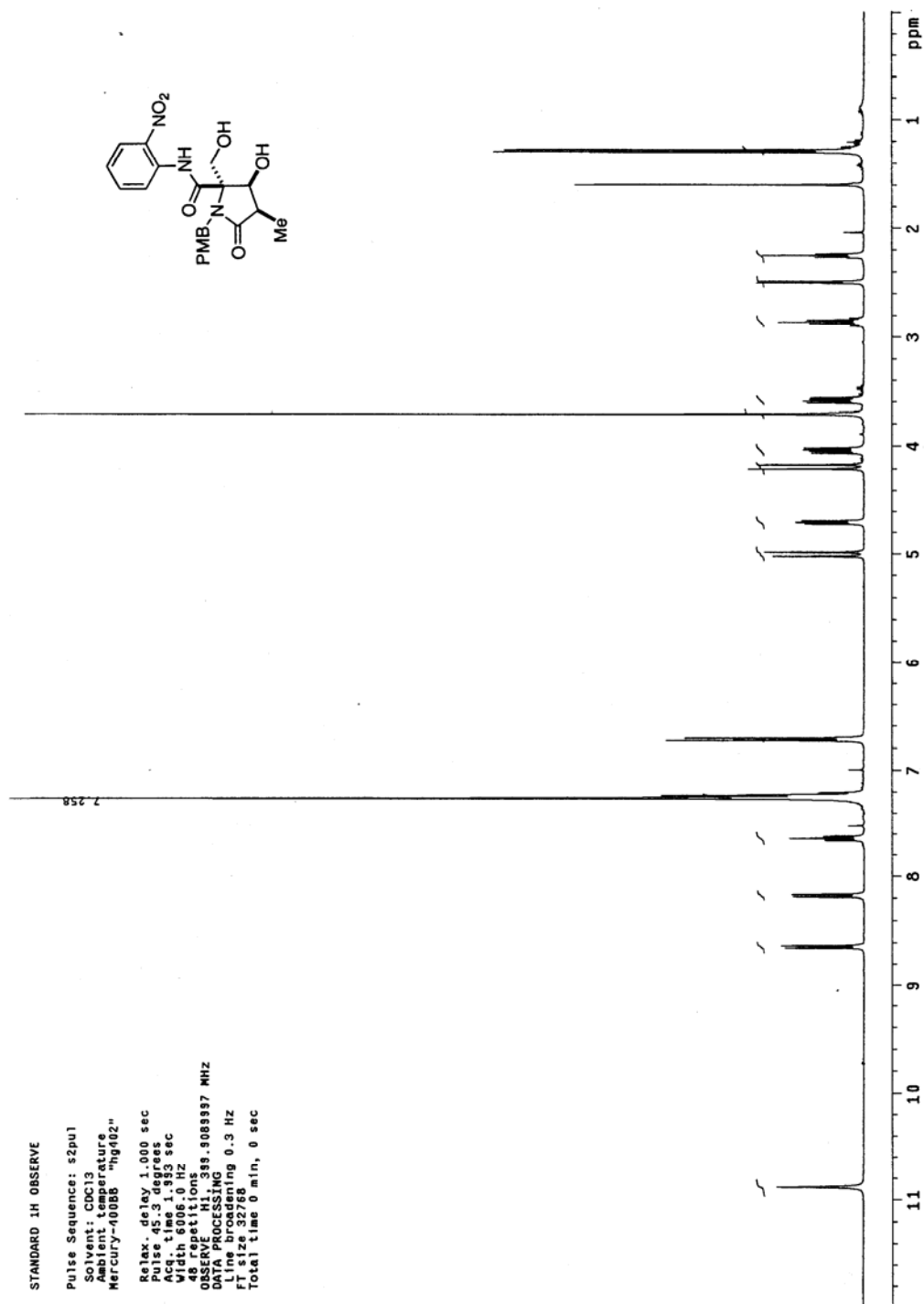
Pulse sequence: s2pu1
Solvent: CDCl3
Temp: 25.0 C / 298.1 K
UNITY-500 "un500"
Pulse 51.5 degrees
Acq. time 1.892 sec
Width 8000.0 Hz
OBSERVED F1: 500.136199 MHz
DATA PROCESSING 0.3 Hz
Line broadening 0.3 Hz
FT size 32768
Total time 31 min, 42 sec

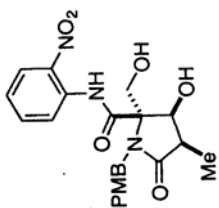


^{13}C NMR spectrum of compound 346

¹H NMR spectrum of compound **350**

¹³C NMR spectrum of compound 350

¹H NMR spectrum of compound **351**

^{13}C NMR spectrum of compound 351

^{13}C OBSERVE

Pulse Sequence: szpul

Solvent: CDCl₃

Ambient temperature

Mercury-400BB "hg402"

Pulse 53.4 degrees

Acq. time 1.19 sec

Width 25000.0 Hz

280 repetitions

OBSERVE C13, 100.5571740 MHz

DECOUPLE H1, 399.9110254 MHz

Power 38 dB

continuously on

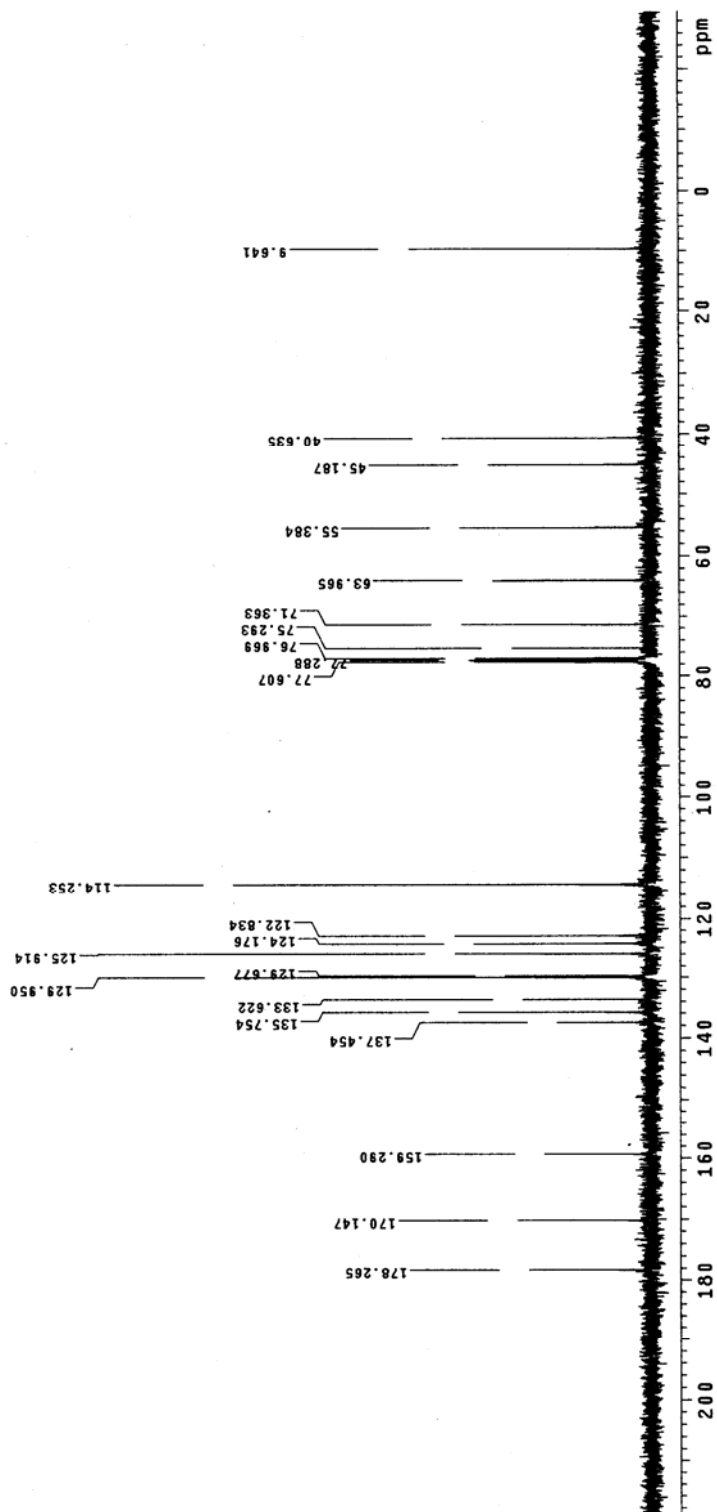
residuals listed

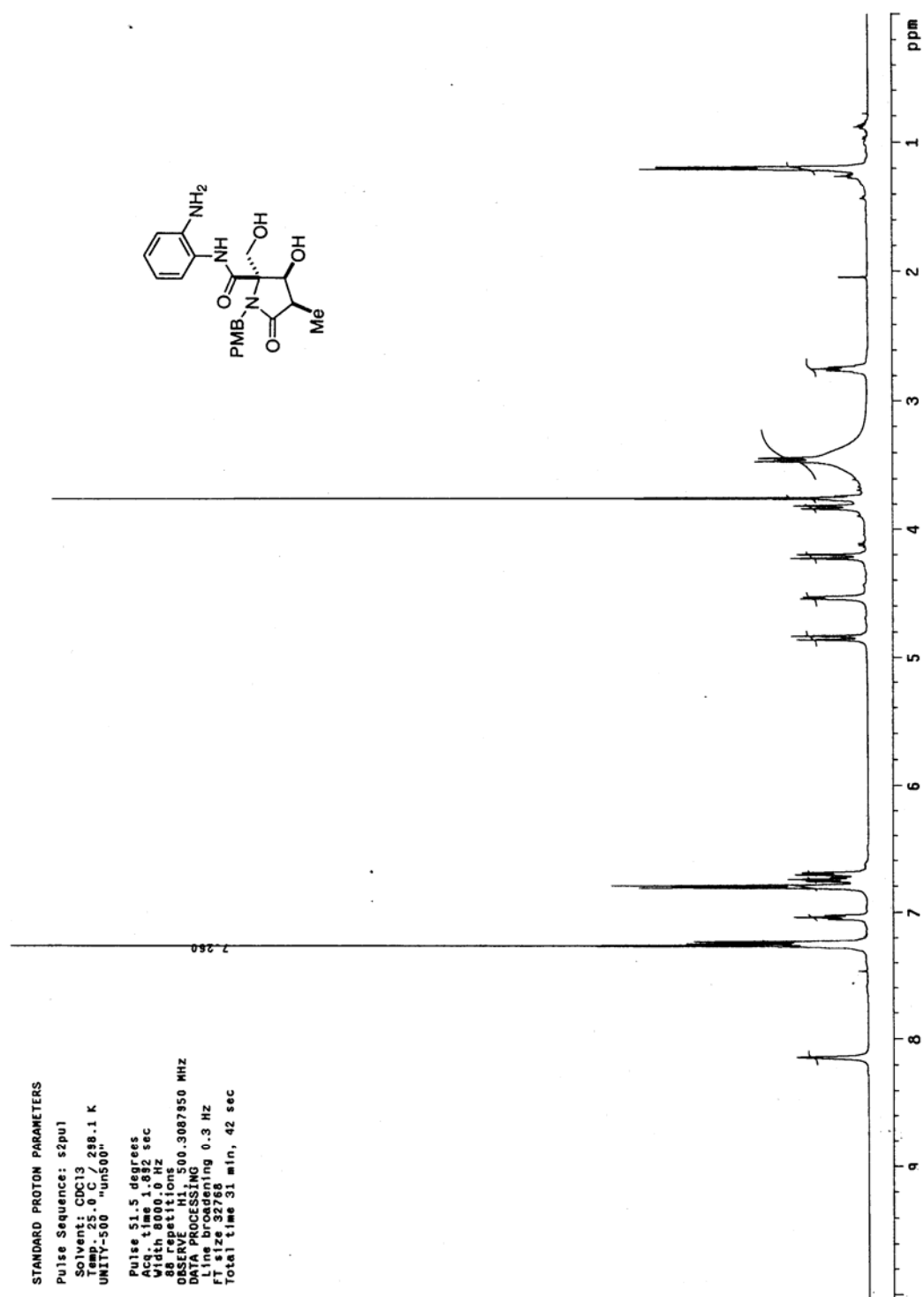
DATA PROCESSING

Line broadening 1.0 Hz

FT size 65536

Total time 1 hr, 12 min, 30 sec



¹H NMR spectrum of compound 352

^{13}C NMR spectrum of compound **352**

^{13}C OBSERVE

Pulse Sequence: s2pu1

Solvent: CDCl₃

Ambient temperature

Mercury-4008B "hg402"

Pulse 52.4 degrees

Acq. time 0.239 sec

1288 Freq 101.625 MHz

OBSERVE C13 100.5571740 MHz

DECOUPLE H1 399.5110254 MHz

Power 38 dB

continuously on

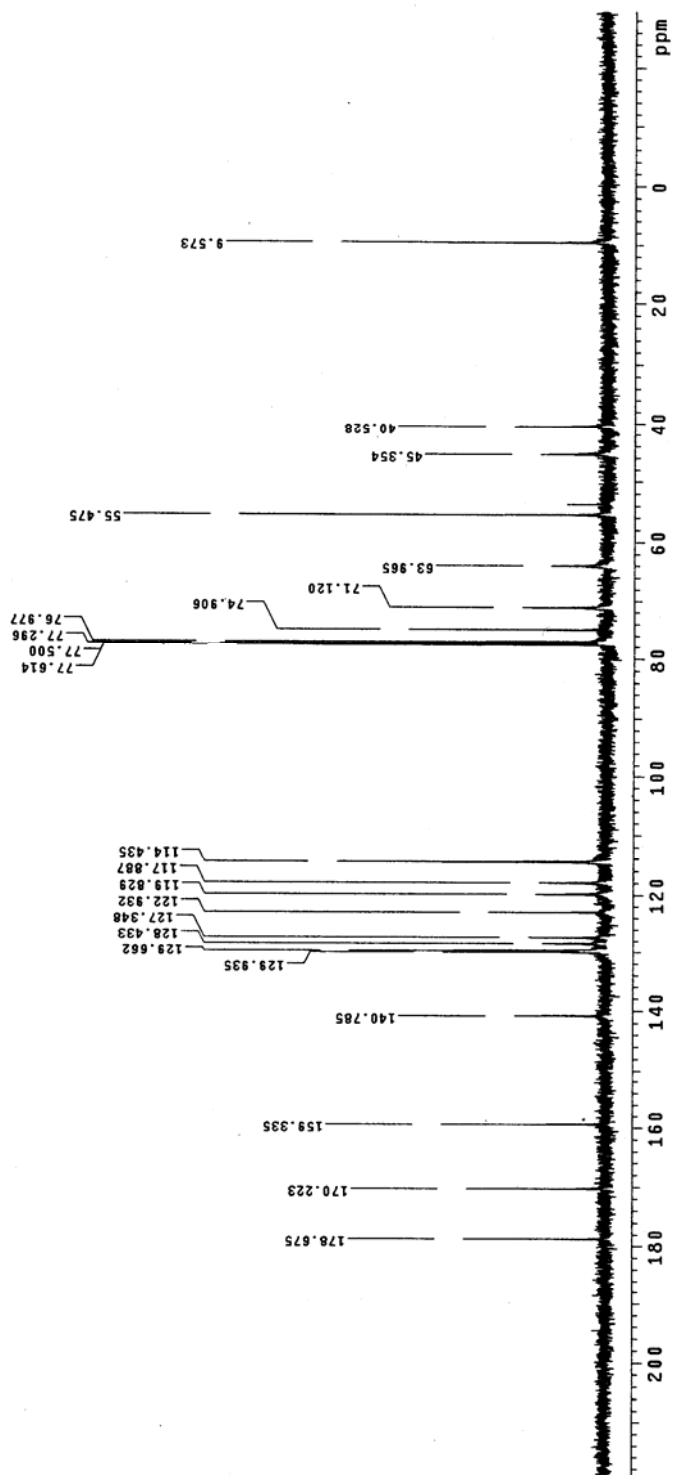
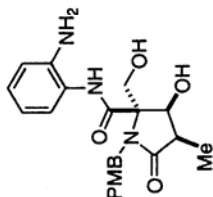
DW 17.16 modulated

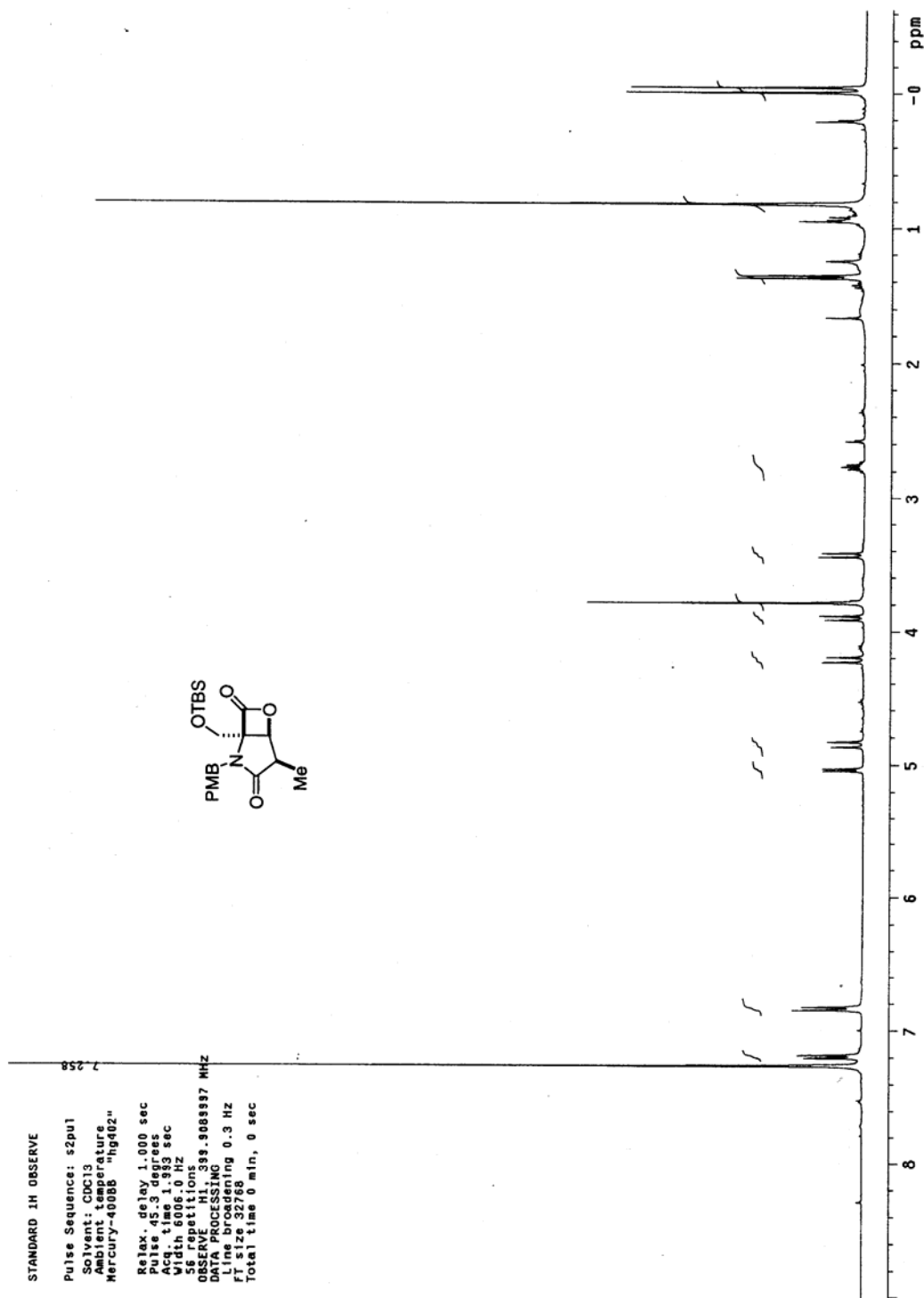
WALTZ16

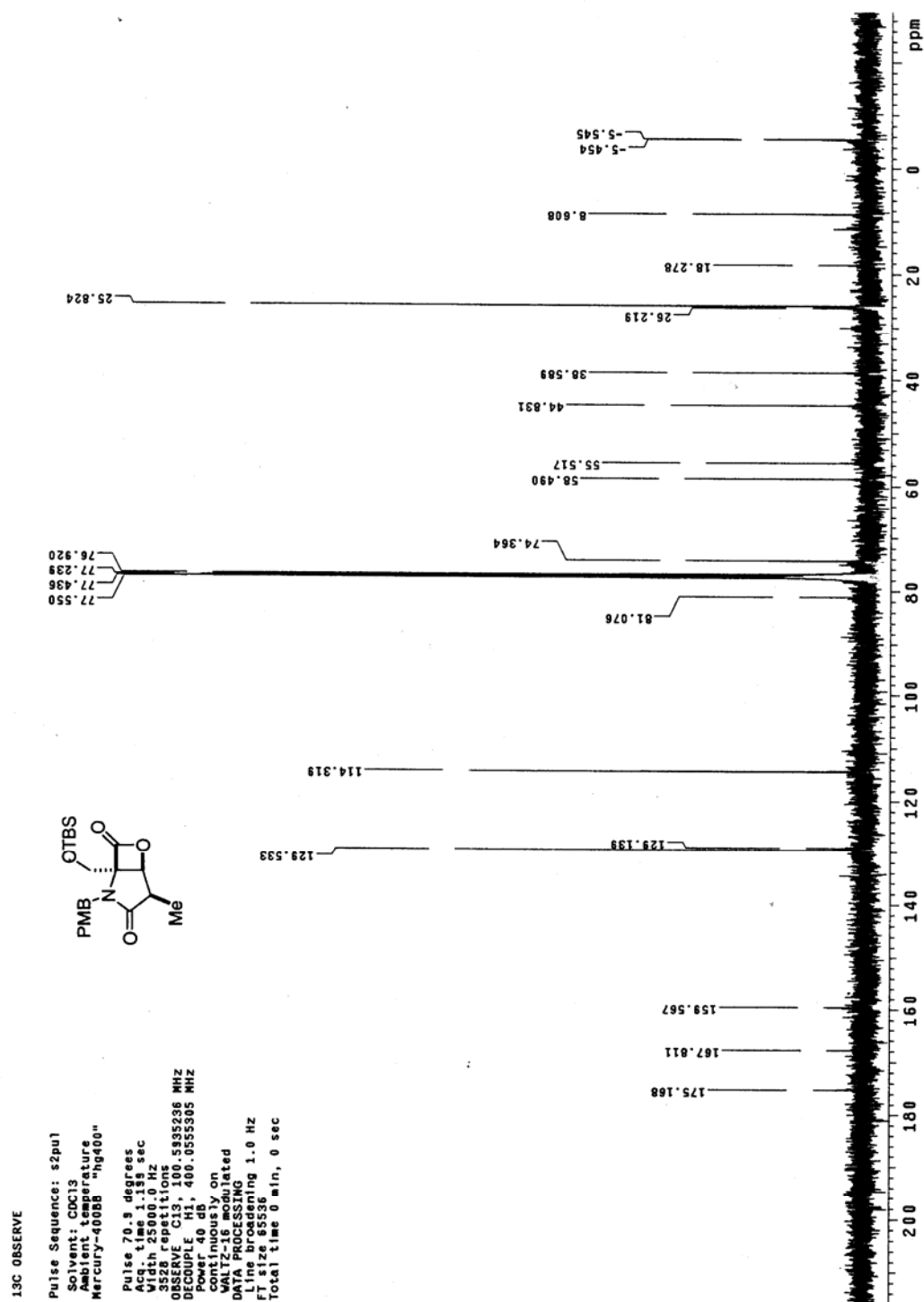
Line Prodigy 1.0 Hz

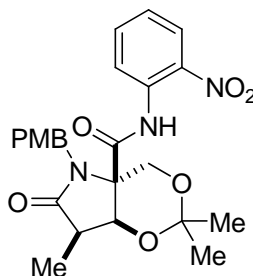
FT size 55536

Total time 1 hr, 12 min, 30 sec



¹H NMR spectrum of compound 354

¹³C NMR spectrum of compound 354

X-ray Crystal Structure Report for Ugi Adduct **350****350**

A colorless needle 0.12 x 0.08 x 0.04 mm in size was mounted on a Cryoloop with Paratone oil. Data were collected in a nitrogen gas stream at 100(2) K using phi and omega scans. Crystal-to-detector distance was 60 mm and exposure time was 30 seconds per frame using a scan width of 1.0°. Data collection was 97.4% complete to 67.00° in θ . A total of 10250 reflections were collected covering the indices, $-24 \leq h \leq 24$, $-9 \leq k \leq 9$, $-16 \leq l \leq 16$. 3817 reflections were found to be symmetry independent, with an R_{int} of 0.0609. Indexing and unit cell refinement indicated a C-centered, monoclinic lattice. The space group was found to be C2 (No. 5). The data were integrated using the Bruker SAINT software program and scaled using the SADABS software program. Solution by direct methods (SIR-2004) produced a complete heavy-atom phasing model consistent with the proposed structure. All non-hydrogen atoms were refined anisotropically by full-matrix least-squares (SHELXL-97). All hydrogen atoms were placed using a riding model. Their positions were constrained relative to their parent atom using the appropriate HFIX command in SHELXL-97.

Table 1. Crystal data and structure refinement for kob12.

X-ray ID	kob12	
Sample/notebook ID	KOB12	
Empirical formula	C ₂₄ H ₂₇ N ₃ O ₇	
Formula weight	469.49	
Temperature	100(2) K	
Wavelength	1.54178 Å	
Crystal system	Monoclinic	
Space group	C2	
Unit cell dimensions	a = 20.5404(13) Å	α = 90°.
	b = 7.9786(5) Å	β = 105.377(5)°.
	c = 14.1152(10) Å	γ = 90°.
Volume	2230.4(3) Å ³	
Z	4	
Density (calculated)	1.398 Mg/m ³	
Absorption coefficient	0.865 mm ⁻¹	
F(000)	992	
Crystal size	0.12 x 0.08 x 0.04 mm ³	
Crystal color/habit	colorless needle	
Theta range for data collection	4.46 to 68.18°.	
Index ranges	-24 ≤ h ≤ 24, -9 ≤ k ≤ 9, -16 ≤ l ≤ 16	
Reflections collected	10250	
Independent reflections	3817 [R(int) = 0.0609]	
Completeness to theta = 67.00°	97.4 %	
Absorption correction	Semi-empirical from equivalents	
Max. and min. transmission	0.9662 and 0.9033	
Refinement method	Full-matrix least-squares on F ²	
Data / restraints / parameters	3817 / 1 / 324	
Goodness-of-fit on F ²	1.021	
Final R indices [I > 2σ(I)]	R1 = 0.0490, wR2 = 0.1034	
R indices (all data)	R1 = 0.0693, wR2 = 0.1145	
Absolute structure parameter	-0.2(3)	
Largest diff. peak and hole	0.282 and -0.303 e.Å ⁻³	

Table 2. Atomic coordinates ($\times 10^4$) and equivalent isotropic displacement parameters ($\text{\AA}^2 \times 10^3$) for kob12. $U(\text{eq})$ is defined as one third of the trace of the orthogonalized U^{ij} tensor.

	x	y	z	$U(\text{eq})$
C(1)	7914(2)	7936(4)	5776(3)	24(1)
C(2)	7345(2)	7962(4)	6283(3)	23(1)
C(3)	7613(2)	6626(4)	7070(2)	20(1)
C(4)	8385(2)	6793(4)	7325(2)	21(1)
C(5)	9097(2)	6930(4)	6074(3)	25(1)
C(6)	9363(2)	5148(4)	6090(2)	23(1)
C(7)	10049(2)	4864(4)	6285(2)	24(1)
C(8)	10314(2)	3262(4)	6296(3)	25(1)
C(9)	9875(2)	1909(4)	6142(2)	22(1)
C(10)	9182(2)	2157(4)	5949(2)	22(1)
C(11)	8931(2)	3771(4)	5904(2)	22(1)
C(12)	10781(2)	-55(4)	6289(3)	28(1)
C(13)	7196(2)	9702(4)	6624(3)	29(1)
C(14)	7633(2)	5174(4)	8509(3)	24(1)
C(15)	7511(2)	5533(5)	9501(3)	35(1)
C(16)	7294(2)	3541(4)	8070(3)	28(1)
C(17)	8636(2)	5135(4)	7861(2)	21(1)
C(18)	8684(2)	8384(4)	7941(2)	20(1)
C(19)	9053(2)	9471(4)	9650(2)	21(1)
C(20)	8979(2)	11167(4)	9429(3)	23(1)
C(21)	9184(2)	12370(4)	10155(3)	27(1)
C(22)	9475(2)	11920(5)	11124(3)	28(1)
C(23)	9559(2)	10258(4)	11368(2)	23(1)
C(24)	9352(2)	9055(4)	10645(3)	23(1)
N(1)	8456(1)	7027(3)	6332(2)	20(1)
N(2)	8821(2)	8210(3)	8942(2)	24(1)
N(3)	9467(2)	7329(4)	10971(3)	45(1)
O(1)	10079(1)	260(3)	6165(2)	26(1)
O(2)	7893(1)	8586(3)	4981(2)	31(1)
O(3)	7369(1)	6619(3)	7913(2)	23(1)

O(4)	8352(1)	5074(3)	8691(2)	23(1)
O(5)	8788(1)	9642(3)	7530(2)	28(1)
O(6)	9837(10)	7050(30)	11737(19)	44(3)
O(6A)	9612(10)	6850(30)	11768(19)	44(3)
O(7)	8977(3)	6277(6)	10611(4)	31(1)
O(7A)	9714(3)	6369(6)	10297(4)	33(1)

Table 3. Bond lengths [\AA] and angles [$^\circ$] for kob12.

C(1)-O(2)	1.226(4)	C(13)-H(13C)	0.9800
C(1)-N(1)	1.384(4)	C(14)-O(4)	1.433(4)
C(1)-C(2)	1.524(5)	C(14)-O(3)	1.445(4)
C(2)-C(13)	1.527(5)	C(14)-C(15)	1.514(5)
C(2)-C(3)	1.532(4)	C(14)-C(16)	1.528(5)
C(2)-H(2)	1.0000	C(15)-H(15A)	0.9800
C(3)-O(3)	1.408(4)	C(15)-H(15B)	0.9800
C(3)-C(4)	1.535(4)	C(15)-H(15C)	0.9800
C(3)-H(3)	1.0000	C(16)-H(16A)	0.9800
C(4)-N(1)	1.460(4)	C(16)-H(16B)	0.9800
C(4)-C(17)	1.543(4)	C(16)-H(16C)	0.9800
C(4)-C(18)	1.569(4)	C(17)-O(4)	1.442(4)
C(5)-N(1)	1.459(4)	C(17)-H(17A)	0.9900
C(5)-C(6)	1.521(5)	C(17)-H(17B)	0.9900
C(5)-H(5A)	0.9900	C(18)-O(5)	1.206(4)
C(5)-H(5B)	0.9900	C(18)-N(2)	1.374(4)
C(6)-C(7)	1.382(5)	C(19)-C(20)	1.388(5)
C(6)-C(11)	1.392(5)	C(19)-N(2)	1.409(4)
C(7)-C(8)	1.388(5)	C(19)-C(24)	1.414(5)
C(7)-H(7)	0.9500	C(20)-C(21)	1.386(5)
C(8)-C(9)	1.386(5)	C(20)-H(20)	0.9500
C(8)-H(8)	0.9500	C(21)-C(22)	1.387(5)
C(9)-O(1)	1.379(4)	C(21)-H(21)	0.9500
C(9)-C(10)	1.391(5)	C(22)-C(23)	1.369(5)
C(10)-C(11)	1.381(5)	C(22)-H(22)	0.9500
C(10)-H(10)	0.9500	C(23)-C(24)	1.384(5)
C(11)-H(11)	0.9500	C(23)-H(23)	0.9500
C(12)-O(1)	1.428(4)	C(24)-N(3)	1.452(4)
C(12)-H(12A)	0.9800	N(2)-H(2A)	0.8800
C(12)-H(12B)	0.9800	N(3)-O(6A)	1.15(2)
C(12)-H(12C)	0.9800	N(3)-O(6)	1.17(3)
C(13)-H(13A)	0.9800	N(3)-O(7)	1.305(6)
C(13)-H(13B)	0.9800	N(3)-O(7A)	1.416(7)

O(7A)-O(7A)#1	1.613(11)		
O(2)-C(1)-N(1)	124.7(3)	C(9)-C(8)-C(7)	118.6(3)
O(2)-C(1)-C(2)	125.3(3)	C(9)-C(8)-H(8)	120.7
N(1)-C(1)-C(2)	110.0(3)	C(7)-C(8)-H(8)	120.7
C(1)-C(2)-C(13)	113.8(3)	O(1)-C(9)-C(8)	123.9(3)
C(1)-C(2)-C(3)	99.2(3)	O(1)-C(9)-C(10)	115.4(3)
C(13)-C(2)-C(3)	117.9(3)	C(8)-C(9)-C(10)	120.6(3)
C(1)-C(2)-H(2)	108.5	C(11)-C(10)-C(9)	119.4(3)
C(13)-C(2)-H(2)	108.5	C(11)-C(10)-H(10)	120.3
C(3)-C(2)-H(2)	108.5	C(9)-C(10)-H(10)	120.3
O(3)-C(3)-C(2)	118.4(3)	C(10)-C(11)-C(6)	121.0(3)
O(3)-C(3)-C(4)	112.3(3)	C(10)-C(11)-H(11)	119.5
C(2)-C(3)-C(4)	105.0(3)	C(6)-C(11)-H(11)	119.5
O(3)-C(3)-H(3)	106.8	O(1)-C(12)-H(12A)	109.5
C(2)-C(3)-H(3)	106.8	O(1)-C(12)-H(12B)	109.5
C(4)-C(3)-H(3)	106.8	H(12A)-C(12)-H(12B)	109.5
N(1)-C(4)-C(3)	98.4(3)	O(1)-C(12)-H(12C)	109.5
N(1)-C(4)-C(17)	118.3(3)	H(12A)-C(12)-H(12C)	109.5
C(3)-C(4)-C(17)	103.4(3)	H(12B)-C(12)-H(12C)	109.5
N(1)-C(4)-C(18)	107.7(3)	C(2)-C(13)-H(13A)	109.5
C(3)-C(4)-C(18)	115.4(3)	C(2)-C(13)-H(13B)	109.5
C(17)-C(4)-C(18)	113.0(3)	H(13A)-C(13)-H(13B)	109.5
N(1)-C(5)-C(6)	112.9(3)	C(2)-C(13)-H(13C)	109.5
N(1)-C(5)-H(5A)	109.0	H(13A)-C(13)-H(13C)	109.5
C(6)-C(5)-H(5A)	109.0	H(13B)-C(13)-H(13C)	109.5
N(1)-C(5)-H(5B)	109.0	O(4)-C(14)-O(3)	111.0(3)
C(6)-C(5)-H(5B)	109.0	O(4)-C(14)-C(15)	105.1(3)
H(5A)-C(5)-H(5B)	107.8	O(3)-C(14)-C(15)	105.0(3)
C(7)-C(6)-C(11)	118.3(3)	O(4)-C(14)-C(16)	111.2(3)
C(7)-C(6)-C(5)	119.9(3)	O(3)-C(14)-C(16)	112.6(3)
C(11)-C(6)-C(5)	121.8(3)	C(15)-C(14)-C(16)	111.5(3)
C(6)-C(7)-C(8)	122.0(3)	C(14)-C(15)-H(15A)	109.5
C(6)-C(7)-H(7)	119.0	C(14)-C(15)-H(15B)	109.5
C(8)-C(7)-H(7)	119.0	H(15A)-C(15)-H(15B)	109.5

C(14)-C(15)-H(15C)	109.5	C(23)-C(22)-H(22)	120.3
H(15A)-C(15)-H(15C)	109.5	C(21)-C(22)-H(22)	120.3
H(15B)-C(15)-H(15C)	109.5	C(22)-C(23)-C(24)	119.5(3)
C(14)-C(16)-H(16A)	109.5	C(22)-C(23)-H(23)	120.2
C(14)-C(16)-H(16B)	109.5	C(24)-C(23)-H(23)	120.2
H(16A)-C(16)-H(16B)	109.5	C(23)-C(24)-C(19)	122.5(3)
C(14)-C(16)-H(16C)	109.5	C(23)-C(24)-N(3)	115.6(3)
H(16A)-C(16)-H(16C)	109.5	C(19)-C(24)-N(3)	121.9(3)
H(16B)-C(16)-H(16C)	109.5	C(1)-N(1)-C(5)	121.9(3)
O(4)-C(17)-C(4)	105.8(3)	C(1)-N(1)-C(4)	109.9(3)
O(4)-C(17)-H(17A)	110.6	C(5)-N(1)-C(4)	124.1(3)
C(4)-C(17)-H(17A)	110.6	C(18)-N(2)-C(19)	126.6(3)
O(4)-C(17)-H(17B)	110.6	C(18)-N(2)-H(2A)	116.7
C(4)-C(17)-H(17B)	110.6	C(19)-N(2)-H(2A)	116.7
H(17A)-C(17)-H(17B)	108.7	O(6A)-N(3)-O(6)	24.9(12)
O(5)-C(18)-N(2)	124.4(3)	O(6A)-N(3)-O(7)	98.1(9)
O(5)-C(18)-C(4)	120.0(3)	O(6)-N(3)-O(7)	118.9(9)
N(2)-C(18)-C(4)	115.6(3)	O(6A)-N(3)-O(7A)	115.6(13)
C(20)-C(19)-N(2)	122.7(3)	O(6)-N(3)-O(7A)	104.9(12)
C(20)-C(19)-C(24)	116.4(3)	O(7)-N(3)-O(7A)	76.6(4)
N(2)-C(19)-C(24)	120.8(3)	O(6A)-N(3)-C(24)	127.0(13)
C(21)-C(20)-C(19)	121.0(3)	O(6)-N(3)-C(24)	119.1(11)
C(21)-C(20)-H(20)	119.5	O(7)-N(3)-C(24)	116.2(3)
C(19)-C(20)-H(20)	119.5	O(7A)-N(3)-C(24)	110.9(4)
C(20)-C(21)-C(22)	121.2(3)	C(9)-O(1)-C(12)	117.5(3)
C(20)-C(21)-H(21)	119.4	C(3)-O(3)-C(14)	109.4(2)
C(22)-C(21)-H(21)	119.4	C(14)-O(4)-C(17)	118.2(2)
C(23)-C(22)-C(21)	119.4(3)	N(3)-O(7A)-O(7A)#1	142.1(4)

Symmetry transformations used to generate equivalent atoms:

#1 -x+2,y,-z+2

Table 4. Anisotropic displacement parameters ($\text{\AA}^2 \times 10^3$) for kob12. The anisotropic displacement factor exponent takes the form: $-2\pi^2 [h^2 a^{*2} U^{11} + \dots + 2 h k a^* b^* U^{12}]$

U ¹¹	U ²²	U ³³	U ²³	U ¹³	U ¹²
C(1)31(2)	18(2)	20(2)	1(1)	1(2)	-1(1)
C(2)22(2)	21(2)	21(2)	3(1)	-3(2)	-3(1)
C(3)20(2)	18(2)	18(2)	1(1)	-1(1)	-1(1)
C(4)23(2)	21(2)	16(2)	1(1)	1(1)	-3(1)
C(5)29(2)	22(2)	24(2)	-1(1)	8(2)	-4(1)
C(6)26(2)	23(2)	19(2)	0(1)	4(1)	-2(1)
C(7)25(2)	27(2)	18(2)	-2(1)	0(1)	-6(1)
C(8)20(2)	29(2)	23(2)	2(1)	2(2)	-2(1)
C(9)27(2)	22(2)	15(2)	1(1)	1(1)	0(1)
C(10)27(2)	22(2)	18(2)	-3(1)	5(1)	-6(1)
C(11)24(2)	22(2)	19(2)	-2(1)	2(1)	-2(1)
C(12)27(2)	25(2)	30(2)	2(1)	3(2)	2(1)
C(13)30(2)	21(2)	33(2)	3(2)	1(2)	4(1)
C(14)29(2)	21(2)	24(2)	8(1)	7(2)	6(1)
C(15)46(2)	30(2)	32(2)	11(2)	16(2)	13(2)
C(16)28(2)	20(2)	31(2)	9(1)	-1(2)	-3(1)
C(17)19(1)	24(2)	17(2)	0(1)	-1(1)	5(1)
C(18)22(2)	17(2)	20(2)	-1(1)	2(1)	0(1)
C(19)21(2)	22(2)	15(2)	-2(1)	-2(1)	-3(1)
C(20)23(2)	23(2)	17(2)	1(1)	-4(2)	2(1)
C(21)31(2)	18(2)	28(2)	-1(1)	1(2)	-1(1)
C(22)31(2)	27(2)	22(2)	-7(2)	-2(2)	-1(2)
C(23)23(2)	26(2)	16(2)	0(1)	0(1)	1(1)
C(24)24(2)	20(2)	21(2)	2(1)	-2(2)	0(1)
N(1)22(1)	21(1)	17(1)	-1(1)	3(1)	-1(1)
N(2)31(2)	18(1)	17(1)	-2(1)	-5(1)	1(1)
N(3)57(2)	22(2)	33(2)	2(1)	-27(2)	1(2)
O(1)24(1)	23(1)	28(1)	2(1)	1(1)	1(1)
O(2)40(1)	30(1)	21(1)	8(1)	4(1)	-1(1)
O(3)27(1)	19(1)	23(1)	5(1)	5(1)	4(1)
O(4)27(1)	21(1)	17(1)	2(1)	2(1)	4(1)

O(5)34(1)	23(1)	25(1)	-3(1)	6(1)	-8(1)
O(6)91(11)	23(5)	24(2)	13(3)	23(7)	0(6)
O(6A)	91(11)	23(5)	24(2)	13(3)	23(7)
0(6)					
O(7)43(3)	23(2)	21(3)	2(2)	-2(2)	-6(2)
O(7A)	42(3)	22(3)	29(3)	-4(2)	-1(2)
4(2)					

Table 5. Hydrogen coordinates ($\times 10^4$) and isotropic displacement parameters ($\text{\AA}^2 \times 10^3$) for kob12.

	x	y	z	U(eq)
H(2)	6926	7523	5814	27
H(3)	7497	5512	6745	24
H(5A)	9436	7622	6541	30
H(5B)	9038	7405	5408	30
H(7)	10349	5794	6417	29
H(8)	10786	3096	6406	29
H(10)	8883	1226	5849	27
H(11)	8457	3943	5745	27
H(12A)	10914	366	5715	42
H(12B)	10866	-1263	6354	42
H(12C)	11045	518	6881	42
H(13A)	7603	10152	7083	44
H(13B)	6832	9624	6952	44
H(13C)	7056	10447	6054	44
H(15A)	7707	4631	9960	53
H(15B)	7024	5597	9432	53
H(15C)	7723	6601	9753	53
H(16A)	7355	3388	7409	42
H(16B)	6811	3590	8031	42
H(16C)	7500	2598	8487	42
H(17A)	8481	4166	7421	25
H(17B)	9136	5117	8082	25
H(20)	8784	11509	8770	27
H(21)	9125	13523	9986	32
H(22)	9614	12758	11615	34
H(23)	9759	9934	12029	28
H(2A)	8758	7209	9165	29